Edited by Patrick Theato
and Harm-Anton Klok

WILEY-VCH

Functional Polymers by Post-Polymerization Modification

Concepts, Guidelines, and Applications

Edited by
Patrick Theato and Harm-Anton Klok

**Functional Polymers by
Post-Polymerization Modification**

Related Titles

Schlüter, D. A., Hawker, C., Sakamoto, J. (eds.)

Synthesis of Polymers

New Structures and Methods

2 Volumes
2012
ISBN: 978-3-527-32757-7

Mittal, V. (ed.)

In-situ Synthesis of Polymer Nanocomposites

2012
ISBN: 978-3-527-32879-6

Friedrich, J.

The Plasma Chemistry of Polymer Surfaces

2012
ISBN: 978-3-527-31853-7

Mathers, R. T., Meier, M. A. R. (eds.)

Green Polymerization Methods

Renewable Starting Materials, Catalysis and Waste Reduction

2011
ISBN: 978-3-527-32625-9

Barner-Kowollik, C., Gruendling, T., Falkenhagen, J., Weidner, S. (eds.)

Mass Spectrometry in Polymer Chemistry

Advanced Techniques for Surface Design

2011
ISBN: 978-3-527-32924-3

Leclerc, M., Morin, J.-F. (eds.)

Design and Synthesis of Conjugated Polymers

2010
ISBN: 978-3-527-32474-3

Dubois, P., Coulembier, O., Raquez, J.-M. (eds.)

Handbook of Ring-Opening Polymerization

2009
ISBN: 978-3-527-31953-4

Barner-Kowollik, C. (ed.)

Handbook of RAFT Polymerization

2008
ISBN: 978-3-527-31924-4

Coqueret, X., Defoort, B. (eds.)

High Energy Crosslinking Polymerization

Applications of Ionizing Radiation

2006
ISBN: 978-3-527-31838-4

Edited by Patrick Theato and Harm-Anton Klok

Functional Polymers by Post-Polymerization Modification

Concepts, Guidelines, and Applications

WILEY-VCH

WILEY-VCH Verlag GmbH & Co. KGaA

The Editors

Prof. Dr. Patrick Theato
Techn. & Macromol. Chemistry
Bundesstraße 45
20146 Hamburg
Germany

Prof. Dr. Harm-Anton Klok
EPFL, Lab. des Polymères
STI-IMX-LP, MXD 112
Station 12
1015 Lausanne
Switzerland

Contents

3   Thiol–ene Based Functionalization of Polymers   *65*
Nikhil K. Singha and Helmut Schlaad

4   Thiol–yne Chemistry in Polymer and Materials Science   *87*
Andrew B. Lowe and Justin W. Chan

List of Abbreviations

2Box	2-(3-Butenyl)-2-oxazoline
2EOx	2-Ethyl-2-oxazoline
2MOx	2-Methyl-2-oxazoline
αAl $\in$ CL	6-Allyl-$\in$-caprolactone
αCl $\in$ CL	α-Chloro-$\in$-caprolactone
α-GP-alkyne	2-(α-ᴅ-Glucopyranosyloxy)-N-2-propyn-1-yl acetamide
αN$_3$ $\in$ CL	α-Azido-$\in$-caprolactone
αP $\in$ CL	α-Propargyl-$\in$-caprolactone
αPδVL	α-Propargyl-δ-valerolactone
$\in$ CL	$\in$-caprolactone
γAεCL	γ-Acryloyloxy-ε-caprolactone
AAm	Acrylamide
AARS	Aminoacyl tRNA synthetase
AC	Acryloyl carbonate
ADC	2,6-Anthracenedicarboxylate
ADTC	2,2-Bis(azidomethyl)trimethylene carbonate
AGE	Allyl glycidyl ether
Aha	Azidohomoalanine
AHMA	6-Azidohexyl methacrylate
AIBN	2,2′-Azobis(2-methylpropionitrile)
AMA	Anthrylmethyl methacrylate
Amp	Ampicillin
AN	Acrylonitrile
AOA	Acetone oxime acrylate
AOI	2-(Acryloyloxy)ethylisocyanate
AP	Anionic polymerization
APMOS	Anthracen-9-ylmethyl 2-((2-bromo-2-methyl-propanoyloxy)methyl)-2-methyl-3-oxo-3-(prop-2-ynyloxy)-propyl succinate
AROP	Anionic ring-opening polymerization
ATRA	Atom transfer radical addition
ATRP	Atom transfer radical polymerization
AzDXO	5,5-Bis(azidomethyl)-1,3-dioxan-2-one
AzEMA	2-Azidoethyl methacrylate

AzHMA	6-Azidohexyl methacrylate
AzPMA	3-Azidopropyl methacrylate
B3MA	But-3-enyl methacrylate
BMVB	1-[(3-Butenyloxy)methyl]-4-vinylbenzene
BP2TF	Benzyl pyridine-2-yldithioformate
Bpa	*p*-Benzoylphenylalanine
BPNorb	3-(Bromo)propyl *exo*-bicyclo[2.2.1]hept-5-ene-2-carboxylate
bPP	Brominated *p*-phenylene
BrS	4-Bromostyrene
Bu	Butadiene
CAA	Chloroallyl azide
CAT	Chloramphenicol acetyltransferase
CD	Cyclodextrin
CHMFS	4-(6′-Methylcyclohex-3-′enylmethoxy)-2,3,5,6-tetrafluorostyrene
Cm	Chloramphenicol
CROP	Cationic ring opening polymerization
CuAAC	Copper catalyzed azide/alkyne cycloaddition
D3	Hexamethylcyclotrisiloxane
DAPA	*N*-[3-(dimethylamino)propyl]-acrylamide
DBCO-NHS	Aza-dibenzocyclooctyne *N*-hydroxy succinimide ester
DBTDL	Dibutyltin dilaureate
DBU	1,8-Diazabicyclo[5.4.0]undec-7-ene
DBz	*β*-Benzyl aspartate-*ω*-benzylamide
DEAEMA	2-(Diethylamino)ethyl methacrylate
DecEnOx	2-(Dec-9-enyl)-2-oxazoline
DHFR	Dihydrofolate reductase
DIC	Diisopropylcarbodiimide
DIEA	*N,N*-Diisopropylethylamine
DMAEMA	2-(Dimethylamino)ethyl methacrylate
DMPA	2,2-Dimethoxy-2-phenylacetophenone
dPGL	3,6-Dipropargyl-1,4-dioxane-2,5-dione
DTC	2,2-Bis(methyl)trimethylene carbonate
DVB	Divinylbenzene
EdMA	Ethylene dimethacrylate
EG	Ethylene glycol
EGMA	Ethylene glycol methacrylate
EPL	Expressed protein ligation
EO	Ethylene oxide
EOP	Ethylene/olefin copolymerization
ET	Ethylene terephthalate
EVGE	Ethoxy vinyl glycidyl ether
FMA	Furfuryl methacrylate
FRP	Free radical polymerization
Fu-PU	Furan containing polyurethanes
FVFC	2-Formal-4-vinylphenyl ferrocenecarboxylate
GA	Glycidyl acrylate
GalNac	*N*-Acetylgalactosamine

GFP	Green fluorescent protein
GI	Globalide
GlcAc$_4$-SH	2,3,4,6-Tetra-*O*-acetyl-1-thio-*β*-D-glucopyranose
GlcNAc	N-acetylglucosamine
GMA	Glycidyl methacrylate
GPE	Glycidyl phenyl ether
GST	Glutathione S-transferase
HB-I (PPV-PPE)	Hyperbranched iodinated poly(phenylene vinylene-phenylene ethynylene)
HMPA	Hexamethylphosphoramide
Hpg	Homopropargylglycine
HPMA	*N*-(2-hydroxypropyl)methacrylamide
IBBL	2,8-Dioxa-1-isopropenylbicyclo[3.3.0]octane-3,7-dione
IMK	Isopropenyl methyl ketone
LA	L-lactide
LCST	Lower critical solution temperature
MA	Methyl acrylate
MAA	Methacrylic acid
MAC	5-Methyl-5-allyoxycarbonyl-1,3-dioxanone
MAC$_2$AE	*N*-methacryloyl-*β*-alanine [*N′*]−oxysuccinimide ester
MAn	Maleic anhydride
MAPTT	3-(3-Methacrylamidopropanoyl)-thiazolidine-2-thione
MBPS-A	Polystyrene-anthracene multiblock copolymer
ME$_6$TREN	Tris[2-(dimethylamino)-ethyl]amine
MI	Maleimide
MMA	Methyl methacrylate
MVI	1-Methylvinylisocycanate
N$_3$MPA	2-[(2-Deoxy-2-azido-α-D-mannopyranosyloxy)ethanamido]-ethyl acrylamide
Na$_{asc}$	Sodium ascorbate
NAA	Non-natural amino acid
nAChR	Nicotinic acetylcholine receptor
NAS	*N*-acryloxysuccinimide
*n*BA	*N*-butyl acrylate
NBAz	2-(Norborn-2-en-5-yl)-4,4-dimethyl-5-oxazoline
NCL	Native chemical ligation
NHNS	Bicyclo[2.2.1]hept-5-ene-*exo*-2-carboxylic acid *N*-hydroxysuccinimide ester
NMAS	*N*-methacryloxysuccinimide
NMM	4-Methylmorpholine
NMP	Nitroxide-mediated polymerization
NNC	4-Nitro-1-naphthyl cinnamate
NPA	*p*-Nitrophenyl acrylate
NPC	4-Nitrophenyl cinnamate
NPMA	*p*-Nitrophenyl methacrylate
NPME	5-Norbornene-2-methyl-propargyl ether
NSVB	*N*-oxysuccinimide *p*-vinyl benzoate
OBNorb	3-Oxobutyl *exo*-bicyclo[2.2.1]hept-5-ene-2-carboxylate
OEGMA	Oligo(ethylene glycol methacrylate)
OP	Oxidative polymerization

p-AcF	*p*-Acetylphenylalanine
p-AzF	*p*-Azidophenylalanine
p-FF	*p*-Fluorophenylalanine
p-NH$_2$F	*p*-Aminophenylalanine
PA	Polyaddition
PBS	Phosphate buffered saline
PC	Polycondensation
PCDO	5-Methyl-5-propargyloxycarbonyl-1,3-dioxan-2-one
PDA	2-(Pyridyldithio)-ethylamine
PDS	Pyridyl disulfide
PDSA	Pyridyl disulfide propyl acrylate
PDSM	Pyridyl disulfide ethyl methacrylate
PDTEMA	*N*-[2-(2-pyridyldithio)]ethyl methacrylamide
PEG	Poly(ethylene glycol)
PFA	Pentafluorophenyl acrylate
PFMA	Pentafluorophenyl methacrylate
PFPNorb	*exo*-5-Norbornene-2-carboxylic acid pentafluorophenyl ester
PFS	Pentafluorostyrene
PFVB	Pentafluorophenyl 4-vinyl benzoate
PGL	3-Methyl-6-propargyl-1,4-dioxane-2,5-dione
PgMA	Propargyl methacrylate
PKE	Poly(keto ester)
PLG	γ-Propargyl-L-glutamate
PMDETA	*N,N,*[*N′*],[*N′*],[*N*]″-pentamethyldiethylenetriamine
PMNorb	3-(Maleimidyl)propyl *exo*-bicyclo[2.2.1]hept-5-ene-2-carboxylate
PP	Photopolymerization
PPh	*p*-Phenylene
PPP	Pulsed-plasma polymerization
ProDOT-H	3,3-dihexyl-3,4-dihydro-2H-thieno[3,4-b][1,4]dioxepine
ProDOT-P	3-methyl-3-((prop-2-yn-1-yloxy)methyl)-3,4-dihydro-2H-thieno[3,4-b][1,4]dioxepine
PS	Polystyrene
PTM	Posttranslational modification
PTSA	*p*-Toluene sulfonic acid
PTXL	Paclitaxel
PU(ArAll$_3$-HMDI)	2,3,4-Tri-O-allyl-L-arabinitol based polyurethane
PU-DPPD	2,2-Di(prop-2-ynyl)propane-1,3-diol based polyurethane
PU-MPPD	2-Methyl-2-propargyl-1,3-propanediol based polyurethane
PU-PBM	3,5-Bis(hydroxymethyl)-1-propargyloxybenzene based polyurethane
Py	Pyridine
PynOx	2-(Pent-4-ynyl)-2-oxazoline
RAFT	Reversible addition-fragmentation chain transfer
ROMP	Ring-opening metathesis polymerization
ROP	Ring-opening polymerization
RSI	Residue-specific incorporation
SAE	Succinic acid ester
SCEMA	2-(*N*-succinimidylcarboxyoxy)ethyl methacrylate
SI	Surface-initiated

SMANCS	Styrene-*alt*-maleic anhydride copolymer conjugated neocarzinostatin
SPAAC	Strain promoted azide/alkyne cycloaddition
SSI	Site-specific incorporation
St	Styrene
t-BA	*t*-Butyl acrylate
TCEP	Tris(2-carboxyethyl)phosphine
TEA	Triethylamine
TFA	Trifluoroacetic acid
TFPMA	Tetrafluorophenyl methacrylate
TMC	Trimethylene carbonate
TMI	*m*-Isopropenyl-α-α-dimethylbenzyl isocyanate
TMS	Trimethylsilyl
*tt*HA	*trans,trans*-Hexa-2,4-dienylacrylate
V1D2	1-Vinyl-1,3,3,5,5-pentamethylcyclotrisiloxane
V4	1,3,5,7-Tetramethyl-1,3,5,7-tetravinylcyclotetrasiloxane
VBA	Vinylbenzaldehyde
VDF	Vinyldiene fluoride
VDM	2-Vinyl-4,4-dimethyl-5-oxazoline
VI	Vinylisocyanate
VMK	Vinylmethylketone
VP	Vinyl pyridine
VSC	Vinyl sulfone carbonate

List of Contributors

Rachelle Arnold
University of Georgia
Department of Chemistry
Faculty Engineering
220 Riverbend Road
Athens, GA 30602
USA

Mehmet Arslan
Bogazici University
Department of Chemistry
34342 Istanbul
Turkey

C. Remzi Becer
University of Warwick
Department of Chemistry
Gibbet Hill Road
Coventry CV4 7AL
United Kingdom

Adam H. Broderick
University of Wisconsin
–Madison
Department of Chemical and
Biological Engineering
1415 Engineering Drive
Madison, WI 53706
USA

James A. Burns
University of Warwick
Department of Chemistry
Gibbet Hill Road
Coventry CV4 7AL
United Kingdom

Neil R. Cameron
Durham University
Department of Chemistry
South Road
Durham DH1 3LE
UK

Justin W. Chan
DuPont Central Research and
Development Experimental
Station
200 Powder Mill Road
Wilmington, DE 19880-0328
USA

Delphine Chan-Seng
Institut Charles Sadron
Precision Macromolecular
Chemistry Group
23 rue du Loess
67034 Strasbourg Cedex 2
France

Tugce Nihal Gevrek
Bogazici University
Department of Chemistry
34342 Istanbul
Turkey

Matthew I. Gibson
University of Warwick
Department of Chemistry
Gibbet Hill Road
Coventry CV4 7AL
United Kingdom

Joe Grubbs
University of Georgia
Department of Chemistry
Faculty of Engineering
220 Riverbend Road
Athens, GA 30602
USA

Kemal Arda Günay
University of Hamburg
Institute for Technical and
Macromolecular Chemistry
Bundesstrasse 45
20146 Hamburg
Germany

Ryohei Kakuchi
University of Hamburg
Institute for Technical and
Macromolecular Chemistry
Bundesstrasse 45
20146 Hamburg
Germany

Toyoji Kakuchi
Hokkaido University
Faculty of Engineering
Division of Biotechnology and
Macromolecular Chemistry
Polymer Chemistry Laboratory
Kita 13
Nishi 8
Sapporo
Hokkaido 060-8628
Japan

Ravi S. Kane
Rensselaer Polytechnic Institute
The Howard P. Isermann
Department of Chemical and
Biological Engineering
Center for Biotechnology and
Interdisciplinary Studies
110 8th St.
Troy, NY 12180
USA

Andreas F. M. Kilbinger
University of Fribourg
Chemistry Department
Chemin du musée 9
1700 Fribourg
Switzerland

Linda Kircher
University of Mainz
Institute for Organic Chemistry
Duesbergweg 10-14
55099 Mainz
Germany

and

Durham University
Department of Chemistry
South Road
Durham DH1 3LE
UK

Harm-Anton Klok
Ecole Polytechnique Fédérale de
Lausanne (EPFL)
Institut des Matériaux et Institut
des Sciences et Ingénierie
Chimiques
Laboratoire des Polymères
Batiment MXD, Station 12
1015 Lausanne
Switzerland

Jason Locklin
University of Georgia
Department of Chemistry
Faculty of Engineering
220 Riverbend Road
Athens, GA 30602
USA

Andrew B. Lowe
University of New South Wales
School of Chemical Engineering
Centre for Advanced
Macromolecular Design (CAMD)
School of Chemical Engineering
High Street, Sydney
New South Wales 2052
Australia

Jean-François Lutz
Institut Charles Sadron
Precision Macromolecular
Chemistry Group
23 rue du Loess BP84047
67034 Strasbourg Cedex 2
France

David M. Lynn
University of Wisconsin–
Madison
Department of Chemical and
Biological Engineering
1415 Engineering Drive
Madison, WI 53706
USA

Jacob T. Martin
Rensselaer Polytechnic Institute
The Howard P. Isermann
Department of Chemical and
Biological Engineering
Center for Biotechnology and
Interdisciplinary Studies
110 8th St.
Troy, NY 12180
USA

Jin Kim Montclare
Polytechnic Institute of
New York University
Department of Chemical and
Biological Sciences
6 MetroTech Center
Brooklyn, NY 11201
USA

Bongjin Moon
Sogang University
Department of Chemistry
1-1 Shinsoo-Dong
Mapo-Gu
Seoul 121-742
Korea

Haresh More
Polytechnic Institute of
New York University
Department of Chemical and
Biological Sciences
6 MetroTech Center
Brooklyn, NY 11201
USA

Sara Orski
University of Georgia
Department of Chemistry
Faculty of Engineering
220 Riverbend Road
Athens, GA 30602
USA

Ryosuke Sakai
Asahikawa National College of
Technology
Department of Materials
Chemistry
2-2-1-6 Shunkodai
Asahikawa
Hokkaido 071-8142
Japan

Amitav Sanyal
Bogazici University
Department of Chemistry
34342 Istanbul
Turkey

Helmut Schlaad
Max Planck Institute of
Colloids and Interfaces
Department of Colloid Chemistry
Research Campus Golm
14424 Potsdam
Germany

Gareth Sheppard
University of Georgia
Department of Chemistry
Faculty of Engineering
220 Riverbend Road
Athens, GA 30602
USA

Nikhil K. Singha
Indian Institute of Technology
Rubber Technology Centre
Kharagpur 721302
India

Patrick Theato
University of Hamburg
Institute for Technical and
Macromolecular Chemistry
Bundesstrasse 45
20146 Hamburg
Germany

Ching-Yao Yang
Polytechnic Institute of New York
University
Department of Chemical and
Biological Sciences
6 MetroTech Center
Brooklyn, NY 11201
USA

Mirela Zamfir
Institut Charles Sadron
Precision Macromolecular
Chemistry Group
23 rue du Loess
67034 Strasbourg Cedex 2
France

1
History of Post-polymerization Modification

Kemal Arda Günay, Patrick Theato, and Harm-Anton Klok

1.1
Introduction

The history of post-polymerization modification, also known as *polymer analogous modification*, is arguably as long as the history of polymer science. As early as 1840, Hancock and Ludersdorf independently reported the transformation of natural rubber into a tough and elastic material on treatment with sulfur [1]. In 1847, Schönbein exposed cellulose to nitric acid and obtained nitrocellulose [2], which was later employed as an explosive. In 1865, Schützenberger prepared cellulose acetate by heating cellulose in a sealed tube with acetic anhydride. The resulting material has found widespread use as photographic film, artificial silk, and membrane material, among others [3]. Although the post-polymerization modification of these natural polymers was widely used in the late nineteenth and early twentieth centuries, the nature of these materials and their modification reactions were only poorly understood. This comes as no surprise, as it was at the same time that Staudinger [4], one of the pioneers of modern polymer science, was struggling to gain acceptance for the notion of the existence of macromolecules. Staudinger [5] also coined the term *polymer analogous reaction* and studied these reactions as an attractive approach to fabricate functional materials.

The general acceptance of the concept of macromolecules also marked the beginning of an increased use of post-polymerization modification reactions to engineer synthetic polymers. Serniuk *et al.* [6] reported the functionalization of butadiene polymers with aliphatic thiols via thiol–ene addition in 1948. Chlorinated polystyrene–divinylbenzene beads were first used in the 1950s as ion exchange resins [7] and later by Merrifield to develop solid-state peptide synthesis [8]. The modification of halogenated or lithiated poly(meth)acrylates was first investigated in the early 1960s [9, 10] and followed by Iwakura's studies on the post-polymerization modification of polymers bearing pendant epoxide groups [11–13]. Although many of the early developments in polymer science can be attributed to the utilization of post-polymerization modifications, the variety of chemical reactions that was available for post-polymerization modification was relatively limited (Figure 1.1). This, however, rapidly changed in the early 1990s with the emergence
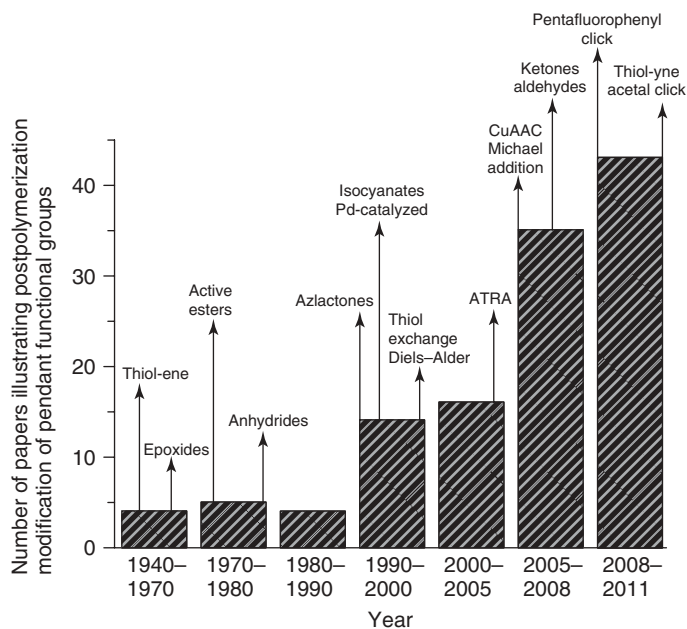
Figure 1.1 Historical overview of the development of post-polymerization modification. The work on post-polymerization modification increased with a skyrocketing pace starting from the late 1990s as a result of development of functional-group-tolerant (controlled radical) polymerization techniques combined with the (re)discovery of highly efficient coupling chemistries. This figure was prepared based on the articles cited in this chapter and last updated in September 2011.

of living/controlled radical polymerization techniques such as atom-transfer radical polymerization (ATRP), reversible addition-fragmentation chain transfer (RAFT), and nitroxide-mediated polymerization (NMP) [14–16]. The improved functional group tolerance of these methods as compared to conventional polymerization techniques allowed the fabrication of well-defined polymers bearing a wide variety of functional groups that can be quantitatively and selectively modified using relatively mild conditions without any side reactions.

The emergence of living/controlled radical polymerization techniques coincided with the discovery/revival of several chemoselective coupling reactions such as copper-catalyzed azide/alkyne cycloaddition (CuAAC), thiol–ene addition, and many others, which are now commonly referred to as *click* reactions. Together, these two developments provided the basis for the explosive growth in use and versatility of post-polymerization reactions since the 1990s. The aim of this chapter is to give a historical account of the development of nine main classes of post-polymerization modification reactions (Scheme 1.1). For the selection of these reactions, strategies that involve the use of, for example, poorly controlled nucleophilic substitution reactions and the modification of relatively inert groups, such as alcohols and carboxylic acids, were not considered. Instead, emphasis was placed on readily
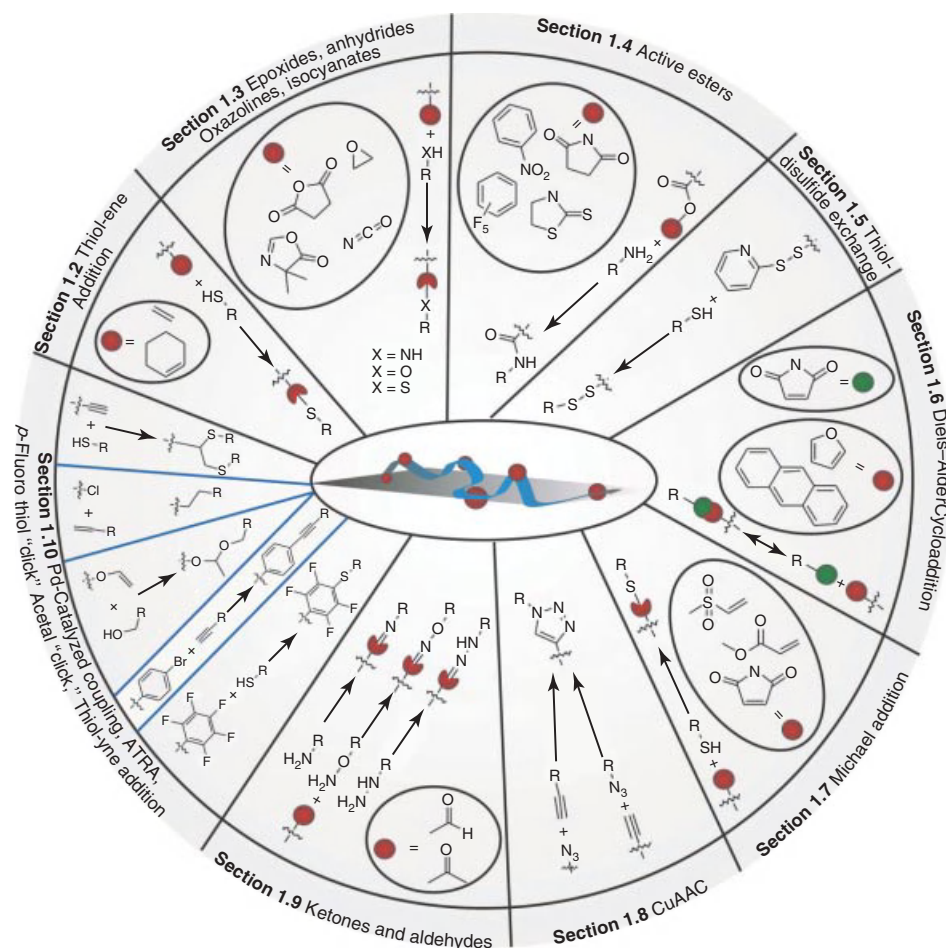
Scheme 1.1 Nine different classes of reactions that can be used for the preparation of functionalized polymers via post-polymerization modification.

available reactive groups that do not require an additional deprotection step before post-polymerization modification.

1.2
Post-polymerization Modification via Thiol-ene Addition

The anti-Markovnikov addition of thiols to alkenes is usually mediated by a radical source or by ultraviolet (UV) irradiation [17]. One of the earliest systematic studies regarding the post-polymerization modification of polyBu via radical thiol addition was reported by Serniuk and coworkers in 1948 [6]. They proposed that only the vinyl

groups generated by 1,2-addition of butadiene units (i.e., pendant vinyl groups) were functionalized, which was later confirmed by Romani and coworkers [18]. Since these early studies, thiol–ene post-polymerization modification has developed into a powerful synthetic tool. Table 1.1 provides an overview of different alkene functional polymers that have been used as substrates for post-polymerization modification.

A drawback of thiol–ene addition to poly(1,2-Bu) is that because of the close proximity of the neighboring vinyl groups, the radical formed after the addition of the thiol may attack an adjacent vinyl group, leading to an intramolecular cyclization [20]. One possibility to suppress this side reaction is to carry out the post-polymerization modification at low temperature and at relatively high concentrations [24]. Schlaad and coworkers further illustrated that, by increasing the distance between pendant alkene groups, intramolecular cyclization could also be supressed, which revolutionized the via thiol–ene post-polymerization modification [22]. This was demonstrated by the post-polymerization modification of poly2Box, which was quantitatively modified using 1.2–1.5 equivalents thiol under mild conditions (radicals generated with UV light at room temperature).

Radicals that mediate the thiol–ene addition can either be generated by thermal or photochemical initiation. Hawker and coworkers illustrated that, although both initiation pathways lead to the complete conversion of pendant alkenes, milder conditions and shorter reaction times are sufficient when photoinitiators are used (Scheme 1.2) [23]. Furthermore, they also demonstrated the orthogonality of the radical thiol addition and CuAAC and the compatibility of the alkene group with controlled radical polymerization (CRP) techniques.

Recently, Heise reported the preparation of an unsaturated polyester (polyGI) via enzymatic ring-opening polymerization (ROP) of the corresponding cyclic ester monomer containing backbone alkene groups. He demonstrated that these backbone alkene groups are also susceptible to post-polymerization modification via thiol–ene addition, but near-quantitative conversion of these groups is only possible when a high excess of thiol is used, as these backbone alkene groups have decreased reactivity compared to pendant alkenes [31].

1.3
Post-polymerization Modification of Epoxides, Anhydrides, Oxazolines, and Isocyanates
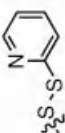
Epoxides, anhydrides, oxazolines, and isocyanates represent a class of reactive groups that have a relatively long history in polymer science. A common feature of these groups is that they are tolerant toward radical-based polymerization techniques, which explains why polymers containing these groups were extensively used for the fabrication of functional polymers via post-polymerization modification already since the 1960/1970s. Table 1.2 provides an overview of polymers bearing epoxide, anhydride, oxazoline, and isocyanate groups that have been used for post-polymerization modification.

Table 1.1 Post-Polymerization modification of (co)polymers via radical thiol addition.

Functional group(s)	Monomer	Comonomer	Polymerization method	Reagents – reaction conditions	Post-Polymerization modification	
					Conversion (%)	Comments
(alkene ∿=)	Bu	St	FRP	Thioglycolic acid, air, r.t. 3–144 h	38–47	Only the vinyl double bonds (generated by 1,2-addition) were assumed to undergo functionalization [6]
		AN		C8–C16 chain length mercaptans (2.0 equivalents), 180–200°C	35–52	
	Bu	St	FRP	Thioglycolic acid, ethyl mercaptoacetate, AIBN, or benzoyl peroxide, 90–100°C, 2.5 h	24–40	Post-Polymerization modification only proceeds from the vinyl double bonds. Side reactions are possible [18]
	V4 V1D2	D3	ROP	1-Octanethiol, 2-(4-pyridyl)ethanethiol (2.0–3.0 equivalents), AIBN (0.12–0.26 equivalents), 65°C, 2–24 h	100	Excess thiol was used to suppress the side reactions [19]
	1,2-Bu	EO	AP	A library of thiols (5.0–40.0 equivalents), AIBN (0.3 equivalents), 70°C, 24 h	70–86	Side reactions are possible [20, 21]
	2BOx	2EOx	CROP	A library of thiols (1.2–1.5 equivalents), UV, 24 h	96–100	Mild reaction conditions. No side reactions. Radical thiol addition was proposed as a click reaction [22]
	B3MA	MMA	ATRP	Library of thiols (5.0–10.0 equivalents), DMPA (0.2 equivalents), UV, r.t., 0.5–2 h	46–100	Photochemical initiation warrant access to greater yields at milder conditions compared to thermal initiation. Orthogonality of the thiol–ene and CuAAC reactions was demonstrated [23]
	αAleCL	εCL	ROP	Library of thiols (5.0–10.0 equivalents), AIBN (0.2 equivalents), 80°C, 3–24 h	17–100	
	BMVB	St	RAFT	Methyl 3-mercaptopropionate (2.0 equivalents), UV, −35°C, 24 h	86	Carried out in concentrated media and at low temperature to suppress side reactions [24]
	1,2-Bu	—	—	A library of thiols (2.0 equivalents), AIBN (0.1 equivalents), 90°C, 24 h	Quantitative	Excess thiol was used to suppress side reactions [25]
	MAC	—	—	2-Mercaptoethanol (47 equivalents), AIBN (2.0 equivalents), 80°C, 24 h	Quantitative	
	U(ArAll3-HMDI)	—	PA	A library of thiols (20.0 equivalents), AIBN (0.75 equivalents), 75°C, 24 h	Quantitative	Polymer bears three allyl groups per repeating unit [26]
	AGE	EO	AROP	A library of thiols (20.0 equivalents), AIBN (0.75 equivalents), 75°C, overnight	90–98	Excess thiol was used to suppress the side reactions [27]
	EVGE	EO	AROP	Benzyl mercaptan (0.5–10.0 equivalents), AIBN (0.75 equivalents), 75°C, 12 h	Quantitative	No side reactions [28]
	DecEnOx	2EOx	CROP	Ac4GlcSH (1.2 equivalents), DMPA (0.2 equivalent), UV, 6 h	100	Polymer contains three chemoselective handles allowing sequential functionalization [29]

Table 1.1 (*continued.*)

Functional group(s)	Monomer	Comonomer	Polymerization method	Post-Polymerization modification		
				Reagents – reaction conditions	Conversion (%)	Comments
(structure)	CHMFS	—	RAFT	$C_{12}H_{25}SH$ (3.0 equivalents), DMPA (2 mol%), UV, 30 min	85	[30]
(structure)	GI	—	ROP	6-Mercapto-1-hexanol, butyl-3-mercapto propionate, N-acetylcysteamine (excess), AIBN, 80 °C	75–95	Excess thiol is necessary for high degree of functionalization [31]
(structure)	PDSM	—	RAFT	PEG_{2000}-acrylate (1.2 equivalents), DMPA (0.20 equivalent), TCEP (1.0 equivalents), UV, 1h	68	Side reactions are possible [32]
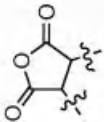
AIBN, 2,2′-Azobis(2-methylpropionitrile); AP, anionic polymerization; CROP, cationic ring-opening polymerization; DMPA, 2,2-dimethoxy-2-phenylacetophenone; and AROP, anionic ring-opening polymerization.
For each functional group/substrate, entries are listed in chronological order.
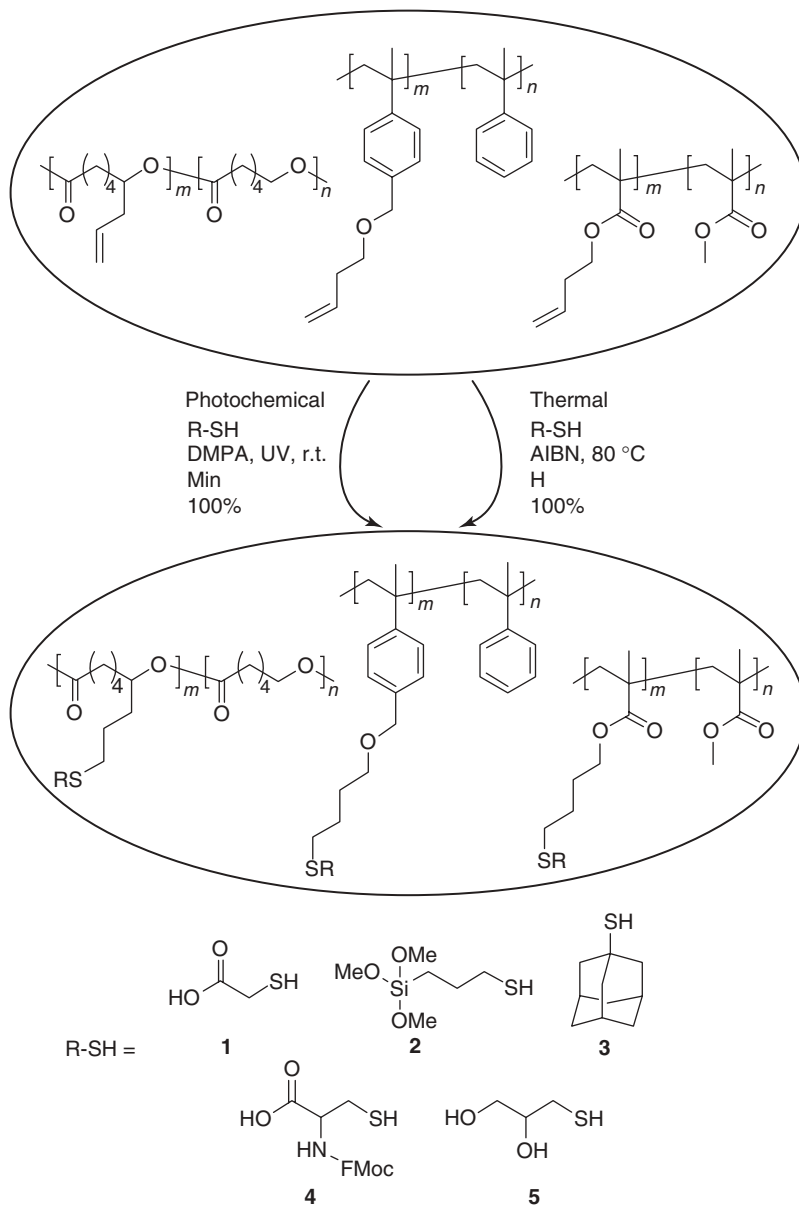
Scheme 1.2 Post-Polymerization modification of polymers bearing alkene groups via thiol–ene addition either mediated by photochemical or thermal initiation [23].

Table 1.2 Post-Polymerization modification of (co)polymers bearing epoxide, anhydride, oxazoline, and isocyanate groups.

Functional group(s)	Monomer	Comonomer	Polymerization method	Reagents – reaction conditions	Post-Polymerization modification	
					Conversion (%)	Comments
(epoxide)	GA	AN	FRP	Di-n-butylamine, diethanolamine (4.0 equivalents), 70°C, 10–14 h	45–80	Conversion depends on copolymer composition [11, 12]
	GMA	MMA	FRP	Di-n-butylamine, N-butylhexylamine (1.0 equivalent), 70°C, 2.5 h	20–35	[13]
	GMA	St	FRP	A library of amines and carboxylic acids (excess), 80°C, 20 h	20–80	Addition of TEA improved the rate of post-polymerization modification with carboxylic acids [33].
	GMA	MMA	FRP	NPC, NNC (1.0 equivalent), base (1.0 equivalent), 90–130°C, 24 h	35–95	Side reactions are possible [34].
	GMA	MMA	FRP	4-Hydroxy-4'-methoxybiphenyl (1.3 equivalents), Na (1.3 equivalents), refluxed in 1,4-dioxane, 6 h	75–100	Copolymer is more reactive than homopolymer [35]
	GMA	MMA	SI-ATRP	Octylamine (1.0 M), 60°C, 4 h	58	Cross-linking occurs between neighboring chains [36]
	GMA	DEAEMA	SI-ATRP	A library of primary amines (0.5–1.0 M), r.t., 48 h	10–79	Tertiary amine groups of DEAEMA catalyzes the reaction [37]

MAn	St	FRP	Neocarzinostatin (0.2 equivalent), 4°C, pH 8.5, 24 h	97 (Amino group)	MAn is partially hydrolyzed. Polymer–drug conjugate was prepared (SMANCS) [38, 39]
MAn	St	FRP	Octylamine, 0–40°C, 3 h	90	Functionalization with sterically hindered amines is not possible [40]
MAn	St	FRP	4-Aminobenzoic acid (1.5 equivalents), TEA (2.0 equivalents), 90°C, 48 h	Quantitative	Near-quantitative functionalization with aromatic amines is possible. Conversion of MAn with amines is greater compared to alcohols [41]
MAn	St	—	A library of amine-functionalized sugars (2.0 equivalents), r.t., 3 h	54–94	Obtained glycopolymers showed improved hepatic cell adhesion compared to hydrolyzed MAn-alt-St [42]
MAn	St	FRP	Propylamine, butylamine, pentylamine, r.t., 5 h	Quantitative	[43]
VDM	MMA	FRP	4-Methoxy-4'-(β-aminoethoxy) biphenyl (1.1 equivalents), 70°C, 24 h	65–90	No side reactions [44]
VDM	AAm EdMA St	SI-FRP	Benzylamine (0.3 equivalent), 30 min	100	Functionalized porous disks were developed to scavenge excess amines from the reaction mixtures [45]
VDM	—	FRP	Benzylamine, Jeffamine M600®, DBz10, 40°C, 72 h	Quantitative	Aqueous post-polymerization modification [46]
VDM	St	NMP	Benzylamine, morpholine (1.2 equivalents), r.t., 24 h	Quantitative	[47]
NBAz	—	ROMP	Glycine methyl ester hydrochloride (1.5 equivalents), TEA (1.5 equivalents), r.t., 20 h; Diethylamine (1.1 equivalents), r.t., 20 h	Quantitative	[48]
VDM	St	SI-ATRP	Benzylamine (1.0 equivalent), r.t., 24 h	66–98	M_n of the copolymer influences the extent of post-polymerization modification [49]

Table 1.2 (continued.)

Functional group(s)	Monomer	Comonomer	Polymerization method	Reagents – reaction conditions	Post-Polymerization modification	
					Conversion (%)	Comments
O=C=N– (structure)	TMI	St	FRP	PEG$_{750}$-OCH$_3$, hydroxymethyl(benzo-18-crown-6) (5.0 equivalents), DBTDL (catalyst), 85°C, 20 h	Quantitative	Post-Polymerization modification of a cross-linked network [50]
	MVI	MA	FRP	A library of hydroxyl-functionalized hemicyanines (0.3 equivalent), 40°C, 3 d	30–35	Allows the fabrication of polymeric multilayers containing nonlinear optical (NLO) chromophores [51]
	MVI	MI	FRP	A library of undemanding alcohols and hydroxyl-functionalized chromophores (1.0 equivalent), DBTDL (0.02 equivalent), 50°C, 1–2 d	Quantitative	Reactivity of isocyanates toward alcohols and amines were demonstrated in different reaction conditions [52]
	VI			A library of amines (1.0 equivalent), 50°C, 2–3 h	80–100	
	TMI	St	ATRP	9-Methyl-(aminomethyl)anthracene, r.t., 4 h	Quantitative	[53]
	AOI	—	RAFT	Hexanol (1.5 equivalents), 0.1% (wt) DBTDL, overnight; Hexylamine (1.0 equivalent), overnight; Hexanethiol (1.0 equivalent), 0.5% (wt) TEA, overnight	Quantitative	Reactivity and chemoselectivity of isocyanates toward alcohols, amines, and thiols were demonstrated in different reaction conditions [54]
	AOI	—	SI-PP	A library of thiols, DBU (0.2 mol% with respect to thiol), r.t., minutes	Quantitative	Proposed as a click reaction. Faster functionalization when DBU was used as a catalyst compared to TEA [55]

SI-ATRP, surface-initiated atom-transfer radical polymerization; SI-FRP, surface-initiated free-radical polymerization.
For each functional group/substrate, entries are listed in chronological order.

Although thermosetting epoxy resins were already being used in the 1950s for many applications such as tissue embedding for electron microscopy [56] or as dental restoratives [57], it was only in the 1960s that Iwakura and coworkers for the first time systematically studied the post-polymerization modification of polymers containing epoxide groups, such as polyGA and polyGMA. They reported that the post-polymerization modification of polyGA or polyGMA with simple secondary amines (1.0–4.0 equivalents of amine) proceeded with low to moderate yields [11–13]. In 1974, Kalal [33] illustrated that the post-polymerization modification via epoxide ring opening can be catalyzed by a tertiary amine (TEA) and reported up to 80% conversion of epoxide groups of polyGMA with carboxylic acids in the presence of TEA. More recently, Barbey and Klok [37] exploited the catalytic effect of the TEA groups on epoxide ring opening by preparing polyGMA-*co*-polyDMAEMA brushes, which contained pendant TEA groups that were demonstrated to accelerate the rate of post-polymerization modification via epoxide ring opening with amines in aqueous media at room temperature. A drawback of epoxide-functionalized polymers is that they are prone to cross-linking on modification with primary amines because of the reaction between the secondary amines formed after the epoxide ring opening with another unreacted epoxide group [36]. While amines are most frequently employed for the post-polymerization modification of polymers bearing epoxide groups, epoxide groups themselves are reactive toward, for example, alcohols and carboxylic acids [33, 35].

Maleic anhydride (MAn) copolymers have attracted significant attention since the late 1970s and early 1980s with the work carried out by Maeda and coworkers [38, 39], who prepared the anticancer agent poly(styrene-*co*-maleic anhydride) conjugated neocarzinostatin (SMANCS). Functionalization of MAn copolymers with undemanding primary amines was reported to proceed almost quantitatively at ambient temperatures [40, 42, 43], whereas N-substituted maleimide (MI) formation was observed at elevated temperatures on ring closure of the maleamic acid (i.e., amine-modified MAn) [58, 59].

Polymers bearing pendant oxazoline groups can be prepared by the polymerization of 2-vinyl-4,4-dimethyl-5-oxazoline (VDM), which was first illustrated by Taylor and coworkers in the early 1970s [60]. Similar to MAn copolymers, quantitative modification of polyVDM with amines is possible at room temperature [47, 48]. Furthermore, the hydrolytic stability of the oxazoline group allows aqueous post-polymerization modification without side reactions [46]. For instance, this selectivity toward amines in aqueous media was utilized for rapid and high-density immobilization of protein A onto polyVDM-functionalized beads at pH 7.5 [61].

The isocyanate group is another attractive handle that allows post-polymerization modification with amines, alcohols, and thiols. While the modification of isocyanates with amines or thiols proceeds rapidly and quantitatively and can be further facilitated by the addition of TEA or 1,8-diazabicyclo[5.4.0]undec-7-ene (DBU), quantitative conversion with alcohols is only possible in the presence of a catalyst such as dibutyltin dilaureate (DBTDL) (**1** in Scheme 1.3) [51, 54]. *m*-Isopropenyl-*α*-*α*-dimethylbenzyl isocyanate (TMI), vinylisocyanate (VI), and
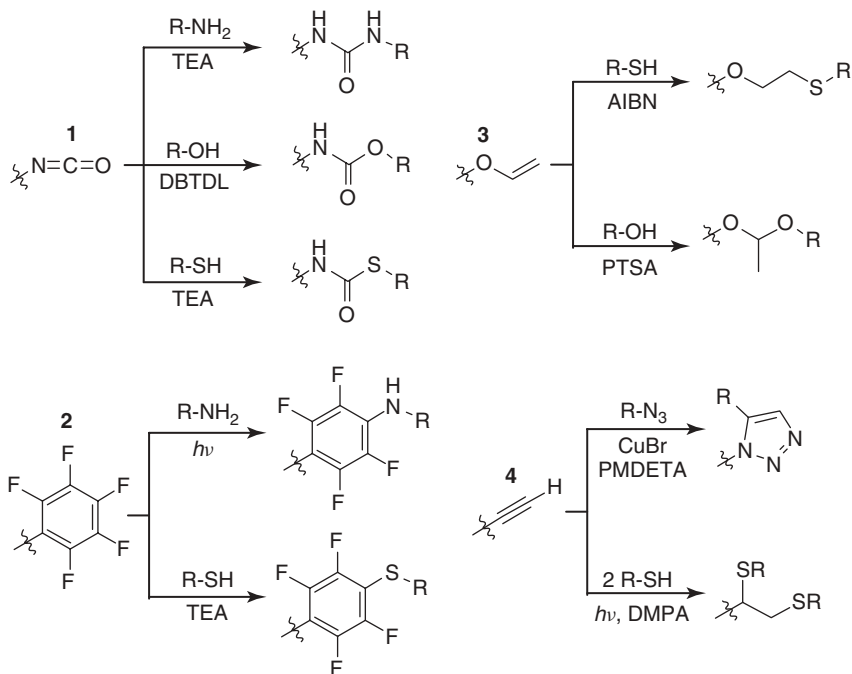
Scheme 1.3 Polymers bearing isocyanate, *n*-alkyl pentafluorophenyl, allyl ether, and alkyne groups that can be quantitatively modified with various reagents, but under different reaction conditions [28, 51, 54, 65, 66].

1-methylvinylisocycanate (MVI) are examples of commonly employed monomers for the synthesis of isocyanate-containing (co)polymers (Table 1.2). A special feature of these isocyanate monomers, which they share with MAn, is that their homopolymerization is more demanding compared to their copolymerization. While the homopolymerization of VI by conventional polymerization techniques can be accompanied by a variety of side reactions because of the competing reactivity of the vinyl double bond and isocyanate group [62], TMI homopolymerization does not yield high-molecular-weight polymer because of the steric hindrance imposed by the α-methyl group to the radical propagation site [63, 64]. Beyer and coworkers [51] synthesized MVI-*alt*-MAn, in which the isocyanate and anhydride groups were sequentially modified with an alcohol and amine, respectively (**1** in Scheme 1.4). More recently, Flores *et al.* reported that a novel isocyanate-containing monomer (2-(acryloyloxy)ethylisocyanate, AOI) can be readily homopolymerized via RAFT polymerization [54] unlike VI, TMI, and MI, and Hensarling and coworkers [55] demonstrated the quantitative modification of polyAOI with thiols within minutes at room temperature.
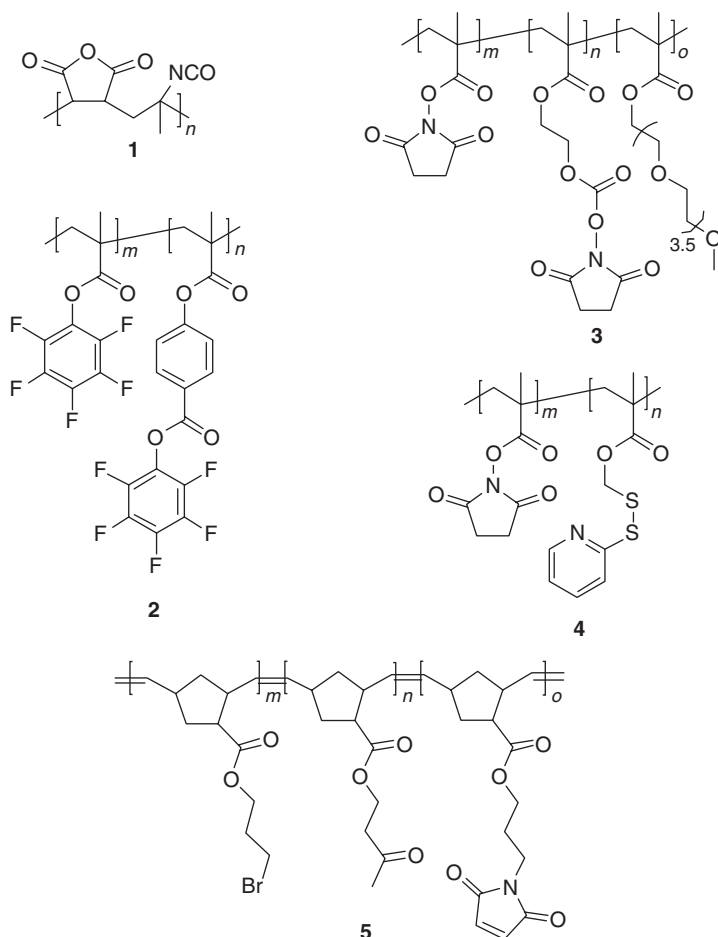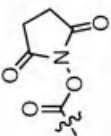
Scheme 1.4 Polymers bearing multiple orthogonal and chemoselective handles that allow either sequential or one-pot post-polymerization modification with different functional groups [51, 67–70].

1.4
Post-polymerization Modification of Active Esters

The synthesis and post-polymerization modification of active ester polymers was pioneered by Ferruti and Ringsdorf in the 1970s [71, 72]. Since then, a broad variety of active ester polymers has been developed utilizing essentially the complete spectrum of available polymerization techniques (Table 1.3). The reaction of active ester polymers with amines is probably the most frequently used post-polymerization modification strategy. Amines are most often used for the post-polymerization modification of active ester polymers since they can react selectively even in the presence of weaker nucleophiles, such as alcohols.

Table 1.3 Postpoymerization modification of (co)polymers bearing active ester groups.

Functional group(s)	Monomer	Comonomer	Polymerization method	Post-Polymerization modification		
				Reagents – reaction conditions	Conversion (%)	Comments
	NAS NMAS	— —	FRP	Piperidine, allylamine, r.t., 4 h N-Butylamine, 60 °C, 6 h	Quantitative	Side reactions are possible [72]
	NAS NMAS	— —	FRP	Cyclohexylamine (2.0 equivalents), r.t., 5 d	60–70	PolyNAS is more reactive than polyNMAS [71]
	NAS NSVB	St	NMP	[G-4]-NH$_2$ (1.1 equivalents), heat, 24 h	50–100	Side reactions are possible. Conversion depends on copolymer composition [73]
	NHNS		ROMP	Aminoethyl mannoside (1.2 equivalents), NMM (1.1 equivalents), 24 h, followed by the addition of DIC (1.0 equivalent) to the reaction mixture, overnight	—	Post-Polymerization modification yielded polymers with greater biological activity compared to the polymer generated by prefunctionalization strategy [74]

NMAS	—	ATRP	H-Gly-Gly-β-naphthylamide. HBr·0.6H$_2$O (0.10 equivalent), TEA (0.2 equivalent), 50°C, 2.5 h, followed by the addition of 1-amino-2-propanol (2 equivalents) to the reaction mixture, 50°C, 1.25 h	Quantitative	Well-defined polymer–drug conjugates were synthesized [75]
NMAS	—	ATRP	A library of primary aliphatic amines bearing charged groups, r.t., overnight	Quantitative	Sequential modification with two different charged amines yielded pH-responsive polymers [76]
NAS	—	ATRP	Galactosamine (0.2 equivalent), TEA (2.0 equivalents), 60°C, 6 h	Quantitative	[77]
NMAS	HPMA	RAFT	Peptide Ac-HTSTYWWLDGAPK-Am (130.0 equivalents), TEA (excess), 50°C, 24 h	14	Polymer peptide conjugate exhibits 3 orders of magnitude higher affinity toward antrax toxin compared to the unbound peptide [78]
MAC$_2$AE	—	SI-FRP	A library of n-alkylamines (C$_3$-C$_{18}$), biomolecules, dyes, complexing agents, PEG-NH$_2$ (50 mg or 50 µl), TEA (50 µl), 40°C, 16 h	34–100	The relationship between the polymer brush thickness and the molar mass of the polymer repeating unit was demonstrated [79]
NSVB	—	RAFT	Terpy-NH$_2$ (2.5 equivalents), 50°C, 16 h	95–99	No side reactions [80]
NSVB	—	SI-ATRP	1-Amino-methylpyrene, octadecylamine (0.12 M), TEA, 40°C, overnight	Quantitative	[81]
NMAS	PEGMA AHMA SCEMA	FRP	Allylamine (5.0 equivalents), TEA (5.0 equivalents), r.t., 18 h	Quantitative	Polymers bearing multiple chemoselective handles allowing orthogonal functionalization [68]

Contd.
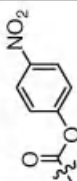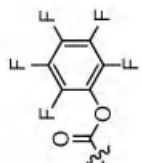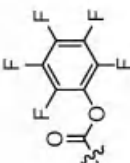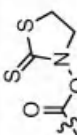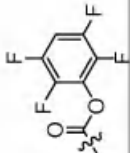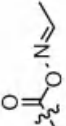
Table 1.3 *(continued.)*

Functional group(s)	Monomer	Comonomer	Polymerization method	Post-Polymerization modification		
				Reagents – reaction conditions	Conversion (%)	Comments
(4-nitrophenyl ester structure, NO_2)	NPA	St	FRP	Benzyloxyamine, 120–140 °C, 25 h	Quantitative	Harsh conditions. Side reactions are possible [82]
	NPA, NPMA	HPMA	FRP	t-Butylamine, diisopropylamine (100.0 equivalents), 25 °C	75–100	Polymers are more reactive than the monomers toward diisopropylamine [83]
	NPMA	St	ATRP	N-Butylamine (9.0 equivalents), 50 °C, 24 h	Quantitative	[84]
	NPMA	—	RAFT	Glycine methyl ester (10.0 equivalents), TEA, 50 °C, 12 h	86	[85]
(pentafluorophenyl ester structure, F)	PFMA PFA	—	FRP	Hexylamine, n-hexylmethylamine (1.0 equivalent), base (1.0 equivalent), 50 °C, 24 h	65–99	PolyPFA is more reactive than polyPFMA. Functionalization with secondary amines is not possible [86]
	PFMA	—	PPP	1,6-Diaminohexane (0.01 M) in 10.0 mM PBS, 10 min	Quantitative	High-energy process. Side reactions and hydrolysis are possible [87]

Structure	Polymer		Method	Conditions	Yield (%)	Notes
(pentafluorophenyl ester, Contd.)	PFPNorb	—	ROMP	Hexylamine, n-hexylmethylamine (2.0 equivalents), 50 °C, 24 h	Quantitative	[88]
	PFMA	—	RAFT	Library of primary aliphatic amines (2.0 equivalents), TEA (2.0 equivalents), 50 °C, 16 h	47–100	Steric effects limit the extent of post-polymerization modification [89]
	PFVB	—	FRP	A library of primary, secondary and cyclic amines (2.0 equivalents), r.t., 12 h	100	More reactive than polyPFA and polyPFMA. Functionalization with aromatic amines is possible [90]
	PFVB	PFMA	RAFT	Aniline (2.0 equivalents), 50 °C, 12 h; A library of aromatic amines, 60 °C, 6 d	100	Sequential functionalization of the copolymer was achieved. Functionalization with secondary aromatic amines is not possible [67]
(thiazolidine-2-thione ester)	MAPTT	HPMA	FRP	1-Amino-2-propanol, methyl esters of amino acids (2.0 equivalents), 25 °C, 1–60 min	Quantitative	Aqueous post-polymerization modification is possible. Side reactions in the copresence of amines and thiols [91]
(trifluorophenyl ester)	TFPMA	DMAEMA	ATRP	Benzylamine, cyclohexylamine (2.0 equivalents), 60 °C, 6 h; t-Butylamine (3.0 equivalents), 80 °C, 24 h	Quantitative	Less reactive than pentafluorophenyl ester polymers [92].

Table 1.3 *(continued.)*

Functional group(s)	Monomer	Comonomer	Polymerization method	Post-Polymerization modification		
				Reagents – reaction conditions	Conversion (%)	Comments
	AOA	—	FRP RAFT NMP	Diisopropylamine (0.19 equivalent), 50 °C, 48 h followed by ammonia (excess), 50 °C, 24 h	Quantitative	polyAOA partially modified with diisopropylamine exhibits an LCST [93]
	AOA	—	RAFT	Hydrazide (10.0 equivalents), 0 °C, 1 h	Quantitative	Hydrazide-functionalized polyAOA employed as an intermediate for the covalent immobilization of a glycan library [94]

PBS, phosphate-buffered saline.
For each functional group/substrate, entries are listed in chronological order.

The most frequently employed active ester polymers are *N*-hydroxysuccinimide derivatives (NHS), such as polyNAS and polyNMAS. A drawback of these polymers, however, is that their solubility is limited to DMF and DMSO. Furthermore, the post-polymerization modification of these active ester polymers can be accompanied by side reactions, such as succinimide ring-opening or the formation of N-substituted glutarimide groups [95]. These side reactions can be suppressed by using an excess of amine or proton acceptor, such as TEA or DMAP [96].

Polymers bearing pentafluorophenyl (PFP) ester groups are attractive alternatives to NHS ester polymers, as polyPFMA was demonstrated to have higher reactivity and better hydrolytic stability and is soluble in a wide range of solvents as compared to polyNMAS [86]. Nevertheless, similar to NHS, PFP ester homopolymers are insoluble in water and thus cannot be functionalized in aqueous media.

Another class of active ester polymers that form an interesting alternative to polyNAS and polyNMAS are those that contain thiazolidine-2-thione (TT) groups. Subr and Ulbrich [91] reported that polymers bearing TT groups allow rapid aminolysis in aqueous media while displaying good hydrolytic stability. The difference between the rates of aminolysis and hydrolysis was found to be greatest between pH 7.4 and 8.0. A drawback of TT esters is that they display low selectivity between amines and thiols under identical reaction conditions.

Active ester polymers based on 4-vinyl benzoate (VB) often exhibit higher reactivity compared to their (meth)acrylates. For instance, Hawker *et al.* [73] used polyNSVB to fabricate dendrimer-functionalized polymers with high yields. Theato and Nilles [90] illustrated that, unlike polyPFMA and polyPFA, polyPFVB can quantitatively react with less nucleophilic aromatic amines. In a subsequent study, the same authors prepared statistical and block copolymers from pentafluorophenyl 4-vinyl benzoate (PFVB) and pentafluorophenyl methacrylate (PFMA) and demonstrated that these polymers could be sequentially modified with an aromatic and aliphatic amine, respectively (**2** in Scheme 1.4) [67].

An alternative strategy toward orthogonally functionalizable active ester-based polymers was developed by Sanyal and coworkers [68]. These authors prepared copolymers of *N*-methacryloxysuccinimide (NMAS) with PEGMA and the carbonate functional monomer 2-(N-succinimidylcarboxyoxy)ethyl methacrylate (SCEMA) (**3** in Scheme 1.4). Exposure of this copolymer to allylamine in THF at room temperature led to complete conversion of the carbonate groups with near-quantitative preservation of the active ester moieties, which could be subsequently modified by adding an excess of propargylamine at 50 °C.

1.5
Post-polymerization Modification via Thiol-Disulfide Exchange

Thiol–disulfide exchange is ubiquitous in biology where it is involved in a variety of processes such as modulation of enzyme activity [97], viral entry [98], and protein folding [99]. Although this reaction has been known since the 1920s from a study of Lecher on alkalisulfides/alkalithiols [100] as well as from the work of Hopkins on

the biochemistry of glutathione [101], it was not until the late 1990s that Wang and coworkers first demonstrated that polymers bearing pyridyl disulfide groups could be employed as an appealing platform for post-polymerization modification via thiol−disulfide exchange, as it could proceed quantitatively and selectively in mild conditions and in aqueous media below pH 8 [102]. Table 1.4 gives an overview of various pyridyl disulfide-containing polymers that have been used as substrates for post-polymerization modification.

Thiol−disulfide exchange post-polymerization modification is strongly pH dependent. There are opposing claims, however, regarding the optimum pH for quantitative functionalization. While Wang and coworkers [102] first illustrated that the rate of post-polymerization modification was highest between pH 8 and 10, Bulmus *et al.* [103] later reported higher conversions of pyridyl disulfide groups with terminal cysteine residues at pH 6 compared to pH 10.

One of the assets of the thiol−disulfide exchange reaction is that it allows the introduction of functional groups via a disulfide bond that is reversible and can be cleaved, either via reduction or with an exchange with another thiol. For instance, Langer [104] first demonstrated the reduction of pyridyl disulfide-containing poly(β-amino ester)s modified with glutathione in intracellular media, which led to a 50% decrease in the DNA binding capacity of the polymer. Ghosh *et al.* [69] later illustrated the quantitative release of incorporated thiols from the polymer backbone on reduction of the newly formed disulfide bonds by DTT. Furthermore, they also illustrated the orthogonality of thiol−disulfide exchange and aminolysis of active esters (**4** in Scheme 1.4).
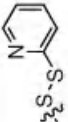
1.6
Post-polymerization Modification via Diels-Alder Reactions

The cycloaddition reaction between a diene and a substituted alkene (dienophile), which was discovered in 1928 by Diels and Alder and distinguished with a Nobel Prize in Chemistry in 1950 [106], emerged as an attractive tool for post-polymerization modification in the 1990s [107, 108]. The Diels−Alder reaction fulfills the ''click'' criteria [109], as it can proceed with quantitative yields without any side reactions, is tolerant to a wide variety of functional groups, and is orthogonal with many other chemistries, such as CuAAC [110, 111]. Furthermore, many Diels−Alder reactions are reversible and the Diels−Alder adduct can decompose into the starting diene and dienophile at higher temperatures as compared to the temperature required for the forward reaction [112]. The reversibility of the Diels−Alder reaction has been extensively utilized to prepare thermoresponsive macromolecular architectures such as gels [107, 113−116], as well as in the synthesis of dendrimers [117] and smart copolymers [118].

Polymers that can be postmodified using Diels−Alder chemistry can be prepared either via a precursor route based on the deprotection of masked MI groups following polymerization of the corresponding monomers [116, 119] or by direct

Table 1.4 Post-Polymerization modification of (co)polymers via thiol–disulfide exchange.

Functional group(s)	Polymerization			Post-Polymerization modification		
	Monomer	Comonomer	Polymerization method	Reagents – reaction conditions	Conversion (%)	Comments
(pyridyl disulfide structure)	PDTEMA	HPMA	FRP	Peptide pAntp-SH (0.1 equivalent), pH 3–8, min; Oligo-SH (0.1 equivalent, pH 9, 5 min	Quantitative 50	Extent of post-polymerization modification is highly pH dependent. PDTEMA content in copolymer: 8.3 mol% [102]
	PDSA	MAA	FRP	Peptide 5-FAM-(Gly)$_3$-Cys (excess), overnight	100	Extent of post-polymerization modification is highly pH dependent. PDSA content in copolymer: 3–8 mol% [103]
		nBA		Peptide (Lys)$_6$-(Gly)$_3$-Cys (0.53–0.90 equivalent), pH 6 or 10, r.t., 16 h	35–86	
				Oligo-SH (0.30–1.0 equivalent), pH 7.4 or 9.0, r.t., 16 h	27–50	
	PDA(β-amino ester)	—	PA	Mercaptoethylamine (excess), r.t., 0.5 h; Peptide RGDC (2 equivalents), r.t., 28 h	Quantitative	Biodegradable polymer bearing thiol-reactive handles [104]
	PDSM	NMAS	ATRP	1-Undecanethiol, thiomethylanthracene (1.2 equivalents), AcOH (catalyst), r.t., 4 h	Quantitative	Reversibility of the reaction was demonstrated. Synthesized polymer bears two chemoselective handles allowing simultaneous functionalization [69]
	PDSM	—	RAFT	A library of thiols (0.06–1.0 equivalent), r.t., 14 h	65–100	Simultaneous functionalization with two different thiols is possible [105]

For each functional group/substrate, entries are listed in chronological order.

polymerization of the monomers containing unmasked dienes, such as furan or anthracene groups (Table 1.5). In an early example, Laita and coworkers demonstrated the post-polymerization modification of various furan-containing polyurethanes in which the furan group was either incorporated in the backbone or in the side chain of these polymers. While modification of the pendant furans with MIs proceeded to completion, conversion of backbone furan groups was limited to 30–60% at 40 °C using 3.0 equivalents of MI [120]. Jones *et al.* [114] later reported higher conversions (60–85%) of the post-polymerization modification of backbone anthracene groups with MIs in stoichiometric conditions when the reaction temperature was increased to 120 °C. Kim and coworkers [121] prepared copolymers bearing pendant anthracene groups, which were quantitatively modified with relatively bulky MI-functionalized chromophores at 120 °C by using stoichiometric amount of MI.

Another interesting class of functional groups for the Diels–Alder post-polymerization modification is pyridinedithioesters. These are attractive since they can act both as a chain transfer agent in RAFT polymerization [124] as well as a heterodienophile in [4 + 2] cycloaddition [125, 126]. Bousquet and coworkers [123] exploited this unique feature to quantitatively modify poly*tt*HA at 50 °C by using 4.0–5.0 equivalents of poly*t*BA (M_n = 3500–13500 g/mol), which was prepared by RAFT polymerization by using benzyl pyridine-2-yl dithioformate as a chain transfer agent.
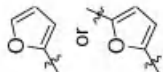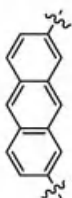
1.7
Post-polymerization Modification via Michael-Type Addition

Michael-type addition reactions have been frequently employed in polymer science starting from the early 1970s to fabricate a variety of macromolecular architectures including step-growth polymers, dendrimers, and cross-linked networks [127]. However, it is only more recently that this reaction has found use in preparing side-chain functional polymers, as only CRP techniques enable the preparation of polymers bearing Michael acceptors, such as acrylates, MIs, and vinyl sulfones. Table 1.6 gives an overview of different polymers that have been used in Michael-type post-polymerization modification. Post-polymerization modification of these polymers with thiols is particularly attractive, as this reaction can proceed quantitatively and selectively in aqueous media at room temperature [128].
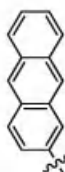
Jérôme and coworkers [129] first demonstrated the synthesis of acrylate-bearing polyesters via ROP. Quantitative functionalization of these polymers without any backbone degradation was achieved in the presence of a large excess of thiol and pyridine (10.0–25.0 equivalents) at room temperature. Weck and coworkers showed that unmasked MI groups are compatible with ring-opening metathesis polymerization (ROMP) conditions. Quantitative modification of MI-bearing poly(norbornene)-based terpolymers was achieved when 2.0 equivalents of the thiol was used at 25 °C. Furthermore, these authors also demonstrated that Michael-type addition, CuAAC, and hydrazone formation are orthogonal chemistries that allow both sequential as well as one-pot modification with different functionalities

Table 1.5 Post-Polymerization modification of (co)polymers via Diels–Alder reactions.

Functional group(s)	Monomer	Comonomer	Polymerization method	Post-Polymerization modification		
				Reagents – reaction conditions	Conversion (%)	Comments
(furan structure) or (furan structure)	A library of Fu-PU	—	PC	N-Methylmaleimide, N-phenylmaleimide (3.0 equivalents), 40 °C, 4–5 h	30–100	The extent of modification of pendant furan groups is greater compared to the ones in the backbone [120]
	FMA	—	FRP	A library of maleimides and bismaleimides (1.0 equivalent), 55 °C, 48 h	60–85	Reversibility of the reaction was demonstrated. Post-Polymerization modification generated two different stereoisomeric Diels–Alder adducts [115]
(anthracene structure)	ADC	ET	PC	N-Phenylmaleimide (1.0 equivalent), 120 °C, 12 h N-Phenylmaleimide (1.0 equivalent), 250 °C (melt), 5–10 min	94 23–51	[114]
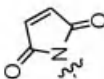
Table 1.5 (*continued.*)

Functional group(s)	Monomer	Comonomer	Polymerization method	Post-Polymerization modification		
				Reagents – reaction conditions	Conversion (%)	Comments
(anthracene structure)	PAMA	MMA	FRP	A library of maleimide-functionalized chromophores, 120 °C, 3 h	Quantitative	Bulky substituents were incorporated [121]
	APMOS	St	CuAAC	PolytBA-MI ($M_n = 2300$ g mol^{-1}), PEG-MI ($M_n = 750$ g mol^{-1}) (1.3 equivalents), 110 °C, 48 h	92–96	Comb-shaped polymers were synthesized [122]
(alkene structure)	ttHA	St	RAFT	PolynBA-BP2TF ($M_n = 3500$–13000 g mol^{-1}) (4.0–5.0 equivalents), TFA (2 equivalents), 50 °C, 12–24 h	75–100	Hetero Diels–Alder reaction. Comb-shaped polymers were synthesized [123]
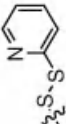
PC, polycondensation.
For each functional group/substrate, entries are listed in chronological order.

Table 1.6 Post-Polymerization modification of (co)polymers via Michael-type addition.

Functional group(s)	Monomer	Comonomer	Polymerization method	Post-Polymerization modification		
				Reagents – reaction conditions	Conversion (%)	Comments
	γAεCL	εCL	ROP	Mercaptoacetic acid (10 equivalents), Py (15 equivalents), r.t., 75 h	100	No backbone degradation [129]
				PEG900-SH (20 equivalents), Py (25 equivalents), r.t., 60 h	80	
	AC	εCLLA	ROP	A library of thiols (10 equivalents), Py (10 equivalents), r.t., 2–3 d	30–100	Post-Polymerization modification with thiols bearing neighboring carboxylic acid groups proceed with low yields [130]
				Peptide RGDC (1.0 equivalents), Py (10 equivalents), 7 d	58	
	IBBL	GPE	AROP	Dodecanethiol, benzylmercaptan (1.0 equivalent), AlCl$_3$ (0.1 equivalent), r.t., 24 h	97–100	Mild reaction conditions [131]
	PMNorb	OBNorb BPNorb	ROMP	Benzenethiol (2.0 equivalents), 25 °C, 18 h	Quantitative	Polymer bears three chemoselective handles warrant access to orthogonal functionalization [70]

(continued overleaf)

Table 1.6 (*continued.*)

Functional group(s)	Monomer	Comonomer	Polymerization method	Post-Polymerization modification		
				Reagents – reaction conditions	Conversion (%)	Comments
(pyridine disulfide structure)	PDSM	—	RAFT	PEG$_{(454-2000)}$-acrylate (1.2 equivalents), ethylamine (0.03 equivalent), TCEP (1.0 equivalent), overnight	70–73	Side reactions are possible. Steric effects limit the extent of post-polymerization modification [32]
(vinyl sulfone structure)	VSC	εCL LA TMC	ROP	A library of thiols (2.0 equivalents), r.t., 24 h	Quantitative	Quantitative post-polymerization modification with bulky thiols is possible [132]

For each functional group/substrate, entries are listed in chronological order.

(**5** in Scheme 1.4) [70]. Polyesters bearing α,β unsaturated ketone groups have recently been prepared by the copolymerization of glycidyl phenyl ether and bicyclic bis(δ-butyrolactone) monomers by Ohsawa and coworkers. These polyesters contain pendant isopropenyl groups that were shown to react quantitatively with thiols in stoichiometric conditions when $AlCl_3$ was used as a catalyst at room temperature [131]. Wang *et al.* prepared vinyl sulfone-functionalized poly(ester carbonate)s by ring-opening copolymerization of a vinyl sulfone carbonate monomer with ε-caprolactone, L-lactone, or trimethylene carbonate. Post-polymerization modification was reported to proceed quantitatively even with bulky thiols (2.0 equivalents of the thiol used) at room temperature [132].

1.8
Post-polymerization Modification via Azide Alkyne Cycloaddition Reactions

The discovery that the Huisgen 1,3-dipolar cycloaddition (CuAAC) reaction between azides and alkynes can be carried out at mild conditions and in regioselective manner when Cu(I) salts are used as catalyst can be considered as the origin of what is now commonly referred to as *click chemistry*. As already predicted by Sharpless and Meldal in 2002 [133, 134], the scope of the CuAAC reaction turned out to be enormous. CuAAC often proceeds with quantitative yields both in aqueous and organic media under mild conditions and is orthogonal with almost any type of functionalization strategy. Table 1.7 gives an overview of azide- and alkyne-functionalized polymers that have been postmodified using CuAAC.

In 2004, Binder reported that the ROMP of oxynorbonenes bearing unmasked alkyne groups proceeds with poor control owing to the competing reactivity of the alkyne group with the ROMP catalyst. This problem was circumvented by preparing alkyne-bearing polymers via a precursor route that involves side-chain modification of a precursor poly(norbornene) via alkylation with propargy bromide. These authors also prepared azide-bearing poly(oxynorbonene)s via another precursor route based on the modification of pendant alkyl bromide chains with sodium azide [158]. In 2005, Parrish and coworkers first demonstrated the compatibility of the alkyne groups with ROP by copolymerizing $\alpha P\delta VL$ with ε-caprolactone. Quantitative modification of the alkyne groups was achieved with an azide-functionalized poly(ethylene glycol) (PEG) ($M_n = 1100 \mathrm{\,g\,mol}^{-1}$) in stoichiometric conditions at $80\,^\circ C$ when $CuSO_4 \cdot 5H_2O/Na_{asc}$ was used as catalyst [143]. Matyjaszewski illustrated that, while an azide-containing monomer (3-azidopropyl methacrylate, AzPMA) can be successfully polymerized with ATRP, polymerization of propargyl methacrylate proceeded with poor control presumably owing to the side reactions involving the pendant acetylene group. Modification of polyAzPMA proceeded quantitatively with a library of alkynes (1.1 equivalents of the alkynes used) at room temperature in the presence of CuBr [135]. Riva and coworkers reported the compatibility of the azide groups with ROP by preparing copolymers of an azide-functionalized caprolactone ($\alpha N_3 \varepsilon CL$) with ε-caprolactone, which reacts quantitatively with propargyl

Table 1.7 Post-Polymerization modification of (co)polymers via azide/alkyne cycloaddition reactions.

Functional group(s)	Monomer	Comonomer	Polymerization method	Reagents – reaction conditions	Post-Polymerization modification	
					Conversion (%)	Comments
N_3	AzPMA	DMAEMA	ATRP	A library of alkynes (1.1 equivalents), CuBr (0.5 equivalent), r.t., 2 h	Quantitative	polyAzPMA is more reactive than AzPMA [135]
	$\alpha N_3 \varepsilon CL$	εCL	ROP	Propargyl benzoate (1.2 equivalents), CuI (0.1 equivalent), DBU, or TEA (0.1 equivalent), 35 °C, 2 h	Quantitative	Terminal hydroxyl group was esterified to prevent side reactions before post-polymerization modification [136]
	AzEMA	—	RAFT	Phenyl acetylene (1.1 equivalents), CuI (0.1 equivalent), r.t., overnight	Quantitative	Copper catalyst is difficult to remove [137]
	AzHMA	—	SI-RAFT	Phenylacetylene, oligoaniline-alkyne, PS-alkyne (2.0 equivalents), CuBr/PMDETA (0.5 equivalent), r.t., 20 min	50–90	Steric effects have a greater impact to the extent of reaction for polyAzHMA brush compared to free polyAzHMA in solution [138]
	CAA	MA	RAFT	PEG_{750}-SAE-Propargyl (1.1 equivalents), $CuSO_4 \cdot 5H_2O$/Na$_{asc}$ (0.07/0.14 equivalent), 50 °C	Quantitative	[139]
	N_3MPA	—	RAFT	α-GP-alkyne (1.5 equivalents), $CuSO_4 \cdot 5H_2O$/Na$_{asc}$ (0.1/4.0 equivalents), r.t., 18 h	Quantitative	[140]
	ADTC	DTC	ROP	A library of alkynes (1.2 equivalents), CuBr/TEA (1.0 equivalent) 35 °C	Quantitative	Polymer bears two alkyne groups per repeating unit [141]
	AzDXO	LA	ROP	(1)5-hexyn-1-ol (17.6 equivalents), CuBr, r.t., 24 h. (2)DBCO-NHS (3 equivalents), r.t. 12 h	Quantitative	Cu-free functionalization via SPAAC was achieved. Polymer bears two azide groups per repeating unit [142]

			Conditions		Comments
αPδVL	εCL	ROP	PEG$_{1100}$·N$_3$ (1.0 equivalent), CuSO$_4$·5H$_2$O/Na$_{asc}$ (0.1/0.2 equivalent), 80°C, 10–12 h Peptide GRGDS-N$_3$ (0.05 equivalent). CuSO$_4$·5H$_2$O/Na$_{asc}$ (0.5/0.8 equivalent), 80°C, 10–12 h	Quantitative	No backbone degradation [143]
PynOx	2MOx	CROP	TMS-N$_3$, Ac-N$_3$ (7.3–13.7 equivalents), CuSO$_4$·5H$_2$O/Na$_{asc}$ (0.3–0.8/0.5–1.4 equivalents) r.t., overnight	Quantitative	Quantitative modification in aqueous media [144]
αPδVL	εCL	ROP	Camptothecin-N$_3$ (0.2 equivalent), DIEA (0.08 equivalent), CuBrPPh$_3$ (0.04 equivalent), r.t., 48 h, followed by the addition of PEG$_{1100}$·N$_3$ (1.1 equivalents). CuSO$_4$·5H$_2$O/Na$_{asc}$ (0.4 equivalent), 80°C, overnight	Quantitative	No backbone degradation. Improved solubility of the polymer-drug conjugate on functionalization with PEG [145]
PCDO	LA	ROP	Azide-functionalized sugars (1.0 equivalent), CuSO$_4$·5H$_2$O/Na$_{asc}$ (0.9/1.8 equivalents), 80°C, 5 h	Quantitative	[146]
PgMA	PEGMA	RAFT	Pyrenyl-N$_3$ (1.2 equivalents), CuBr/PMDETA (0.2 equivalent), r.t., 24 h	Quantitative	Comb-shaped polymers assembling into electron donor–acceptor (EDA) supramolecules were synthesized [147]
dPGL	LA	ROP	1-Azidododecane, PEG$_{550}$-N$_3$ (3.0 equivalents), CuSO$_4$·5H$_2$O/Na$_{asc}$ (0.05 equivalent), r.t., 3 h	Quantitative	No backbone degradation [148]
U-PBM U-DPPD	—	PA	A library of azides (2.0 equivalents), CuBr/PMDETA (0.1 equivalent), or CuSO$_4$·5H$_2$O/Na$_{asc}$ (0.05/0.1 equivalent), 50°C, overnight	Quantitative	PolyU-DPPD bears two alkyne groups per repeating unit [149]
U-MPPD	—	PC	Benzyl azide, PEG$_{550}$-N$_3$ (2.0 equivalents), CuBr/PMDETA (0.2–1.0 equivalent), 50°C, 2–600 min	Quantitative	[150]
ProDOT-P	ProDOT-H	OP	A library of azides (9.0–24.5 equivalents), CuSO$_4$·5H$_2$O/Na$_{asc}$ (7.0/24.0 equivalents), 80°C, 5 d	Quantitative	Low atom economy. Improved solubility of the polymer on functionalization [151]

(continued overleaf)

Table 1.7 *(continued.)*

Functional group(s)	Monomer	Comonomer	Polymerization method	Post-Polymerization modification		
				Reagents – reaction conditions	Conversion (%)	Comments
(Contd.)	PLG	—	ROP	$PEG_{750-5000}$-N_3 (1.0–2.0 equivalents), CuBr/PMDETA (0.3 equivalent)	95–99	Conformation of the polymer allows quantitative functionalization with PEG [152]
	$\alpha P\varepsilon CL$	εCL	ROP	poly$DMAEMA_{6500}$-N_3, CuBr/PMDETA, r.t., 24 h	Quantitative	Comb-shaped polymers were synthesized [153]
	$\alpha P\varepsilon CL$	εCL	ROP	β-CD-N_3 (5.0 equivalents), $CuSO_4 \cdot 5H_2O$/Na_{asc} (0.05/0.10 equivalent), 95 °C, 24 h	90–100	Polymer was end-capped to prevent side reactions before post-polymerization modification [154]
	PGL	LA	ROP	PEG_{2000}-PTXL-N_3 (0.50 equivalent), CuBr/PMDETA (0.6 equivalent), 35 °C, 24 h	95	A biodegradable polymer–drug conjugate was synthesized [155]
	NPME	Ethylene	EOP	PEG_{1700}-N_3, PS_{2600}-N_3 (1.8 equivalents), CuBr/PMDETA (0.9/2.7 equivalents), 80 °C, 12–24 h	91–100	[156]
	PgMA	—	SI-FRP	A library of azides, CuBr/PMDETA, 80 °C, 8 h	70	[157]

For each functional group/substrate, entries are listed in chronological order.

benzoate (1.2 equivalents) at 35 °C when CuI was used [136]. The possibility to synthesize azide-/alkyne-functionalized polymers via direct polymerization of the corresponding monomers, as demonstrated in these last three examples, marked the beginning of an explosive growth of the use of CuAAC post-polymerization modification strategy (Table 1.7).

A drawback of the CuAAC post-polymerization modification reaction is that removal of the copper catalyst can be demanding, as it can form complexes with the triazole ring, which hampers the solubility of the functionalized polymer [137]. Furthermore, toxicity of the copper catalyst to cells limits the applicability of CuAAC reaction in biological media [159, 160]. An attractive, copper-free functionalization strategy is the *strain-promoted azide alkyne cycloaddition* (SPAAC) reaction [161]. Recently, Song and coworkers [142] demonstrated that the functionalization of pendant azide groups of polyAzDXO via SPAAC reaches quantitative conversion at shorter reaction times compared to CuAAC and at lower equivalents of the cyclooctyne/alkyne used (Scheme 1.5).
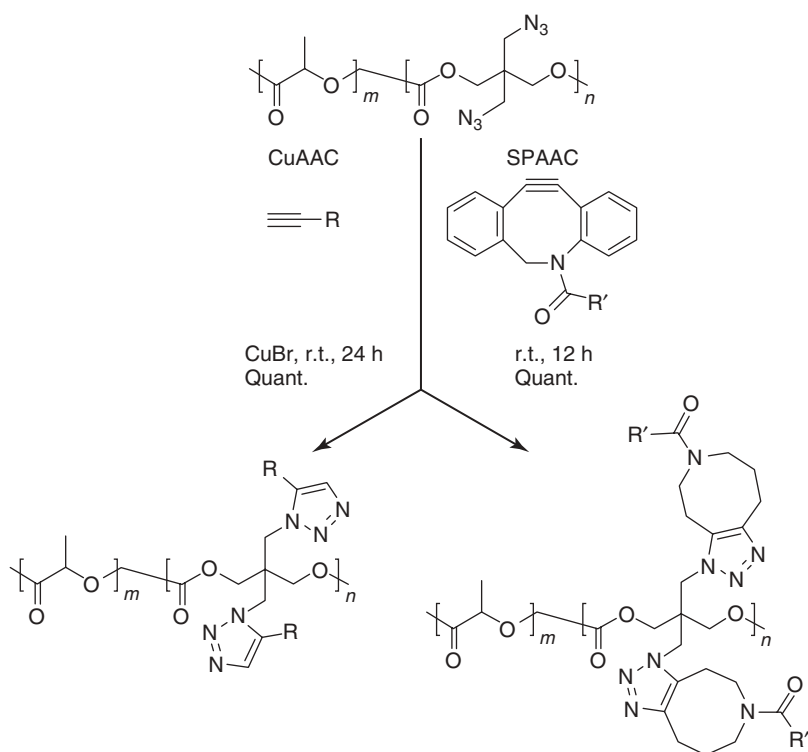
Scheme 1.5 Post-Polymerization modification of polyAzDXO via CuAAC and SPAAC reaction [142].

1.9
Post-polymerization Modification of Ketones and Aldehydes

Ketones and aldehydes can selectively react with primary amines, alkoxyamines, and hydrazines to form imines, oximes, and hydrazones, respectively. While imines are usually prone to hydrolysis, oximes and hydrazones are hydrolytically stable between slightly acidic to neutral pH [162, 163]. Nevertheless, imines can be further converted to stable secondary amines via reductive amination in the presence of a reducing agent, such as borohydride derivatives [164, 165]. Table 1.8 gives an overview of aldehyde and ketone functional polymers that have been modified via post-polymerization modification.

Although the preparation of polymers bearing pendant ketone groups was already reported by Overberger and Tsurata in the 1960s [171, 172], these polymers have only recently found use as a platform for post-polymerization modification. Bertozzi and coworkers [166, 173] prepared copolymers containing vinylmethylketone (VMK) and isopropenyl methyl ketone (IMK) both via free-radical polymerization (FRP) as well as via RAFT polymerization and demonstrated that the resulting polymers could be quantitatively modified with aminoxy-functionalized sugars at 95 °C when 2.8 equivalents of the sugar was used (Table 1.8). Yang and Weck [70, 167] reported the synthesis of aldehyde- and ketone-functionalized polynorbornenes via Ru-catalyzed ROMP of the corresponding aldehyde- and ketone-substituted norbornene monomer. Post-polymerization modification of the ketone-substituted polymer with a library of hydrazines proceeded quantitatively at 25 °C. Barrett and Yousaf prepared a library of poly(ketoester)s that contain ketone groups as part of the backbone of the polymer. Modification of these backbone ketone groups proceeded quantitatively with a library of oximes (1.5 equivalents used) at room temperature (Scheme 1.6) [170].

The first example of the polymerization of monomers containing aldehyde groups was reported as early as in 1950s by Wiley and Hobson [174] as well as by Schulz *et al.* [175]. The research activities of the latter authors concentrated on poly(acrolein), which was obtained via redox polymerization, and also included first studies on the post-polymerization modification of these polymers. Polymerization of unprotected aldehyde monomers by conventional polymerization techniques, however, can be accompanied by a variety of side reactions, because of the competing reactivity between the vinyl double bond and the aldehyde group [176]. To overcome these problems, precursor routes based on deprotection of masked aldehyde functionalities, such as acetal or dioxolane groups, following polymerization of the corresponding monomers by oxidation were employed to prepare well-defined aldehyde-bearing polymers starting from 1980s [85, 177–180]. In 2007, Wooley *et al.* [181], for the first time, reported the direct RAFT polymerization of an unprotected aldehyde-containing monomer (vinylbenzaldehyde, VBA). Fulton demonstrated that polyVBA prepared via RAFT polymerization could be quantitatively modified using an excess of various acylhydrazides. Furthermore, Fulton demonstrated the dynamic nature of the reaction between an aldehyde and *n*-acylhydrazone, and therefore, probed the potential of polyVBA as a platform

Table 1.8 Post-Polymerization modification of (co)polymers bearing ketone and aldehyde groups.

Functional group(s)	Monomer	Comonomer	Polymerization method	Post-Polymerization modification		
				Reagents – reaction conditions	Conversion (%)	Comments
	VMK	DAPA	FRP	α-Aminoxy GalNac (2.8 equivalents), AcOH (0.1%), 95°C, 96h	96–100	Conformation of the polymer changed on post-polymerization modification [166]
	IMK		RAFT	α-Aminoxy GalNac (1.03 equivalents), pH 5.5, 50°C, 20h	80	
	OBNorb	BPNorb	ROMP	A library of hydrazides, 25°C, 2–24h	97–99	Orthogonality of the hydrazone formation and CuAAC was demonstrated. Aldehyde derivative of the polymer is insoluble in common organic solvents [167]
	OBNorb	BPNorb PMNorb	ROMP	Benzylhydrazide (2.0 equivalents), 25°C, 4h	98	Polymer synthesized bears three chemoselective handles warrant access to orthogonal functionalization [70]

(continued overleaf)

Table 1.8 *(continued.)*

Functional group(s)	Monomer	Comonomer	Polymerization method	Post-Polymerization modification		
				Reagents – reaction conditions	Conversion (%)	Comments
[structure]	VBA	—	RAFT	N-Acylhydrazides (C₅,C₁₀,C₁₇, 100.0 equivalents), TFA (catalyst), 2 h	Quantitative	Low atom economy. Reversible post-polymerization modification [168]
	FVFC	PEGMA	RAFT	O-Benzylhydroxylamine hydrochloride (1.2 equivalents), 25 °C, 12 h	Quantitative	[169]
[structure]	A library of PKE's	—	CP	A library of alkoxyamines (1.5 equivalents), r.t, 5 h	Quantitative	Direct functionalization of the backbone. Mild reaction conditions. Biocompatible polymer [170]

For each functional group/substrate, entries are listed in chronological order.

Polymer	x	y
1	0	0
2	0	2
3	1	1
4	2	2
5	3	3
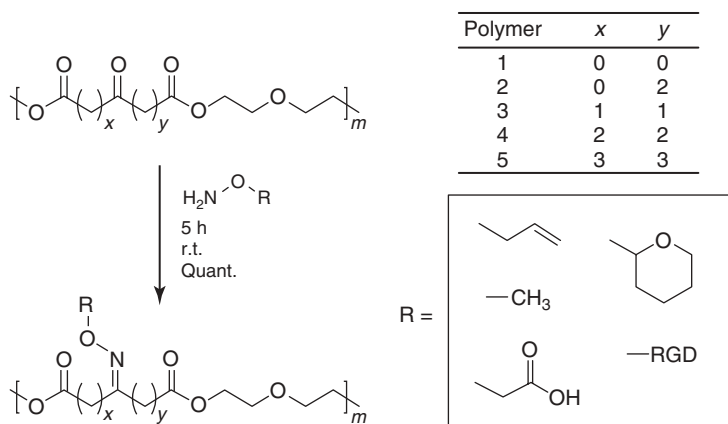
Scheme 1.6 Quantitative modification of various poly(keto esters) via a library of alkoxyamines [170].

for the construction of combinatorial libraries [168]. Xiao *et al.* [169] reported the preparation of polyFVFC-*co*-polyEGMA, which could be quantitatively modified with 1.2 equivalents of *O*-benzylhydroxylamine at 25 °C.
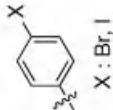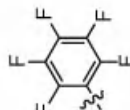
1.10
Post-polymerization Modifications via Other Highly Efficient Reactions

In the previous sections, we attempted to summarize the emergence and historical development of eight of the most prominent reactions that are used for post-polymerization modification. In addition to these more established post-polymerization modification reactions, there are also other reactions that have received less attention or which have been developed more recently. This final section provides an overview of several of these reactions (Table 1.9) and discusses their potential for post-polymerization modification.

The discovery of the catalytic effect of organopalladium compounds for the formation of stable C—C bonds with high yields and at milder conditions compared to many other coupling strategies, which was rewarded with the Nobel Prize in Chemistry in 2010, has enormously expanded the scope of organic synthesis as well as polymer science. Although palladium-catalyzed coupling reactions tolerate a wide variety of functional groups including halides, alkenes, alkynes as well as organoboron and organotine compounds [189–192], the post-polymerization modification of polymers bearing pendant phenyl halide groups with alkynes (Sonogashira coupling) has been investigated most extensively (Table 1.9). Stephens and Tour [182] reported that the conversion of brominated poly(*p*-phenylene) with various alkynes proceeds with moderate to high yields at elevated temperatures when phenylphosphine-based palladium catalysts were used. Grubbs later demonstrated near-quantitative functionalization of low-molecular-weight polyBrS

Table 1.9 Post-Polymerization modification of (co)polymers via Pd-catalyzed coupling, ATRA, *p*-fluoro thiol, acetal, and thiol–yne reactions.

Functional group(s)	Monomer	Comonomer	Polymerization method	Post-Polymerization modification		
				Reagents – reaction conditions	Conversion (%)	Comments
![structure] X : Br, I	bPP	PPh	HMPA-Promoted	A library of alkynes (3.5 equivalents), diisopropylamine (3.5 equivalents), CuI (0.04 equivalent), PdCl$_2$(PPh$_3$)$_2$, or Pd(PPh$_3$)$_4$ (0.04 equivalent), 60–100 °C, 5–10 h	56–84	Polymer does not have a well-defined structure. Cross-linking is possible [182]
	BrS	VPSt	NMP	Phenylacetylene, 1-hexyne (1.5 equivalents), diisopropylamine (1.7 equivalents), CuI (0.04 equivalent), [PdCl$_2$(PhCN)$_2$] (0.08 equivalent), r.t., 96 h	47–99	High-molecular-weight polyBrS cross-links on moderate functionalization with 1-hexyne [183]
	HB-I(PV-PE)	—	Pd-catalyzed	A diverse library of alkynes, CuI, PdCl$_2$(PPh$_3$)$_2$, r.t., overnight	85–95	Polymerization and post-polymerization modification was carried under identical conditions [184]

				Conditions	Yield	Comments
(Cl structure)	αClεCL	εCL	ROP	3-Butenyl benzoate (4.0 equivalents), CuBr (1.0 equivalent), Me6TREN, 60 °C, 90–240 min	Quantitative	No backbone degradation [185, 186]
	αClεCL	εCL	ROP	PEG750-alkene (4.0 equivalents), CuBr (1.0 equivalent), Me6TREN (1.0 equivalent), 60 °C, 240 min	19	Side reactions are possible [187]
(pentafluorophenyl structure)	PFS	St	NMP	GlcAc4-SH (1.2 equivalents), TEA (3.0 equivalents), 40 °C, 30–60 min	Quantitative	Thiol bearing molecules selectively react with the *para*-fluorine position [66]. Functionalization with amines is also possible [65]
	PFS	OEGMA	NMP	Thiophenol (0.2 equivalents), TEA (1.2 equivalents), r.t., 15 h	Quantitative	Quantitative functionalization with aromatic thiols is possible [188]
(vinyl ether structure)	EVGE	EO	AROP	Benzyl alcohol (10.0 equivalents), PTSA (0.01 equivalent), r.t., 10 min	Quantitative	Acetal-click reaction [28]
(alkyne structure)	PgMA	—	SI-FRP	A library of thiols, DMPA, 28 °C, 1 h	80	Thiol–yne reaction proceeds faster than CuAAC [157]

For each functional group/substrate, entries are listed in chronological order.

at room temperature when the reaction was mediated by [PdCl$_2$(PhCN)$_2$]. However, cross-linking of high-molecular-weight polyBrS was observed on modification with 1-hexyne [183]. Bunz *et al.* [184] extended the Pd-catalyzed post-polymerization modification to the functionalization of various hyperbranched polyI(PV-PE) copolymers.

Another attractive reaction for the post-polymerization modification of polymers is atom-transfer radical addition (ATRA), which takes place between alkyl halides and alkenes in the presence of a transition-metal catalyst and can be considered as a predecessor of ATRP [193]. Jérome and coworkers [185, 186] prepared poly(αClεCL-*co*-εCL) and investigated the modification of this polymer with various alkenes (Table 1.9). They demonstrated that, although ATRA post-polymerization modification is tolerant to many functional groups, such as alcohols, esters, epoxides, and carboxylic acids, the extent of modification can be limited by the competing reduction of C–Cl bonds to C–H bonds [187].

The development of the CuAAC reaction has stimulated the search for alternative ''click reactions.'' Examples of ''click'' reactions that have recently emerged and which have found use for post-polymerization modification include the PFP click [194], the acetal-click, and the thiol–yne addition reactions (Table 1.9) [195]. A common feature of these reactions is that they proceed very rapidly and quantitatively at mild conditions. Schubert and coworkers extensively studied the modification of polyPFS copolymers via PFP click reactions. Quantitative substitution of the *p*-fluoro position can be rapidly achieved both with amines and thiols, but milder conditions are sufficient when thiols are used (**2** in Scheme 1.3) [65, 66]. Furthermore, quantitative modification with less nucleophilic aromatic thiols was also achieved at longer reaction times [188]. Recently, Wurm and coworkers [28] prepared a polyether derivative bearing pendant vinyl ether groups (polyEVGE, ethoxy vinyl glycidyl ether), which was not only susceptible to modification via radical thiol addition but could also be functionalized with alcohols to form side-chain acetal groups (**3** in Scheme 1.3). These authors reported quantitative conversion of vinyl ether groups within 10 min in the presence of the *p*-toluene sulfonic acid (PTSA) catalyst with an excess of benzyl alcohol at room temperature. Although the reaction between alkynes and thiols in the presence of a radical source has already been known since the1930s [196], it was only recently that it was revived as a ''click'' reaction and started to find widespread use for the fabrication of macromolecular architectures [195, 197–199]. Hensarling and coworkers [200] illustrated that the post-polymerization modification of polyPgMA brushes with a library of thiols proceeded quantitatively within minutes under UV irradiation and a photoinitiator at ambient conditions. Cai and coworkers [157] showed that quantitative functionalization of polyPgMA brushes can be achieved both via thiol–yne and CuAAC reactions, whereas milder conditions are sufficient when thiol–yne modification was employed (**4** in Scheme 1.3).

1.11
Concluding Remarks

Many of the early developments in polymer science can be attributed to the use of post-polymerization modification reactions. The (re)discovery of many highly efficient and orthogonal chemistries, combined with the development of various functional-group-tolerant living/controlled polymerization techniques, has enormously expanded the scope of post-polymerization modification and resulted in an enormous increase in the use of this approach to synthesize functional polymers. Looking at the developments in this field from an historical perspective, the aim of this chapter was to highlight the significant advances and breakthroughs and to provide the reader with a flavor of what has been accomplished and all the possibilities that are yet to be explored.

References

1. Cunningham, W.A. (1935) *J. Chem. Educ.*, **12**, 120.
2. Oesper, R.E. (1929) *J. Chem. Educ.*, **6**, 677.
3. Rustemeyer, P. (2004) *Macromol. Symp.*, **208**, 1–6.
4. Staudinger, H. (1953) Nobel Lecture.
5. Staudinger, H. (1939) *Rubber Chem. Technol.*, **12**, 117–118.
6. Serniuk, G.E., Banes, F.W., and Swaney, M.W. (1948) *J. Am. Chem. Soc.*, **70**, 1804–1808.
7. Pepper, K.W., Paisley, H.M., and Young, M.A. (1953) *J. Am. Chem. Soc.*, 4097–4105.
8. Merrifield, R.B. (1963) *J. Am. Chem. Soc.*, **85**, 2149–2154.
9. Kern, W., Schulz, R.C., and Braun, D. (1960) *J. Polym. Sci.*, **48**, 91–99.
10. Blatz, P.E. (1962) *J. Polym. Sci.*, **58**, 755–768.
11. Iwakura, Y., Kurosaki, T., and Nakabayashi, N. (1961) *Makromolekul. Chem.*, **44-6**, 570–590.
12. Iwakura, Y., Kurosaki, T., and Imai, Y. (1965) *Makromolekul. Chem.*, **86**, 73–79.
13. Iwakura, Y., Kurosaki, T., Ariga, N., and Ito, T. (1966) *Makromolekul. Chem.*, **97**, 128–138.
14. Wang, J.-S. and Matyjaszewski, K. (1995) *J. Am. Chem. Soc.*, **117**, 5614–5615.
15. Chiefari, J., Chong, Y.K., Ercole, F., Krstina, J., Jeffery, J., Le, T.P.T., Mayadunne, R.T.A., Meijs, G.F., Moad, C.L., Moad, G., Rizzardo, E., and Thang, S.H. (1998) *Macromolecules*, **31**, 5559–5562.
16. Hawker, C.J., Bosman, A.W., and Harth, E. (2001) *Chem. Rev.*, **101**, 3661–3688.
17. Griesbaum, K. (1970) *Angew. Chem. Int. Ed.*, **9**, 273–287.
18. Romani, F., Passaglia, E., Aglietto, M., and Ruggeri, G. (1999) *Macromol. Chem. Phys.*, **200**, 524–530.
19. Herczynska, L., Lestel, L., Boileau, S., Chojnowski, J., and Polowinski, S. (1999) *Eur. Polym. J.*, **35**, 1115–1122.
20. Justynska, J., Hordyjewicz, Z., and Schlaad, H. (2005) *Polymer*, **46**, 12057–12064.
21. Justynska, J. and Schlaad, H. (2004) *Macromol. Rapid Commun.*, **25**, 1478–1481.
22. Gress, A., Völkel, A., and Schlaad, H. (2007) *Macromolecules*, **40**, 7928–7933.
23. Campos, L.M., Killops, K.L., Sakai, R., Paulusse, J.M.J., Damiron, D., Drockenmuller, E., Messmore, B.W., and Hawker, C.J. (2008) *Macromolecules*, **41**, 7063–7070.
24. ten Brummelhuis, N., Diehl, C., and Schlaad, H. (2008) *Macromolecules*, **41**, 9946–9947.

25. Tempelaar, S., Mespouille, L., Dubois, P., and Dove, A.P. (2011) *Macromolecules*, **44**, 2084–2091.

26. Ferris, C., De Paz, M.V., and Galbis, J.A. (2011) *J. Polym. Sci. Polym. Chem.*, **49**, 1147–1154.

27. Obermeier, B. and Frey, H. (2011) *Bioconjugate Chem.*, **22**, 436–444.

28. Mangold, C., Dingels, C., Obermeier, B., Frey, H., and Wurm, F. (2011) *Macromolecules*, **44**, 6326–6334.

29. Kempe, K., Hoogenboom, R., Jaeger, M., and Schubert, U.S. (2011) *Macromolecules*, **44**, 6424–6432.

30. Ma, J., Cheng, C., and Wooley, K.L. (2009) *Macromolecules*, **42**, 1565–1573.

31. Ates, Z., Thornton, P.D., and Heise, A. (2011) *Polym. Chem.*, **2**, 309–312.

32. Wong, L.J., Sevimli, S., Zareie, H.M., Davis, T.P., and Bulmus, V. (2010) *Macromolecules*, **43**, 5365–5375.

33. Kalal, J., Švec, F., and Maroušek, V. (1974) *J. Polym. Sci. Polym. Symp.*, **47**, 155–166.

34. Nishikubo, T., Iizawa, T., Takahashi, E., and Nono, F. (1985) *Macromolecules*, **18**, 2131–2135.

35. Navarro-Rodriguez, D., Rodriguez-Gonzalez, F.J., Romero-Garcia, J., Jimenez-Regalado, E.J., and Guillon, D. (1998) *Eur. Polym. J.*, **34**, 1039–1045.

36. Edmondson, S. and Huck, W.T.S. (2004) *J. Mater. Chem.*, **14**, 730–734.

37. Barbey, R. and Klok, H.-A. (2010) *Langmuir*, **26**, 18219–18230.

38. Maeda, H., Takeshita, J., and Kanamaru, R. (1979) *Int. J. Pept. Protein Res.*, **14**, 81–87.

39. Maeda, H., Ueda, M., Morinaga, T., and Matsumoto, T. (1985) *J. Med. Chem.*, **28**, 455–461.

40. Hu, G.H. and Lindt, J.T. (1992) *Polym. Bull.*, **29**, 357–363.

41. Jeong, J.H., Byoun, Y.S., Ko, S.B., and Lee, Y.S. (2001) *J. Ind. Eng. Chem.*, **7**, 310–315.

42. Donati, I., Gamini, A., Vetere, A., Campa, C., and Paoletti, S. (2002) *Biomacromolecules*, **3**, 805–812.

43. Henry, S.M., El-Sayed, M.E.H., Pirie, C.M., Hoffman, A.S., and Stayton, P.S. (2006) *Biomacromolecules*, **7**, 2407–2414.

44. Guichard, B., Noël, C., Reyx, D., Thomas, M., Chevalier, S., and Senet, J.-P. (1998) *Macromol. Chem. Phys.*, **199**, 1657–1674.

45. Tripp, J.A., Stein, J.A., Svec, F., and Fréchet, J.M.J. (1999) *Org. Lett.*, **2**, 195–198.

46. Fontaine, L., Lemele, T., Brosse, J.-C., Sennyey, G., Senet, J.-P., and Wattiez, D. (2002) *Macromol. Chem. Phys.*, **203**, 1377–1384.

47. Tully, D.C., Roberts, M.J., Geierstanger, B.H., and Grubbs, R.B. (2003) *Macromolecules*, **36**, 4302–4308.

48. Lapinte, V., Brosse, J.-C., and Fontaine, L. (2004) *Macromol. Chem. Phys.*, **205**, 824–833.

49. Fournier, D., Pascual, S., Montembault, V., Haddleton, D.M., and Fontaine, L. (2006) *J. Comb. Chem.*, **8**, 522–530.

50. Xu, W.Y. and Smid, J. (1993) *Macromolecules*, **26**, 7004–7008.

51. Beyer, D., Paulus, W., Seitz, M., Maxein, G., Ringsdorf, H., and Eich, M. (1995) *Thin Solid Films*, **271**, 73–83.

52. Dörr, M., Zentel, R., Dietrich, R., Meerholz, K., Bräuchle, C., Wichern, J., Zippel, S., and Boldt, P. (1998) *Macromolecules*, **31**, 1454–1465.

53. Yin, Z., Koulic, C., Pagnoulle, C., and Jérome, R. (2002) *Macromol. Chem. Phys.*, **203**, 2021–2028.

54. Flores, J.D., Shin, J., Hoyle, C.E., and McCormick, C.L. (2010) *Polym. Chem.*, **1**, 213–220.

55. Hensarling, R.M., Rahane, S.B., LeBlanc, A.P., Sparks, B.J., White, E.M., Locklin, J., and Patton, D.L. (2011) *Polym. Chem.*, **2**, 88–90.

56. Luft, J.H. (1961) *J. Biophys. Biochem. Cytol.*, **9**, 409–414.

57. Bowen, R.L. (1956) *J. Dent. Res.*, **35**, 360–369.

58. Häußler, L., Wienhold, U., Albrecht, V., and Zschoche, S. (1996) *Thermochim. Acta*, **277**, 17–27.

59. Lee, W.-F. and Lee, C.-H. (1997) *Polymer*, **38**, 971–979.

60. Taylor, L.D., Chiklis, C.K., and Platt, T.E. (1971) *J. Polym. Sci. Polym. Lett.*, **9**, 187–190.

61. Coleman, P.L., Walker, M.M., Milbrath, D.S., Stauffer, D.M., Rasmussen, J.K.,

Krepski, L.R., and Heilmann, S.M. (1990) *J. Chromatogr.*, **512**, 345–363.

62. Schulz, V.R.C. and Stenner, R. (1964) *Makromolekul. Chem.*, **72**, 202–204.

63. Barner, L., Perera, S., Sandanayake, S., and Davis, T.P. (2006) *J. Polym. Sci. Polym. Chem.*, **44**, 857–864.

64. Kukulj, D., Davis, T.P., and Gilbert, R.G. (1998) *Macromolecules*, **31**, 994–999.

65. Ott, C., Hoogenboom, R., and Schubert, U.S. (2008) *Chem. Commun.*, 3516–3518.

66. Becer, C.R., Babiuch, K., Pilz, D., Hornig, S., Heinze, T., Gottschaldt, M., and Schubert, U.S. (2009) *Macromolecules*, **42**, 2387–2394.

67. Nilles, K. and Théato, P. (2010) *J. Polym. Sci. Polym. Chem.*, **48**, 3683–3692.

68. Cengiz, N., Kabadayioglu, H., and Sanyal, R. (2010) *J. Polym. Sci. Polym. Chem.*, **48**, 4737–4746.

69. Ghosh, S., Basu, S., and Thayumanavan, S. (2006) *Macromolecules*, **39**, 5595–5597.

70. Yang, S.K. and Weck, M. (2009) *Soft Matter*, **5**, 582–585.

71. Batz, H.G., Franzmann, G., and Ringsdorf, H. (1972) *Angew. Chem. Int. Ed.*, **11**, 1103–1104.

72. Ferruti, P., Bettelli, A., and Feré, A. (1972) *Polymer*, **13**, 462–464.

73. Desai, A., Atkinson, N., Rivera, F., Devonport, W., Rees, I., Branz, S.E., and Hawker, C.J. (2000) *J. Polym. Sci. Polym. Chem.*, **38**, 1033–1044.

74. Strong, L.E. and Kiessling, L.L. (1999) *J. Am. Chem. Soc.*, **121**, 6193–6196.

75. Godwin, A., Hartenstein, M., Müller, A.H.E., and Brocchini, S. (2001) *Angew. Chem. Int. Ed.*, **40**, 594–597.

76. Pedone, E., Li, X., Koseva, N., Alpar, O., and Brocchini, S. (2003) *J. Mater. Chem.*, **13**, 2825–2837.

77. Hu, Z., Liu, Y., Hong, C., and Pan, C. (2005) *J. Appl. Polym. Sci.*, **98**, 189–194.

78. Yanjarappa, M.J., Gujraty, K.V., Joshi, A., Saraph, A., and Kane, R.S. (2006) *Biomacromolecules*, **7**, 1665–1670.

79. Murata, H., Prucker, O., and Rühe, J. (2007) *Macromolecules*, **40**, 5497–5503.

80. Aamer, K.A. and Tew, G.N. (2007) *J. Polym. Sci. Polym. Chem.*, **45**, 5618–5625.

81. Orski, S.V., Fries, K.H., Sheppard, G.R., and Locklin, J. (2010) *Langmuir*, **26**, 2136–2143.

82. Narita, M., Teramoto, T., and Okawara, M. (1972) *Bull. Chem. Soc. Jpn.*, **45**, 3149–3155.

83. Rejmanová, P., Labský, J., and Kopeèek, J. (1977) *Makromol. Chem.*, **178**, 2159–2168.

84. Liu, Y., Wang, L., and Pan, C. (1999) *Macromolecules*, **32**, 8301–8305.

85. Hwang, J.Y., Li, R.C., and Maynard, H.D. (2007) *J. Controlled Release*, **122**, 279–286.

86. Eberhardt, M., Mruk, R., Zentel, R., and Théato, P. (2005) *Eur. Polym. J.*, **41**, 1569–1575.

87. Francesch, L., Borros, S., Knoll, W., and Förch, R. (2007) *Langmuir*, **23**, 3927–3931.

88. Vogel, N. and Théato, P. (2007) *Macromol. Symp.*, **249-250**, 383–391.

89. Gibson, M.I., Fröhlich, E., and Klok, H.-A. (2009) *J. Polym. Sci. Polym. Chem.*, **47**, 4332–4345.

90. Nilles, K. and Théato, P. (2007) *Eur. Polym. J.*, **43**, 2901–2912.

91. Šubr, V. and Ulbrich, K. (2006) *React. Funct. Polym.*, **66**, 1525–1538.

92. Li, X.S., Gan, L.H., and Gan, Y.Y. (2008) *Polymer*, **49**, 1879–1884.

93. Metz, N. and Theato, P. (2007) *Eur. Polym. J.*, **43**, 1202–1209.

94. Godula, K. and Bertozzi, C.R. (2010) *J. Am. Chem. Soc.*, **132**, 9963–9965.

95. Devenish, S.R.A., Hill, J.B., Blunt, J.W., Morris, J.C., and Munro, M.H.G. (2006) *Tetrahedron Lett.*, **47**, 2875–2878.

96. Wong, S.Y. and Putnam, D. (2007) *Bioconjugate Chem.*, **18**, 970–982.

97. Gilbert, H.F. (1982) *J. Biol. Chem.*, **257**, 2086–2091.

98. Markovic, I., Stantchev, T.S., Fields, K.H., Tiffany, L.J., Tomiç, M., Weiss, C.D., Broder, C.C., Strebel, K., and Clouse, K.A. (2004) *Blood*, **103**, 1586–1594.

99. Wedemeyer, W.J., Welker, E., Narayan, M., and Scheraga, H.A. (2000) *Biochemistry*, **39**, 4207–4216.

100. Lecher, H. (1920) *Ber. Dtsch. Chem. Ges.*, **53**, 591–593.

101. Hopkins, F.G. (1925) *Biochem. J.*, **19**, 787–819.

102. Wang, L., Kristensen, J., and Ruffner, D.E. (1998) *Bioconjugate Chem.*, **9**, 749–757.

103. Bulmus, V., Woodward, M., Lin, L., Murthy, N., Stayton, P., and Hoffman, A. (2003) *J. Controlled Release*, **93**, 105–120.

104. Zugates, G.T., Anderson, D.G., Little, S.R., Lawhorn, I.E.B., and Langer, R. (2006) *J. Am. Chem. Soc.*, **128**, 12726–12734.

105. Wong, L., Boyer, C., Jia, Z., Zareie, H.M., Davis, T.P., and Bulmus, V. (2008) *Biomacromolecules*, **9**, 1934–1944.

106. Diels, O. and Alder, K. (1928) *Liebigs Ann. Chem.*, **460**, 98–122.

107. Chujo, Y., Sada, K., and Saegusa, T. (1990) *Macromolecules*, **23**, 2636–2641.

108. Ritter, H. and Sperber, R. (1994) *Macromolecules*, **27**, 5919–5920.

109. Kolb, H.C., Finn, M.G., and Sharpless, K.B. (2001) *Angew. Chem. Int. Ed.*, **40**, 2004–2021.

110. Durmaz, H., Dag, A., Altintas, O., Erdogan, T., Hizal, G., and Tunca, U. (2007) *Macromolecules*, **40**, 191–198.

111. Durmaz, H., Dag, A., Hizal, A., Hizal, G., and Tunca, U. (2008) *J. Polym. Sci. Polym. Chem.*, **46**, 7091–7100.

112. Sauer, J. (1966) *Angew. Chem. Int. Ed.*, **5**, 211–230.

113. Canary, S.A. and Stevens, M.P. (1992) *J. Polym. Sci. Polym. Chem.*, **30**, 1755–1760.

114. Jones, J.R., Liotta, C.L., Collard, D.M., and Schiraldi, D.A. (1999) *Macromolecules*, **32**, 5786–5792.

115. Canadell, J., Fischer, H., De With, G., and Van Benthem, R.A.T.M. (2010) *J. Polym. Sci. Polym. Chem.*, **48**, 3456–3467.

116. Kosif, I., Park, E.J., Sanyal, R., and Sanyal, A. (2010) *Macromolecules*, **43**, 4140–4148.

117. Szalai, M.L., McGrath, D.V., Wheeler, D.R., Zifer, T., and McElhanon, J.R. (2007) *Macromolecules*, **40**, 818–823.

118. Gacal, B., Durmaz, H., Tasdelen, M.A., Hizal, G., Tunca, U., Yagci, Y., and Demirel, A.L. (2006) *Macromolecules*, **39**, 5330–5336.

119. Dispinar, T., Sanyal, R., and Sanyal, A. (2007) *J. Polym. Sci. Polym. Chem.*, **45**, 4545–4551.

120. Laita, H., Boufi, S., and Gandini, A. (1997) *Eur. Polym. J.*, **33**, 1203–1211.

121. Kim, T.-D., Luo, J., Tian, Y., Ka, J.-W., Tucker, N.M., Haller, M., Kang, J.-W., and Jen, A.K.-Y. (2006) *Macromolecules*, **39**, 1676–1680.

122. Durmaz, H., Dag, A., Hizal, G., and Tunca, U. (2011) *J. Polym. Sci. Polym. Chem.*, **49**, 1195–1200.

123. Bousquet, A., Barner-Kowollik, C., and Stenzel, M.H. (2010) *J. Polym. Sci. Polym. Chem.*, **48**, 1773–1781.

124. Benaglia, M., Rizzardo, E., Alberti, A., and Guerra, M. (2005) *Macromolecules*, **38**, 3129–3140.

125. Bastin, R., Albadri, H., Gaumont, A.-C., and Gulea, M. (2006) *Org. Lett.*, **8**, 1033–1036.

126. Inglis, A.J., Sinnwell, S., Stenzel, M.H., and Barner-Kowollik, C. (2009) *Angew. Chem. Int. Ed.*, **48**, 2411–2414.

127. Mather, B.D., Viswanathan, K., Miller, K.M., and Long, T.E. (2006) *Prog. Polym. Sci.*, **31**, 487–531.

128. Friedman, M., Cavins, J.F., and Wall, J.S. (1965) *J. Am. Chem. Soc.*, **87**, 3672–3682.

129. Rieger, J., Van Butsele, K., Lecomte, P., Detrembleur, C., Jérôme, R., and Jérôme, C. (2005) *Chem. Commun.*, 274–276.

130. Chen, W., Yang, H., Wang, R., Cheng, R., Meng, F., Wei, W., and Zhong, Z. (2010) *Macromolecules*, **43**, 201–207.

131. Ohsawa, S., Morino, K., Sudo, A., and Endo, T. (2011) *Macromolecules*, **44**, 1814–1820.

132. Wang, R., Chen, W., Meng, F., Cheng, R., Deng, C., Feijen, J., and Zhong, Z. (2011) *Macromolecules*, **44**, 6009–6016.

133. Rostovtsev, V.V., Green, L.G., Fokin, V.V., and Sharpless, K.B. (2002) *Angew. Chem. Int. Ed.*, **41**, 2596–2599.

134. Tornøe, C.W., Christensen, C., and Meldal, M. (2002) *J. Org. Chem.*, **67**, 3057–3064.

135. Sumerlin, B.S., Tsarevsky, N.V., Louche, G., Lee, R.Y., and Matyjaszewski, K. (2005) *Macromolecules*, **38**, 7540–7545.

136. Riva, R., Schmeits, P., Stoffelbach, F., Jérôme, C., Jérôme, R., and Lecomte, P. (2005) *Chem. Commun.*, 5334–5336.

137. Li, Y., Yang, J., and Benicewicz, B.C. (2007) *J. Polym. Sci. Polym. Chem.*, **45**, 4300–4308.

138. Li, Y. and Benicewicz, B.C. (2008) *Macromolecules*, **41**, 7986–7992.

139. Li, G., Wang, H., Zheng, H., and Bai, R. (2010) *J. Polym. Sci. Polym. Chem.*, **48**, 1348–1356.

140. Abdelkader, O., Moebs-Sanchez, S., Queneau, Y., Bernard, J., and Fleury, E. (2011) *J. Polym. Sci. Polym. Chem.*, **49**, 1309–1318.

141. Zhang, X., Zhong, Z., and Zhuo, R. (2011) *Macromolecules*, **44**, 1755–1759.

142. Xu, J., Prifti, F., and Song, J. (2011) *Macromolecules*, **44**, 2660–2667.

143. Parrish, B., Breitenkamp, R.B., and Emrick, T. (2005) *J. Am. Chem. Soc.*, **127**, 7404–7410.

144. Luxenhofer, R. and Jordan, R. (2006) *Macromolecules*, **39**, 3509–3516.

145. Parrish, B. and Emrick, T. (2007) *Bioconjugate Chem.*, **18**, 263–267.

146. Lu, C., Shi, Q., Chen, X., Lu, T., Xie, Z., Hu, X., Ma, J., and Jing, X. (2007) *J. Polym. Sci. Polym. Chem.*, **45**, 3204–3217.

147. Zhang, X., Lian, X., Liu, L., Zhang, J., and Zhao, H. (2008) *Macromolecules*, **41**, 7863–7869.

148. Jiang, X., Vogel, E.B., Smith, M.R., and Baker, G.L. (2008) *Macromolecules*, **41**, 1937–1944.

149. Fournier, D. and Du Prez, F. (2008) *Macromolecules*, **41**, 4622–4630.

150. Billiet, L., Fournier, D., and Du Prez, F. (2008) *J. Polym. Sci. Polym. Chem.*, **46**, 6552–6564.

151. Sinha, J., Sahoo, R., and Kumar, A. (2009) *Macromolecules*, **42**, 2015–2022.

152. Engler, A.C., Lee, H.-I., and Hammond, P.T. (2009) *Angew. Chem. Int. Ed.*, **48**, 9334–9338.

153. Darcos, V., El Habnouni, S., Nottelet, B., El Ghzaoui, A., and Coudane, J. (2010) *Polym. Chem.*, **1**, 280–282.

154. Jazkewitsch, O., Mondrzyk, A., Staffel, R., and Ritter, H. (2011) *Macromolecules*, **44**, 1365–1371.

155. Yu, Y., Zou, J., Yu, L., Jo, W., Li, Y., Law, W.-C., and Cheng, C. (2011) *Macromolecules*, **44**, 4793–4800.

156. Hong, M., Liu, J.-Y., Li, B.-X., and Li, Y.-S. (2011) *Macromolecules*, **44**, 5659–5665.

157. Cai, T., Neoh, K.G., and Kang, E.T. (2011) *Macromolecules*, **44**, 4258–4268.

158. Binder, W.H. and Kluger, C. (2004) *Macromolecules*, **37**, 9321–9330.

159. Agard, N.J., Baskin, J.M., Prescher, J.A., Lo, A., and Bertozzi, C.R. (2006) *ACS Chem. Biol.*, **1**, 644–648.

160. Kele, P., Li, X., Link, M., Nagy, K., Herner, A., Lõrincz, K., Béni, S., and Wolfbeis, O.S. (2009) *Org. Biomol. Chem.*, **7**, 3486–3490.

161. Agard, N.J., Prescher, J.A., and Bertozzi, C.R. (2004) *J. Am. Chem. Soc.*, **126**, 15046–15047.

162. Rose, K. (1994) *J. Am. Chem. Soc.*, **116**, 30–33.

163. Shao, J. and Tam, J.P. (1995) *J. Am. Chem. Soc.*, **117**, 3893–3899.

164. Abdel-Magid, A.F., Carson, K.G., Harris, B.D., Maryanoff, C.A., and Shah, R.D. (1998) *Abstr. Pap. Am. Chem. Soc.*, **216**, U934–U934.

165. Gribble, G.W. (1998) *Chem. Soc. Rev.*, **27**, 395–404.

166. Rabuka, D., Parthasarathy, R., Lee, G.S., Chen, X., Groves, J.T., and Bertozzi, C.R. (2007) *J. Am. Chem. Soc.*, **129**, 5462–5471.

167. Yang, S.K. and Weck, M. (2008) *Macromolecules*, **41**, 346–351.

168. Fulton, D.A. (2008) *Org. Lett.*, **10**, 3291–3294.

169. Xiao, Z.-P., Cai, Z.-H., Liang, H., and Lu, J. (2010) *J. Mater. Chem.*, **20**, 8375–8381.

170. Barrett, D.G. and Yousaf, M.N. (2008) *Biomacromolecules*, **9**, 2029–2035.

171. Overberger, C.G. and Schiller, A.M. (1961) *J. Polym. Sci.*, **54**, S30–S31.

172. Tsuruta, T., Fujio, R., and Furukawa, J. (1964) *Makromolekul. Chem.*, **80**, 172–184.

173. Godula, K., Umbel, M.L., Rabuka, D., Botyanszki, Z., Bertozzi, C.R., and

Parthasarathy, R. (2009) *J. Am. Chem. Soc.*, **131**, 10263–10268.

174. Wiley, R.H. and Hobson, P.H. (1950) *J. Polym. Sci.*, **5**, 483–486.

175. Schulz, v.R.C., Fauth, H., and Kern, W. (1956) *Makromolekul. Chem.*, **20**, 161–167.

176. Schulz, R.C. (1964) *Angew. Chem. Int. Ed.*, **3**, 416–423.

177. Zábranský, J., Houska, M., and Kálal, J. (1985) *Makromol. Chem.*, **186**, 215–222.

178. Zábranský, J., Houska, M., and Kálal, J. (1985) *Makromol. Chem.*, **186**, 223–229.

179. Taubmann, C., Luxenhofer, R., Cesana, S., and Jordan, R. (2005) *Macromol. Biosci.*, **5**, 603–612.

180. Li, R.C., Broyer, R.M., and Maynard, H.D. (2006) *J. Polym. Sci. Polym. Chem.*, **44**, 5004–5013.

181. Sun, G.R., Cheng, C., and Wooley, K.L. (2007) *Macromolecules*, **40**, 793–795.

182. Stephens, E.B. and Tour, J.M. (1993) *Macromolecules*, **26**, 2420–2427.

183. Sessions, L.B., Cohen, B.R., and Grubbs, R.B. (2007) *Macromolecules*, **40**, 1926–1933.

184. Kub, C., Tolosa, J., Zucchero, A.J., McGrier, P.L., Subramani, C., Khorasani, A., Rotello, V.M., and Bunz, U.H.F. (2010) *Macromolecules*, **43**, 2124–2129.

185. Lenoir, S., Riva, R., Lou, X., Detrembleur, C., Jérôme, R., and Lecomte, P. (2004) *Macromolecules*, **37**, 4055–4061.

186. Riva, R., Lenoir, S., Jérôme, R., and Lecomte, P. (2005) *Polymer*, **46**, 8511–8518.

187. Riva, R., Rieger, J., Jérôme, R., and Lecomte, P. (2006) *J. Polym. Sci. Polym. Chem.*, **44**, 6015–6024.

188. Becer, C.R., Kokado, K., Weber, C., Can, A., Chujo, Y., and Schubert, U.S. (2010) *J. Polym. Sci. Polym. Chem.*, **48**, 1278–1286.

189. Heck, R.F. and Nolley, J.P. (1972) *J. Org. Chem.*, **37**, 2320–2322.

190. Sonogashira, K., Tohda, Y., and Hagihara, N. (1975) *Tetrahedron Lett.*, **16**, 4467–4470.

191. Stille, J.K. (1986) *Angew. Chem. Int. Ed.*, **25**, 508–523.

192. Miyaura, N. and Suzuki, A. (1995) *Chem. Rev.*, **95**, 2457–2483.

193. Matyjaszewski, K. and Xia, J. (2001) *Chem. Rev.*, **101**, 2921–2990.

194. Gan, D., Mueller, A., and Wooley, K.L. (2003) *J. Polym. Sci. Polym. Chem.*, **41**, 3531–3540.

195. Lowe, A.B., Hoyle, C.E., and Bowman, C.N. (2010) *J. Mater. Chem.*, **20**, 4745–4750.

196. Kohler, E.P. and Potter, H. (1935) *J. Am. Chem. Soc.*, **57**, 1316–1321.

197. Fairbanks, B.D., Scott, T.F., Kloxin, C.J., Anseth, K.S., and Bowman, C.N. (2009) *Macromolecules*, **42**, 211–217.

198. Yu, B., Chan, J.W., Hoyle, C.E., and Lowe, A.B. (2009) *J. Polym. Sci. Polym. Chem.*, **47**, 3544–3557.

199. Hoogenboom, R. (2010) *Angew. Chem. Int. Ed.*, **49**, 3415–3417.

200. Hensarling, R.M., Doughty, V.A., Chan, J.W., and Patton, D.L. (2009) *J. Am. Chem. Soc.*, **131**, 14673–14675.

2
Post-polymerization Modifications via Active Esters

Ryohei Kakuchi and Patrick Theato

2.1
Introduction

A rapidly growing interdisciplinary science demands a wide range of functional materials. In particular, functional polymers have played indispensable roles. In general, the synthesis of functional polymers can be achieved by two routes: (i) direct polymerization of functional monomers or (ii) installation of functional groups onto the presynthesized polymers via the so-called post-polymerization modification or polymer analogous reactions. Although the direct polymerization of functional monomers can avoid the possibility of structural defects in the synthesized polymers, the route sometimes suffers from the decrease in the polymerizability of the functionalized monomer because of steric hindrance and/or incompatibility with solvents, or the polymerization process itself. Furthermore, by employing the former approach, the diversity in the monomeric structure is limited because the monomer synthesis is a mandatory – and sometimes very tedious – step to obtain the corresponding polymers. In clear contrast to this, the post-polymerization modification provides several advantages over the former approach, such as polymerization of a single *reactive* monomer and the ease of diversification in chemical structure. However, post-polymerization reactions also encounter the problem of potential defects in chemical structures of the obtained polymers by an insufficient efficiency of the reaction in installing functional groups. Thus, highly efficient reactions are required for any post-polymerization modification. Among the reactions with high efficiency (nowadays called, *click* reactions), the Cu(I)-catalyzed 1,3-dipolar cycloaddition reaction between organo azides and alkynes is one of the most well-established click reactions in both polymer chemistry and materials science. However, this reaction requires in most cases an organometallic catalyst, which potentially limits the practical use of such polymers in electro- and bio-related materials.

In this context, active esters are very classical reactive groups but still represent one of the most useful groups for post-polymerization modifications because the reaction between amines with active esters proceeds under very mild conditions (such as room temperature) yielding practically 100% conversion of the

corresponding amides. In addition to this, the reaction of active esters with amines clearly provides the advantage of proceeding without the auxiliary usage of a metal catalyst.

The advent of controlled radical polymerizations, which encompass nitroxide-mediated polymerization (NMP), atom-transfer radical polymerization (ATRP), and reversible addition fragmentation chain-transfer (RAFT) polymerization, has equipped polymer chemists with the synthetic tools to achieve an unprecedented precision at the molecular level when it comes to the polymerization of vinyl monomers. In contrast to cationic or anionic living polymerizations, the radical-based methods of NMP, ATRP, and RAFT polymerization are very tolerant toward functional groups and especially reactive groups.

Research efforts combining controlled radical polymerizations with the versatility of active ester chemistry are in the focus of this chapter. Thus, based on the rapidly increasing importance of polymeric active ester not only in polymer chemistry but also in material and bio-related sciences, it is the aim of this chapter to highlight the recent advances by using active ester groups in the preparation of precisely defined polymer architectures.

2.2
Active Esters in the Side Group

Inspired by the pioneering work by the groups of Ringsdorf and Ferruti, who demonstrated in 1972 the utilization of the active ester functionality, scientists have found broad application of polymeric active esters from simple polymer chemistry to materials and life science and beyond. Over the years, polymer scientists have studied and polymerized numerous monomers based on active esters by different polymerization methods. The following list of monomers is intended to provide a selection of particularly useful monomers that have frequently been used for the synthesis of functional polymer materials (Scheme 2.1): *N*-hydroxy succinimide acrylate (NHSA) (also called *N-acryloxysuccinimide* or *N-succinimidyl acrylate*) and *N*-hydroxy succinimide methacrylate (NHSMA) [1–8], pentafluorophenyl acrylate (PFPA) and pentafluorophenyl methacrylate (PFPMA) [9], 2,3,5,6-tetrafluorophenyl methacrylate (TFPMA) [10], endo-*N*-hydroxy-5-norborene-2,3-dicarboxyimidacrylate (NorbNHSA) [11], *p*-nitrophenyl acrylate (PNPA) and *p*-nitrophenyl methacrylate (PNPMA) [12–14], acetonoxime acrylate (AOA) [15, 16], *N*-succinimidyl 4-vinylbenzoate (NHS4VB) [3, 17, 18], pentafluorophenyl 4-vinylbenzoate (PFP4VB) [19–21], 4-acryloxyphenyl-dimethylsulfonium triflate (DMSPA) [22], pentafluorophenyl 5-methyl-2-oxo-1,3-dioxane-5-carboxylate (MTC-OPhF5) [23], 5-methyl-5-(succinimide-*N*-oxycarbonyl)-1,3-dioxan-2-one (MSTC) [24], pentafluorophenyl 5-norbornene-2-carboxylate (PFPNorb) [25], *N*-hydroxysuccinimidyl 5-norbornene-2-carboxylate (NHSNorb) [26–29], pentafluorophenyl 4-ethynylbenzoate (PFPEB) [30], perfluorophenyl 6-(4-ethynylphenoxy)hexanoate, perfluorophenyl 11-(4-ethynylphenoxy)undecanoate [31], and perfluorophenyl 4-(2-phenylethynyl)benzoate [32].
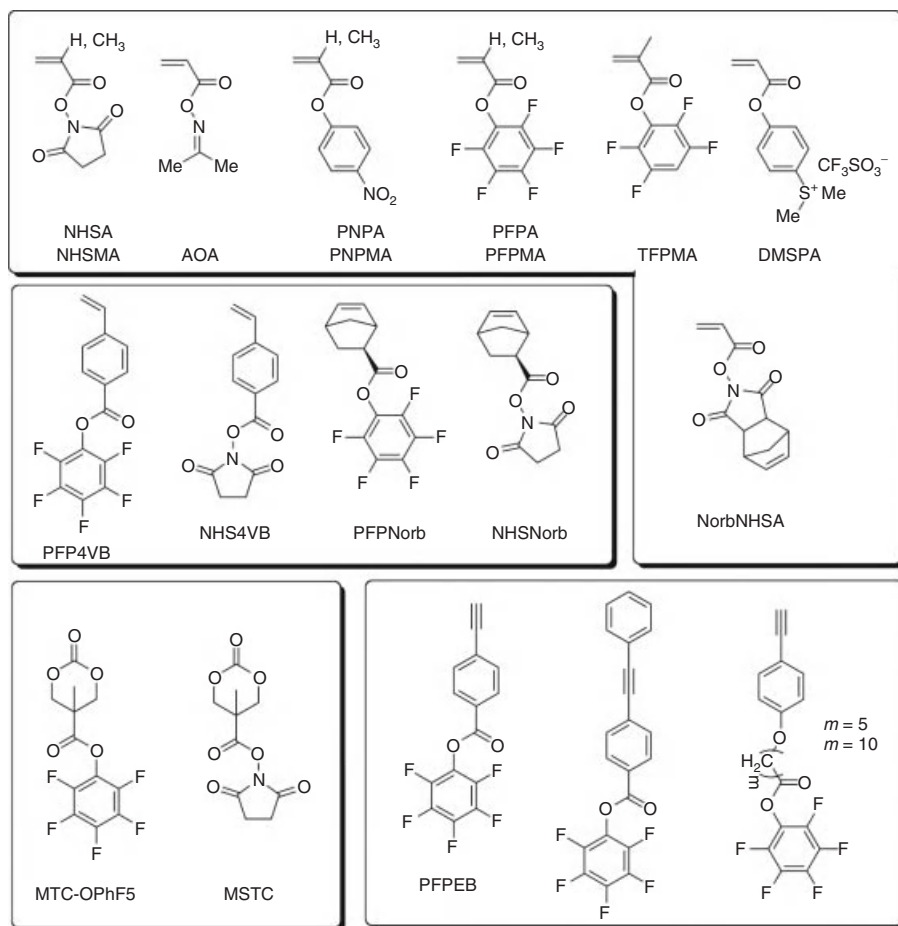
Scheme 2.1 Collection of various types of monomers featuring an active ester group.

While the list encompasses monomers suitable for various different polymerizations, in the following sections we mainly concentrates on developments in the area of vinyl-based monomers that can be polymerized by controlled radical polymerization techniques. Nevertheless, whenever suitable, we will look beyond and will not restrict our thinking.

2.2.1
Homopolymers

2.2.1.1 General

The polymerization of active ester monomers yields reactive precursor polymers, which can be employed in the synthesis of functional polymers by a post-polymerization modification. The simple conversion with amines results in copolymers whose composition essentially depends on the feed ratio of the added

amines [33]. Practically, one mostly performs a sequential conversion with different amines, which enables a better control of the incorporated amounts of the different amines [6]. First, the minor component is added, which is allowed to react to completion. In most reported cases, this first step is performed with the precious, that is, expensive, amine in order to guarantee a quantitative conversion of the amine. In a second step, another amine is then added, and so forth. Finally, in the last step, a slight excess of the major amine component is added, which is allowed to react with the remaining active ester units. Purification then yields the functional copolymer. It has to be noted here that homopolymers based on NHSA and NHSMA suffer from solubility issues. The polymers poly(NHSA) and poly(NHSMA) are only soluble in dimethylformamide (DMF) or dimethylsulfoxide (DMSO), which makes the purification step rather tedious. Thus, it is a common practice, when NHSA or NHSMA is employed, to copolymerize these monomers in the first place to obtain copolymers, with NHSA or NHSMA being the reactive comonomer unit [34]. These reactive copolymers are then soluble in a wider variety of common organic solvents and allow the conversion with various amines.

Apparently, the synthetic possibilities derived from the post-polymerization functionalization of active ester polymers are nearly endless. As such, only selected examples are mentioned in the following to provide the reader a small glimpse of the recent applications of active ester homo- and copolymers. These are categorized into the following by their application area.

2.2.1.2 Stimuli-Responsive Polymers

The most commonly used method is the copolymerization of NHSA with *N*-isopropylacrylamide (NIPAM), which results in reactive poly(NIPAM). Furthermore, functionalization with amines leads to functionalized poly(NIPAM) [35]. Poly(NIPAM) is the most popular thermosensitive polymer because of its lower critical solution temperature (LCST) in water at 32 °C, which is close to body temperature [36]. Depending on the functional unit that has been introduced via the amine in the functionalized poly(NIPAM), the LCST can be shifted to a higher or lower value with hydrophilic units or hydrophobic groups, respectively.

For example, a quadpolymer consisting of NIPAM, NHSA, acrylic acid, and polylactide-grafted hydroxyethyl methacrylate was prepared and used as a protein-reactive, partly biodegradable thermoresponsive copolymer in a reaction with collagen [37]. Thiol-modified poly(NIPAM) has been obtained by the conversion of poly(NIPAM-*co*-NHSA) with cysteamine, which was subsequently used in a Michael-addition reaction with vinyl-modified poly(NIPAM-*co*-HEMA) to yield a thermosensitive hydrogel [38]. Multiresponsive polymers based on active ester polymers have also been synthesized. Starting from poly(PFPA) or poly(NHSA), various dual- or triple-responsive polymers have been synthesized by sequential conversion with amine-functionalized photochromic dyes, amino-TEMPO, and/or isopropylamine and cyclopropylamine (Scheme 2.2) [39–44]. Temperature- and pH-responsive poly(methacrylamide) microgels have been described using PNPA units to install the required functionality, such as folate, for targeting purposes [45–49].
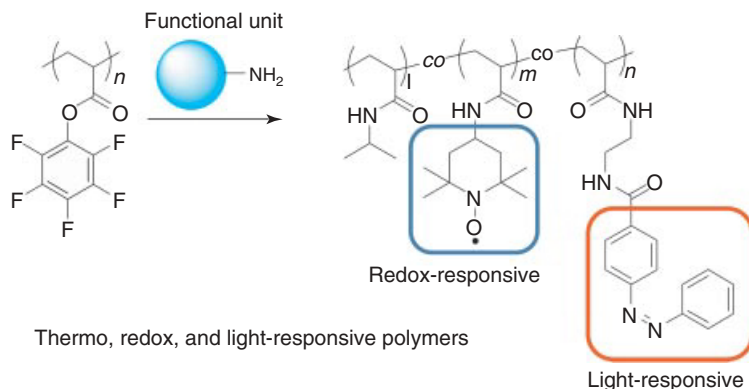
Scheme 2.2 Synthesis of multiresponsive polymers via post-polymerization functionalization of poly(PFPA).

2.2.1.3 Biologically Active Polymers

Active-ester-containing copolymers, in particular thermoresponsive copolymers, have frequently been used for conjugation with proteins or peptides [50–53]. Examples include polyvalent anthrax toxin inhibitors [54] and also polymers that promote cellular internalization [28, 29]. In particular, the possibility to easily prepare multivalent polymeric ligands for cell interactions or inhibitors provides opportunities for active ester polymers [55–61].

Thermoreversible copolymers of NIPAM with a collagenase-sensitive solubility behavior have been prepared by the post-polymerization modification of poly(NIPAM-*co*-NHSA) with a peptide containing the collagenase substrate peptide sequence Ala-Pro-Gly-Leu. The LCST increased after enzymatic degradation of the side-chain peptide.

Defined poly(*N*-(2-hydroxypropyl)-methacrylamide) (poly(HPMA)) folate conjugates have been prepared by sequential conversion of poly(PFPMA) with Oregon Green 488 cadaverine as a fluorescent label, a folate spacer conjugate, and 2-hydroxypropylamine [62]. A receptor-mediated endocytosis process was observed, which was deduced from the colocalization with lysosomal markers. Similarly, various poly(HPMA) multifunctional derivatives have been prepared by post-polymerization modification [8, 63, 64].

Polymer–DNA conjugates have also been prepared via active ester chemistries [65–69]. Poly(NIPAM) copolymerized with NHSA and propargyl acrylate was also used to prepare defined DNA–poly(NIPAM) micelles [70].

Besides peptide-functionalized polymers, active ester polymers have also been used to prepare glycosylated polymers (Scheme 2.3) by conversion of poly(PFPA) or poly(NHSA) with D-glucosamine, D-galactosamine [71–74], amino-functionalized mannose [60], chitosan [75], or even more complex aminated saccharides [58, 61].

But defined functional polymers have also been synthesized for the selective detection of proteins based on multiple loading of Ln^{3+} of the polymer chain conjugated to the protein to be detected [76].
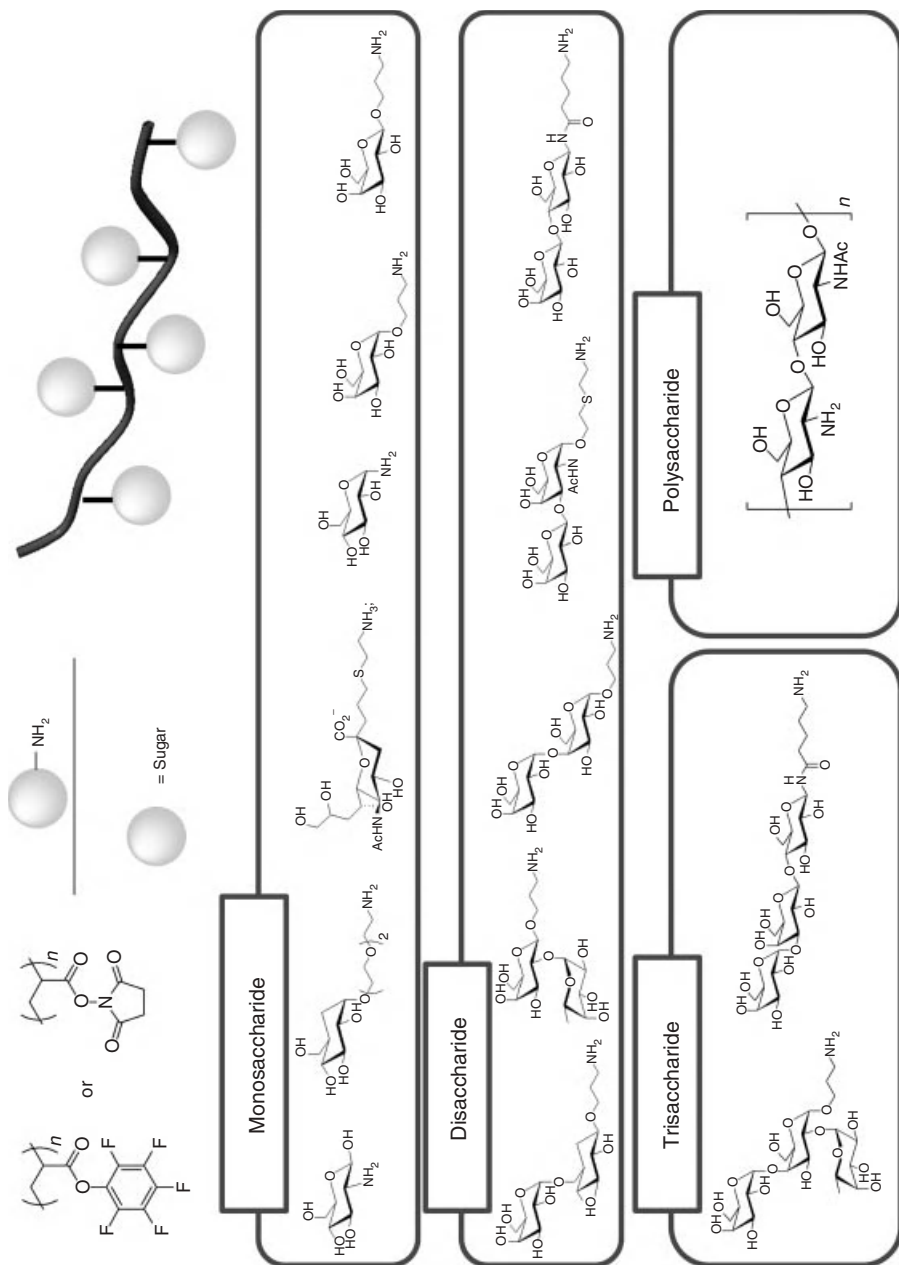
Scheme 2.3 General synthetic strategy for the synthesis of glycopolymers via post-polymerization modification of poly(PFPA) or poly(NHSA).

2.2.1.4 **Thin Films**

Post-Polymerization modification reactions have also been employed for the modification of surfaces by surface-grafting of polymers [77]. Thin films of plasma-polymerized PFPMA are frequently used for the immobilization of biomolecules, such as peptides and proteins, and such functionalized [78–81] swellable hydrogel thin films find application as, for example, a platform for cell studies [81]. Similarly, poly(NIPAM-*co*-NHSA) films have been grafted from polypropylene substrates by γ-irradiation, providing a biological platform [82]. Furthermore, poly(NHSA) can also be grown from conductive substrates by an electrografting method [83, 84]. Growing the chain from an AFM tip enabled the deposition of single poly(NHSA) chains onto amino-coated substrates [85]. In addition, the post-polymerization of the poly(NHSA) chains on the AFM tip allowed the preparation of chemically modified AFM tips by simple conversion with various amines [86].

NHS ester hydrogel-coated glass slides were prepared by the copolymerization of NHSA, acryloylmorpholine, and bis-acrylamidoprop-1-yl-PEG$_{1900}$ between two glass slides of which one glass slide was modified with 3-(trimethoxysilyl) propyl methacrylate to afford sufficient attachment between the glass slides [87]. Also, PNPA has been utilized in the formation of functional hydrogel layers [88].

Another way to deposit active-ester-containing polymers onto substrates takes advantage of a terpolymer consisting of dimethylacrylamide, 3-(trimethoxysilyl) propyl methacrylate, and NHSA [89, 90]. The trimethoxysilyl group provides an efficient route not only for the attachment on SiO$_2$ surfaces but also for the modification of AFM cantilevers, yielding molecular recognition sensors (Scheme 2.4) [91].

Stimuli-responsive nanocomposite films composed of poly(NIPAM) have been prepared by covalent layer-by-layer self-assembly of poly(NIPAM-*co*-NHSA) with amino-modified silica nanoparticles [92, 93]. Such a covalent bonding approach had also been utilized for the formation of nanostructured protein hydrogel films. A copolymer of NHSA and acryloylmorpholine was deposited simultaneously with a protein [94, 95]. The amino groups exposed at the protein surface reacted with the active ester groups, and as a result, a cross-linked hydrogel film was obtained.
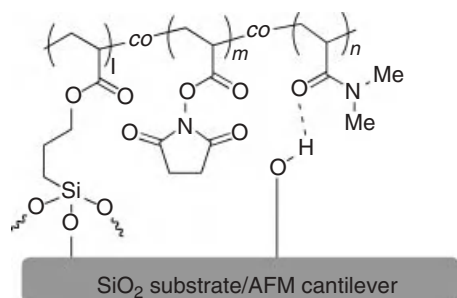
Scheme 2.4 Chemical immobilization of a copolymer featuring NHSA groups on a substrate.

Grafting-from approaches have also been employed in the fabrication of reactive surfaces based on active esters. These surfaces can be used in various applications, depending on the amine used for the functionalization. Examples are antibacterial surfaces [96] and molecular recognition probes [86].

Lahann and coworkers [97] have utilized chemical vapor deposition (CVD) copolymerization of [2.2]paracyclophanes with pentafluorophenyl ester and alkyne groups to prepare orthogonally reactive surfaces, which can be used to coimmobilize biomolecules.

Theato and coworkers presented another very versatile approach. They combined a grafting-to and post-modification step on the basis of polysilsesquioxane-based hybrid polymers. These hybrid polymers consist predominately of poly(PFPA) chains that had been grown from a polysilsesquioxane precursor polymer. The secondary condensation reactions of the polysilsesquioxane part allow the deposition on various surfaces, and the subsequent conversion with amines results in surfaces with adjustable wettability [98–100] or biological activity [101].

Surfaces containing active ester polymer brushes were utilized by Locklin and coworkers [102] in a double post-polymerization modification. First, the active ester polymer brushes were reacted with an amine-functionalized cyclopropenone, which was then successfully used in a second functionalization step via a catalyst-free cycloaddition with azides [18].

2.2.1.5 Polymeric Ligands for Nanoparticles

Decoration of magnetic nanoparticles with polymers bearing either NHSMA or PFPA units (Scheme 2.5) has been the basis for an effective bioseparation process or immobilization process of proteins [103]. Similarly, such a grafting of NHSA has been conducted by a grafting-from RAFT polymerization from mesoporous silica nanoparticles [104].
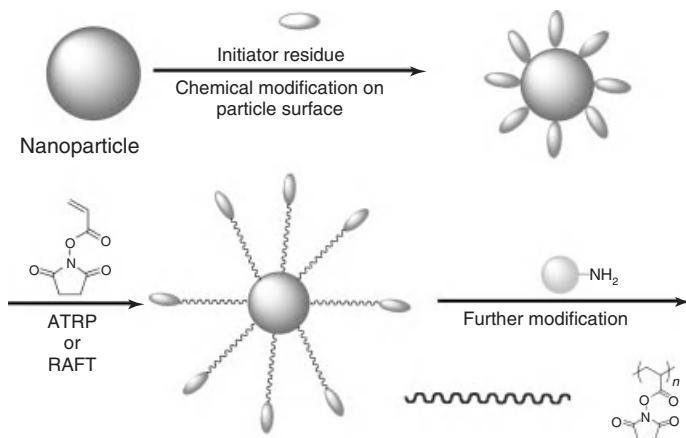
Scheme 2.5 Nanoparticles with grafted reactive polymers via a grafting-from approach. Depending on the nature of the nanoparticle, different ATRP initiators or chain-transfer agents are suitable.

In addition, active ester polymers based on poly(PFPA) have been used for the synthesis of polymeric ligands for a variety of different nanoparticles. Different binding ligands have been incorporated, depending on the type of inorganic material the nanoparticles are composed of [105–109].

Polymeric active esters have also been used as precursors for the functionalization of carbon nanotubes (CNTs), which allowed modification with DNA, for example [110]. Incorporation of pyrene side groups provided a good stabilization of CNTs. Converting the remaining active ester units into a poly(NIPAM) resulted in temperature-dependent solubilization of CNTs [111, 112].

2.2.1.6 Miscellaneous Uses of Active Ester Polymers

A series of 1*H*-benzotriazole-, 1*H*-benzimidazole-, and 1*H*-benzopyrazole-containing polymers has been synthesized by Thayumanavan and coworkers [113] by post-polymerization modification of poly(NHSMA). They compared the polymers as proton conductors and found that the imidazole-like pathway makes a significant contribution to the proton transfer only for the triazole-containing polymer. But also functional polyacetylenes have been synthesized by post-polymerization modifications of reactive precursor polymers that take advantage of active ester groups [30–32, 114].

Last but not least, active ester polymers have been employed in the synthesis of contrast agents for magnetic resonance imaging (MRI). Various approaches have been reported in the literature, which include the binding of Gd(III) chelating moiety to polymers [115, 116] or to proteins or peptides via active esters [117, 118].

2.2.2
Block Copolymers

2.2.2.1 General

Block copolymers are easily accessible by controlled radical polymerization techniques. Sequential polymerization of at least two different monomers leads directly to block copolymers. If one of these blocks consists of repeating units featuring an active ester, then a post-polymerization modification with amines can easily be conducted, leading to various functional block copolymers [3, 19, 119–122]. Noteworthy in this respect is the utilization of NHSMA in cleavable block copolymers [123].

2.2.2.2 Block Copolymers and Inorganic Moieties

Pyrene side groups with a second block have also been used to prepare "hairy" CNTs [124]. In similar approaches, block copolymers comprised of one anchor block have been studied for the modification of inorganic nanoparticles [125–129] and quantum dots [130], which find application as optoelectronic materials. Also, metal-ion-containing block copolymers utilizing pendant terpyridine units were prepared by NHSMA-containing reactive precursor polymers [131, 132].

2.2.2.3 Amphiphilic Block Copolymers

Various amphiphilic block copolymers have been synthesized that allowed versatile functionalization of the hydrophilic block by taking advantage of an active ester precursor block. In particular, biological drug delivery particles have been of interest, because targeting as well as biocompatible units could be installed in a simple post-polymerization modification step [63, 133–135].

The intrinsic formation of micelles of amphiphilic block copolymers in water has triggered the utilization of NHSA- or PFPMA-containing block copolymers [64, 136, 137]. Another example describes the modification of the reactive corona of PS-*b*-poly(PNPA) block copolymer micelles with glucosamine [138, 139]. Pan and coworkers [140] investigated the self-organization of amphiphilic block copolymers consisting of PEO and poly(PNPMA).

The synthesis of orthogonally reactive block copolymers has stimulated research activities in polymer chemistry, because it would allow the synthesis of multifunctional block copolymers from one precursor polymer. As such, active ester groups have been combined with maleimide groups [26], alkyne groups (K. Nilles and P. Theato, in preparation), α-chloroacetamide groups [29], protected acetal groups [141], and even other active ester groups [21], taking advantage of the difference in reactivity.

2.2.2.4 Stimuli-Responsive Block Copolymers

Block copolymers featuring one stimuli-responsive block can form micelles on stimulation. For example, thermoresponsive poly(NIPAM) blocks as well as various derivatives thereof have been in the focus of research as possible delivery objects on micellization in water. Examples are PNIPAM block copolymers featuring poly(acrylic acid) [142], PEO [143], or poly(*n*-butyl acrylate) [144] as a second block (Scheme 2.6).

Double thermoresponsive block copolymers have been synthesized via RAFT polymerization of PFPMA and oligo(ethylene glycol) monomethyl ether methacrylate, followed by post-polymerization modification with amines [145]. Similarly, thermo- and light-responsive block copolymers have been prepared by RAFT polymerization of PFPA and subsequent conversion with amino-functionalized azobenzene and isopropylamine [146].
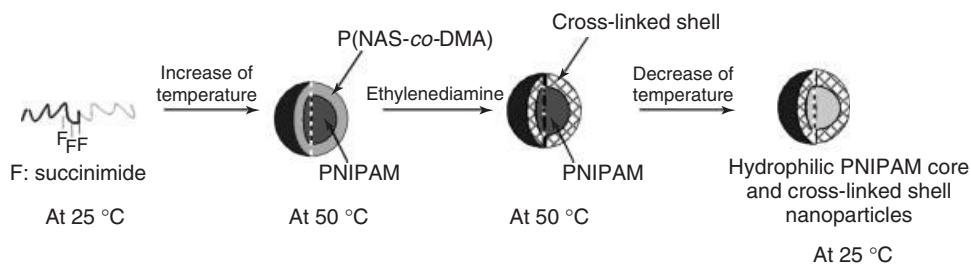
Scheme 2.6 Formation of hydrophilic core micelles with cross-linked shell.

Integration of active ester units allowed the easy introduction of targeting units, such as biotin [147]. Of course, the active ester comonomer unit can also be used to cross-link the micelles or self-assembled objects [148]. A reversible cross-linking was even achieved by conversion of the active ester groups within the self-assembled micelle core with cysteamine, which allowed reversible disulfide formation and cleavage [9, 149]. But also the formation of shell or middle layer cross-linked micelles is possible [9, 150]. This approach is particularly exciting for generating stable delivery particles, as demonstrated by the group of Wooley [136, 151].

2.3
Star Polymers

The synthesis of defined star polymers has rapidly progressed since the establishment of controlled/living polymerization techniques and modern conjugation chemistries [152, 153]. Star polymers are singular, well-defined nanoobjects and have thus found application in various areas such as drug delivery, catalysis, and photonics. In general, star polymers can be synthesized using an ''arm-first'' approach or a ''core-first'' approach. Either synthetic way can be chosen to incorporate active ester units in the polymer arms. Pan and coworkers [154] synthesized a hexa-armed star polymer (s[poly(ʟ-lactide)-*block*-poly(styrene-*co*-*N*-hydroxy succinimide acrylate)], s[PLLA-*b*-P(S-*co*-NHSA)]) with NHSA as a comonomer by a core-first approach. Subsequent cross-linking via the active ester units, followed by the hydrolysis of the PLLA block, resulted in the formation of hollow spheres.

In addition, the arm-first approach has been combined with the versatile chemistry of active esters. For example, Hawker and colleagues prepared core–shell star copolymers in an arm-first approach by starting with well-defined block copolymers composed of NHSA [104]. Functionalization with 1,4,7,10-tetraazacyclododecane-1,4,7-tris(acetic acid-*t*-butyl ester)-10-acetic acid (DOTA) allowed chelation of radioactive ^{64}Cu nuclei, which enabled positron emission tomography (PET) imaging with these star polymers. While this approach used the active ester monomer only as a comonomer, Davis and coworkers demonstrated the synthesis of star polymers via an arm-first approach based on homopolymerization of PFPA (Scheme 2.7) [137, 155]. Subsequent post-polymerization modification led to various functional star polymers, including star glycopolymers.

2.4
Active Esters at the End Groups

One of the apparent advantages of controlled radical polymerization techniques is the easy installation of functional groups at the α-chain end. Starting from an initiator or chain-transfer agent that features a particular functional group will result in polymers that exhibit this functional group at the α-chain end. Consequently, the installation of reactive groups within initiators or chain-transfer
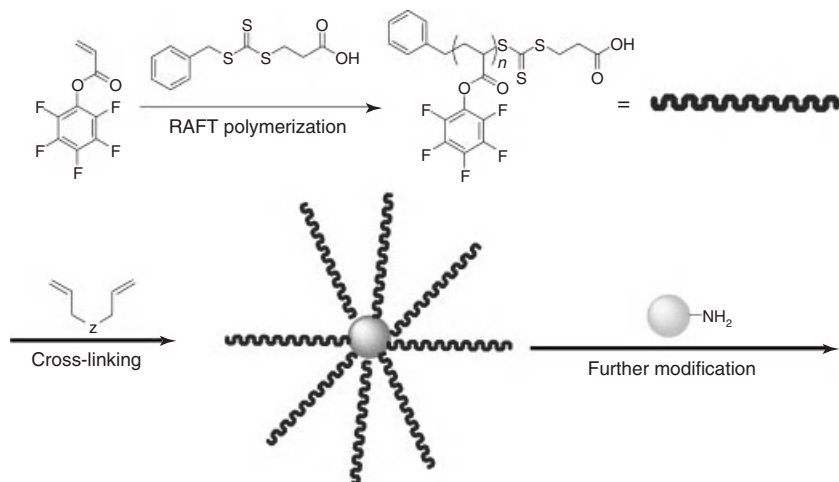
Scheme 2.7 Synthesis of reactive star polymers via an arm-first approach utilizing poly(PFPA) as the arms.

agents leads to potential post-polymerization modification possibilities at the chain end. This allows either the introduction of a particular functional group at the chain end, keeping the degree of polymerization constant, or the conjugation of polymers to proteins/peptides or other synthetic polymers resulting in novel block copolymers.

Modified derivatives of the nitroxide SG1 have been studied for NMP. For example, the NHS ester of MAMA-SG1 was investigated in the NMP of styrene, *n*-butyl acrylate, or methyl methacrylate [156]. The resulting polymers were then grafted onto amino-coated silica particles with grafting densities of 0.1–0.2 chains nm^{-2}. An increased grafting density up to 0.9 chains nm^{-2} could be achieved by a one-pot grafting approach, which consisted of the amino-coated silica, the NHS ester of MAM-SG1, and the respective monomer. The NHS ester of MAMA-SG1 could also be used in the synthesis of polystyrene-*block*-poly(D,L-lactide) or polystyrene-*block*-poly(propylene oxide) block copolymers [157]. Both post-polymerization conjugation and the complementary prepolymerization approach were studied and comparable results obtained, demonstrating the efficiency of the active ester groups.

For ATRP also, the use of initiators bearing active ester units has been explored. Predominantly, NHS 2-bromopropionate and NHS 2-bromoisobutyrate were used as reactive initiators in ATRP. Both have frequently been used for the synthesis of polymer–protein conjugates. Such conjugates have been formed using glycopolymers functionalized at the end active esters [158], biocompatible poly(2-methacryloxethyl phosphorylcholine) [159, 160], or poly(oligo(ethylene glycol) methyl ether methacrylate) [161–164]. It has also been shown that the conjugation can be realized by both grafting-to and grafting-from approaches [165].
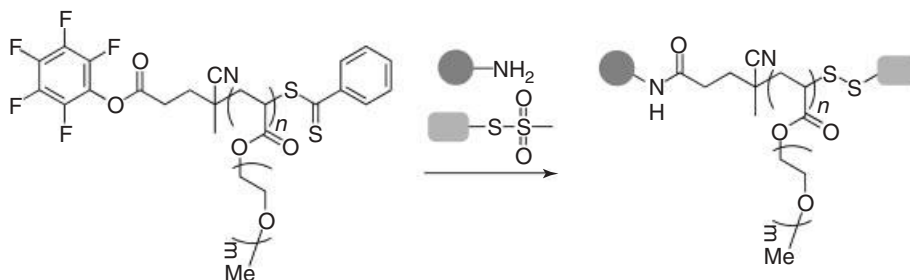
Scheme 2.8 Post-Polymerization modification of orthogonally reactive end groups by active ester/amine and thiol/methanethiosulfonate chemistry.

Last but not least, RAFT polymerizations were also carried out in the presence of chain-transfer agents featuring active ester groups. Both NHS and PFP esters have found frequent application in the synthesis of polymers and block copolymers. For example, NHS-based dithioesters were employed in the synthesis of fluorescently labeled thermoresponsive block copolymers [166] and poly(N-acryloylmorpholine) featuring a biotin or galactose derivative end group [167]. PFP ester-based dithioesters or trithiocarbonates could be used for the synthesis of new functional chain-transfer agents by simple conversion with an aliquot of the respective amine [168, 169]. Stimuli-responsive poly(diethylene glycol methacrylate) featuring a PFP ester at the α-chain end has been investigated in various contexts. The conjugation to collagenlike peptides yielded multiresponsive triblock copolymers that featured a very rich self-organization behavior [170, 171]. A systematic study of the influence of different end groups on the thermoresponsive behavior of poly(oligo(ethylene glycol) methacrylate) was conducted, and a dramatic change of the LCST in water [172] and the UCST in alcohols was observed (Scheme 2.8) [173]. Furthermore, the conjugation of dyes was successful [174, 175] and, in the case of photochromic dyes, led to thermo- and light-responsive polymers [42, 176].

2.5
Controlled Positioning of Active Ester Moieties

Controlled positioning of the active ester side groups along a polymer chain can be realized in the controlled polymerization, that is, NMP, of styrene when 1 equivalent of a maleimide is added at any given time [177]. Pentafluorophenyl 4-maleimidobenzoate is kinetically installed at different stages of the polymerization when 1 equivalent of monomer per growing polymer chain is added (Scheme 2.9) [178]. Successful installation of apolar and polar functional groups was then achieved via post-polymerization functionalization with amines. When combined with the additional positioning of a second monomer, N-propargyl maleimide, it was possible to fold the single chain by sequential conversion of the two orthogonal
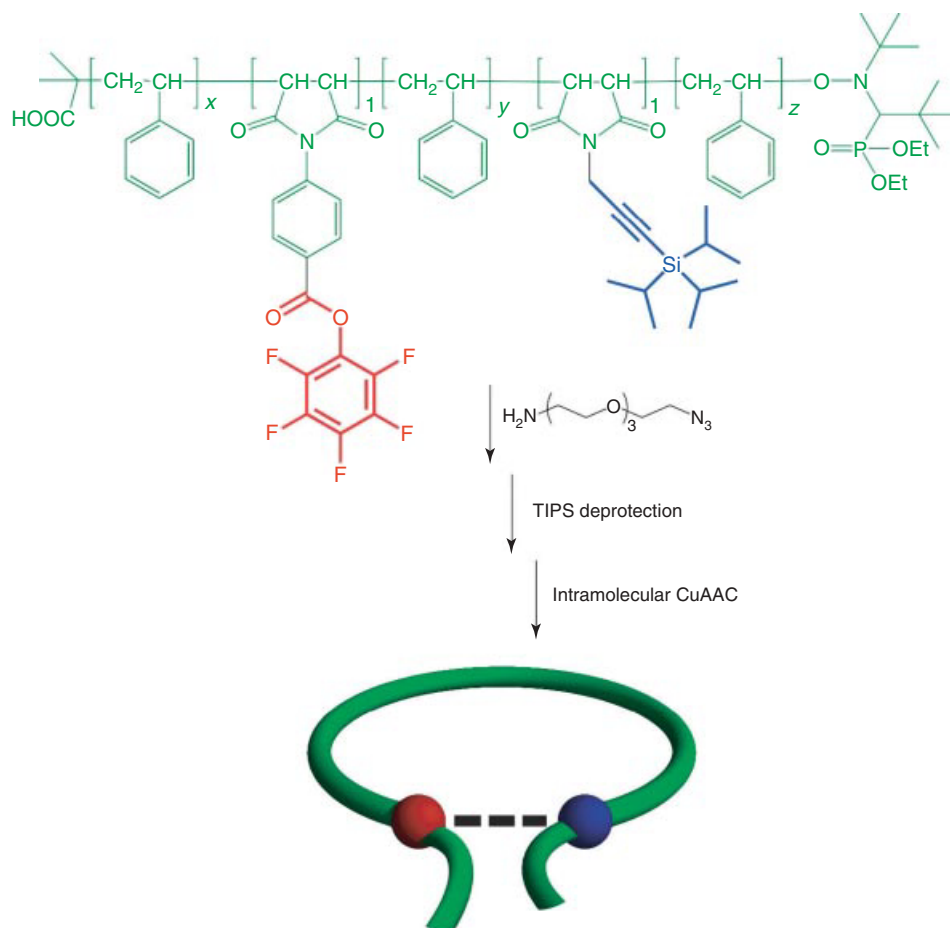
Scheme 2.9 Use of orthogonally reactive active ester and alkyne groups for the intramolecular folding of polymers using asymmetric covalent bridges.

reactive groups with 1 equivalent of 11-azido-3,6,9-trioxaundecan-1-amine [179]. As a result, the second intramolecular azide–alkyne Huisgen cycloaddition led to folded polymer chains containing asymmetric covalent bridges.

2.6
Summary

The advantage of active esters is their broad compatibility with various polymerization techniques. Polymers containing active ester groups are stable and can easily be shipped, which makes them valuable materials for international collaborations. As such, they have found application in almost every scientific area, which surely

is driven by the ubiquitous amine functionality. Furthermore, the reactions can be conducted without the need for an additional catalyst. All these advantages make them ideal candidates for advanced future applications.

Most importantly, the possibility to combine active ester groups in defined polymer architectures with complementary reactive groups has just initiated the first research projects and we are confident that this complementarity will boost future research endeavors.

References

1. Batz, H.-G., Franzmann, G., and Ringsdorf, H. (1972) *Angew. Chem. Int. Ed.*, **11**, 1103–1104.
2. Ferruti, P., Bettelli, A., and Feré, A. (1972) *Polymer*, **13**, 462–464.
3. Desai, A., Atkinson, N., Rivera, F., Devonport, W., Rees, I., Branz, S.E., and Hawker, C.J. Jr. (2000) *J. Polym. Sci., Part A: Polym. Chem.*, **38**, 1033–1044.
4. Cengiz, N., Kabadayioglu, H., and Sanyal, R. (2010) *J. Polym. Sci., Part A: Polym. Chem.*, **48**, 4737–4746.
5. Godwin, A., Hartenstein, M., Müller, A.H.E., and Brocchini, S. (2001) *Angew. Chem. Int. Ed.*, **40**, 594–597.
6. Pedone, E., Li, X., Koseva, N., Alpar, O., and Brocchini, S. (2003) *J. Mater. Chem.*, **13**, 2825–2837.
7. Hu, Z., Liu, Y., Hong, C., and Pan, C. (2005) *J. Appl. Polym. Sci.*, **98**, 189–194.
8. Yanjarappa, M.J., Gujraty, K.V., Joshi, A., Saraph, A., and Kane, R.S. (2006) *Biomacromolecules*, **7**, 1665–1670.
9. Li, Y., Lokitz, B.S., Armes, S.P., and McCormick, C.L. (2006) *Macromolecules*, **39**, 2726–2728.
10. Li, X.S., Gan, L.H., and Gan, Y.Y. (2008) *Polymer*, **49**, 1879–1884.
11. Strong, L.E. and Kiessling, L.L. (1999) *J. Am. Chem. Soc.*, **121**, 6193–6196.
12. Rejmanová, P., Labský, J., and Kopeèek, J. (1977) *Makromol. Chem.*, **178**, 2159–2168.
13. Liu, Y., Wang, L., and Pan, C. (1999) *Macromolecules*, **32**, 8301–8305.
14. Hwang, J., Li, R.C., and Maynard, H.D. (2007) *J. Controlled Release*, **122**, 279–286.
15. Metz, N. and Theato, P. (2007) *Eur. Polym. J.*, **43**, 1202–1209.
16. Godula, K. and Bertozzi, C.R. (2010) *J. Am. Chem. Soc.*, **132**, 9963–9965.
17. Aamer, K.A. and Tew, G.N. (2007) *J. Polym. Sci., Part A: Polym. Chem.*, **45**, 5618–5625.
18. Orski, S.V., Fries, K.H., Sheppard, G.R., and Locklin, J. (2010) *Langmuir*, **26**, 2136–2143.
19. Nilles, K. and Theato, P. (2009) *J. Polym. Sci., Part A: Polym. Chem.*, **47**, 1696–1705.
20. Nilles, K. and Theato, P. (2007) *Eur. Polym. J.*, **43**, 2901–2912.
21. Nilles, K. and Theato, P. (2010) *J. Polym. Sci., Part A: Polym. Chem.*, **48**, 3683–3692.
22. Kakuchi, R. and Theato, P. (2012) *Macromolecules*, **45**, 1331–1338.
23. Sanders, D.P., Fukushima, K., Coady, D.J., Nelson, A., Fujiwara, M., Yasumoto, M., and Hedrick, J.L. (2010) *J. Am. Chem. Soc.*, **132**, 14724–14726.
24. Zhou, Y., Zhuo, R.-X., and Liu, Z.-L. (2005) *Macromol. Rapid Commun.*, **26**, 1309–1314.
25. Vogel, N. and Theato, P. (2007) *Macromol. Symp.*, **249/250**, 383–391.
26. Pontrello, J.K., Allen, M.J., Underbakke, E.S., and Kiessling, L.L. (2005) *J. Am. Chem. Soc.*, **127**, 14536–14537.
27. Coughlin, E.B. and Simon, Y. (2011) *Non-Conventional Functional Block Copolymers*, vol. **1066**, American Chemical Society, pp. 53–70.
28. Kolonko, E.M. and Kiessling, L.L. (2008) *J. Am. Chem. Soc.*, **130**, 5626–5627.
29. Kolonko, E.M., Pontrello, J.K., Mangold, S.L., and Kiessling, L.L. (2009) *J. Am. Chem. Soc.*, **131**, 7327–7333.

30. Pauly, A.C. and Theato, P. (2011) *J. Polym. Sci., Part A: Polym. Chem.*, **49**, 211–224.

31. Zhang, X.A., Chen, M.R., Zhao, H., Gao, Y., Wei, Q., Zhang, S., Qin, A., Sun, J.Z., and Tang, B.Z. (2011) *Macromolecules*, **44**, 6724–6737.

32. Zhang, X.A., Qin, A., Tong, L., Zhao, H., Zhao, Q., Sun, J.Z., and Tang, B.Z. (2012) *ACS Macro Lett.*, **1**, 75–79.

33. Wong, S.Y., Sood, N., and Putnam, D. (2009) *Mol. Ther.*, **17**, 480–490.

34. Chiang, W.-H., Hsu, Y.-H., Lou, T.-W., Chern, C.-S., and Chiu, H.-C. (2009) *Macromolecules*, **42**, 3611–3619.

35. Leon, C.M., Lee, B.H., Preul, M., McLemore, R., and Vernon, B.L. (2009) *Polym. Int.*, **58**, 847–850.

36. Schild, H.G. (1992) *Prog. Polym. Sci.*, **17**, 163–249.

37. Guan, J., Hong, Y., Ma, Z., and Wagner, W.R. (2008) *Biomacromolecules*, **9**, 1283–1292.

38. Wang, Z.-C., Xu, X.-D., Chen, C.-S., Yun, L., Song, J.-C., Zhang, X.-Z., and Zhuo, R.-X. (2010) *ACS Appl. Mater. Interfaces*, **2**, 1009–1018.

39. Jochum, F.D. and Theato, P. (2009) *Polymer*, **50**, 3079–3085.

40. Jochum, F.D., Forst, F.R., and Theato, P. (2010) *Macromol. Rapid Commun.*, **31**, 1456–1461.

41. Jochum, F.D. and Theato, P. (2009) *Macromolecules*, **42**, 5941–5945.

42. Jochum, F.D., zur, B.L., Roth, P.J., and Theato, P. (2009) *Macromolecules*, **42**, 7854–7862.

43. Schattling, P., Jochum, F.D., and Theato, P. (2011) *Chem. Commun.*, **47**, 8859–8861.

44. Fu, H., Policarpio, D.M., Batteas, J.D., and Bergbreiter, D.E. (2010) *Polym. Chem.*, **1**, 631–633.

45. Perez-Alvarez, L., Saez-Martinez, V., Hernaez, E., Herrero, M., and Katime, I. (2009) *Macromol. Chem. Phys.*, **210**, 467–477.

46. Perez-Alvarez, L., Saez-Martinez, V., Hernaez, E., and Katime, I. (2009) *Macromol. Chem. Phys.*, **210**, 1120–1126.

47. Saez-Martinez, V., Perez-Alvarez, L., Merrero, M.T., Hernaez, E., and Katime, I. (2008) *Eur. Polym. J.*, **44**, 1309–1322.

48. Perez-Alvarez, L., Saez-Martinez, V., Hernaez, E., and Katime, I. (2008) *Mater. Chem. Phys.*, **112**, 516–524.

49. Martinez, V.S., Alvarez, L.P., Hernaez, E., Herrero, T., and Katime, I. (2007) *J. Polym. Sci., Part A: Polym. Chem.*, **45**, 3833–3842.

50. Wu, Z. (2008) *J. Appl. Polym. Sci.*, **110**, 777–783.

51. Chen, J.P. and Hoffman, A.S. (1990) *Biomaterials*, **11**, 631–634.

52. Chen, J.P., Yang, H.J., and Hoffman, A.S. (1990) *Biomaterials*, **11**, 625–630.

53. Uludag, H., Wong, M., and Man, J. (2000) *J. Appl. Polym. Sci.*, **75**, 583–592.

54. Gujraty, K.V., Yanjarappa, M.J., Saraph, A., Joshi, A., Mogridge, J., and Kane, R.S. (2008) *J. Polym. Sci., Part A: Polym. Chem.*, **46**, 7249–7257.

55. Puffer, E.B., Pontrello, J.K., Hollenbeck, J.J., Kink, J.A., and Kiessling, L.L. (2007) *ACS Chem. Biol.*, **2**, 252–262.

56. Gestwicki, J.E., Strong, L.E., Borchardt, S.L., Cairo, C.W., Schnoes, A.M., and Kiessling, L.L. (2001) *Bioorg. Med. Chem.*, **9**, 2387–2393.

57. Mammen, M., Dahmann, G., and Whitesides, G.M. (1995) *J. Med. Chem.*, **38**, 4179–4190.

58. Sigal, G.B., Mammen, M., Dahmann, G., and Whitesides, G.M. (1996) *J. Am. Chem. Soc.*, **118**, 3789–3800.

59. Choi, S.-K., Mammen, M., and Whitesides, G.M. (1997) *J. Am. Chem. Soc.*, **119**, 4103–4111.

60. Huang, M., Shen, Z., Zhang, Y., Zeng, X., and Wang, P.G. (2007) *Bioorg. Med. Chem. Lett.*, **17**, 5379–5383.

61. Arranz-Plaza, E., Tracy, A.S., Siriwardena, A., Pierce, J.M., and Boons, G.-J. (2002) *J. Am. Chem. Soc.*, **124**, 13035–13046.

62. Barz, M., Canal, F., Koynov, K., Zentel, R., and Vicent, M.J. (2010) *Biomacromolecules*, **11**, 2274–2282.

63. Barz, M., Luxenhofer, R., Zentel, R., and Kabanov, A.V. (2009) *Biomaterials*, **30**, 5682–5690.

64. Herth, M.M., Barz, M., Moderegger, D., Allmeroth, M., Jahn, M., Thews,

O., Zentel, R., and Rosch, F. (2009) *Biomacromolecules*, **10**, 1697–1703.

65. De, L.B., Chaix, C., Charreyre, M.-T., Laurent, A., Aigoui, A., Perrin-Rubens, A., and Pichot, C. (2005) *Bioconjugate Chem.*, **16**, 265–274.

66. Kondo, S.-i., Shichijyou, D., Sasai, Y., Yamauchi, Y., and Kuzuya, M. (2005) *Chem. Pharm. Bull.*, **53**, 863–865.

67. Minard-Basquin, C., Chaix, C., Pichot, C., and Mandrand, B. (2000) *Bioconjugate Chem.*, **11**, 795–804.

68. Erout, M.-N., Troesch, A., Pichot, C., and Cros, P. (1996) *Bioconjugate Chem.*, **7**, 568–575.

69. Minard-Basquin, C., Chaix, C., D'Agosto, F., Charreyre, M.-T., and Pichot, C. (2004) *J. Appl. Polym. Sci.*, **92**, 3784–3795.

70. Cavalieri, F., Postma, A., Lee, L., and Caruso, F. (2009) *Acs Nano*, **3**, 234–240.

71. Boyer, C. and Davis, T.P. (2009) *Chem. Commun.*, 6029–6031.

72. Baek, M.-G. and Roy, R. (2001) *Macromol. Biosci.*, **1**, 305–311.

73. Baek, M.-G. and Roy, R. (2000) *Biomacromolecules*, **1**, 768–770.

74. Wang, J.-Q., Chen, X., Zhang, W., Zacharek, S., Chen, Y., and Wang, P.G. (1999) *J. Am. Chem. Soc.*, **121**, 8174–8181.

75. Bao, H., Hu, J., Gan, L.H., and Li, L. (2009) *J. Polym. Sci., Part A: Polym. Chem.*, **47**, 6682–6692.

76. Lou, X., Zhang, G., Herrera, I., Kinach, R., Olga, O., Baranov, V., Nitz, M., and Winnik, M.A. (2007) *Angew. Chem. Int. Ed.*, **46**, 6111–6114.

77. Galvin, C.J. and Genzer, J. (2012) *Prog. Polym. Sci.*, **37**, 871–906.

78. Duque, L., Menges, B., Borros, S., and Foerch, R. (2010) *Biomacromolecules*, **11**, 2818–2823.

79. Duque, L., Queralto, N., Francesch, L., Bumbu, G.G., Borros, S., Berger, R., and Förch, R. (2010) *Plasma Processes Polym.*, **7**, 915–925.

80. O'Shaughnessy, W.S., Mari-Buye, N., Borros, S., and Gleason, K.K. (2007) *Macromol. Rapid Commun.*, **28**, 1877–1882.

81. Montero, L., Baxamusa, S.H., Borros, S., and Gleason, K.K. (2009) *Chem. Mater.*, **21**, 399–403.

82. Garcia-Uriostegui, L., Burillo, G., and Bucio, E. (2010) *Eur. Polym. J.*, **46**, 1074–1083.

83. Gabriel, S., Duwez, A.-S., Jerome, R., and Jerome, C. (2007) *Langmuir*, **23**, 159–161.

84. Cuenot, S., Gabriel, S., Jerome, R., Jerome, C., Fustin, C.-A., Jonas, A.M., and Duwez, A.-S. (2006) *Macromolecules*, **39**, 8428–8433.

85. Duwez, A.-S., Cuenot, S., Jerome, C., Gabriel, S., Jerome, R., Rapino, S., and Zerbetto, F. (2006) *Nat. Nanotechnol.*, **1**, 122–125.

86. Cecchet, F., Lussis, P., Jerome, C., Gabriel, S., Silva-Goncalves, E., Jerome, R., and Duwez, A.-S. (2008) *Small*, **4**, 1101–1104.

87. Marsden, D.M., Nicholson, R.L., Ladlow, M., and Spring, D.R. (2009) *Chem. Commun.*, 7107–7109.

88. Guerrero-Ramirez, L.G., Nuno-Donlucas, S.M., Cesteros, L.C., and Katime, I. (2008) *Mater. Chem. Phys.*, **112**, 1088–1092.

89. Cretich, M., di Carlo, G., Longhi, R., Gotti, C., Spinella, N., Coffa, S., Galati, C., Renna, L., and Chiari, M. (2009) *Anal. Chem.*, **81**, 5197–5203.

90. Yalcin, A., Damin, F., Ozkumur, E., di Carlo, G., Goldberg, B.B., Chiari, M., and Unlu, M.S. (2009) *Anal. Chem.*, **81**, 625–630.

91. Oliviero, G., Bergese, P., Canavese, G., Chiari, M., Colombi, P., Cretich, M., Damin, F., Fiorilli, S., Marasso, S.L., Ricciardi, C., Rivolo, P., and Depero, L.E. (2008) *Anal. Chim. Acta*, **630**, 161–167.

92. Fu, H., Hong, X., Wan, A., Batteas, J.D., and Bergbreiter, D.E. (2010) *ACS Appl. Mater. Interfaces*, **2**, 452–458.

93. Liao, K.-S., Fu, H., Wan, A., Batteas, J.D., and Bergbreiter, D.E. (2009) *Langmuir*, **25**, 26–28.

94. Tanaka, H., Hanasaki, M., Isojima, T., Takeuchi, H., Shiroya, T., and Kawaguchi, H. (2009) *Colloids Surf., B*, **70**, 259–265.

95. Tanaka, H., Isojima, T., Hanasaki, M., Ifuku, Y., Takeuchi, H., Kawaguchi, H.,

and Shiroya, T. (2008) *Macromol. Rapid Commun.*, **29**, 1287–1292.

96. Ignatova, M., Voccia, S., Gabriel, S., Gilbert, B., Cossement, D., Jerome, R., and Jerome, C. (2009) *Langmuir*, **25**, 891–902.

97. Deng, X., Eyster, T.W., Elkasabi, Y., and Lahann, J. (2012) *Macromol. Rapid Commun.*, **33**, 640–645.

98. Kessler, D. and Theato, P. (2009) *Langmuir*, **25**, 14200–14206.

99. Kessler, D., Nilles, K., and Theato, P. (2009) *J. Mater. Chem.*, **19**, 8184–8189.

100. Kessler, D., Jochum, F.D., Choi, J., Char, K., and Theato, P. (2011) *ACS Appl. Mater. Interfaces*, **3**, 124–128.

101. Kessler, D., Roth, P.J., and Theato, P. (2009) *Langmuir*, **25**, 10068–10076.

102. Orski, S.V., Poloukhtine, A.A., Arumugam, S., Mao, L., Popik, V.V., and Locklin, J. (2010) *J. Am. Chem. Soc.*, **132**, 11024–11026.

103. Gelbrich, T., Reinartz, M., and Schmidt, A.M. (2010) *Biomacromolecules*, **11**, 635–642.

104. Wan, X., Wang, D., and Liu, S. (2010) *Langmuir*, **26**, 15574–15579.

105. Tahir, M.N., Eberhardt, M., Theato, P., Faiss, S., Janshoff, A., Gorelik, T., Kolb, U., and Tremel, W. (2006) *Angew. Chem. Int. Ed.*, **45**, 908–912.

106. Tahir, M.N., Eberhardt, M., Therese, H.A., Kolb, U., Theato, P., Müller, W.E.G., Schroeder, H.-C., and Tremel, W. (2006) *Angew. Chem. Int. Ed.*, **45**, 4803–4809.

107. Tahir, M.N., Zink, N., Eberhardt, M., Therese, H.A., Kolb, U., Theato, P., and Tremel, W. (2006) *Angew. Chem. Int. Ed.*, **45**, 4809–4815.

108. Shukoor, M.I., Natalio, F., Metz, N., Glube, N., Tahir, M.N., Therese, H.A., Ksenofontov, V., Theato, P., Langguth, P., Boissel, J.-P., Schroeder, H.C., Müller, W.E.G., and Tremel, W. (2008) *Angew. Chem. Int. Ed.*, **47**, 4748–4752.

109. Shukoor, M.I., Natalio, F., Tahir, M.N., Wiens, M., Tarantola, M., Therese, H.A., Barz, M., Weber, S., Terekhov, M., Schroeder, H.C., Müller, W.E.G., Janshoff, A., Theato, P., Zentel, R., Schreiber, L.M., and Tremel, W. (2009) *Adv. Funct. Mater.*, **19**, 3717–3725.

110. Martinez, M.T., Tseng, Y.-C., Ormategui, N., Loinaz, I., Eritja, R., and Bokor, J. (2009) *Nano Lett.*, **9**, 530–536.

111. Etika, K.C., Jochum, F.D., Cox, M.A., Schattling, P., Theato, P., and Grunlan, J.C. (2010) *Macromol. Rapid Commun.*, **31**, 1368–1372.

112. Etika, K.C., Jochum, F.D., Cox, M.A., Schattling, P., Theato, P., and Grunlan, J.C. (2010) *Macromolecules*, **43**, 9447–9453.

113. Nagamani, C., Versek, C., Thorn, M., Tuominen, M.T., and Thayumanavan, S. (2010) *J. Polym. Sci., Part A: Polym. Chem.*, **48**, 1851–1858.

114. Pauly, A.C. and Theato, P. (2012) *Polym. Chem.*, **3**, 1769–1782.

115. Allen, M.J., Raines, R.T., and Kiessling, L.L. (2006) *J. Am. Chem. Soc.*, **128**, 6534–6535.

116. Ratzinger, G., Agrawal, P., Körner, W., Lonkai, J., Sanders, H.M.H.F., Terreno, E., Wirth, M., Strijkers, G.J., Nicolay, K., and Gabor, F. (2010) *Biomaterials*, **31**, 8716–8723.

117. Kundu, A., Peterlik, H., Krssak, M., Bytzek, A.K., Pashkunova-Martic, I., Arion, V.B., Helbich, T.H., and Keppler, B.K. (2010) *J. Inorg. Biochem.*, **105**, 250–255.

118. Yan, G.-P., Liu, M.-L., and Li, L.Y. (2005) *Bioconjugate Chem.*, **16**, 967–971.

119. Eberhardt, M. and Theato, P. (2005) *Macromol. Rapid Commun.*, **26**, 1488–1493.

120. Favier, A., D'Agosto, F., Charreyre, M.-T., and Pichot, C. (2004) *Polymer*, **45**, 7821–7830.

121. Relogio, P., Charreyre, M.-T., Farinha, J.P.S., Martinho, J.M.G., and Pichot, C. (2004) *Polymer*, **45**, 8639–8649.

122. Monge, S. and Haddleton, D.M. (2003) *Eur. Polym. J.*, **40**, 37–45.

123. Klaikherd, A., Ghosh, S., and Thayumanavan, S. (2007) *Macromolecules*, **40**, 8518–8520.

124. Meuer, S., Braun, L., and Zentel, R. (2009) *Macromol. Chem. Phys.*, **210**, 1528–1535.

125. Zorn, M., Meuer, S., Tahir, M.N., Khalavka, Y., Soennichsen, C., Tremel,

W., and Zentel, R. (2008) *J. Mater. Chem.*, **18**, 3050–3058.

126. Zorn, M., Tahir, M.N., Bergmann, B., Tremel, W., Grigoriadis, C., Floudas, G., and Zentel, R. (2010) *Macromol. Rapid Commun.*, **31**, 1101–1107.

127. Zorn, M. and Zentel, R. (2008) *Macromol. Rapid Commun.*, **29**, 922–927.

128. Zorn, M., Weber, S.A.L., Tahir, M.N., Tremel, W., Butt, H.-J., Berger, R., and Zentel, R. (2010) *Nano Lett.*, **10**, 2812–2816.

129. Meuer, S., Fischer, K., Mey, I., Janshoff, A., Schmidt, M., and Zentel, R. (2008) *Macromolecules*, **41**, 7946–7952.

130. Zorn, M., Bae, W.K., Kwak, J., Lee, H., Lee, C., Zentel, R., and Char, K. (2009) *Acs Nano*, **3**, 1063–1068.

131. Shunmugam, R. and Tew, G.N. (2005) *J. Polym. Sci., Part A: Polym. Chem.*, **43**, 5831–5843.

132. Tew, G.N., Aamer, K.A., and Shunmugam, R. (2005) *Polymer*, **46**, 8440–8447.

133. Barz, M., Tarantola, M., Fischer, K., Schmidt, M., Luxenhofer, R., Janshoff, A., Theato, P., and Zentel, R. (2008) *Biomacromolecules*, **9**, 3114–3118.

134. Scheibe, P., Barz, M., Hemmelmann, M., and Zentel, R. (2010) *Langmuir*, **26**, 5661–5669.

135. Barz, M., Wolf, F.K., Canal, F., Koynov, K., Vicent, M.J., Frey, H., and Zentel, R. (2010) *Macromol. Rapid Commun.*, **31**, 1492–1500.

136. Sun, G., Lee, N.S., Neumann, W.L., Freskos, J.N., Shieh, J.J., Dorshow, R.B., and Wooley, K.L. (2009) *Soft Matter*, **5**, 3422–3429.

137. Fukukawa, K.-i., Rossin, R., Hagooly, A., Pressly, E.D., Hunt, J.N., Messmore, B.W., Wooley, K.L., Welch, M.J., and Hawker, C.J. (2008) *Biomacromolecules*, **9**, 1329–1339.

138. Hu, Y.-C., Liu, Y., and Pan, C.-Y. (2004) *J. Polym. Sci., Part A: Polym. Chem.*, **42**, 4862–4872.

139. Hu, Y.-C. and Pan, C.-Y. (2005) *Macromol. Rapid Commun.*, **26**, 968–972.

140. Tang, X., Hu, Y., and Pan, C. (2007) *Polymer*, **48**, 6354–6365.

141. Li, R.C., Hwang, J., and Maynard, H.D. (2007) *Chem. Commun.*, 3631–3633.

142. Rathfon, J.M. and Tew, G.N. (2008) *Polymer*, **49**, 1761–1769.

143. Yoshioka, H., Mikami, M., Mori, Y., and Tsuchida, E. (1994) *J. Macromol. Sci., Pure Appl. Chem.*, **A31**, 109–112.

144. Yoshioka, H., Mikami, M., Mori, Y., and Tsuchida, E. (1994) *J. Macromol. Sci., Pure Appl. Chem.*, **A31**, 113–120.

145. Jochum, F.D., Roth, P.J., Kessler, D., and Theato, P. (2010) *Biomacromolecules*, **11**, 2432–2439.

146. Jochum, F.D. and Theato, P. (2010) *Chem. Commun.*, **46**, 6717–6719.

147. Quan, C.-Y., Wu, D.-Q., Chang, C., Zhang, G.-B., Cheng, S.-X., Zhang, X.-Z., and Zhuo, R.-X. (2009) *J. Phys. Chem. C*, **113**, 11262–11267.

148. Pascual, S. and Monteiro, M.J. (2009) *Eur. Polym. J.*, **45**, 2513–2519.

149. Zhang, J., Jiang, X., Zhang, Y., Li, Y., and Liu, S. (2007) *Macromolecules*, **40**, 9125–9132.

150. Li, Y., Lokitz, B.S., and McCormick, C.L. (2006) *Macromolecules*, **39**, 81–89.

151. Li, Y., Akiba, I., Harrisson, S., and Wooley, K.L. (2008) *Adv. Funct. Mater.*, **18**, 551–559.

152. Altintas, O., Vogt, A.P., Barner-Kowollik, C., and Tunca, U. *Polym. Chem.*, (2012) **3**, 34–45.

153. Cameron, D.J.A. and Shaver, M.P. (2011) *Chem. Soc. Rev.*, **40**, 1761–1776.

154. Yu, X., Tang, X., and Pan, C. (2005) *Polymer*, **46**, 11149–11156.

155. Boyer, C., Whittaker, M., and Davis, T.P. (2011) *J. Polym. Sci., Part A: Polym. Chem.*, **49**, 5245–5256.

156. Parvole, J., Ahrens, L., Blas, H., Vinas, J., Boissiere, C., Sanchez, C., Save, M., and Charleux, B. (2010) *J. Polym. Sci., Part A: Polym. Chem.*, **48**, 173–185.

157. Vinas, J., Chagneux, N., Gigmes, D., Trimaille, T., Favier, A., and Bertin, D. (2008) *Polymer*, **49**, 3639–3647.

158. Ladmiral, V., Monaghan, L., Mantovani, G., and Haddleton, D.M. (2005) *Polymer*, **46**, 8536–8545.

159. Samanta, D., McRae, S., Cooper, B., Hu, Y., Emrick, T., Pratt, J., and Charles, S.A. (2008) *Biomacromolecules*, **9**, 2891–2897.

160. Lewis, A., Tang, Y., Brocchini, S., Choi, J.-w., and Godwin, A. (2008) *Bioconjugate Chem.*, **19**, 2144–2155.

161. Zarafshani, Z., Obata, T., and Lutz, J.-F. (2010) *Biomacromolecules*, **11**, 2130–2135.

162. Lecolley, F., Tao, L., Mantovani, G., Durkin, I., Lautru, S., and Haddleton, D.M. (2004) *Chem. Commun.*, 2026–2027.

163. Tan, I., Zarafshani, Z., Lutz, J.-F., and Titirici, M.-M. (2009) *ACS Appl. Mater. Interfaces*, **1**, 1869–1872.

164. Nicolas, J., Khoshdel, E., and Haddleton, D.M. (2007) *Chem. Commun.*

165. Nicolas, J., Miguel, V.S., Mantovani, G., and Haddleton, D.M. (2006) *Chem. Commun.*

166. Prazeres, T.J.V., Beija, M., Charreyre, M.-T., Farinha, J.P.S., and Martinho, J.M.G. (2010) *Polymer*, **51**, 355–367.

167. Bathfield, M., D'Agosto, F., Spitz, R., Charreyre, M.-T., and Delair, T. (2006) *J. Am. Chem. Soc.*, **128**, 2546–2547.

168. Godula, K., Rabuka, D., Nam, K.T., and Bertozzi, C.R. (2009) *Angew. Chem. Int. Ed.*, **48**, 4973–4976.

169. Wiss, K.T. and Theato, P. (2010) *J. Polym. Sci., Part A: Polym. Chem.*, **48**, 4758–4767.

170. Wiss, K.T., Krishna, O.D., Roth, P.J., Kiick, K.L., and Theato, P. (2009) *Macromolecules*, **42**, 3860–3863.

171. Krishna, O.D., Wiss, K.T., Luo, T., Pochan, D.J., Theato, P., and Kiick, K.L. (2012) *Soft Matter*, **8**, 3832–3840.

172. Roth, P.J., Jochum, F.D., Forst, F.R., Zentel, R., and Theato, P. (2010) *Macromolecules*, **43**, 4638–4645.

173. Roth, P.J., Jochum, F.D., and Theato, P. (2011) *Soft Matter*, **7**, 2484–2492.

174. Roth, P.J., Kim, K.-S., Bae, S.H., Sohn, B.-H., Theato, P., and Zentel, R. (2009) *Macromol. Rapid Commun.*, **30**, 1274–1278.

175. Roth, P.J., Haase, M., Basche, T., Theato, P., and Zentel, R. (2010) *Macromolecules*, **43**, 895–902.

176. Roth, P.J., Wiss, K.T., Zentel, R., and Theato, P. (2008) *Macromolecules*, **41**, 8513–8519.

177. Lutz, J.-F. (2010) *Nat Chem*, **2**, 84–85.

178. Kakuchi, R., Zamfir, M., Lutz, J.-F., and Theato, P. (2012) *Macromol. Rapid Commun.*, **33**, 54–60.

179. Zamfir, M., Theato, P., and Lutz, J.-F. (2012) *Polym. Chem.*, **3**, 1796–1802.

3
Thiol−ene Based Functionalization of Polymers

Nikhil K. Singha and Helmut Schlaad

3.1
Introduction

Efficient polymer-analog or modification reactions are important tools in modern synthetic polymer chemistry [1, 2], even more so since the advent of polymer ''click'' chemistry [3]. Among the myriad of chemistries applied, the ''thiol−ene'' reaction is especially noteworthy, which is the addition of a thiol to an ''ene'' bond, usually a carbon−carbon double bond, through either a radical or a nucleophilic pathway (Scheme 3.1). Typically, however, thiol−ene is associated with the radical pathway, as was discovered in 1905 by Posner [4]. The first application of radical thiol addition to unsaturated polymers, namely Buna rubbers, was reported in 1948 [5]. Until recently, the use of thiol−ene chemistry has been limited to organic synthesis [6] and the modification of polydienes, mainly polybutadienes (PBs), and generation of polymer networks and films [7]. In the early 2000s, the true potential of the reaction has been recognized as a ''click'' reaction not only for the synthesis of polymers [8] and dendrimers [9] but also for the modification of biomacromolecules (peptides/proteins and polysaccharides), particles/colloids, and surfaces [11−12]. The number of publications dealing with thiol−ene chemistry has dramatically increased since 2006, more than 150 papers being published in 2010 (Web of Science, January 2011).
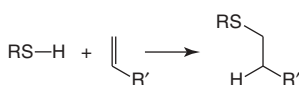
Scheme 3.1 Addition of thiol to olefin (hydrothiolation).

   In this chapter, we present a selected overview on recently published works on the thiol−ene modification of polymers, aiming to highlight the applicability and versatility of this reaction, but also referring to certain limitations.

3.2
General Considerations and Mechanisms

3.2.1
Radical Thiol–ene Addition

The radical addition of thiols to unsaturated carbon–carbon bonds proceeds via a chain process involving initiation, propagation and chain transfer, and termination steps (Scheme 3.2) [6, 7, 11–13].

Addition of the thiyl radical preferentially occurs in anti-Markovnikov orientation, and the intermediate carbon radical reacts with a chain-transfer agent (usually the thiol or solvent molecules, for example, halocarbon and aromatic hydrocarbon), thereby creating a new thiyl radical. The propagation/chain-transfer cycle can turn several hundreds to thousands times until termination by radical–radical recombination. Generally, chain transfer is the rate-limiting step, and therefore the structures of thiol and solvent have a strong impact on the reaction kinetics. Aromatic thiols are far more efficient chain-transfer agents than aliphatic thiols (see a list of compounds in Figure 3.1) because of the possible stabilization of the radical species by resonance. Also, the thiyl radical addition to carbon–carbon double bonds is reversible, and the intermediate carbon radical may eliminate a thiyl radical with the formation of an alkene under cis/trans isomerization. Stereochemistry can be maintained when the intermediate radical cannot disturb this stereochemistry, as, for instance, for unsaturated rings.

The rate of addition to alkenes strongly depends on the substituents, and it decreases in the series from strained cycles (e.g., norbornene), terminal alkenes, cis double bonds to trans double bonds (Figure 3.2, left to right). If other neighboring groups are present, in vinylic as in an allylic position, the prediction of the reactivity becomes more complicated and in some cases also mixtures of products are obtained. The presence of halogens, hetero atoms, or groups containing hetero
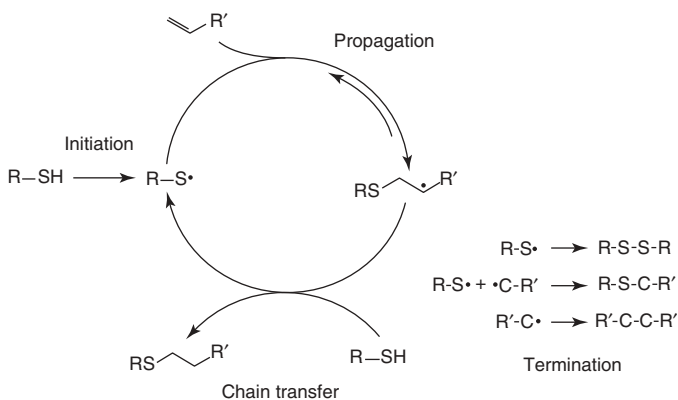
Scheme 3.2 General mechanism of radical thiol–ene addition.
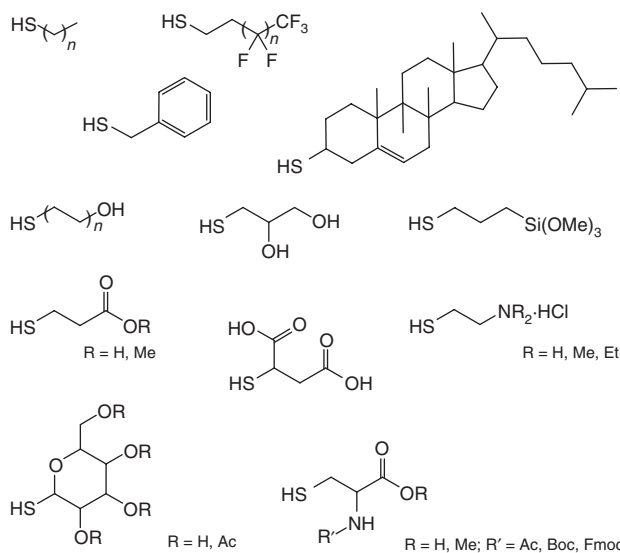
Figure 3.1 Examples of thiols used in thiol−ene chemistry.

atoms results in the formation of products with the sulfide group on the vicinal position. Thioethers or halogens in allylic position can lead to a β-elimination on thiyl radical addition to the double bond, yielding a new radical (either another thiyl or a halogen radical), and a new double bond (allyl-sulfide). The radical addition to conjugated π-systems affords delocalization of the radical, so that chain transfer of a proton can occur on multiple positions, thereby yielding a mixture of products. When strained cycles, for example, cyclopropanes or oxiranes, are present as substituents, the carbon radical formed after addition can also delocalize by a ring-opening mechanism, resulting in the formation of mixtures of isomeric structures after proton transfer.

The type of initiation has also impact on thiol−ene chemistry [14]. Radicals can be generated in a variety of ways, the most straightforward ones involving the use of thermal or photochemical initiators. Radical initiators can be divided into two different classes, namely, initiators undergoing cleavage (Type I) and initiators abstracting hydrogen (Type II). Examples of Type I initiators include azo compounds (e.g., azobisisobutyronitrile, AIBN) and peroxides (e.g., benzoyl peroxide, BPO) and also photoinitiators (e.g., 2,4,6-trimethylbenzoyl-diphenylphosphine oxide and
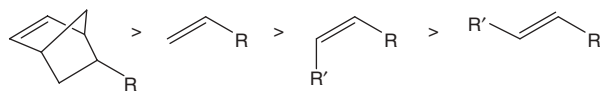
Figure 3.2 Carbon−carbon double bonds used in thiol−ene chemistry.
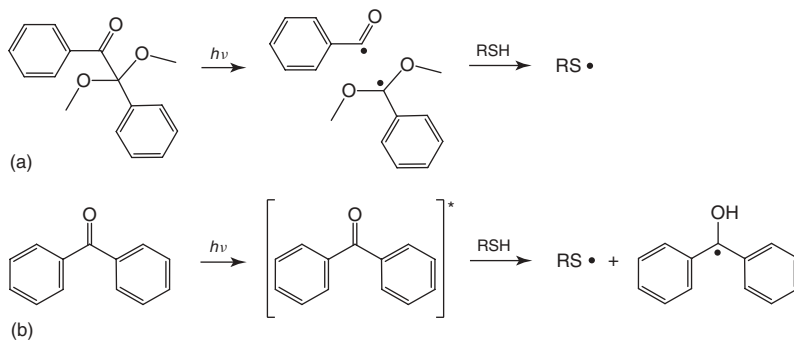
Scheme 3.3 Generation of thiyl radicals through (a) type I photoinitiator (DMPA) and (b) type II photoinitiator (benzophenone) [14].

2,2-dimethoxy-2-phenyl acetophenone, DMPA or DPAP). These compounds undergo cleavage on heating or irradiation with UV light under the formation of two radical species. Either one or both radicals can add to the unsaturated carbon–carbon bond directly or abstract hydrogen from a thiol to initiate the addition reaction (Scheme 3.3a). Type II photoinitiators, for instance, benzophenone, react in their triplet excited state with a hydrogen donor, that is, thiol, to generate the thiyl radical and initiate the addition reaction (Scheme 3.3b). Type II initiators may be less efficient than Type I initiators but produce less side products.

Thiyl radicals can also be directly generated by either applying high temperature (typically far over $100\,^\circ$C) or irradiation with UV light (typically using UV lamps with λ_{max} at 254 or 365 nm) or sunlight [7], or exposure to cobalt-60 radioactive source [6]. Direct generation of thiyl radicals is preferred for thiol–ene ''click'' chemistry, as the formation of undesired by-products from chemical initiator fragments is avoided. However, the rate of direct formation of radicals is low, hence the overall process is slow compared to the process with added initiator.

3.2.2
Nucleophilic Thiol–ene Addition

The thiol–ene reaction can also proceed via a nucleophilic route where a mild base (e.g., triethylamine) or nucleophile (e.g., dimethylphenylphosphine) acts as a catalyst. The proposed mechanisms of the reactions are shown in Scheme 3.4. The key step is the addition of a strongly nucleophilic thiolate anion to an activated carbon–carbon double bond (Michael addition). Activated substrates carry electron-withdrawing groups, for example, esters, amides, nitriles, next to the double bond (Figure 3.3).

In base-catalyzed reaction, for example with triethylamine, the base abstracts a proton from the thiol to produce thiolate anion and triethylammonium cation. The strong thiolate anion attacks the activated carbon–carbon double bond and gives a very strong enolate or carbanion (1,4-addition product). This anion abstracts a
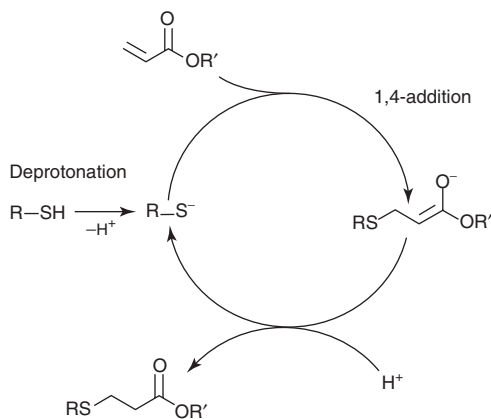
Scheme 3.4 Proposed mechanism of base/nucleophile-catalyzed thiol−ene addition.
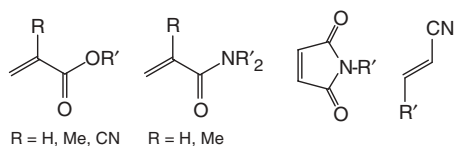
Figure 3.3 Examples of activated double bonds for nucleophilic thiol−ene addition.

proton from either thiol or triethylammonium cation to yield the regioselective anti-Markovnikov thiol−ene adduct. In this catalyzed version of thiol−ene reaction, use of a weak to mild base results in a much stronger base to catalyze the thiol−ene reaction. In the case of nucleophile-catalyzed reaction, the nucleophile attacks the activated double bond to yield a zwitterionic ester enolate species, which then deprotonates the thiol under the formation of the thiolate anion [15].

3.3
Functionalization of Polymers

Thiol−ene functionalization of polymers mainly involves the functionalization of polymer end groups (including polymer−polymer coupling reactions, Section 3.1) and pendent side chains (Section 3.2). Special cases are the functionalization of dendrimers (Section 3.2) and of biomacromolecules (Section 3.3).

3.3.1
Endfunctionalization

Thiol−ene endfunctionalization of polymers can be achieved in two ways: by re-acting a polymer bearing double bond end group(s) with thiol; or, vice versa, a
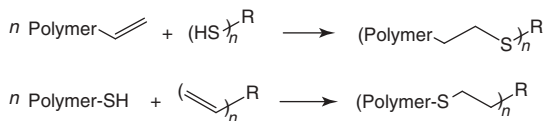
Scheme 3.5 Synthesis of end-functionalized polymers ($n = 1$, R = organic molecule), block copolymers ($n = 1$, R = polymer), and star-shaped polymers ($n \geq 2$, R = organic molecule) by thiol–ene chemistry.

polymer bearing thiol end group(s) with olefin (Scheme 3.5). Diblock copolymers are produced when the olefin or thiol reactant is also a monofunctional polymer (polymer–polymer coupling), while star-shaped polymers are obtained when polymers are reacted with multifunctional olefins/thiols (the ''grafting-onto'' method). The reaction of multifunctional polymers and thiols/olefins yields polymer networks or films (not described here) [7, 11, 12].

3.3.1.1 Polymer–ene/Thiol
Polymers with unsaturated chain ends were synthesized through controlled ionic and radical polymerization techniques using suitable initiators and/or quenching agents.

Poly(ethylene oxide) (PEO) with terminal allyl groups [16] or methyl(n)vinyl ($3 - n$)silyl groups [17] could be quantitatively modified by thermal addition of cysteamine hydrochloride (AIBN, 15 equivalents thiol, *N*,*N*-dimethylformamide (DMF), 70 °C, 24 h), or thioglycolic acid (AIBN, 3 equivalents thiol, toluene, 80 °C, 2 h), respectively. Allyl-PEO was modified with thiols (thioglycolic acid, 3-mercaptopropyl-trimethoxysilane, thio-adamantane, Fmoc-protected cysteine, and thioglycerol) applying both thermal and photochemical procedures, the latter being the more efficient one to give quantitative or near-quantitative (94%, thio-adamantane) conversion within 1 h [18].

Allyl-terminated PEO-*block*-poly(L-lactide) was functionalized with mercaptopropionic acid, thioglycerol, or *N*-Boc-cysteamine in tetrahydrofuran (THF) solution at room temperature within 1–2 h; radicals were generated by irradiation with 254 nm UV light [19].

Poly(2-isopropyl-2-oxazoline) (PIPOX) with terminal allyl group, as synthesized by the cationic ring-opening polymerization of 2-isopropyl-2-oxazoline and quenching with allylmethylamine, was quantitatively functionalized with thiocholesterol using UV light ($\lambda > 300$ nm) in THF solution at room temperature [20].

Polyisobutylene (PIB) with one or two (α,ω-)terminal methylvinylidene groups were available through cationic polymerization (quenching with 1,2,2,6,6-pentamethylpiperidine) and could be quantitatively functionalized with a series of different thiols (Scheme 3.6) [21]. The thiol reactant was used at 1.5 equivalents with respect to double bonds, and the reaction times were on the order of a few minutes.

α-Allyl-ω-bromo PS was prepared by allylbromide-initiated atom transfer radical polymerization (ATRP) of styrene and reacted with 3-mercaptopropionic acid (thermal and photoinitiation) in near quantitative yield [14]. Norbornyl-based
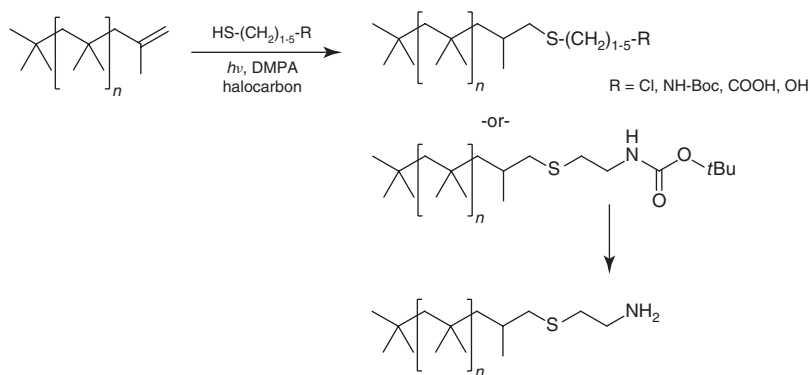
Scheme 3.6 Functionalization of exo-olefin-terminated polyisobutylene [21].
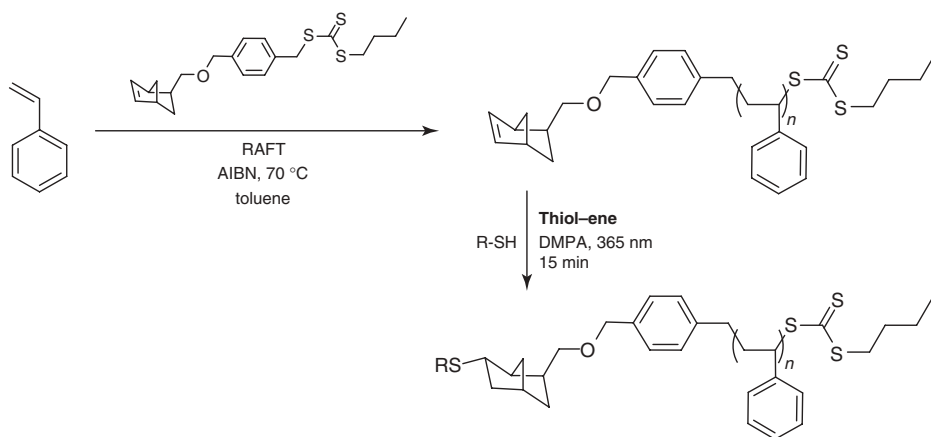
Scheme 3.7 Synthesis of functional polymer via the RAFT and thiol–ene approach [22].

reversible addition fragmentation chain-transfer (RAFT) agents were used for the controlled polymerization of acrylates, styrene, and vinyl acetate. The double bond at the α-chain end was then reacted with 1-dodecanethiol, benzyl mercaptan, or 2-mercaptopropionic acid in THF solution using DMPA/UV-365 nm as radical source (Scheme 3.7). Reaction came to completion, that is, conversion >90%, within 15 min [22].

Despite all the successful examples of polymer functionalization, there are certain limitations to radical thiol–ene reactions for polymer–polymer conjugation [23]. For instance, the thermal coupling of poly(butyl acrylate) (molecular weight about 1.9 kDa) bearing a 1,1-disubstituted vinyl chain end with trimethylpropane *tris*(2-mercaptoacetate) failed to give the three-arm star polymer. The same appeared to be true for the photochemical coupling of ω-allyl-poly(vinylacetate) (1.8 kDa) and PS-thiol (3–6 kDa), as synthesized by RAFT polymerization. Conjugation efficiency was just 25%, as evidenced by ^{1}H NMR spectroscopy and elemental analysis,

although size-exclusion chromatography (SEC) and Fourier transform infrared (FTIR) spectroscopy suggested successful coupling. The reason for the failure of thiol–ene conjugation reaction was thought to be head-to-head coupling reactions causing termination of the propagation cycle (Scheme 3.2). Such limitation does not seem to apply for the base/nucleophile-catalyzed thiol–ene reaction (see below).

ATRP/atom-transfer coupling reaction was used to synthesize α, ω-dimethyl-fulvene-protected maleimide polystyrene. Thermal retro-Diels–Alder deprotection of the maleimide end groups and subsequent Michael addition of benzyl mercaptan or *N*-acetyl-L-cysteine methyl ester yielded *bis*-conjugated PS (Scheme 3.8), as verified by ^{1}H NMR spectroscopy and elemental analysis [24].

3.3.1.2 Polymer–SH/Olefin

Polymers with protected thiol end groups could readily be obtained by (RAFT) polymerization through the use of a sulfur-containing chain-transfer agent [25–27]. For instance, a dithiophenyl end group of a RAFT-generated poly(*N*-isopropyl acrylamide) (PNIPAM) was reacted with octylamine and allyl methacrylate in the presence of dimethylphenylphosphine to effect *in situ* aminolysis of dithiophenyl to thiol and subsequent thiol–ene Michael addition (Scheme 3.9). The obtained PNIPAM-alkene was then treated with thiols (hexanethiol, 6-mercaptohexanol, and 3-mercaptopropyl-POSS) by applying UV (365 nm) light in the presence of a photoinitiator (benzil dimethyl ketal, Irgacure 651) to reach quantitative conversion within 2 h [26].

R = Benzyl or *N*-acetyl-L-cysteine methyl ester
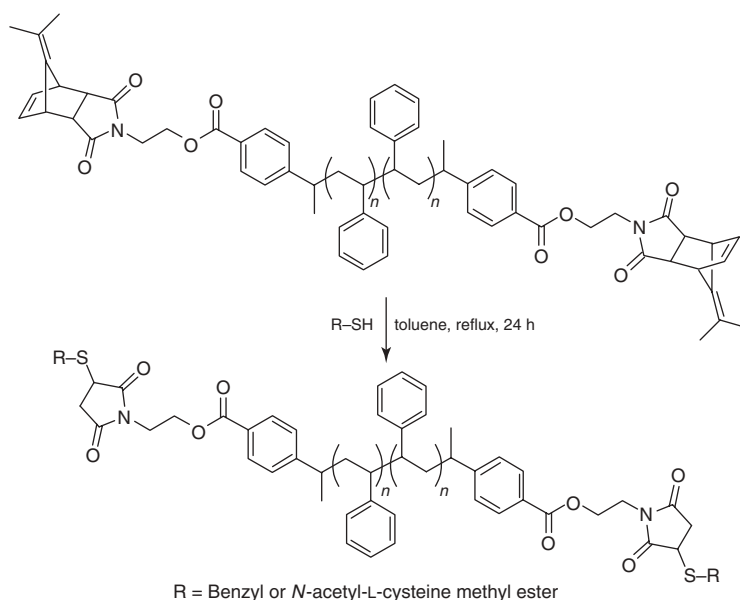
Scheme 3.8 Synthesis of telechelic polymer via ATRP and thiol–ene reaction [24].
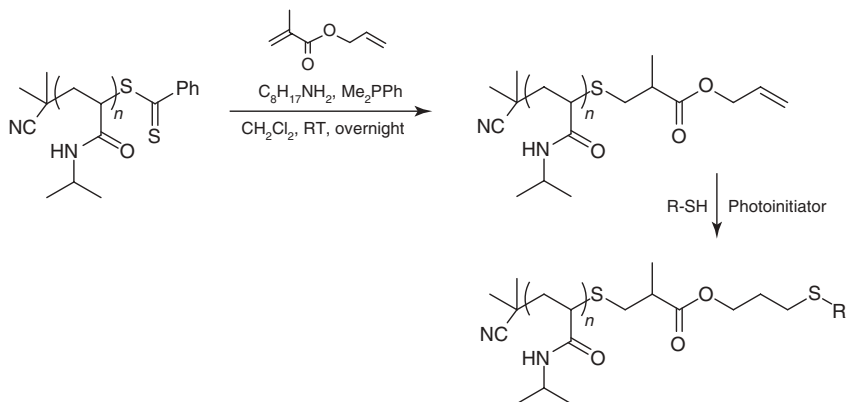
Scheme 3.9 *In situ* nucleophilic-radical thiol−ene functionalization of PNIPAM prepared by RAFT polymerization [26].
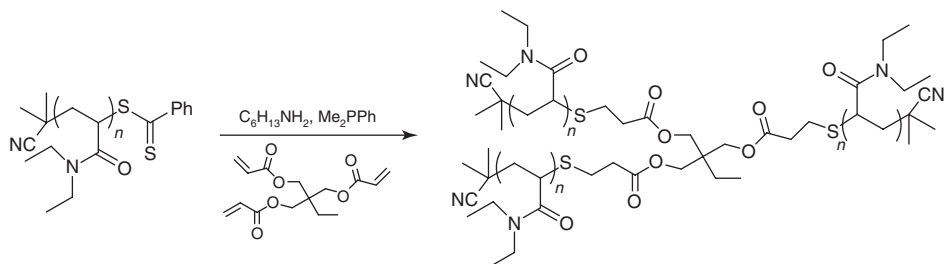
Scheme 3.10 Convergent synthesis of star polymer via nucleophilic thiol−ene addition [28].

Similarly, the trithiocarbonate end group of PNIPAM could be transformed into thiol by aminolysis (2-ethanolamine/tributylphosphine, 1,4-dioxane, RT) and reacted with excess of *bis*-maleimidodiethyleneglycol (catalyst: triethylamine) to yield a maleimido-terminated PNIPAM (see Scheme 3.21) [25]. The polymer could be quantitatively functionalized by a second thiol-Michael addition step with low-molecular-weight thiols (4-methyoxybenzyl mercaptan and 1-dodecanethiol) as well as with thiolated PS (molecular weight 2.5 kDa). Purification of the crude PNIPAM-PS block copolymer was accomplished by scavenging the unreacted PS-thiol by an iodoacetate-functionalized resin.

A similar strategy has further been applied for the convergent synthesis of three-arm star polymers [28]. Poly(*N,N*-diethylacrylamide) (PDEAm) with terminal dithiobenzoate end group, prepared by RAFT polymerization, was subjected to *in situ* aminolysis and thiol-Michael addition to trimethyoylpropanetriacrylate (Scheme 3.10). The successful synthesis of the star polymer was confirmed by ^{1}H NMR spectroscopy and by matrix-assiated laser desorption/ionization time-of-flight (MALDI-TOF) mass spectrometry.
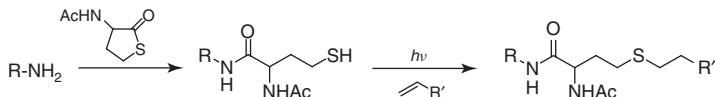
Scheme 3.11 Concept of endfunctionalization of polymers via thiolactone strategy [29].
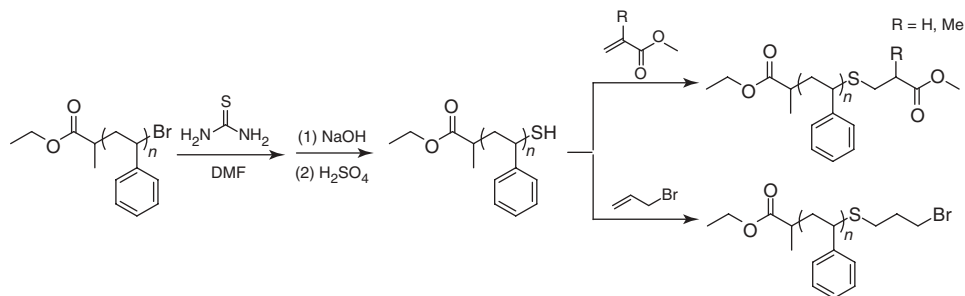
Scheme 3.12 Synthesis of thiol end-functionalized polystyrene via ATRP and subsequent reaction with double bonds [14].

The *in situ* generation of thiols could also be achieved by the reaction of primary amines with thiolactone. Nucleophilic ring opening of the thiolactone and UV-radical thiol–ene addition was performed in a one-pot fashion (Scheme 3.11) [29]. This reaction is in principle applicable for the endfunctionalization of amine-terminated polymers but has only been applied to the formation of polymer networks so far.

ATRP or cationic polymerization procedures were applied to synthesize polymers with halogenated end groups, which were then transformed into thiol by treatment with thiourea. This strategy was used to make, for instance, thiolated polystyrene by ATRP, which was then reacted with (activated) double bonds, that is, methyl (meth)acrylate and allyl bromide, to yield the corresponding thiol–ene adducts (Scheme 3.12) [14]. The radical reactions were initiated by thermal initiators (AIBN) or photoinitiators (e.g., DMPA) by applying 10-fold excess of double bonds with respect to thiol chain ends; the solvent used was dichloromethane. Reactions came to completion within 4 h; however, the products were contaminated with poly(meth)acrylate. A concurrent polymerization of (meth)acrylate should be avoided in base/nucleophile-catalyzed thiol–ene reactions.

Thiol-terminated PIB, prepared by cationic polymerization of isobutylene and subsequent treatment with thiourea, was subjected to a one-pot sequential nucleophilic thiol–ene addition of propargyl acrylate and photochemical thiol–yne addition of 6-mercaptohexanol (Scheme 3.13) [30]. Both reaction steps were confirmed, by ^{1}H NMR spectroscopic analyses, to proceed in quantitative yield.

It should be noted, however, that the presence of ''free'' thiol end groups bears the risk of radical polymer–polymer coupling via disulfide bridging. Disulfide formation does not happen in the case of *in situ* formation of thiols.
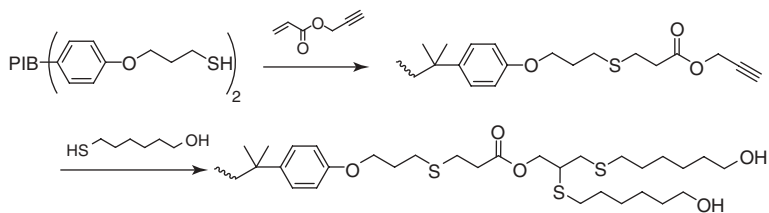
Scheme 3.13 One-pot thiol−ene/yne functionalization of thiol end-functionalized poly-isobutylene [30].

3.3.2
Polymer-Analog Reactions

Polymer-analog or modification reactions are more commonly associated with radical thiol−ene chemistry and less so with nucleophilic thiol-Michael addition. Usually, unsaturated polymers (or dendrimers) with pendent vinyl double bonds are modified with thiols through thermal or photochemical radical pathways. Polythiols, on the other hand, have rarely been used because of possible oxidation and intra-/intermolecular cross-linking reactions.

3.3.2.1 **Polyene/Thiol**

Polymers Radical thiol addition has been widely used for the modification of diene rubbers [5, 31−34], PB [35−41], polyisoprenes [42], polysiloxanes [43, 44], and polyurethanes (PUs) [45]. Recently, the modification of 1,2-PB with various thiols (Figure 3.1) has been explored for the generation of well-defined functional homopolymers and block copolymers, including polyelectrolytes and biohybrid polymers [46−56], as well as polymer particles [57]. The reaction was demonstrated to be modular and wide in scope, a prerequisite for being considered as a ''click'' reaction [58]; however, it is plagued by side reactions, especially intramolecular cyclization on the polymer backbone through the addition of the intermediate carbon radical to a neighboring double bond (Scheme 3.14) [15]. A degree of functionalization of more than 80% at full conversion of double bonds could be achieved when the photochemical thiol addition was performed at high concentration of reactants and low temperatures ($-35\,^{\circ}$C) [52]. It is further noteworthy that the photoaddition of thiol to 1,2-PB could be performed using just 2-fold excess of thiol (not 10-fold or higher excess) and the sun as light source.

However, radical thiol−ene addition can have the characteristics of a click reaction for polymer substrates other than PB, the first reported being poly[2-(3-butenyl)-2-oxazoline] homopolymers and copolymers (Scheme 3.15) [8]. The larger distance between the intermediate radical and the neighboring double bond, as compared to PB, disfavors intramolecular cyclization, thus promoting thiol addition without any side reaction. In order to avoid radiation damage to the polymer and to keep radical concentration low (to avoid radical−radical coupling), thiyl radicals were directly generated by irradiation with UV light ($\lambda > 300$ nm) in
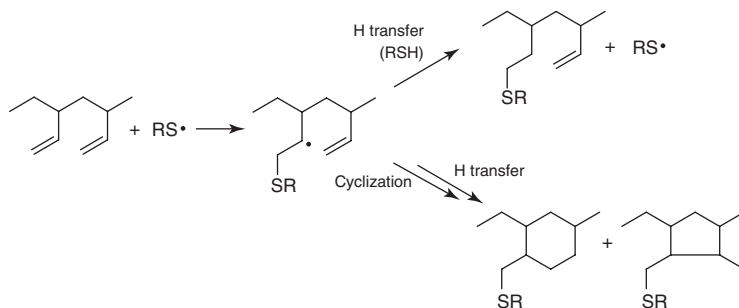
Scheme 3.14 Thiol−ene modification of 1,2-polybutadiene: regular addition step and intramolecular cyclization.
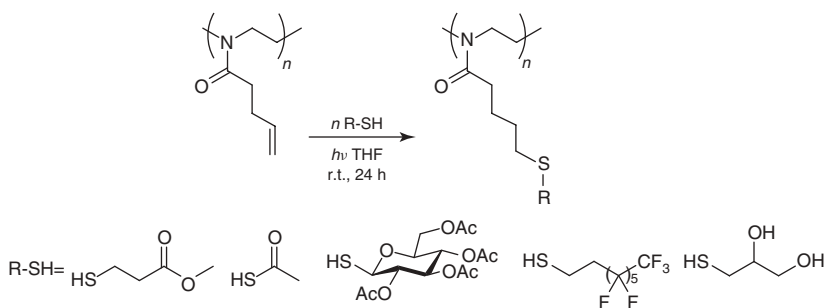
Scheme 3.15 Thiol−ene click modification of poly[2-(3-butenyl)-2-oxazoline] [8].

the absence of a photoinitiator. Reactions were performed in an organic solution, preferably in THF, at room temperature using 1.5−2-fold excess of thiol to double bond. Reaction times were typically in the order of 24 h.

Many other unsaturated (co-)polymers, as obtained by various polymerization methods, could be "click"-modified by radical thiol−ene chemistry, including copolymers based on poly[4-(3-butenyloxymethyl)-styrene] [18], poly(allylglycidyl ether) [59−62], poly(3-butenyl methacrylate) [18], poly[(6-allyl-ε-caprolactone)] [18], poly(2-alkene-2-oxazoline) [63−65], poly(DL-allylglycine) [66], poly(methyl-2-allyloxycarbonyl-propylene carbonate) [19], poly(octylallene-*co*-styrene) [67], and poly[2-methoxy-5-(2-ethylhexyloxy)-1,4-phenylene vinylene] [68] (Figure 3.4).

Thiol−ene polymer-analog reactions were performed using both thermal and photochemical initiation pathways, as described in Section 3.1. It has been reported that photochemical reactions, however, yielded higher efficiencies, required shorter reaction times, and were more tolerant to functional groups and backbones than their thermal counterparts [18].

Interestingly, the thermal addition of 2-mercaptoethanol to poly(styrene-*co*-octylallene) proceeded smoothly to quantitative yield, despite the fact that the backbone contained both terminal and internal double bonds with different reactivities [67]. This particular reaction was performed in toluene solution at 70 °C (initiator: AIBN) with a 40-fold excess of thiol with respect to double bonds. Conjugated
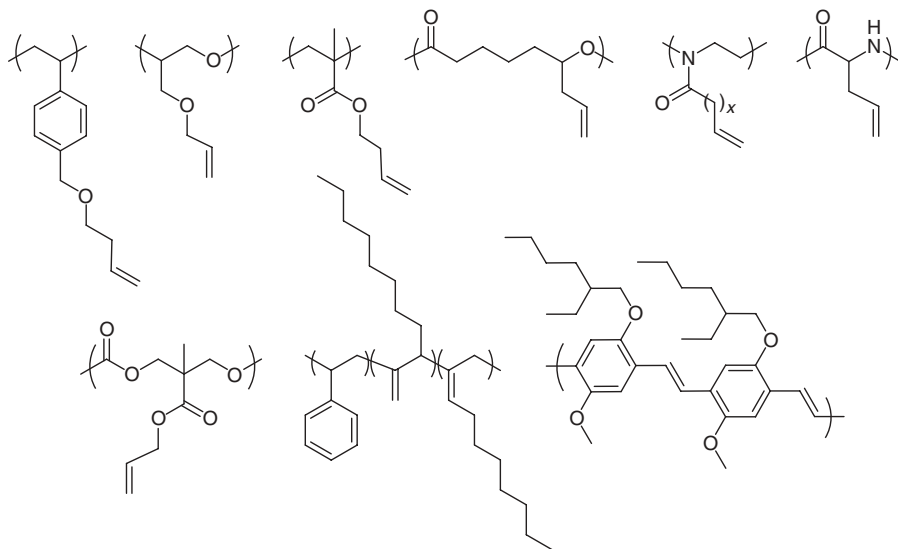
Figure 3.4 Examples of unsaturated copolymers used for radical thiol−ene click modification.

internal double bonds in poly[2-methoxy-5-(2-ethylhexyloxy)-1,4-phenylene viny-lene] were photochemically reacted with dodecanethiol in bulk ($[SH]_0/[C=C]_0 = 4$), reaching quantitative conversion within 40 s [68].

PEO-*block*-poly(DL-allylglycine) could be ''click'' modified with 1-thio-β-D-glucopyranose to yield a well-defined glycopolypeptide without the need for protecting groups [66]. The photoaddition reaction had to be performed in trifluoroacetic acid, a good solvent for both reactants, with a twofold excess of the thio-sugar. The reaction was, however, rather slow reaching full conversion within two days.

Thiol−ene ''clickable'' polymers could also be obtained by chemical modifi-cation, often (trans-)esterification, of readily available polymers. For example, poly(2-hydroxyethyl methacrylate) (PHEMA) was reacted with 4-pentenoic acid anhydride to yield poly[2-(methacryloyloxy)-ethyl pent-4-enoate]. The photochem-ical addition of functional thiols such as glucothiose [69], thioglycolic acid, and 2-mercaptosuccinic acid (Scheme 3.16) [70] was achieved with DMPA/UV light (365 nm) at room temperature within 2 h. Thiol was used in large excess (10−20 equivalents).

Poly(γ-benzyl-L-glutamate) was submitted to a partial trans-esterification reac-tion with allylalcohol to obtain a poly[γ-(benzyl/allyl)-L-glutamate] copolymer [71]. Addition of 2-mercaptoethanol to the allyl side chains ($[SH]_0/[C=C]_0/[AIBN]_0 = 40 : 1 : 2$, toluene, 80 °C, 24 h) was not quantitative, which was attributed to steric hindrance and decreased reactivity of allyl groups.

Cellulose (filter paper) was modified by tartaric acid-catalyzed reaction with either 2-(oct-7-enyl)oxirane or 9-decenoic acid to yield-ene-functionalized cellulose,
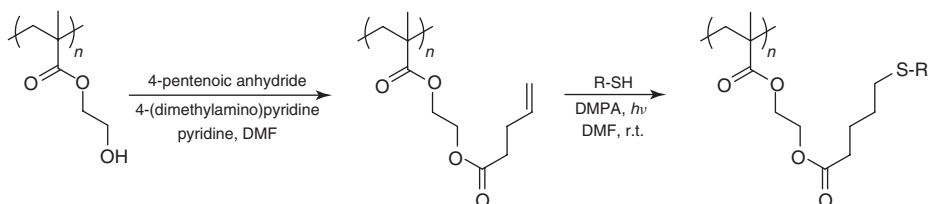
Scheme 3.16 Preparation of carboxyl terminated poly(2-hydroxyethyl methacrylate) via thiol−ene reaction [70].

to which hydrophobic thiols, for example, benzyl mercaptan, were added in a photochemical reaction. The attachment of the thiol to cellulose could be confirmed but not the quantitative conversion of double bonds [72].

10-Undecenoyl chloride was grafted onto lithiated polysulfone followed by thermal addition of 2-(2-benzimidazolyl)ethanethiol (Scheme 3.17) [73]. In order to convert all double bonds into thioether links, 10 days of reaction were required and additional amounts of AIBN were charged every 24 h.

Side-chain peptide−synthetic polymer conjugates were obtained via the tandem "ester−amide/thiol−ene" modification strategy (Scheme 3.18) [74]. Poly(pentafluorophenyl methacrylate), an activated polyester synthesized by ATRP, was reacted with allylamine to yield poly(*N*-allylmethacrylamide), onto which thiol-terminated peptide was added using AIBN as the radical source ($[C=C]_0/[SH]_0/[AIBN]_0 = 1 : 0.3 : 2$, DMF, $70\,^\circ$C, 16 h). The polymer−peptide conjugate material was characterized by ^{1}H NMR, IR spectroscopy, and SEC.
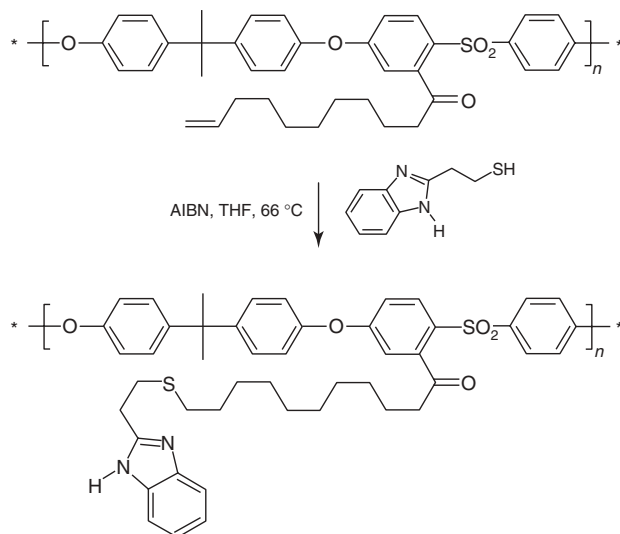
Scheme 3.17 Thermal addition of 2-(2-benzimidazolyl)ethanethiol to undecenoyl-grafted polysulfone [73].
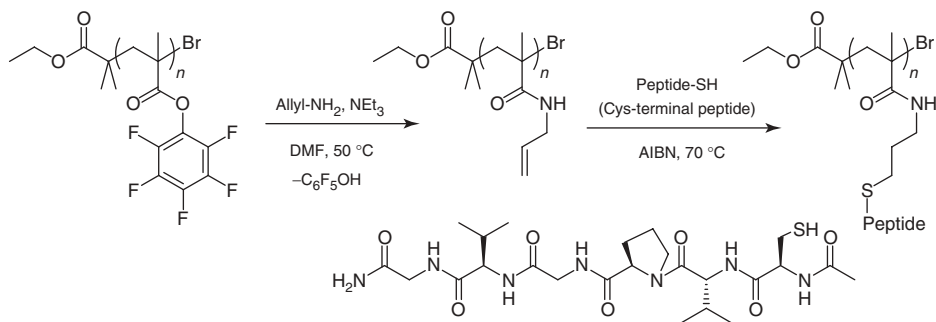
Scheme 3.18 Synthesis of biofunctionalized polymethacrylate by tandem "ester-amide/thiol–ene" strategy [74].

PUs were also functionalized by thiol–maleimide coupling reactions [75]. Linear PU bearing furan-protected maleimide in the side chains were synthesized by polyaddition of diols and diisocyanates. The furan protecting group was removed by heating to 100 °C in vacuum (retro-Diels–Alder) to afford the activated maleimide. The triethylamine-catalyzed addition of various thiols (1-mercaptododecane, benzyl mercaptan, 4-chlorobenzyl mercaptan, 1-thioglycerol, and thiosalicylic acid) was achieved in dimethylsufoxide (DMSO) or *N*-methyl-2-pyrrolidone (NMP) solution at 50 °C. Maximum conversion of more than 90% was obtained with 2 equivalents of thiol.

Dendrimers   Combinations of epoxy–amine or esterifications with thiol–ene photochemistry have been used to prepare dendrimers [9, 76, 77]. For instance, the core molecule 1,4-*bis*(aminomethyl)-benzene was first reacted with allylglycidyl ether (epoxy-amine) reaction and allyl groups were then modified with 2-mercaptoethylamine hydrochloride (thiol–ene) reaction. Repetition of the procedure yielded the final third-generation (G3) dendrimer, which could be further functionalized with monomethyl (triethylene glycol) mercaptan [76].

The synthesis of a G4 polythioether dendrimer starting from a 2,4,6-triallyloxy-1,3,5-triazine tris-alkene core has also been described [9]. 1-Thioglycerol (1.5 equiv.) was added to the core by DMPA/UV (365 nm) within 30 min (reaction performed in air). Esterification of the hydroxyl groups with 4-pentenoic anhydride yielded the G1-ene$_6$. Repetition of the procedure afforded the fourth-generation dendrimer G4-ene$_{48}$. Dendrimers were purified by simple precipitation into diethyl ether and were recovered in more than 90% yield. In addition, the double bonds on the surface of the dendrimer could be click modified with functional thiols (Scheme 3.19).

The combination of thiol–ene chemistry and esterification reactions was further applied for the generation of a dendritic library from different core molecules and monomers [77]. Importantly, these coupling chemistries eliminated the traditional need for protection/deprotection steps and afforded dendrimers in high yield and purity.
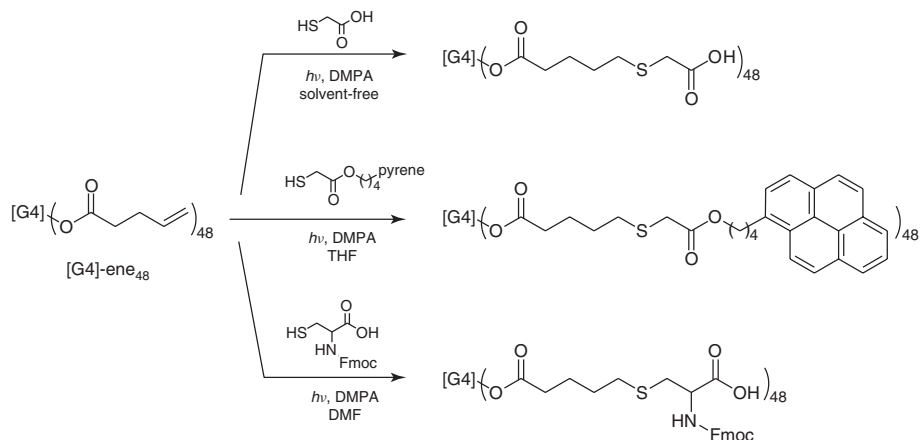
Scheme 3.19 Functionalization of fourth-generation poly(thioether) dendrimer via thiol—ene photochemistry [9].

3.3.2.2 Polythiol/Olefin

Polythiols used in thiol—ene reactions include poly(L-cysteine) copolymers, as synthesized by ring-opening polymerization of the corresponding amino acid *N*-carboxyanhydrides [78], and poly(2-mercapto-ethyl methacrylate), as synthesized via RAFT polymerization of the *S*-alkyl-*O*-ethyl xanthate-protected monomer and via subsequent aminolysis (Figure 3.5) [79].

Copolycysteines were modified by radical/nucleophilic 1 : 1 additions of PEO methyl ether acrylate or fluorescein *O*-acrylate. Reactions were carried out with AIBN as the initiator at 70 °C in DMF solution, in the presence of pyridine as a base, and came to completion within 1 h [78].

Poly(2-mercapto-ethyl methacrylate) copolymer was submitted to photochemical thiol—ene addition. 4-Allylanisole could be added to the thiol side chains ($[C=C]_0/[SH]_0 = 5$) in anisole solution at room temperature using DMPA/UV (365 nm); the reaction was complete after 1 h. The xanthate-protected precursor copolymers were also successfully modified by thiol-Michael addition (5 equivalents benzyl acrylate, butylamine/tributylphosphine, THF, RT, overnight) and by thiol—disulfide exchange reaction (50 equivalents 2,2′-dipyridyl disulfide, THF, RT, overnight) [79].

Poly[2-((3-((2-nitrobenzyl)thio)propanoyl)oxy)ethyl methacrylate], as synthesized by ATRP, could be converted into the polythiol by irradiation with UV light ($\lambda_{max} = 320$ nm) and subsequently reacted with the maleimide 1-(2-hydroxyethyl)-1*H*-pyrrole-2,5-dione at room temperature (Scheme 3.20) [80]. The photodeprotection step was rather slow, reaching almost quantitative conversion (>90%) only
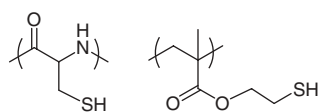
Figure 3.5 Polythiols used for radical thiol—ene modification.
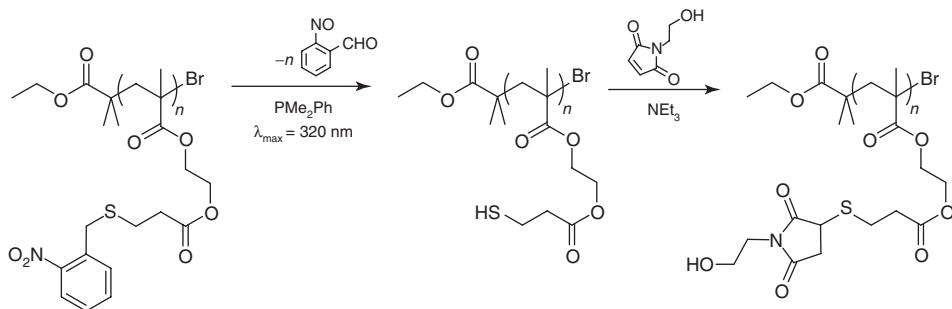
Scheme 3.20 One-pot photodeprotection of polymethacrylate bearing 2-nitro-benzyl thioether moieties and subsequent thiol–ene modification [80].

after 60 h. The thiol-Michael addition step was found to proceed to completion within just 16 h.

3.3.3
Bioconjugation

Thiol–ene reactions have been used in bioorganic synthesis, functionalization of biological materials, bioconjugation, hydrogel formation, and tissue engineering [15]. The applications of thiol–ene reaction in these fields are due to its characteristic nature of high yield, easy implementation, high selectivity, reasonable reaction time under ambient reaction conditions, and inertness toward oxygen and water. The thiol-Michael addition, especially thiol–maleimide, is more commonly applied than radical thiol–ene addition. However, photochemical thiol–ene bioconjugation reactions are recently catching up in attention and importance.

Lipase–polystyrene bioconjugates, referred to as *giant amphiphiles*, were synthesized by coupling maleimide-functionalized PS with the reduced thiol-containing protein [81]. Coupling in aqueous phosphate-buffered solution, however, yielded only ill-defined structures. A controlled coupling could be achieved when the reaction was performed at the air–water interface in a Langmuir–Blodgett trough or in THF/water 92 : 8 (w/w) mixed solvent at room temperature. For the first case, a chloroform solution of PS–maleimide was spread onto the interface, and the protein was added to the aqueous subphase. The reaction was allowed to proceed for 4 h.

Conjugation of RAFT-generated polymers to proteins was achieved by two consecutive nucleophilic thiol–ene reactions (Scheme 3.21) 82. A thiol-terminated PNIPAM was prepared by RAFT polymerization and subsequent aminolysis with hexylamine/tributylphosphine in 1,4-dioxane solution. PNIPAM-SH was then reacted with a large excess of 1,8-*bis*-maleimido-diethylenethylene glycol (1,4-dioxane, RT, 13 h) to yield a maleimide-terminated PNIPAM. This PNIPAM could then be successfully conjugated to either bovine serum albumin (BSA) or ovalbumin (OVA), as confirmed by gel electrophoresis (sodium dodecyl sulfate polyacrylamide gel
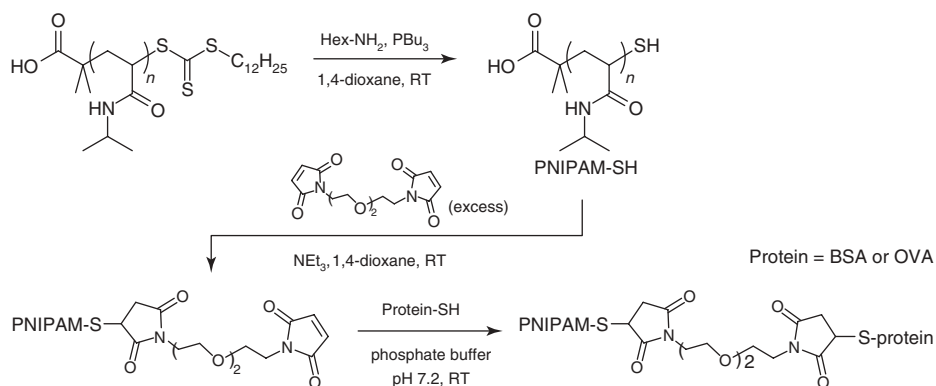
Scheme 3.21 Synthesis of PNIPAM−protein conjugates via RAFT polymerization and thiol−maleimide addition [82].
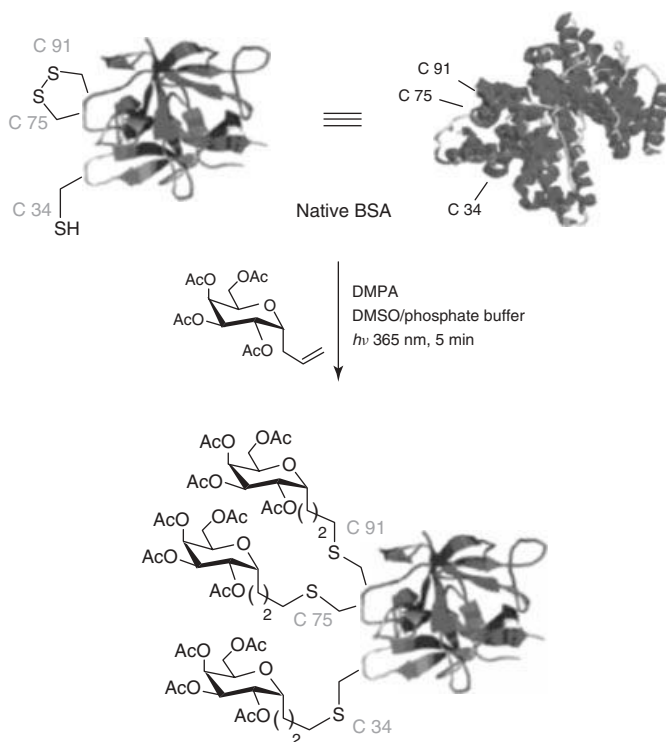
Scheme 3.22 Photochemical glycosylation of native bovine serum albumin (BSA) [83].

electrophoresis, SDS-PAGE) and SEC. However, coupling was not quantitative and samples needed to be purified by dialysis and gel filtration.

The radical thiol–ene reaction could be applied for the coupling of allyl *C*-glycosides with cysteine units [83]. Yields of 90% or higher were achieved when the reactions were performed in DMF solution with irradiation at 365 nm and DMPA as sensitizer; thiol was used in threefold excess with respect to double bonds. This procedure could also be successfully applied for the photoinduced glycosylation of native globular BSA (Scheme 3.22), as confirmed by MALDI-TOF mass spectrometry. Reaction was run in a mixture of DMSO, although the sulfoxide could act as radical scavenger and thiol oxidation agent, and phosphate buffer under argon atmosphere.

The photochemical coupling of protected cysteine derivatives to 1-alkenes was also initiated using irradiation at 254 nm or thermal starters in aqueous or alcoholic solutions; the yields of purified compounds were 31–88%. Coupling of a thiol-terminated glycopeptide antigen to allylether-modified BSA was done with UV 254 nm irradiation in an aqueous phosphate buffer solution under argon atmosphere. The antigen–BSA conjugate contained on average eight glycopeptides per BSA molecule, as indicated by MALDI-TOF mass spectrometry, corresponding to a degree of functionalization of 32% [84].

3.4
Summary

Thiol–ene chemistry has become an efficient tool for the preparation of different polymeric material with varying interest, especially for bio and engineering applications. Radical and base/nucleophile-catalyzed thiol–ene reactions are quite complementary to each other regarding their applicability for the functionalization of polymers. Radical, especially photochemical, thiol–ene chemistry is certainly more widely applicable, less stringent in experimental conditions, and more tolerant to functional groups, but appears to be limited to the coupling of polymers with low-molecular-weight thiols/olefins. The method of choice for polymer–polymer conjugation and bioconjugation is thiol–Michael addition. Photoinitiated and base/nucleophile-catalyzed thiol–ene reactions have a bright future in the preparation of high-performance materials through surface as well as bulk functionalization of polymers.

Acknowledgments

References

1. Förster, S. and Antonietti, M. (1998) *Adv. Mater.*, **10**, 195−217.
2. Gauthier, M.A., Gibson, M.I., and Klok, H.-A. (2009) *Angew. Chem. Int. Ed.*, **48**, 48−58.
3. Kolb, H.C., Finn, M.G., and Sharpless, K.B. (2001) *Angew. Chem. Int. Ed.*, **40**, 2004−2021.
4. Posner, T. (1905) *Chem. Ber.*, **38**, 646−657.
5. Serniuk, G.E., Banes, F.W., and Swaney, M.W. (1948) *J. Am. Chem. Soc.*, **70**, 1804−1808.
6. Griesbaum, K. (1970) *Angew. Chem. Int. Ed.*, **9**, 273−287.
7. Hoyle, C.E., Lee, T.Y., and Roper, T. (2004) *J. Polym. Sci., Part A: Polym. Chem.*, **42**, 5301−5338.
8. Gress, A., Völkel, A., and Schlaad, H. (2007) *Macromolecules*, **40**, 7928−7933.
9. Killops, K.L., Campos, L.M., and Hawker, C.J. (2008) *J. Am. Chem. Soc.*, **130**, 5062−5064.
10. Dondoni, A. (2008) *Angew. Chem. Int. Ed.*, **47**, 8995−8997.
11. Hoyle, C.E. and Bowman, C.N. (2010) *Angew. Chem. Int. Ed.*, **49**, 1540−1573.
12. Hoyle, C.E., Lowe, A.B., and Bowman, C.N. (2010) *Chem. Soc. Rev.*, **39**, 1355−1387.
13. Ten Brummelhuis, N. and Schlaad, H. (2012) in *Encyclopedia of Radicals in Chemistry, Biology and Materials* (eds C. Chatgilialoglu and A. Studer), John Wiley & Sons Ltd, Chichester, pp. 2017−2056.
14. Uygun, M., Tasdelen, M.A., and Yagci, Y. (2010) *Macromol. Chem. Phys.*, **211**, 103−110.
15. Lowe, A.B. (2010) *Polym. Chem.*, **1**, 17−36.
16. Cammas, S., Nagasaki, Y., and Kataoka, K. (1995) *Bioconjugate Chem.*, **6**, 226−230.
17. Vadala, M.L., Thompson, M.S., Ashworth, M.A., Lin, Y., Vadala, T.P., Ragheb, R., and Riffle, J.S. (2008) *Biomacromolecules*, **9**, 1035−1043.
18. Campos, L.M., Killops, K.L., Sakai, R., Paulusse, J.M.J., Damiron, D., Drockenmuller, E., Messmore, B.W., and Hawker, C.J. (2008) *Macromolecules*, **41**, 7063−7070.
19. Yue, J., Li, X., Mo, G., Wang, R., Huang, Y., and Jing, X. (2010) *Macromolecules*, **43**, 9645−9654.
20. Schlaad, H., Diehl, C., Gress, A., Meyer, M., Demirel, A.L., Nur, Y., and Bertin, A. (2010) *Macromol. Rapid Commun.*, **31**, 511−525.
21. Magenau, A.J.D., Chan, J.W., Hoyle, C.E., and Storey, R.F. (2010) *Polym. Chem.*, **1**, 831−833.
22. Stamenović, M.M., Espeel, P., Camp, W.V., and Du Prez, F.E. (2011) *Macromolecules*, **44**, 5619−5630.
23. Koo, S.P.S., Stamenoviæ, M.M., Prasath, R.A., Inglis, A.J., Du Prez, F.E., Barner-Kowollik, C., Van Camp, W., and Junkers, T. (2010) *J. Polym. Sci. Part A: Polym. Chem.*, **48**, 1699−1713.
24. Tolstyka, Z.P., Kopping, J.T., and Maynard, H.D. (2007) *Macromolecules*, **41**, 599−606.
25. Li, M., De, P., Gondi, S.R., and Sumerlin, B.S. (2008) *J. Polym. Sci., Part A: Polym. Chem.*, **46**, 5093−5100.
26. Yu, B., Chan, J.W., Hoyle, C.E., and Lowe, A.B. (2009) *J. Polym. Sci. Part A: Polym. Chem.*, **47**, 3544−3557.
27. Boyer, C., Granville, A., Davis, T.P., and Bulmus, V. (2009) *J. Polym. Sci. Part A: Polym. Chem.*, **47**, 3773−3794.
28. Chan, J.W., Yu, B., Hoyle, C.E., and Lowe, A.B. (2008) *Chem. Commun.*, 4959−4961.
29. Espeel, P., Goethals, F., and Du Prez, F.E. (2011) *J. Am. Chem. Soc.*, **133**, 1678−1681.
30. Magenau, A.J.D., Hartlage, T.R., and Storey, R.F. (2010) *J. Polym. Sci. Part A: Polym. Chem.*, **48**, 5505−5513.
31. Cunneen, J.I. and Shipley, F.W. (1959) *J. Polym. Sci.*, **36**, 77−90.
32. Kularatne, K.W.S. and Scott, G. (1979) *Eur. Polym. J.*, **15**, 827−832.
33. Ajiboye, O. and Scott, G. (1982) *Polym. Degrad. Stab.*, **4**, 397−413.
34. Ceausescu, E., Bittman, S., Fieroiu, V., Badea, E.G., Gruber, E., Ciupitoiu, A., and Apostol, V. (1985) *J. Macromol. Sci. Chem.*, **A22**, 525−539.

35. Boutevin, B., Hervaud, Y., and Nouiri, M. (1990) *Eur. Polym. J.*, **26**, 877–882.

36. Ameduri, B., Boutevin, B., and Nouiri, M. (1993) *J. Polym. Sci., Part A: Polym. Chem.*, **31**, 2069–2080.

37. Schapman, F., Couvercelle, J.P., and Bunel, C. (1998) *Polymer*, **39**, 4955–4962.

38. Boutevin, B., Hervaud, Y., and Mouledous, G. (1998) *Polym. Bull.*, **41**, 145–152.

39. Romani, F., Passaglia, E., Aglietto, M., and Ruggeri, G. (1999) *Macromol. Chem. Phys.*, **200**, 524–530.

40. Boutevin, G., Ameduri, B., Boutevin, B., and Joubert, J.-P. (2000) *J. Appl. Polym. Sci.*, **75**, 1655–1666.

41. Ciardelli, F., Aglietto, M., Passaglia, E., and Picchioni, F. (2000) *Polym. Adv. Technol.*, **11**, 371–376.

42. Wang, G.W., Fan, X.S., and Huang, J.L. (2010) *J. Polym. Sci. Part A: Polym. Chem.*, **48**, 3797–3806.

43. Herczynska, L., Lestel, L., Boileau, S., Chojnowski, J., and Polowinski, S. (1999) *Eur. Polym. J.*, **35**, 1115–1122.

44. Boileau, S., Mazeaud-Henri, B., and Blackborow, R. (2003) *Eur. Polym. J.*, **39**, 1395–1404.

45. Alibeik, S., Rizkalla, A.S., and Mequanint, K. (2007) *Eur. Polym. J.*, **43**, 1415–1427.

46. Justynska, J. and Schlaad, H. (2004) *Macromol. Rapid Commun.*, **25**, 1478–1481.

47. Justynska, J., Hordyjewicz, Z., and Schlaad, H. (2005) *Polymer*, **46**, 12057–12064.

48. Geng, Y., Discher, D.E., Justynska, J., and Schlaad, H. (2006) *Angew. Chem. Int. Ed.*, **45**, 7578–7581.

49. You, L. and Schlaad, H. (2006) *J. Am. Chem. Soc.*, **128**, 13336–13337.

50. Hordyjewicz-Baran, Z., You, L., Smarsly, B., Sigel, R., and Schlaad, H. (2007) *Macromolecules*, **40**, 3901–3903.

51. Justynska, J., Hordyjewicz, Z., and Schlaad, H. (2006) *Macromol. Symp.*, **210**, 41–46.

52. Ten Brummelhuis, N., Diehl, C., and Schlaad, H. (2008) *Macromolecules*, **41**, 9946–9947.

53. Schlaad, H., You, L., Sigel, R., Smarsly, B., Heydenreich, M., Mantion, A.,

and Mašić, A. (2009) *Chem. Commun.*, 1478–1480.

54. David, R.L.A. and Kornfield, J.A. (2008) *Macromolecules*, **41**, 1151–1161.

55. Lotti, L., Coiai, S., Ciardelli, F., Galimberti, M., and Passaglia, E. (2009) *Macromol. Chem. Phys.*, **210**, 1471–1483.

56. Yang, H., Jia, L., Zhu, C., Di-Cicco, A., Levy, D., Albouy, P.-A., Li, M.-H., and Keller, P. (2010) *Macromolecules*, **43**, 10442–10451.

57. Korthals, B., Morant-Minñana, M.C., Schmid, M., and Mecking, S. (2010) *Macromolecules*, **43**, 8071–8078.

58. Barner-Kowollik, C., Du Prez, F.E., Espeel, P., Hawker, C.J., Junkers, T., Schlaad, H., and Van Camp, W. (2011) *Angew. Chem. Int. Ed.*, **50**, 60–62.

59. Persson, J.C. and Jannasch, P. (2006) *Chem. Mater.*, **18**, 3096–3102.

60. Hruby, M., Konak, C., and Ulbrich, K. (2005) *J. Appl. Polym. Sci.*, **95**, 201–211.

61. Lee, B.F., Kade, M.J., Chute, J.A., Gupta, N., Campos, L.M., Fredrickson, G.H., Kramer, E.J., Lynd, N.A., and Hawker, C.J. (2011) *J. Polym. Sci. Part A: Polym. Chem.*, **49**, 4498–4504.

62. Obermeier, B. and Frey, H. (2011) *Bioconjugate Chem.*, **22**, 436–444.

63. Diehl, C. and Schlaad, H. (2009) *Macromol. Biosci.*, **9**, 157–161.

64. Diehl, C. and Schlaad, H. (2009) *Chem. Eur. J.*, **15**, 11469–11472.

65. Kempe, K., Hoogenboom, R., and Schubert, U.S. (2011) *Macromol. Rapid Commun.*, **32**, 1484–1489.

66. Sun, J. and Schlaad, H. (2010) *Macromolecules*, **43**, 4445–4448.

67. Ni, X., Zhu, W., and Shen, Z. (2010) *Polymer*, **51**, 2548–2555.

68. Pogantsch, A., Rentenberger, S., Langer, G., Keplinger, J., Kern, W., and Zojer, E. (2005) *Adv. Funct. Mater.*, **15**, 403–409.

69. Chen, G., Amajjahe, S., and Stenzel, M.H. (2009) *Chem. Commun.*, 1198–1200.

70. Huynh, V.T., Chen, G., Souza, Pd., and Stenzel, M.H. (2011) *Biomacromolecules*, **12**, 1738–1751.

71. Guo, J., Huang, Y., Jing, X., and Chen, X. (2009) *Polymer*, **50**, 2847–2855.

72. Zhao, G.-L., Hafrén, J., Deiana, L., and Córdova, A. (2010) *Macromol. Rapid Commun.*, **31**, 740–744.

73. Persson, J.C., Josefsson, K., and Jannasch, P. (2006) *Polymer*, **47**, 991–998.

74. Singha, N.K., Gibson, M.I., Koiry, B.P., Danial, M., and Klok, H.-A. (2011) *Biomacromolecules*, **12**, 2908–2913.

75. Billiet, L., Gok, O., Dove, A.P., Sanyal, A., Nguyen, L.-T.T., and Du Prez, F.E. (2011) *Macromolecules*, **44**, 7874–7878.

76. Kang, T., Amir, R.J., Khan, A., Ohshimizu, K., Hunt, J.N., Sivanandan, K., Montanez, M.I., Malkoch, M., Ueda, M., and Hawker, C.J. (2010) *Chem. Commun.*, **46**, 1556–1558.

77. Montañez, M.I., Campos, L.M., Antoni, P., Hed, Y., Walter, M.V., Krull, B.T., Khan, A., Hult, A., Hawker, C.J., and Malkoch, M. (2010) *Macromolecules*, **43**, 6004–6013.

78. Habraken, G.J.M., Koning, C.E., Heuts, J.P.A., and Heise, A. (2009) *Chem. Commun.*, 3612–3614.

79. Nicolaÿ, R. (2012) *Macromolecules*, **45**, 821–827.

80. Pauloehrl, T., Delaittre, G., Bastmeyer, M., and Barner-Kowollik, C. (2012) *Polym. Chem.*, **3**, 1740–1749.

81. Velonia, K., Rowan, A.E., and Nolte, R.J.M. (2002) *J. Am. Chem. Soc.*, **124**, 4224–4225.

82. Li, M., De, P., Li, H., and Sumerlin, B.S. (2010) *Polym. Chem.*, **1**, 854–859.

83. Dondoni, A., Massi, A., Nanni, P., and Roda, A. (2009) *Chem. Eur. J.*, **15**, 11444–11449.

84. Wittrock, S., Becker, T., and Kunz, H. (2007) *Angew. Chem. Int. Ed.*, **46**, 5226–5230.

4
Thiol−yne Chemistry in Polymer and Materials Science

Andrew B. Lowe and Justin W. Chan

4.1
Introduction

The gradual movement away from high-volume, low-functional polymers and materials to lower volume and highly functional species has, in many instances, necessitated the development of new synthetic procedures for both efficient materials synthesis and modification. This movement has been aided by the discovery and development of new polymerization procedures, perhaps most notably the development of a suite of reversible deactivation radical polymerization processes including atom-transfer radical polymerization (ATRP) [1], reversible addition-fragmentation chain transfer (RAFT) [2−7], radical polymerization, stable free radical polymerization (SFRP) [8], and tellurium-mediated radical polymerization (TERP) [9] as well as the (re)emergence of a range of ''click'' chemistries [10−19]. These polymerization processes, many of which are now well established and practiced routinely, have revolutionized advanced polymer and materials synthesis, facilitating the preparation of new macromolecular species that were in many instances previously inaccessible.

In recent years, a number of thiol-based chemistries have attracted significant attention from the polymer science community as efficient tools for polymer and materials synthesis and in post-polymerization modification. Examples of these chemistries include the thiol−ene (including the thiol−Michael variant), thiol−halo, thiol−isocyanate, and thiol−yne reactions (Scheme 4.1) [11−15, 20−27].

The best developed of these reactions is, without doubt, the thiol−ene reaction with the radical-mediated version having received the most attention with literature reports dating back to the early 1900s [28]. The thiol−ene reaction is, simply, the hydrothiolation of a C=C bond and can proceed under a broad range of conditions with an impressive range of both ene and thiol substrates. Several excellent reviews have been written on the topic recently, and readers are directed to these papers for further information [11, 14, 15]. Since the topic of this chapter is the thiol−yne reaction, at this point we simply note that the radical version is very much a sister reaction to the radical thiol−ene reaction while it also bears some distinctive features that are highlighted below. The reaction between a thiol and an isocyanate
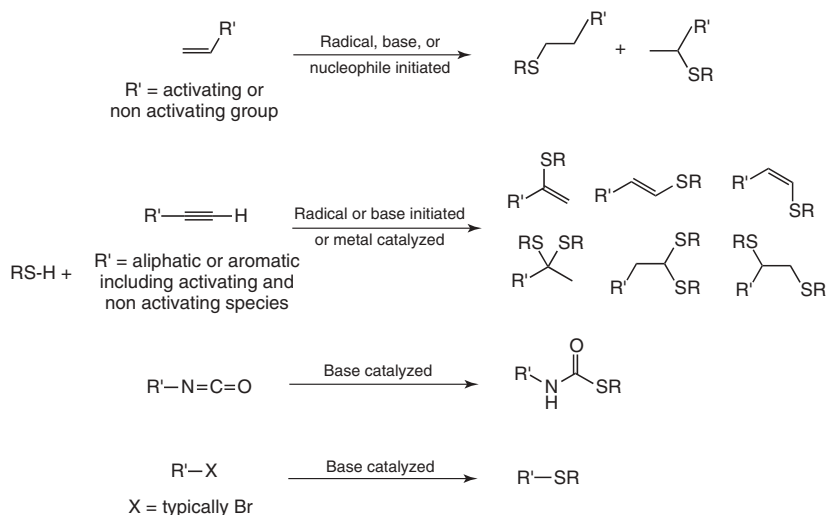
Scheme 4.1 Examples of efficient thiol-based coupling chemistries.

is an extremely rapid process that proceeds to give quantitative formation of the thiocarbamate and is not plagued by the same side reactions associated with alcohol−isocyanate reactions. Little can be found in the current mainstream polymer literature in which this extremely facile reaction is used, although there are descriptions of its use for end-group and side chain modification. The final example, shown in Scheme 4.1, is simply the nucleophilic substitution of an alkyl halide, typically a bromide, by a thiol. As with all these reactions, this is well-established chemistry with recent examples in the polymer literature describing dendrimer, multiblock, and hyperbranched polymer syntheses.

4.2
The Thiol−yne Reaction in Small-Molecule Chemistry

The thiol−yne reaction is, simply, the hydrothiolation of a carbon−carbon triple bond. From a practical standpoint, the reaction has many similarities to the more well-established thiol−ene reaction and can be performed on both activated and nonactivated substrates under a range of catalytic and noncatalytic conditions. However, a distinguishing feature of the thiol−yne reaction is the possible modes of addition that can be achieved. The primary product in such reactions is dictated by the nature of the substrates and the experimental conditions under which the hydrothiolations are accomplished.

For example, Scheme 4.2 shows the six general possible products for the addition of a thiol to a C≡C bond. There are three possible monohydrothiolation products of a terminal acetylenic bond – the Markovnikov product (**A**) – and

Possible monoaddition products
including E/Z stereoisomers for internal
alkynyl substrates

Possible double-addition products
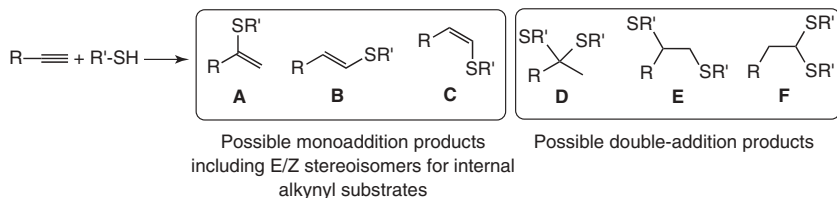
Scheme 4.2 Possible modes of addition in the hydrothiolation of carbon–carbon triple bonds.
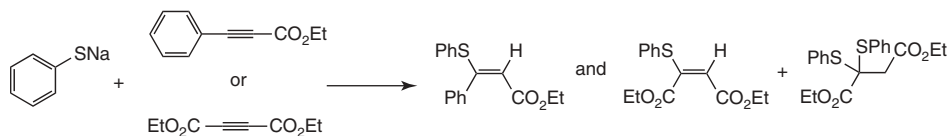
Scheme 4.3 Reported products from the reaction of sodium thiophenolate with ethyl phenylpropiolate and ethyl acetylene dicarboxylate.

two anti-Markovnikov species (**B** and **C**), namely, the cis and trans isomers of the resulting vinyl sulfide. In the case of internal alkynes, this translates to possible (*E*) and (*Z*) stereoisomers. For the addition of 2 equivalents of thiol, the addition reaction can occur to give the α-disubstituted dithioacetal (**D**), the β-disubstituted dithioacetal (**F**), or the α,β-disubstituted dithioether (**E**). Below, we describe examples of the experimental conditions that have been examined for effecting C≡C hydrothiolation and note, where applicable, the regio- and stereoselective nature of these processes.

Some of the earliest literature reports concerning small-molecule thiol–yne reactions relate to the hydrothiolation of activated alkyne bonds and date from the turn of the twentieth century [29, 30]. In 1900, Rhuemann and coworkers described the reactions between sodium thiophenolate and two activated alkynes, namely, ethyl phenylpropiolate and ethyl acetylenedicarboxylate – both examples of internal alkyne substrates (Scheme 4.3).

In the case of ethyl phenylpropiolate, Ruhemann reported the formation of the monoaddition product, with C–S bond formation occurring at the more electrophilic carbon atom as expected for such conjugate additions, whereas in the case of ethyl acetylenedicarboxylate, both the monoaddition and double-addition products were reported with, in the case of the latter, addition occurring at the same carbon atom yielding the dithioacetal derivative. Kohler and Potter noted the preparation of *cis*- and *trans*-benzal methyltolyl sulfide (the β-mono adducts) via the reaction of phenylacetylene with thiocreosol as part of their studies on the reactions of α,β-unsaturated sulfones [31]. The addition of toluene-ω-thiol to propiolic acid was later examined by Owen and Sultanbawa under several different catalytic conditions [32]. The authors reported the formation of β-mono adducts although they could not dismiss the possible formation of a diadduct. In the same paper, the authors noted that the addition of thiolacetic acid to propiolic acid yielded only the cis and trans β-(acetylthiol)acrylic acids, whereas with methylpropiolate the cis and trans isomers

were formed along with the double-addition product α,β-bisacetylthiopropionate. The reaction of 2 equivalents of thiolacetic acid with acetylene dicarboxylic acid (or the bis methyl ester) yielded in both instances the α,α′-double addition products (**D**-like species). All of these later Michael-type addition reactions were performed in the absence of any added catalyst.

In 1949, Bader *et al.* [33] described the reaction of thiolacetic acid with a series of acetylenes including 1-hexyne, phenylacetylene, *p*-methoxyphenylacetylene, 1,7-octadiyne, and methyl propargyl ether in the presence of peroxides and/or UV irradiation. For example, in the case of 1-hexyne, both mono (β-substituted) and di-(α,β-substituted) adducts were obtained in reasonable yields. The mono adduct was shown to be readily converted to the di adduct by further heating with additional thiolacetic acid. Reactions performed under UV irradiation or in the presence of peroxides were found to increases the reaction yields. The effect of peroxide catalysis was most pronounced in the reactions with phenylacetylene and *p*-methoxyphenylacetylene, where significant improvements in the yield were observed; however, in both instances only β-substituted mono adducts were obtained.

Sauer detailed the radical-initiated reactions of acetylene with butanethiol, benzylmercaptan, and thiophenol, reporting the formation of the α,β-double addition products. It was also shown that when the acetylene–thiol reaction was performed in the presence of CO it was possible to form thiopropenals although the preferred reaction product was still the bis-thioether [34]. Blomquist and Wolinsky [35] described a study on the addition of ethylmercaptan to a range of acetylenic species including propargyl alcohol, propargyl acetate, 2-butyn-1,4-diol, 1-hexyne, 2-methyl-3-butyn-2-ol, propiolic acid, dimethyl acetylenedicarboxylate, and phenylacetylene. All reactions were performed under UV irradiation for 14–28 days in a molar ratio of 1 : 2, yne:thiol. Vicinial (α,β) bis-ethylmercapto derivatives were obtained wholly or as the major product in all but two cases. Only the mono adduct was obtained in the reaction with methyl acetylenedicarboxylate, whereas the β,β-dithioacetal derivative, C_6H_5-CH_2-$CH(SEt)_2$, was obtained in the reaction with phenylacetylene.

Nucleophilic-type additions of thiols to acetylenes have been reported by Cristol *et al.* [36] and by Truce and Simms [37]. The base-catalyzed reaction of *p*-toluenethiol to phenylacetylene, 2-butyne, and 1-hexyne yielded, in all instances, monoaddition species in a stereospecific manner with *cis*-ω-styryl *p*-tolylsulfide being the only product obtained from phenylacetylene and (*Z*)-but-2-en-2-yl(*p*-tolyl)sulfane the sole isolated product from 2-butyne, for example [37].

Clearly, the majority of these reports dating to the first half of the twentieth century were focused on determining the general scope and features of the reactions between thiols and alkynes under both radical-mediated and non-radical-mediated conditions. Evidently, the nature of the substrates and the mediating conditions play an important role in determining the nature of the products and their distribution. Since these early reports, chemists have continued to examine the hydrothiolation of alkynes but have focused, understandably, on developing new catalytic systems

promoting regio- and or stereospecific addition and also applying the chemistry in the general synthesis of more complex molecules.

Ichinose described the BEt_3-induced radical hydrothiolation of a series of terminal alkynes, demonstrating efficient regioselective formation of the mono adducts with addition occurring at the terminal carbon atom but yielding a mixture of (*E*) and (*Z*) stereoisomers [38]. The first example of a transition-metal-catalyzed hydrothiolation of an alkyne was reported by Kuniyasu *et al.* [39]. A range of catalysts were evaluated, including $Pd(OAc)_2$, $Pd(PPh_3)_4$, $Pt(PPh_3)_4$, $Ni(PPh_3)_2Cl_2$, and $RhCl(PPh_3)_3$, for the reaction of thiophenol with 1-octyne. In general, $Pd(OAc)_2$ yielded Markovnikov addition products; other Pd, Pt, and Ni complexes yielded the internal vinyl sulfides via an isomerization process; and Rh gave, predominantly, the anti-Markovnikov product.

Since this seminal report, a number of groups have more closely evaluated many of these catalytic systems as well, actively developing new homo- and heterogeneous catalysts. Bäckvall and Ericsson [40] detailed the regioselective $Pd(OAc)_2$-catalyzed monoaddition between thiophenol and conjugated enynes as a route to both 2-(phenylsulfinyl)- and 2-(phenylsulfonyl)-1,3-dienes. Hydrothiolation was reported to occur exclusively at the α-position (Markovnikov-type addition). Expanding on these findings, Ogawa *et al.* [41] detailed the regio- and stereo-controlled formation of vinyl sulfides employing a wide range of catalysts based on Pd, Pt, and Rh. $RhCl(PPh_3)_3$ was shown to exhibit excellent activity, effecting anti-Markovnikov addition of ArSH to alkynes, yielding vinylic sulfides regio- and stereoselectively (*trans*-RCH=CHSAr). $PdCl_2(PhCN)_2$-catalyzed hydrothiolation of aromatic alkynes with ArSH yielded the Markovnikov adducts $R(ArS)C=CH_2$ with very good regioselectivity. In the case of alkynes with propargylic hydrogens, it is also possible to get a sequential addition/isomerization reaction, yielding internal vinylic sulfides. This work, as with the work of Kuniyasu *et al.* [39], very nicely demonstrated how simply changing the catalyst affords an easy route to controlling and selectively synthesizing specific target vinyl sulfides. Cao *et al.* [42] described the use of a Rh complex to effect the Markovnikov addition of aromatic and aliphatic thiols to terminal alkynes, and the same group reported anti-Markovnikov addition, yielding trans vinyl sulfides (or (*E*)-vinyl sulfides for internal alkynes) using Wilkinson's catalyst [43]. Han *et al.* [44] gave one example of the reaction between 1-octyne and thiophenol in the presence of a Ni species, which proceeded with >91% selectivity for the Markovnikov addition product. Also highlighting the effectiveness of Ni-based catalytic systems, Ananikov *et al.* [45] reported regioselective arylthio addition to terminal alkynes to give β-vinyl sulfides under solvent-free conditions, employing a cheap and readily available catalyst precursor. In a similar vein, Malyshev and coworkers [46] described Ni catalysts bearing N-heterocyclic carbene ligands as homogeneous systems for the Markovnikov addition of arylthiols to a series of terminal alkynes.

Kondoh and coworkers described the Cs_2CO_3/TEMPO-mediated hydrothiolation of a series of aromatic alkynes with a range of thiols. Reactions were performed in near 1 : 1 M ratios and were found to proceed to give, generally, anti-Markovnikov monoaddition products with a pronounced selectivity for the (*Z*)

stereoisomer [47]. The same group have also reported the Pd(OAc)$_2$-catalyzed hydrothiolation of 1-alkynylphosphines to give the corresponding (*Z*)-1-phosphino-2-thio-1-alkenes [48].

In addition to late-transition-metal-catalyzed reactions, Weiss *et al.* [49] have reported the organoactinide-catalyzed hydrothiolation of terminal aliphatic, aromatic, and conjugated ynes with aliphatic, aromatic, and benzylic thiols with a Th complex. In all instances, the reactions, essentially, proceeded with a very high degree of Markovnikov selectivity. Beyond the transition metals and actinides, there are reports describing hydrothiolation of ynes with GP III and GP VI catalysts. Manarin *et al.* [50] detailed the solvent-free, room temperature, PhSeBr-catalyzed synthesis of vinyl sulfides employing a range of aromatic thiols as well as with internal and terminal alkynes bearing both alkyl and aryl groups. Isolated yields of products were moderate to high but stereoselectivity appeared to be low. Interestingly, we have seen that, in general, transition-metal-catalyzed reactions tend to favor the formation of β-vinyl sulfides (Markovnikov addition) and radical-mediated conditions tend to lead to the formation of 1,2-double addition adducts. Yadav and coworkers [51] reported the InBr$_3$-catalyzed reaction of aromatic thiols with aliphatic unactivated alkynes and found that double addition occurred at the β-position giving dithioacetals in essentially quantitative yields. However, in reactions of aromatic thiols with phenylacetylene, only the monoaddition products, with anti-Markovnikov orientation, were formed in high yields.

In the past few years, the thiol–yne reaction has also received attention as a useful ligation tool in the synthesis of complex highly functional molecules and nonnatural sugars, and also in the modification of peptides and proteins. Chan *et al.* [52] reported the synthesis of star-shaped polyfunctional molecules via a sequential phosphine catalyzed thiol-Michael reaction between a multifunctional thiol and propargyl acrylate followed by a radical thiol–yne reaction with a range of functional thiols. Scheme 4.4 shows an example with a tetrafunctional thiol and also the range of possible thiols evaluated below this example.

Both the initial thiol–Michael and subsequent thiol–yne reactions were shown to be extremely rapid, and quantitative formation of the product molecules was confirmed using a combination of NMR spectroscopy and matrix-assisted laser desorption/ionization time-of-flight mass spectrometry (MALDI-TOF MS).

Recently, Fairbanks *et al.* [53] conducted a fundamental classical study evaluating the relative reactivities of a series of terminal and internal alkynes, with functionality likely to be of interest to polymer chemists, in reactions with octanethiol under photoinitiated radical conditions (Figure 4.1).

It was demonstrated that 2 equivalents of 1-octanethiol react, essentially quantitatively, with 1 equivalent of 1-octyne to give the 1,2-double hydrothiolation products. The same results were observed with propargyl acetate and methyl propargyl ether, although the rates of reaction were lower than those observed for 1-octyne. However, the authors noted that such behavior was not universal to all alkyne substrates. In the case of ethyl propiolate and methyl propargylamine, the addition of a second thiyl radical species was not observed with reactions yielding only the monohydrothiolated vinyl sulfide products. The exact reason for this difference in
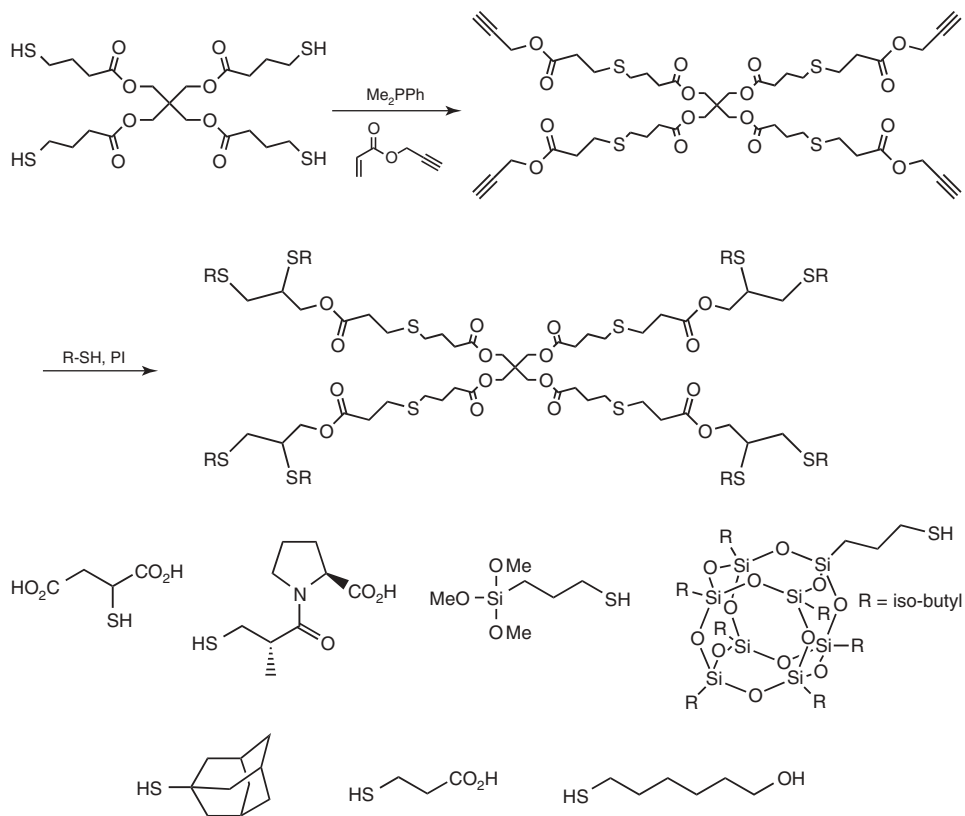
Scheme 4.4 Sequential thiol–Michael/thiol–yne couplings and the rapid, efficient synthesis of star-shaped highly functional molecules.

Photoinitiator

1-Octanethiol

Butyl 3-mercaptopropanoate

1-Octyne

Propargyl acetate

Methyl propargyl ether

Ethyl propiolate

Methyl propargylamine

2-Octyne

Cyclooctyne
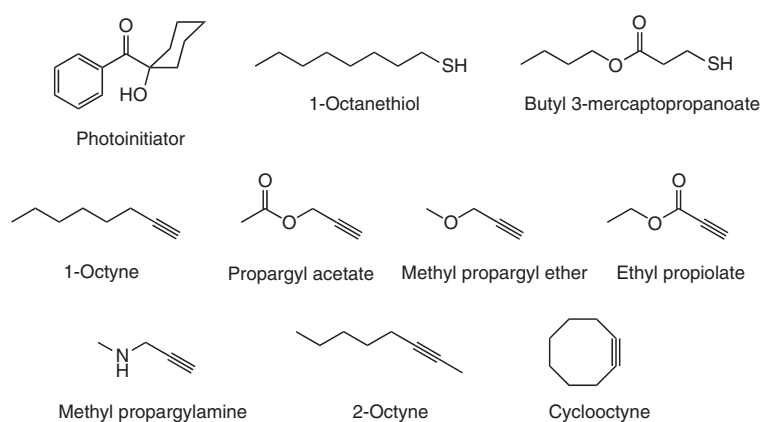
Figure 4.1 Chemical structures of photoinitiator and substrates employed in the fundamental evaluation of the radical-mediated thiol–yne reaction.
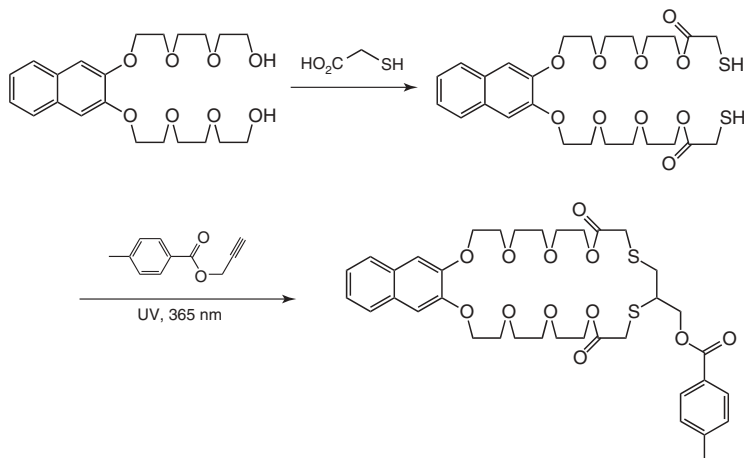
Scheme 4.5 Synthesis of thioether-based macrocycles via radical-mediated thiol—alkyne coupling.

reactivity is still unclear, but it was noted that under different conditions (higher light intensities, more efficient initiators) it was likely that double addition could be induced. In the case of the internal alkyne, 2-octyne, reactions with 1-octanethiol did proceed to give the double-addition products although at a much reduced rate, which is consistent with observations made in reactions of thiols with terminal versus internal ene bonds in thiol—ene reactions. In the case of cyclooctyne, it was found that the addition of a thiyl radical occurred relatively quickly which was attributed to the release of ring strain. However, the addition of a second equivalent of thiol was not observed to occur as judged by ^{1}H NMR spectroscopy, which was rationalized in terms of steric hindrance coupled with the little to low ring strain associated with cyclooctenes. Interestingly, it was also noted that cyclooctyne and 1-octanethiol react spontaneously under dark conditions (absence of light or added photoinitiator) in an unpurged atmosphere. This is due, presumably, to advantageous reactive oxygen species and suggests that copper-less click reactions with azides in biological media containing thiols may not be completely (bio)orthogonal.

Zhou and coworkers recently detailed the synthesis of thioether-based macrocycles and a rotaxane employing radical-mediated thiol—yne chemistry (Scheme 4.5) [54], while cyclic multivalent Arg-Gly-Asp peptides have been reported by Aimetti, Feaver, and Anseth via sequential thiol—ene and thiol—yne photoreactions [55].

Conte and coworkers [56] described the double glycosylation of cysteine-containing peptides via a one-pot, two-stage process involving initial propargylation followed by thiol—yne coupling with glucosylthiols (Scheme 4.6).

In the case of this example the double-hydrothiolated product was isolated by column chromatography in a 53% yield as a ~1 : 1 mixture of diastereoisomers. This strategy was extended to the natural tripeptide glutathione (GSH) and the synthetic tetrapeptide Arg-Gly-Asp-Cys. Interestingly, the authors noted that in the initial syntheses with the yne functional cysteine and the thio-sugar, at short
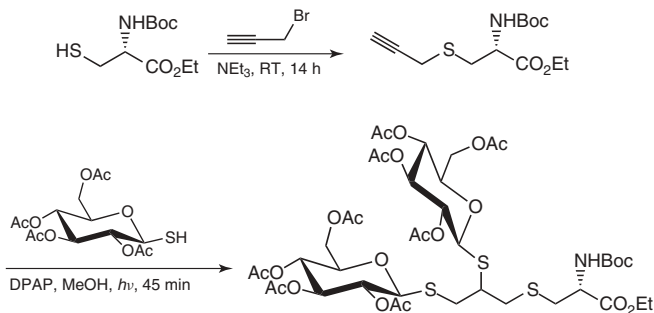
Scheme 4.6 Double hydrothiolation of an alkyne functional cysteine derivative.

reaction times significant amounts of the intermediate vinyl thioether were present, suggesting that the addition of the second sugar thiyl radical was slow relative to the initial addition, which was attributed to steric hindrance (this observation is in contrast to model studies in which the intermediate vinyl thioether is observed to be ∼ 3× more reactive than a terminal alkyne). However, this observation opened up the possibility of performing sequential thiol–yne/thiol–ene reactions with *different* thiols after isolation of the monoaddition product. The authors demonstrated this was indeed feasible by reacting *S*-propargyl GSH with the above glucosyl thiol (1.1 equivalents) with 2,2-dimethoxy-2-phenylacetophenone (DPAP) as photoinitiator in MeOH for 15 min. Subsequently, the product was treated with biotin thiol (also with DPAP in MeOH but for 45 min), yielding the hetero 1,2-dithioether in a 34% isolated yield. The same species could also be obtained in the reverse order (biotin thiol first followed by glucosyl thiol). The same group [57] extended this double-modification approach with cysteine, GSH, and bovine serum albumin (BSA) to give hetero double-conjugated species with sugar residues as well as a fluorescent tag. Similar glycosylation has also been achieved with other cysteine-containing peptides [58].

4.3
The Thiol–yne Reaction in Polymer and Material Synthesis

While it is evident that the thiol–yne reaction, in its various forms, has been known for over 100 years and employed somewhat routinely in small-molecule organic synthesis, it is only recently that the reaction has begun to attract significant attention from the polymer science community. Additionally, current efforts have focused almost exclusively on the radical-mediated version of the reaction, although there are several recent reports extending the application of alkyne hydrothiolation in polymer synthesis and modification beyond radical-based reactions; these limited examples are discussed below.

One of the earliest reports describing the use of the thiol–yne reaction in polymer synthesis/modification comes from Ochiai *et al.* [59]. Conjugated enynes of general formula $CH_2 = CH–C≡C–R$ (R = Ph or *n*-butyl) were polymerized radically,

yielding the 1,2-polymerized species, that is, polymers with pendent internal yne functionality. The authors subjected these homopolymers to hydrothiolation, hydrosilylation, and hydroalumination. In the case of hydrothiolation, reactions with 1 equivalent of dodecanethiol, in the presence of 2,2′-azobis(2-methylpropionitrile) (AIBN) at 60 °C, resulted in the formation of pendent vinyl sulfides, that is, monoaddition, the extent of which was determined by the nature of the R group in the conjugated enyne, with the smaller less sterically hindered *n*-butyl substrate resulting in higher degrees of monohydrothiolation (64% monohydrothiolation of pendent yne groups).

4.3.1
Network Polymers

Following this report, the thiol–yne reaction appears to have been essentially forgotten in polymer science until its recent re-emergence beginning with the work of Fairbanks *et al.* [60] and Chan and coworkers [61], who prepared and studied highly cross-linked thioether-based networks based on thiol–yne chemistry. The radical-mediated thiol–ene reaction has been employed routinely to prepare highly cross-linked, uniform polymeric networks with unique thermal and mechanical properties such as low stress shrinkage and uniform thermal transitions, with much of the work having been performed by the research groups of Prof. Charles Hoyle and Prof. Christopher Bowman. Extending this thiol–ene work, Bowman *et al.* [60] reported on the use of thiol–yne radical chemistry to prepare novel highly cross-linked networks and also evaluated the mechanism and kinetics of the basic hydrothiolation reaction. Similar to the radical thiol–ene reaction, the radical-mediated thiol–yne reaction was shown to proceed via a step-growth pathway, the general mechanism of which is shown in Scheme 4.7. Thiyl radicals, R-S•, are initially generated by employing any of the common methods for radical generation (thermal, photoinitiated – with or without added photoinitiator, etc.). These thiyl radicals then add to an alkyne in a predominantly anti-Markovnikov manner, forming the intermediate carbon-centered vinyl sulfide radical which undergoes a chain-transfer event with additional thiol forming the monohydrothiolated alkenylsulfide. As a vinylthioether, this is also extremely reactive toward thiyl radicals and can undergo reaction with another equivalent of R-S•, ultimately yielding the double hydrothiolation product after a second transfer event whilst also regenerating thiyl radicals. It should be noted, however, that such double hydrothiolations do result in the formation of a stereogenic center which may be of significance in small-molecule syntheses.

Bowman and coworkers [60] showed that thiyl addition of pentaerythritol tetra(3-mercaptopropionate to the intermediate vinyl thioether is approximately three times faster than that of the addition to an alkyne (octadiyne). This difference in reactivity and formation of an intermediate reactive species leads to unique and complex kinetics that were investigated and reported in this work. As a comparison, a tetrafunctional thiol was photopolymerized with either a dialkyne (octadiyne) or a diene (octadiene), and the mechanical and thermal properties were examined
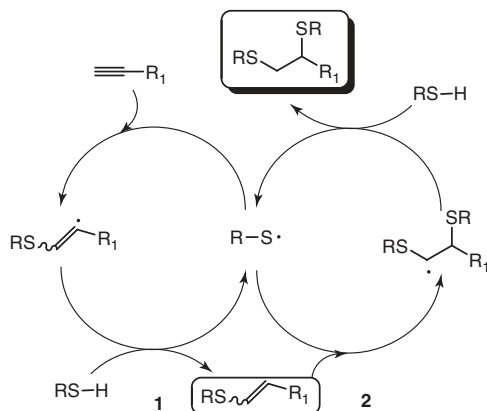
Scheme 4.7 Proposed mechanism for the radical-mediated thiol–yne reaction resulting in double hydrothiolation.

for each resulting thermoset. Owing to the increase in cross-link density with the system employing the dialkyne, the cross-link density was six times greater than the system employing the dialkene. It was also observed that the glass-transition temperature (T_g) (and modulus) of the thiol–yne networks was higher than in the corresponding thiol–ene network. The authors also noted a delay in gel point during network formation for the thiol–yne system, a common feature of networks prepared via the thiol–ene chemistry. The result is a highly homogeneous polymeric network usually accompanied by resulting narrow T_gs. This work illustrated the novelty and utility of the thiol–yne reaction for preparing highly cross-linked polymer networks.

Around the same time, Chan *et al.* [61] highlighted the utility of the radical thiol–yne reaction in the synthesis of high refractive index polymeric materials. Hydrocarbon networks bearing thioether linkages were prepared using the thiol–yne reaction in a simple single step. Commercially available dithiols and dialkynes with increasing hydrocarbon lengths were polymerized using photoinitiator and UV light. Near-quantitative conversion were apparent by real-time Fourier transform infrared (FTIR) spectroscopy, illustrating the click-like nature of the thiol–yne reaction. The narrow T_gs measured by dynamic mechanical thermal analysis (DMTA) indicated that all polymeric systems had uniform network density and structure. Additionally, the T_gs increased as the cross-link density increased. The use of purely hydrocarbon-based substrates ensured that high weight percentages of thioether linkages (>50%) were incorporated into the hydrocarbon networks. Structure–property relationships were determined correlating refractive index and bulk density to the polymer sulfur content. Results indicated a linear relationship between both refractive index and the sulfur content. Additionally, refractive indices of these polymer networks were remarkably high, with some values >1.65. This work highlighted how the radical thiol–yne reaction can serve as a useful tool for preparing highly complex materials from simple, commercially

available materials while developing true structure–property relationships of high refractive index polymers.

In more recent work, Chan *et al*. [62] described sequential nucleophilic thiol-Michael addition and radical-mediated thiol–yne reactions for preparing novel multifunctional photocurable monomers and networks. Propargyl acrylate was initially reacted, with Me$_2$PPh initiation, with ethylene glycol di(3-mercaptopropionate), trimethylolpropane tris(3-mercaptopropionate), and pentaerythritol tetra(3-mercaptopropionate) to yield the corresponding 2-, 3-, and 4-functional alkynes respectively in high yield and purity. Each was subsequently reacted under photochemical conditions with added photoinitiator with the above 2-, 3-, and 4-functional thiols, giving a series of high-density thiol–yne networks. The resulting networks displayed unique thermal and mechanical properties with tailored T_g values, for example, ranging from −10 to 42 °C, and moduli of 6–23 MPa.

Bowman and coworkers investigated the polymerization-induced shrinkage stress of cross-linked polymeric networks via the radical-mediated thiol–yne and addition-fragmentation chain transfer (AFCT) reactions [63]. Often, polymeric network thermosets undergo shrinkage stress whereby volumetric shrinkage can cause cracking in the final materials. Bowman and coworkers employed a technique termed *"addition-fragmentation chain transfer"*, whereby thiyl radicals can add across an allyl sulfide bond and subsequently fragment to regenerate a thiyl radical and an allyl sulfide bond. This resulting rearrangement of bonds proceeds to reduce the volumetric shrinkage while still maintaining constant cross-link density. Bowman and coworkers have utilized AFCT in other thiol–ene systems, which typically have T_g's lower than room temperature. By using thiol–yne systems with similar components, the authors were able to increase the T_gs to produce glassy networks (i.e., T_g greater than room temperature) that exhibit this unique response to stress. The proposed concurrent thiol–yne, thiol–ene, and AFCT reactions are shown in Scheme 4.8.

Lovelady *et al*. [64] described the synthesis of highly porous polymeric network materials employing high internal phase emulsion templates via both thiol–yne and thiol–ene chemistry. Network-forming reactions were shown to be efficient for both chemistries, although the resulting materials displayed different properties from those prepared via thiol–yne chemistry displaying enhanced strength and toughness due to the increased cross-link density.

4.3.2
Surface-Initiated Polymerizations and Modifications

Surface-initiated polymerizations (SIPs) and surface modifications are unique tools for providing functionality and utility to the surfaces of glass, silica, and other seemingly inert materials. Patton and coworkers [65] were the first to report the application of thiol–yne chemistry for the modification of surfaces in a modular manner (Scheme 4.9). Silica wafers were functionalized with photoinitiators for subsequent SIP. A protected alkyne-containing methacrylate monomer
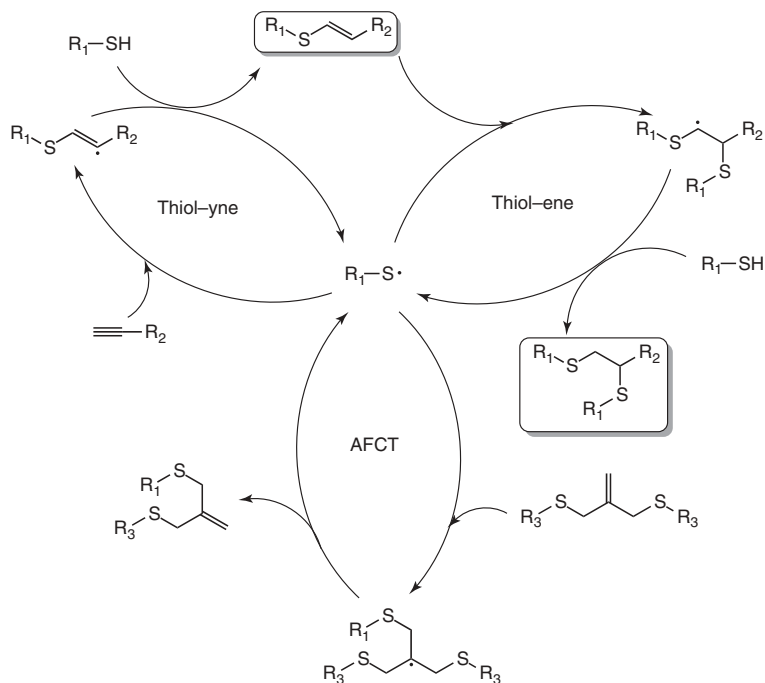
Scheme 4.8 Proposed three-stage radical mechanism for concurrent thiol–yne and addition-fragmentation chain-transfer reactions in network-forming polymers.

was then polymerized forming brushes from the surface of the wafer with the protecting groups subsequently removed post-polymerization. The radical-initiated thiol–yne reaction was then employed to graft various thiols to the polymer brushes, generating many unique surfaces on the silica and subsequent unique surface behaviors.

Reactions were monitored by attenuated total reflection (ATR) FTIR, which showed complete disappearance of the alkyne functionality within 60 s. In a unique example, silica surfaces bearing alkyne groups were reacted with mercaptopropionic acid (MPA), forming acid-functionalized brushes. By modulating the pH, the surfaces were tuned to various degrees of hydrophobicity, as demonstrated by contact angle measurements. In this case, the resulting surfaces showed unique reversible pH-responsive behavior. Additionally, the unique spatial control afforded by the thiol–yne reaction was demonstrated by creating a gridlike pattern as shown in Figure 4.2. The authors were able to create unique surfaces with discrete areas of hydrophilicity and various sizes using a UV mask, first by coating the surface with a hydrophilic thiol, applying light (either UV or sunlight), removing the mask, washing off any unreacted thiol, applying a hydrophobic thiol-containing molecule, and, finally, applying a second dose of light.

In a similar manner, the radical-mediated thiol–yne reaction was successfully utilized for surface modifications by photochemical microcontact printing by
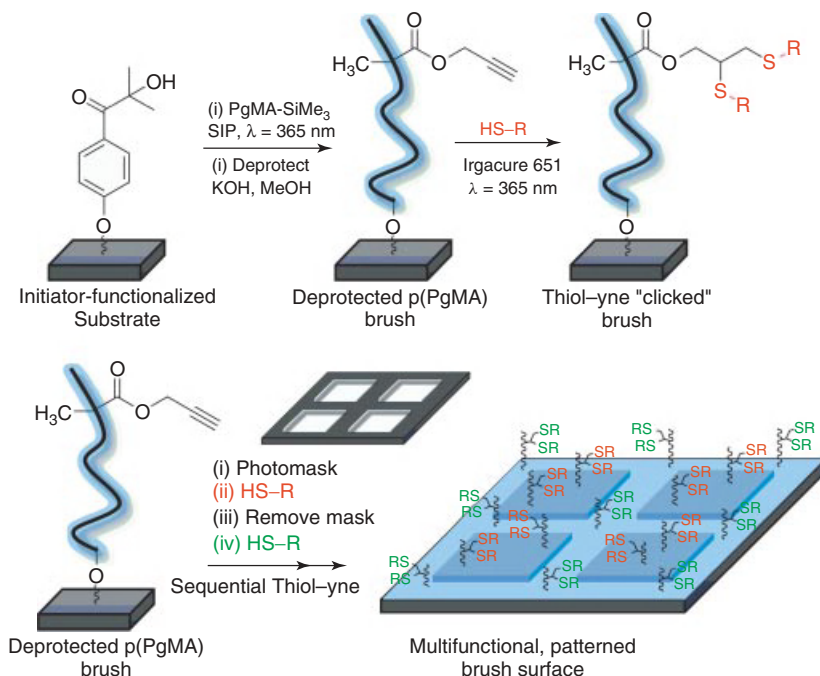
Scheme 4.9 Surface-initiated polymerization of TMS-protected propargyl methacrylate (trimethylsilyl) followed by deprotection and subsequent radical thiol–yne modification to give surfaces with tunable properties. (Source: Reprinted with permission from [65]. Copyright 2009 American Chemical Society.)

Wendeln and coworkers [66]. Here, glass and silica surfaces were modified to display alkyne pendant small molecules via a sol–gel type reaction. A series of thiol-containing compounds, including thiol sugars, were immobilized onto the surfaces, yielding materials with unique properties and surface features. By applying a coated stamp and UV light, areas that were exposed to both the thiol and light reacted to produce the thioether. On removal of the stamp, areas not in contact with thiol remained unchanged. The edge resolution of the patterns was determined to be <100 nm.

Subsequently Mehlich and Ravoo compared catalyzed and noncatalyzed "click" reactions for microcontact printing of inks onto self-assembled monolayers (SAMs) [67]. The authors compared the efficiency of several click and click-like reactions given that chemistry on surfaces is unique and may not correlate with solution chemistry. Glass or silica wafers were modified using standard SAM chemical methods to display either thiol or yne tethered functional groups. In the case of the yne-functionalized SAMs, each substrate was then dip-coated with a thiol-containing fluorescent molecule and the saturated samples were photoirradiated. The resulting patterned materials exhibited properties, such as contact angle
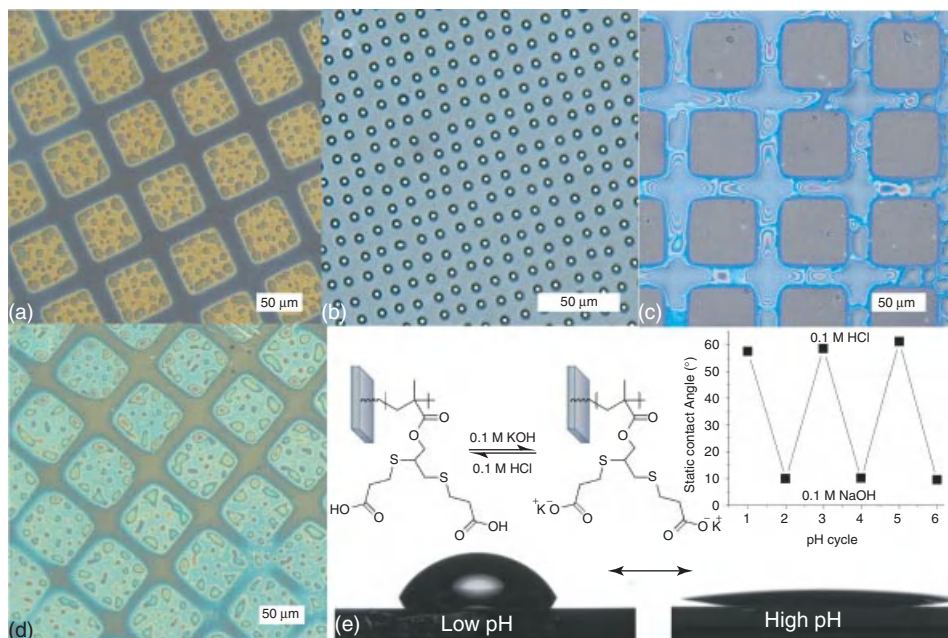
Figure 4.2 Optical condensation images of thiol−yne patterned brushes demonstrating nucleation of water droplets on hydrophilic areas: (a) mercaptopropionic acid (MPA)/1-dodecanethiol (DDT) (square/bars), 300 mesh; (b) MPA/DDT (squares/bars), 2000 mesh; (c) inverse DDT/MPA (squares/bars), 300 mesh; (d) sunlight initiated MPA/DDT (squares/bars); and (e) static water contact angle measurements. (Source: Reprinted with permission from [65]. Copyright 2009 American Chemical Society.)

and fluorescence, consistent with the corresponding thiol-containing molecules. This work compared the thiol−yne reaction to other well-investigated click reactions including the thiol−ene, Huisgen cycloaddition, and Diels−Alder reactions (Figure 4.3).

Wang *et al.* [68] described the use of the radical thiol−yne reaction for the glycosylation of microporous polypropylene membranes for the affinity adsorption of lectin. The authors indicated that the thiol−yne reaction offers a significant advantage over the alkyne−azide cycloaddition because of the undesirable hydrogen bonding between the triazole that forms during the cycloaddition reaction and typical amino acid residues of proteins. Surface glycosylation was demonstrated to be successful through the significant recognition specificity and affinity adsorption toward fluorescein isothiocyanate Concanavalin A (FITC-Con A).

Cai *et al.* [69] highlighted the synthesis of poly(vinylidene fluoride)-*g*-poly (propargyl methacrylate) by the thermally initiated graft polymerization of propargyl methacrylate from an ozone-activated poly(vinylidene fluoride) backbone. Microporous membranes were subsequently prepared from the graft copolymers
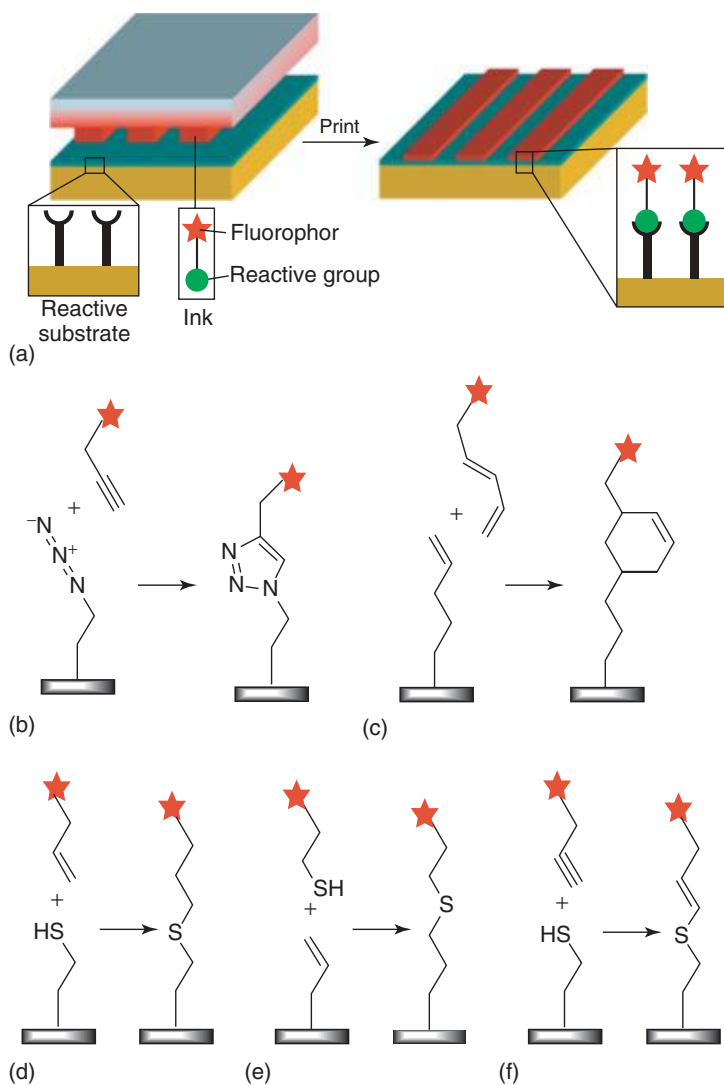
Figure 4.3 Formation of a series of surface-modified substrates employing a range of highly efficient click and click-like reactions including alkyne azide (b), Diels-Alder (c), thiol-ene (d) and (e), and thiol-yne (f) chemistries.

by phase inversion in aqueous media. The pendent yne functionality was further reacted with several acidic and basic thiols including 3-mercapto-1-propanesulfonic acid, 3-MPA, and 2-mercaptoethylamine (cysteamine) in the presence of 2,2-dimethoxy-2-phenylacetophenone (DMPA) as photoinitiator. Membranes modified with 3-mercapto-1-propanesulfonic acid exhibited electrolyte-dependent permeability.
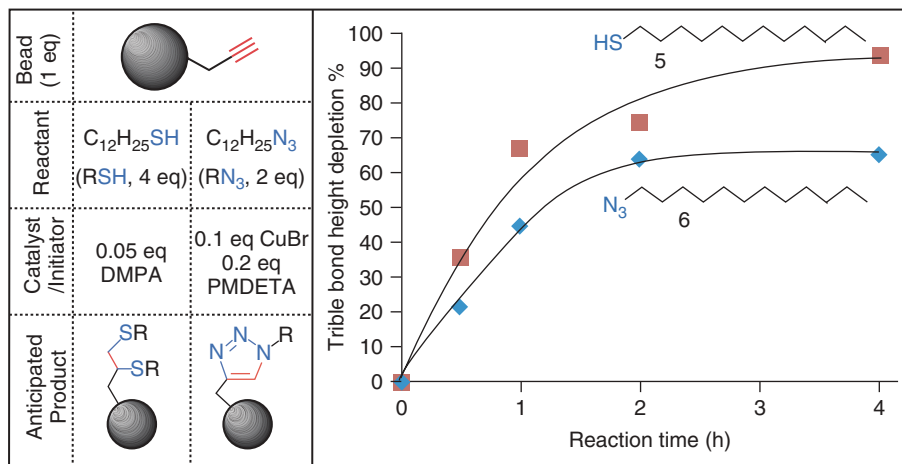
Figure 4.4 Kinetic comparison of the Cu(I)-catalyzed alkyne–azide and photoinitiated thiol–yne reactions for the surface modification of yne functional polymer beads (eq, equivalent).

4.3.3
Polymer Beads

We described in Section 4.3.1 how the radical thiol–yne reaction can be readily implemented for the preparation of highly cross-linked polymeric networks with tunable cross-link density, glass-transition temperatures, and mechanical properties. Since the tuning of these properties can be easily controlled, the thiol–yne reaction is a great potential synthetic procedure for the preparation of nano/micro-sized particles where control over submicrometer features is desirable.

Prasath and coworkers [70] highlighted the preparation of near-monodisperse polymeric beads of varying porosity and functionality employing a combination of thiol–yne chemistry and microfluidic engineering. The beads were prepared in a microfluidic chamber in a single step with a range of multifunctional thiols and alkynes. For example, amine, alcohol, and acid groups were readily detected on the resulting bead surfaces via FTIR. The authors also described the successful coupling of Fmoc-glycine onto the thiol–yne beads, alluding to the potential use of these materials in solid-phase peptide syntheses. In subsequent work, the same group [71] compared the reactivity of the Cu(I)-catalyzed alkyne–azide reaction and thiol–yne chemistry in the preparation of functional microporous beads. Near-monodisperse functionalized beads, with pendant thiol or yne functionality, were prepared using microfluidic techniques. Beads prepared with pendent yne functionality were reacted with 1-dodecaneazide and 1-dodecanethiol. The formation of the bis-thioether was found to be faster than triazole formation (Figure 4.4).

The use of thiol-functionalized beads allowed a direct comparison of nine different thiol-based reactions. Specifically, the kinetics of the reaction between
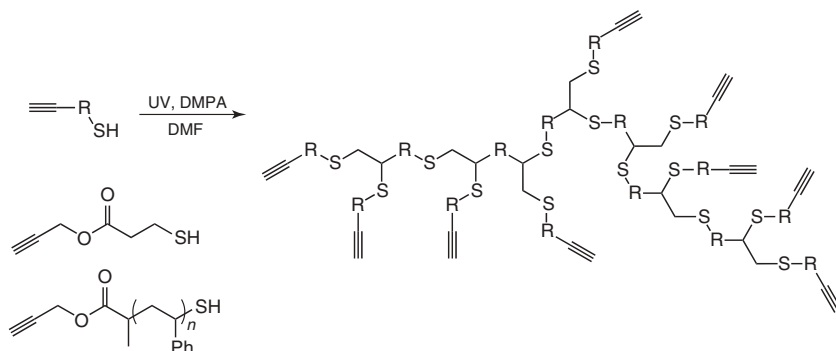
Scheme 4.10 Formation of hyperbranched molecules and polymers via photoinitiated radical thiol–yne reaction.

surface-bound thiol and examples of a terminal ene (radical conditions with photoinitiator), norbornene (radically with photoinitiator), acrylate (Michael addition under phosphine initiation), maleimide (Michael addition under base catalysis), bromo (base-catalyzed S_N2), epoxide (base-catalyzed ring-opening – S_N2), aziridine (base-catalyzed ring-opening – S_N2), isocyanate (base-catalyzed carbonyl addition), and isothiocyanate (base-catalyzed thiocarbonyl addition) substrates were evaluated. Even though these substrates react under different catalytic conditions and via different mechanistic pathways, it was found that the fastest reaction was with the isocyanate followed by norbornene > acrylate ≈ isothiocyanate > maleimide ≈ terminal ene > α-bromoester > epoxide ≈ aziridine.

4.3.4
Hyperbranched Polymers

Hyperbranched polymers are nonlinear materials in which the branches are distributed randomly within the polymer. In contrast to more structurally well-defined dendrimers, such (co)polymers, are typically straightforward to prepare. The first report describing the use of radical thiol–yne chemistry for the preparation of hyperbranched materials came from Konkolewicz, Gray-Weale, and Perrier (Scheme 4.10) [72].

Hyperbranched materials were readily prepared at room temperature, from both small molecules with yne and thiol functionality such as prop-2-yn-1-yl 3-mercaptopropanoate as well as polymeric analogs based on RAFT-prepared polystyrene. An important feature of this system is that the ratio of thiol:yne is 1 : 1 (as opposed to 2 : 1 in typical thiol–yne formulations). As noted previously, the addition of a thiol to an yne is three times slower than that for the addition of a thiol to an alkenylsulfide (formed from the addition of the first thiol to an alkyne). As such, the authors noted that in the above system the resulting hyperbranched species contained either fully reacted ynes (double-hydrothiolated species) or fully intact ynes with little if any monoaddition species detectable. This

approach, therefore, clearly offers the opportunity for preparing hyperbranched materials containing a high density of unreacted yne functionality that is available for further modification either via a second thiol–yne process or a cycloaddition reaction such as a Cu(I)-catalyzed alkyne–azide coupling.

Utilizing the hyperbranched materials derived from prop-2-yn-1-yl 3-mercaptopropanoate, Konkolewicz and coworkers [73] reported the preparation of polymers containing a gold–alkynyl complex. Treatment of the hyperbranched material with an N-heterocyclic carbene–gold–OH complex results in the elimination of water via alkyne deprotonation and loss of OH from the gold complex, resulting in the formation of the gold-alkynyl complexes with high luminescent properties (Scheme 4.11).

The possibility of post-polymerization modification was further demonstrated in a subsequent study combining RAFT radical polymerization, hyperbranched polymer syntheses, followed by subsequent modification (Scheme 4.12) [74].

For example, trimethylsilylpropargyl acrylate was copolymerized with a small amount of ethyleneglycol dimethacrylate, yielding a highly branched copolymer that, after deprotection of the trimethylsilyl groups, yielded the corresponding branched species with free alkyne functionality. Coupling with 2-azidoethyl-2,3,4,6-tetraacetyl-β-D-galactopyranoside followed by deacetylation yielded the corresponding polysugar with ∼85% functionalization of the free yne units. Reaction with thioglucose in the presence of DMPA under photoirradiation resulted in the complete consumption of the free yne functional groups; however, ∼10% of the residues were estimated to be mono-, as opposed to bis-, hydrothiolated species. This less than quantitative formation of the double thioether was attributed to steric hindrance.

Liu and Dong [75] demonstrated the synthesis of biodegradable hyperbranched polycaprolactones designed with alkyne groups along the periphery using AB_2 type macromonomers containing α-thiol and ω-alkyne groups and the radical-mediated thiol–yne reaction. Additionally, hyperbranched polypseudorotaxanes were synthesized via thiol–yne chemistry by decorating the AB_2 macromonomer in a host/guest complex with rotaxane (α-cyclodextrin) molecules. Interestingly, the decorated and nondecorated macromonomers cross-linked to form hyperbranched polymers with different kinetics: those macromonomers decorated with the cyclodextrans exhibited slower kinetics and lower degrees of cross-linking because of the increased rigidity in comparison to the nonmodified species. By tuning the irradiation time, the authors were able to control polymer molecular weights and degrees of crystallization, as evidenced by thermal transitions.

In a further demonstration of the ability to combine RAFT radical polymerization with thiol–yne chemistry, Konkolewicz *et al.* [76] prepared AB diblock copolymers of styrene and *N,N*-dimethyl acrylamide (DMA) or *tert*-butyl acrylate (*t*-BA) (the tert-butyl groups were removed post-polymerization to give the corresponding acrylic acid residues) using an alkyne functional chain-transfer agent (CTA), (prop-2-ynyl propanoate)yl butyl trithiocarbonate. The authors note that there was essentially no polymerization through the alkyne group on the CTA, indicating that the alkyne does not couple with any radical species generated
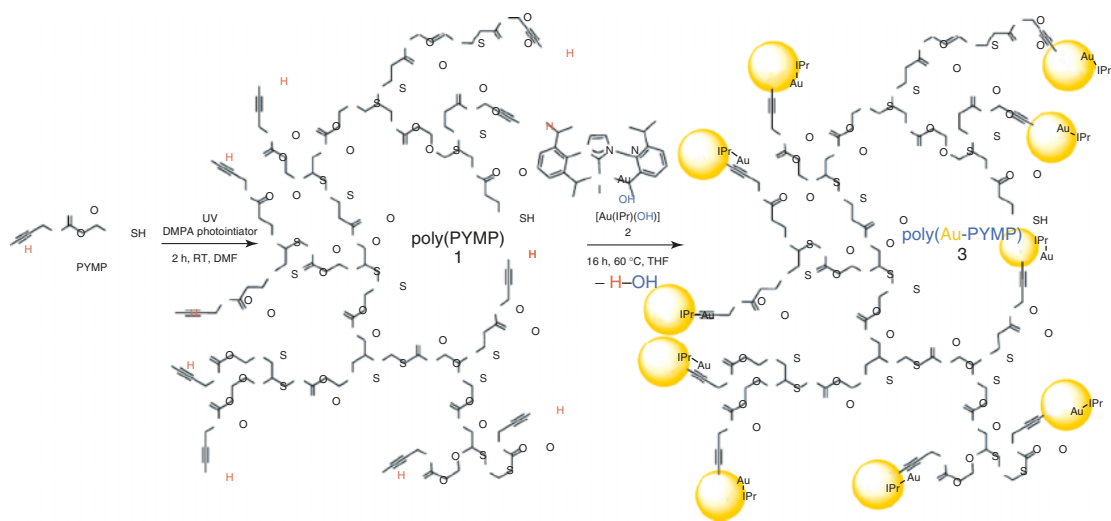
Scheme 4.11 Formation of gold-complex-modified hyperbranched polymers.
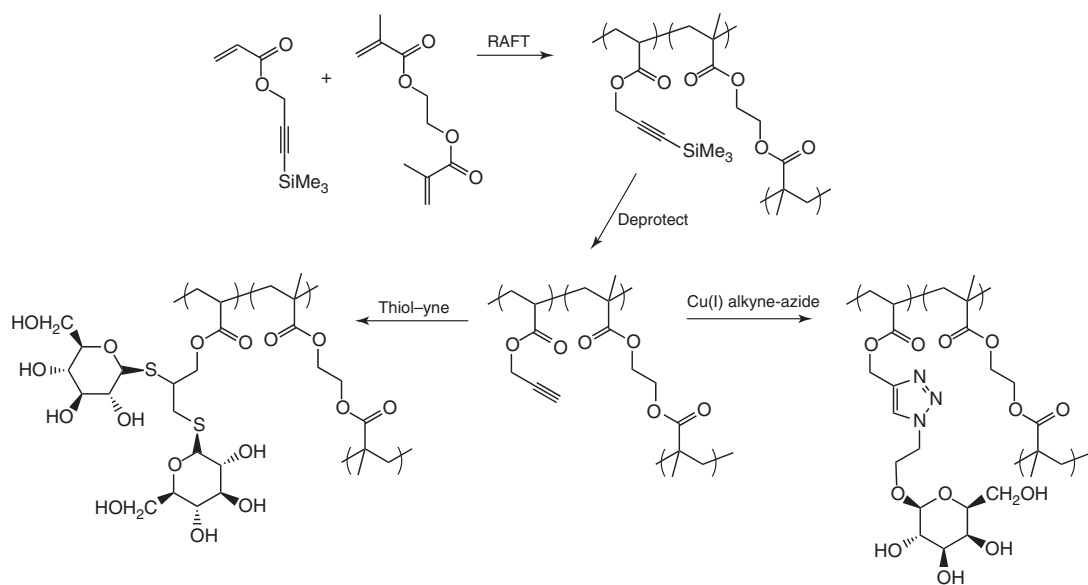
Scheme 4.12 Post-polymerization of RAFT-prepared hyperbranched, yne-containing (co)polymers with sugar residues employing both Cu(I)-catalyzed alkyne azide coupling and radical thiol–yne chemistry.

during the RAFT polymerization. Following polymerization, the trithiocarbonate groups were transformed to thiol groups through simple aminolysis, yielding α-yne, ω-thiol functional copolymers. These linear polymers were then mixed with a photoinitiator and subjected to 365 nm light at room temperature to afford the hyperbranched structures containing block copolymer building blocks. Formation of the hyperbranched species was confirmed by monitoring the increase by molecular weight by size exclusion chromatography (SEC).

In an approach similar to that reported by Konkolewicz *et al.* [72], Han *et al.* [77] prepared hyperbranched polymers employing a molecule containing both thiol and yne functionalities. This species was prepared from the reaction of a dithiol with propargyl acrylate (thiol-Michael reaction) and subsequently polymerized thermally in the presence of AIBN, giving the hyperbranched polymers with unreacted yne functional groups. The same group described a complementary approach to similar materials using a combination of thiol–halogen and thiol–yne chemistries. A dithiol was initially reacted with either propargyl chloride or bromide to give a thiol/yne species, which was subsequently copolymerized, as the major component, with a dithiol and diyne (minor components) to give the target thioether-based, yne functional hyperbranched copolymers [78].

4.3.5
Dendrimers and Dendritic Polymers

Dendrimers are extremely well-defined branched (co)polymers with many interesting properties and potential applications. Unfortunately, their well-defined nature, while desirable in many instances, is often associated with challenging syntheses. The very nature of dendritic molecules requires the use of highly efficient chemistry, be they convergent or divergent syntheses, to minimize structural defects, and as such it is perhaps not surprising that thiol–yne chemistry has been evaluated as a synthetic tool in this field. Chen and coworkers [79] described a combination of esterification and thiol–yne chemistries for the preparation of dendritic polymers for use as platinum drug delivery vehicles (Scheme 4.13). The reaction of tri(prop-2-yn-1-yl)benzene-1,3,5-tricarboxylate with 1-thioglycerol under UV irradiation (the radical thiol–yne reaction) gives the corresponding 12-functional alcohol, tris(2,3-bis((2,3dihydroxypropyl)thio)propyl) benzene-1,3,5-tricarboxylate. Esterification of this multifunctional alcohol with 4-oxo-4-(prop-2-yn-1-yloxy)butanoic anhydride yields the corresponding 12-functional yne, which after further reaction with 1-thioglycerol gives the 48-functional alcohol. Repetition of the esterification and thiol–yne reactions can also give the 192-functional alcohol. Employing a combination of SEC and MALDI-TOF MS, these dendritic polymers were shown to be extremely well defined with very few structural defects. Reaction of the 12-functional yne dendrimer with thiolglycolic acid yielded a 24-functional carboxylic acid functional dendrimer which was shown to be able to complex *cis*-dichlorodiammineplatinum (II), thus demonstrating the potential of these thioether-based dendrimers to serve as drug delivery vehicles.
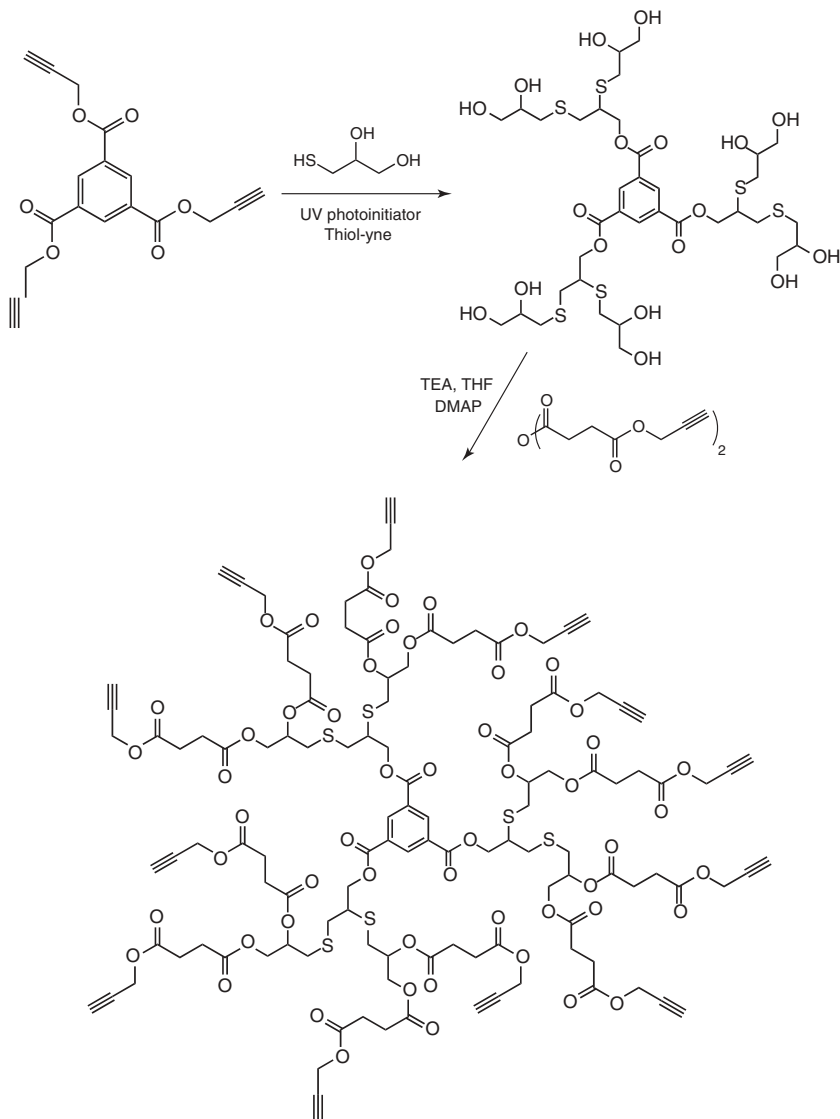
Scheme 4.13 Formation of thioether-based dendrimers via sequential thiol–yne/esterification reactions.

Amir *et al.* [80] described the synthesis of dendrimers employing a combination of amine–epoxy and thiol–yne coupling reactions (Scheme 4.14).

Reaction of a bis-amine-terminated poly(ethylene glycol) with 2-((prop-2-yn-1-yloxy)methyl)oxirane yielded the 4-functional yne with internal OH functional groups. Subsequent treatment with cysteamine hydrochloride in the presence of a photoinitiator (DMPA) under UV irradiation gave the corresponding
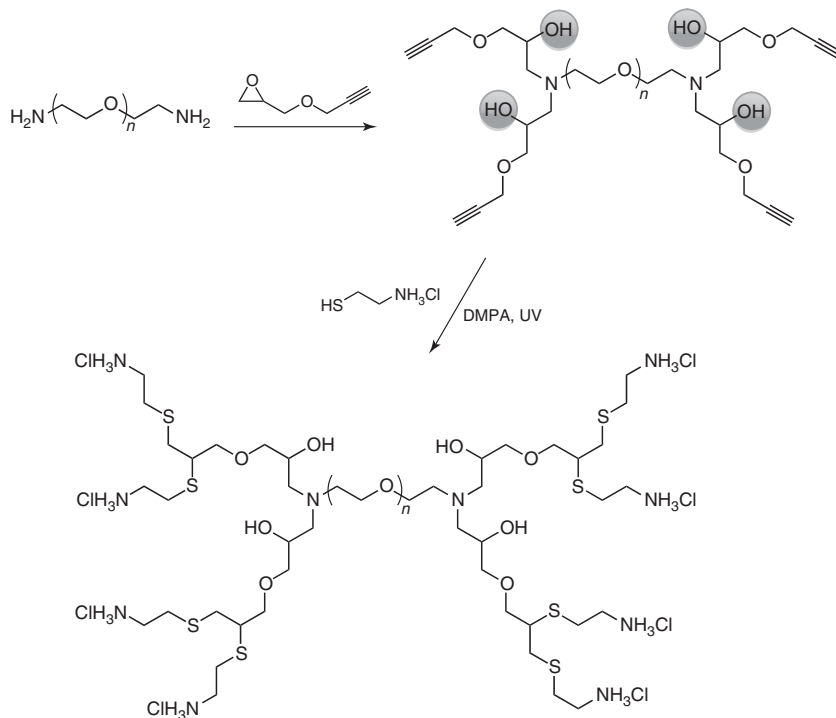
Scheme 4.14 Preparation of functional dendrimers employing sequential amine–epoxy and radical thiol–yne reactions.

8-functional amino species. Repetition of this reaction sequence yields the higher order dendritic structures. The authors demonstrated that it was possible to react the internal OH groups (before the thiol–yne coupling) with 7-(diethylamino)coumarin-3-carbonyl chloride – a potential fluorescence probe. Incubation of the coumarin-functionalized dendrimer with porcine liver esterase resulted in a steady release of the coumarin payload, as monitored by fluorescence at 480 nm, indicating that the internalized ester linkages were susceptible to enzymatic degradation, thus highlighting the potential of these dendritic structures to serve as payload carriers bearing suitable functional groups enabling controlled release.

4.3.6
Main chain α- and ω-Functional (co)Polymers

The ability to precisely and quantitatively functionalize polymers, either along the main chain, on pendent groups, or at the α and or ω-chain ends, has, in many instances, been a challenging synthetic goal. There are, of course, many routes for achieving such functionalizations, including the use of suitably functional initiators or terminating agents or employing post-polymerization functionalization
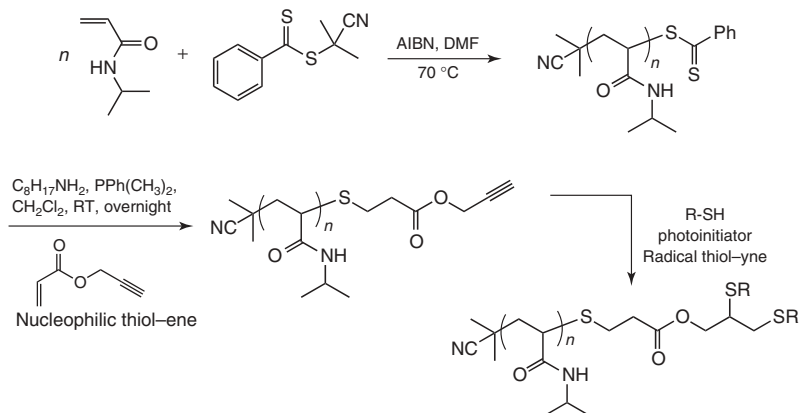
Scheme 4.15 Outline for the preparation of doubly end-functional RAFT-prepared poly(*N*-isopropylacrylamide) via sequential thiol–Michael and thiol–yne reactions.

chemistries for instilling the desired functionality. The use of the latter approach requires, ideally, highly efficient and preferably facile chemistry. Several research groups have evaluated thiol–yne chemistry as a means of preparing side, main chain, and end-functional polymers employing the approaches noted above. The first report detailing the use of thiol–yne chemistry for the preparation of such materials came from Yu *et al.* [81]. *N*-Isopropylacrylamide (NIPAM) was homopoly-merized via RAFT with 2-cyanopropan-2-yl benzodithioate (Scheme 4.15) to give the corresponding phenyldithioester end-capped homopolymer. Such dithioester end groups are extremely useful reactive handles, being readily cleaved to the analogous macromolecular thiols that are then available for a range of thiol-based chemistries. The authors reacted the dithioester-end-capped polyNIPAM in a one-pot reaction with octylamine (to cleave the dithioester to the thiol) and propargyl acrylate in the presence of dimethylphenylphosphine (PPh(CH₃)₂) (a potent catalyst for thiol-Michael addition reactions [23]). This one-pot process yielded the correspond-ing yne-end-functional polyNIPAM via the sequential aminolysis/Michael addition reactions.

The ω-yne functional homopolymer was then reacted with 6-mercapto-1-hexanol, 1-hexanethiol and 3-mercaptopropyl polyhedral oligomeric silsesquioxane (100% excess based on yne functional groups) in the presence of Irgacure 651 photoinitia-tor. This resulted in the quantitative formation, as judged by ^{1}H NMR spectroscopy, of the corresponding bis-ω-thioether adducts.

In an example highlighting the combination of living cationic polymerization, thiol-Michael chemistry, and thiol–yne modification, Magenau *et al.* [82] prepared α,ω-thiol end-functionalized polyisobutylene (PIB) and subsequently employed the material in a range of further chemical transformations (Scheme 4.16).

The authors initially prepared α,ω-primary bromide functional PIB via quenching of quasi-living PIB with a suitable alkoxybenzene [83]. Subsequent reaction with thiourea followed by base hydrolysis of the intermediate alkylisothiouronium salt
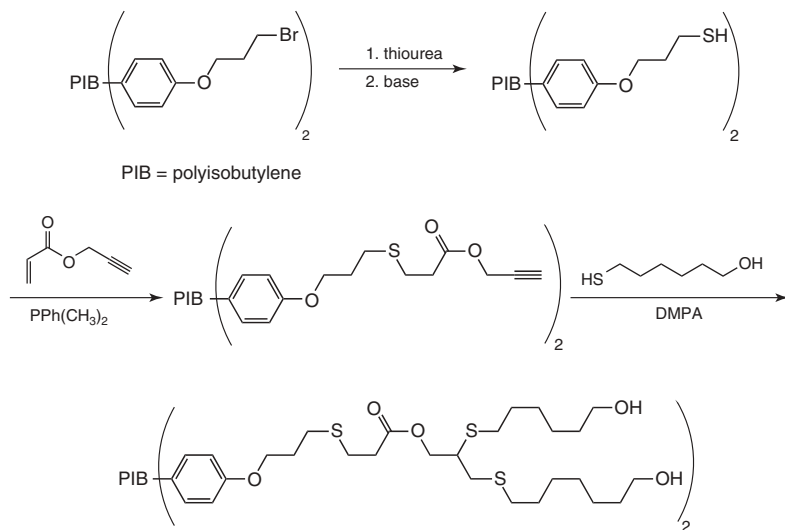
Scheme 4.16 α,ω-End-functional polyisobutylene prepared via a four-step process involving selective termination, functional group transformation, thiol–Michael addition, and thiol–yne chemistries.

yielded the α,ω-thiol end-modified PIB. Following the method described above for the modification of polyNIPAM (PNIPAM) prepared by RAFT, the authors treated the thiol-terminated PIB with propargyl acrylate under phosphine initiation to give the yne-end-modified PIB followed by reaction with 6-mercapto-1-hexanol in the presence of MPA under UV irradiation to give the α,ω-modified 4-functional alcohol.

Naik and coworkers [84] described the use of thiol–yne chemistry to prepare α-functional lipid-mimetic materials via both the functional imitator and post-polymerization routes (Scheme 4.17).

Propargylamine was first reacted with 1-dodecanthiol in the presence of a photoinitiator at 365 nm to give the double-hydrothiolated primary amine 2,3-bis(dodecylthio)propan-1-amine. This was then employed as an initiator in the *N*-carboxyanhydride (NCA) ring-opening polymerization of benzyl 3-(2,5-dioxooxazolidin-4-yl)propanoate to give the bis-α-functional homopolymer. Exactly the same material could be obtained via a post-polymerization route in which polymerization of the same substrate was first accomplished using propargylamine as the initiator followed by radical thiol–yne reaction of the α-alkyne functional homopolymer with 1-dodecanethiol. These hydrophobically end-modified polymers were shown to undergo self-directed assembly in aqueous media, forming spherical vesicles with a relatively narrow size distribution.

Huang *et al.* [85] described the side chain functionalization of polypeptides using a combination of NCA ring-opening polymerization and thiol–yne coupling. A new yne functional monomer, γ-propargyl-L-glutamate NCA, was prepared and polymerized using amine-terminated poly(ethylene glycol) and α,ω-amine-terminated
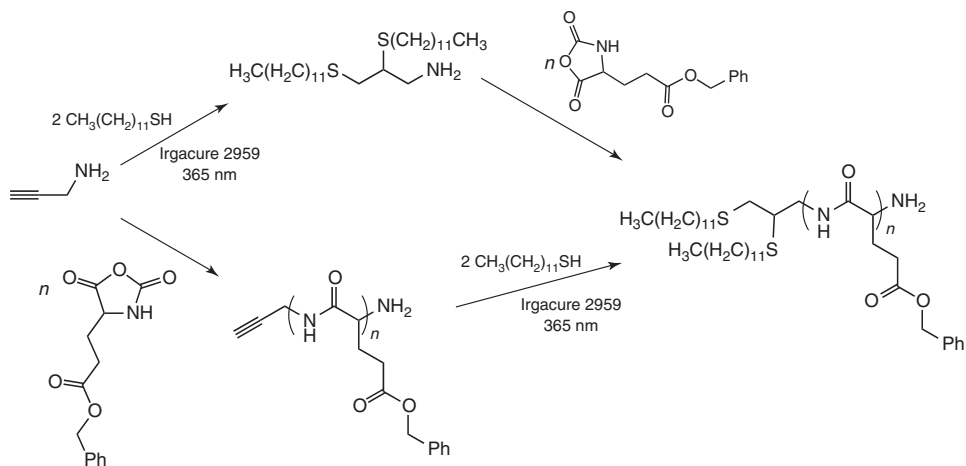
Scheme 4.17 Pre- and post-polymerization initiator functionalization with thiol–yne chemistry as a route to α-bis functional poly(*N*-carboxyanhydrides).

poly(propylene oxide) as initiators, yielding linear polymers with pendent yne functional groups. These were reacted, post-polymerization, with MPA in the presence of DMPA and with UV irradiation. ^{1}H NMR spectroscopy indicated complete consumption of the alkyne functional group and formation of the corresponding 1,2-dithioether adduct.

Kiskan and Weber very recently detailed the post-polymerization modification of microporous conjugated polymers using thiol–yne chemistry. The precursor yne-containing network polymers were prepared by Sonogashira–Hagihara coupling between 1,3,5-triethynylbenzene and 1,4-dibromobenzene (Scheme 4.18). It was anticipated that subsequent thiol–yne modification of the microporous materials would affect both the porosity (due to the change in hybridization state of the connecting carbon atoms) and the optical properties. Reactions of the main chain yne-containing network polymers with 2-mercaptoethanol or 6-mercaptohexanol resulted in rather low degrees of modification with, on average, $\sim$1 in 8–9 C$\equiv$C bonds reacting with a thiol (with 1.5 equiv. of thiol per triple bond), as judged by elemental analysis. Successful modification was also qualitatively confirmed using FTIR spectroscopy. Interestingly, no evidence could be discerned for the formation of the double-addition product.

However, these relatively low degrees of modification did have a measurable effect on the network microporosity as judged by CO_2 and N_2 adsorption/desorption at 273.15 and 77.3 K, respectively.

Side chain modification of yne-containing (co)polymers has been described by Brummelhuis and Schlaad [86] and Huynh *et al.* [87]. In the case of the former contribution, radical thiol–yne chemistry was employed for the concurrent functionalization and core cross-linking of AB diblock copolymers of 2-(3-butinyl)-2-oxazoline and 2-ethyl-2-oxazoline-based micelles. The internally confined yne double bonds were reacted, for example, with 3-MPA, giving the desired
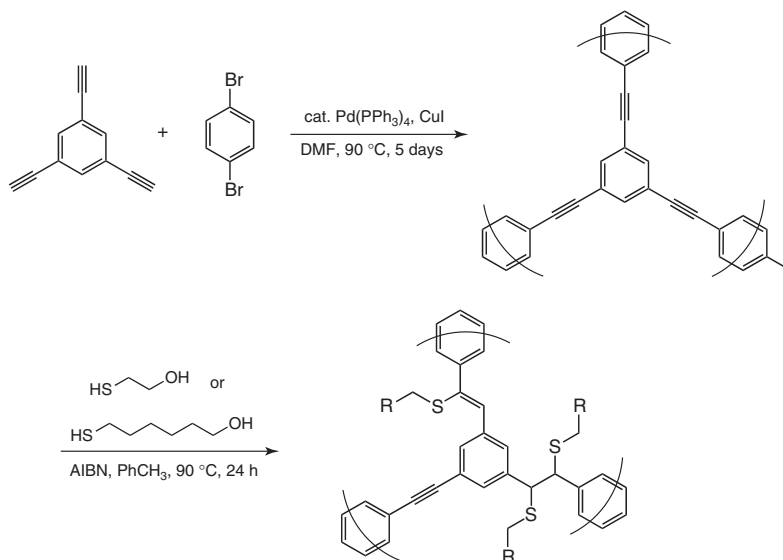
Scheme 4.18 Synthesis and post-polymerization modification of conjugated microporous polymers based on arylene–ethynylene building blocks.

functional cross-linked materials. Cross-linking was hypothesized to occur via the reaction of an intermediate vinyl thioether radical with either an unreacted C≡C bond or a C=C bond in an intermediate vinyl thioether. In the latter case, statistical and block copolymers, prepared via RAFT, containing 2-hydroxyethyl methacrylate and oligo(ethylene glycol) methyl ether methacrylate, were modified with 4-oxo-4-(prop-2-ynyloxy)butanoic anhydride, yielding copolymers with pendent yne functionality. Thiol–yne reaction with thioglycolic acid or 2-mercaptosuccinic acid yields copolymers with pendent carboxylic acid residues which were shown to be able to complex *cis*-platin, and subsequently demonstrated to serve as carrier vehicles for the delivery of the anticancer drug in A549 lung cancer cells.

4.3.7
Nonradical Thiol–yne Click Polymerization

It is evident that the application of thiol–yne chemistry in polymer and materials science has focused, almost exclusively, to date on the radical-mediated version of the process effecting, in most instances, 1,2-double hydrothiolation. However, as discussed in Section 4.1, there are, in fact, six possible hydrothiolation products with monoaddition species (vinyl thioethers) being readily accessible via certain transition-metal-mediated processes. Only very recently have such transition-metal-catalyzed reactions been adopted to polymer synthesis. Liu and coworkers [88] reported the Rh-mediated polymerization of aromatic diynes with 4,4′-thiodibenzenethiol (Scheme 4.19). Polymerization proceeded at room temperature in a regioselective manner, yielding solely anti-Markovnikov poly(vinylene
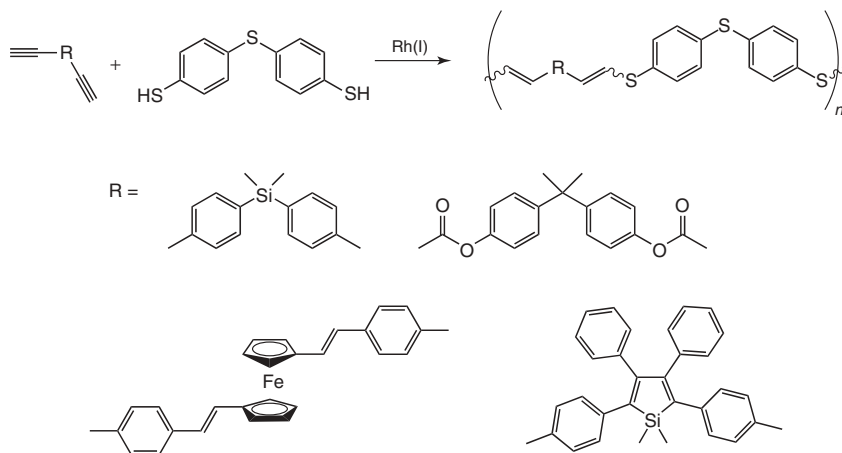
Scheme 4.19 Synthesis of novel poly(vinylene thioether)s via the Rh-catalyzed hydrothiolation of C≡C bonds in reactions between aromatic diynes and dithiols.

thioether)s of intermediate to high molecular weight and with (*E*) stereoselectivities up to 100% in the case of Wilkinson's catalyst Rh(PPh$_3$)$_3$Cl.

In contrast, polymers with (*Z*)-rich isomeric structures were obtained with [Rh(nbd)Cl]$_2$ and [Rh(nbd)(PPh$_3$)$_2$]$^+$PF$_6^-$. Starting with a polymer obtained from the dithiol and bis(4-ethynylphenyl)dimethylsilane with Wilkinson's catalyst (100% (*E*) poly(vinylene thioether)) the authors demonstrated that irradiation with either UV or visible light induced an (*E*)−(*Z*) isomerization process. Starting with the parent polymer ((*E*)/(*Z*) = 100/0), UV irradiation resulted in a gradual increase of the (*Z*) content, reaching a final composition of (*E*)/(*Z*) = 42/58. Subsequent visible light irradiation resulted in a reversal of this isomerization process. The poly(vinylene thioether)s were also shown to possess interesting properties such as aggregation, enhanced emission characteristics, and interesting optical properties, and were also demonstrated to be curable under thermal and UV conditions giving thick films with high refractive indices.

4.3.8
Summary and Outlook

Herein we have discussed and highlighted the use of the thiol–yne reaction in both small-molecule and macromolecular synthesis and modification. While known and studied for over 100 years in more traditional small-molecule organic chemistry, it has only been in the past 2–3 years that the chemistry has been adopted and applied in mainstream polymer chemistry. However, we have already seen impressive demonstrations of the power of this chemical reaction. In network formation, we see that the radical thiol–yne reaction is very similar to its sister thiol–ene reaction but gives materials with enhanced thermal and mechanical properties.

Surface modifications, whether on flat planar surfaces or nonplanar substrates, has been demonstrated to be a powerful approach not only for introducing a range of functionalities but also for preparing patterned surfaces with variable and tunable responsiveness. The chemistry has also been shown to be a reliable and robust route to both hyperbranched and dendritic (co)polymers, offering a facile route to such materials. It is also a useful chemical transformation for end-group, main chain, and side chain modification, although is not without its potential problems in main chain and pendent chain modifications. Interestingly, while the focus has been on almost exclusively the radical-mediated version of the reaction with the aim of effecting 1,2-dihydrothiolation, very recently researchers have begun evaluating nonradical versions of the reaction in polymer synthesis.

There is little doubt that the thiol–yne reaction will continue to attract synthetic polymer chemists in the coming years, with many new exciting applications of this click, or click-like, process inevitably to be reported. The radical version of the reaction is currently the favored manifestation of the process, effecting 1,2-bishydrothiolation, but is not without its problems. Side chain modification can be problematic with high concentrations of yne functionality and is analogous to the similar reactions on (co)polymers with a high concentration of the ene functionality in the side chains. While barely evaluated, there appears to be significant opportunity for transition-metal-catalyzed monohydrothiolation as a route to either new (co)polymers or as a modification protocol, although in this modern age of intense interest in synthetic routes employing metal-free or catalyst-free syntheses these may not attract the attention they deserve. However, it is clear that this somewhat forgotten reaction has, in a short time, proven itself to be a reliable and powerful synthetic tool, which will undoubtedly continue to grow in popularity.

References

1. Matyjaszewski, K. and Xia, J. (2001) *Chem. Rev.*, **101**, 2921.
2. Moad, G., Rizzardo, E., and Thang, S.H. (2005) *Aust. J. Chem.*, **58**, 379.
3. Moad, G., Rizzardo, E., and Thang, S.H. (2006) *Aust. J. Chem.*, **59**, 669.
4. Moad, G., Rizzardo, E., and Thang, S.H. (2008) *Polymer*, **49**, 1079.
5. Moad, G., Rizzardo, E., and Thang, S.H. (2009) *Aust. J. Chem.*, **62**, 1402.
6. Lowe, A.B. and McCormick, C.L. (2007) *Prog. Polym. Sci.*, **32**, 283.
7. Lowe, A.B., Torres, M., and Wang, R. (2007) *J. Polym. Sci., Part A: Polym. Chem.*, **45**, 5864.
8. Hawker, C.J., Bosman, A.W., and Harth, E. (2001) *Chem. Rev.*, **101**, 3661.
9. Yamago, S. (2006) *J. Polym. Sci., Part A: Polym. Chem.*, **44**, 1.
10. Kolb, H.C., Finn, M.G., and Sharpless, K.B. (2001) *Angew. Chem. Int. Ed.*, **40**, 2004.
11. Lowe, A.B. (2010) *Polym. Chem.*, **1**, 17.
12. Lowe, A.B. and Harvison, M.A. (2010) *Aust. J. Chem.*, **63**, 1251.
13. Lowe, A.B., Hoyle, C.E., and Bowman, C.N. (2010) *J. Mater. Chem.*, **20**, 4745.
14. Hoyle, C.E. and Bowman, C.N. (2010) *Angew. Chem. Int. Ed.*, **49**, 1540.
15. Hoyle, C.E., Lowe, A.B., and Bowman, C.N. (2010) *Chem. Soc. Rev.*, **39**, 1355.
16. Binder, W.H. and Sachsenhofer, R. (2007) *Macromol. Rapid Commun.*, **28**, 15.

17. Droumaguet, B.L. and Velonia, K. (2008) *Macromol. Rapid Commun.*, **29**, 1073.

18. Franc, G. and Kakkar, A.K. (2010) *Chem. Soc. Rev.*, **39**, 1536.

19. Harvison, M.A. and Lowe, A.B. (2011) *Macromol. Rapid Commun.*, **32**, 779.

20. Dondoni, A. (2008) *Angew. Chem. Int. Ed.*, **47**, 8995.

21. Hoyle, C.E., Lee, T.Y., and Roper, T. (2004) *J. Polym. Sci., Part A: Polym. Chem.*, **42**, 5301.

22. Hoogenboom, R. (2010) *Angew. Chem. Int. Ed.*, **49**, 3415.

23. Chan, J.W., Hoyle, C.E., Lowe, A.B., and Bowman, M. (2010) *Macromolecules*, **43**, 6381.

24. Chan, J.W., Yu, B., Hoyle, C.E., and Lowe, A.B. (2008) *Chem. Commun.*, 4959.

25. Li, H., Yu, B., Matsushima, H., Hoyle, C.E., and Lowe, A.B. (2009) *Macromolecules*, **42**, 6537.

26. Flores, J.D., Sing, J., Hoyle, C.E., and McCormick, C.L. (2010) *Polym. Chem.*, **1**, 213.

27. Xu, J., Tai, L., Boyer, C., Lowe, A.B., and Davis, T.P. (2010) *Macromolecules*, **43**, 20.

28. Posner, T. (1905) *Dtsch. Chem. Ges.*, **38**, 646.

29. Ruhemann, S. and Stapleton, H.E. (1900) *J. Chem. Soc. Dalton Trans.*, **77**, 1179.

30. Ruhemann, S. (1905) *J. Chem. Soc. Dalton Trans.*, **87**, 461.

31. Kohler, E.P. and Potter, H. (1935) *J. Am. Chem. Soc.*, **57**, 1316.

32. Owen, L.N. and Sultanbawa, M.U.S. (1949) *J. Chem. Soc.*, 3109.

33. Bader, H., Cross, L.C., Heilbron, I., and Jones, E.R.H. (1949) *J. Chem. Soc.*, 619.

34. Sauer, J.C. (1957) *J. Am. Chem. Soc.*, **79**, 5314.

35. Blomquist, A.T. and Wolinsky, J. (1958) *J. Org. Chem.*, **23**, 551.

36. Cristol, S.J., Begoon, A., Norris, A.P., and Ramey, P.S. (1954) *J. Am. Chem. Soc.*, **76**, 4558.

37. Truce, W.E. and Simms, J.A. (1956) *J. Am. Chem. Soc.*, **78**, 2756.

38. Ichinose, Y., Wakamatsu, K., Nozaki, K., and Birbaum, J.-L. (1987) *Chem. Lett.*, 1647.

39. Kuniyasu, H., Ogawa, A., Sato, K.-I., Ryu, I., Kambe, N., and Sonoda, N. (1992) *J. Am. Chem. Soc.*, **114**, 5902.

40. Bäckvall, J.-E. and Ericsson, A. (1994) *J. Org. Chem.*, **59**, 5850.

41. Ogawa, A., Ikeda, T., Kimura, K., and Hirao, T. (1999) *J. Am. Chem. Soc.*, **121**, 5108.

42. Cao, C., Fraser, L.R., and Love, J.A. (2005) *J. Am. Chem. Soc.*, **127**, 17614.

43. Shoai, S., Bichler, P., Kang, B., Buckley, H., and Love, J.A. (2007) *Organometallics*, **26**, 5778.

44. Han, L.-B., Zhang, C., Yazawa, H., and Shimada, S. (2004) *J. Am. Chem. Soc.*, **126**, 5080.

45. Ananikov, V.P., Orlov, N.V., and Beletskaya, I.P. (2006) *Organometallics*, **25**, 1970.

46. Malyshev, D.A., Scott, N.M., Marion, N., Stevens, E.D., Ananikov, V.P., Beletskaya, I.P., and Nolan, S.P. (2006) *Organometallics*, **25**, 4462.

47. Kondoh, A., Takami, K., Yorimitsu, H., and Oshima, K. (2005) *J. Org. Chem.*, **70**, 6468.

48. Kondoh, A., Yorimitsu, H., and Oshima, K. (2007) *Org. Lett.*, **9**, 1383.

49. Weiss, C.J., Wobser, S.D., and Marks, T.J. (2009) *J. Am. Chem. Soc.*, **131**, 2063.

50. Manarin, F., Roehrs, J.A., Marina, P., Alves, D., Nogueira, C.W., and Zeni, G. (2007) *Tetrahedron Lett.*, **48**, 4805.

51. Yadav, J.S., Subba Reddy, B.V., Raju, A., Ravindar, K., and Baishya, G. (2007) *Chem. Lett.*, **36**, 1474.

52. Chan, J.W., Hoyle, C.E., and Lowe, A.B. (2009) *J. Am. Chem. Soc.*, **131**, 5751.

53. Fairbanks, B.D., Sims, E.A., Anseth, K.S., and Bowman, C.N. (2010) *Macromolecules*, **43**, 4113.

54. Zhou, W., Zheng, H., Li, Y., Liu, H., and Li, Y. (2010) *Org. Lett.*, **12**, 4078.

55. Aimetti, Aa., Feaver, K.R., and Anseth, K.S. (2010) *Chem. Commun.*, **46**, 5781.

56. Conte, M.L., Pacifico, S., Chambery, A., Marra, A., and Dondoni, A. (2010) *J. Org. Chem.*, **75**, 4644.

57. Conte, M.L., Staderini, S., Marra, A., Sanchez-Navarro, M., Davis, B.G., and Dondoni, A. (2011) *Chem. Commun.*, **47**, 11086.

58. Minozzi, M., Monesi, A., Nanni, D., Spagnolo, P., Marchetti, N., and Massi, A. (2011) *J. Org. Chem.*, **76**, 450.

59. Ochiai, B., Tomita, I., and Endo, T. (2004) *Polym. Bull.*, **51**, 263.

60. Fairbanks, B.D., Scott, T.F., Kloxin, C.J., Anseth, K.S., and Bowman, C.N. (2009) *Macromolecules*, **42**, 211.

61. Chan, J.W., Zhou, H., Hoyle, C.E., and Lowe, A.B. (2009) *Chem. Mater.*, **21**, 1579.

62. Chan, J.W., Hoyle, C.E., Bowman, C.N., and Lowe, A.B. (2010) *Macromolecules*, **43**, 4937.

63. Park, H.Y., Kloxin, C.J., Scott, T.F., and Bowman, C.N. (2010) *Macromolecules*, **43**, 10188.

64. Lovelady, E., Kimmins, S.D., Wu, J., and Cameron, N.R. (2011) *Polym. Chem.*, **2**, 559.

65. Hensarling, R.M., Doughty, V.A., Chan, J.W., and Patton, D.L. (2009) *J. Am. Chem. Soc.*, **131**, 14673.

66. Wendeln, C., Rinnen, S., Schulz, C., Arlinghaus, H.F., and Ravoo, B.J. (2010) *Langmuir*, **26**, 15966.

67. Mehlich, J. and Ravoo, B.J. (2011) *Org. Biomol. Chem.*, **9**, 4108.

68. Wang, C., Ren, P.-F., Huang, X.-J., Wua, J., and Xu, Z.-Z. (2011) *Chem. Commun.*, **47**, 3930.

69. Cai, T., Neoh, K.G., and Kang, E.T. (2011) *Macromolecules*, **44**, 4258.

70. Prasath, R.A., Gokmen, M.T., Espeel, P., and Du Prez, F.E. (2010) *Polym. Chem.*, **1**, 685.

71. Gokmen, T., Brassinne, J., Prasath, R.A., and Du Prez, F.E. (2011) *Chem. Commun.*, **47**, 4652.

72. Konkolewicz, D., Gray-Weale, A., and Perrier, S.B. (2009) *J. Am. Chem. Soc.*, **131**, 18075.

73. Konkolewicz, D., Gaillard, S., West, A.G., Cheng, Y.Y., Gray-weale, A.,

Schmidt, T.W., and Nolan, S.P. (2011) *Organometallics*, **30**, 1315.

74. Semsarilar, M., Ladmiral, V., and Perrier, S.B. (2010) *Macromolecules*, **43**, 1438.

75. Liu, W. and Dong, C.-M. (2010) *Macromolecules*, **43**, 8447.

76. Konkolewicz, D., Poon, C.K., Gray-Weale, A., and Perrier, S. (2011) *Chem. Commun.*, **47**, 239.

77. Han, J., Zhao, B., Gao, Y., Tang, A., and Gao, C. (2011) *Polym. Chem.*, **2**, 2175.

78. Han, J., Zhao, B., Tang, A., Gao, Y., and Gao, C. (2012) *Polym. Chem.*, **3**, doi: 10.1039/c1py00367d

79. Chen, G., Kumar, J., Gregory, A., and Stenzel, M.H. (2009) *Chem. Commun.*, 6291.

80. Amir, R.J., Albertazzi, L., Willis, J., Khan, A., Kang, T., and Hawker, C.J. (2011) *Angew. Chem. Int. Ed.*, **50**, 3425.

81. Yu, B., Chan, J.W., Hoyle, C.E., and Lowe, A.B. (2009) *J. Polym. Sci., Part A: Polym. Chem.*, **47**, 3554.

82. Magenau, A.J.D., Hartlage, T.R., and Storey, R.F. (2010) *Polymer*, **48**, 5505.

83. Morgan, D.L. and Storey, R.F. (2009) *Macromolecules*, **42**, 6844.

84. Naik, S.S., Chan, J.W., Comer, C., Hoyle, C.E., and Savin, D.A. (2011) *Polym. Chem.*, **2**, 303.

85. Huang, Y., Zeng, Y., Yang, J., Zeng, Z., Zhu, F., and Chen, X. (2011) *Chem. Commun.*, **47**, 7509.

86. Brummelhuis, N.T. and Schlaad, H. (2011) *Polym. Chem.*, **2**, 1180.

87. Huynh, V.T., Chen, G., de Souza, P., and Stenzel, M.H. (2011) *Biomacromolecules*, **12**, 1738.

88. Liu, J., Lam, J.W.Y., Jim, C.K.W., Ng, J.C.Y., Shi, J., Su, H., Yeung, K.F., Hong, Y., Faisal, M., Yu, Y., Wong, K.S., and Tang, B.Z. (2011) *Macromolecules*, **44**, 68.

5

Design and Synthesis of Maleimide Group Containing Polymeric Materials via the Diels-Alder/Retro Diels-Alder Strategy

Tugce Nihal Gevrek, Mehmet Arslan, and Amitav Sanyal

5.1
Introduction

Efficient post-polymerization functionalization of polymeric materials is of utmost importance to impart the desired functional attributes to these materials. In recent years, such reactive polymeric materials have found applications in areas such as polymer therapeutics, biomolecular arrays, drug delivery platforms, and tissue engineering scaffolds. Conjugation of biomolecules such as peptides, proteins, and oligonucleotides onto polymers has been extensively explored because such conjugation improves the stability and circulation time in blood of these materials *in vivo* [1–3]. Similarly, conjugation of drug molecules to polymers has been exploited to increase the bioavailability, stability, and half-life of the drug *in vivo* [4, 5]. Furthermore, it has been observed that polymer–drug conjugates accumulate preferentially in tumor tissues because of their leaky vasculature via the enhanced permeability and retention (EPR) effect [6]. All aforementioned applications depend on the availability of efficient conjugation methods of polymeric materials with small molecules such as drugs and peptides or large molecules such as proteins and growth factors. The past decade has witnessed an immense increase in the adaptation of post-polymerization functionalization to decorate polymeric materials. This has been largely propelled by the advent of ''click'' chemistry and the renewed interest to adapt efficient organic reactions and transformation into synthetic polymer chemistry [7].

Usually, incorporation of reactive functional groups onto the polymer chain ends has been accomplished by (i) using a reactive group containing initiator, (ii) quenching the polymerization by a chain-capping reagent containing a reactive functional group, or (iii) by post-polymerization chain-end modification of the polymer. Introduction of reactive groups as side chains has been accomplished with the utilization of monomers containing a reactive functional group. In all these approaches, it is imperative that the reactive functional group remains intact under the polymerization conditions or during its introduction via post-polymerization modification. While most reactive groups such as activated esters do not interfere with radical reactions, some reactive groups need to be protected during the

synthetic steps involving free radical chemistry. Polymer chemists can use the same protecting group strategies that are routinely used by synthetic organic chemists.

5.2
### Maleimide Functional Group Containing Polymeric Materials

Maleimide groups are excellent handles for post-polymerization functionalization of polymeric materials because of their easy reaction with (i) thiol-containing molecules and biomolecules via the nucleophilic thiol–ene reaction as well as (ii) molecules containing electron-rich diene units via the Diels–Alder cycloaddition reaction (Scheme 5.1) [8]. Both these modifications can be effected under mild and ''metal-free'' reaction conditions. Furthermore, the reactions proceed in a clean manner, that is, they do not generate any side products or by-products.

Synthesis of maleimide-containing polymers is not trivial because the reactive double bond of the maleimide group that provides an efficient handle for polymer functionalization also makes the maleimide unit an excellent monomer toward polymerization. This necessitates the use of a protecting group for the maleimide moiety during the polymerization process. Importantly, the deprotection should be very efficient and devoid of any side reactions to render this a viable methodology. This chapter explains how the sequential use of the Diels–Alder cycloaddition reaction and the retro Diels–Alder cycloreversion reaction enables the synthesis of maleimide-containing polymeric materials.

5.3
The Diels-Alder/Retro Diels-Alder Cycloaddition-Cycloreversion Reactions

More than 80 years ago, Diels and Alder reported the [4 + 2] cycloaddition reaction between a diene and a dienophile (Scheme 5.2) [9]. The Diels–Alder reaction has been one of the most widely exploited reactions by organic chemists to synthesize simple and complex natural products. The reaction is reversible, and the cycloadduct can be thermally fragmented to obtain the starting materials or new products via the retro Diels–Alder reaction. The reactivity between the diene and dienophiles depends on the energy gap between the highest occupied molecular orbital (HOMO) of the diene and the lowest unoccupied molecular orbital (LUMO) of the dienophile. Thus electron-rich dienes are good dienes, and electron-deficient double bonds are good dienophiles. Thus combination of different dienes and dienophiles allows one to obtain the cycloadduct at different temperatures. Furthermore, the stability of the cycloadduct also largely depends on this diene–dienophile combination. Hence, the temperature at which the retro Diels–Alder reaction occurs can be tuned to the polymer by appropriate choice of the cycloadduct. The most commonly used diene–dienophile pairs that have been widely utilized in polymer chemistry are the furan–maleimide and the
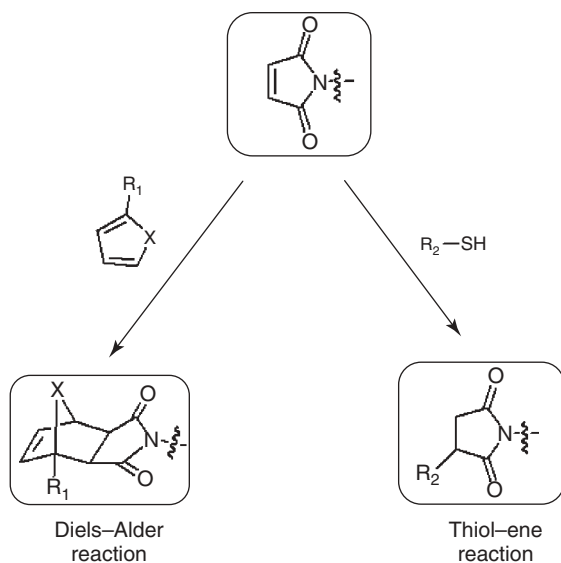
Scheme 5.1 Maleimide group functionalization via the Diels−Alder and the "thiol-ene" reaction.
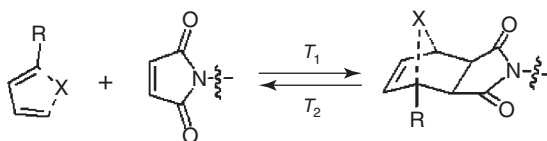
Scheme 5.2 The Diels−Alder/retro Diels−Alder cycloaddition/cycloreversion reaction.

anthracene−maleimide combinations. The furan−maleimide cycloadduct can be formed over a wide range of temperatures (room temperature to 80 °C) with varying reaction kinetics. The anthracene−maleimide cycloadducts are usually formed by heating them at 110 °C. These reaction temperatures can be fine-tuned by utilizing electron-donating or electron-withdrawing substituents on the diene moiety. Furthermore, employment of a Lewis acid catalyst or high pressure during the cycloaddition reaction can enhance the reaction rate at lower temperatures. For using the cycloaddition/cycloreversion sequence as a viable protection−deprotection strategy, the temperature at which the retro Diels−Alder reaction takes place is crucial. The cycloreversion should proceed in a quantitative manner at reasonable temperatures with no degradation of the polymers. The exo cycloadduct of furan and maleimide undergoes cycloreversion near 100 °C, whereas the cycloreversion of the anthracene−maleimide pair takes place at temperatures above 200 °C. Consequently, the furan−maleimide cycloadduct is generally the candidate of choice when a cycloreversion step is involved to unmask the thiol-reactive maleimide group.

5.4
## Application of Diels-Alder/Retro Diels-Alder Reaction to Synthesize Maleimide-Containing Polymers

The electron-deficient double bond of the maleimide functional group can be protected using the Diels–Alder cycloaddition reaction with an electron-rich diene. The cycloaddition masks the reactive double bond of the maleimide group, thus ensuring the protection of the maleimide unit from free radicals during the polymerization process or the post-polymerization introduction step. Once the polymer containing a protected maleimide group is obtained, a retro Diels–Alder cycloreversion reaction unmasks the maleimide group by removing the protective diene unit. Thus a strategy based on the combination of a Diels–Alder/retro Diels–Alder reaction allows fabrication of various maleimide-containing polymeric materials [10]. The particular synthetic protocol utilized to install a maleimide group in the polymer depends largely on the topology of the polymer and the location of the maleimide group in the polymer. For example, a maleimide group can be located at the chain termini of a linear or multiarm polymer, the core of a star polymer, or as pendant side chains along the backbone of the polymer (Scheme 5.3).

5.4.1
Synthesis of Polymers Containing the Maleimide Group at the Chain Termini

Advances in living polymerization techniques such as atom-transfer radical polymerization (ATRP) [11], reversible–addition fragmentation chain-transfer (RAFT) polymerization [12], nitroxide-mediated polymerization (NMP) [13], and ring-opening polymerization (ROP) [14] have not only enabled the synthesis of polymers with control of molecular weights and polydispersity but also allowed easy introduction of end groups. The use of appropriately functionalized initiators have enabled easy introduction of the end groups. The incorporation of reactive end groups into polymers affords a modular approach to obtain polymers with the desired terminal groups. In recent years, a wide range of initiators containing reactive functional groups have been employed toward this end. The most commonly used functional groups have been activated esters and azides that can undergo facile post-polymerization modification via amidation and Huisgen-type [3 + 2] alkyne–azide click reaction, respectively. This section outlines the recent advances in the synthesis of polymers containing the maleimide functional group at chain ends, thus allowing facile post-polymerization modification via the Diels–Alder reaction or the nucleophilic thiol–ene click reaction.

Among the several available strategies to introduce the maleimide groups at chain termini, the most commonly used one involves the use of an initiator containing a masked maleimide functional group (Scheme 5.4). An appropriate initiator can be designed by the modification of a typical free radical initiator or a chain-transfer agent (CTA) with a diene-protected, maleimide-based fragment. Polymerizations that are initiated from such modified initiators will yield polymers containing a
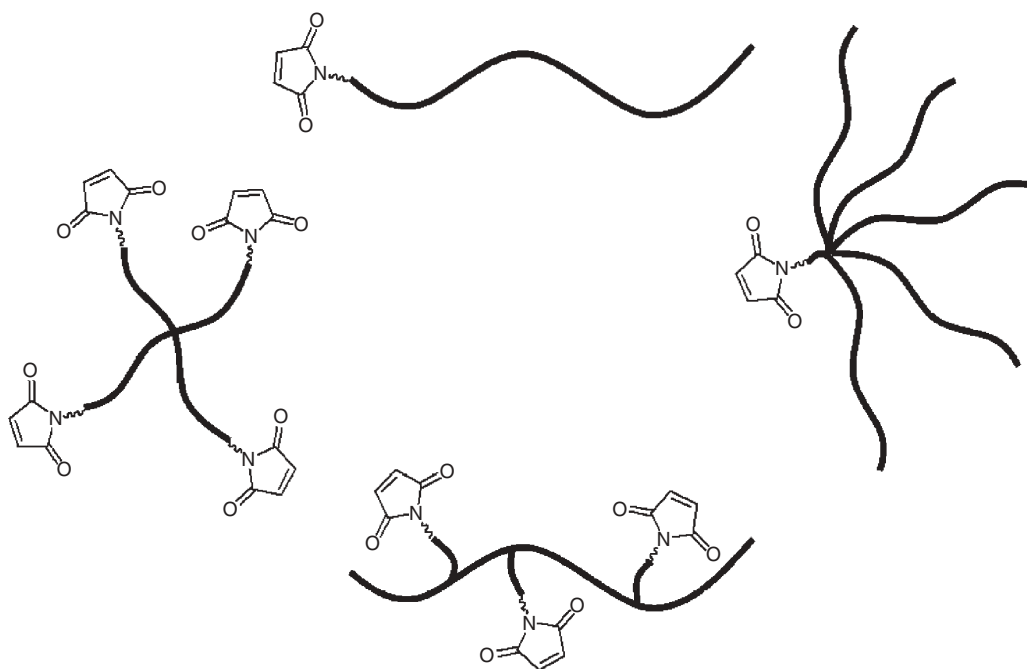
Scheme 5.3 Illustration exemplifying various possible locations of the maleimide functional groups in polymers.
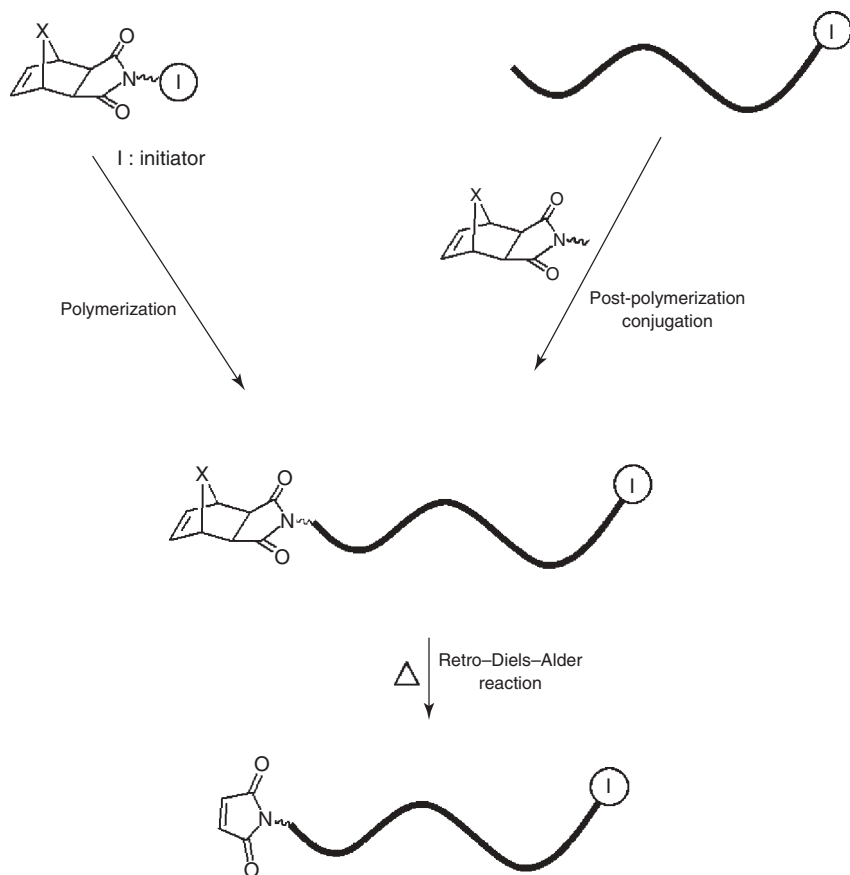
Scheme 5.4 Illustrative synthetic strategies to obtain polymers with maleimide functional groups at the chain termini.

masked maleimide unit at the chain ends. Alternatively, polymerizations such as RAFT, when conducted in the presence of CTAs incorporating a masked maleimide unit, will also provide polymers containing masked maleimide groups at chain ends. As an alternative, it is also possible to install masked maleimide units using effective post-polymerization strategies that involve chain-end termination strategies. It is also possible to quench the polymerization reaction with an appropriate quenching agent containing a masked maleimide moiety. Reactive maleimide groups can be obtained by subjecting these polymers to a retro Diels–Alder cycloreversion step. All these strategies are discussed in the following paragraphs by highlighting examples from recent literature.

The first example using the strategy based on the Diels–Alder/retro Diels–Alder reaction sequence to synthesize a maleimide chain-end-terminated polymer was reported by Haddleton and coworkers [15] (Scheme 5.5). A furan-protected maleimide-containing radical initiator that initiates ATRP in the presence of a
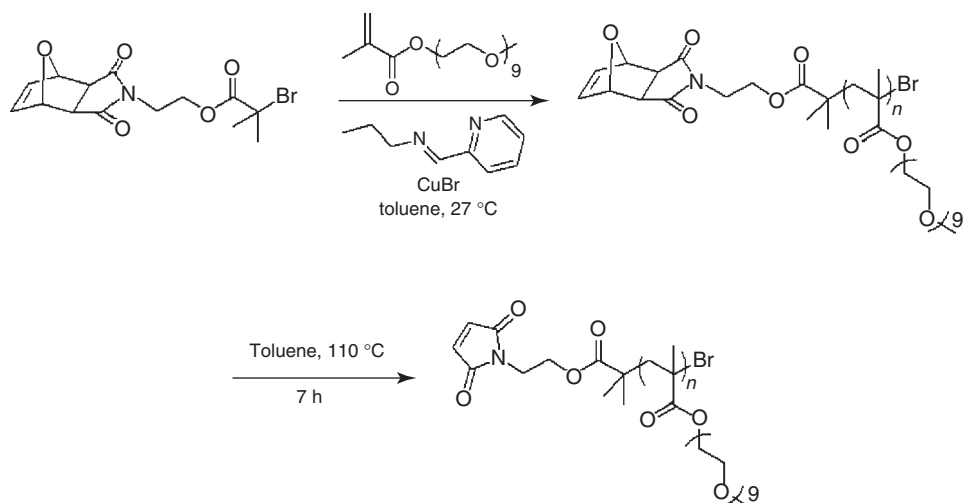
Scheme 5.5 Synthesis of maleimide end-functionalized polyPEG polymers using a furan-protected, maleimide-containing ATRP initiator.

Cu(I) catalyst was synthesized. Polymerization of poly(ethylene glycol)methacrylate (PEGMA) using this initiator containing the masked maleimide unit yields water-soluble polymers that contain furan-protected maleimide units at their chain ends. The furan protecting group is removed in a clean and quantitative manner by refluxing in toluene at 110 °C to yield the thiol-reactive maleimide-group-containing polymers. The maleimide group at the chain end of this water-soluble polymer provides an excellent handle for obtaining protein–polymer conjugates.

As an alternative strategy, the reactive maleimide group was also introduced onto the polymer ends via a post-polymerization functionalization reaction. First, an amine-terminated polymer was synthesized using an ATRP initiator containing the protected amine. Deprotection of the amine group followed by conversion of the free amine group to the maleimide unit using an excess of maleic anhydride resulted in the installation of maleimide units with an efficiency of 80–85%. It should be noted that the above approach ensures that each polymer chain is terminated with a thiol-reactive maleimide functional group. Needless to say, the chemical purity of such well-defined polymers will play an important role in the efficiency of subsequent conjugation reactions. Thus obtained water-soluble polyPEG polymers terminated by maleimide were conjugated to bovine serum albumin (BSA), a thiol-containing protein. Successful protein–polymer conjugation was demonstrated using sodium dodecyl sulfate polyacrylamide gel electrophoresis (SDS/PAGE) and fast protein liquid chromatography (FPLC) analysis. In another study, these maleimide-terminated polymers were efficiently conjugated to salmon calcitonin via an N-terminal cysteine to afford peptide–polymer conjugates with improved half-life and resistance to metabolism [16]. In a subsequent study, thiol-functionalized aptamers were conjugated to these polymers in order to improve the *in vivo* residence time of these small and highly charged molecules that

are prone to rapid renal elimination [17]. The coupling of disulfide-modified, 25-base DNA aptamer to maleimide-terminated polymers was achieved in high yields (70–80%) with tris[2-carboxyethyl]phosphine hydrochloride (TCEP) as reducing agent at pH 4. The effect of the structure and conformation of the PEG polymers on the binding affinity of the aptamer toward its target glycoprotein was investigated.

The methodology was thereafter extended to obtain glycopolymers that could also be conjugated with thiol-group-containing proteins to afford glycoprotein conjugates [18]. Maleimide-terminated polymers containing sugar units as pendant groups were synthesized by one of the two routes (Scheme 5.6). A hydrophobic polymer containing two orthogonally reactive groups, namely, a maleimide group at the chain end and the alkyne groups as pendant side chains, was synthesized. A silyl-protected alkyne-based monomer was used to avoid undesirable side reactions during polymerization. Removal of the silyl groups was efficiently achieved using tetrabutyl ammonium fluoride (TBAF) to yield the desired pendant groups with terminal alkyne units. A Huisgen-type click reaction using the copper-catalyzed azide-alkyne $[3 + 2]$ cycloaddition was used to modify the side chains with azide-containing sugar molecules.

Velonia and Haddleton utilized these polymers to fabricate protein–polymer conjugate-based giant amphiphiles [19]. Clickable protein–polymer conjugates were obtained by conjugation of thiol-containing BSA with polymers containing a maleimide group at their chain end and reactive side chains, which could be modified using the copper-catalyzed Huisgen-type $[3 + 2]$ azide–alkyne cycloaddition reaction (Scheme 5.7). A solketal methacrylate monomer, a trimethylsilyl-protected alkyne monomer, and a fluorescent-dye-containing monomer were copolymerized using the furan-protected maleimide-containing ATRP initiator. The solketal-based monomer was used to provide hydrophilicity to the polymer after post-polymerization hydrolysis of the ketal group. The silyl-protected monomer was used to enable functionalization of the polymer by the copper-catalyzed azide–alkyne cycloaddition reaction, after removal of the silyl protection group. The dye molecule containing the methacrylate monomer was incorporated into the copolymer in ≤ 1 mol% as a fluorescent tag. The hydrophilic polymer was conjugated to BSA to obtain the protein–polymer conjugate. Alkyl $(C_{10}H_{21}N_3)$ and benzyl $(C_7H_7N_3)$ azides were clicked onto the alkyne groups on the polymer component of the protein–polymer conjugate using $CuSO_4$/sodium ascorbate as catalyst in phosphate buffer at pH 7.4 at 7 °C for two days. During the course of the reaction, the hydrophobic character of the polymeric component increased as a result of the attachment of alkyl side chains. The reaction mixtures became opaque because of the formation of aggregates composed of amphiphilic protein–polymer conjugates.

Most of the early work relating to the synthesis of maleimide-terminated copolymers involved the use of methacrylate-based monomers. Synthesis of a styrene-based telechelic polymer containing maleimide groups at both chain ends was reported by Maynard and coworkers [20] (Scheme 5.8). The synthetic strategy involved the synthesis of a diene-protected maleimide unit containing styrene polymer using ATRP. Thus the obtained polymer will have a diene-protected
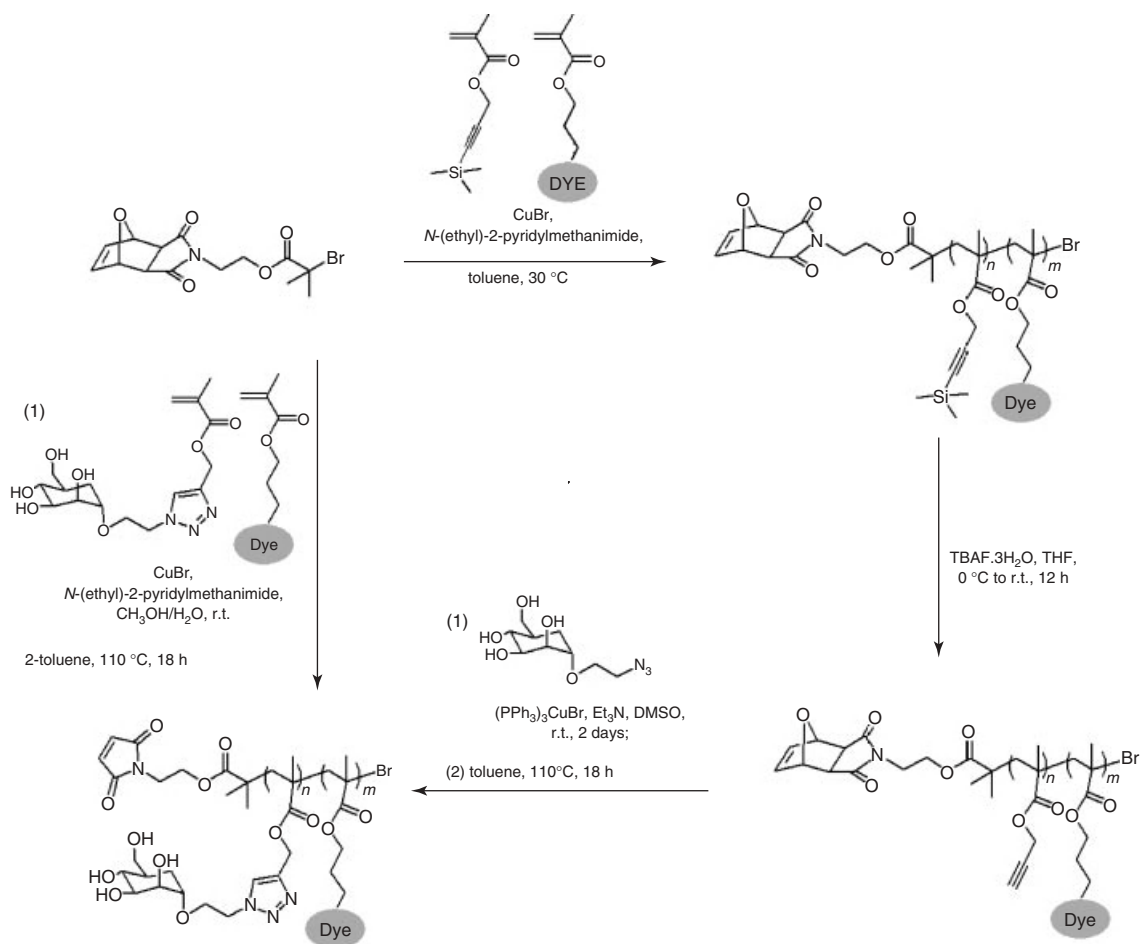
Scheme 5.6 Synthesis of maleimide end-functionalized glycopolymers.
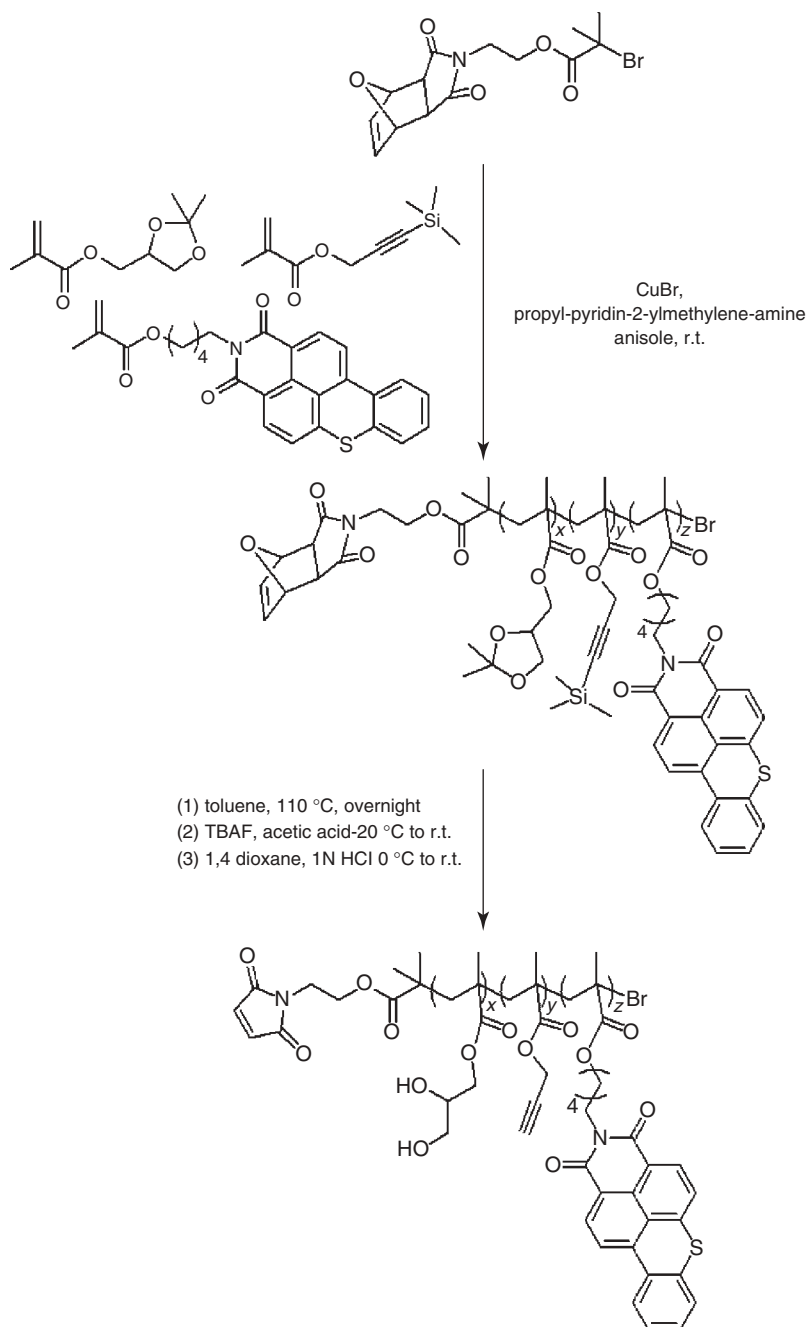
Scheme 5.7 Synthesis of maleimide end-functionalized polymers with clickable side chains utilized to produce protein–polymer amphiphiles.
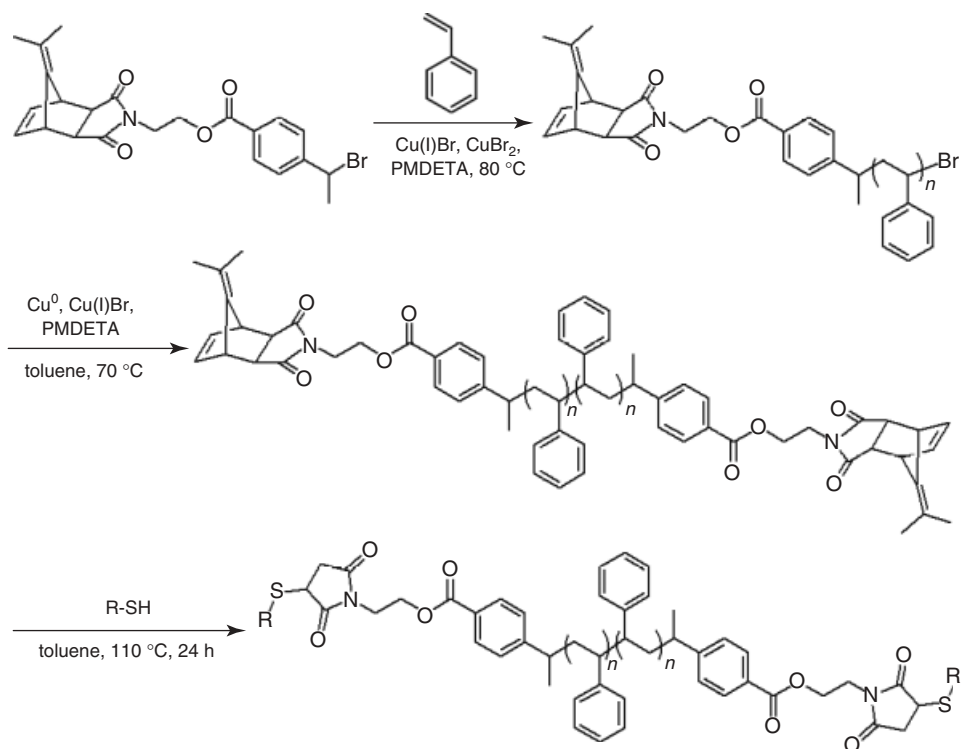
Scheme 5.8 Synthesis of styrene-based telechelic polymers containing the dimethylfulvalene−maleimide cycloadduct.

maleimide unit at one of the chain ends, while the other chain end will contain a halogen such as bromine. A Cu(I)-induced radical−radical polymer chain coupling, namely, the atom-transfer coupling (ATR) reaction, would provide the desired telechelic polymer. Interestingly, a furan-protected, maleimide-based initiator was unable to provide well-defined styrene-based polymers. This was presumably due to the instability of the furan−maleimide cycloadduct under the polymerization conditions around 80 °C. In order to achieve a cycloadduct that would undergo the retro Diels−Alder reaction at a higher temperature than the polymerization temperature, the dimethylfulvalene protecting group was used. The use of a dimethylfulvalene−maleimide cycloadduct-based initiator yielded the desired polystyrene polymer. Polymer chain coupling under ATR conditions resulted in dimethylfulvene-protected, maleimide-containing, styrene-based telechelic polymers. These polymers were functionalized by thiol-containing molecules such as benzyl mercaptan and *N*-acetyl-L-cysteine methyl ester via *in situ* removal of the dimethylfulvalene group and Michael addition by refluxing in toluene at 110 °C. This example highlights the versatility of the use of the Diels−Alder reaction as a protection step where the thermal stability of the masked maleimide group can be tuned by choosing the appropriate capping diene moiety.

The use of controlled living free radical polymerization techniques not only provides polymers with control over molecular weights and narrow polydispersity but, as demonstrated in the examples above, also allows facile installation of desirable end-group functionalities by the choice of appropriate initiators. An additional advantage of these polymerization techniques is that a variety of different macromolecular architectures such as star and graft copolymers can be obtained by using multifunctional initiators. In a recent study, Sanyal and coworkers [21] used the Diels–Alder/retro Diels–Alder strategy in combination with ATRP to prepare multiarm star polymers bearing a thiol-reactive maleimide core (Scheme 5.9). Polymers were synthesized with ATRP, a controlled living polymerization technique, which, as demonstrated in earlier examples, provides an excellent method to place the desired functional group at the polymer chain ends. Dendritic ATRP initiators containing a furan-protected maleimide unit at their focal point were used to obtain multiarm star polymers with a thiol reactive core. Two-, four-, and eight-arm polymers were synthesized using methyl methacrylate (MMA), poly(ethylene glycol) methylether methacrylate (PEGMA), and *tert*-butylacrylate (*t*-BA) as monomers. After the polymerization step, deprotection of the maleimide functional group was achieved by simply heating the polymers at 100 °C under vacuum. Efficient postfunctionalization of the maleimide unit at the core of these multiarm polymers was demonstrated by conjugating a thiol-containing tripeptide glutathione.

RAFT polymerization is another widely used controlled polymerization technique that allows synthesis of polymers that have well-defined structures with low-molecular-weight distributions [22]. Since ATRP requires the use of a metal catalyst such as Cu(I), the polymers obtained oftentimes contain residual metal impurities, which can interfere with further application of these polymers. RAFT polymerization provides a good metal-free alternative for synthesizing polymers in a controlled manner. In RAFT polymerization, introducing a functional group to the polymer end is accomplished by choosing a functional group containing a CTA. Maynard and coworkers [23] investigated the synthesis of maleimide end-functionalized polymers via RAFT polymerization to obtain polymers capable of site-specific conjugation to free cysteine residues on proteins. A trithiocarbonate CTA containing a furan-protected maleimide group was used during polymerization of poly(ethylene glycol) methylether acrylate in dimethyformamide (DMF) at 60 °C to yield poly(ethylene glycol)acrylate (PEGA)s (Scheme 5.10). Postpolymerization retro Diels–Alder reaction provides polymers containing thiol-reactive maleimide group at chain ends. The maleimide groups in the obtained polymers were shown to undergo effective conjugation to thiol-containing proteins.

The majority of the protein–polymer conjugates reported in the literature consist of examples where one protein is bound to one or more polymers. Dimeric and multimeric protein–polymer conjugates, where more than one protein is bound to a single macromolecule, would allow fabrication of protein multimers commonly found in biological systems. Scarcity of such examples has probably been due to the lack of synthetic strategies, until recently, to obtain well-defined polymers with a precise number of reactive groups at chain ends. RAFT polymerization yields polymers that are amenable to facile end-group modification. Perrier and coworkers
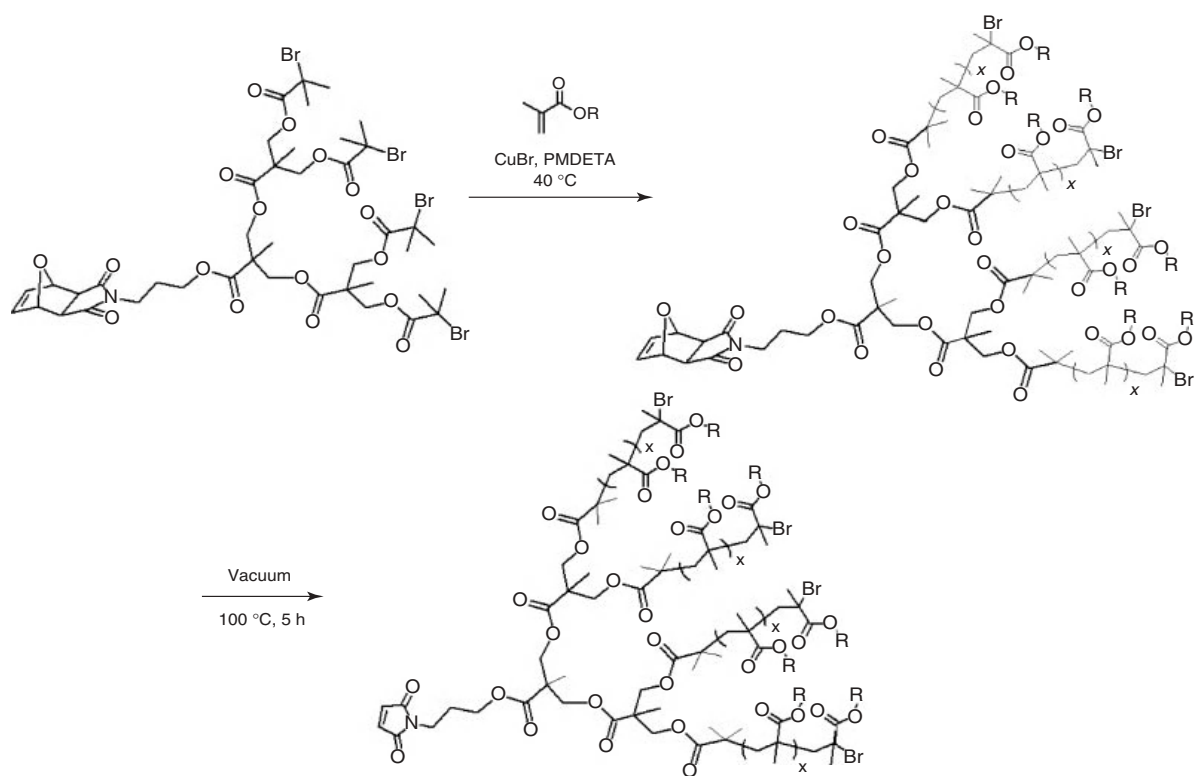
Scheme 5.9 Synthesis of multiarm polymers containing a thiol-reactive maleimide functional group at the core.
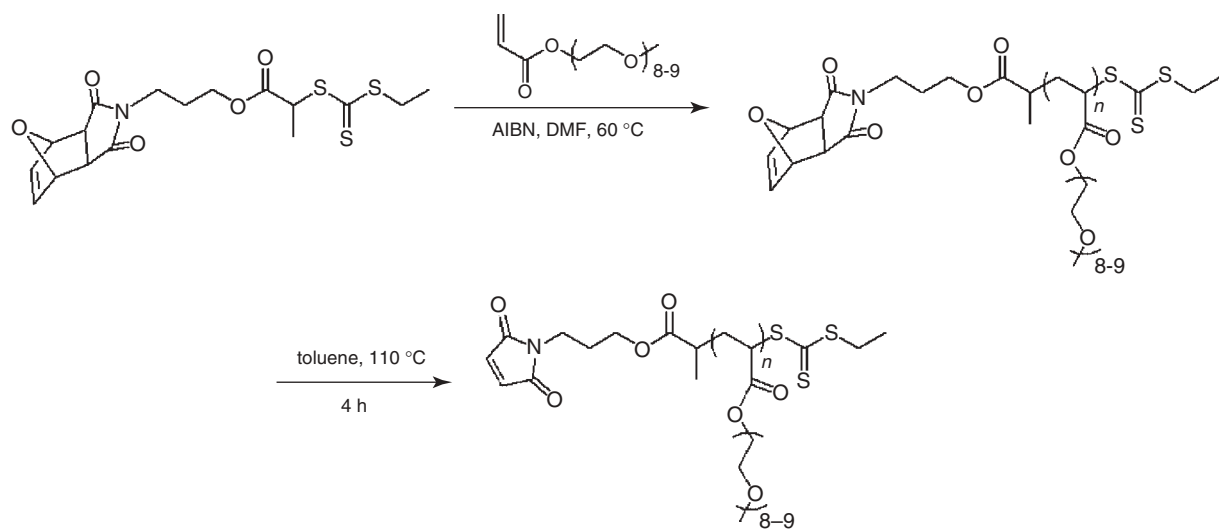
Scheme 5.10 Synthesis of maleimide group-terminated polymers via RAFT polymerization.

[24] demonstrated that the RAFT end group can be replaced by another functional group through a radical cross-coupling reaction with azo-based radical initiators. Maynard and coworkers [25] used this strategy to synthesize telechelic maleimide end-functionalized polymers to fabricate homodimeric protein–polymer conjugates (Scheme 5.11). Copolymerization of NIPAM and a dye-appended monomer from a bistrithiocarbonate CTA yields thermoresponsive polymers. The telechelic trithiocarbonate end-functionalized polymer thus obtained is heated at 70 °C in the presence of an excess amount of an azo initiator containing a furan-protected maleimide group. Retro Diels–Alder reaction is not observed at this temperature, thus preventing any possible side reactions leading to cross-linking of polymers during the end-group exchange. Maleimide units are unmasked by the removal of the furan protection by heating these polymers at 120 °C under vacuum. The obtained polymers containing maleimide groups at both chain ends were reacted with a V131C mutant T4 lysozyme containing one free cysteine residue. SDS-PAGE analysis coupled with fluorescence quantification revealed that a mixture of monomeric (79%) and dimeric (21%) protein–polymer conjugates were obtained. Formation of the monomeric conjugate was attributed to a hindered macromolecular reaction. Filtration using a cation-exchange resin was utilized to separate the monomer and dimeric conjugates.

The methodology was extended by Maynard and coworkers [26] to synthesize maleimide end-functionalized star polymers. Star polymers with thiol-reactive maleimide groups at chain ends of each polymeric arm were designed to obtain multimeric protein–polymer conjugates. A four-arm poly(*N*-isopropylacrylamide) (pNIPAAm) star polymer was synthesized via RAFT polymerization in the presence of a tetrafunctional CTA (Scheme 5.12). Furan-protected maleimide functional groups were installed at the chain ends by heating the trithiocarbonate chain end-terminated polymer in the presence of an excess of an appropriate azo initiator. A four-arm pNIPAAm with thiol-reactive maleimide groups at chain ends was obtained by the removal of the furan protecting groups by heating the polymer at 105 °C in vacuum for 2 h. Attachment of V131C T4L lysozyme onto these star polymers was investigated. It was found that, on average, three proteins were conjugated to each of the tetra-arm star polymers. It was suggested that increased steric hindrance around the star polymer core or hydrolysis of the maleimide group under the reaction conditions employed for conjugation could be the reason for lower than expected protein conjugation.

An elegant extension of the above-mentioned approach by Maynard and coworkers allowed the synthesis of heterotelechelic polymers using RAFT polymerization [27]. In order conjugate two different biomolecules to polymer ends, telechelic biotin-maleimide pNIPAAm polymers were prepared (Scheme 5.13). RAFT polymerization of NIPAAm in the presence of a biotinylated-trithiocarbonate-based CTA was conducted to yield polymers bearing biotin at one of the chain ends and a trithiocarbonate group at the other end. The trithiocarbonate group was replaced with a furan-protected maleimide moiety using an appropriate azo initiator via a radical cross-coupling reaction. Maleimide group activation was then performed via the retro Diels–Alder reaction to free the masked maleimide group. Two different
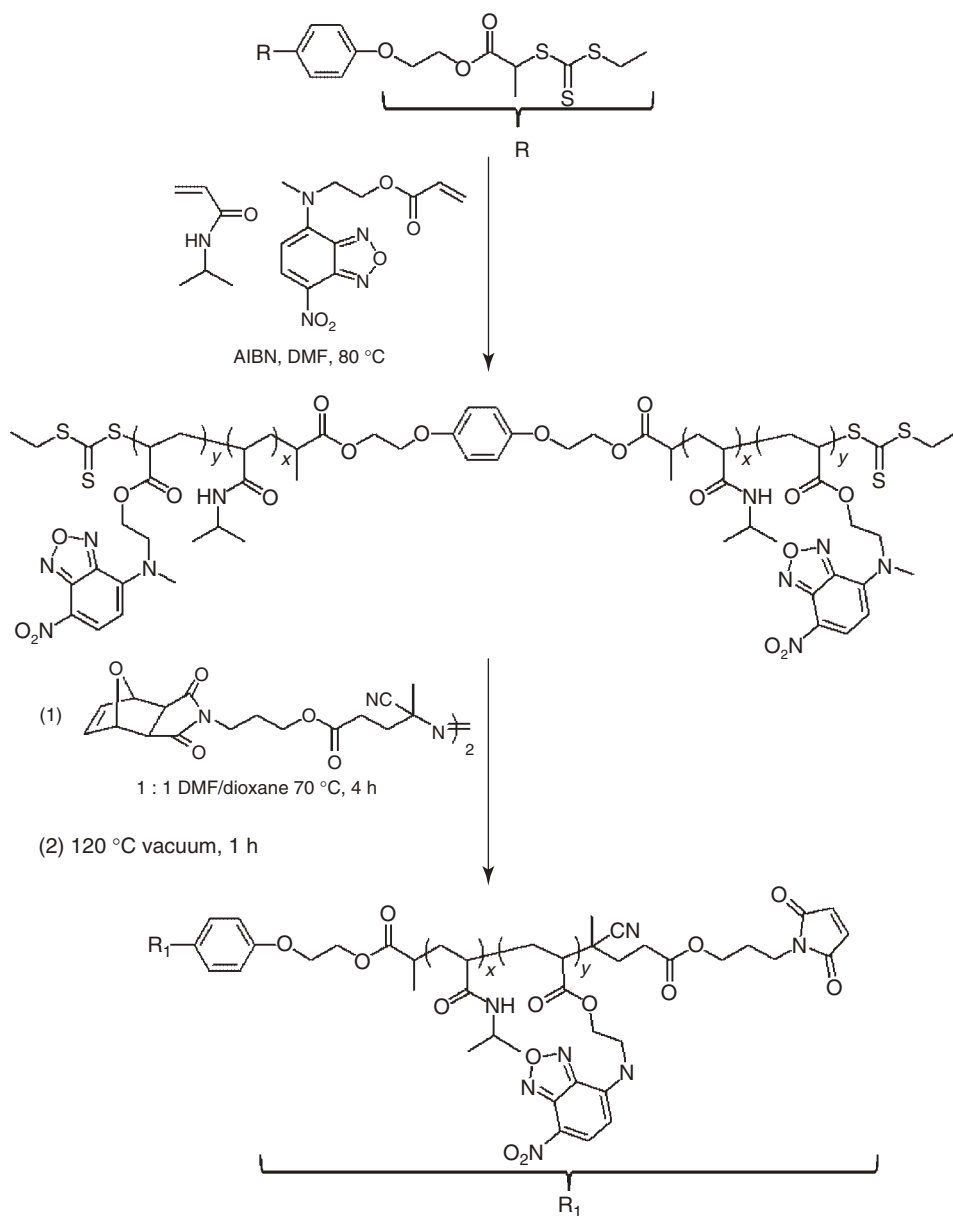
Scheme 5.11 Synthesis of telechelic polymers containing the maleimide end group via RAFT polymerization.
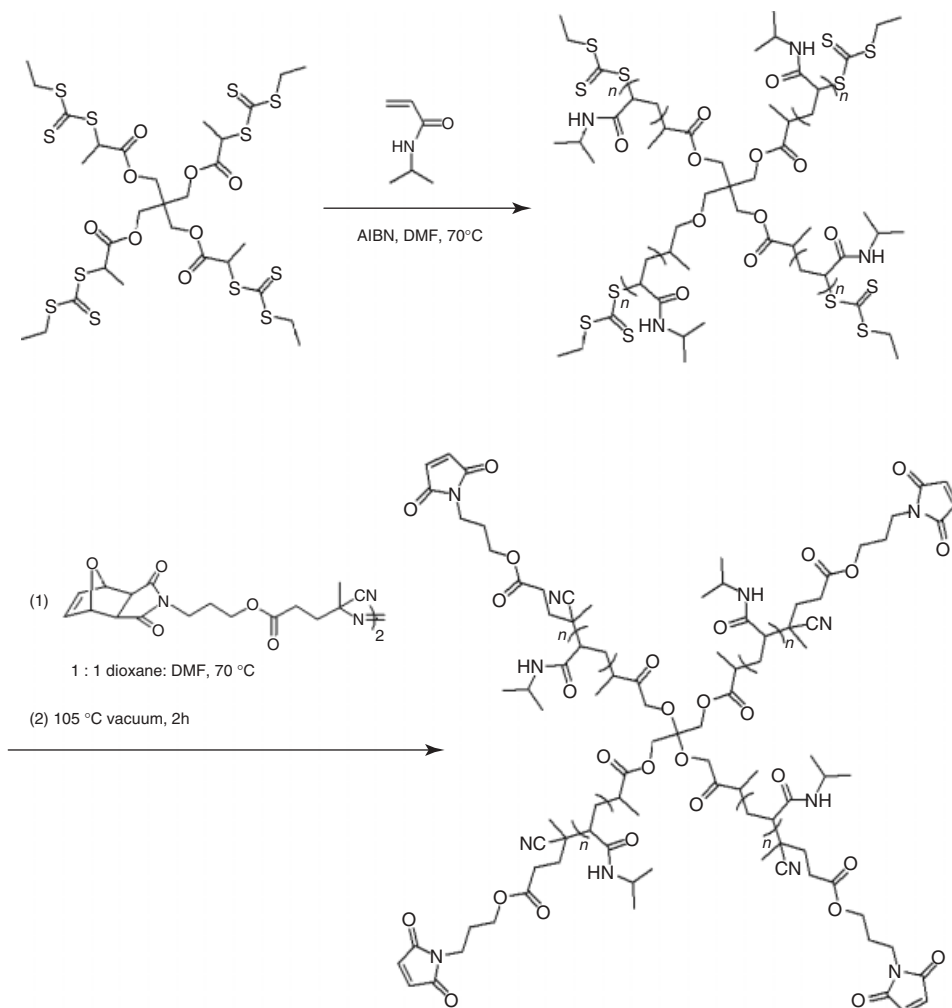
Scheme 5.12 Synthesis of four-armed maleimide chain-end functional star polymers.

proteins, namely, streptavidin and BSA, were successfully conjugated to the polymer ends to obtain protein–heterodimer conjugates. Streptavidin is a protein that has an extraordinarily high affinity for biotin. As mentioned earlier, BSA bears a cysteine residue that couples to the maleimide unit through thiol–ene conjugation.

Recently, this construct was elaborated to fabricate a heterotelechelic biotin–maleimide polymer containing a cleavable disulfide bond (Scheme 5.14) [28]. Conjugation of a mutant V131C T4 lysozyme to the maleimide end afforded protein–polymer conjugates that could bind to a streptavidin-coated surface through the biotin moiety at the polymer chain end. Successful reduction of the disulfide bond to release the protein from the surfaces in the presence of either TCEP hydrochloride or glutathione was demonstrated.
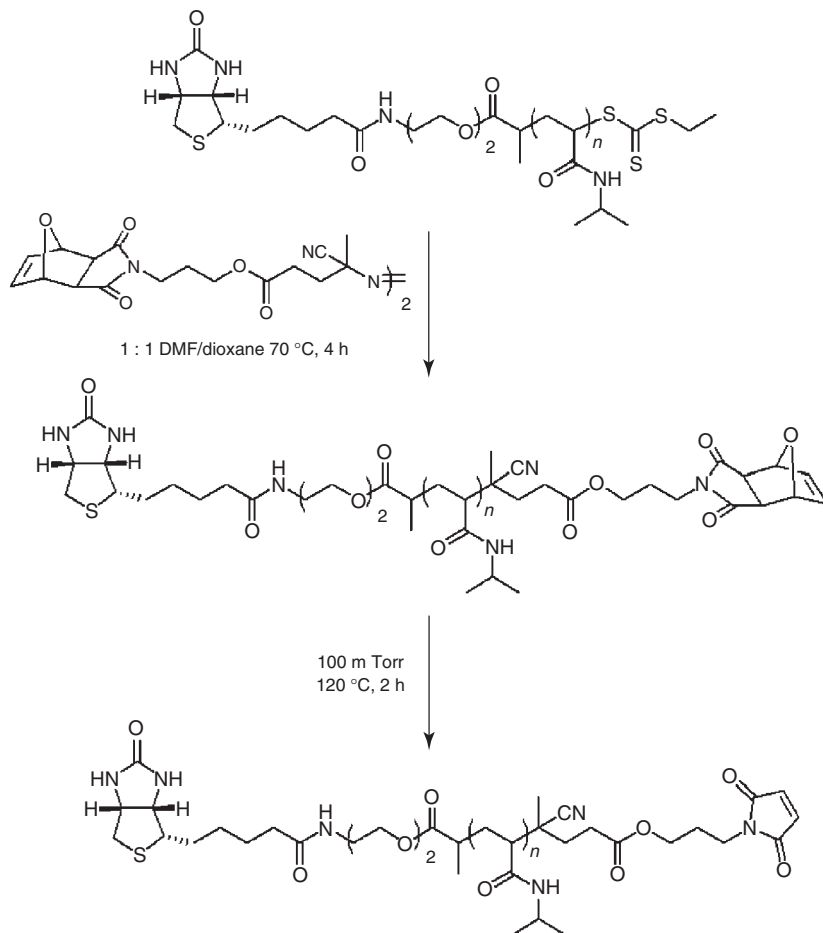
Scheme 5.13 Synthesis of heterotelechelic biotin−maleimide-functionalized polymers.

In recent years, the Diels−Alder/retro Diels−Alder reaction-based strategy to obtain maleimide-appended polymers has also been combined with non-radical-based living polymerization techniques such as ROP. This combination allows the facile preparation of functionalizable, biocompatible, and biodegradable polyesters, which find applications in areas such as drug delivery and fabrication of tissue engineering scaffolds. In a seminal study, Dove and coworkers [29] described the synthesis of poly(lactide)s via organocatalytic ROP of lactide monomers using a furan-protected maleimide-containing alcohol initiator (Scheme 5.15). The obtained maleimide-terminated PLAs were amenable to functionalization with thiol-containing molecules under mild conditions via the metal-free thiol−maleimide nucleophilic click reaction. Importantly, size-exclusion chromatography (SEC) and matrix-assisted laser desorption/ionization time-of-flight (MALDI-ToF) mass spectrometry analysis proved that no degradation of the

(1)   NIPAAM, AIBN, DMF 70 °C, 4 h

(2)

1 : 1 DMF/dioxane 70 °C, 4 h

120 °C, vacuum
4 h
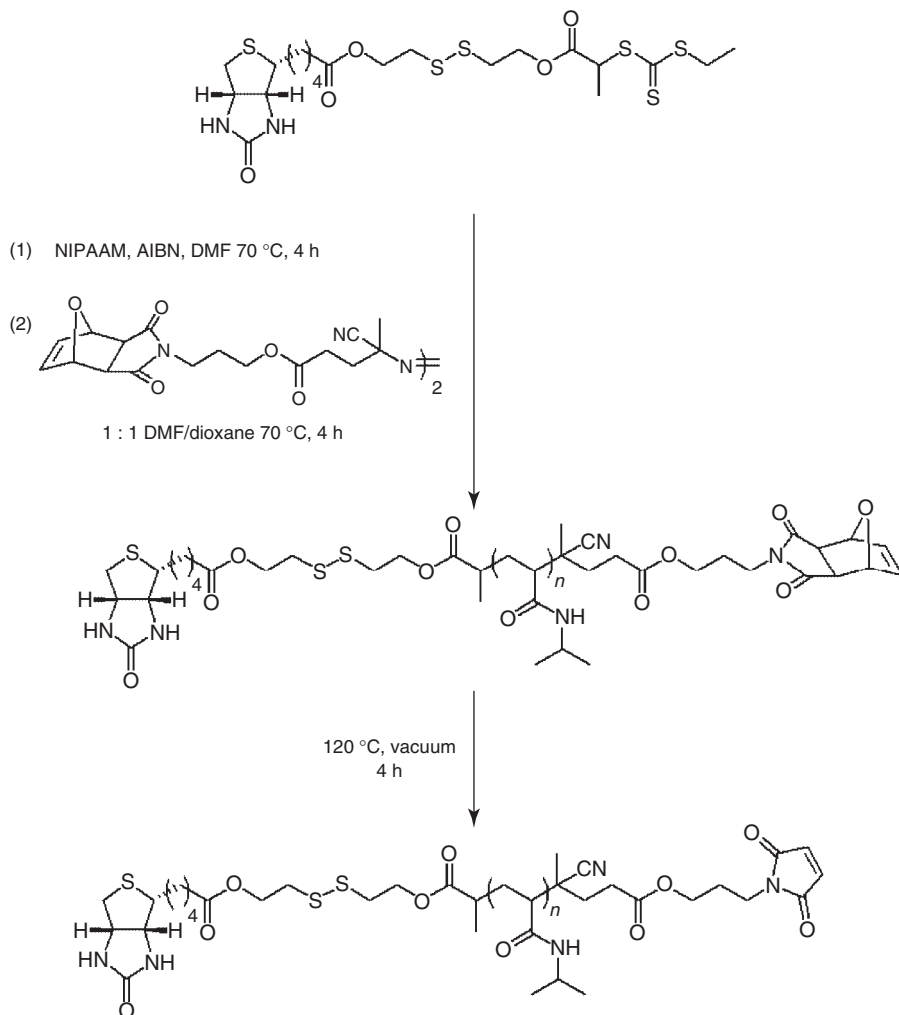
Scheme 5.14 Synthesis of cleavable heterotelechelic biotin–maleimide-functionalized polymers.

sensitive polyester backbone occurred during these conjugation reactions. Furthermore, these maleimide-terminated poly(lactides) were conjugated with molecules containing two or three thiol groups to obtain telechelic and three-arm polymers.

Dove and coworkers also demonstrated that ROP of lactide monomer can be carried out using aluminum methyl complexes using isopropyl alcohol as initiating species [30]. After polymerization, while the initiating species forms one end of the polymer chain, the other chain end is an aluminum alkoxide species that can be quenched with a judiciously chosen acid chloride to install
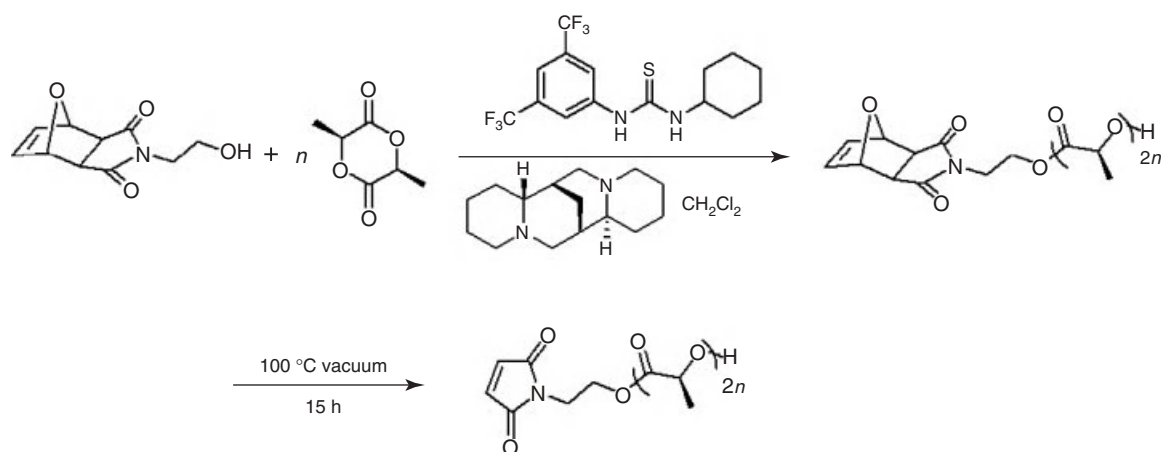
Scheme 5.15 Synthesis of thiol-reactive maleimide group-terminated PLA polymers.
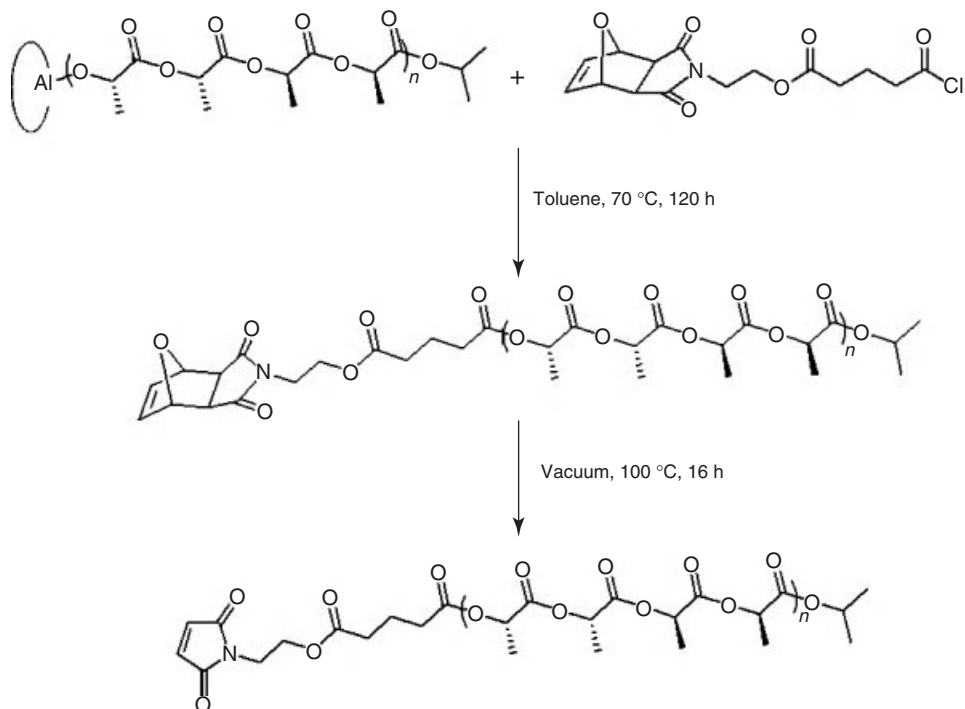
Scheme 5.16 Synthesis of thiol-reactive maleimide group–terminated PLA polymers.

a desirable functional group (Scheme 5.16). Post-polymerization quenching with acid chloride bearing a furan-protected maleimide unit yields polymers terminated with protected maleimide moiety. Retro Diels–Alder reaction removes the furan protection to furnish PLAs with maleimide group at chain ends. Linear, telechelic, and star-shaped stereoregular PLAs with maleimide groups at chain termini were obtained using this methodology. Conjugation of thiophenol to these polymers was accomplished under mild conditions, without any deterioration of the polyester polymers.

Dove and coworkers [31] extended the methodology to prepare telechelic maleimide-containing stereoregular PLAs as precursors for obtaining PLA macrocycles (Scheme 5.17). Aluminum complex-catalyzed ROP of lactide initiated from an alcohol-containing furan-protected initiator containing the maleimide group, on post-polymerization quenching with an acid chloride derivative of furan-protected maleimide cycloadduct, provides telechelic PLAs bearing protected maleimide units at both chain ends. Retro Diels–Alder reaction under vacuum at 100 °C was utilized to obtain PLAs with maleimide group at both chain ends. Since these polymers were now prone to "thiol–ene" reaction from both ends, cyclization reaction with a dithiol in the presence of Et$_3$N yielded cyclic stereoregular PLAs.
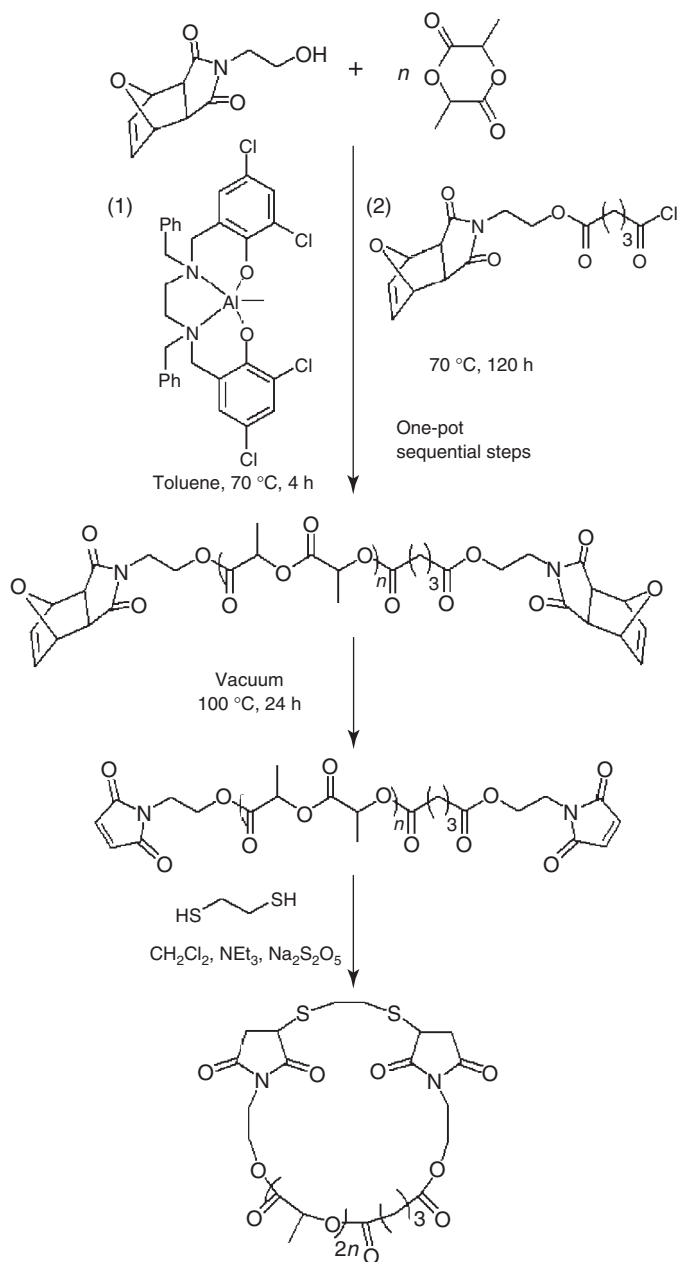
Scheme 5.17 Synthesis of cyclic PLA polymers via maleimide-terminated telechelic polymers.

5.4.2
Polymers Containing Maleimide Groups as Side Chains

Polymers provide scaffolds that enable the design of multivalent and multifunctional systems that are similar to the ones frequently encountered in biological macromolecules. This is achieved by the attachment of multiple copies of the same or different functional molecules as side chains dangling off the polymeric backbone. A simple way to achieve this is through the use of efficient post-polymerization functionalization. Varying the degree of functionalization allows facile preparation of a library of polymers that are derived from the same parent polymer. A variety of reactive functional groups such as activated esters that allow the attachment of amine-containing molecules, as well as alkyne and azide groups that allow functionalization via the copper-catalyzed Huisgen type click chemistries, have been incorporated into polymers as pendant side chains. Introduction of the maleimide functional group as side chains would expand the tool box of reactive polymers. Until recently, such polymers were not realized because of the lack of efficient strategies to incorporate the maleimide functional group into polymeric materials. The use of monomers containing a diene-protected maleimide unit allows one to obtain polymers that have the maleimide group precursor units as side chains. Post polymerization, retro Diels–Alder cycloreversion reaction allows easy removal of the diene capping functional groups to furnish polymers appended with reactive maleimide units. As mentioned earlier, the maleimide units are protected to circumvent any side reactions with the electron-deficient reactive double bond during the polymerization.

Bailey and Swager [32] reported the synthesis of maleimide-appended conjugated poly(phenyleneethynylene)s (PPEs) via the palladium-catalyzed Sonogashira–Hagihara reaction. PPEs have the ability of energy funneling and transport, which makes them useful in sensor applications. Appropriate functionalization of these polymers with ligand molecules capable of specific recognition will enable fabrication of specific sensors. The pendant maleimide groups provide an efficient handle to decorate the polymer using the thiol–ene reaction. A furan-protected monomer containing a maleimide functional group was synthesized to obtain the desired polymers (Scheme 5.18). During the polymerization step, masked aryl diiodides containing the maleimide group were cross-coupled with dialkynes in the presence of a palladium catalyst. Attempts of polymerization with unmasked maleimide monomer cross-coupling polymerization resulted only in the formation of short-chain oligomers with side reactions. Maleimide groups were deprotected by removing furan moieties under thermal conditions. The postfunctionalization efficiency of maleimide-containing polymers was investigated by conjugating a thiol-modified carboxy-X-rhodamine (ROX) dye. Effective conjugation was demonstrated via absorbance, fluorescence spectra, and gel permeation chromatography (GPC) analyses. The Diels–Alder/retro Diels–Alder reaction-based strategy affords thiol-reactive PPEs, which enables the preparation of diverse libraries of PPEs with pendant functionalities.
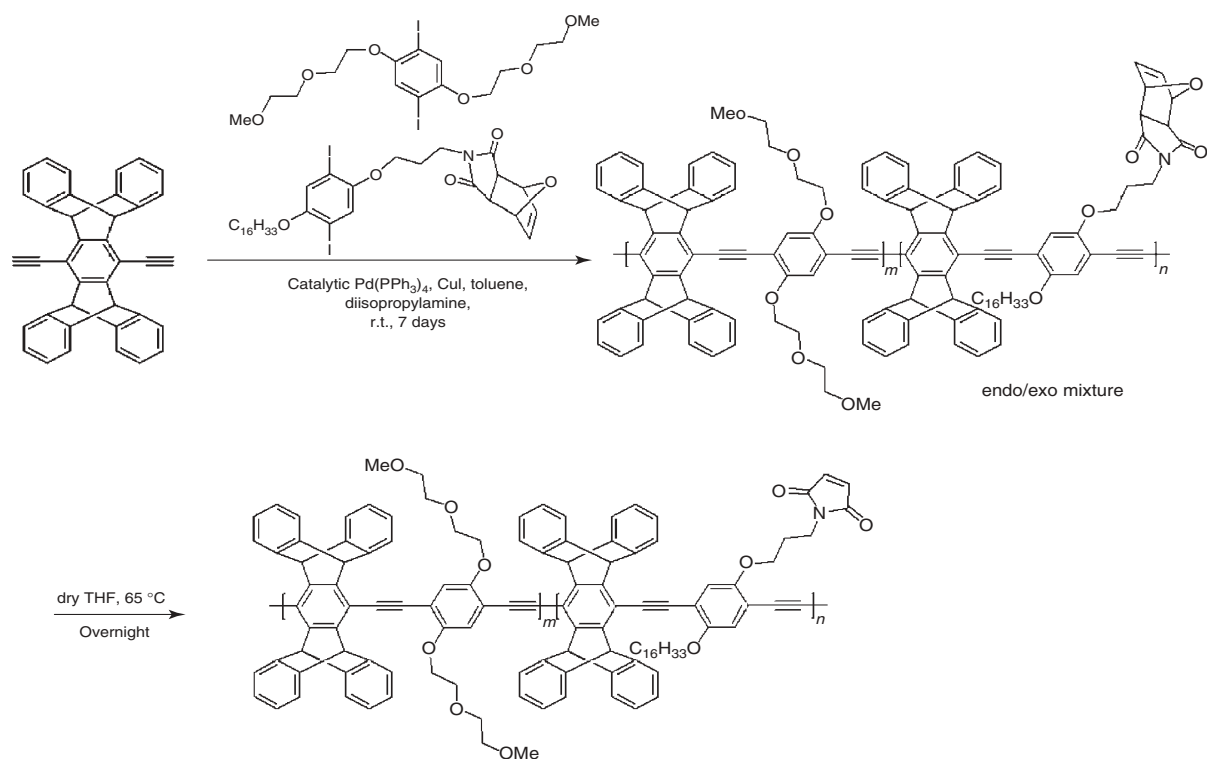
Scheme 5.18 Synthesis of maleimide-containing poly(phenyleneethynylene) polymer.
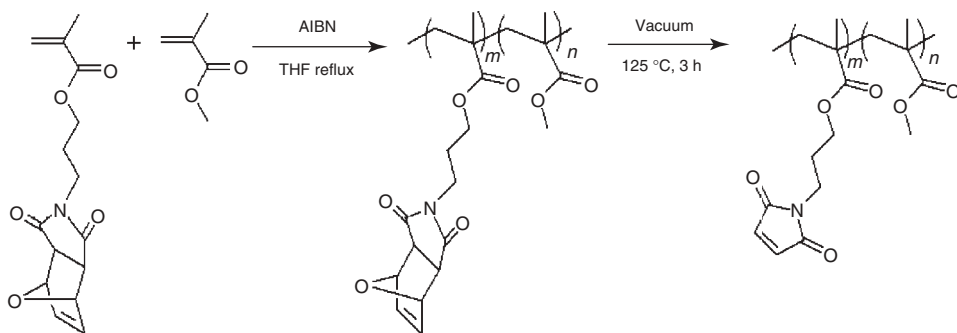
Scheme 5.19 Synthesis of methacrylate-based polymers containing pendant maleimide groups.

Synthesis of methacrylate-based polymers containing thiol-reactive maleimide units as side chains was reported by Sanyal and coworkers [33] by utilization of a monomer containing a masked maleimide group . The maleimide functional group in a methacrylate monomer was protected by a furan group through a Diels−Alder reaction (Scheme 5.19). A variety of copolymers containing pendant masked maleimide groups were prepared via 2,2'-azobis(isobutyronitrile) (AIBN) initiated polymerization. Post-polymerization retro Diels−Alder reaction by heating the polymer removes the furan protecting groups in a quantitative manner to unmask all the side-chain maleimide units to their reactive form.

As an extension of this work, clickable thiol-reactive polymeric micropatterns were obtained using thermal nanoimprint lithography (NIL) of copolymers containing masked maleimide functional groups as side chains [34]. These patterns can be utilized for the generation of functional and biofunctional interfaces by postfunctionalization with thiol-containing molecules and biomolecules. A copolymer synthesized using the furan-protected, maleimide-containing methacrylate monomer, MMA, and poly(ethyleneglycol) methacrylate was used to produce reactive patterns (Figure 5.1). The poly(ethyleneglycol)-based monomer was added to provide these surfaces with antibiofouling characteristics. The polymer was spin-coated onto a surface, and thermal NIL was performed at 175 °C under 400 psi for 5 min. The high temperature during patterning led to deprotection of the maleimide units to directly furnish thiol-reactive polymeric micropatterns. The efficient derivatization of these reactive patterned surfaces was demonstrated by attachment of thiol-containing fluorescent dyes. These patterns could be easily modified with thiol-containing carboxylic acid ligands to enable anchoring of magnetic nanoparticles. Decoration of the patterns with thiol-containing RGD peptides enabled immobilization of cells onto these surfaces with improved cellular adhesion and alignment as a result of their topography.

Polystyrene polymers containing maleimide groups on their side chains were obtained by utilization of a novel styrenic monomer containing a masked maleimide unit (Scheme 5.20) [35]. AIBN-initiated free radical polymerization was used for the synthesis of copolymers containing masked maleimide groups as side chains.
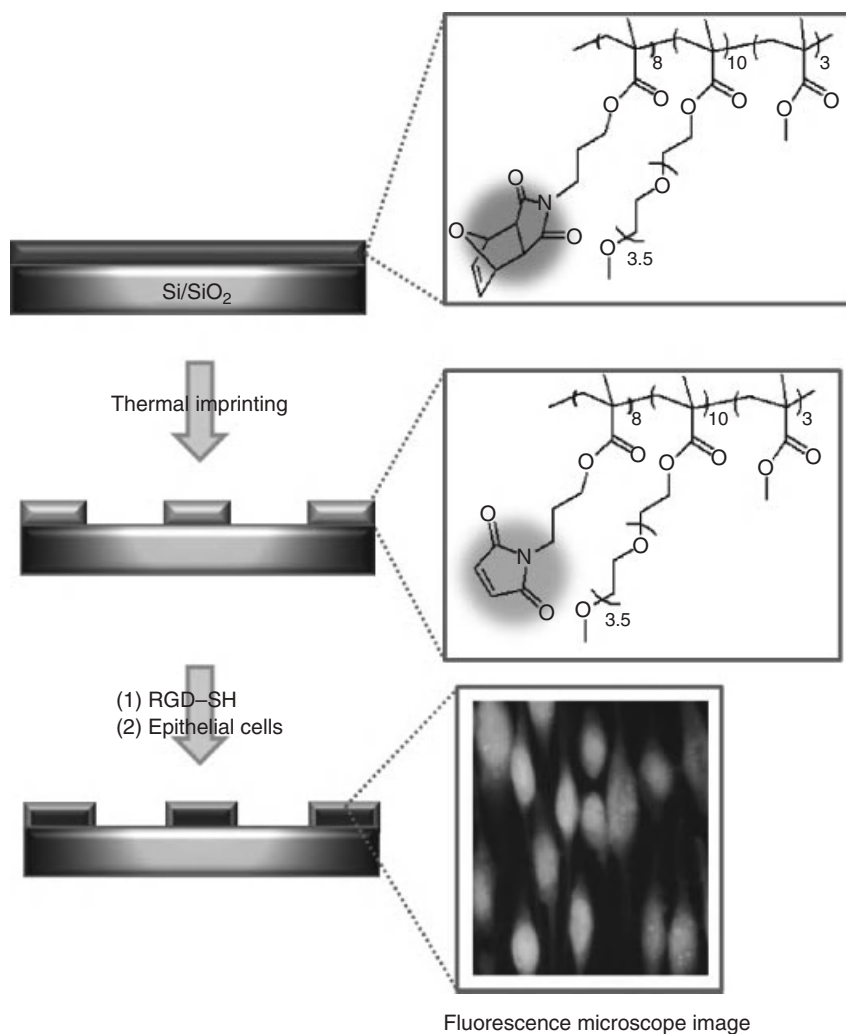
Figure 5.1 Synthesis of thiol-reactive micropatterns via thermal nanoimprint lithography.

The maleimide groups in the side chain of the polymers were unmasked into their reactive form by thermal cycloreversion. Orthogonally functionalizable copolymers were obtained by the copolymerization of the maleimide-based monomer with either *N*-hydroxysuccinimide-containing or an alkene-containing styrene-based monomer. The former combination of monomers yielded copolymers that were orthogonally reactive toward thiol- and amine-containing molecules, and the latter combination yielded copolymers containing two orthogonally thiol-reactive functional groups. This allowed sequential attachment of two different thiol-containing molecules onto the copolymers via the nucleophilic thiol–ene followed by the free radical thiol–ene click reactions.

(1) AIBN, 70 °C, THF
(2) toluene, 110 °C,
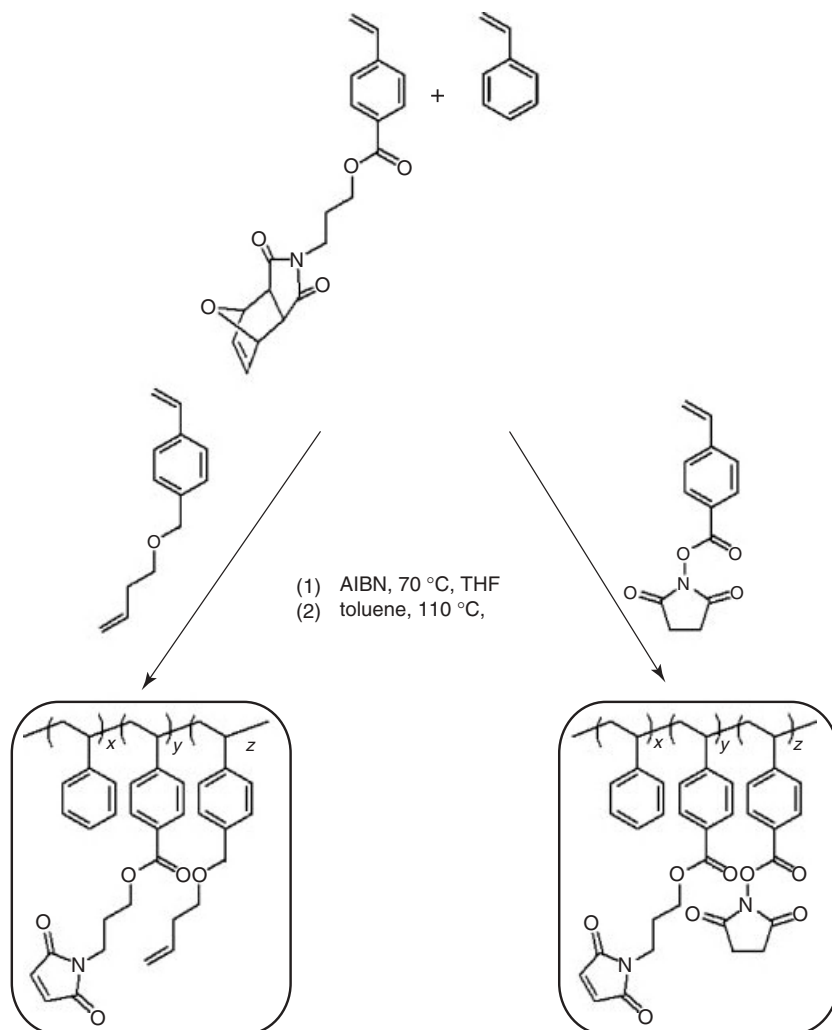
Scheme 5.20 Synthesis of maleimide-containing "orthogonally" functionalizable copolymers.

Functional polyurethanes reactive toward the thiol–ene conjugations were recently reported by Du Prez and coworkers [36]. Polyurethanes were synthesized by the addition of diisocyanates with diols under tin-catalyzed reaction conditions (Scheme 5.21). A furan-protected, maleimide-containing diol monomer and 1,4-butanediol was added to hexamethylenediisocyanate in ethylacetate and heated to 50 °C in the presence of dibutyltin dilaurate catalyst to yield linear polyurethanes. The obtained polymers were heated at 100 °C under vacuum to yield aliphatic polyurethanes with pendant maleimide functional groups. Functionalization of these maleimide groups was conducted using a variety of thiols via
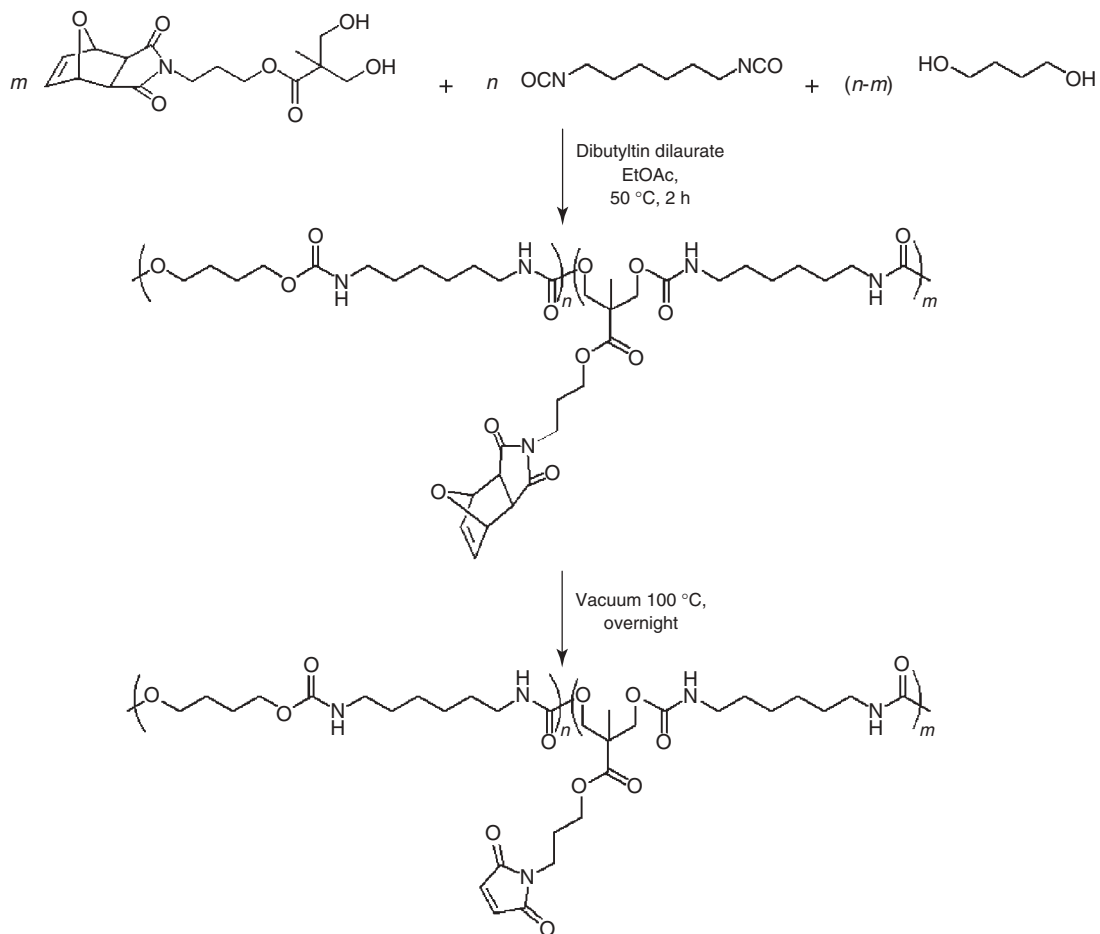
Scheme 5.21 Synthesis of pendant maleimide group-containing linear polyurethanes.

the Michael-addition reaction in the presence or an organobase triethylamine. At room temperature, the efficiency of coupling reaction was found to be around 75% in dimethylsulfoxide (DMSO), which could be increased to 92% at slightly elevated temperatures (50 °C) using *N*-methyl-2-pyrrolidone (NMP) as a solvent.

Facile functionalization of biodegradable polymers such as polyesters are highly desirable because these materials are used in a variety of applications ranging from fabrication of drug delivery systems to tissue engineering scaffolds [37]. Despite their widespread utilization for a variety of biomedical purposes, until recently, only a limited number of functionalizable poly(ester)s have been available [38]. Some of them undergo post-polymerization functionalization via the copper-catalyzed Huisgen-type click reaction. The presence of residual metal impurities and possible polymer degradation under these functionalization conditions necessitates the development of alternative ''metal-free'' approaches. Since the nucleophilic thiol−ene addition is accomplished under mild reaction conditions, it does not lead to degradation of fragile polymeric materials such as polyesters. Toward this end, a maleimide-containing thiol-reactive biodegradable polymer was synthesized by the organocatalyzed polymerization of a novel furan-protected maleimide-functional carbonate monomer (Scheme 5.22) [39]. Polymers obtained via 1,8-diazabicycloundec-7-ene (DBU) catalyzed ROP have pendant groups containing furan-protected maleimide units which, on being subjected to retro Diels−Alder reaction, yielded maleimide groups that were ready to react with thiol-containing molecules. Importantly, no degradation of these polyester-based copolymers was observed during the retro Diels−Alder reaction carried out at 100 °C under vacuum. Addition of 6-(ferrocenyl)hexanethiol and 1-hexanethiol was carried out to demonstrate that the maleimide units could be modified in a quantitative manner without any degradation of the parent polymers. The use of a maleimide-containing carbonate monomer with no furan protection led to the formation of cross-linked materials under the polymerization conditions, thus highlighting the importance of the protection−deprotection strategy.

5.4.3
Synthesis of Maleimide-Containing Hydrogels Obtained Using the Diels−Alder/Retro Diels−Alder Reaction-Based Strategy

Hydrogels are polymeric materials that are widely used in areas such as biomolecular immobilizations, tissue engineering, implant coatings, and drug delivery systems. Control of chemical attachment of molecules and biomolecules of interest is desirable for many applications. While considerable advancements have been made in the synthesis of functionalizable hydrogels, most of the strategies involve development of hydrogels that contain reactive functional groups such as activated esters that are compatible with free radical polymerization techniques. Recently, we demonstrated that the furan-protected, maleimide-containing methacrylate monomer can be used to fabricate hydrogels incorporating tailored amount of maleimide groups (Scheme 5.23) [40]. Interestingly, polymerization with a hydrophilic monomer such as PEGMA under high concentration leads to gelation.
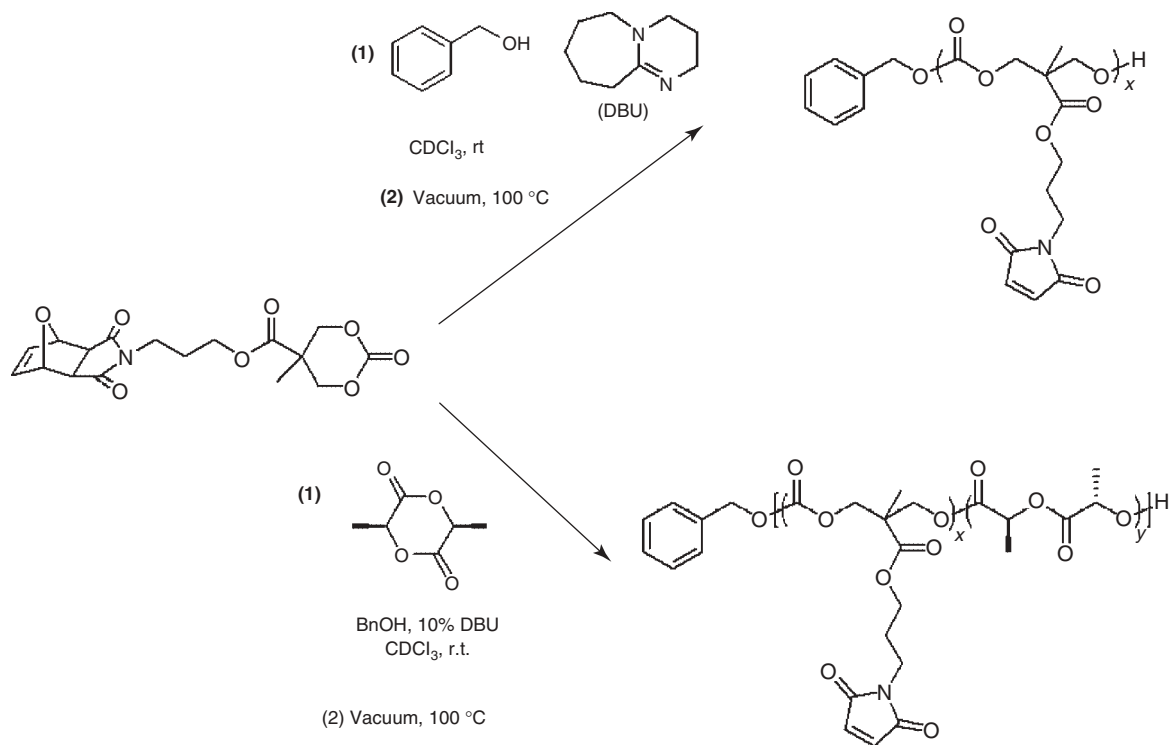
Scheme 5.22 Synthesis of pendant maleimide group-containing biodegradable polyesters.
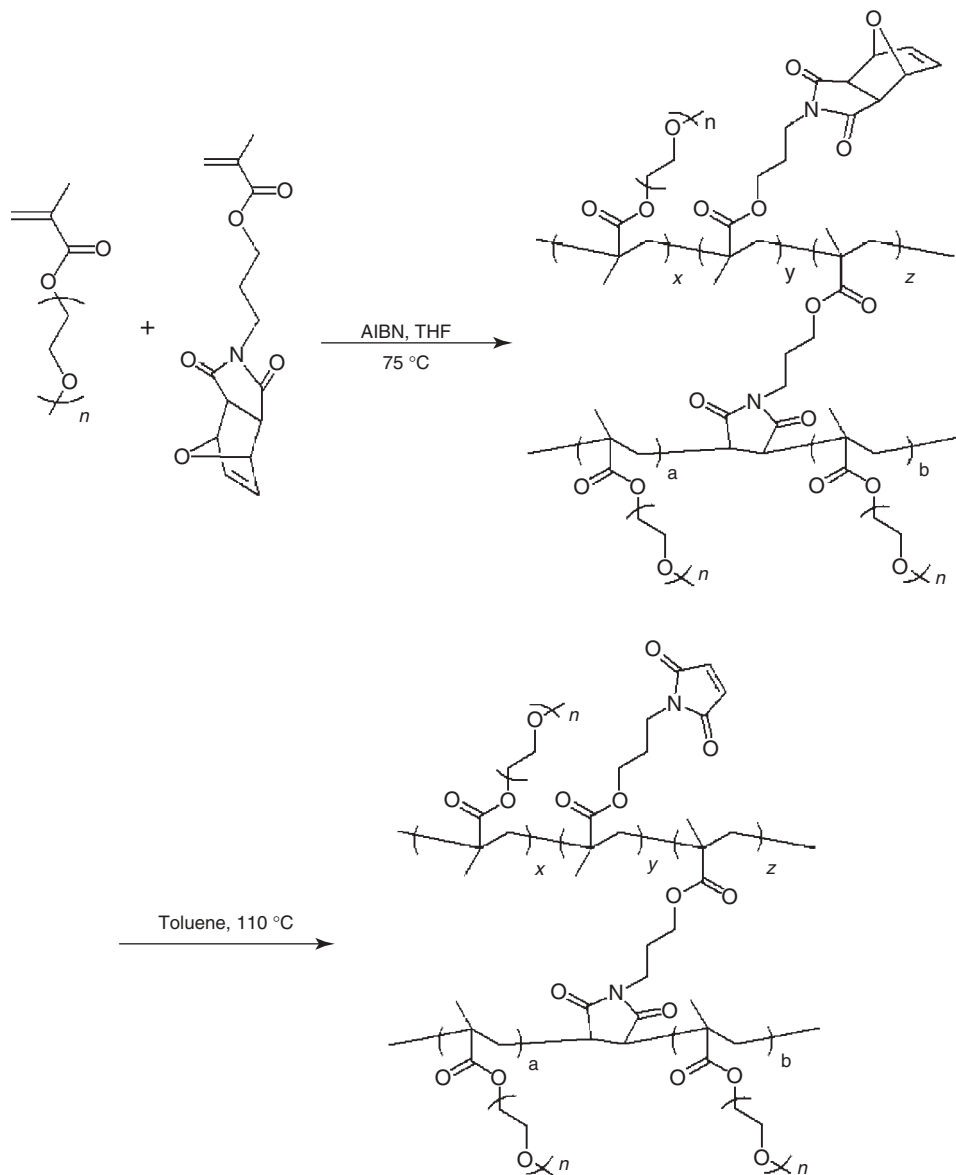
Scheme 5.23 The Diels–Alder/retro Diels–Alder reaction-based strategy for the synthesis of maleimide-containing, thiol-reactive hydrogels.

Gelation occurs presumably because of the slight amount of cross-linker generated *in situ* via the retro Diels–Alder reaction of the monomer under these conditions. Control experiments, where the monomer was designed so that it was unable to undergo a retro Diels–Alder reaction, led to soluble polymers. The formed hydrogels were heated to 110 °C to unmask all the maleimide groups. The amount of

maleimide groups in the hydrogel matrix could be tailored by varying the feed ratio of monomers during gelation. Varying the amount of reactive maleimide groups in the hydrogels could be used to control the level of bioimmobilization. Hydrogels with different maleimide content were modified by reaction with a thiol-containing biotin via the nucleophilic thiol–ene reaction to enable immobilization of the enzyme streptavidin in a controlled manner.

5.5
Conclusions

Recent years have witnessed an increased interest in the incorporation of the maleimide functional group into various polymeric materials. The maleimide group enables facile functionalization of these materials with either electron-rich dienes via the Diels–Alder reaction or by conjugation of thiols via the nucleophilic thiol–ene reaction. The maleimide moiety needs to be protected using the Diels–Alder reaction with a diene during the polymerization step to minimize side reactions. The retro Diels–Alder cycloreversion reaction is utilized as a powerful post-polymerization modification to afford reactive maleimide-containing polymers that are amenable to further functionalization. Given the wide areas of application of maleimide-appended polymeric materials, we will continue to witness further application of this strategy in the fabrication of reactive polymeric materials.

References

1. Caliceti, P. and Veronese, F.M. (2003) *Adv. Drug Deliv. Rev.*, **55**, 1261–1277.
2. Vandermeulen, G.W.M. and Klok, H.A. (2004) *Macromol. Biosci.*, **4**, 383–398.
3. Gauthier, M.A. and Klok, H.A. (2008) *Chem. Commun.*, 2591–1611.
4. Duncan, R. (2003) *Nat. Rev. Drug Deliv.*, **2**, 347–360.
5. Pasut, G. and Veronese, F.M. (2007) *Prog. Polym. Sci.*, **32**, 933–961.
6. Maeda, H., Wu, J., Sawa, T., Matsumura, Y., and Hori, K. (2000) *J. Controlled Release*, **65**, 271–284.
7. Hawker, C.J. and Wooley, K.L. (2005) *Science*, **309**, 1200–1205.
8. Hall, D.J., Van Den Berghe, H.M., and Dove, A.P. (2011) *Polym. Int.*, **60**, 1149–1157.
9. Diels, O. and Alder, K. (1928) *Justus Liebigs Ann. Chem.*, **460**, 98–105.
10. Sanyal, A. (2010) *Macromol. Chem. Phys.*, **211**, 1417–1425.
11. Matyjaszewski, K. and Xia, J.H. (2001) *Chem. Rev.*, **101**, 2921–2990.
12. Moad, G., Rizzardo, E., and Thang, S.H. (2008) *Acc. Chem. Res.*, **41**, 1133–1142.
13. Hawker, C.J., Bosman, A.W., and Harth, E. (2001) *Chem. Rev.*, **101**, 3661–3688.
14. Dechy-Cabaret, O., Martin-Vaca, B., and Bourissou, D. (2004) *Chem. Rev.*, **104**, 6147–6176.
15. Mantovani, G., Lecolley, F., Tao, L., Haddleton, D.M., Clerx, J., Cornelissen, J.J., and Velonia, K. (2005) *J. Am. Chem. Soc.*, **127**, 2966–2973.
16. Ryan, S.M., Wang, X., Mantovani, G., Sayers, C.T., Haddleton, D.M., and Braydon, D.J. (2009) *J. Controlled Release*, **135**, 51–59.
17. Da Pieve, C., Williams, P., Haddleton, D.M., Palmer, R.M.J., and Missailidis, S. (2010) *Bioconjugate Chem.*, **21**, 169–174.
18. Geng, J., Mantovani, G., Tao, L., Nicolas, J., Chen, G., Wallis, R., Mitchell, D.A.,

Johnson, B.R.G., Evans, S.D., and Haddleton, D.M. (2007) *J. Am. Chem. Soc.*, **129**, 15156–15163.

19. Le Drougaguet, B., Mantovani, G., Haddleton, D.M., and Velonia, K. (2007) *J. Mater. Chem.*, **17**, 1916–1922.

20. Tolstyka, Z.P., Kopping, J.T., and Maynard, H.D. (2008) *Macromolecules*, **41**, 599–606.

21. Gok, O., Durmaz, H., Ozdes, E.S., Hizal, G., Tunca, U., and Sanyal, A. (2010) *J. Polym. Sci. Part A: Polym. Chem.*, **48**, 2546–2556.

22. Moad, G., Rizzardo, E., and Thang, S.H. (2005) *Aust. J. Chem.*, **58**, 379–410.

23. Bays, E., Tao, L., Chang, C.W., and Maynard, H.D. (2009) *Biomacromolecules*, **10**, 1777–1781.

24. Perrier, S., Takolpuckdee, P., and Mars, C.A. (2005) *Macromolecules*, **38**, 2033–2036.

25. Tao, L., Kaddis, C.S., Loo, R.R.O., Grover, G.N., Loo, J.A., and Maynard, H.D. (2009) *Chem. Commun.*, 2148–2150.

26. Tao, L., Kaddis, C.S., Loo, R.R.O., Grover, G.N., Loo, J.A., and Maynard, H.D. (2009) *Macromolecules*, **42**, 8028–8033.

27. Heredia, K.L., Grover, G.N., Tao, L., and Maynard, H.D. (2009) *Macromolecules*, **42**, 2360–2367.

28. Heredia, K.L., Tao, L., Grover, G.N., and Maynard, H.D. (2010) *Polym. Chem.*, **1**, 168–170.

29. Pounder, R.J., Stanford, M.J., Brooks, P., Richards, S.P., and Dove, A.P. (2008) *Chem. Commun.*, 5158–5160.

30. Stanford, M.J. and Dove, A.P. (2009) *Macromolecules*, **42**, 141–147.

31. Stanford, M.J., Pflughaupt, R.L., and Dove, A.P. (2010) *Macromolecules*, **43**, 6538–6541.

32. Bailey, G.C. and Swager, T.M. (2006) *Macromolecules*, **39**, 2815–2818.

33. Dispinar, T., Sanyal, R., and Sanyal, A. (2007) *J. Polym. Sci. Part A: Polym. Chem.*, **45**, 4545–4551.

34. Subramani, C., Cengiz, N., Saha, K., Gevrek, T.N., Yu, X., Jeong, Y., Bajaj, A., Sanyal, A., and Rotello, V.M. (2011) *Adv. Mater.*, **23**, 3165–3169.

35. Yilmaz, I.I., Arslan, M., and Sanyal, A. (2012.) *Macromol. Rapid Commun.*, **33**, 856–862.

36. Billiet, L., Gok, O., Dove, A.P., Sanyal, A., Nguyen, L.-T.T., and Du Prez, F. (2011) *Macromolecules*, **44**, 7874–7878.

37. Kamber, N.E., Jeong, W., Waymouth, R.M., Pratt, R.C., Lohmeijer, B.G.G., and Hedrick, J.L. (2007) *Chem. Rev.*, **107**, 5813–5840.

38. Dove, A.P. (2008) *Chem. Commun.*, 6446–6470.

39. Onbulak, S., Tempelaar, S., Pounder, R.J., Gok, O., Sanyal, R., Dove, A.P., and Sanyal, A. (2012) *Macromolecules*, **45**, doi: 10.1021/ma2019528

40. Kosif, I., Park, E.J., Sanyal, R., and Sanyal, A. (2010) *Macromolecules*, **43**, 4140–4148.

6
The Synthesis of End-Functional Ring-Opening Metathesis Polymers

Andreas F. M. Kilbinger

6.1
Introduction

Olefin metathesis catalysts are used in polymer chemistry to prepare polymers via a step-growth or a chain-growth polymerization process. The first one follows step-growth polymerization kinetics and is called acyclic diene metathesis (AD-MET). Polymers prepared via this process can therefore easily be end-functionalized using functional chain stoppers. The ADMET step-growth polymerization process will necessarily lead to much broader molecular weight distributions than can typically be obtained with living ring-opening metathesis polymerization (ROMP), a living chain-growth process. Mono end functionality, that is, the controlled functionalization of just one of the two end groups, cannot be achieved following step-growth kinetics. Owing to these mechanistic limitations, step-growth olefin metathesis is not reviewed in this chapter. The field of ADMET has recently been reviewed elsewhere [1, 2].

ROMP follows a chain-growth mechanism and can be carried out in a living manner, that is, with fast initiation and negligible unintended termination or chain transfer if carried out under appropriate conditions. The area of living ROMP has recently been reviewed by Bielawski and Grubbs [3].

Several reviews dealing with the subject of precision end-functionalization in living ROMP have recently been published [4, 5]. The relevant literature up until 2010 has been reviewed in these reports. This chapter aims to review all aspects of end-functionalization in living olefin metathesis polymerization up until the end of 2011.

The earliest well-defined transition-metal carbene initiators were based on titanium complexes [6]. These were followed by Schrock's well-defined tungsten and molybdenum initiators, imido alkylidene complexes in high oxidation states [7]. As can be seen from Table 6.1, the early transition-metal carbene initiators (titanium and less pronounced tungsten and molybdenum) show a highly oxophilic behavior and do not, therefore, tolerate water, air, and many polar functional groups (after all, it is this oxophilicity of titanium that is exploited in the McMurry reaction [8] or the Tebbe's reagent [9]).

Table 6.1 The functional group tolerance of transition-metal−carbene complexes.

Titanium	Tungsten	Molybdenum	Ruthenium
Carboxylic acids	Carboxylic acids	Carboxylic acids	Olefins
Alcohols, water	Alcohols, water	Alcohols, water	Carboxylic acids
Aldehydes	Aldehydes	Aldehydes	Alcohols, water
Ketones	Ketones	Olefins	Aldehydes
Esters, amides	Olefins	Ketones	Ketones
Olefins	Esters, amides	Esters, amides	Esters, amides

Increasing reactivity →
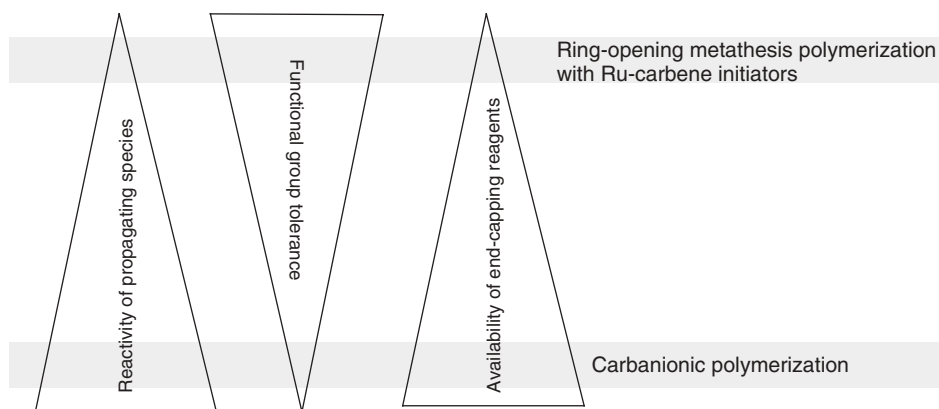
Figure 6.1 A schematic comparison of living ring-opening metathesis polymerization with ruthenium carbenes as the propagating species and living carbanionic polymerization.

Molybdenum carbene initiators, for example, tolerate the presence of ketones but react readily with aldehydes in a Wittig-like reaction. Such well-behaved reactions can be exploited for the introduction of end-group functionalities as will be seen later on. The ruthenium carbene complexes developed by Grubbs are the most functional-group-tolerant metathesis initiators known today. Table 6.1 shows that all carbonyl functional groups listed are tolerated by the Ru−carbene complex.

While this behavior of the ruthenium carbene catalysts is of great importance for their use in organic synthesis of highly functional olefins or the polymerization of monomers carrying such functional groups, it poses a severe limitation on possible functional end-capping reactions. This is illustrated in the example given in Figure 6.1, where reactivity, functional group tolerance, and availability of end-capping reagents are compared for living ROMP with ruthenium initiators and
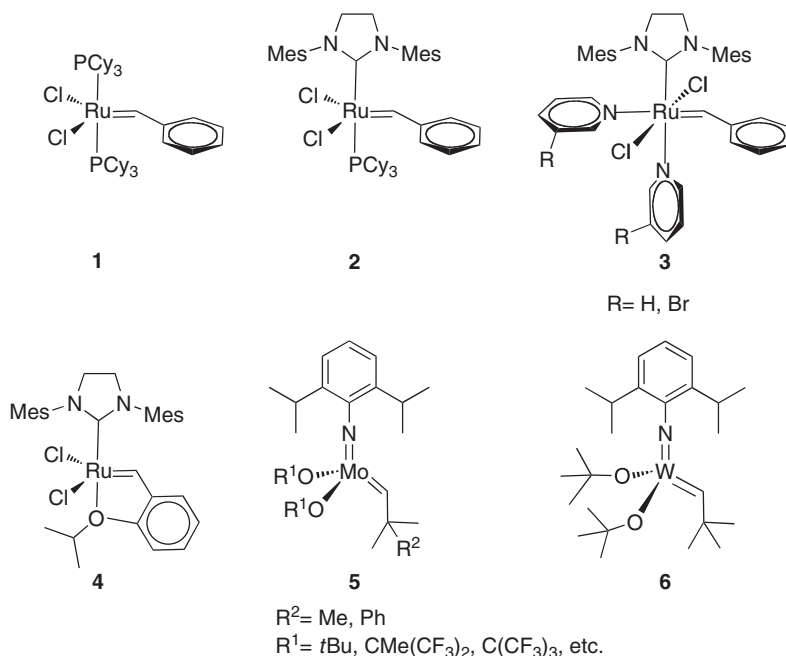
Figure 6.2 Commonly used transition-metal carbene initiators for living ROMP. Cy, cyclohexyl; Mes, mesityl.

living carbanionic polymerization. In carbanionic polymerization, the highly reactive carbanion represents the propagating species. As its reactivity (nucleophilicity) is very high, it severely limits the functional groups that can be present in the monomer structure. Yet, because of its high reactivity, there are many functional groups/reagents that react in a well-defined manner with the carbanion to give functional end groups. The situation is reversed for living ROMP, with ruthenium carbenes as the propagating species. Their predominant feature is the tolerance of functional groups which, in many cases, are allowed to be present in the monomer structure during propagation. However, the availability of many functional groups that are nonreactive toward the ruthenium–carbene complex drastically limits the number of reagents that can be used as functional end-capping reagents.

Figure 6.2 shows a selection of commonly used transition-metal carbene initiators for living ROMP. Many more carbene initiators have been reported but are not mentioned here because of their similar reactivity as far as introduction of end-functionalities is concerned. Ruthenium initiators **1–3** (Figure 6.2) are also often referred to as *Grubbs first-, second-, and third-generation initiators*. The Hoveyda–Grubbs second-generation initiator (**4**) carries a chelating carbene but no phosphine ligand and is often used in cross-metathesis reactions because of its longer lifetime compared to catalysts **3**. A vast number of ruthenium-based metathesis catalysts exist that carry different types of heterocyclic carbene ligands [10, 11].

Imido alkylidene initiators **5** and **6** were developed by Schrock [12]. They show very high reactivity but suffer from the functional group tolerances, as shown in Table 6.1. It is only the most commonly used ruthenium, molybdenum, and tungsten carbene initiators that are discussed in this chapter. Group VIII and group VI metathesis-active transition-metal complexes have been reviewed [13].

6.2
End-Functionalization Methods in General

When trying to place a functional group onto the chain end of a polymer, several synthetic strategies can be used.

One could use a *functional carbene initiator* that carries the functional group covalently attached to the initiating carbene ligand. This will ensure that all initiated chains carry the correct end group (or better, the start group). The chain end could be terminated nonfunctionally after completion of the propagation to ensure mono-end-functionalization.

A *terminating reagent* could be used that terminates propagation while introducing a suitable functional group to the chain end. This only works on those living chains that have ''survived'' the propagation process. Premature termination or chain-transfer processes will lead to non-end-functional chains, that is, reduced end-group functionality.

A *functional symmetric chain-transfer agent* (CTA) can place a functional group at the chain end of one polymer chain while cleaving the ruthenium–carbene complex off the chain end and turning it into a new functional initiator. Subsequent functional initiation will result in polymer chains carrying a functionality at the start group. After propagation, the reaction with the CTA will functionally modify the chain end, leading to a bis-end-functional polymer, and the whole process starts all over again.

This means that symmetrical CTAs can do both: they can produce functional initiators and act as functional terminating agents. Chain-growth reactions that aim at functionalizing both chain ends are in most cases best carried out until thermodynamic equilibrium has been reached so that potential differences in the reactivity of monomer and CTA with the metal carbene are overcome. These reactions will, however, yield broader molecular weight distributions, as they do not represent a living polymerization process. Some special cases where the monomer is added periodically are reported later in this chapter. There, narrow molecular weight distribution telechelics can be achieved. The symmetric olefin can also just be added at the end of the propagation reaction. This terminal cross-metathesis reaction will then lead to a mono-end-functional polymer.

A general method for end-functionalizing a living ROMP is shown in Scheme 6.1. The functional group R_{start} can be introduced during initiation and the group R_{end} via a termination step. The group R_{dead} deactivates the olefin metathesis activity of the metal complex.
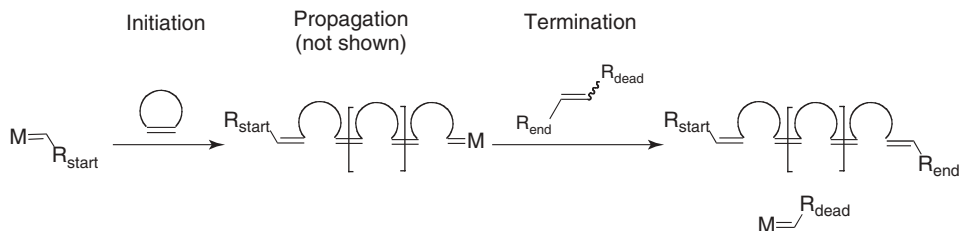
Scheme 6.1 A functional initiator transfers the functional group R_{start} onto one end of the polymer. During the termination step, the group R_{end} is transferred onto the other chain end while deactivating the metal complex with the group R_{dead}.
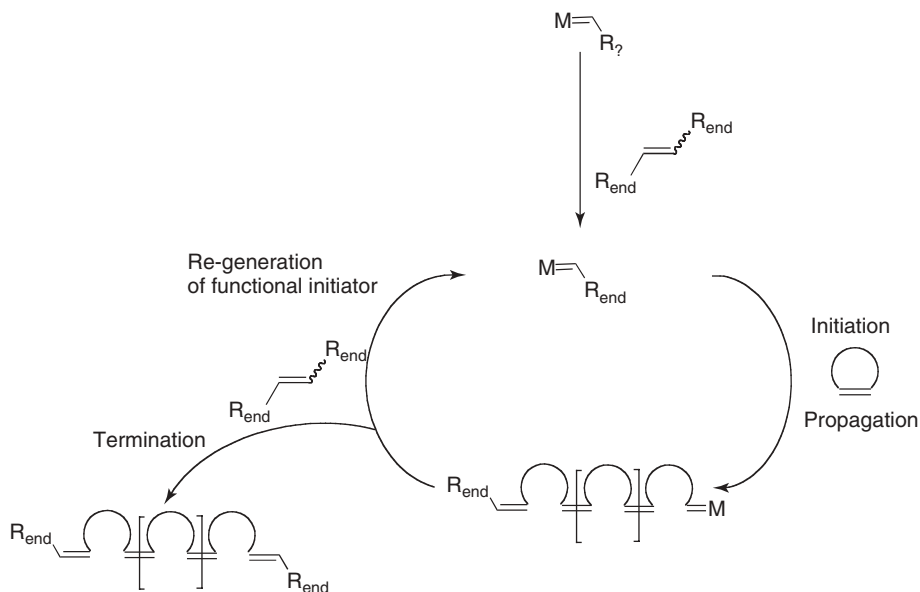
Scheme 6.2 A general method of synthesizing telechelic polymers using symmetrical acyclic olefins.

Another method of introducing a chain-end functionality in a nonliving manner is functional chain transfer using symmetrical acyclic olefins, as depicted in Scheme 6.2. The process is started with a metal carbene initiator (the functionality $R_?$ is not important as far as chain-end functionality is concerned) that is typically added in substoichiometric amounts with respect to the number of chains produced. This metal carbene reacts with a CTA, which is a symmetrical olefin that turns the metal carbene into the functional initiating species M $= R_{end}$. This is followed by a reaction with the monomer (= propagation) until the metal carbene reacts once more with the symmetrical olefin CTA. Half the symmetrical olefin gets transferred onto the chain end of the polymer, and the other half regenerates the functional initiator which can now initiate the growth of a new polymer chain. The molecular
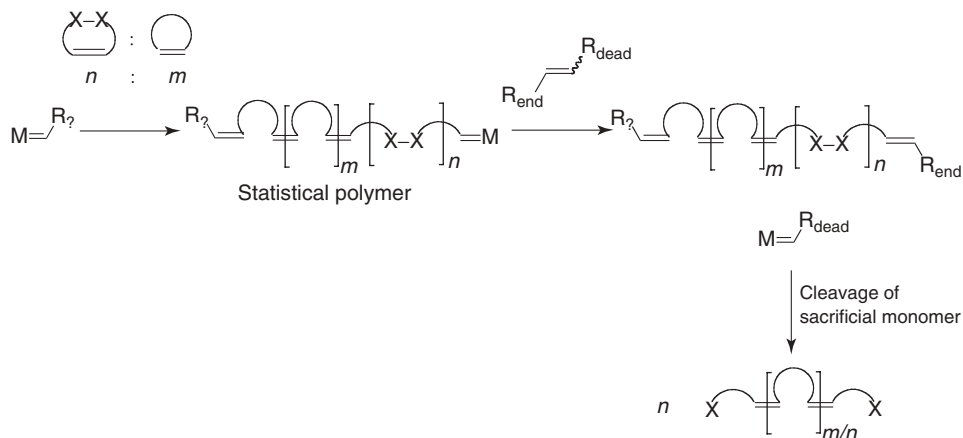
Scheme 6.3 A general synthetic method of preparing telechelic polymers using symmetric cyclic olefins that can be cleaved after polymerization to liberate the desired functionality.

weight is determined by the ratio of the CTA to the monomer. As the reactivity of the monomer and the CTA can differ significantly, it is often necessary to equilibrate the reaction via secondary metathesis reactions. This necessarily leads to broader molecular weight distributions.

Both of the procedures described above use acyclic olefins to introduce functionality at either end of the polymer chain. Another approach is the use of cyclic olefins where the functionality is hidden as part of the cyclic structure. These cyclic olefins react with the metal carbene initiator and propagate together with other cyclic monomers in a chain-growth manner. At the end of the polymerization, the hidden functionality can be liberated by cleaving the polymer in those places where the functional monomer was incorporated into the polymer chain.

Such monomers can be employed in two different processes: one allowing narrow molecular weight distributions and mono-end-functionality; the other always leading to telechelic, that is, bis-end-functional, polymers with broader molecular weight distributions. For the latter case, a cyclic monomer and a cleavable functional cyclic monomer are polymerized statistically, leading to segments of the polymer separated by units of the cleavable monomer (Scheme 6.3). Cleavage at these positions yields the bis-end-functional telechelic polymer.

Scheme 6.4 shows the second method using cleavable cyclic olefins. Here, a metal carbene initiator M=CH₂ (= carrying any metathesis-active residue) initiates the polymerization of the cleavable cyclic olefin to form a first polymer block. The so-formed macroinitiator then polymerizes a cyclic monomer in a living manner. This can be followed either by the introduction of the same or another cleavable cyclic olefin to give a triblock copolymer, or simply by the addition of a functional or nonfunctional termination reagent leading to a diblock copolymer.

Cleavage of the sacrificial monomers yields a telechelic, that is, bis-end-functional, polymer in the case of the triblock copolymer and a mono- or di-end-functional
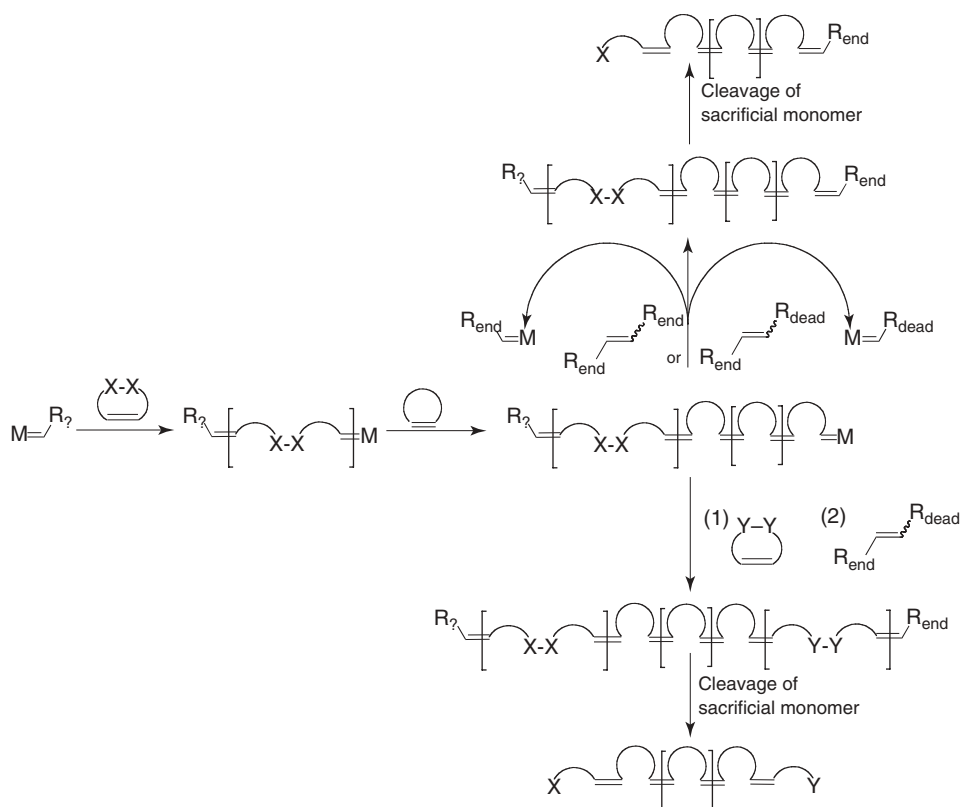
Scheme 6.4 The synthesis of mono- or bis-end-functional polymers employing sacrificial block copolymers. The polymer blocks composed of the symmetrical cyclic functional olefin are broken down after polymerization. This leaves but one functional group at the original place of the polymer block. $R_?$ = any metathesis-active residue, R_{end} = end − group functionality, and R_{dead} = residue that deactivates metathesis activity of the complex.

polymer in the case of the diblock copolymer. It is important to point out that the end-functional polymers prepared in this manner show all the characteristic features of a living polymer, in particular a narrow molecular weight distribution.

6.3
Functionalization during Initiation

In this chapter, reagents are discussed that are represented in the general reaction pathway depicted in Scheme 6.1. A functional initiator $R = CHR_{start}$ transfers the functionality R_{start} to the end (the start) of the polymer chain. Despite the high

degrees of functionalization, functional initiation is probably the least common method of introducing a functional end group. The reasons for this might be the difficulty in obtaining pure functional initiators and the fact that synthesis and purification protocols need to be optimized anew for each differently functionalized initiator.

Very few functional initiators based on titanium metal centers have been reported. Because titanium carbenes are very sensitive toward oxygen-containing functional groups, only inert alkyl- or aryl-substituted initiators have been reported [14].

Titanium–carbene complexes prepared from Tebbe's reagent [9] are also not tolerant toward functional groups and hence not useful for functional polymerization initiation.

Amass *et al.* used the carbanion of living anionic polystyrene to react with WCl_6. The resulting tungsten-alkyl species eliminated HCl and formed a metathesis-active tungsten carbene which was used to polymerize norbornene [15, 16]. This represents the first successful block copolymer synthesis using a conversion of polymerization technique involving ROMP.

Owing to the commercial availability of the Grubbs-type ruthenium-based initiators, several strategies have been pursued to prepare prefunctionalized catalysts. A very versatile method relying on commercially available complexes uses a cross-metathesis reaction between a ruthenium benzylidene and a functionalized olefin, yielding a new carbene complex and styrene. This method has been used by Slugovc and coworkers who attached luminescent dyes to Grubbs' first-generation catalyst in order to study their behavior on different polymeric materials [17]. Bai *et al.* used symmetrical *Z*-olefins to prefunctionalize a Grubbs third-generation initiator with a trimethylsilyl TMS-protected amine [18].

A functionalized carbene can also be synthesized by reacting the respective functional diazoalkane to the precursor complex $RuCl_2(PPh_3)_3$ [19]. This method has been used by the Grubbs group for the synthesis of a catalyst that can be used both in ROMP and atom-transfer radical polymerization (ATRP) polymerization, as well as for the formation of block copolymers using both methods [20].

In a similar approach to Amass, Hutchings and Koshravi prepared a styrene-terminated poly(ethylene oxide), which they converted into a ruthenium benzylidene macroinitiator. This was achieved via a highly reactive ruthenium propylidene intermediate [21].

6.4
Functionalization after Propagation

This section refers to the general reaction pathway shown in Scheme 6.1. The termination agent R_{end}-CH=CH-R_{dead} reacts with the propagating metal–carbene complex in a regioselective manner to transfer the functional group R_{end} onto the polymer chain and to diminish the metathesis activity of the metal complex.

6.4.1
Reaction with Carbonyl Groups

Titanium metathesis catalysts show the same reactivity as that of Tebbe's reagent [9]. This reagent can transfer its methylene group onto carbonyls in exchange for their oxo group in a Wittig-like reaction, thereby forming an olefin and titanium oxide. Amides and esters have been transformed to the respective enamines and vinyl ethers in this manner [22, 23]. Grubbs *et al.* were able to place a diphenylethenyl end group on polynorbornene by adding benzophenone to a living titanium-initiated polymerization [14, 24]. The same group could show that the addition of an excess of a dialdehyde resulted in selective end-capping to give an aldehyde-terminated polymer. The obtained terminal aldehyde was subsequently reduced to an alcohol end group [25].

In the same paper, the authors reported polyaldehydes and aldehyde end-capped polymers as core molecules for block- and graft-copolymer synthesis. The very high reactivity of the Ti-alkylidene groups toward aldehydes and ketones was exploited by adding the living chains to a multifunctional quencher, thereby building more complex polymeric architectures [26].

Molybdenum–carbene and tungsten–carbene complexes are also conveniently functionally terminated with the addition of a suitable aldehyde [27]. The first application of this reaction using tungsten catalysts was reported by Schrock and Grubbs using benzaldehyde as the quencher [28].

With molybdenum carbenes, benzaldehyde was also used with similar success [29]. The general applicability of this reaction was later on shown with different alkyl-substituted aldehydes such as pivalonaldehyde [30, 31]. Addition of pyrenealdehyde allowed the introduction of a fluorescence label at the chain end of a polynorbornene [32].

Functional aldehyde quenching has been established as the standard termination reaction for metathesis polymerizations involving molybdenum or tungsten initiators [33]. While some aldehydes such as pyrenealdehyde can be introduced directly, others need to be suitably protected to avoid side reactions [34]. Bifunctional carbene initiators could also be terminated in this manner, giving rise to the introduction of functionalities at either end of the polymer chain (= telechelic polymer) [35, 36].

Nomura *et al.* employed this strategy in a number of applications featuring hydroxy-functionalized polynorbornenes and sugar conjugates [37]. They chose a TMS-protected *p*-hydroxybenzaldehyde as the terminating agent followed by mild liberation of the hydroxy group. This terminal hydroxy group was used to attach another norbornene residue, which was polymerized by ROMP to give a graft copolymer. Attachment of poly(ethylene glycol) gave the corresponding diblock copolymer [38–40].

Star-shaped polymers were synthesized by Dounis and Feast by adding the trifunctional aldehyde-quencher 1,3,5-benzene-tricarbaldehyde to a molybdenum-initiated polynorbornene [41]. Other complex polymeric architectures could be synthesized using functional aldehyde quenchers carrying moieties that allowed the initiation or termination of a second polymerization following a

different polymerization mechanism. *p*-Fluorobenzaldehyde was used to form a terminal fluoride which could undergo a subsequent polycondensation [33]. *p*-Bromomethylbenzaldehyde and *p*-vinylbenzaldehyde were added to synthesize polymers, which could function as initiators for ATRP or anionic polymerization [42, 43].

Notestein and Register prepared an anionic polymer terminated with an aldehyde end group. This polymer was added to a living ROMP polymer to form the conjugate between both types of polymers. Block copolymers combining polynorbornene and polystyrene or polyisoprene were realized using this macrotermination reaction [44].

Ruthenium carbene initiators are inert toward aldehydes and ketones as can be seen from Table 6.1. Carbonyl-carrying solvents such as ethyl acetate, DMF, or acetone can even be used for polymerizations [45]. Functional termination can also be achieved for ruthenium carbenes using different strategies, as are reported in the following sections.

6.4.2
Reaction with Molecular Oxygen

Feast *et al.* found that exposure of the propagating molybdenum and tungsten carbenes to traces of molecular oxygen resulted in bimodal gel permeation chromatography (GPC) curves. These represented the molecular weight aimed for and also double of the aimed for molecular weight. Molecular oxygen can react with the Mo and W carbenes to form aldehyde end groups that act as macro-terminating agents giving rise to the doubling of molecular weight.

While this was initially considered an unwanted side reaction, it was soon studied as a coupling reaction by Feast *et al.* [46].

Biagini *et al.* [47] observed the same aldehyde formation for ruthenium carbenes. As aldehydes are inert toward propagating ruthenium carbenes, this reaction can be used for the synthesis of aldehyde end-capped polymers. The reaction is, however, rather slow. Reaction times of 24 h were reported, which can limit the scope of this reaction in some cases.

6.4.3
Reaction with Functional Vinyl Ethers

Ethylvinyl ether is employed in virtually every ruthenium-carbene-initiated polymerization to nonfunctionally terminate the polymerization. The reaction that takes place transfers the nonfunctional methylene group (= R_{end}, Scheme 6.1) to the polymer chain end and the ''ether portion'' (= R_{dead}, Scheme 6.1) onto the ruthenium initiator, yielding a Fischer–carbene complex which under most conditions shows little or no metathesis activity [48].

The same can be achieved when substituted vinyl ethers are employed that carry a suitable functionality (= R_{end}, Scheme 6.1) attached to the vinyl group. In

addition to the formation of the Fischer carbene, the attached functionality is now transferred onto the polymer chain end.

This reaction was reported for the first time using ethyl vinyl ether and 2,3-dihydrofurane, a cyclic vinyl ether that reacted stoichiometrically with uninitiated ruthenium catalyst forming Fischer carbenes [49]. Commercially available ethyl vinyl ether quickly became the standard nonfunctional terminating agent for Grubbs-type ruthenium-complex-initiated metathesis polymerizations [19]. It is typically added at the end of the polymerization in excess quantities, which cleaves the ruthenium center from the polymer to be worked-up. Ethyl vinyl ether reacts regioselectively with the ruthenium–carbene complexes giving the Fischer carbene and transfer of a methylene group to the end of the polymer chain. The origin of this regioselectivity has not yet been established.

Substituted vinyl ethers are very useful termination reagents, as they are readily prepared from the corresponding aldehydes in a Wittig reaction involving the phosphorus ylide of chloromethyl ethyl ether [50]. Vinyl ether termination has therefore established itself as a versatile strategy for the introduction of complex functional end groups. The Kiessling group, in particular, has used this strategy in a number of reports. The end groups attached to metathesis polymers ranges from fluorescent labels [51] to ketones [52–55] to biotin [56] and many other bioactive groups [57–61]. The functional vinyl ethers reported are typically (*E*)/(*Z*) mixtures, with a higher percentage of the *E* isomer. The reaction times with the ruthenium carbene and the degrees of polymer end functionality vary considerably among the examples given. This is most likely a function of the type of substituent present on the vinyl ether. Contrary to ruthenium, titanium, molybdenum, and tungsten carbene catalysts are not terminated by vinyl ethers.

6.4.4
Reaction with Functional Vinyl Esters

Similar to vinyl ethers, vinyl esters also form metathesis-inactive and also unstable Fischer carbenes. They decompose readily to the respective carboxylic acid and a ruthenium complex carrying a carbido ligand [62]. This carbido complex is metathesis-inactive unless it is reactivated by addition of a strong acid or an oxidant [63, 64].

A special case of vinyl esters are cyclic vinyl esters, that is, vinyl lactones. In contrast to cyclic vinyl ethers, cyclic vinyl esters have the advantage that the acyl carbene that is initially attached to the end of the polymer chain is spontaneously cleaved to form a ruthenium–carbido complex and a carboxylic acid-terminated polymer (Scheme 6.5).

A further advantage of using small ring cyclic terminating agents is the exclusive presence of *Z*-olefins that generally react faster with the propagating ruthenium carbene than the corresponding *E*-olefins. Two vinyl ester terminating agents have been investigated in detail [65]. Vinylene carbonate is commercially available and reacts as depicted in Scheme 6.5 (bottom). After the formation of an acyl carbene
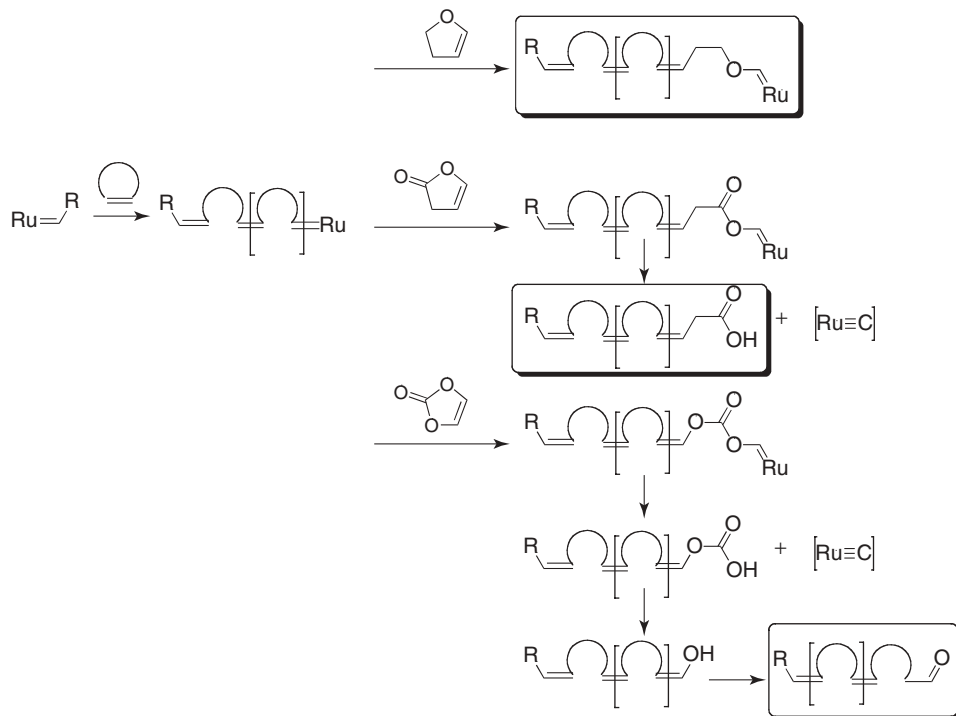
Scheme 6.5 Comparison between the termination of a propagating ruthenium carbene and a cyclic vinyl ether (top), a cyclic vinyl ester (middle), and vinylene carbonate (bottom).

and decomposition into the carbido complex, the vinyl alcohol tautomerizes into an aldehyde.

The second example is 3*H*-furanone (Scheme 6.5, middle), which can be prepared from furfural via a Bayer–Villiger oxidation. Reaction of the propagating carbene with this reagent results in an acyl carbene, which, after carbido complex formation, gives the terminal carboxylic acid. Polymers carrying either aldehyde or carboxylic acid end groups are therefore readily available with this quenching method.

For the reaction with the propagating ruthenium carbene with vinylene carbonate, only one metallacyclobutane intermediate can be formed because of the symmetry of the reagent. In the case of 3*H*-furanone, two metallacyclobutanes are, in principle, conceivable. However, only the reaction leading to the acyl carbene has been observed experimentally [65]. Similar to the case of the reaction of ruthenium carbenes with vinyl ethers, the reason for the stereoselectivity is not known.

Hilf *et al.* prepared polynorbornenes carrying pendant alcohol groups that were functionally terminated with *3H*-furanone to give carboxylic acid end groups [66]. A subsequent polycondensation of these AB*x*-type macromonomers (A representing the one carboxylic acid and B the *x* alcohol groups) yielded hyperbranched polymers but no gelation, which is a further indicator for true mono-end-functionality.

6.4.5
Reaction with Nondeactivating Olefins

Reactions of this kind are essentially special cases of the reaction shown in Scheme 6.1. In the mechanism shown, the metal carbene gets deactivated by the group R_{dead}. When using a nondeactivating olefin, as shown in Scheme 6.6, one of the substituents of the olefin gets transferred onto the polymer (here R_1) and the other (R_2) is attached to a metathesis-active carbene complex. The overall process can be described as a terminal cross-metathesis reaction.

This type of reaction works best if there is no residual monomer left for the complex $M=CHR_2$ to react with. Polymers that easily undergo secondary metathesis reactions are also poor choices for this kind of reaction, as the active metal carbene complex can also react with the olefins of the polymer backbone itself.

Acrylates have been used as functionalization reagents in a terminal cross-metathesis reaction. In acrylates, the group R_1 (Scheme 6.6) represents the ester group and R_2 a nonfunctional methylene unit (CH_2). Owing to the lack of stereoselectivity in the cross-metathesis step, only moderate degrees of functionalization are obtained [67].

Symmetrically substituted olefins in which the substituents R_1 and R_2 are identical (Scheme 6.6) give much better end-functionalization results. In this manner, initiator groups for ATRP [68, 69] and building blocks for "click" reactions [70] have been attached to the chain ends of polynorbornenes. Amine-terminated polynorbornenes were recently synthesized via a terminal cross-metathesis step by Bai *et al.* using a symmetrical *Z*-olefin [18]. Using terminal cross-metathesis and a very similar approach, Madkour *et al.* used symmetrical *Z*-olefins carrying pentafluorophenyl ester groups to install an active ester at the chain end of a polymer [71]. Kurzhals *et al.* used homo-metathesis to prepare symmetrical olefins for terminal cross-metathesis. Barbiturate and thymine polymer end groups were introduced in this way [72]. Lee *et al.* prepared biotin end-functionalized glycopolymers based on a polynorbornene backbone using terminal cross-metathesis [73]. Matson and Grubbs carried out a study in which they compared the degree of end-functionalization of polymers [74]. They investigated two procedures: In the first, the propagating ruthenium carbene was directly reacted with the symmetrical
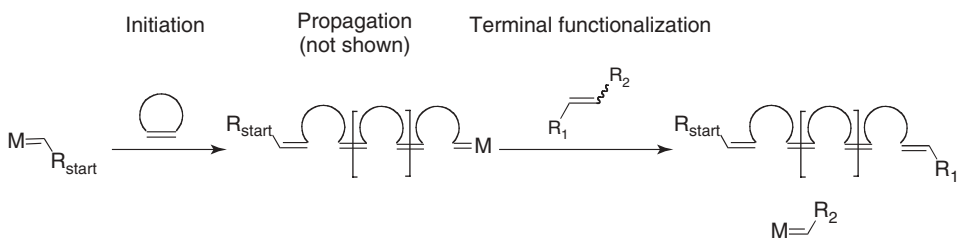
Scheme 6.6 Polymer chain end-functionalization via terminal cross-metathesis.

Z-olefin, giving the end-functional polymer. In the second case, the propagating polymer was first nonfunctionally terminated with ethylvinyl ether to yield a polymer with a terminal double bond. In a second step, this terminal olefin was reacted with catalyst **4** (Figure 6.2) and a symmetrical *Z*-olefin in a cross-metathesis reaction. Overall, the degrees of functionality were lower for the two-step procedure. However, this procedure can theoretically be applied to many other polymers carrying terminal olefins.

6.5
Functionalization during Propagation

6.5.1
Using Chain-Transfer Agents

The use of acyclic symmetrically substituted olefins, the so-called CTAs, to synthesize telechelic polymers is shown in Scheme 6.2.

An early example in which molybdenum carbenes were used as polymerization initiators was given by Schrock *et al.* [75]. In this case, the CTA used did not represent a symmetrical olefin but rather a cyclopentene to which a substituted olefin was attached via a linker. In a tandem ring-opening–ring-closing reaction, the propagating Mo carbene opened the cyclopentene ring and formed a six-membered ring with the pendant-substituted olefin. This resulted in a cyclohexene group at the polymer chain end and a substituted Mo carbene initiator that would consume more monomer. The chain transferring activity of these agents, however, proved to be rather poor.

In a later example, Crowe *et al.* could show that styrene and 1,3-butadiene could be used successfully as CTAs in the polymerization of norbornene [76]. Narrow molecular weight distributions were obtained but no functional groups were attached to the polymeric chain ends.

Functional telechelic polymers can be readily prepared using symmetrical acyclic olefins in a ruthenium carbene-catalyzed ROMP. The mechanism of this reaction has been theoretically and experimentally investigated by the Grubbs group [77, 78].

Many functional groups have been introduced at the polymer chain end in this manner. The first applications involved protected reactive functional groups such as alcohols [79], amines, and carboxylic acids [80]. Also, less reactive functional groups were introduced without protection. Especially, groups such as halides, pseudo-halides [81], methacrylates, and epoxides [82], which can function as initiating sites for different polymerization techniques such as ATRP, free-radical, or ionic polymerization, were introduced this way. Furthermore, more complex CTA-carrying polymers [83] or groups that exhibit liquid crystalline properties [84] have been employed.

Matson *et al.* used a third-generation Grubbs ruthenium carbene initiator (**3**, R = H) to carry out a pulsed addition ROMP in which precisely defined

quantities of monomer were added to a catalyst–CTA mixture at defined time intervals [85]. This procedure allowed the synthesis of polymers with narrow molecular weight distribution that carried the nonfunctional residues of the CTA at either chain end. This approach could drastically increase the number of well-defined polymer chains per catalyst molecule and has shown the impressive reactivity and selectivity of the latest catalyst developments.

A similar method that was first reported by Fraser *et al.* [86] is depicted in Scheme 6.3. A cyclic cleavable monomer is incorporated into the polymer chain in a statistical manner. After work-up, the polymer chain cleaved at the positions where the cleavable monomer was incorporated, yielding telechelics. The molecular weight distributions are generally expected to be rather broad, as a statistical process takes place.

6.5.2
Sacrificial Synthesis

In sacrificial synthesis, cleavable cyclic monomers are incorporated in a block copolymer structure as shown in Scheme 6.4 [87]. After polymerization, the polymer blocks composed of cleavable monomer can be broken down into low-molecular-weight compounds (= sacrificed) leaving just one functionality at the former junction between the cleavable and the noncleavable block. Telechelic polymers can be synthesized as shown in Scheme 6.4. In this case, a triblock copolymer has to be prepared, starting and ending with a sacrificial block. Mono-end-functional polymers are also accessible using diblock copolymers in which the sacrificial block typically follows the noncleavable polymer block.

The first report of this strategy described the introduction of terminal allylic alcohols [87, 88]. 1,3-Dioxepines, which are similar to the cyclic acetals used in the copolymerization technique (see above), were used to form the sacrificial block. Acidic hydrolysis or hydrogenation decomposed the sacrificial block and yielded the allylic alcohol. The degree of functionalization is directly given by the degree of macroinitiation of the sacrificial block. All further additions of sacrificial monomer, that is, propagation of sacrificial monomer, do not contribute to the degree of end-functionalization. In order to determine the minimum amount of sacrificial monomer necessary to obtain high degrees of end-group functionality, an efficiency study was carried out [89].

Hydroxy-terminated polymers prepared in this manner were used to build more complex macromolecular architectures such as graft copolymers [90] or block copolymers [91].

Using a 1,3-dithiepine instead of a 1,3-dioxepine as sacrificial monomer, allylic thiol polymer end groups could be obtained [92]. The poly(1,3-dithiepine) block was cleaved (sacrificed) under hydrogenation conditions using Raney nickel.

As mentioned earlier (Scheme 6.4), this method can also be used to place a functional group at the beginning of the polymer chain. Hydroxy-homotelechelic polymers, or polymers bearing an alcohol group at either end, have been realized in this manner from sacrificial triblock copolymers where the outer blocks

consisted of polyacetals. Using this method, the first well-defined telechelic materials showing narrow molecular weight distribution have been synthesized by ruthenium-catalyzed ROMP [93].

By combining sacrificial synthesis with vinyl lactone termination, Hilf *et al.* could prepare diblock copolymers in which the initiating block consisted of a poly(methyldioxepine) and the second block of a polynorbornene imide [94]. Functional termination with vinyl lactones (*3H*-furanone and vinylene carbonate) installed aldehydes or carboxylic acids at the chain ends. The initial polydioxepine blocks were subsequently sacrificed, liberating the allyl alcohol functionality at the beginning of the chain. In this way, heterotelechelic polymers carrying alcohols at one end and carboxylic acids or aldehydes at the other could be prepared.

6.6
Conclusions and Outlook

ROMP, particularly using ruthenium carbene initiators, used to be a polymerization method for which very few end-functionalization methods were available. This picture has changed completely over the last 10 years.

The most common ROMP polymerization initiators today are based on ruthenium, molybdenum, and tungsten carbene complexes. For tungsten and molybdenum, the problem of polymer end-functionalization had been addressed early on with functional aldehydes. The ruthenium carbene initiators were more tolerant to functional groups but at the same time lacked reagents to be terminated with in a functional manner.

In addition to the functional vinyl ethers that have been used the longest, there are vinyl lactone quenching, terminal cross-metathesis, and sacrificial synthesis. All these methods and reagents are able to introduce functionality at the chain end of a ROMP polymer. Nonetheless, care has to be taken to select the correct catalyst because different catalyst types and generations vary in terms of functional-group tolerance, polymerization activity, and general reactivity toward substrates. Every catalyst type requires its specific functionalization techniques.

Most of the techniques described here introduce the functionality at the chain end, that is, after monomer propagation. However, in principle, functional initiation is even more attractive, as it ensures very high degrees of end-group functionality. It is conceivable that clean and reliable methods of converting commercial catalysts into functionalized derivatives will fill this gap in the future.

Acknowledgments

References

1. Mutlu, H., Montero de Espinosa, L., and Meier, M.A.R. (2011) *Chem. Soc. Rev.*, **40**, 1404–1445.
2. Baughman, T.W. and Wagener, K.B. (2005) *Adv. Polym. Sci.*, **176**, 1–42.
3. Bielawski, C.W. and Grubbs, R.H. (2007) *Prog. Polym. Sci.*, **32**, 1–29.
4. Hilf, S. and Kilbinger, A.F.M. (2009) *Nat. Chem.*, **1**, 537–546.
5. Nomura, K. and Abdellatif, M.M. (2010) *Polymer*, **51**, 1861–1881.
6. Calderon, N., Ofstead, E.A., Ward, J.P., Judy, W.A., and Scott, K.W. (1968) *J. Am. Chem. Soc.*, **90**, 4133–4140.
7. Schrock, R.R. (2006) *Angew. Chem., Int. Ed.*, **45**, 3748–3759.
8. McMurry, J.E. and Fleming, M.P. (1974) *J. Am. Chem. Soc.*, **96**, 4708–4709.
9. Tebbe, F.N., Parshall, G.W., and Reddy, G.S. (1978) *J. Am. Chem. Soc.*, **100**, 3611–3613.
10. Vougioukalakis, G.C. and Grubbs, R.H. (2010) *Chem. Rev.*, **110**, 1746–1787.
11. Samojlowicz, C., Bieniek, M., and Grela, K. (2009) *Chem. Rev.*, **109**, 3708–3742.
12. Schrock, R.R. (2009) *Chem. Rev.*, **109**, 3211–3226.
13. Buchmeiser, M.R. (2000) *Chem. Rev.*, **100**, 1565–1604.
14. Gilliom, L.R. and Grubbs, R.H. (1986) *J. Am. Chem. Soc.*, **108**, 733–742.
15. Amass, A.J. and Gregory, D. (1987) *Br. Polym. J.*, **19**, 263–268.
16. Amass, A.J., Bas, S., Gregory, D., and Mathew M.C. (1985) *Makromol. Chem.*, **186**, 325–330.
17. Burtscher, D., Saf, R., and Slugovc, C. (2006) *J. Polym. Sci. Part A: Polym. Chem.*, **44**, 6136–6145.
18. Bai, Y., Lu, H., Ponnusamy, E., and Cheng, J. (2011) *Chem. Commun.*, **47**, 10830–10832.
19. Schwab, P., Grubbs, R.H., and Ziller, J.W. (1996) *J. Am. Chem. Soc.*, **118**, 100–110.
20. Bielawski, C.W., Louie, J., and Grubbs, R.H. (2000) *J. Am. Chem. Soc.*, **122**, 12872–12873.
21. Castle, T.C., Hutchings, L.R., and Khosravi, E. (2004) *Macromolecules*, **37**, 2035–2040.
22. Pine, S.H., Zahler, R., Evans, D.A., and Grubbs, R.H. (1980) *J. Am. Chem. Soc.*, **102**, 3270–3272.
23. Brown-Wensley, K.A., Buchwald, S.L., Cannizzo, L.F., Clawson, L., Ho, S., Meinhardt, D., Stille, J.R., Straus, D., and Grubbs, R.H. (1983) *Pure Appl. Chem.*, **55**, 1733–1744.
24. Cannizo, L.F. and Grubbs, R.H. (1987) *Macromolecules*, **20**, 1488.
25. Risse, W. and Grubbs, R.H. (1991) *J. Mol. Catal.*, **65**, 211–217.
26. Risse, W. and Grubbs, R.H. (1989) *Macromolecules*, **22**, 4462–4466.
27. Schrock, R.R. (1990) *Acc. Chem. Res.*, **23**, 158–165.
28. Schrock, R.R., Feldman, J., Cannizzo, L.F., and Grubbs, R.H. (1987) *Macromolecules*, **20**, 1169–1172.
29. Murdzek, J.S. and Schrock, R.R. (1987) *Macromolecules*, **20**, 2640–2642.
30. Schrock, R.R., Murdzek, J.S., Bazan, G.C., Robbins, J., DiMare, M., and O'Reagan, M.B. (1990) *J. Am. Chem. Soc.*, **112**, 3875–3886.
31. Bazan, G.C., Khosravi, E., Schrock, R.R., Feast, W.J., Gibson, V.C., O'Reagan, M.B., Thomas, J.K., and Davis, W.M. (1990) *J. Am. Chem. Soc.*, **112**, 8378–8387.
32. Albagli, D., Bazan, G.C., Schrock, R.R., and Wrighton, M.S. (1993) *J. Phys. Chem.*, **97**, 10211–10216.
33. Albagli, D., Bazan, G.C., Schrock, R.R., and Wrighton, M.S. (1993) *J. Am. Chem. Soc.*, **115**, 7328–7334.
34. Mitchell, J.O., Gibson, V.C., and Schrock, R.R. (1991) *Macromolecules*, **24**, 1220–1221.
35. Fox, H.H., Lee, J.-K., Park, L.Y., and Schrock, R.R. (1993) *Organometallics*, **12**, 759–768.
36. Singh, R., Verploegen, E., Hammond, P.T., and Schrock, R.R. (2006) *Macromolecules*, **39**, 8241–8249.
37. Murphy, J.J. and Nomura, K. (2005) *Chem. Commun.*, 4080–4082.
38. Murphy, J.J., Takahashi, S., and Nomura, K. (2001) *Macromolecules*, **34**, 4712–4723.

39. Murphy, J.J., Kawasaki, T., Fujiki, M., and Nomura, K. (2005) *Macromolecules*, **38**, 1075–1083.

40. Murphy, J.J., Furusho, H., Paton, R.M., and Nomura, K. (2007) *Chem. Eur. J.*, **13**, 8985–8997.

41. Dounis, P. and Feast, W.J. (1996) *Polymer*, **37**, 2547.

42. Coca, S., Paik, H.-J., and Matyjaszewski, K. (1997) *Macromolecules*, **30**, 6573–6576.

43. Myers, S.B. and Register, R.A. (2008 *Macromolecules*, **41**, 5283.

44. Notestein, J.M., Lee, L.-B.W., and Register, R.A. (2002) *Macromolecules*, **35**, 1985–1987.

45. Slugovc, C., Demel, S., and Stelzer, F. (2002) *Chem. Commun.*, 2572–2573.

46. Feast, W.J., Gibson, V.C., Khosravi, E., Marshall, E.L., and Mitchell, J.P. (1992) *Polymer*, **33**, 872–873.

47. Biagini, S.C.G., Davies, R.G., Gibson, V.C., Giles, M.R., Marshall, E.L., and North, M. (2001) *Polymer*, **42**, 6669–6671.

48. Katayama, H., Yonezawa, F., Nagao, M., and Ozawa, F. (2002) *Macromolecules*, **35**, 1133–1136.

49. Wu, Z., Nguyen, S.T., Grubbs, R.H., and Ziller, J.W. (1995) *J. Am. Chem. Soc.*, **117**, 5503–5511.

50. Earnshaw, C., Wallis, C.J., and Warren, S. (1979) *J. Chem. Soc., Perkin Trans. 1*, **12**, 3099–3106.

51. Gordon, E.J., Gestwicki, J.E., Strong, L.E., and Kiessling, L.L. (2000) *Chem. Biol.*, **7**, 9–16.

52. Kolonko, E.M., Pontrello, J.K., Mangold, S.L., and Kiessling, L.L. (2009) *J. Am. Chem. Soc.*, **131**, 7372–7333.

53. Kolonko, E.M. and Kiessling, L.L. (2008) *J. Am. Chem. Soc.*, **130**, 5626–5627.

54. Allen, M.J., Raines, R.T., and Kiessling, L.L. (2006) *J. Am. Chem. Soc.*, **128**, 6534–6535.

55. Yang, Z.-Q., Puffer, E.B., Pontrello, J.K., and Kiessling, L.L. (2002) *Carbohydr. Res.*, **337**, 1605–1613.

56. Chen, B., Metera, K., and Sleiman, H.F. (2005) *Macromolecules*, **38**, 1084–1090.

57. Gestwicki, J.E., Cairo, C.W., Mann, D.A., Owen, R.M., and Kiessling, L.L. (2002) *Anal. Biochem.*, **305**, 149–155.

58. Pontrello, J.K., Allen, M.J., Underbakke, E.S., and Kiessling, L.L. (2005) *J. Am. Chem. Soc.*, **127**, 14536–14537.

59. Mangold, S.L., Carpenter, R.T., and Kiessling, L.L. (2008) *Org. Lett.*, **10**, 2997–3000.

60. Owen, R.M., Gestwicki, J.E., Young, T., and Kiessling, L.L. (2002) *Org. Lett.*, **4**, 2293–2296.

61. Kiessling, L.L., Gordon, E.J., and Strong, L.E. (2001) United States Patent U.S. Pat. 6, 291, 616 B1.

62. Caskey, S.R., Stewart, M.H., Kivela, J.E., Sootsman, J.R., Johnson, M.J.A., and Kampf, J.W. (2005) *J. Am. Chem. Soc.*, **127**, 16750–16751.

63. Caskey, S.R., Stewart, M.H., Johnson, M.J.A., and Kampf, J.W. (2006) *Angew. Chem. Int. Ed.*, **45**, 7422–7424.

64. Macnaughtan, M.L., Johnson, M.J.A., and Kampf, J.W. (2007) *J. Am. Chem. Soc.*, **129**, 7708–7709.

65. Hilf, S., Grubbs, R.H., and Kilbinger, A.F.M. (2008) *J. Am. Chem. Soc.*, **130**, 11040–11048.

66. Hilf, S., Wurm, F., and Kilbinger, A.F.M. (2009) *J. Polym. Sci. Part A: Polym. Chem.*, **47**, 6932–6940.

67. Lexer, C., Saf, R., and Slugovc, C. (2009) *J. Polym. Sci. Part A: Polym. Chem.*, **47**, 299–305.

68. Li, M.-H., Keller, P., and Albouy, P.-A. (2003) *Macromolecules*, **36**, 2284–2292.

69. Matson, J.B. and Grubbs, R.H. (2008) *Macromolecules*, **41**, 5626–5631.

70. Gozgen, A., Dag, A., Durmaz, H., Sirkecioglu, O., Hizal, G., and Tunca, U. (2009) *J. Polym. Sci. Part A: Polym. Chem.*, **47**, 497–504.

71. Madkour, A.E., Koch, H.R., Lienkamp, K., and Tew, G.N. (2010) *Macromolecules*, **43**, 4557–4561.

72. Kurzhals, S. and Binder, W.H. (2010) *J. Polym. Sci. Part A: Polym. Chem.*, **48**, 5522–5532.

73. Lee, S.-G., Brown, J.M., Rogers, C.J., Matson, J.B., Krishnamurthy, C., Rawat, M., and Hsieh-Wilson, L.C. (2010) *Chem. Sci.*, **1**, 322–325.

74. Matson, J.B. and Grubbs, R.H. (2010) *Macromolecules*, **43**, 213–221.

75. Schrock, R.R., Yap, K.B., Yang, D.C., Sitzmann, H., Sita, L.R., and Bazan,

G.C. (1989) *Macromolecules*, **22**, 3191–3200.

76. Crowe, W.E., Mitchell, J.P., Gibson, V.C., and Schrock, R.R. (1990) *Macromolecules*, **23**, 3534–3536.

77. Benedicto, A.D., Claverie, J.P., and Grubbs, R.H. (1995) *Macromolecules*, **28**, 500–511.

78. Bielawski, C.W., Benitez, D., Morita, T., and Grubbs, R.H. (2001) *Macromolecules*, **34**, 8610–8618.

79. Hillmyer, M.A., Nguyen, S., and Grubbs, R.H. (1997) *Macromolecules*, **30**, 718–721.

80. Morita, T., Maughon, B.R., Bielawski, C.W., and Grubbs, R.H. (2000) *Macromolecules*, **33**, 6621–6623.

81. Ji, S., Hoye, T.T., and Macosko, C.W. (2004) *Macromolecules*, **37**, 5458–5489.

82. Maughon, B.R., Morita, T., Bielawski, C.W., and Grubbs, R.H. (2000) *Macromolecules*, **33**, 1929–1935.

83. Scherman, O.A., Rutenberg, I.M., and Grubbs, R.H. (2003) *J. Am. Chem. Soc.*, **125**, 8515–8522.

84. Xia, Y., Verduzco, R., Grubbs, R.H., and Kornfield, J.A. (2008) *J. Am. Chem. Soc.*, **130**, 1735–1740.

85. Matson, J.B., Virgil, S.C., and Grubbs, R.H. (2009) *J. Am. Chem. Soc.*, **131**, 3355–3362.

86. Fraser, C., Hillmyer, M.A., Gutierrez, E., and Grubbs, R.H. (1995) *Macromolecules*, **28**, 7256–7261.

87. Hilf, S., Berger-Nicoletti, E., Grubbs, R.H., and Kilbinger, A.F.M. (2006) *Angew. Chem., Int. Ed.*, **45**, 8045–8048.

88. Perrier, S. and Wang, X. (2007) *Nature*, **445**, 271.

89. Hilf, S., Grubbs, R.H., and Kilbinger, A.F.M. (2008) *Macromolecules*, **41**, 6006–6011.

90. Hilf, S. and Kilbinger, A.F.M. (2007) *Macromol. Rapid Commun.*, **28**, 1225–1230.

91. Hilf, S., Hanik, N., and Kilbinger, A.F.M. (2008) *J. Polym. Sci. Part A: Polym. Chem.*, **46**, 2913–2921.

92. Hilf, S. and Kilbinger, A.F.M. (2009) *Macromolecules*, **42**, 4127–4133.

93. Hilf, S. and Kilbinger, A.F.M. (2009) *Macromolecules*, **42**, 1099–1106.

94. Hilf, S. and Kilbinger, A.F.M. (2010) *Macromolecules*, **43**, 208–212.

7

Functional Polymers with Controlled Microstructure Based on Styrene and *N*-Substituted Maleimides

Delphine Chan-Seng, Mirela Zamfir, and Jean-François Lutz

7.1
Introduction

Biopolymers, such as proteins and nucleic acids, have a precise structure, where the exact chemical composition and the sequence of each composing unit, called primary structure, are precisely defined. Many of these polymers can fold spontaneously into well-arranged compact shapes, due to their secondary and tertiary structures, which are responsible for their specific biological functions. The folding of these biomacromolecules mainly relies on their primary structure rather than on the architecture of the macromolecules.

Polymer chemists look at synthesizing polymers that will be able to perform a specific function, such as biopolymers, responding to the application targeted either by developing original materials or by mimicking Nature [1]. The current toolbox of the polymer chemist allows synthesizing macromolecules with precise molecular weight, composition, and architecture, which could bear a large variety of functional groups. Various techniques have been developed to incorporate functional moieties on macromolecules, including the preparation of the polymer using functional initiators and/or monomers [2, 3] or post-polymerization modification of the polymer [4]. While the presence of functional moieties on the polymer is an important factor to adapt the properties of the polymer to the targeted application, the precise positioning of these functionalities on the polymer backbone could also bring further contribution to its efficacy.

However, the degree of control of the primary structure (i.e., order of the comonomer sequences) of synthetic polymers still does not rival with those of macromolecules produced in Nature [5, 6]. Various synthetic routes to prepare sequence-controlled polymers have been explored [7, 8]. One of the widely used methods is the solid-phase synthesis technique developed for peptide synthesis, consisting in its assemblage by successive additions of the various amino acids in the order of the desired sequence involving protection/deprotection steps for each amino acid incorporation [9]. This solid-phase synthesis technique has been further exploited by numerous research groups to prepare various types of nonnatural sequence-defined oligomers such as oligoesters, oligoamides, oligoureas, or

oligocarbamates [7, 10, 11]. For example, classic synthetic polymers such as polyamides – traditionally prepared by step-growth chemistry – can be prepared by solid-phase synthesis, for example, (i) by stepwise addition of succinic anhydride and a diamine, either a poly(ethylene glycol)-based diamine or 1,6-diaminohexane, without requiring any protection/deprotection steps [12] or (ii) by using succinic anhydride and a diamine, (*S*)-2-(9-fluorenylmethoxycarbonyl-amino)-1-propylamine, the diamine being protected to control the orientation of the chiral center [13]. The use of supported chemistry for the elaboration of well-defined polymers prepared by step-growth copolymerization is essential, since unsupported step-growth copolymerization of A-A and B-B comonomers, while allowing the preparation of alternating copolymers, do not lead to polymers with well-controlled molecular weight and architecture.

The control of the primary structure of copolymers in the case of chain-growth copolymerization is more challenging. Generally, the high reactivity of the propagating chain centers leads to a random distribution of the comonomers on the polymer backbone. An exception is the synthesis of alternating copolymers, which can be prepared using certain monomer pairs favoring cross-propagation [14]. Several examples of alternating comonomer pairs have been described in radical and cationic chain-growth polymerizations [5, 14, 15]. An interesting recent example concerns the metal-catalyzed synthesis of alternating polyesters [16]. As an illustration, Kramer *et al.* described the polymerization of two different enantiopure comonomers (derived from β-lactones) of opposite stereochemistry in the presence of a syndiospecific catalyst based on yttrium, yielding a polymer with a high degree of alternation [17].

Another example of alternating copolymers has been largely reported for some polymers prepared by radical-initiated copolymerizations of electron-donor and electron-acceptor comonomers [14]. Our research group has been especially interested in using styrene and maleimides as comonomer pairs and taking advantages of their specific copolymerization behavior to prepare well-defined copolymers with controlled microstructure (Figure 7.1) [18]. In this chapter, we first review the copolymerization of these monomer pairs under conventional and controlled radical polymerization conditions before introducing the strategy developed in our laboratory allowing the precise positioning of various *N*-substituted maleimides on a polystyrene backbone. Then, we present the recent achievements employing this strategy, including polyelectrolytes and folded macromolecules, and the elaboration of more sophisticated functional polymers prepared by post-polymerization modification techniques such as copper-catalyzed 1,3-dipolar cycloaddition or reactions promoted by monomers bearing activated esters.

7.2
Background on Radical Copolymerization of Styrene and Maleimides

Common comonomer pairs allowing the preparation of alternating copolymers include *N*-vinylcarbazole–fumaronitrile [19–21], styrene–maleic anhydride
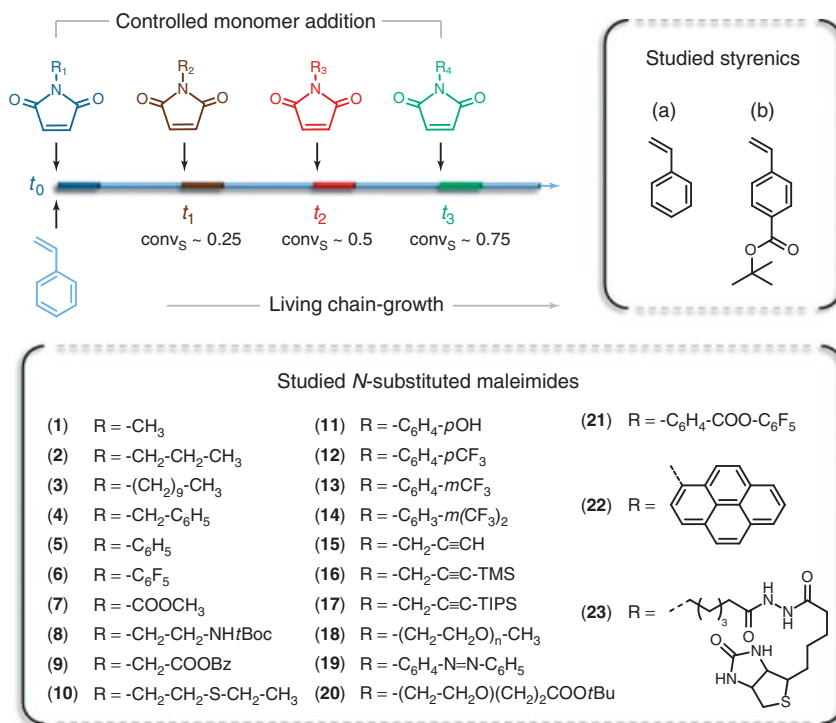
Figure 7.1 General concept for the synthesis of sequence-controlled polymers by controlled radical copolymerization of donor (styrenes) and acceptor (*N*-substituted maleimides) comonomers. The insets show the molecular structures of the monomers that have already been tested in our laboratory.

[14, 15, 22, 23], and styrene–maleimides. This section focuses on the copolymerization of styrene with *N*-substituted maleimides under either conventional or controlled radical polymerization conditions.

7.2.1
Conventional Radical Polymerization

The alternating phenomenon observed for radical-initiated copolymerization has been explained by different factors favoring the cross-propagation of the comonomers. It includes factors such as resonance stability – in other words, an unstable propagating species preferring to react with a resonance-stabilized monomer and vice versa – and polarity of the double bond – in other words, a propagating species formed from a monomer with a double bond bearing a partially positive charge preferring to add to a monomer whose double bond is partially negatively charged and vice versa [14]. Thus, strong electron acceptors, such as maleimides, will prefer to react with propagating chains whose radicals

are next to an electron-donating substituent, such as styryl radicals, rather than with propagating chains whose radical is next to an electron-accepting substituent.

The tendency toward alternation was studied using different approaches. Mayo and Lewis [24] were among the first to evaluate the relative reactivity of propagating chains formed from each comonomer, with the comonomers providing information on their own arrangement on the polymer backbone. The alternating copolymerization is characterized by the product $r_1 \times r_2 = 0$, where r_1 and r_2 are the monomer reactivity ratios, with r_1 and r_2 both not >1. However, a strong tendency toward alternation can also occur if the product $r_1 \times r_2$ is very small, that is, close to zero. Alfred and Price attempted to correlate the monomer reactivity with the structure of the comonomers in the *Q-e* scheme, *Q* representing the intrinsic reactivity and *e* the polarity of each comonomer/propagating chain [25]. Alternating copolymers are usually predicted by similar *Q* values accompanied with a large difference in polarity expressed by the *e* values of each comonomer, in other words, high values and of opposite sign. For example, the reactivity ratios for the copolymerization of styrene with maleimide were determined as $r_{styrene} = 0.1$ and $r_{maleimide} = 0.1$ according to the Mayo and Lewis method, while using the Price–Alfred scheme, the reactivity and the polarity of styrene and maleimide were calculated as $Q_{styrene} = 1$ and $e_{styrene} = -0.8$ and $Q_{maleimide} = 1.8$ and $e_{maleimide} = 1.34$ [26]. In this case, an abnormal value of $Q_{maleimide}$ was observed, which was explained by the formation of an electron donor–electron acceptor complex in the transition state between styrene and maleimide.

A large variety of *N*-substituted maleimides have been copolymerized with styrene, leading to polymers with a strong tendency toward alternation. One of the first examples was reported by Coleman and Conrady [27], who homopolymerized and copolymerized *N*-butyl maleimide and *N*-dodecyl maleimide with various vinyl monomers including styrene, leading to alternating copolymers. Using the method developed by Mayo and Lewis, they determined the reactivity ratio of *N*-butyl maleimide with styrene as $r_{styrene} = 0.025$ and $r_{N\text{-butyl maleimide}} = 0.06$. Yamada *et al.* [28] copolymerized *N*-hydroxymethyl maleimide, *N*-hydroxyethyl maleimide, and *N*-(4-hydroxyphenyl) maleimide with styrene, vinyl acetate, methyl methacrylate, and *N*-vinylpyrrolidone. Alternating copolymers were obtained when these maleimides were copolymerized with styrene or *N*-vinylpyrrolidone. Urushido *et al.* [29] reported the preparation of alternating copolymers when copolymerizing *N*-allyl maleimide with styrene. While all the maleic double bonds were consumed during the polymerization, the allylic double bonds remained untouched. *N*-carboxyphenyl maleimide was copolymerized with styrene, but the alternating tendency was reported to be lower compared to other styrene copolymerization with *N*-substituted maleimides. This phenomenon was observed even though the Alfred–Price *Q* and *e* values remained similar to those of other styrene-*N*-substituted maleimide systems in which copolymers with a higher degree of alternation were obtained [30]. Other *N*-substituted maleimides copolymerized with styrene included *N*-*n*-hexyl maleimide [31], *N*-cyclohexyl maleimide [31], *N*-benzyl maleimide [31], *N*-phenyl maleimide [32–35], *N*-(alkyl-substituted phenyl) maleimides [33], *N*-(substituted phenyl)

maleimides [36], *N*-(1-naphtyl) maleimide [37], *N*-(2-chlorophenyl) maleimide [38], *N*-pentafluorophenyl maleimide [39], *N*-[3,5-bis(trifluoromethyl)phenyl] maleimide [39], *N*-(3-trifluoromethylphenyl) maleimide [39], *N*-(4-trifluoromethylphenyl) maleimide [39], and *N*-maleoyl amino acids prepared from maleic anhydride and an amino acid, either L-alanine or L-phenylalanine [40]. Alternating copolymers prepared from styrene and *N*-substituted maleimides bearing an initiator allowing the introduction of grafts from the copolymer backbone by atom-transfer radical polymerization (ATRP) have been described first by Çakir *et al.* using (2,5-dioxo-2,5-dihydro-1*h*-pyrrole-1-yl)methyl 2-bromopropanoate as the *N*-substituted maleimide followed by polymerization of methyl methacrylate by ATRP to create the grafts [41]. Deng and Chen [42] employed *N*-[2-(2-bromoisobutyryloxy)ethyl] maleimide as comonomer of styrene and polymerized *tert*-butyl acrylate from the ATRP initiator to prepare brushes. Besides bulk and solution polymerizations, styrene and *N*-butyl maleimide have been copolymerized under microemulsion conditions [43].

7.2.2
Controlled Radical Polymerization

Polymers with well-defined molecular weight and narrow molecular weight distribution can be synthesized by controlled radical polymerizations. The most common techniques include stable free radical polymerization (SFRP, also known as nitroxide-mediated polymerization or NMP) [44–46], ATRP [47–50], and reversible addition-fragmentation chain-transfer polymerization (RAFT) [51–53]. Styrene and *N*-substituted maleimides have been copolymerized using these three controlled radical polymerization systems.

Schmidt-Naake *et al.* [55] reported the copolymerization of styrene and various *N*-substituted maleimides, that is, *N*-cyclohexyl maleimide [54, 55], *N*-butyl maleimide, and *N*-phenyl maleimide in the presence of the stable free radical 2,2,6,6-tetramethylpiperidin-1-yloxyl (TEMPO) initiated by benzoyl peroxide, while Lokaj *et al.* studied the copolymerization of styrene with maleimide [56], *N*-butyl maleimide [57], or *N*-phenyl maleimide [58] in the presence of TEMPO and initiated by autopolymerization (i.e., styrene thermal initiation). As in the case of conventional radical polymerization, an alternating copolymer was observed, but the polymerization technique employed allowed better control over the molecular weight and molecular weight distribution. Alternating copolymers with controlled molecular weight and molecular weight distribution were also obtained under ATRP conditions. Styrene was copolymerized with *N*-(2-acetoxyethyl)maleimide [59], *N*-phenyl maleimide [59], *N*-cyclohexyl maleimide [60]. Zhao *et al.* reported the copolymerization of styrene with *N*-phenyl maleimide in the presence of an ATRP initiator bearing a polyarylether dendron in anisole [61] or with *N*-hexyl maleimide [62], *N*-phenyl maleimide [63], *N*-cyclohexyl maleimide [63], and *N*-butyl maleimide [63] in the ionic liquid 1-butyl-3-methylimidazolium hexafluorophosphate. Block copolymers of *N*-phenyl maleimide and styrene were prepared under RAFT conditions using 2,2′-azobisisobutyronitrile as the initiator and 2-cyanopropyl-2-yl

dithiobenzoate as chain-transfer agent [64]. Homopolymerization of *N*-phenyl maleimide was first evaluated, which indicated the ability to reach relatively high monomer conversion up to 65% with good control over the molecular weight distribution while following first-order kinetics. Nevertheless, the chain extension of this homopolymer with styrene led to very low styrene conversion even after a long period, that is, 2.5% after 24 h. The authors succeeded, however, to prepare poly(*N*-phenyl maleimide-*b*-styrene) with narrow molecular weight distributions by chain extension of a polystyrene macroinitiator prepared by RAFT with *N*-phenyl maleimide.

Furthermore, the choice of the substituent on the *N*-substituted maleimide to prepare copolymers with styrene allowed the preparation of polymers having a nonlinear architecture, such as graft and hyperbranched polymers. *N*-(4-Hydroxyphenyl) maleimide, *N*-(4-(α-chloropropionyloxy)]phenyl maleimide, and *N*-(4-(α-bromopropionyloxy)]phenyl maleimide were copolymerized with styrene under RAFT conditions to form alternating copolymers used as precursor of graft copolymers prepared by polymerization of styrene from the ATRP initiators present on the copolymer backbone [65]. Hyperbranched polymers were prepared by self-condensing vinyl polymerization (SCVP) under ATRP conditions of styrene in the presence of *N*-[2-(2-bromoisobutyryloxy)ethyl] maleimide [66], *N*-(4-α-bromobutyryloxy phenyl) maleimide [67–69], *N*-[4-(α-chloropropionyloxy)]phenyl maleimide [69], or *N*-[4-(α-bromopropionyloxy)] phenyl maleimide [69] as inimer. The use of an excess of styrene favored the consumption of the *N*-[2-(2-bromoisobutyryloxy)ethyl] maleimide to form a core of the corresponding copolymer and the formation of polystyrene branches from this core [66]. Another approach to synthesize branched copolymers has been reported by Wenyan *et al.* [70], which consisted in copolymerizing styrene and *N*-phenyl maleimide in the presence of divinylbenzene under ATRP conditions.

As described previously in this section, radical copolymerization of styrene and *N*-substituted maleimides can lead to a large variety of structures such as alternating or hyperbranched copolymers. However, an interesting case of copolymerization was reported when styrene and maleic anhydride were used as comonomers in a nonequimolar ratio. Benoit *et al.* [71] reported the copolymerization of maleic anhydride with nine times excess of styrene by NMP using 2,2,5-trimethyl-3-(1-phenylethoxy)-4-phenyl-3-azahexane as alkoxyamine. Contrary to conventional radical polymerization where homopolystyrene and a variety of copolymers would be formed under this comonomer feed ratio, all the chains formed by NMP had the same composition. At the early stage of the polymerization, maleic anhydride was consumed fast and preferentially, while the conversion of styrene in the same time frame remained low; that is, when all maleic anhydride was completely depleted, only around 30% of styrene was polymerized. Once all the maleic anhydride was used, homopolymerization of styrene occurred, leading to the one-pot preparation of the block copolymer poly[(styrene-*r*-maleic anhydride)-*b*-styrene]. The first block, poly(styrene-*r*-maleic anhydride), was composed randomly of two styrene repeat unit per maleic anhydride repeat unit, and

the randomness of this copolymer was assigned to the high polymerization temperature employed to conduct NMP. Zhu *et al.* prepared a similar block copolymer by RAFT copolymerization of maleic anhydride and styrene with a comonomer feed ratio of 1–9 and followed the consumption of each comonomer by gas chromatography, observing that the copolymer was predominantly alternating until full conversion of maleic anhydride followed by polymerization of pure styrene forming a second block [72]. The authors observed a similar behavior when performing RAFT copolymerization of styrene with *N*-phenyl maleimide. Preparation of poly[(styrene-*alt*-maleic anhydride)-*b*-styrene] was also reported by various groups under RAFT [73, 74] and NMP [75] conditions. The ability to prepare one-pot block copolymers due to this feature of controlled radical copolymerization of styrene with maleic anhydride led to the strategy developed in our laboratory to prepare polymers with a controlled microstructure, which is described in the following section.

7.3
Precise Incorporation of Maleimide Units on Polystyrene Backbone

7.3.1
Strategy

Our research group and others have been exploring methods to prepare polymers with a controlled microstructure [7, 76]. Our approach is based on the controlled radical copolymerization of styrene derivatives with strong electron-acceptor monomers that will be locally and precisely incorporated on the polymer backbone (Figure 7.1). Furthermore, we chose *N*-substituted maleimides as electron-acceptor monomers because they are more favorable to cross-propagation with styrene than homopolymerization [14, 15] and offered a wide range of monomers to explore by varying the substituent present at the *N*-position of the maleimide. This monomer pair, that is, styrene derivatives and *N*-substituted maleimides, presents a strong tendency toward alternation even if the *N*-substituted maleimide is present in a discrete amount as discussed previously. We reduced the fraction of *N*-substituted maleimide to the point where a single electron-acceptor monomer will be incorporated on the polystyrene chain, that is, 1 equivalent relative to the initiator in the presence of a large excess of styrene. This system was expected to be viable because the consumption of *N*-substituted maleimide when copolymerized with styrene is extremely fast compared to styrene and will be incorporated locally on the growing polymer chain. This strategy was developed first for the ATRP system [77, 78] because the homopolymerization of styrene [79–81] and copolymerization of styrene and maleimides [59, 61, 63] are largely reported in the literature, but it was then extended to the NMP system [82, 83].

The feasibility of this approach considered first the kinetic study of the copolymerization of styrene and various *N*-substituted maleimides, that is, *N*-methyl maleimide (**1**), *N*-propyl maleimide (**2**), or *N*-benzyl maleimide (**4**), under bulk ATRP conditions where all the monomers are introduced at once at the beginning

of the polymerization [77]. Similar to the work of Benoit *et al.* [71], in which they followed the evolution of the conversion of styrene and maleic anhydride during their copolymerization under NMP conditions by ^{1}H NMR, we looked at the conversion of each comonomer during the polymerization. The plots of conversion versus time for all the *N*-substituted maleimides copolymerized with styrene clearly demonstrated the very fast consumption of the *N*-substituted maleimides at the early stage of the copolymerization; that is, more than 99% *N*-substituted maleimides was converted in 15 min, while the conversion of styrene was low (10%). Afterward, only the homopolymerization of styrene was observed.

To evaluate whether each copolymer chain prepared from 100 equivalents of styrene and 1 equivalent of *N*-benzyl maleimide possessed one maleimide repeat unit per chain, matrix-assisted laser desorption/ionization time-of-flight (MALDI-TOF) mass spectrometry was performed [77]. The spectrum recorded indicated that the polymer chains with no *N*-benzyl maleimide or containing three or more maleimides represented only a small fraction of the polymer sample. The predominant peaks corresponded to polymer chains bearing one or two maleimides, and the presence of two maleimides per polymer chain could be partially due to the polymer fractions formed by bimolecular termination. However, these data suggested that the targeted number of maleimide units per polymer chain is obtained within a narrow sequence distribution during the copolymerization of styrene with *N*-benzyl maleimide.

While the system described until now considered only the incorporation of the functional maleimide at the α extremity of the polystyrene chain, it has been proved that the *N*-substituted maleimide can be positioned anywhere along the growing polystyrene chain. In fact, the *N*-substituted maleimide can be added to the polymerization medium at any precise time during the homopolymerization of styrene. For example, styrene polymerization can be started without any functional maleimide and, once a certain conversion of styrene is reached, for example, 35%, 1 equivalent of *N*-propyl maleimide is added to the polymerization medium [78]. Since the consumption of functional maleimides during their copolymerization with styrene is very fast, *N*-propyl maleimide was incorporated in a precise location determined by the time of its addition. ^{1}H NMR confirmed the fast quantitative conversion of the functional maleimide, while the styrene conversion was low. The styrene polymerization continued then until the full conversion of styrene.

In summary, this strategy allowed creating polystyrene chains bearing discrete locally positioned *N*-substituted maleimides with a narrow sequence distribution, whose location could be controlled by the time of addition of the functional maleimide.

7.3.2
Maleimides

This concept can be utilized with maleimides bearing a wide range of functional groups, including functional moieties that allow post-polymerization modifications

such as protected alkynes or activated esters. The *N*-substituted maleimides evaluated with this technique in our laboratory are shown in Figure 7.1 [78, 83, 84]. Since a fast and local incorporation of the maleimide is required to promote the precise positioning of this monomer on the polystyrene backbone, high cross-propagation between these monomer pairs is needed. This phenomenon was investigated for each *N*-substituted maleimide by following the kinetics of their copolymerization with styrene and the consumption of each comonomer during the polymerization. While most of the *N*-substituted maleimides exhibited very favorable cross-propagation with styrene and performed well using our strategy, a few of them were more challenging to prepare well-defined polymers with controlled microstructure.

When *N*-(4-hydroxyphenyl) maleimide (**11**) was used as the *N*-substituted maleimide for the copolymerization with styrene, low monomer conversion was observed [78]. The phenol moiety on the functional maleimide may have induced inhibition of the radical polymerization, which explains this phenomenon.

An attempt was made to copolymerize a maleimide bearing a biotin moiety **23** with styrene. Since this functional maleimide had a poor solubility in styrene, the incorporation of this maleimide on the polystyrene backbone was very low when the copolymerization was performed under bulk conditions. When the copolymerization was performed in *N,N*-dimethylformamide, the polymerization was homogeneous, but this functional maleimide interfered with the ATRP catalyst, inhibiting the polymerization. However, the biotin could be introduced on the polymer backbone by post-polymerization modification [83].

N-Propargyl maleimide (**15**), a precursor for post-polymerization modification by copper-catalyzed 1,3-dipolar cycloaddition, was copolymerized with styrene, but led to the formation of copolymers with a broad bimodal molecular distribution [78]. The perturbation of the radical polymerization, due to the coupling reactions occurring at the terminal acetylene functions, leading to cross-linking when using a monomer bearing unprotected alkyne, had been observed previously by others [85, 86]. This difficulty could be overcome by using protected alkynes with either trimethylsilyl (TMS) or triisopropylsilyl (TIPS) protecting groups (see Structures **16** and **17** in Figure 7.1), which could be deprotected after polymerization in the presence of tetrabutylammonium fluoride (TBAF) [84].

7.3.3
Styrene Derivatives

As indicated in the previous section, a wide range of *N*-substituted maleimides were investigated. Furthermore, this technique was also broadened by using other donor monomers, especially para-substituted styrene derivatives.

In the attempt to prepare well-defined polyelectrolytes with controlled microstructure, *tert*-butyl 4-vinyl benzoate (**b**), a protected version of vinyl benzoic acid, was synthesized and was subsequently sequentially copolymerized with *N*-substituted maleimides, that is, *N*-benzylmaleimide **4**, *N*-(1-pyrenyl)maleimide (**22**), and TIPS-protected *N*-propargyl maleimide (**17**), under NMP using the commercially available initiator BlocBuilder MA (Figure 7.2) [82]. The reactivity ratio calculation
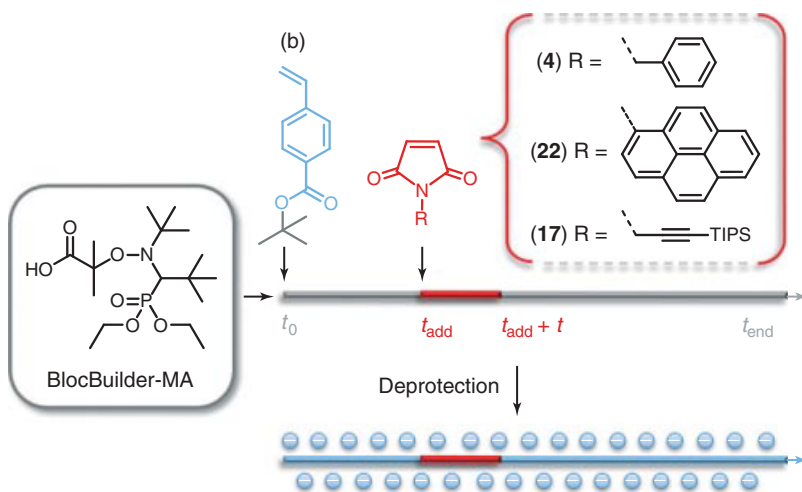
Figure 7.2 General strategy for the synthesis of well-defined polyelectrolytes with a controlled microstructure. Well-defined non-ionic precursors were first synthesized by sequence-controlled radical polymerization of *tert*-butyl 4-vinyl benzoate (**b**) with various *N*-substituted maleimides (structures **4**, **17**, and **22** in Figure 7.1). Afterward, these macromolecules were hydrolyzed into polyanions [82].

indicated a pronounced alternating tendency for the *tert*-butyl 4-vinyl benzoate and *N*-benzylmaleimide pair, but the value obtained ($r_{t\text{-BuVBA/BzMI}} = 0.14$) was slightly higher than the one previously obtained for styrene and *N*-substituted maleimides [18] suggesting a lower incorporation precision. *N*-substituted maleimides were added to polymerization medium at the beginning of the polymerization or 2 h after the homopolymerization of *tert*-butyl 4-vinyl benzoate, corresponding to approximately half conversion of this monomer. After two additional hours of reaction, *N*-substituted maleimides were almost fully consumed, while *tert*-butyl 4-vinyl benzoate conversion increased by 15%. The polymerization was conducted until high conversion of all the monomers was reached, leading to well-defined polymers with controlled microstructures. The *tert*-butyl protecting groups were then removed under acidic conditions without interfering with the functional groups present on the polymer, affording well-defined polyelectrolytes bearing precisely positioned functional groups such as pyrene or protected alkyne.

7.4
Tuning a Simple Technique for the Preparation of Sequence-Controlled Polymers to the Elaboration of Functionalized Well-Defined Macromolecules

The previous section described the controlled radical polymerization of styrene and maleimides, where the controlled addition of discrete amounts of maleimide during styrene polymerization led to their incorporation with a precise positioning

on the polystyrene backbone. In this section, the versatility of this technique to prepare more elaborate macromolecules is presented.

7.4.1
Incorporation of Different Functionalities on the Same Polymer Backbone of a Well-Defined Polymer Possessing a Controlled Microstructure

The preparation of well-defined polymers with a controlled microstructure described up to now incorporated one unit of *N*-substituted maleimide per polymer chain. This strategy can, however, handle the introduction of several *N*-substituted maleimides that can be positioned on the polystyrene backbone [77].

As described previously, *N*-substituted maleimides are consumed extremely fast after their addition to the polymerization medium, allowing their precise positioning along the polystyrene backbone when a discrete amount of this monomer is used. As the addition of the *N*-substituted maleimide can be done at the beginning of the polymerization or at any time during the polymerization, it can be positioned either at the extremity of the polymer chain or anywhere along the polymer backbone. This technique also permitted the preparation of polystyrene bearing multiple *N*-substituted maleimides precisely positioned at different locations, and its feasibility was demonstrated using *N*-propyl maleimide [78]. A discrete amount of *N*-propyl maleimide was introduced to the polymerization medium at the beginning of the polymerization and was incorporated rapidly in the polymer backbone, that is, at the α-end of the polymer chain. Once styrene conversion reached ~60%, a second equivalent of *N*-propyl maleimide was added to the polymerization medium. The monomer conversion of styrene and *N*-propyl maleimide was monitored during the polymerization, confirming the proper local incorporation of *N*-propyl maleimide after each addition along the polystyrene backbone.

An example considered the introduction of four *N*-substituted maleimides, that is, *N*-propyl maleimide (**2**), *N*-benzyl maleimide (**4**), *N*-methyl maleimide (**1**), and *N*-[3,5-bis(trifluoromethyl) phenyl] maleimide (**14**), added at precise times during the ATRP of styrene. The efficiency of the preprogrammed insertion of different *N*-substituted maleimides was monitored by ^{1}H NMR (Figure 7.3). Immediately after each addition of the *N*-substituted maleimide, the characteristic peaks of this functional monomer were observed by ^{1}H NMR and they disappeared with time indicating the proper incorporation and consumption of each *N*-substituted maleimide after their respective additions. These results demonstrated the ability of this strategy to prepare well-defined, tailored polymers with controlled microstructures.

7.4.2
Designing 1D Periodic Molecular Arrays

While the preparation of sequence-controlled poly(styrene-*co*-*N*-substituted maleimide)s is well developed for a library of *N*-substituted maleimides [78], this synthetic route is challenging when attempting to synthesize long, well-defined
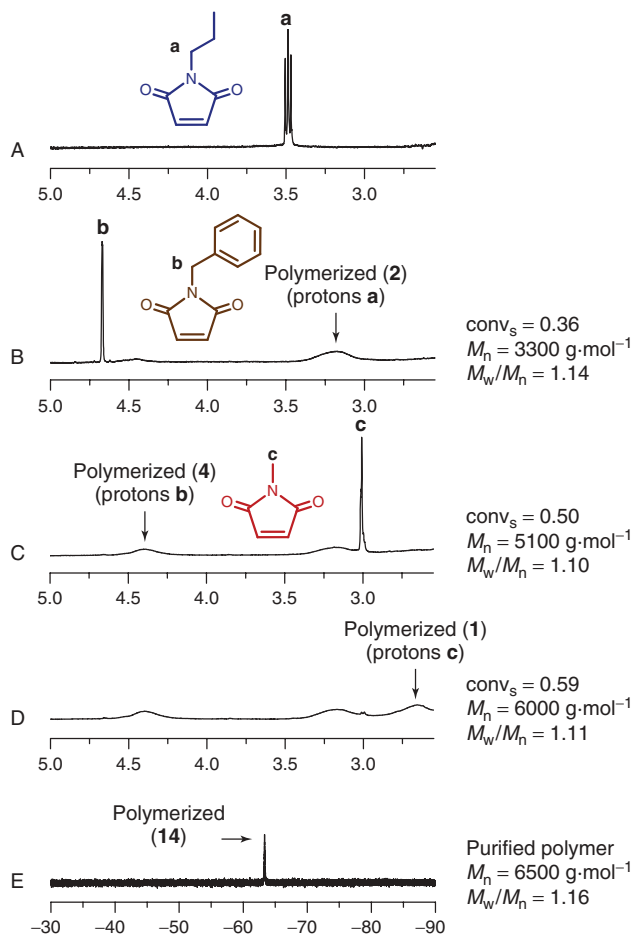
Figure 7.3 NMR spectra recorded in CDCl$_3$ at different stages of the sequential copolymerization of styrene (**a**) with the *N*-substituted maleimides **2**, **4**, **1**, and **14** (added in this particular order; see Figure 7.1 for detailed molecular structures): (a) ^{1}H spectrum (zoom of the region 2.55–5.0 ppm) of the initial reaction mixture, (b) ^{1}H spectrum recorded shortly after the addition of **4** ($t = 1$ h), (c) ^{1}H spectrum recorded shortly after the addition of **1** ($t = 2$ h45 min), (d) ^{1}H spectrum recorded 15 min before the addition of **14** ($t = 5$ h45 min), and (e) ^{19}F spectrum recorded for the final purified copolymer (isolated after 21 h of polymerization) [77].

polymer chains with controlled microstructures. To overcome this difficulty, high-molecular-weight polymers with controlled sequences can be prepared by covalently assembling short sequence-controlled oligomers (Figure 7.4). Various coupling strategies have been reported in the literature [87], and the copper-catalyzed azide–alkyne cycloaddition [88–90] was selected to prepare high-molecular-weight poly(styrene-*co*-*N*-substituted maleimide)s with precise positioning of the *N*-substituted maleimides.
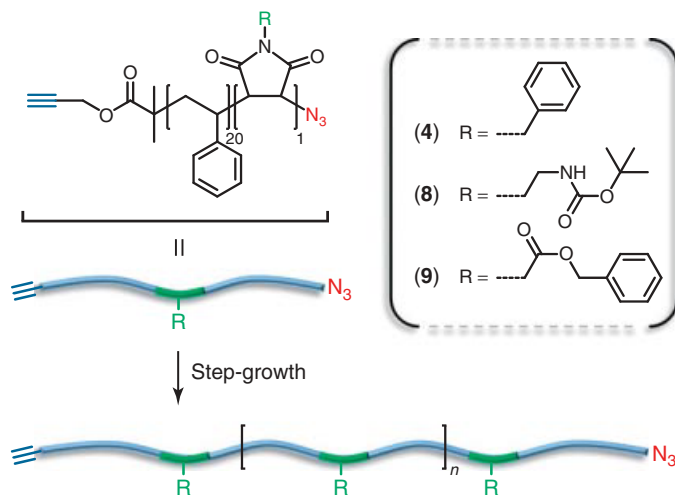
Figure 7.4 General strategy for preparing functional periodic copolymers by step-growth ''click'' coupling of sequence-controlled heterotelechelic copolymers. The polystyrene precursors were first synthesized by sequence-controlled copolymerization of styrene (**a**) with functional *N*-substituted maleimides (structures **4**, **8**, and **9** in Figure 7.1) [91].

Styrene and *N*-substituted maleimide, using either *N*-(2-(amino-*t*Boc)-ethylen) maleimide (**8**) or benzyl *N,N*-maleoylglycinate (**9**), were sequentially copolymerized by ATRP in the presence of a TMS-protected alkyne-functionalized initiator, that is, 3-(1,1,1-trimethylsilyl)-2-propynyl 2-bromo-2-methylpropanoate [91]. The *N*-substituted maleimide was locally introduced into the polymerization medium when conversion of styrene had reached ∼40–45%. The obtained oligo(styrene-*co*-*N*-substituted maleimide) ($DP_n = 20$) possessing a functional *N*-substituted maleimide in the middle of the oligomer chain was then converted to α-alkyne ω-azido telechelic oligo(styrene-*co*-*N*-substituted maleimide). A nucleophilic substitution was first performed on the bromine chain end from the ATRP-formed oligomer in the presence of sodium azide, which was followed by the cleavage of TMS-protected group present on the alkyne function using TBAF. These functional telechelic oligomers were polymerized at room temperature by step-growth ''click'' coupling. After one day, ^{1}H NMR indicated the presence of triazole linkages, while size-exclusion chromatography (SEC) confirmed the formation of higher molecular weight macromolecules corresponding to the attachment of 5–10 oligomers together.

7.4.3
Elaboration of New Materials by Post-polymerization Modification

Post-polymerization modification is an attractive alternative for the synthesis of macromolecules decorated with functional groups and can surmount the low

tolerance of a variety of polymerization conditions to certain functional groups as well as offering a number of advantages when compared to copolymerization strategies [4]. This method refers to the polymerization of monomers bearing functional groups that are inert toward the polymerization conditions but offering the possibility to be quantitatively transformed into a wide range of other functional groups in a subsequent reaction step. Thus, a single reactive polymer precursor can be employed to generate a diverse library of functional polymers with identical degree of polymerization and chain-length distributions.

7.4.3.1 Activated Esters as Precursor of Post-polymerization Modification

Polymers bearing activated carbonyl compounds have proved to be an attractive chemical tool for post-polymerization modification [92]. Early examples of highly ester-activated polymers were pioneered by Ferruti *et al.* [93] and Ringsdorf *et al.* [94]. Another interesting coupling approach was stressed by the group of Theato using monomers bearing activated esters, such as *N*-hydroxy succinimide esters or pentafluorophenyl esters, which can react in post-polymerization with primary and secondary amines functionalized with the desired moiety [95–97]. Therefore, by choosing a substituent on the maleimide that is capable of promoting post-polymerization modification, a wide range of functional polymers can be prepared.

In a recent study, a maleimide functionalized with pentafluorophenyl ester, in particular pentafluorophenyl 4-maleimidobenzoate (**21**), was synthesized and copolymerized with styrene under NMP in the presence of BlocBuilder MA [83]. The active ester moiety was kinetically installed at the early stage of polymerization (i.e., near the α-chain end) and in the middle of highly defined polystyrene chains. Moreover, the pentafluorophenyl 4-maleimidobenzoate unit remained unaffected by the conditions of the polymerization as confirmed by the observation of the characteristic peaks of the pentafluorobenzyl ester moiety by ^{19}F NMR. The exact positioning of this functional monomer was dictated by the precise timing of the addition of the *N*-substituted maleimide, permitting the local incorporation of pentafluorophenyl 4-maleimidobenzoate on the polystyrene backbone. On the basis of the well-established post-polymerization modification chemistry using pentafluorophenyl ester moieties, the successful installation of both apolar and polar groups (i.e., 2,4-dimethoxy-benzyl amine and *N*-(+)-biotinyl-3-aminopropylammoniumtrifluoroacetate) was achieved. The full conversion of the pentafluorobenzyl ester groups in the presence of functional amines into amide moieties was confirmed by Fourier transform infrared (FTIR) spectroscopy and ^{1}H NMR.

7.4.3.2 Formation of Positionable Covalent Bridges

A more sophisticated example showing the ability to tune this system, where reactive functional groups can be introduced either at the extremity of the chain or along the polymer backbone, concerns the formation of positionable covalent bridges [84]. This approach requires the preparation of single polymer chains containing azide and alkyne functional groups susceptible to efficient post-polymerization
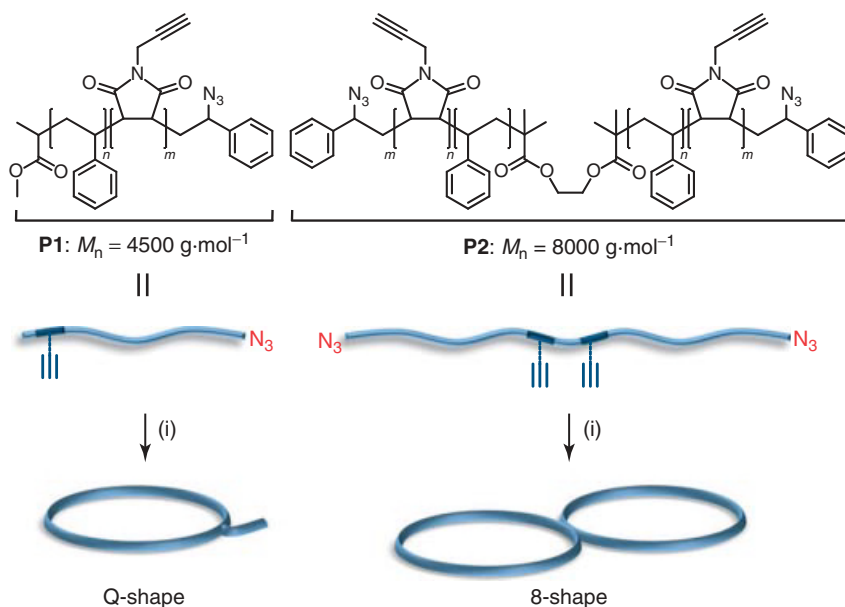
Figure 7.5 Covalent folding of linear synthetic polymer chains. Top: Molecular structures of foldable linear polystyrene chains prepared by ATRP. For simplicity, these structural formulae display only the average comonomer composition of the precursors and do not give information about the localization of the maleimide units in the chains. Bottom: Schematic representation of the folded macromolecules. Experimental conditions: (i) copper-catalyzed azide–alkyne 1,3-dipolar cycloaddition: CuBr, bipy, DMF, ultradiluted conditions, 80 °C [84].

modification chemistries such as copper-catalyzed 1,3-dipolar cycloaddition [89] or Glaser coupling [98], leading to the formation of different types of precise folded topologies.

The precursor was prepared by sequential copolymerization of styrene and protected N-propargyl maleimide (i.e., **16** or **17**) under ATRP conditions using a monofunctional ATRP initiator, followed by the nucleophilic substitution of the bromine chain end with sodium azide. After cleavage of the protecting group of the alkyne functions, copper-catalyzed 1,3-dipolar cycloaddition was performed under very dilute conditions to favor intramolecular reaction [99]. Depending on the location of the reactive alkyne functions in the polymer chains, the precursors were folded into P-shaped or Q-shaped macromolecules (Figure 7.5). The successful formation of covalent bridges was confirmed by FTIR measurements, while in SEC chromatograms, an apparent decrease of molecular weight was observed because of a hydrodynamic volume decrease caused by chain cyclization [100].

The monofunctional ATRP initiator was also replaced by a bifunctional one, and two different polymer precursors were obtained. The first polymer was prepared by the sequential copolymerization of styrene and a protected N-alkyne maleimide, followed by nucleophilic substitution of the bromine chain ends with sodium azide
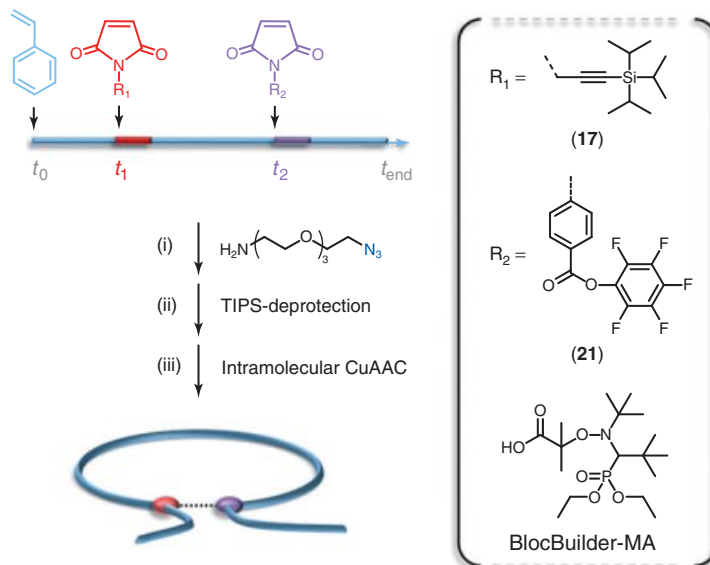
Figure 7.6 General strategy studied for folding polystyrene chains using asymmetric covalent bridges. The linear polystyrene precursors containing precisely incorporated reactive functions were first synthesized by sequence-controlled copolymerization of styrene (**a**) with functional *N*-substituted maleimides (structures **17** and **21** in Figure 7.1). Experimental conditions: (i) THF, RT, overnight; (ii) TBAF, THF, RT, overnight; and (iii) CuBr/bipy, 80 °C, ultradilute conditions in DMF [101].

and the cleavage of the protecting group of the alkyne function leading to an α, ω-diazido polystyrene bearing at least two *N*-propargyl maleimides on the polymer. A second polymer was prepared similarly but without modification of the bromine chain ends, affording α, ω-dibromo polystyrene bearing at least two *N*-propargyl maleimides on the polymer. The folding of these polymers was performed under different conditions. Copper-catalyzed 1,3-dipolar cycloaddition was performed on α, ω-diazido poly(styrene-*co*-*N*-propargyl maleimide) forming a bicyclic structure (8-shape, Figure 7.5), while α, ω-dibromo poly(styrene-*co*-*N*-propargyl maleimide) underwent a Glaser coupling, folding the polymer into a knot (α shape). In the latter case, a relatively high fraction of intermolecular defects was observed.

A very recent contribution describes a simple folding strategy for designing α-shaped polystyrene origamis stabilized by asymmetric covalent bridges, with variable sizes and loop diameters, which involves a series of subsequent efficient chemical steps (Figure 7.6) [101]. This approach relies on the synthesis of sequence-defined linear polystyrene precursors bearing two precisely localized reactive *N*-substituted maleimide comonomers, namely, TIPS-protected *N*-propargyl maleimide (**17**) and pentafluorophenyl 4-maleimidobenzoate (**21**), using sequence-controlled nitroxide-mediated copolymerization in the presence of BlocBuilder MA. Afterward, the first post-modification of the obtained polymer involved the reaction of the pentafluorophenyl-activated

ester function with an α,ω-difunctionalized oligoethylene glycol, that is, 11-azido-3,6,9-trioxaundecan-1-amine. Once the TIPS protecting group was removed to free the alkyne function, the polymer folding was performed by intramolecular copper-based 1,3-dipolar cycloaddition under dilute conditions. The successful formation of α-shaped folded origamis was confirmed by SEC, ^{1}H NMR, and FTIR spectroscopy measurements. In some of the described samples, nearly defect-free intramolecular folding could be obtained (i.e., <2% of intermolecular defects).

7.5
Summary and Outlook

The controlled radical polymerization of styrene with the addition of discrete amounts of *N*-substituted maleimides at well-determined time of reaction is an interesting method to prepare polymers with a well-defined microstructure. The introduction of large variety of *N*-substituted maleimides and styrene derivatives allows the synthesis of a library of functional polymers that can have broad applications. Furthermore, post-modifications of these polymers open the door to new well-defined architectures, such as precise folding of macromolecules.

References

1. Ouchi, M., Badi, N., Lutz, J.-F., and Sawamoto, M. (2011) *Nat. Chem.*, **3**, 917–924.

2. Coessens, V., Pintauer, T., and Matyjaszewski, K. (2001) *Prog. Polym. Sci.*, **26**, 337–377.

3. Chung, T.C. (2002) *Prog. Polym. Sci.*, **27**, 39–85.

4. Gauthier, M.A., Gibson, M.I., and Klok, H.-A. (2009) *Angew. Chem., Int. Ed.*, **48**, 48–58.

5. Lutz, J.-F. (2010) *Polym. Chem.*, **1**, 55–62.

6. Lutz, J.-F. (2010) *Nat. Chem.*, **2**, 84–85.

7. Badi, N. and Lutz, J.-F. (2009) *Chem. Soc. Rev.*, **38**, 3383–3390.

8. Brudno, Y. and Liu, D.R. (2009) *Chem. Biol.*, **16**, 265–276.

9. Merrifield, R.B. (1963) *J. Am. Chem. Soc.*, **85**, 2149–2154.

10. Börner, H.G. (2011) *Macromol. Rapid Commun.*, **32**, 115–126.

11. Hartmann, L. (2011) *Macromol. Chem. Phys.*, **212**, 8–13.

12. Rose, K. and Vizzavona, J. (1999) *J. Am. Chem. Soc.*, **121**, 7034–7038.

13. Mosca, S., Wojcik, F., and Hartmann, L. (2011) *Macromol. Rapid Commun.*, **32**, 197–202.

14. Cowie, J.M.G. (1985) *Alternating Copolymers*, Plenum Press, New York.

15. Rzaev, Z.M.O. (2000) *Prog. Polym. Sci.*, **25**, 163–217.

16. Brulé, E., Guo, J., Coates, G.W., and Thomas, C.M. (2011) *Macromol. Rapid Commun.*, **32**, 169–185.

17. Kramer, J.W., Treitler, D.S., Dunn, E.W., Castro, P.M., Roisnel, T., Thomas, C.M., and Coates, G.W. (2009) *J. Am. Chem. Soc.*, **131**, 16042–16044.

18. Lutz, J.-F., Schmidt, B.V.K.J., and Pfeifer, S. (2011) *Macromol. Rapid Commun.*, **32**, 127–135.

19. Shirota, Y., Matsumoto, A., and Mikawa, H. (1972) *Polym. J.*, **3**, 643–644.

20. Shirota, Y., Yoshimura, M., Matsumoto, A., and Mikawa, H. (1974) *Macromolecules*, **7**, 4–11.

21. Yoshimura, M., Mikawa, H., and Shirota, Y. (1978) *Macromolecules*, **11**, 1085–1091.

22. Alfred, T. and Lavin, T. (1945) *J. Am. Chem. Soc.*, **67**, 2044–2045.

23. Walling, C. and Mayo, F.R. (1947) *Discuss. Faraday Soc.*, **2**, 295–303.

24. Mayo, F.R. and Lewis, F.M. (1944) *J. Am. Chem. Soc.*, **66**, 1594–1601.

25. Alfred, T. Jr. and Price, C.C. (1947) *J. Polym. Sci.*, **2**, 101–106.

26. Van Paesschen, G. and Timmerman, D. (1964) *Makromol. Chem.*, **78**, 112–120.

27. Coleman, L.E. Jr. and Conrady, J.A. (1959) *J. Polym. Sci.*, **38**, 241–245.

28. Yamada, M., Takase, I., Tsukano, T., Ueda, Y., and Koutou, N. (1969) *Kobunshi Kagaku*, **26**, 593–601.

29. Urushido, K., Koike, K., Kitano, H., Kobayashi, M., and Kuribayashi, S. (1990) *Kobunshi Ronbunshu*, **47**, 79–82.

30. Oishi, T., Iwahara, M., and Fujimoto, M. (1991) *Polym. J.*, **23**, 1409–1417.

31. Oishi, T. and Kimura, T. (1976) *Kobunshi Ronbunshu*, **33**, 685–691.

32. Prementine, G.S., Jones, S.A., and Tirrell, D.A. (1989) *Macromolecules*, **22**, 770–775.

33. Matsumoto, A., Kubota, T., and Otsu, T. (1990) *Macromolecules*, **23**, 4508–4513.

34. Iwatsuki, S., Kubo, M., Wakita, M., Matsui, Y., and Kanoh, H. (1991) *Macromolecules*, **24**, 5009–5014.

35. Mori, H., Ii, Y., Yokohama, H., Tsuneshige, Y., Fujii, S., and Nakazato, T. (1999) United States Patent U.S. Pat. 5, 948, 879.

36. Yamada, M., Takase, I., and Mishima, T. (1967) *Kobunshi Kagaku*, **24**, 326–332.

37. Oishi, T. and Kimura, T. (1975) *Kobunshi Ronbunshu*, **32**, 380–383.

38. Mohamed, A.A., Jebrael, F.H., and Elsabeé, M.Z. (1986) *Macromolecules*, **19**, 32–37.

39. El-Guweri, M., Hendlinger, P., and Laschewsky, A. (1997) *Macromol. Chem. Phys.*, **198**, 401–418.

40. Oishi, T., Matsusaki, K., and Fujimoto, M. (1992) *Polym. J.*, **24**, 1281–1291.

41. Çakir, T., Serhatli, I.E., and Önen, A. (2006) *J. Appl. Polym. Sci.*, **99**, 1993–2001.

42. Deng, G. and Chen, Y. (2009) *J. Polym. Sci. Part A: Polym. Chem.*, **47**, 5527–5533.

43. Zhao, Y., Liu, P., Liu, H., Jiang, J., Chen, C., and Xi, F. (2001) *Macromol. Rapid Commun.*, **22**, 633–637.

44. Solomon, D.H., Rizzardo, E., and Cacioli, P. (1985) United States Patent U.S. Pat. 4, 581, 429.

45. Georges, M.K., Veregin, R.P.N., Kazmaier, P.M., and Hamer, G.K. (1993) *Macromolecules*, **26**, 2987–2988.

46. Tebben, L. and Studer, A. (2011) *Angew. Chem. Int. Ed.*, **50**, 5034–5068.

47. Kato, M., Kamigaito, M., Sawamoto, M., and Higashimura, T. (1995) *Macromolecules*, **28**, 1721–1723.

48. Wang, J.-S. and Matyjaszewski, K. (1995) *J. Am. Chem. Soc.*, **117**, 5614–5615.

49. Matyjaszewski, K. and Tsarevsky, N.V. (2009) *Nat. Chem.*, **1**, 276–288.

50. Ouchi, M., Terashima, T., and Sawamoto, M. (2009) *Chem. Rev.*, **109**, 4963–5050.

51. Chiefari, J., Chong, Y.K., Ercole, F., Krstina, J., Jeffery, J., Le, T.P.T., Mayadunne, R.T.A., Meijs, G.F., Moad, C.L., Moad, G., Rizzardo, E., and Thang, S.H. (1998) *Macromolecules*, **31**, 5559–5562.

52. Perrier, S. and Takolpuckdee, P. (2005) *J. Polym. Sci., Part A: Polym. Chem.*, **43**, 5347–5393.

53. Moad, G., Rizzardo, E., and Thang, S.H. (2008) *Polymer*, **49**, 1079–1131.

54. Schmidt-Naake, G. and Butz, S. (1996) *Macromol. Rapid Commun.*, **17**, 661–665.

55. Butz, S., Baethge, H., and Schmidt-Naake, G. (2000) *Macromol. Chem. Phys.*, **201**, 2143–2151.

56. Lokaj, J., Krakovský, I., Holler, P., and Hanyková, L. (2004) *J. Appl. Polym. Sci.*, **92**, 1863–1868.

57. Lokaj, J., Vlèek, P., and Kříž, J. (1999) *J. Appl. Polym. Sci.*, **74**, 2378–2385.

58. Lokaj, J., Holler, P., and Kříž, J. (2000) *J. Appl. Polym. Sci.*, **76**, 1093–1099.

59. Chen, G.-Q., Wu, Z.-Q., Wu, J.-R., Li, Z.-C., and Li, F.-M. (2000) *Macromolecules*, **33**, 232–234.

60. Jiang, X., Xia, P., Liu, W., and Yan, D. (2000) *J. Polym. Sci. Part A: Polym. Chem.*, **38**, 1203–1209.

61. Zhao, Y.-L., Jiang, J., Liu, H.-W., Chen, C.-F., and Xi, F. (2001) *J. Polym. Sci. Part A: Polym. Chem.*, **39**, 3960–3966.

62. Zhao, Y.-L., Zhang, J.-M., Jiang, J., Chen, C.-F., and Xi, F. (2002) *J. Polym. Sci. Part A: Polym. Chem.*, **40**, 3360–3366.

63. Zhao, Y.-L., Chen, C.-F., and Xi, F. (2003) *J. Polym. Sci. Part A: Polym. Chem.*, **41**, 2156–2165.

64. Li, A. and Lu, J. (2009) *J. Appl. Polym. Sci.*, **114**, 2469–2473.

65. Fang, Y., Cao, Y., Zhang, A., Zhai, G., Kong, L., and Zhang, D. (2010) *Acta Polym. Sin.*, **10**, 51–58.

66. Deng, G. and Chen, Y. (2004) *Macromolecules*, **37**, 18–26.

67. Qiang, R., Fanghong, G., Bibiao, J., Dongliang, Z., Jianbo, F., and Fudi, G. (2006) *Polymer*, **47**, 3382–3389.

68. Qiang, R., Bibiao, J., Dongliang, Z., Qiang, Y., Jianbo, F., Yang, Y., and Jianhai, C. (2005) *Eur. Polym. J.*, **41**, 2742–2752.

69. Zhai, G., Li, C., Fang, Y., Jiang, B., Jin, C., and Song, H. (2011) *J. Appl. Polym. Sci.*, **121**, 2957–2968.

70. Wenyan, H., Huili, P., Bibiao, J., Qiang, R., Guangqun, Z., Lizhi, K., Dongliang, Z., and Jianhai, C. (2011) *J. Appl. Polym. Sci.*, **119**, 977–982.

71. Benoit, D., Hawker, C.J., Huang, E.E., Lin, Z., and Russell, T.P. (2000) *Macromolecules*, **33**, 1505–1507.

72. Zhu, M.-Q., Wei, L.-H., Li, M., Jiang, L., Du, F.-S., Li, Z.-C., and Li, F.-M. (2001) *Chem. Commun.*, 365–366.

73. Harrisson, S. and Wooley, K.L. (2005) *Chem. Commun.*, 3259–3261.

74. Chernikova, E., Terpugova, P., Bui, C., and Charleux, B. (2003) *Polymer*, **44**, 4101–4107.

75. Lessard, B. and Mariæ, M. (2010) *Macromolecules*, **43**, 879–885.

76. Hartmann, L. and Börner, H.G. (2009) *Adv. Mater.*, **21**, 3425–3431.

77. Pfeifer, S. and Lutz, J.-F. (2007) *J. Am. Chem. Soc.*, **129**, 9542–9543.

78. Pfeifer, S. and Lutz, J.-F. (2008) *Chem. Eur. J.*, **14**, 10949–10957.

79. Matyjaszewski, K., Patten, T.E., and Xia, J. (1997) *J. Am. Chem. Soc.*, **119**, 674–680.

80. Lutz, J.-F. and Matyjaszewski, K. (2002) *Macromol. Chem. Phys.*, **203**, 1385–1395.

81. Lutz, J.-F. and Matyjaszewski, K. (2005) *J. Polym. Sci. Part A: Polym. Chem.*, **43**, 897–910.

82. Srichan, S., Oswald, L., Zamfir, M., and Lutz, J.-F. (2012) *Chem. Commun.*, **48**, 1517–1519.

83. Kakuchi, R., Zamfir, M., Lutz, J.-F., and Theato, P. (2012) *Macromol. Rapid Commun.*, **33**, 54–60.

84. Schmidt, B.V.K.J., Fechler, N., Falkenhagen, J., and Lutz, J.-F. (2011) *Nat. Chem.*, **3**, 234–238.

85. Malkoch, M., Thibault, R.J., Drockenmuller, E., Messerschmidt, M., Voit, B., Russell, T.P., and Hawker, C.J. (2005) *J. Am. Chem. Soc.*, **127**, 14942–14949.

86. Quémener, D., Le Hellaye, M., Bissett, C., Davis, T.P., Barner-Kowollik, C., and Stenzel, M.H. (2008) *J. Polym. Sci. Part A: Polym. Chem.*, **46**, 155–173.

87. Binauld, S., Damiron, D., Connal, L.A., Hawker, C.J., and Drockenmuller, E. (2011) *Macromol. Rapid Commun.*, **32**, 147–168.

88. Kolb, H.C., Finn, M.G., and Sharpless, K.B. (2001) *Angew. Chem. Int. Ed.*, **40**, 2004–2021.

89. Lutz, J.-F. (2007) *Angew. Chem. Int. Ed.*, **46**, 1018–1025.

90. Binder, W.H. and Sachsenhofer, R. (2007) *Macromol. Rapid Commun.*, **28**, 15–54.

91. Berthet, M.-A., Zarafshani, Z., Pfeifer, S., and Lutz, J.-F. (2010) *Macromolecules*, **43**, 44–50.

92. Kern, W., Schulz, R.C., and Braun, D. (1960) *J. Polym. Sci.*, **48**, 91–99.

93. Ferruti, P., Bettelli, A., and Feré, A. (1972) *Polymer*, **13**, 462–464.

94. Batz, H.-G., Franzmann, G., and Ringsdorf, H. (1972) *Angew. Chem., Int. Ed. Engl.*, **84**, 1189–1190.

95. Eberhardt, M., Mruk, R., Zentel, R., and Theato, P. (2005) *Eur. Polym. J.*, **41**, 1569–1575.

96. Eberhardt, M. and Theato, P. (2005) *Macromol. Rapid Commun.*, **26**, 1488–1493.

97. Theato, P. (2008) *J. Polym. Sci. Part A: Polym. Chem.*, **46**, 6677–6687.

98. Siemsen, P., Livingston, R.C., and Diederich, F. (2000) *Angew. Chem. Int. Ed.*, **39**, 2632–2657.

99. Laurent, B.A. and Grayson, S.M. (2006) *J. Am. Chem. Soc.*, **128**, 4238–4239.

100. Kricheldorf, H.R. (2010) *J. Polym. Sci. Part A: Polym. Chem.*, **48**, 251–284.

101. Zamfir, M., Theato, P., and Lutz, J.-F. (2012) *Polym. Chem.*, **3**, 1796–1802.

8
Temperature-Triggered Functionalization of Polymers

Bongjin Moon

8.1
Introduction

The importance of functional polymers is growing much faster than ever before because they have found so many potential applications in various areas such as nanoscience, electronic device fabrication, and biomaterials. In general, two major strategies can be employed for introducing functional groups into polymer chains. The first one is to carry the desired functional groups from the monomer preparation stage. If the desired functional group on the monomer is tolerable to the polymerization conditions and the subsequent purification steps, one can directly obtain the polymer functionalized with the desired functional group. However, if the functional group is too sensitive or reactive to survive the polymerization conditions, this strategy may not be practical. Therefore, in many cases, one needs to install the desired functional groups by chemically modifying the preexisting polymer [1]. However, in contrast to the reactions with small molecules, the chemical reactions on polymer chains can be limited in many cases by slow reaction kinetics, poor solubility, and incompatible purification process.

Two typical examples are illustrated in Scheme 8.1. Polyvinyl alcohol (PVA) is a well-known hydrophilic polymer that has repeating vinyl alcohol units. However, PVA cannot be made from vinyl alcohol because vinyl alcohol is practically a very unstable enol form of acetaldehyde. Therefore, PVA is prepared by performing the hydrolysis of the precursor polymer, namely, poly(vinyl acetate), as a post-polymerization modification step. In this case, the hydrolysis reaction may proceed to completion even if an aqueous base is used because the reaction becomes more accelerated because of the increased solubility of PVA in water. On the other hand, an opposite situation can be met in the second example. Although polyethylene (PE) can be made by Ziegler−Natta type polymerization, sometimes it is necessary to prepare it by hydrogenation of poly(1,4-butadiene) (PB), which is prepared by anionic polymerization, especially when block copolymer containing a PE block is required. However, complete hydrogenation of PB using a heterogeneous catalyst is known to be very difficult because the solubility of the resulting polymer becomes very poor because of its high crystallinity as the reaction proceeds.

Polyvinyl alcohol (PVA) from poly(vinyl acetate)
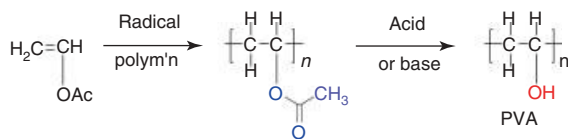
Polyethylene (PE) from polybutadiene (PB)

- • Difficult to complete the reaction due to limited solubility of PE.

PB
Rubber

PE
Waxy crystalline solid
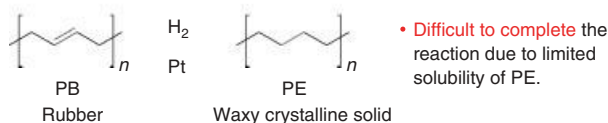
Scheme 8.1 Two examples of chemical modification of polymers.

In this regard, it is highly desirable to devise a strategy that allows modifying the functional groups in polymer chains in a nonchemical manner, where neither chemical reagents nor solvents are employed. Two representative strategies are photochemical reaction and thermal reaction. Photochemical reaction has a merit that the location of the reaction site can be accurately registered by using a photomask within a range of the wavelength of the irradiated light, which is the key aspect in photolithography and has been already well documented in the literature [2]. On the other hand, temperature-triggered functionalization of polymers has been paid less attention although this protocol has a great potential in preparing novel functional materials in both thin-film and bulk phase.

8.2
Temperature-Triggered Alteration of Polymer Property

8.2.1
Thermolysis of *t*-Butyl Esters, Carbonates, and Carbamates

The *t*-butyl group is one of the most popular protecting groups for carboxylic acids. While *t*-butyl esters are stable to mild basic hydrolysis, they can be readily cleaved under moderately acidic conditions [3]. The acid-promoted cleavage step releases the *t*-butyl cation subsequently regenerating proton and isobutene, which makes the reaction catalytic. The same transformation can be achieved by heating the substrate at a high temperature (>200 °C) (Scheme 8.2). The first example of thermal elimination of isobutene from *t*-butyl ester was reported by Baumgarten and Hauser in 1944 [4]. When they heated mono-*t*-butyl dimethylmalonate at 140–150 °C for 2 h, they obtained dimethylmalonic acid along with the evolution of isobutene gas. The lower pyrolysis temperature was attributed to the presence of an acid group in the substrate, since ordinary *t*-butyl esters were stable at that temperature. Non-acid-catalyzed thermolytic cleavage of *t*-butyl ester was reported by Klemm *et al.* in 1962, where they obtained various naphthoic acids by the pyrolysis of the corresponding *t*-butyl esters at 190–220 °C [5]. While these thermal
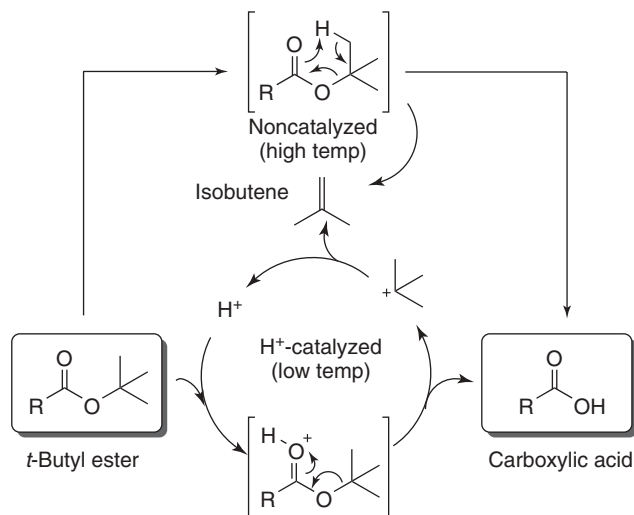
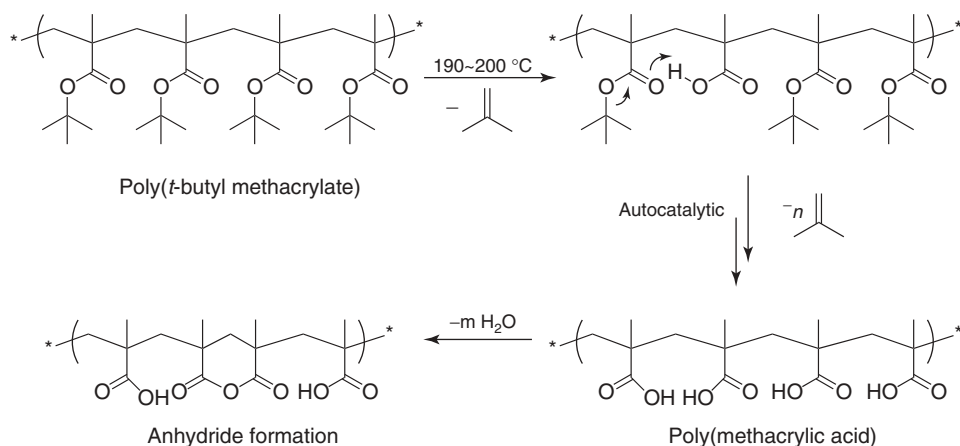**Scheme 8.2** *t*-Butyl ester cleavage mechanism either by acid catalysis or by thermolysis.

deprotection methods have been rarely employed in small-molecule chemistry because of the harsh conditions, they have found a large number of applications in polymer and materials science because many polymers and materials are thermally more robust and less volatile than small molecules.

In 1960, Grant and Grassie [6] pioneered the thermal decomposition of poly(*t*-butyl methacrylate) at ~200 °C and reported that the decomposition process occurs in two consecutive stages: release of isobutene, and the subsequent liberation of water. Since the initial release of isobutene produces carboxylic acid units, subsequent decomposition of *t*-butyl esters is accelerated by the acids, and therefore this process is autocatalytic. Once most of the *t*-butyl ester groups are converted to carboxylic acid groups, thermal dehydration takes place, producing glutaric anhydride units [7] (Scheme 8.3).

The same type of thermal deesterification also takes place in poly(*tert*-butyl acrylate) following an analogous mechanism [8], and its intermolecular autocatalytic mechanism has been investigated [9].

In a similar manner, a versatile protecting group for alcohol or amine, namely, the *t*-butyloxycarbonyl (*t*-Boc) group, can also be thermally removed. In these cases, the reaction produces carbon dioxide as a side product in addition to isobutene (Scheme 8.4).

In 1983, Fréchet and coworkers [10] demonstrated the utility of the *t*-Boc group as a phenol protecting group in polymer systems (Scheme 8.5). They prepared poly(*p-tert*-butoxycarbonyloxystyrene) (P(*p-t*-BocOSt)) via radical or cationic polymerization and the polymer was thermally postmodified into poly(*p*-hydroxystyrene) (P(*p*-HOSt)), which is otherwise difficult to synthesize via direct polymerization of *p*-hydroxystyrene because of its air sensitivity and inhibitory effect to radical species.

Poly(*t*-butyl methacrylate)

190~200 °C

Autocatalytic

Poly(methacrylic acid)

−*n*

−*m* H₂O

Anhydride formation

Scheme 8.3 Two-stage thermal decomposition of poly(*t*-butyl methacrylate).

RO*t*Boc

or

RNH*t*Boc

cat H⁺ or Δ

, CO₂

R−OH

or

R−NH₂
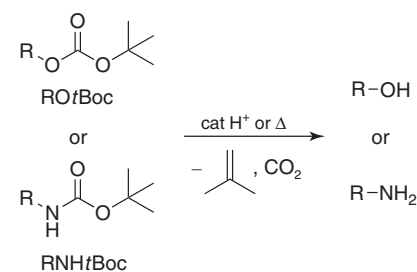
Scheme 8.4 *t*-Butyloxycarbonyl (*t*-Boc) protecting groups for alcohol or amine and their deprotecting conditions.

p-*t*BocOSt

AIBN, tol
or
BF₃EtO, SO₂

P(*p*-*t*BocOSt)

~200 °C
−CO₂
−isobutene

Poly(*p*-hydroxystyrene)
P(*p*-HOSt)
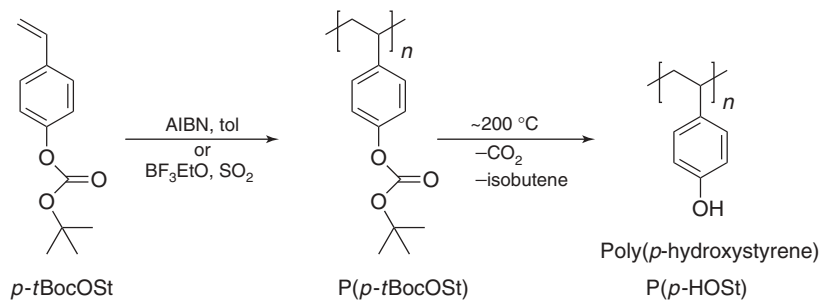
Scheme 8.5 Synthesis of poly(*p*-hydroxystyrene) via thermolysis of the precursor polymer poly(*p*-*tert*-butoxycarbonyloxystyrene).

When P(*p*-*t*-BocOSt) was subjected to thermal gravimetric analysis (TGA), a sharp loss of 45% of the mass at ~190 °C was observed, which is consistent with evolution of 1 mol of carbon dioxide and 1 mol of isobutene per *t*-Boc group (which amounts to 45% of the total mass of P(*p*-*t*-BocOSt)). A newly developed strong
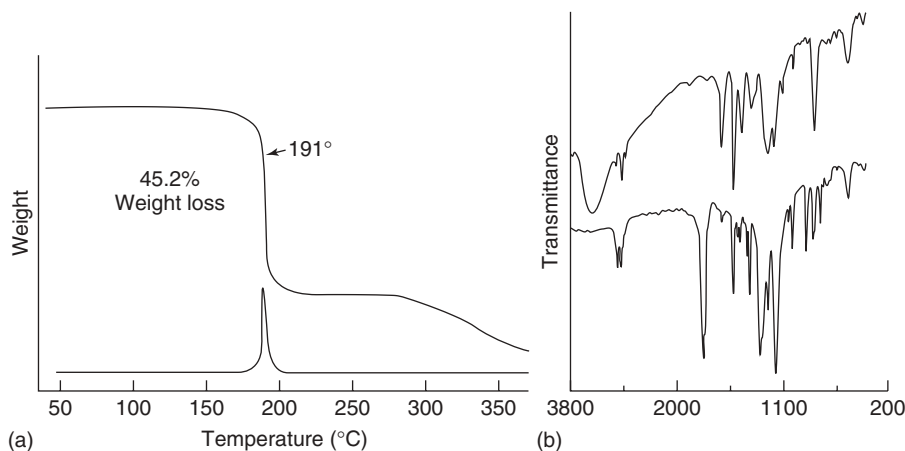
Figure 8.1 Thermal gravimetric analysis (TGA) data of P(*p-t*-BocOSt) (a) and IR spectra of P(*p-t*-BocOSt) (b) before (bottom) and after (top) thermolysis. (Source: Reprinted from [10] with permission from Elsevier.)

broad band at ~3380 cm^{-1} and no residual carbonate band at 1758 cm^{-1} in the IR spectrum after the thermolysis also supported the clean removal of *t*-Boc groups (Figure 8.1).

It is noteworthy that the autocatalytic feature of this transformation gave a birth to the concept of "chemical amplification" in the design of sensitive resist systems for microelectronic devices. Because the transformation dramatically changes the bulk property of the polymer from highly hydrophobic to highly hydrophilic, this type of reactions has been utilized in the photoresist field with concomitant use of photo acid generators [11].

Recently, it has been reported that thermolytic cleavage of *tert*-butyl esters and carbonates can be greatly enhanced under microwave-assisted conditions in fluorinated alcohols [12]. Various *tert*-butyl esters or carbonates were cleanly cleaved under microwave-assisted conditions at 100 °C in a couple of hours using either trifluoroethanol or hexafluoroisopropanol as a solvent.

8.2.2
Thermolysis of Miscellaneous Esters, Carbonates, and Carbamates

In an effort to find a system where thermolysis can take place at lower temperature than in the case of *t*-butyl esters or carbonates, Ito and Ueda studied the structural effect of polymethacrylates in thermolysis [13]. As shown in the TGA profiles of the polymers in Figure 8.2, polymethacrylates comprising the primary or secondary benzyl esters (polymer I and polymer II) did not exhibit distinct steps of deesterification below 280 °C in the TGA profile, while the polymer comprising the tertiary benzyl ester (polymer III) showed two distinct stages of weight loss between 200 and 260 °C. The first sharp weight loss at ~210 °C was assigned to the loss of
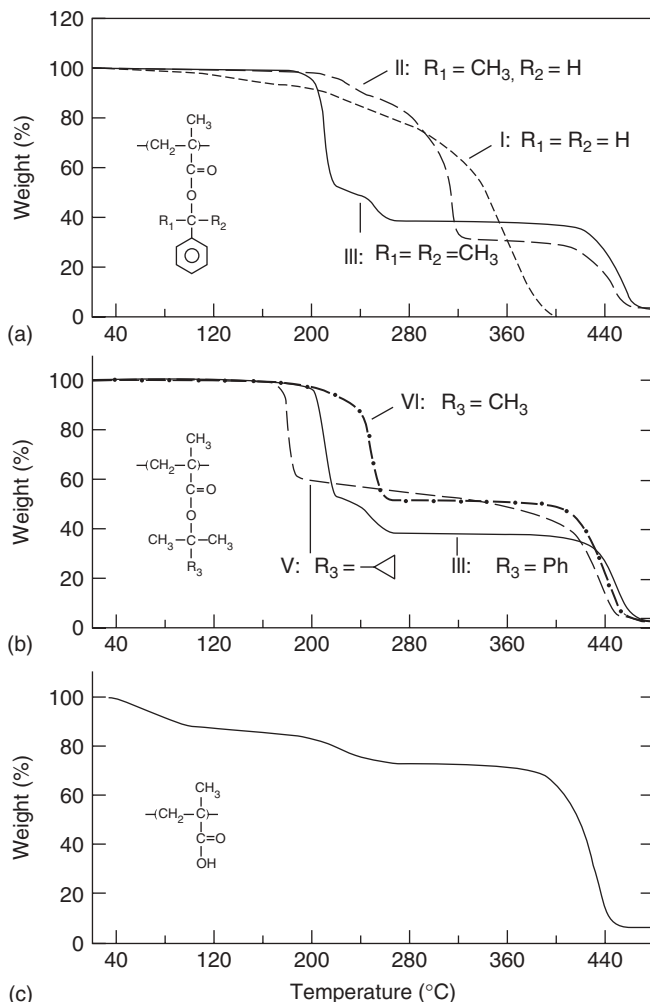
Figure 8.2 TGA of various polymethacrylates comprising primary (I), secondary (II), and tertiary benzyl esters (III) (a) *t*-butyl (IV) and 1-cyclopropyl-1-methylethyl (V) esters (b) poly(methyl methacrylic acid) (PMAA) (c) (heating rate 5 °C min^{-1}). (Source: Reprinted from [13] with permission from the American Chemical Society.)

α-methyl styrene, and the subsequent weight loss in the range of 240–260 °C was attributed to dehydration to form poly(methacrylic anhydride). The dehydration step was verified by running the same TGA experiment with poly(methyl methacrylic acid) (PMAA). It was observed that the thermal deesterification and dehydration of poly(*tert*-butyl methacrylate) (polymer VI) take place almost concomitantly at ∼240 °C, which is about 30 °C higher than the temperature for polymer III. Replacement of one of the methyl groups in the *tert*-butyl group with a cyclopropyl group (polymer V) dramatically decreased the deesterification temperature by 80 °C.
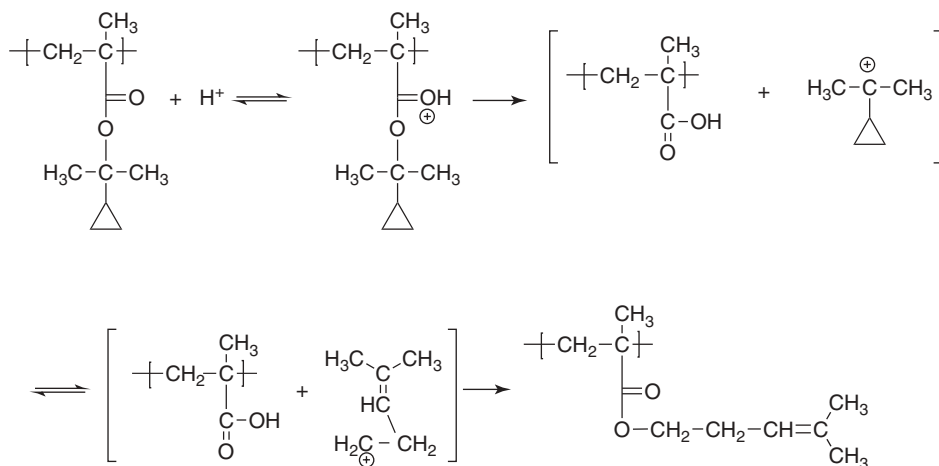
Scheme 8.6 Deesterification, rearrangement, and reesterification mechanism during the thermolysis of polymer V. (Source: Redrawn from [13].)

However, the deesterification of polymer V did not take place completely. For example, isothermal TGA at $180\,°C$ of polymer V indicated 37% weight loss within 13 min, which corresponds to 76% of deesterification and 68% of quantitative anhydride formation, but prolonged heating for 2 h resulted in only a minor additional weight loss of 3%. This incomplete thermolysis was rationalized by self-acid-catalyzed heterolytic C−O bond cleavage to generate the dimethyl cyclopropyl carbenium ion and retrapping the homoallylic carbocation after rearrangement (Scheme 8.6). The same type of ester was also applied to a styrenic polymer, poly(2-cyclopropyl-2-propyl-4-vinylbenzoate) (PCPPVB), and its thermolysis and acidolysis were found to behave in the same manner as in the case of polymethacrylate [14].

8.2.3
Thermolysis of Acetals

Hemiacetal type protecting groups for phenol and carboxylic acid also proved to be useful thermally cleavable groups. Initially, hemiacetal type protecting groups drew immediate attention to the field of photoresists because these groups could be used as a chemically amplified photoresist arising from their autocatalytic deprotection behavior in the presence of photoacid generators. Tetrahydropyranyl (THP) [15–17] and acyclic alkoxy-ethyl groups [18] were among the early screened protecting groups for polyhydroxystyrene (PHS) in photoresist applications. While polymers protected with *t*-butyl groups show high thermal stability but low acid decomposition efficiency, THP-protected polymers exhibited high acid decomposition efficiency but low thermal stability. Nakane and coworkers [19] have synthesized various 1-alkoxyethyl methacrylates from methacrylic acid with alkyl vinyl ethers and copolymerized the monomers with butyl methacrylates by conventional radical
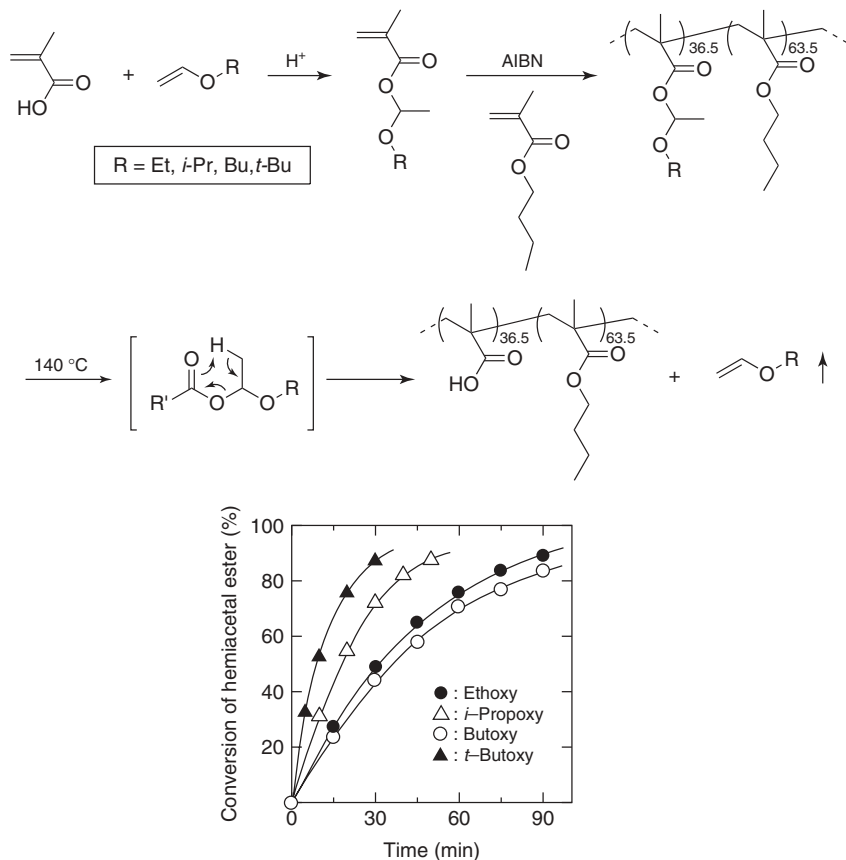
Figure 8.3 Synthesis of alkoxyethyl-protected methacrylates, copolymerization with *n*-butyl methacrylate, and thermal deprotection. (Source: Reprinted from [19] with permission from John Wiley & Sons, Inc.)

polymerization. Thermal dissociation of the hemiacetal groups in the side chain readily occurred at 140 °C following first-order reaction kinetics. Their reactivities were in the following order: 1-(*tert*-butoxy)ethyl > 1-isopropoxyethyl > 1-ethoxyethyl > 1-butoxyethyl ester (Figure 8.3).

Since the thermolysis temperature of these hemiacetal-protected polymers is quite low, this thermolytic chemistry has been widely used in preparing well-defined poly(methacrylic acid) by atom-transfer radical polymerization (ATRP) [20] and poly(acrylic acid)-derived block copolymers by reversible addition-fragmentation chain-transfer (RAFT) polymerization [21]. Selective thermal deprotection of ethoxyethyl groups from thin films of poly(isobornyl acrylate)-*block*-poly(ethoxyethyl acrylate) (PiBA-*b*-PEEA) block copolymers exhibited *in situ* morphological transition during the thermal deprotection [22].

The thermolysis chemistry was also applied to micro or nanolithography using the atomic force microscope (AFM) with heatable probe tips [23]. In 2007,

Riedo and coworkers [24] demonstrated thermochemical nanolithography, which allowed the alternation of the local surface property by thermally cleaving THP groups in poly(tetrahydro-2*H*-pyran-2-yl methacrylate) poly(3-{4-[(*E*)-3-methoxy-3-oxoprop-1-enyl]phenoxy}propyl 2-methacrylate) [*p*(THP-MA)*p*(PMC-MA)] copolymer film by an AFM equipped with a heatable probe tip. In 2008, Duvigneau and coworkers employed a similar technique to achieve local surface functionalization of thin block copolymer films of polystyrene-*block*-poly(*tert*-butyl acrylate) and verified the functionality by immobilizing PEG-NH$_2$ and fluoresceinamine on the surface [25].

8.3
Temperature-Triggered Generation of Reactive Groups

Most of the thermal transformations shown in the previous section are accompanied by alterations of their bulk properties. For example, thermal deprotection of *t*-butyl esters in poly(*p*-*tert*-butoxycarbonyloxystyrene) (P(*p*-*t*-BocOSt)) alters their solubility from water-insoluble to water-soluble, which makes the polymer useful in photoresist applications [10]. However, not many examples have involved generation of reactive functional groups that could be further utilized in the subsequent reactions. It should be noted that one of the most advantageous features of thermolysis is that the conditions do not require additional reagents or solvents other than raising the temperature. This feature makes thermal chemical transformation invaluable for generating reactive functional groups in polymeric materials.

8.3.1
Thermolytic Generation of Anhydride Group in Polymers

A good example appears in preparing a well-defined end-functional polymer. Cernohous and coworkers [26] developed a clever strategy to introduce an anhydride group at the polymer chain end via an anionic polymerization–thermolysis sequence. Since the anhydride group is a very reactive electrophile, introduction of a single anhydride group at the polymer chain end is a challenging task, because even a conventional purification method such as precipitation can kill the anhydride functionality by the reaction with residual moisture or nucleophilic solvent itself (i.e., methanol). The key to the strategy was to trap the anionically growing polymer chain by di-*t*-butyl maleate and the subsequent thermolysis of the diester group to the succinic anhydride moiety (Scheme 8.7). The trapping reagent, di-*t*-butyl maleate, reacted only once with anionically growing poly(methyl methacrylate) (PMMA) chain (PMMA-Li) and did not propagate further under the anionic polymerization conditions. Therefore, the subsequent quenching with methanol provided di-*t*-butyl succinate (DTBS) terminated PMMA (PMMA-DTBS). Thermolysis of PMMA-DTBS at 230 °C under vacuum for 3 h provided the desired anhydride end-functional PMMA (PMMA-anh) with high functionality. This polymer showed very fast coupling reaction kinetics with amine-functionalized
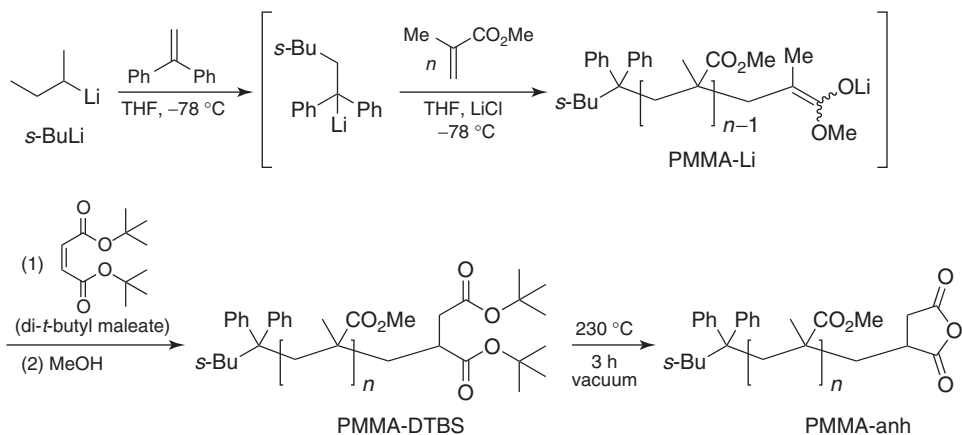
Scheme 8.7 Synthesis of alkoxyethyl-protected methacrylates, copolymerization with *n*-butyl methacrylate, and thermal deprotection. (Source: Redrawn from [26].)
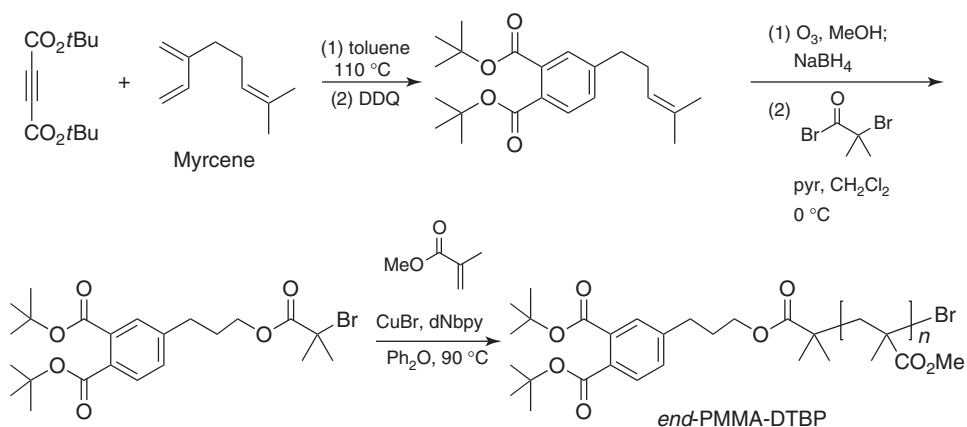
Scheme 8.8 Synthesis of di-*t*-butyl phthalate (DTBP)-functionalized ATRP initiator and PMMA. (Source: Redrawn from [29].)

polystyrene in reactive blending [27]. A similar strategy was also successfully applied to the preparation of anhydride end-functional polystyrene [28].

In an effort to develop a strategy that allowed the production of an anhydride group at a lower thermolysis temperature, Moon and coworkers employed di-*t*-butyl phthalate (DTBP) as a precursor for a phthalic anhydride group [29]. The synthesis started from the Diels–Alder reaction between commercially available di-*tert*-butyl acetylenedicarboxylate with myrcene, as shown in Scheme 8.8. The subsequent oxidative aromatization of the Diels–Alder product with 2,3-dichloro-5,6-dicyano-1,4-benzoquinone (DDQ) afforded 4-isoprenyl-di-*tert*-butyl phthalate. After the double bond in the isoprenyl
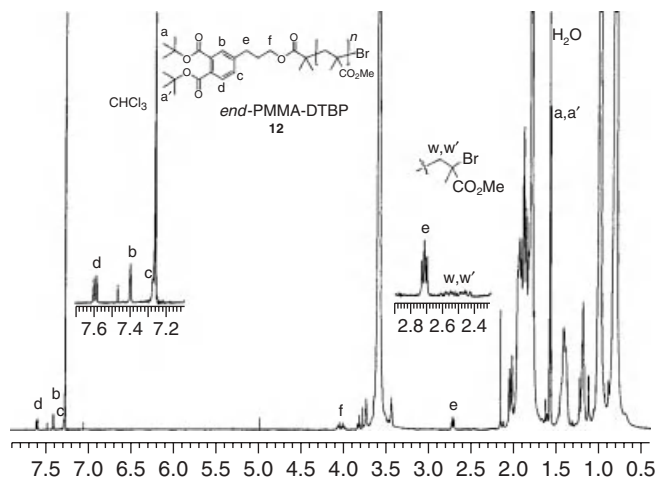
Figure 8.4 ^{1}H NMR (500 MHz) spectrum of *end*-PMMA-DTBP ($M_n = 21\,000\,\mathrm{g\,mol}^{-1}$) in CDCl$_3$. (Source: Reprinted from [29] with permission from the American Chemical Society.)

group was cleaved by ozonolysis and reduced to alcohol, it was derivatized with 2-bromoisobutyryl bromide to afford the ATRP initiator containing a DTBP group. PMMA containing the DTBP group at the chain end was successfully prepared under standard ATRP conditions using this initiator.

The presence of the DTBP group in *end*-PMMA-DTBP could be clearly verified by ^{1}H NMR because most of the resonance peaks from the end group did not overlapped with those from polymer backbone (Figure 8.4). Owing to this unique feature, the thermolysis of the DTBP group could be monitored by ^{1}H NMR, as shown in Figure 8.5. The DTBP group was gradually converted into the phthalic anhydride group (PMMA-PA) in 1 h at 200 °C along with the observation of a temporary phthalic acid intermediate (PMMA-DA).

From this experiment, it was discovered that the thermolysis of DTBP group progressed following the mechanism shown in Scheme 8.9. The pyrolysis of one of the two *tert*-butyl groups in PMMA-DTBP releases an isobutene and provides PMMA-MTBP (PMMA-mono-*tert*-butyl phthalate). Owing to the self-catalytic feature arising from the newly generated carboxylic acid, the second thermolysis was much faster than the first one, which was why PMMA-MTBP intermediate had not been observed. Because the rate of the thermolytic dehydration step from PMMA-DA to PMMA-PA was comparable to that of the first thermolysis step, accumulation of PMMA-DA species was observed in the early stage. This kinetic feature corresponds to typical two consecutive first-order reactions. The half-lives for the initial thermolysis of PMMA-DTBP species were measured to be 30, 11, and 4.3 min at three different thermolysis temperatures (190, 200, and 210 °C, respectively). From these data, the activation enthalpy ($\Delta H^{\ddagger}$) and activation entropy ($\Delta S^{\ddagger}$) were also calculated to be about 42 kcal mol^{-1} and 16 cal/(mol K), respectively. It
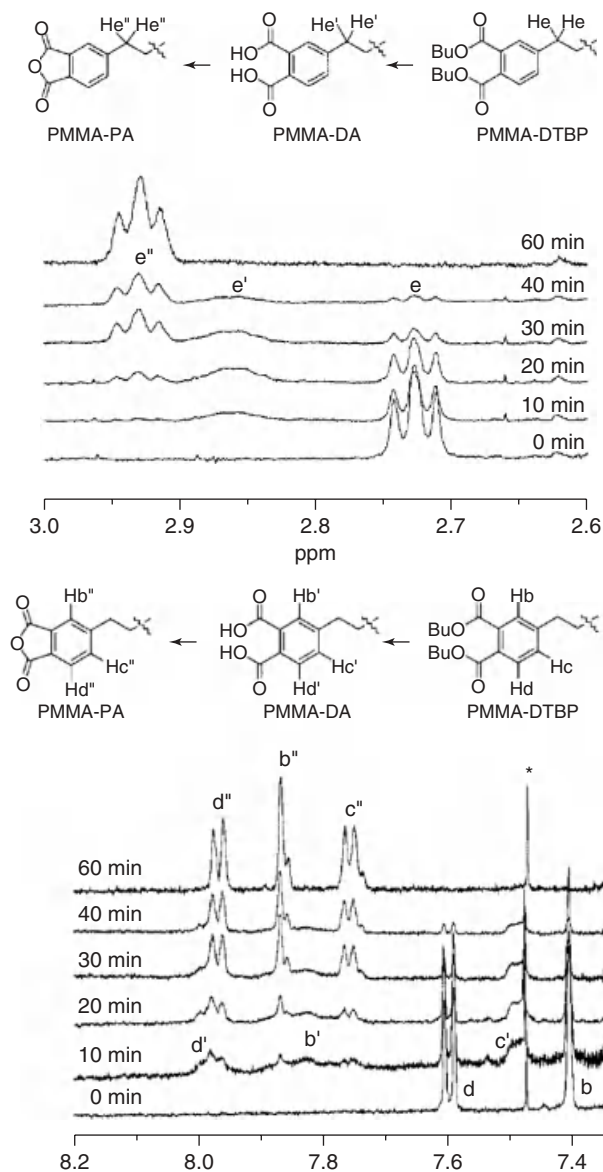
Figure 8.5 ¹H NMR monitoring of thermolysis of *end*-PMMA-DTBP at 200 °C. (Source: Reprinted from [29] with permission from the American Chemical Society.)

should be noted that the thermal conversion of the DTBP group to the PA group was significantly faster than that of DTBS to succinic anhydride. In addition, it was learned from a competition experiment that the phthalic anhydride group reacted with the aliphatic amine approximately five times faster than the succinic anhydride group [29].
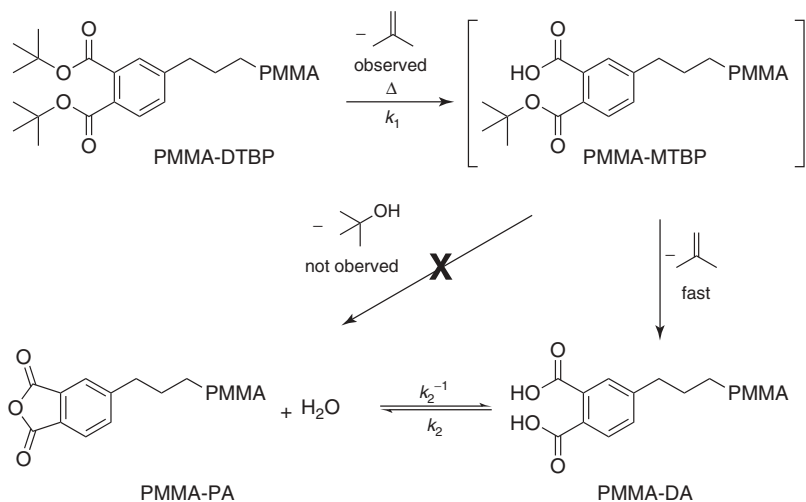
Scheme 8.9 Proposed mechanism for the thermal conversion of PMMA-DTBP to PMMA-PA. (Source: Redrawn from [29].)
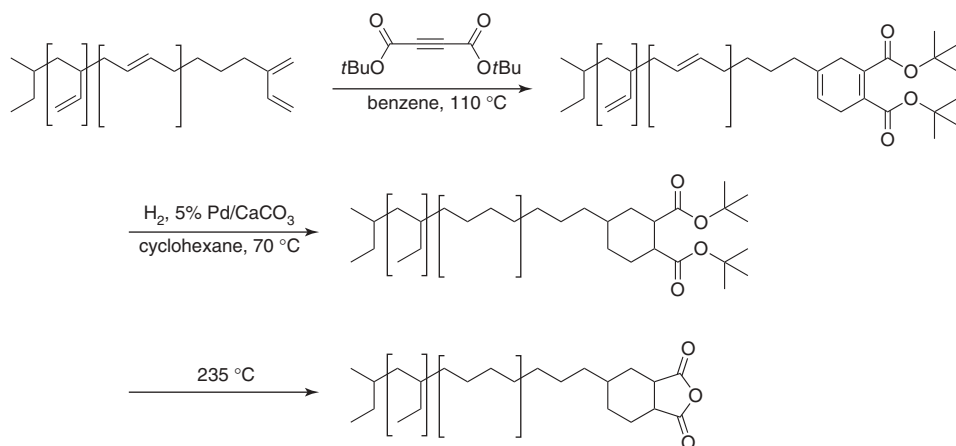
Scheme 8.10 Synthesis of anhydride-functionalized polyethylethylene (PEE) via post-polymerization modification with di-*tert*-butyl acetylenedicarboxylate, hydrogenation, and thermolysis. (Source: Redrawn from [30].)

The Diels–Alder reaction with di-*tert*-butyl acetylenedicarboxylate turned out to be also useful as a post-polymerization modification reaction. In order to prepare well-defined polyethylethylene (PEE) with an anhydride group at the chain end, Jones and coworkers [30] synthesized 1,3-diene-functionalized PB by anionic polymerization and reacted the terminal 1,3-diene group with di-*tert*-butyl acetylenedicarboxylate (Scheme 8.10). The resulting polymer was subjected to hydrogenation to produce di-*tert*-butyl 1,2-dicarboxylate-functionalized PEE
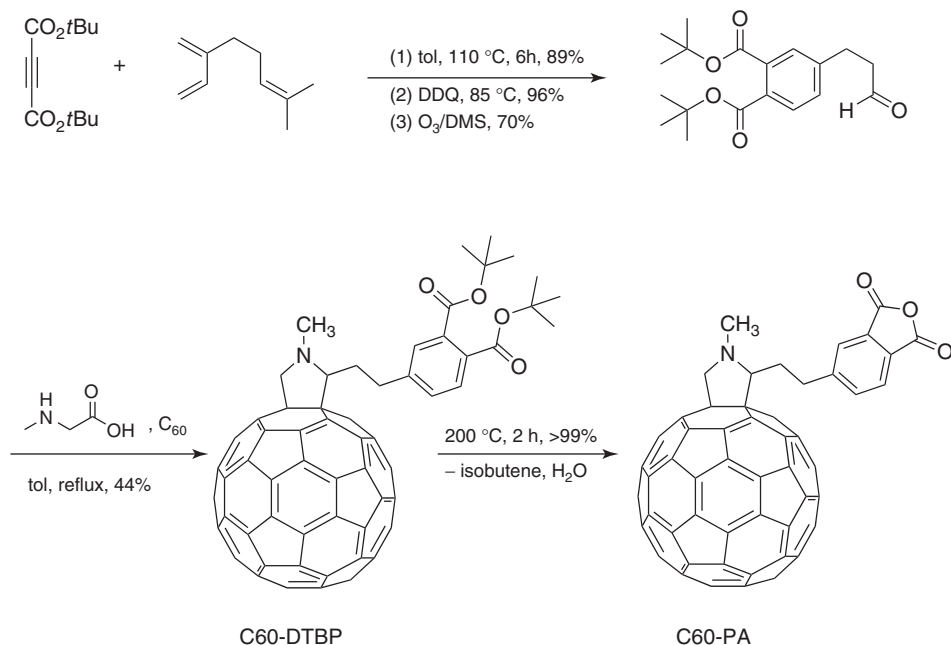
Scheme 8.11 Synthesis of anhydride-functionalized fullerene via thermolysis. (Source: Redrawn from [31].)

and the subsequent thermolysis provided the desired anhydride-functionalized PEE. Considering the poor solubility of PEE in organic solvents, the non-chemical thermolytic generation of anhydride group was of great value in this case.

A similar strategy was also applied to the preparation of anhydride-functionalized fullerene (C_{60}), as shown in Scheme 8.11 [31]. The aldehyde adduct obtained from the Diels−Alder reaction between di-*tert*-butyl acetylenedicarboxylate and myrcene was immobilized onto C_{60} by the Prato reaction [32]. The resulting DTBP-functionalized fullerene (C60-DTBP) was soluble in most conventional organic solvents and easy to handle. Thermolysis of C60-DTBP under typical thermolysis conditions (200 °C, 2 h) cleanly provided phthalic anhydride-functionalized C_{60} (C60-PA).

8.3.2
Thermolytic Generation of Ketenes in Polymers

Ketene is another well-known, versatile electrophile in organic chemistry and has a very rich chemistry [33]. One of the synthetic routes to dialkyl ketene is pyrolysis of 5,5-dialkyl-2,2-dimethyl-1,3-dioxa-4,6-dione (or 5,5-dialkyl Meldrum's acid) under flash vacuum pyrolysis (FVP) conditions (Scheme 8.12) [34, 35]. In general, ketenes are highly reactive and can be easily trapped with various nucleophiles
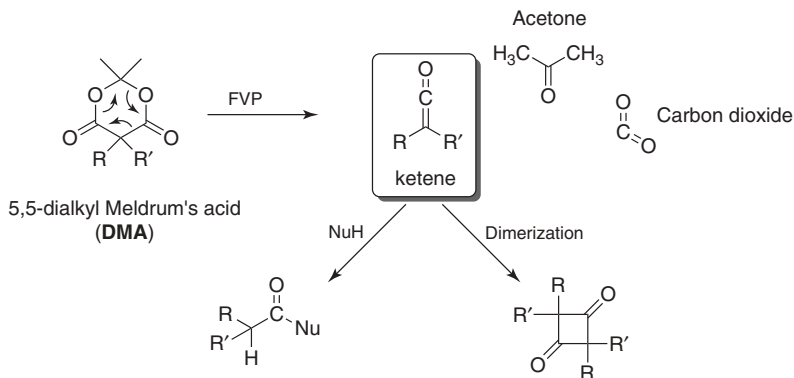
Scheme 8.12 Thermolysis of 5,5-dialkyl Meldrum's acid to dialkyl ketene under flash vacuum pyrolysis conditions and the reactivity of ketene.

(NuH), such as amine and alcohol, forming amide and ester, respectively. In the absence of nucleophilic trapping reagent, ketenes gradually dimerize to mainly form 1,3-cyclobutanedione derivatives. Owing to the high reactivity, ketenes have been considered as a transient chemical species rather than a stable reactive group.

However, this preconception was dispelled after Leibfarth and coworkers demonstrated that free ketenes can be thermally produced in a polymer matrix starting from polymers containing Meldrum's acid (Scheme 8.13). The presence of free ketene in the polymer matrix at ambient temperature was verified by IR spectroscopy, where a distinct signal for ketene was observed at $2103 \, \text{cm}^{-1}$ for a polymer film thermolyzed at $240 \, °C$ for ~ 30 s. However, prolonged heating over ~ 30 s at this temperature diminished the ketene concentration in the polymer matrix because of the consumption of the ketenes via dimerization (cross-linking) pathway [36].

Once the ketenes are produced at high temperature and cooled down below the glass-transition temperature of polymer matrix, they kept their reactivity until being trapped with nucleophiles. The dual role of the ketene-functionalized polymer, namely, the reaction to the nucleophile and the cross-linking ability, allows the fabrication of a reactive surface strongly adhered to the surface, as demonstrated in a microcontact printing (μ-CP) experiment shown in Figure 8.6.

Since the thermolysis temperature range of the Meldrum's acid moiety falls into that of polyolefin melt processing, the heat-induced cross-linking via ketene intermediate was successfully employed in preparation of cross-linked PE (Scheme 8.14) [37]. Copolymerization of ethylene with Meldrum's acid-functionalized norbornene using [N-(2,6-diisopropylphenylimino)isobutanamidato] Ni(η^1-CH$_2$Ph) (PMe$_3$) activated with Ni(COD)$_2$ proceeded smoothly, incorporating the Meldrum's acid moieties up to 0.8 mol%. When the resulting Meldrum's acid-functionalized PE
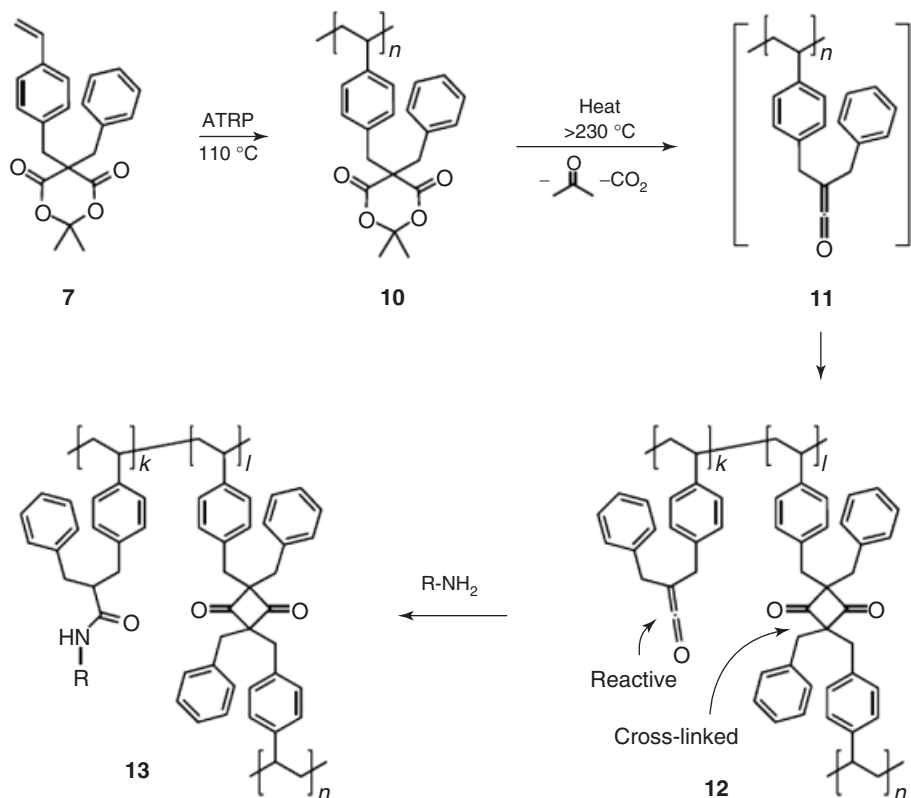
Scheme 8.13 Synthesis of Meldrum's acid-containing polymer and its thermolytic properties. (Source: Reprinted from [36] with permission from Macmillan Publishers Ltd.)

was subjected to melt processing conditions (185 °C, 1 h), the cross-linking efficiency was determined to be over 90% as there existed more than one Meldrum's acid unit per 300 ethylene repeat units.

On the other hand, this efficient thermal cross-linking protocol was applied to other Meldrum's acid-containing polymers [38] that had been prepared by transition-metal-initiated cyclopolymerization of 5,5-diallyl Meldrum's acid regulating the tacticity of the backbones [39–41]. Interestingly, the *threo*-disyndiotactic sequence-rich (st_{rich}) polymer exhibited successful cross-linking in μ-CP while maintaining their preformed dimensional integrity. In contrast, *threo*-diisotactic sequence-rich (it_{rich}) polymer showed poor dimensional stability on heating (Scheme 8.15) [38].

Recently, two thermal reactions having distinct thermolysis temperature regimes, namely, thermal azide–alkyne cycloaddition (TAAC) and thermolytic retrocyclization generation of acyl ketenes followed by nucleophilic trapping (Scheme 8.16),
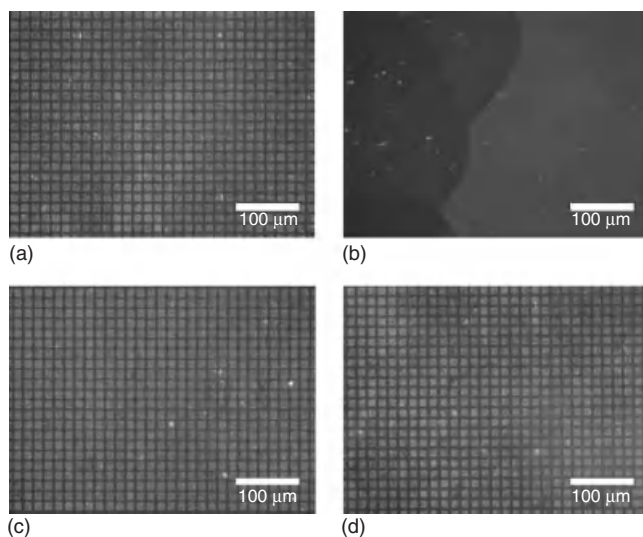
Figure 8.6 Covalent attachment of fluorescent dye on μ-CP surface. An amine-functionalized fluorescent dye, TAMRA cadaverine, was patterned to the surfaces of non-heat-treated film (a) and heat-treated film (c) of Meldrum's acid-functionalized polymer. After extensive rinsing with water for 5 min along with sonication, the pattern on heat-treated film remained intact (d), while non-heat-treated film completely lost the printed pattern (b). (Source: Reprinted from [36] with permission from Macmillan Publishers Ltd.)
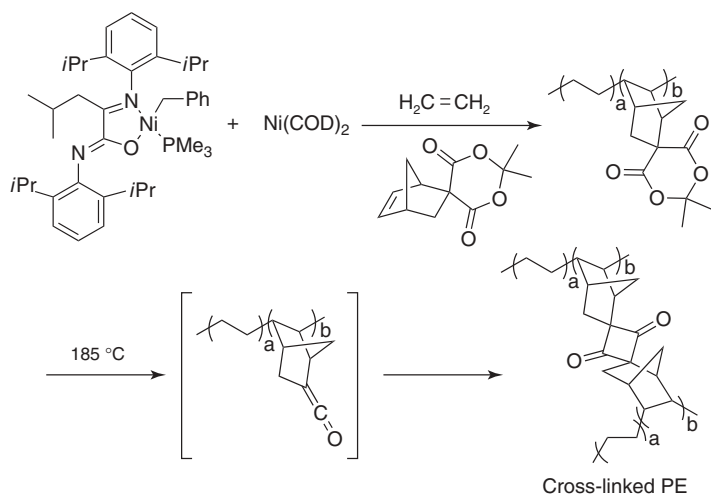
Scheme 8.14 Synthesis of Meldrum's acid-containing polyethylene (PE) and its thermal cross-linking via ketene dimerization. (Source: Redrawn from [37].)

(a)

(b)   (c)
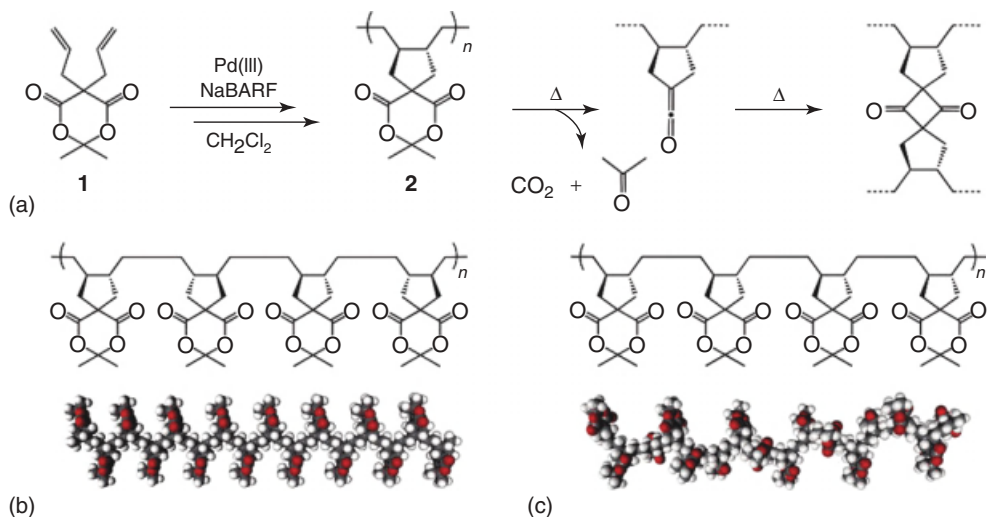
Scheme 8.15 (a) Polymerization of diallyl Meldrum's acid (**1**) initiated by Pd(II) complexes and thermal cross-linking of the resulting cycloolefinic polymer (**2**). (b,c) Structures and corresponding computer-generated CPK models of 16 mers of **1** composed exclusively of (b) *threo*-disyndiotactic (*st*) and (c) *threo*-diisotactic (*it*) sequences. (Source: Reprinted from [38] with permission from the American Chemical Society.)

(a)   Thermal azide–alkyne cycloaddition (TAAC)

(b)   Acyl ketene formation
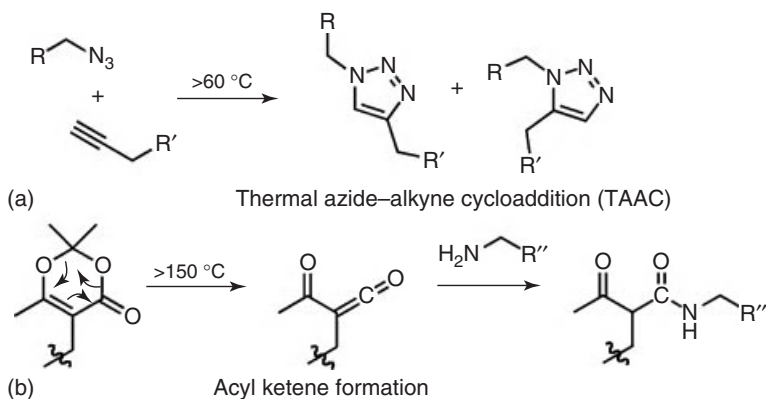
Scheme 8.16 Mild and orthogonal covalent bond formation chemistries. (a) Thermal azide–alkyne cycloaddition (TAAC). (b) Thermolytic retrocyclization generation of acyl ketenes followed by nucleophilic trapping. (Source: Reprinted from [42] with permission from the American Chemical Society.)

were used in fabricating a single trifunctional polymer film that could orthogonally react with three different reagents in sequence [42].

Polystyrene having three functional groups, namely, alkyne, azide, and [1, 3]-dioxin-4-one, were synthesized by radical polymerization, as shown in Scheme 8.17. The thin films fabricated with this trifunctional polymer exhibited
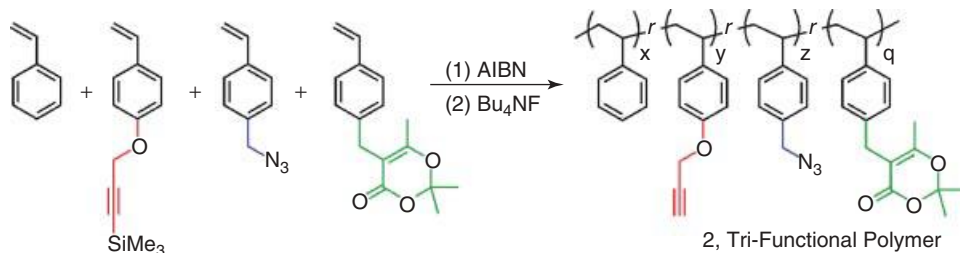
Scheme 8.17 Synthesis of trifunctional linear polymer used in Ref. [42]. (Source: Reprinted from [42] with permission from the American Chemical Society.)
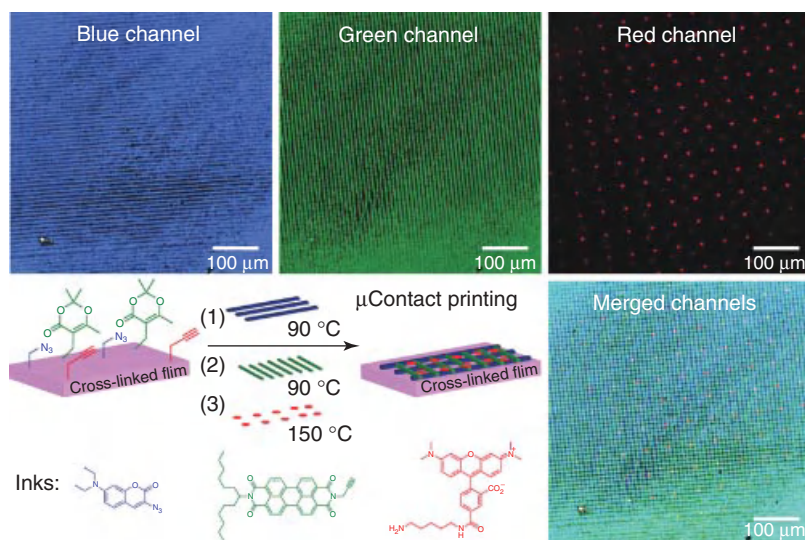

Figure 8.7 Single trifunctional polymer film functionalized in a three-step process with blue, green, and red fluorescent dyes through thermal μ-CP-mediated covalent bond formation. (Source: Reprinted from [42] with permission from the American Chemical Society.)

excellent orthogonal reactivity toward three different fluorescent dyes by using temperature as another controlling factor for selective reactions (Figure 8.7). It should be noted that the film becomes insoluble by partial thermal cross-linking between azides and alkynes in the early stage, which allows sequential μ-CP with dimensional film integrity.

8.3.3
Thermolytic Generation of Transient Reactive Groups

In contrast to the above-mentioned cases, there are some examples that involve very reactive transient intermediates during the thermal treatment. In most cases,
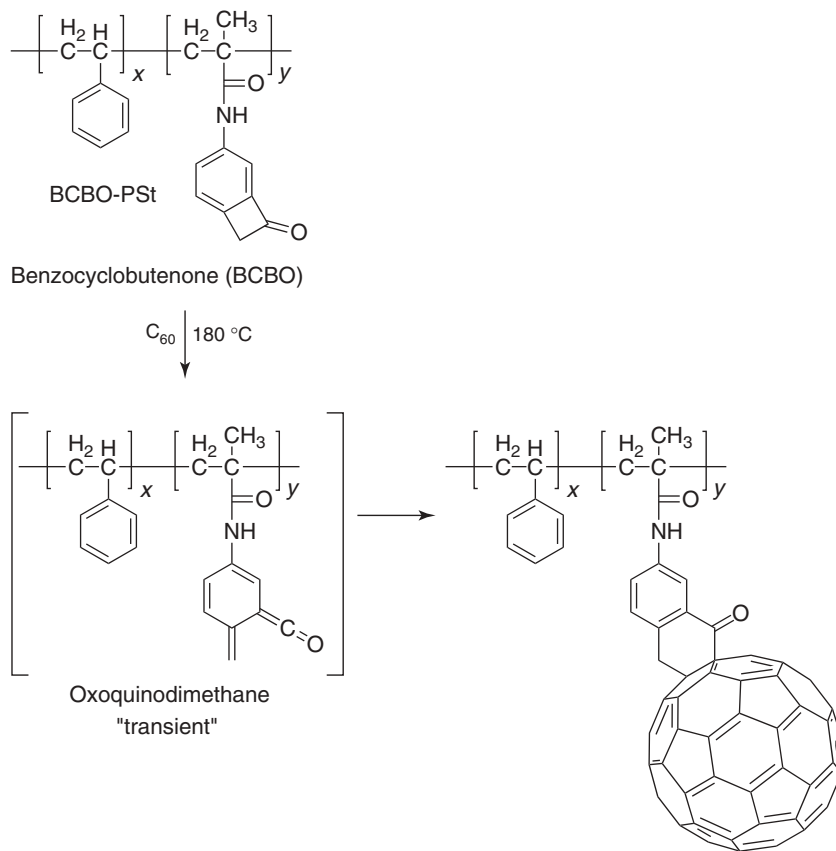
Scheme 8.18 Synthesis of C_{60}-functionalized copolymer via transient oxoquinodimethane intermediate. (Source: Redrawn from [43].)

the intermediates are not observable. However, the presence of the intermediates can be indirectly verified either by chemical trapping or by a self-coupling reaction (cross-linking in polymer matrix).

For example, thermal treatment of the benzocyclobutenone (BCBO) system is known to provide the α-oxo-*o*-quinodimethane intermediate that can be trapped with a dienophile such as fullerene (Scheme 8.18). This turned out to be an efficient way of preparing C_{60}-functionalized polymers [43].

In a similar manner, benzocyclobutene (BCB) acts as a precursor for *o*-quinodimethane by thermal activation [44]. Since the transient intermediate *o*-quinodimethane is highly reactive and tends to dimerize when it approaches another in proximity very rapidly as shown in Scheme 8.19, BCB has been widely used in thermosetting materials [45, 46], intramolecularly collapsed nanoparticles [47–49], and selective cross-linking of polymer matrices [50–52]. A typical thermally cross-linkable polymer based on BCB moiety is shown in Scheme 8.20 [50]. Nitroxide-mediated radical polymerization (NMRP) of methyl methacrylate,
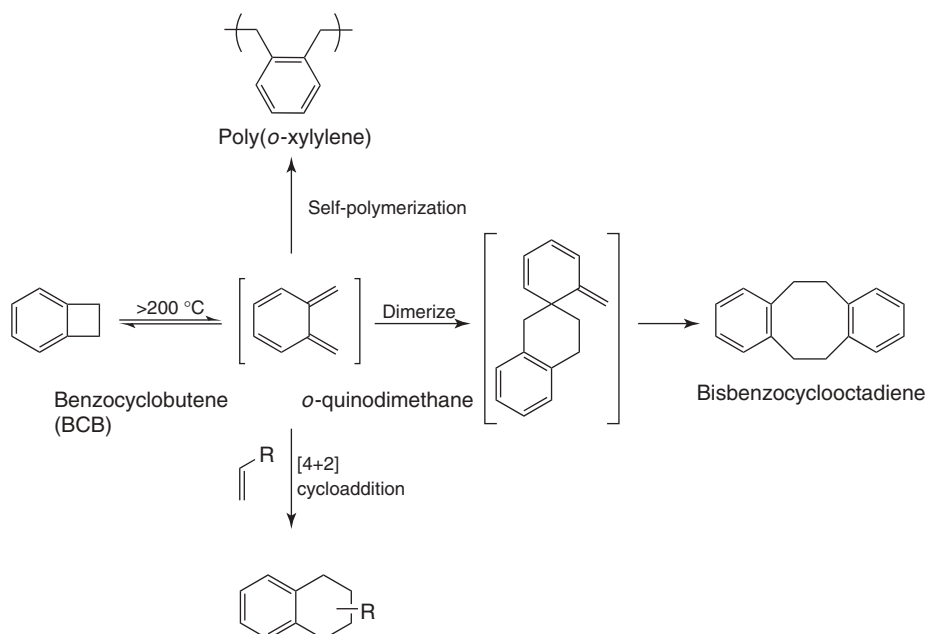
Scheme 8.19 Thermal chemistry of benzocyclobutene (BCB). (Source: Redrawn from [45].)

4-vinyl benzocyclobutene, and styrene in the ratio of 56 : 2 : 42 provided a random copolymer of these three components. A short thermal treatment (250 °C, 10 min) of the polymer resulted in efficient cross-linking and provided an insoluble thin film with neutral surface property for fabricating PS-*b*-PMMA block copolymer self-assembly.

8.4
Conclusions

Since most polymers are nonvolatile and more tolerable to high temperature than small molecules, modification of the functionality of the polymer by heat-induced reactions becomes quite practical. In addition, these thermal modification processes can circumvent many problems that can be encountered when chemical modification is attempted, because the processes do not require any reagents but only heating. As more efficient controlled polymerization methods become available, installation of thermally activable precursors into polymer chains at a designated position also with desired architecture will be easily achievable. These novel thermally activable functional polymers are finding many potential applications in many areas.
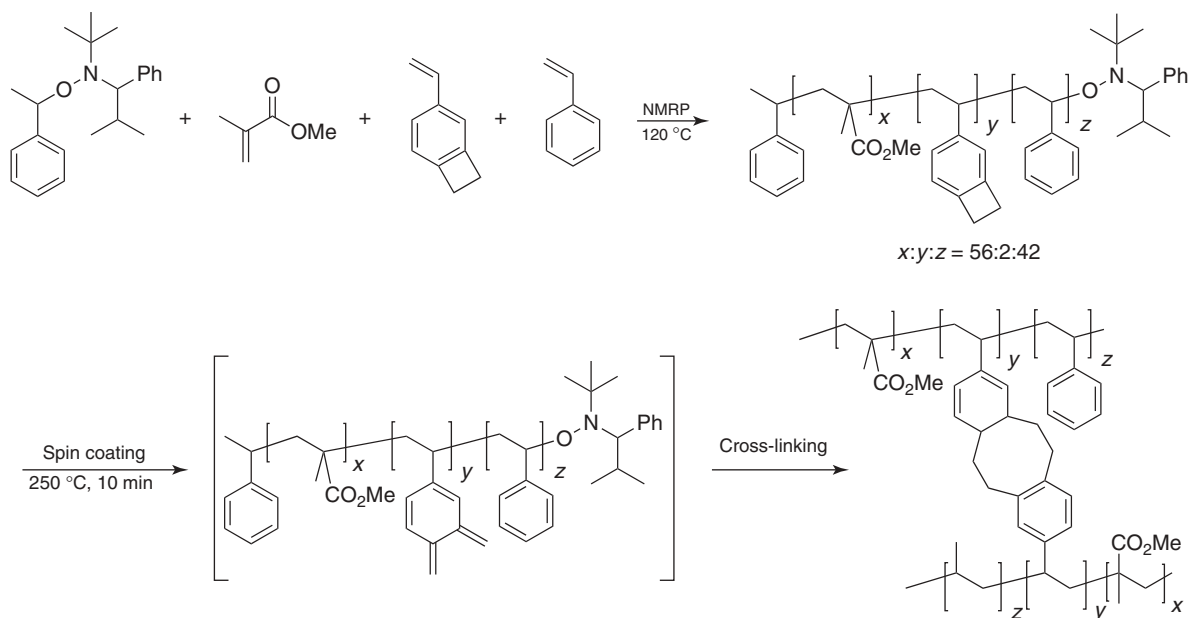
Scheme 8.20 Synthesis of cross-linkable neutral random brush polymer, P(S-r-BCB-r-MMA) (BCB) (*x*/*γ*/*z* = 56/2/42) for PS-*b*-PMMA self-assembled film fabrication. (Source: Redrawn from [50].)

References

1. Gauthier, M.A., Gibson, M.I., and Klok, H.-A. (2009) *Angew. Chem. Int. Ed.*, **48** (1), 48–58.
2. Mack, C. (2007) *Fundamental Principles of Optical Lithography*, John Wiley & Sons, Ltd, Chichester.
3. Greene, T.W. and Wuts, P.G.M. (1999) *Protective Groups in Organic Synthesis*, John Wiley & Sons, Inc., New York.
4. Baumgarten, E. and Hauser, C.R. (1944) *J. Am. Chem. Soc.*, **66**, 1037–1038.
5. Klemm, L.H., Antoniates, E.P., and Lind, C.D. (1962) *J. Org. Chem.*, **27**, 519–526.
6. Grant, D.H. and Grassie, N. (1960) *Polymer*, **1**, 445–455.
7. Grant, D.H. and Grassie, N. (1960) *Polymer*, **1**, 125–134.
8. Schaefgen, J.R. and Sarasohn, I.M. (1962) *J. Polym. Sci.*, **58**, 1049–1061.
9. Litmanovich, A.D. and Cherkezyan, V.O. (1984) *Eur. Polym. J.*, **20** (11), 1041–1044.
10. Fréchet, J.M.J., Eichler, E., Ito, H., and Willson, C.G. (1983) *Polymer*, **24** (8), 995–1000.
11. Ito, H. (2005) *Adv. Polym. Sci.*, **172**, 37–245.
12. Choy, J., Jaime-Figueroa, S., and Lara-Jaime, T. (2010) *Tetrahedron Lett.*, **51** (17), 2244–2246.
13. Ito, H. and Ueda, M. (1988) *Macromolecules*, **21** (5), 1475–1482.
14. Ito, H., Ueda, M., and England, W.P. (1990) *Macromolecules*, **23** (9), 2589–2598.
15. Hayashi, N., Ueno, T., Hesp, S., Toriumi, M., and Iwayanagi, T. (1992) *Polymer*, **33** (8), 1583–1587.
16. Sakamizu, T., Shiraishi, H., Yamaguchi, H., Ueno, T., and Hayashi, N. (1992) *Jpn. J. Appl. Phys.*, **31**, 428.
17. Hattori, T., Schegel, L., Imai, A., Hayashi, N., and Ueno, T. (1992) *Proc. SPIE*, **1925**, 146.
18. Iwasa, S., Maeda, K., Nakano, K., Ohfuji, T., and Hasegawa, E. (1996) *J. Photopolym. Sci. Technol.*, **9** (3), 447–456.
19. Nakane, Y., Ishidoya, M., and Endo, T. (1999) *J. Polym. Sci., Part A: Polym. Chem.*, **37** (5), 609–614.
20. Van Camp, W., Du Prez, F.E., and Bon, S.A.F. (2004) *Macromolecules*, **37** (18), 6673–6675.
21. Hoogenboom, R., Schubert, U.S., Van Camp, W., and Du Prez, F.E. (2005) *Macromolecules*, **38** (18), 7653–7659.
22. Wouters, D., Van Camp, W., Dervaux, B., Du Prez, F.E., and Schubert, U.S. (2007) *Soft Matter*, **3** (12), 1537–1541.
23. Jungchul, L., Beechem, T., Wright, T.L., Nelson, B.A., Graham, S., and King, W.P. (2006) *J. Microelectromech. Syst.*, **15** (6), 1644–1655.
24. Szoszkiewicz, R., Okada, T., Jones, S.C., Li, T.-D., King, W.P., Marder, S.R., and Riedo, E. (2007) *Nano Lett.*, **7** (4), 1064–1069.
25. Duvigneau, J., Schoenherr, H., and Vancso, G.J. (2008) *Langmuir*, **24** (19), 10825–10832.
26. Cernohous, J.J., Macosko, C.W., and Hoye, T.R. (1997) *Macromolecules*, **30** (18), 5213–5219.
27. Schulze, J.S., Cernohous, J.J., Hirao, A., Lodge, T.P., and Macosko, C.W. (2000) *Macromolecules*, **33** (4), 1191–1198.
28. Moon, B., Hoye, T.R., and Macosko, C.W. (2000) *J. Polym. Sci., Part A: Polym. Chem.*, **38** (12), 2177–2185.
29. Moon, B., Hoye, T.R., and Macosko, C.W. (2001) *Macromolecules*, **34** (23), 7941–7951.
30. Jones, T.D., Macosko, C.W., Moon, B., and Hoye, T.R. (2004) *Polymer*, **45** (12), 4189–4201.
31. Heo, G.S. and Moon, B. (2008) *Tetrahedron Lett.*, **49** (38), 5540–5543.
32. Prato, M. and Maggini, M. (1998) *Acc. Chem. Res.*, **31** (9), 519–526.
33. Tidwell, T.T. (2006) *Ketenes*, John Wiley & Sons, Inc., New Jersey.
34. Brown, R.F.C., Eastwood, F.W., and Harrington, K.J. (1974) *Aust. J. Chem.*, **27** (11), 2373–2384.
35. Baxter, G.J., Brown, R.F.C., Eastwood, F.W., and Harrington, K.J. (1975) *Tetrahedron Lett.*, **48**, 4283–4284.
36. Leibfarth, F.A., Kang, M., Ham, M., Kim, J., Campos, L.M., Gupta, N., Moon, B., and Hawker, C.J. (2010) *Nat. Chem.*, **2** (3), 207–212.

37. Leibfarth, F.A., Schneider, Y., Lynd, N.A., Schultz, A., Moon, B., Kramer, E.J., Bazan, G.C., and Hawker, C.J. (2010) *J. Am. Chem. Soc.*, **132** (42), 14706–14709.

38. Miyamura, Y., Park, C., Kinbara, K., Leibfarth, F.A., Hawker, C.J., and Aida, T. (2011) *J. Am. Chem. Soc.*, **133** (9), 2840–2843.

39. Park, S., Takeuchi, D., and Osakada, K. (2006) *J. Am. Chem. Soc.*, **128** (11), 3510–3511.

40. Okada, T., Park, S., Takeuchi, D., and Osakada, K. (2007) *Angew. Chem. Int. Ed.*, **46** (32), 6141–6143.

41. Miyamura, Y., Kinbara, K., Yamamoto, Y., Praveen, V.K., Kato, K., Takata, M., Takano, A., Matsushita, Y., Lee, E., Lee, M., and Aida, T. (2010) *J. Am. Chem. Soc.*, **132** (10), 3292–3294.

42. Spruell, J.M., Wolffs, M., Leibfarth, F.A., Stahl, B.C., Heo, J., Connal, L.A., Hu, J., and Hawker, C.J. (2011) *J. Am. Chem. Soc.*, **133** (41), 16698–16706.

43. Wang, Z.Y., Kuang, L., Meng, X.S., and Gao, J.P. (1998) *Macromolecules*, **31** (16), 5556–5558.

44. Segura, J.L. and Martin, N. (1999) *Chem. Rev.*, **99** (11), 3199–3246.

45. Deeter, G.A., Venkataraman, D., Kampf, J.W., and Moore, J.S. (1994) *Macromolecules*, **27** (10), 2647–2657.

46. Kraus, A., Guegel, A., Belik, P., Walter, M., and Muellen, K. (1995) *Tetrahedron*, **51** (36), 9927–9940.

47. Harth, E., Van Horn, B., Lee, V.Y., Germack, D.S., Gonzales, C.P., Miller, R.D., and Hawker, C.J. (2002) *J. Am. Chem. Soc.*, **124** (29), 8653–8660.

48. Kim, Y., Pyun, J., Frechet, J.M.J., Hawker, C.J., and Frank, C.W. (2005) *Langmuir*, **21** (23), 10444–10458.

49. Pyun, J., Tang, C., Kowalewski, T., Frechet, J.M.J., and Hawker, C.J. (2005) *Macromolecules*, **38** (7), 2674–2685.

50. Ryu, D.Y., Shin, K., Drockenmuller, E., Hawker, C.J., and Russell, T.P. (2005) *Science*, **308** (5719), 236–239.

51. Leiston-Belanger, J.M., Russell, T.P., Drockenmuller, E., and Hawker, C.J. (2005) *Macromolecules*, **38** (18), 7676–7683.

52. Kim, E., Shin, C., Ahn, H., Ryu, D.Y., Bang, J., Hawker, C.J., and Russell, T.P. (2008) *Soft Matter*, **4** (3), 475–479.

9
New Functional Polymers Using Host–Guest Chemistry

Ryosuke Sakai and Toyoji Kakuchi

9.1
Introduction

Host–guest chemistry is defined as a chemistry that deals with the complex formation of two or more molecules through multiple noncovalent bonding such as hydrogen bonds, ionic bonds, van der Waals forces, and hydrophobic interactions [1–14]. On the basis of the multiplicity of the noncovalent interaction and spatial regulation of the host molecule, the resulting complex often forms a specific three-dimensional structure. In addition, the host–guest complexation triggers dramatic changes in the electronic states and/or the three-dimensional structure of the host molecule, thus providing a responsive ability. Furthermore, the noncovalent bonding imparts reversibility and mobility to the formed complex. On the basis of these characteristic features, molecules with specifically designed host moieties exhibit transcendent functions that are not realized by covalently bonded molecular systems. Therefore, polymers bearing specially designed host moieties can become functional polymers through a specific host–guest complexation with certain guest molecules. Thus, the host–guest complexation of the polymer could be regarded as a *noncovalent modification* of the polymers.

   This chapter provides a broad overview of functional polymers using host–guest chemistry, where new concept in this area is particularly described in detail. Because ''functional'' polymers are mainly dealt in this book, polymer syntheses using host–guest chemistry including supramolecular polymers are excluded from this chapter, which have already been summarized in excellent reviews [15–19]. In addition, this chapter focuses only on host–guest complexation, and thus simple acid–base interaction, metal–ligand coordinations, and biological interactions are not described. The polymers introduced here will attract a great deal of attention from the viewpoint of scientific research. In addition, such polymers have tremendous potentials for applications as advanced materials including smart and intelligent materials, thus contributing to practical materials development. The research area in this chapter involves various topics and therefore a brief introduction is included in each section.

9.2
Polymers with Responsive Three-Dimensional Structures

Naturally occurring polymers often form a one-handed helix as a higher order structure, for example, a left-handed helical structure for amylose, an α-helix for a polypeptide, and a right-handed double helix for DNA. Similar to the naturally occurring polymers, helical structure is observed as one of the fundamental higher-order structures for synthetic polymers, whereas some special regulations are basically required for realization of the one-handed helical structure [20–24]. It should be noted that the one-handed helical structure itself has chirality. Thus, helical polymers with a one-handed helical conformation on their main chain show another class of chirality, that is, a helical chirality. This section deals with polymers forming helical structures that are susceptible to host–guest complexation with certain molecules.

9.2.1
Helicity Induction

In 1995, Yashima *et al.* [25, 26] developed a conceptually new strategy to induce a helical structure on an optically inactive polymer, that is, macromolecular helicity induction. A *cis*-transoidal stereoregular poly(phenylacetylene) bearing carboxyl groups **1** demonstrated the first example of the macromolecular helicity induction (Figure 9.1). The polymer formed a predominantly one-handed helical structure on complexation with optically active compounds capable of interacting with carboxyl groups, and the complexes exhibited a characteristic-induced circular dichroism (ICD) in the UV–visible region of the conjugated polymer backbone. For the helicity induction, the induced helical sense was basically controllable by the chirality of the employed chiral small molecules. Thus, the helicity induction technique is quite valuable as a versatile approach for preparing a helical polymer with the desired helical sense after the polymer preparation. Furthermore, such an ability of responding to the presence of small chiral molecules is expected to be used as a chiral sensing material.

This helicity induction is accomplished by a simple acid–base interaction. For the helicity induction, the chiral information of the optically active guest molecules is transmitted via the specific interaction between the functional groups in the polymer and guest molecules, so that the rational design of the interaction site is required for realizing the sensitive and selective helicity induction. On the basis of this concept, a number of polymers featuring rationally designed crown ether hosts have also been fabricated.

The first example was reported for poly(phenylacetylene) with aza-18-crown-6 (**2**), in which a macromolecular helicity was induced on the main chain through the host–guest complexation with the perchlorate salts of amino acids [27, 28]. For this helicity induction system, an unprecedented sensitivity was observed, that is, the polymer could respond to an extremely small amount of chiral information. For example, the polymer formed an almost perfect single-handed helical conformation
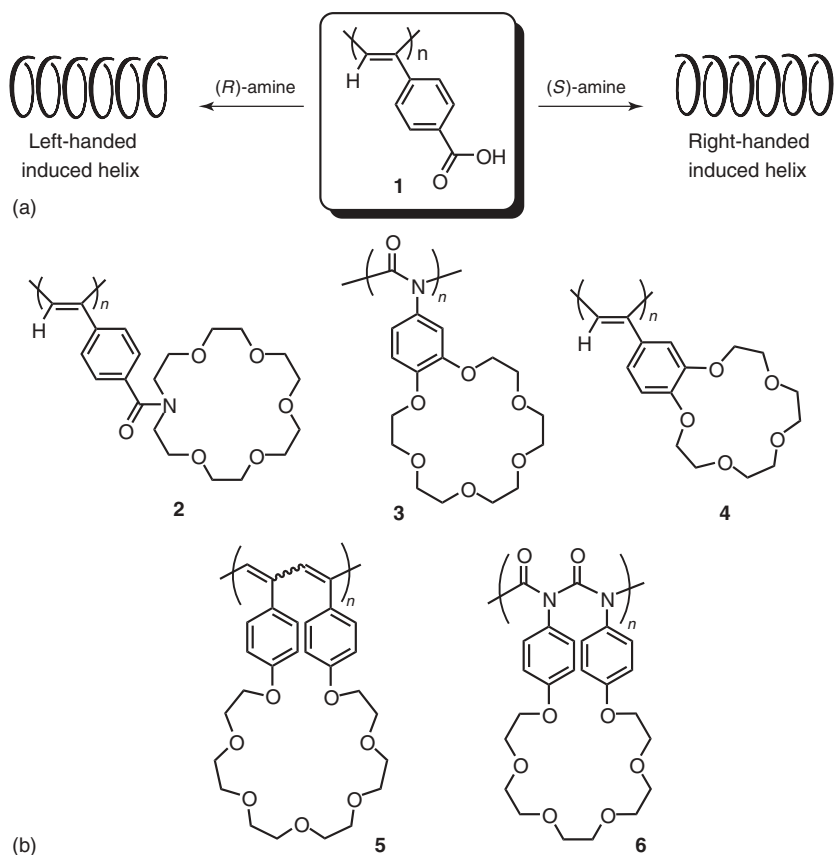
Figure 9.1 (a) Helicity induction of poly(phenylacetylene) bearing carboxyl groups driven by the interaction with chiral amines. (b) Typical polymers capable of forming the helical structure via the host–guest complexation with small chiral guest molecules.

in the presence of only a 0.1 equiv. of L-alanine (L-Ala) relative to the azacrown ether units. This extremely high sensitivity is explained by the chiral amplification phenomenon based on the so-called "sergeants and soldiers effect." In this helicity induction, a large amount of uncomplexed crown units takes part in the construction of a one-handed helical structure that is favorable to a small amount of crown units complexed with L-Ala. Therefore, on the basis of this cooperative phenomenon, the tiny chiral information of a small chiral molecule is significantly amplified by transforming it into the chirality of the entire polymer chain, resulting in an extremely higher chiral output than that expected from the original chirality. In addition to Ala, the polymer could complex with all the common 19 amino acids with a chirality and show intense ICDs. It should be noted that the sign of the ICD is totally dependent on the chirality of the amino acids. Thus, the polymer can be used as a practical probe for determining the amino acid chirality. Moreover, the polymer also shows another chiral amplification based on

the ''majority rule,'' which arises from the phenomenon that the polymer chain predominantly forms a helical structure with a single-handedness that is preferred for the major enantiomer. In fact, an even 5% *ee* ($L/D = 52.5/47.5$) of Ala produced the full ICD intensity in the CD spectrum. In addition, the apparent ICD can be observed even if the Ala has an extremely small enantiomeric imbalance of less than 0.005% *ee* ($L/D = 50.0025/49.9975$).

Similar helicity inductions driven by the host–guest complexation are applicable to a wide variety of crown-ether-conjugated polymers. Poly(phenyl isocyanate) featuring 18-crown-6 pendants (**3**) also forms a one-handed helical structure through the host–guest complexation with chiral guest molecules [29]. The smaller size crown ether, 15-crown-5, was capable of being used as a host for chiral amines and amino acid derivatives, and the complexes formed a one-handed helical conformation [30, 31]. However, the sensitivity was lower than the above-mentioned poly(phenylacetylene) bearing aza-18-crown-6, presumably because of the low binding ability of the 15-crown-5 unit. For example, on complexation with chiral guest molecules, poly(4′-ethynylbenzo-15-crown-5) (**4**) showed an induced helical chirality, which drastically depended on the temperature change and disappeared at 30 °C or higher [31]. Although the induced helix is not stable, it is of great interest that the construction and collapse of the induced helical structure is reversibly tunable with temperature modulation. Kakuchi *et al.* [32, 33] reported that poly(phenylacetylene)s (**5**) and polyisocyanates (**6**) with a crown ether on their main chain, which were prepared by the cyclopolymerization technique, formed a single-handed helical structure driven by the complexation with chiral guests. In these helicity induction systems, the complexed chiral guest directly endows the twisting of the main chain conformation, leading to another class of helicity induction.

9.2.2
Helix Inversion

For the above-mentioned helix formation, the main chain forms a single-handed helical conformation through the host–guest complexation with small chiral molecules. Therefore, the off–on switching of the helical chirality is realized by responding to the chirality of the employed guest molecules. In addition to the helicity induction concept, helix inversion, which is the inversion of the macromolecular helicity between right- and left-handed helical conformations, is also important as a unique stimulus-responsive property observed in the helical polymers, resulting in the characteristic chiroptical switching [24]. The first example of the helix inversion through host–guest interaction was achieved for poly(phenylacetylene) bearing β-cyclodextrin (CyD) pendants (**7**), in which the macromolecular helicity was inverted in response to the complexation with achiral and chiral guest molecules (Figure 9.2) [34]. Interestingly, this helix inversion was accompanied by a drastic color change. Thus, the details of the chirality and colorimetric response of this polymer are described in the subsequent section.
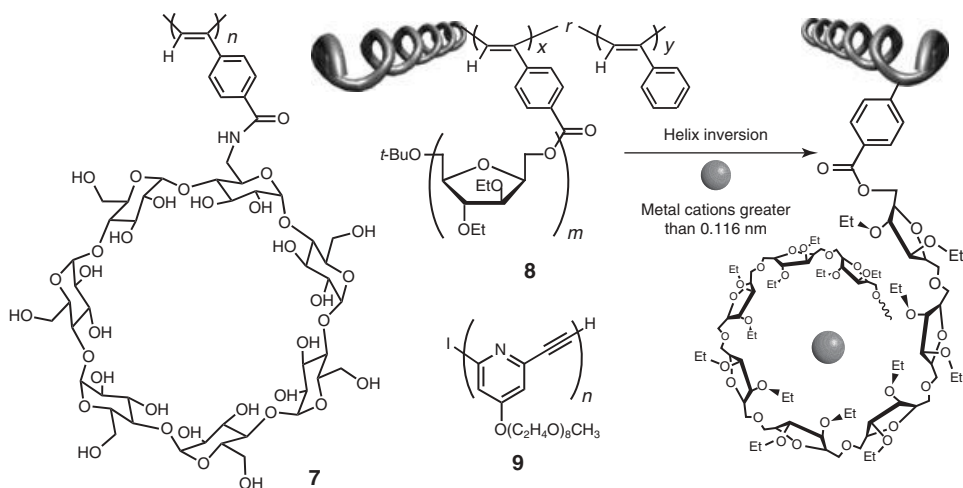
Figure 9.2 Helical polymers that can invert their helical conformations driven by the interaction with chiral and achiral small molecules. The metal cation-triggered helix inversion of **8** is illustrated as an example.

Kakuchi and coworkers [35, 36] reported helix inversion caused by the complex formation between a pendant acyclic host and metal cation. Poly(phenylacetylene) with a polycarbohydrate ionophore as the graft chain **8** was prepared by the copolymerization of an end-functionalized $(1 \rightarrow 6)$-2,5-anhydro-3,4-di-*O*-ethyl-D-glucitol having a 4-ethynylbenzoyl group with phenylacetylene. The polymer showed a split-type CD pattern in the absorption region of the conjugated polymer backbone (280–500 nm), indicating that the polymer had a predominantly one-handed helical conformation in the backbone because of the chirality of the pendant polycarbohydrates. The CD pattern of the polymer was completely inverted by the addition of certain metal cations, such as Ba^{2+}, Pb^{2+}, Sr^{2+}, Na^+, and Li^+. This is considered to be based on the helix inversion of the polymer main chain, which is triggered by the complex formation between the polycarbohydrate ionophore and these cations. Interestingly, the above cations have relatively larger ionic radii among the examined cations, which are greater than 0.116 nm except for Li^+. The polycarbohydrate ionophore on the side chain is originally an acyclic host that can form a pseudo-helix structure suitable for coordinating the given cation. Thus, this ionophore shows a good binding ability to various cations. In this host–guest complexation, the spatial size of the pendant ionophore is highly dependent on the size of the bound cation, thus influencing the main chain conformation. The larger cation presumably produced the destabilization of the original helical conformation, realizing the size-selective helix inversion.

Helix inversion in a foldamer was also reported for poly(*m*-ethynylpyridine) (**9**). The polymer could encapsulate both α- and β-D-glucoses within the cylindrical cavity, whereas the Cotton effect sign of the polymer in the case of α-glucose was opposite to that for β-D-glucose [37]. On the addition of α-D-glucose, the aqueous

solution of the polymer showed a strong ICD, which inverted with time, indicative of the helix inversion based on the anomerization of D-glucose between the α- and β-forms. This demonstration highlighted the fact that the helical polymers with a stimulus-responsive ability can be applicable to even real-time information translator.

9.3
Polymer Probes for Specific Chemical Sensing

The most straightforward application of molecular recognition would be sensing probes. Also, small molecular and supramolecular systems, both colorimetric and fluorescent polymer probes, have been designed and fabricated using responsive conjugated polymers, of which the conjugated main chains are used as a signaling component [38–42]. The characteristic feature of such polymer probes is that a significant number of binding sites is conjugated to one signaling unit (polymer chain). Therefore, the polymer probes sometimes show a significantly enhanced sensitivity based on a signal amplification phenomenon that is not realized by small molecular systems.

9.3.1
Colorimetric Probes

Marsella and Swager [43] have achieved the colorimetric sensing of metal cations based on a π-conjugated polymer (Figure 9.3). Polythiophene consisting of bithiophene repeating units integrated into a crown ether (**10**) showed a good binding ability to Li^+, Na^+, and K^+. Interestingly, these complexations provided clear bathochromic shifts in the absorption band corresponding to the main chain π-conjugation, and thus resulting in visible color changes. This is considered to be based on the changes in the π-conjugation length via twisting the thiophene units that is triggered by the cation complexation event. Furthermore, the redshift was highly dependent on the cations and estimated to be 46 nm for Li^+, 91 nm for Na^+, and 22 nm for K^+. This indicated that the rational design of a host moiety is useful for the specific detection of a certain analyte.

Colorimetric cation detection has also been accomplished using a unique and simple strategy, which uses supramolecular assemblies consisting of polydiacetylene vesicles and an ionophore [44]. 10,12-Tricosadiynoic acid (**11**) and phospholipids formed vesicles in an aqueous solution, which was photopolymerized by UV irradiation to give a blue-colored polydiacetylene vesicle solution. To this solution, ionophores, such as monensin (**12**) or valinomycin (**13**), were added to impart a cation binding ability, which did not affect the solution color. In this system, the ionophores were found to be embedded in a matrix of the polymerized diacetylene lipids. The resulting solution was shown to undergo visible color changes from blue to red in the presence of certain cations. The color transitions of the vesicles were based on the conformation change in the polydiacetylene vesicles, which
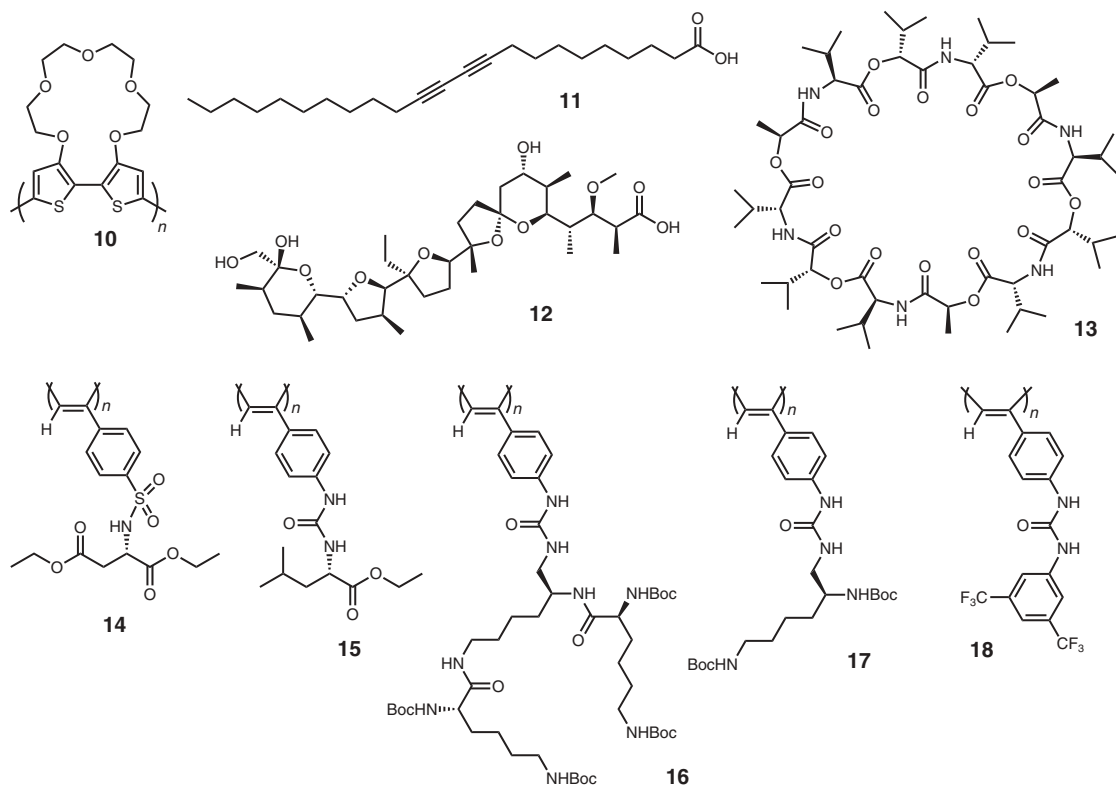
Figure 9.3 Structures of polymer-based colorimetric probes.

were directly related to the binding of the cations to the ionophores. The system detected cations of submillimolar concentrations and demonstrated a significant ionic selectivity dependent on the employed ionophores. The probe design used in this system is based on just mixing the ionophore binding component with the polydiacetylene signaling unit, thus providing a facile and valuable route in the probe fabrication.

As mentioned above, poly(phenylacetylene) bearing β-CyD pendants (**7**) exhibited a visible color change as well as changes in the helical conformation in the main chain [34, 45]. The polymer possessed a yellow-orange color due to the effective conjugation of the main chain and one-handed helical structure based on the chirality of the pendant β-CyD, which is a cyclic host molecule consisting of seven glucose units. When 1-adamantanol or (−)-borneol was added to the polymer solution, an immediate color change from yellow-orange to red was observed, which was accompanied by the inversion of the Cotton effect signs. This color change was concluded to be caused by the structural change in the twist angle of the conjugated double bonds. In contrast, cyclooctanol and cyclohexanol brought about neither such a dramatic color change nor CD inversion. Thus, both the color change and helix inversion events were suggested to be stimulated by an inclusion of guest molecules inside the CyD cavity.

Moreover, the polymer showed a superior chiral-sensing ability. The addition of racemic and (*R*)-1-phenylethylamine induced a negligible conformational change in the polymer, resulting in no essential change in the absorption and CD spectra. On the contrary, the polymer showed a clear CD inversion and redshift in response to the addition of the (S)-isomer. On the basis of the fact that a large amount of (*S*)-1-phenylethylamine was required for these changes in the CD and the solution color, a chiral solvation effect rather than an enantioselective inclusion complexation in the β-CyD residues were implied to be the driving force for the observed color change. Therefore, these findings well demonstrated that a rationally designed polymeric receptor is very useful for the specific detection of certain molecules including chiral compounds.

Similar to poly(phenylacetylene) bearing β-CyD hosts, sulfonamide-functionalized poly(phenylacetylene) (**14**) demonstrated a colorimetric sensing of anions, in which sulfonamide units act as binding sites for the anions [46, 47]. As expected, **14** produced a yellow-colored solution, which is caused by the effective π-conjugation on the polymer backbone. Moreover, a split-type Cotton effect was observed in the CD spectrum of the polymer, indicating the biased helical structure in the main chain. On the addition of F^-, a significant bathochromic shift occurred in the UV–vis absorption spectrum. Therefore, this spectral change reflected a distinct color change in the polymer solution from yellow to red, which can be easily visually recognized. Furthermore, the F^- addition produced a CD-spectral pattern completely different from the original one. Given that the absorption change was accompanied by a drastic CD change, the observed color change was found to be attributable to the extension of the main chain conjugation length based on the conformation change in the polymer main chain. Similar to F^-, a bathochromic shift was observed in the presence of $CH_3CO_2^-$, whereas the

shift was smaller than that for F$^-$, thus resulting in the orange-colored solution. In addition, other anions including Br$^-$, NO$_3$$^-$, N$_3$$^-$, and ClO$_4$$^-$ did not influence the absorption change. This selectivity in the colorimetric response was concluded to be dictated by the basicity of the anions.

Owing to the significance of anion sensed in diverse fields including environmental, industrial, biological, and medical ones, the design and construction of synthetic receptors with a selective anion detection ability is highly required today [6,48–52]. However, the realization of such a selective and specific anion binding has been recognized as a remarkably challenging task because of the diversity in the chemical and physical properties of anions, which includes basicity, size, and shape. In anion reception chemistry, the selectivity in anion recognition is basically dictated by the basicity of anions, as mentioned earlier. Therefore, it is quite difficult to realize the anion detection with a different specificity.

As one of the effective approaches, size-specific colorimetric anion detection was realized by the polymer-based receptor using poly(phenylacetylene) bearing urea binding sites derived from ʟ-Leu (**15**) [53]. A tetrahydrofuran (THF) solution of the polymer was pale yellow because of the small absorption around 400 nm in the absorption spectrum. In spite of the chirality at the ʟ-Leu pendants, the CD spectrum of **15** showed no essential Cotton effect around 400 nm, thus indicating that the polymer possesses a nonbiased helical conformation. On the addition of CH$_3$CO$_2$$^-$, the pale yellow polymer solution immediately turned red, which is based on a drastic bathochromic shift from 400 to 520 nm. In addition, an intense split-type Cotton effect was developed in the range from 340 to 630 nm, indicating that a biased one-handed helical structure was induced in the backbone by the CH$_3$CO$_2$$^-$ addition. This accompanying CD change indicated that the colorimetric response is based on the conformational change. In addition to CH$_3$CO$_2$$^-$, other anions including F$^-$, Cl$^-$ and Br$^-$, I$^-$, HSO$_4$$^-$, NO$_3$$^-$, and N$_3$$^-$ produced distinctive changes in the absorption and CD spectra. In particular, the anion-triggered bathochromic shifts were highly dependent on the type of anion, thus providing a brilliant color variation. On the basis of several experiments, the authors concluded that this unprecedented colorimetric response was dictated by the employed anion size as well as the basicity of the anions. Furthermore, a close arrangement of multiple urea receptors with the helical polymer backbone was found to be necessary for such a colorimetric response based on the observations that the poly(phenylacetylene) hemi-functionalized with urea binding sites showed no color changes by the addition of any anions. This would be one of the results that well demonstrate the significance and value of fabricating a macromolecular receptor for the realization of significant ability unattainable by small molecule-based receptors.

Similar to **15**, a series of poly(phenylacetylene)s bearing urea functionalities derived from other amino acids, such as ʟ-Ala, ʟ-Phe, ʟ-Ile, ʟ-Glu, ʟ-Asp, ʟ-Leu, were found to also show CD and colorimetric responses to anions [54]. Although the color changes were almost the same for all the polymers, the CD spectral changes were strongly dependent on the pendant structure of the amino acids. The pattern recognition methodology using both the color and CD responses obtained

from all the above polymers was reported to be useful for the discrimination of anions.

Furthermore, Kakuchi *et al.* [55] demonstrated that poly(phenylacetylene) bearing second generation lysine dendrons through urea groups **16** was a superior anion receptor possessing a stricter size specificity for colorimetric anion detection. On the addition of $CH_3CO_2^-$, F^-, and Cl^-, an almost colorless polymer solution immediately turned red. In contrast to the above three anions, Br^-, NO_3^-, N_3^-, and ClO_4^- apparently caused no essential changes in both their CD and absorption spectra. In sharp contrast to **16**, control polymer with first generation lysine dendrons (**17**) exhibited obvious colorimetric responses to N_3^-, NO_3^-, and Br^- as well as to $CH_3CO_2^-$, F^-, and Cl^-. Given that the structural difference between **16** and **17** is only the generation of the lysine dendron, the size of the pendant dendron was concluded to play an important role in governing the selectivity of the colorimetric anion detection for these macromolecular receptors. Particularly, for **16**, the steric hindrance of the bulky G2 dendron would highly restrict the interaction of the larger anions with the urea group and/or the complexation-triggered conformational change in the polymer chain, thus realizing the anion detection with an unprecedented strict size-specificity. Although some effective methodologies for size-specific anion detection have been established, such strict size specificity has never been achieved in anion reception chemistry.

The conjugated-polymer-based chemical sensor generally consists of a polymer backbone as a signaling component and a significant number of binding sites at the side pendants. This structural feature provides a unique nonlinear response including the chiral amplification described above, which is fundamentally different from small molecule-based sensors. Such a nonlinear response was also observed in the colorimetric anion sensing based on poly(phenylacetylene) with [bis(trifluoromethyl)phenyl]urea pendants (**18**) [56].

On the addition of $CH_3CO_2^-$, $C_6H_5CO_2^-$, F^-, Cl^-, Br^-, NO_3^-, N_3^-, and HSO_4^-, **18** exhibited a large bathochromic shift depending on the type of anion. To elucidate the anion-binding ability of the polymer, an absorption titration experiment was conducted with varying amounts of anions. The resulting titration curves displayed a sigmoidal curvature particularly for $CH_3CO_2^-$, $C_6H_5CO_2^-$, F^-, and Cl^-, indicative of a cooperative binding mode [57, 58]. On the basis of the consideration of these binding processes using the Hill equation, a cooperative and positive homotropic allosteric binding was found to occur between the polymer and these four anions. For this binding system, the partially formed urea/anion complex units in the polymer chain should produce a change in the entire main chain conformation, which is more suitable for further anion binding.

9.3.2
Fluorescent Probes

A conjugated-polymer-based sensor for potassium ions that operates via an ion-induced aggregation was reported [59]. 15-Crown-5-functionalized poly(*p*-phenylene ethynylene) (**19**) was designed and used as the fluorescent polymer
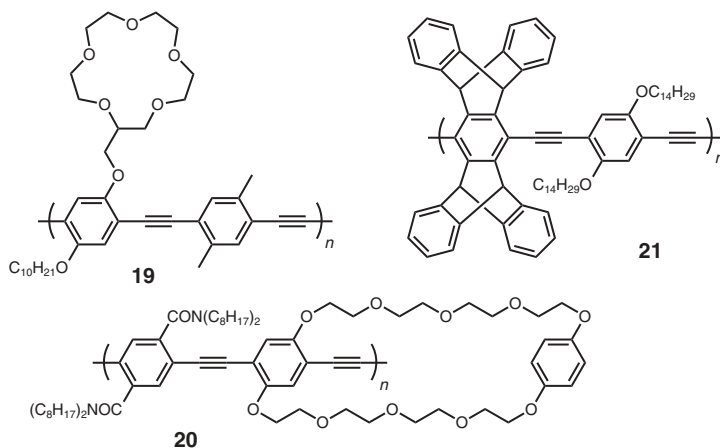
Figure 9.4 Typical examples of polymer-based fluorescent probes.

sensor (Figure 9.4). On the basis of the ability of 15-crown-5 to form a 2 : 1 complex with K^+ ions, the K^+ addition was found to generate potassium-bridged polymer aggregates. The aggregated polymer displayed a redshift in the absorption spectrum in which λ_{max} shifted from 434 to 459 nm. In addition to this absorption change, the ion-induced aggregation resulted in a drastic fluorescence quenching, in which the emission intensity decreased 82% for a 2 : 1 crown ether/K^+ molar ratio. In sharp contrast, a 1500-fold excess of either Li^+ or Na^+ did not significantly influence the fluorescence emission spectrum of the polymer, probably because these cations form 1 : 1 complexes with 15-crown-5. On the basis of this fact and some additional experimental observations, the fluorescence quenching is confirmed to be caused by the K^+ − induced aggregate formation of the polymer.

A common goal in sensory materials is increased sensitivity. Therefore, a number of strategies has been developed to realize this objective. Among them, chemical sensors based on amplifying fluorescent conjugated polymers are recognized as a unique and rather practical approach for sensitive sensor fabrication [40]. The first demonstration was reported by Swager and Zhou [60] in 1995. Poly(phenylene ethynylene) bearing cyclophane receptors **20** showed a fluorescence emission due to the main chain conjugation. On the addition of paraquat, which is a powerful electron acceptor and well-known electron-transfer-quenching agent, a drastic fluorescence quenching occurred as a result of the binding of the paraquat by the cyclophane through a pseudo-rotaxane complex formation. To better understand this fluorescence quenching, studies were conducted in parallel on a small model compound containing a single cyclophane receptor with the same local environment. Although this monomeric analog also showed a fluorescence quenching behavior to paraquat, the quenching effect was much lower than that observed for the polymer. By conducting detailed photophysical studies, this effect was found to be a result of the facile energy migration along the polymer backbone. In this system, the polymer need only to have a small fraction of complexed receptor

sites to affect complete quenching, in sharp contrast to the monomeric indicator in which every receptor must be occupied for the complete quenching. Therefore, this signal amplification phenomenon realized for the fluorescent polymer sensor enables a significantly enhanced sensitivity over a small molecular indicator, thus offering the practical and reliable approach for the highly sensitive detection of certain analytes.

As the most brilliant example of this sensing strategy, a practicable detection method of explosives, particularly 2,4,6-trinitrotoluene (TNT) and 2,4-dinitrotoluene (DNT), was developed in 1998 by Yang and Swager [61, 62]. The developed sensory material was a solid-state (thin film) fluorescent sensor consisting of a pentiptycene-derived phenylene ethynylene polymer **21**. The rigid three-dimensional pentiptycene moieties play crucial roles in the solid-state application, which are (i) maintenance of high fluorescence quantum yields based on the prevention of self-assembly of the polymer chains, (ii) sufficient solubility due to the reduced interpolymer interactions, and (iii) construction of cavities between the adjacent polymers for diffusion of the analytes. For example, the 70% fluorescence quenching of the polymer film occurred on exposure to TNT vapor (10 ppb) for 60 s. Furthermore, the sensor film was found to be particularly selective toward nitro-aromatic compounds. The authors considered that the electrostatic interaction between the electron-rich polymer and the electron-deficient nitro-aromatic compounds are critical in both the rapid response processes and the explosives specificity. For the practical detection of trace amount of explosives, modified probe polymers with a superior sensitivity have been further fabricated by the Swager *et al.* [40] and others.

9.4
Responsive Soft Materials

Materials that can respond to a molecular recognition event and change their macroscopic figurations are categorized as smart and intelligent materials. As such materials, smart gels with molecular recognition ability have been extensively studied, which have enormous potentials for actual applications in diverse fields [63–66]. In addition to the smart gels, materials capable of responding to both a temperature change and molecular recognition are now described [67–69].

9.4.1
Responsive Smart Gels

Gels are recognized as viscoelastic solidlike materials consisting of a solid 3D matrix and a solvent, which is the major component. The formation of the solid matrix is generally a result of cross-linking of the polymeric strands of macromolecules by covalent chemical bonding. In fact, this strategy is employed to manufacturing a significant number of both common and advanced materials that are necessary for our life. Similar to the covalently cross-linking gels, gel materials that are based

on noncovalent binding have attracted a great deal of attention at present from the viewpoint of smart material development [70–74].

The simplest approach for the preparation of such gel materials is the use of noncovalent bonding as the cross-linking. A supramolecular gelation was realized based on the complex formation between CyD polymers and copolymers containing pendant azobenzene groups [75]. Poly(allylamine) with pendant β-CyD groups (**22**) was prepared as a host polymer (Figure 9.5). A guest polymer **23** was separately synthesized by the copolymerization of acrylamide with *p*-azobenzene acrylamide. The mixture of these polymers was found to produce gels through the noncovalent host–guest complexation between the β-CyD unit and azobenzene pendant. However, this phenomenon was limited to *trans*-azobenzene pendants, and gelations did not occur for the guest polymer with *cis*-azobenzene pendants. This is due to the fact that the binding ability of β-CyD to *trans*-azobenzene was greater than that to *cis*-azobenzene.

A noncovalently cross-linking organogel with a unique chirality dependency was also fabricated [76]. The aforementioned poly(phenylacetylene) bearing aza-18-crown-6 pendants (**2**) formed a predominantly one-handed helical conformation on the complexation with an optically active bis(amino acid)s cross-linker, such as L-homocystine perchlorate, thus producing gels through the intermolecular cross-linking due to host–guest complexation. In this gel, the polymer was found to form a one-handed helical structure in response to the chirality of the cross-linker. In sharp contrast, racemic bis(amino acid)s did not produce such gels at all. On the basis of some examinations, a one-handed helical structure induced by chiral bis(amino acid)s was considered to be essential for the gelation. This insight into the gelation mechanism was also supported by the fact that no gelations occurred after the addition of various achiral diamines.

Enantioselective gelation was further achieved for poly(phenylacetylene) bearing β-CyD pendants through ester linkages **24** [77]. The polymer gradually gelled in a few minutes on the addition of (*S*)-1-phenylethylamine. On the contrary, the polymer solution never gelled even in the presence of an excess amount of (*R*)-1-phenylethylamine. The scanning electron microscopy (SEM) measurement suggested that the polymer in the presence of (*S*)-1-phenylethylamine further formed hierarchical superstructured helical assemblies on a micrometer scale with a controlled helix-sense, which lead to the physical gel formation. For this enantioselective gelation, the chiralities of both β-CyD and helical polymer chain were suggested to play crucial roles in such an enantioselectivity.

Harada *et al.* [78, 79] succeeded in the macroscopic self-assembly of gels through molecular recognition. Acrylamide-based gels functionalized with either host rings (α-, β-, and γ-CyDs) or guest hydrocarbon groups were synthesized for this investigation. For example, by simply contacting a piece of the host gel with β-CyD units **25** to a piece of the guest gel with adamantyl groups **26** in water, both gels firmly adhered to form a combined gel in which the complex formation between the β-CyD unit and adamantyl group on their surfaces is the driving force for this adhesion. The adhesion phenomenon was tunable by changing the size and shape of the host and guest units. Thus, selective self-assembly (adhesion) of
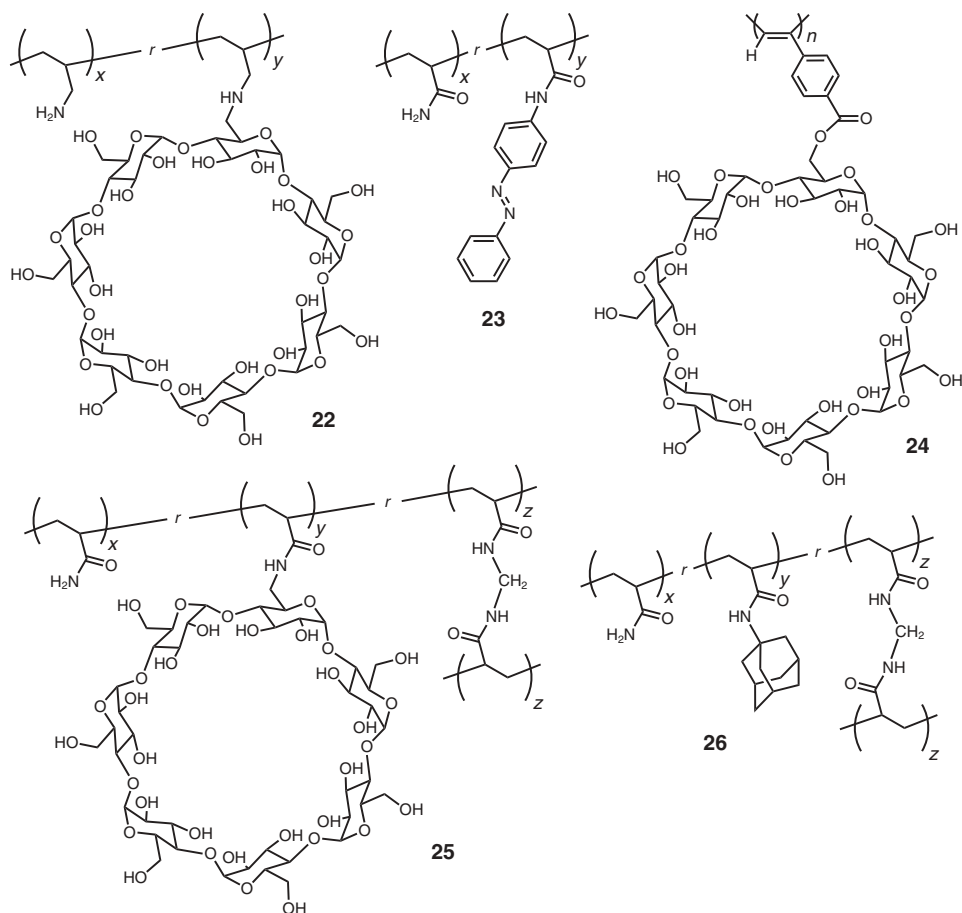
Figure 9.5 Smart gels based on the host–guest chemistry.

host gels and guest gels were demonstrated by the result that four types of gel pieces consisting of two different host gels and two different guest gels selectively assembled to produce two types of complementary combined gels with alternating aggregated structures. This is a valuable report in that the host–guest complexation at a molecular level was demonstrated to directly influence macroscopic objects in the order of millimeters to centimeters. In addition, such macroscopic scale recognition is expected to be applicable to other molecular interactions, thus leading to the development of advanced materials with a macroscopic response ability.

9.4.2
Thermoresponsive Materials with Molecular Recognition Ability

Much attention has focused on smart materials that respond to a temperature change, the so-called thermoresponsive materials. Poly(*N*-isopropylacrylamide)
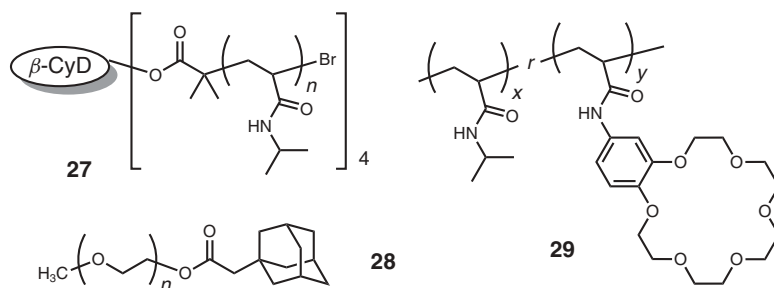
Figure 9.6 Structures of thermoresponsive polymers with molecular recognition ability.

(PNIPAM) is a representative thermoresponsive polymer and exhibits a coil to globule transition of the polymer structure in water at a temperature known as the lower critical solution temperature (LCST), which is generally around 32 °C [67–69]. Owing to its versatility, tremendous applications have been expected in diverse fields of materials science including bioengineering and nanotechnology. Currently, it has been clarified that the LCST of PNIPAM is susceptible to various structure changes. Thus, the thermoresponsive property can be controlled by a molecular recognition event.

Controlling the thermoresponsive property through supramolecular self-assembly was realized for the star-shaped PNIPAM with a β-CyD core (**27**) (Figure 9.6) [80]. The LCST of the star polymer was about 33.5 °C, which shifted to a higher temperature on the addition of the macromolecular guest, poly(ethylene glycol) (PEG) end-functionalized with an adamantyl group **28**. The changes in the LCST were found to be due to the increased solubility driven by the formation of a supramolecular block copolymer composed of the thermoresponsive PNIPAM block and hydrophilic PEG block via host–guest complexation.

Yamaguchi *et al.* [81, 82] fabricated a molecular recognition ion gating membrane. The porous polyethylene film was grafted with a copolymer of *N*-isopropylacrylamide (NIPAM) with benzo-18-crown-6-acrylamide (**29**) by a plasma graft copolymerization technique to produce a porous membrane. The grafted copolymer showed a dramatic volume change in water at its LCST, which further produced changes in the pore size. On the other hand, the LCST of the copolymer complexing with Ba^{2+} was higher than the original one. Therefore, at a constant temperature between the two LCSTs, the membrane changed its pore size in response to Ba^{2+}. This pore size change uniformly occurred in all the pores, leading to a clear cut effect on the solution permeability. Furthermore, owing to the crown ether host, a selective cation response was observed. Thus, this membrane should be useful not only as a molecular recognition ion gate but also as a device for spontaneously controlling the permeation flux and solute size.
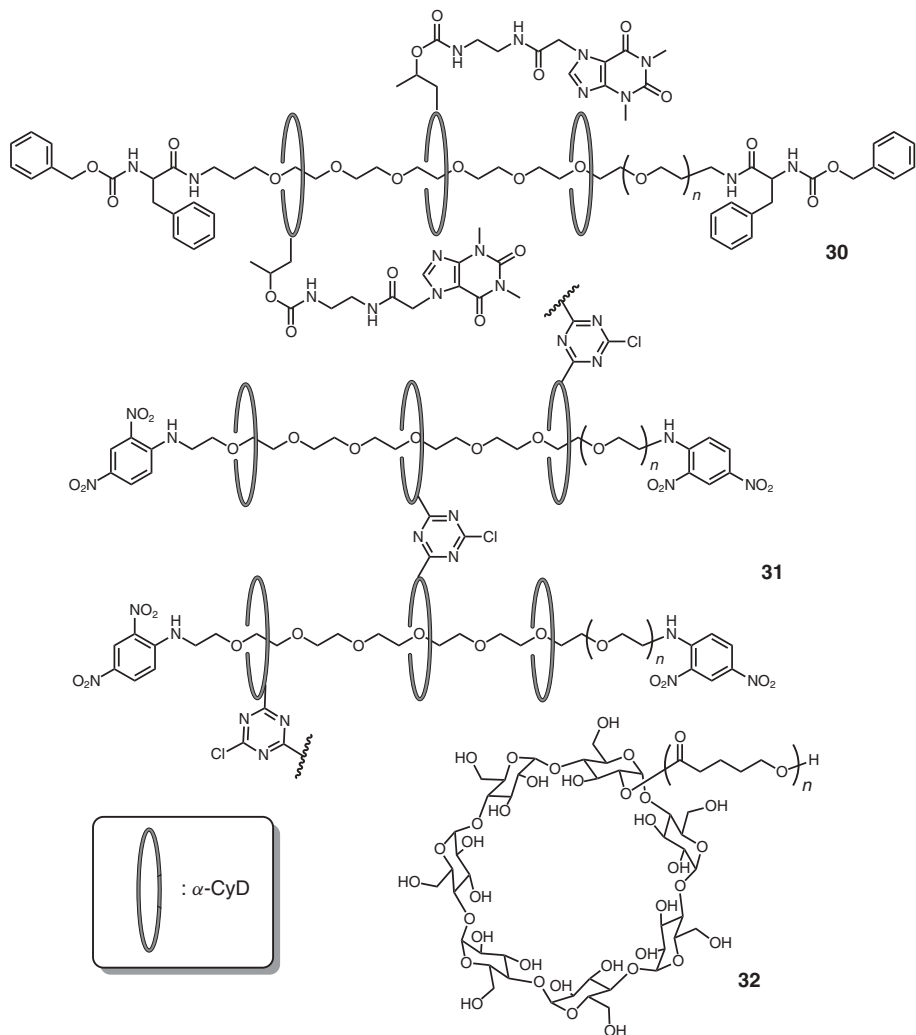
Figure 9.7 Polyrotaxanes with superior functions based on host–guest chemistry.

9.5
Functional Polyrotaxanes

Host–guest complexation is extensively applied as a building block for the synthesis of interlocked compounds, and therefore, a significant number of polyrotaxanes with various molecular designs have already been realized, in which crown ethers and CyDs have often been employed as a host to construct such an interlocked moiety. The synthetic approaches have been summarized in excellent review papers [83–88]. Thus, this section deals with selected examples of polyrotaxanes with superior functions.

Yui and Ooya [89] studied biodegradable polyrotaxanes as a molecular assembly for drug delivery systems. For instance, the theophylline–polyrotaxane conjugate (**30**) was synthesized for a demonstration, in which theophylline, asthma drug, was used as a model drug (Figure 9.7). The polyrotaxane was first prepared in which many α-CyDs are threaded to a PEG chain capped with L-phenylalanine (L-Phe). Subsequently, theophylline was conjugated to the polyrotaxane through the coupling reaction of theophylline with α-CyDs in the polyrotaxane to produce the target theophylline–polyrotaxane conjugates. By the enzymatic treatment using proteases, such as papain, the terminal peptide linkage in the polyrotaxane backbone was revealed to be cleaved off, and the theophylline-immobilized α-CyDs were completely released by this hydrolysis. The main advantage of this polyrotaxane-based drug delivery system is that the drug can be released all at once as soon as stopper cleavage occurs. Thus, this approach could be useful for the realization of the programmed release, which is tunable by the rational design of the drug-polyrotaxane conjugate.

Okumura and Ito [90] developed a methodology for the preparation of a new kind of gel, that is, topological gel with freely movable cross-links **31**. Polyrotaxane consisting of a PEG axis and α-CyD rings was chemically cross-linked with cyanuric chloride to produce transparent gels with a good tensility, low viscosity, and large swellability in water. In this gel, the polymer chains are topologically interlocked by figure-of-eight cross-linkers. Therefore, the cross-linkers can freely pass along the polymer chains in the gel. This mobility enables equalization in the tension of the threaded polymer chains just as pulleys, which is totally different from covalently cross-linking gels. Therefore, this topological gel derived from polyrotaxane is recognized as the third type of gel, being expected to produce high-performance materials.

An artificial molecular chaperone was fabricated using poly-*pseudo*-rotaxane with an extensible axle [91]. As an axis molecule, β-CyD-tethered poly(δ-valerolactone) (**32**) was prepared by the bulk polymerization of δ-valerolactone (δ-VL) initiated with β-CyD. In this polymerization, the inclusion complex between β-CyD and δ-VL was clarified to be essential for the monomer insertion process. Thus, the axis polymer has the potential to further initiate the polymerization of δ-VL, whereas the purified axis polymer did not show any polymerization ability. In sharp contrast, poly-*pseudo*-rotaxane, in which β-CyDs are threaded to the polymer chain of **32**, could initiate the further polymerization to give a longer polymer chain with an increased molecular weight. On the basis of X-ray diffraction and solid-state NMR measurements, the polymer chain of the poly-*pseudo*-rotaxane was found to be an elongated chain, although the polymer chain of **32** without the threaded β-CyDs formed a random coil conformation. Therefore, the polymer chain of **32** was considered to deactivate the polymerization ability by blocking the active cavity of β-CyD at the chain end. On the other hand, for the poly-*pseudo*-rotaxane, the threaded β-CyDs to **32** play an essential role in preventing the polymer chain from getting entangled in order to maintain the initiation ability. Chaperone proteins in biological systems are known to assist in protein folding and allow the functional

state of proteins. Hence, the threaded β-CyDs in this poly-*pseudo*-rotaxane can be regarded as an artificial chaperone.

References

1. Cram, D.J. (1992) *Nature (London)*, **356**, 29–36.
2. Bradshaw, J.S. and Izatt, R.M. (1997) *Acc. Chem. Res.*, **30**, 338–345.
3. MacGillivray, L.R. and Atwood, J.L. (1999) *Angew. Chem., Int. Ed.*, **38**, 1018–1033.
4. Piguet, C. (1999) *J. Inclusion Phenom. Macrocyclic Chem.*, **34**, 361–391.
5. Rebek, J. Jr. (2000) *Chem. Commun. (Cambridge)*, 637–643.
6. Beer, P.D. and Gale, P.A. (2001) *Angew. Chem. Int. Ed.*, **40**, 486–516.
7. Abraham, W. (2002) *J. Inclusion Phenom. Macrocyclic Chem.*, **43**, 159–174.
8. Cooke, G. and Rotello, V.M. (2002) *Chem. Soc. Rev.*, **31**, 275–286.
9. Lee, J.W., Samal, S., Selvapalam, N., Kim, H.-J., and Kim, K. (2003) *Acc. Chem. Res.*, **36**, 621–630.
10. Del, V.E.M.M. (2004) *Process Biochem. (Oxford)*, **39**, 1033–1046.
11. Gokel, G.W., Leevy, W.M., and Weber, M.E. (2004) *Chem. Rev. (Washington, DC)*, **104**, 2723–2750.
12. Kitagawa, S., Kitaura, R., and Noro, S.-I. (2004) *Angew. Chem. Int. Ed.*, **43**, 2334–2375.
13. Pitt, M.A. and Johnson, D.W. (2007) *Chem. Soc. Rev.*, **36**, 1441–1453.
14. Schneider, H.-J. and Yatsimirsky, A.K. (2008) *Chem. Soc. Rev.*, **37**, 263–277.
15. Harada, A. (1996) *Coord. Chem. Rev.*, **148**, 115–133.
16. Brunsveld, L., Folmer, B.J.B., Meijer, E.W., and Sijbesma, R.P. (2001) *Chem. Rev.*, **101**, 4071–4097.
17. Khlobystov, A.N., Blake, A.J., Champness, N.R., Lemenovskii, D.A., Majouga, A.G., Zyk, N.V., and Schroder, M. (2001) *Coord. Chem. Rev.*, **222**, 155–192.
18. Lehn, J.-M. (2002) *Polym. Int.*, **51**, 825–839.
19. Harada, A. and Hashidzume, A. (2010) *Aust. J. Chem.*, **63**, 599–610.
20. Okamoto, Y. and Nakano, T. (1994) *Chem. Rev.*, **94**, 349–372.
21. Nakano, T. and Okamoto, Y. (2001) *Chem. Rev.*, **101**, 4013–4038.
22. Yashima, E., Maeda, K., and Nishimura, T. (2004) *Chem. Eur. J.*, **10**, 42–51.
23. Yashima, E. and Maeda, K. (2008) *Macromolecules*, **41**, 3–12.
24. Yashima, E., Maeda, K., Iida, H., Furusho, Y., and Nagai, K. (2009) *Chem. Rev. (Washington, DC)*, **109**, 6102–6211.
25. Yashima, E., Matsushima, T., and Okamoto, Y. (1995) *J. Am. Chem. Soc.*, **117**, 11596–11597.
26. Yashima, E., Matsushima, T., and Okamoto, Y. (1997) *J. Am. Chem. Soc.*, **119**, 6345–6359.
27. Nonokawa, R. and Yashima, E. (2003) *J. Am. Chem. Soc.*, **125**, 1278–1283.
28. Nonokawa, R. and Yashima, E. (2003) *J. Polym. Sci. A: Polym. Chem.*, **41**, 1004–1013.
29. Sakai, R., Satoh, T., Kakuchi, R., Kaga, H., and Kakuchi, T. (2003) *Macromolecules*, **36**, 3709–3713.
30. Nonokawa, R., Oobo, M., and Yashima, E. (2003) *Macromolecules*, **36**, 6599–6606.
31. Sakai, R., Otsuka, I., Satoh, T., Kakuchi, R., Kaga, H., and Kakuchi, T. (2006) *Macromolecules*, **39**, 4032–4037.
32. Sakai, R., Satoh, T., Kakuchi, R., Kaga, H., and Kakuchi, T. (2004) *Macromolecules*, **37**, 3996–4003.
33. Kakuchi, R., Sakai, R., Otsuka, I., Satoh, T., Kaga, H., and Kakuchi, T. (2005) *Macromolecules*, **38**, 9441–9447.
34. Yashima, E., Maeda, K., and Sato, O. (2001) *J. Am. Chem. Soc.*, **123**, 8159–8160.
35. Otsuka, I., Sakai, R., Satoh, T., Kakuchi, R., Kaga, H., and Kakuchi, T. (2005) *J. Polym. Sci. A: Polym. Chem.*, **43**, 5855–5863.
36. Otsuka, I., Sakai, R., Kakuchi, R., Satoh, T., and Kakuchi, T. (2008) *Eur. Polym. J.*, **44**, 2971–2979.

37. Waki, M., Abe, H., and Inouye, M. (2007) *Angew. Chem., Int. Ed.*, **46**, 3059–3061.

38. McQuade, D.T., Pullen, A.E., and Swager, T.M. (2000) *Chem. Rev. (Washington, DC)*, **100**, 2537–2574.

39. Bunz, U.H.F. (2005) *Adv. Polym. Sci.*, **177**, 1–52.

40. Thomas, S.W. III, Joly, G.D., and Swager, T.M. (2007) *Chem. Rev. (Washington, DC)*, **107**, 1339–1386.

41. Ahn, D.J. and Kim, J.-M. (2008) *Acc. Chem. Res.*, **41**, 805–816.

42. Sun, X., Chen, T., Huang, S., Li, L., and Peng, H. (2010) *Chem. Soc. Rev.*, **39**, 4244–4257.

43. Marsella, M.J. and Swager, T.M. (1993) *J. Am. Chem. Soc.*, **115**, 12214–12215.

44. Kolusheva, S., Shahal, T., and Jelinek, R. (2000) *J. Am. Chem. Soc.*, **122**, 776–780.

45. Maeda, K., Mochizuki, H., Watanabe, M., and Yashima, E. (2006) *J. Am. Chem. Soc.*, **128**, 7639–7650.

46. Kakuchi, R., Kodama, T., Shimada, R., Tago, Y., Sakai, R., Satoh, T., and Kakuchi, T. (2009) *Macromolecules*, **42**, 3892–3897.

47. Kakuchi, R., Shimada, R., Tago, Y., Sakai, R., Satoh, T., and Kakuchi, T. (2010) *J. Polym. Sci., Part A: Polym. Chem.*, **48**, 1683–1689.

48. Amendola, V., Fabbrizzi, L., and Mosca, L. (2010) *Chem. Soc. Rev.*, **39**, 3889–3915.

49. Joyce, L.A., Shabbir, S.H., and Anslyn, E.V. (2010) *Chem. Soc. Rev.*, **39**, 3621–3632.

50. Kubik, S. (2010) *Chem. Soc. Rev.*, **39**, 3648–3663.

51. Schmidtchen, F.P. (2010) *Chem. Soc. Rev.*, **39**, 3916–3935.

52. Gale, P.A. (2011) *Chem. Commun. (Cambridge)*, **47**, 82–86.

53. Kakuchi, R., Nagata, S., Sakai, R., Otsuka, I., Nakade, H., Satoh, T., and Kakuchi, T. (2008) *Chem. Eur. J.*, **14**, 10259–10266.

54. Kakuchi, R., Tago, Y., Sakai, R., Satoh, T., and Kakuchi, T. (2009) *Macromolecules*, **42**, 4430–4435.

55. Sakai, R., Sakai, N., Satoh, T., Li, W., Zhang, A., and Kakuchi, T. (2011) *Macromolecules (Washington, DC)*, **44**, 4249–4257.

56. Sakai, R., Okade, S., Barasa, E.B., Kakuchi, R., Ziabka, M., Umeda, S., Tsuda, K., Satoh, T., and Kakuchi, T. (2010) *Macromolecules (Washington, DC)*, **43**, 7406–7411.

57. Shinkai, S., Ikeda, M., Sugasaki, A., and Takeuchi, M. (2001) *Acc. Chem. Res.*, **34**, 494–503.

58. Takeuchi, M., Ikeda, M., Sugasaki, A., and Shinkai, S. (2001) *Acc. Chem. Res.*, **34**, 865–873.

59. Kim, J., McQuade, D.T., McHugh, S.K., and Swager, T.M. (2000) *Angew. Chem. Int. Ed.*, **39**, 3868–3872.

60. Zhou, Q. and Swager, T.M. (1995) *J. Am. Chem. Soc.*, **117**, 7017–7018.

61. Yang, J.-S. and Swager, T.M. (1998) *J. Am. Chem. Soc.*, **120**, 11864–11873.

62. Yang, J.-S. and Swager, T.M. (1998) *J. Am. Chem. Soc.*, **120**, 5321–5322.

63. Gehrke, S.H. (1993) *Adv. Polym. Sci.*, **110**, 81–144.

64. Ahn, S.-K., Kasi, R.M., Kim, S.-C., Sharma, N., and Zhou, Y. (2008) *Soft Matter*, **4**, 1151–1157.

65. Zhang, X., Zhao, N., Liang, S., Lu, X., Li, X., Xie, Q., Zhang, X., and Xu, J. (2008) *Adv. Mater. (Weinheim)*, **20**, 2938–2946.

66. Tokarev, I. and Minko, S. (2009) *Adv. Mater. (Weinheim)*, **21**, 241–247.

67. Kawaguchi, H., Kisara, K., Takahashi, T., Achiha, K., Yasui, M., and Fujimoto, K. (2000) *Macromol. Symp.*, **151**, 591–598.

68. Zhang, G. and Wu, C. (2006) *Adv. Polym. Sci.*, **195**, 101–176.

69. Cooperstein, M.A. and Canavan, H.E. (2010) *Langmuir*, **26**, 7695–7707.

70. Kato, T., Mizoshita, N., and Kanie, K. (2001) *Macromol. Rapid Commun.*, **22**, 797–814.

71. Foster, J.A. and Steed, J.W. (2010) *Angew. Chem. Int. Ed.*, **49**, 6718–6724.

72. Piepenbrock, M.-O.M., Lloyd, G.O., Clarke, N., and Steed, J.W. (2010) *Chem. Rev. (Washington, DC)*, **110**, 1960–2004.

73. Steed, J.W. (2010) *Chem. Soc. Rev.*, **39**, 3686–3699.

74. Steed, J.W. (2011) *Chem. Commun. (Cambridge)*, **47**, 1379–1383.

75. Takashima, Y., Nakayama, T., Miyauchi, M., Kawaguchi, Y., Yamaguchi, H., and Harada, A. (2004) *Chem. Lett.*, **33**, 890−891.

76. Morino, K., Oobo, M., and Yashima, E. (2005) *Macromolecules*, **38**, 3461−3468.

77. Maeda, K., Mochizuki, H., Osato, K., and Yashima, E. (2011) *Macromolecules (Washington, DC)*, **44**, 3217−3226.

78. Harada, A., Kobayashi, R., Takashima, Y., Hashidzume, A., and Yamaguchi, H. (2011) *Nat. Chem.*, **3**, 34−37.

79. Yamaguchi, H., Kobayashi, R., Takashima, Y., Hashidzume, A., and Harada, A. (2011) *Macromolecules (Washington, DC)*, **44**, 2395−2399.

80. Zhang, Z.-X., Liu, X., Xu, F.J., Loh, X.J., Kang, E.-T., Neoh, K.-G., and Li, J. (2008) *Macromolecules*, **41**, 5967−5970.

81. Yamaguchi, T., Ito, T., Sato, T., Shinbo, T., and Nakao, S.-I. (1999) *J. Am. Chem. Soc.*, **121**, 4078−4079.

82. Ito, T., Hioki, T., Yamaguchi, T., Shinbo, T., Nakao, S.-I., and Kimura, S. (2002) *J. Am. Chem. Soc.*, **124**, 7840−7846.

83. Gibson, H.W., Bheda, M.C., and Engen, P.T. (1994) *Prog. Polym. Sci.*, **19**, 843−945.

84. Huang, F. and Gibson, H.W. (2005) *Prog. Polym. Sci.*, **30**, 982−1018.

85. Wenz, G., Han, B.-H., and Mueller, A. (2006) *Chem. Rev. (Washington, DC)*, **106**, 782−817.

86. Frampton, M.J. and Anderson, H.L. (2007) *Angew. Chem. Int. Ed.*, **46**, 1028−1064.

87. Harada, A., Hashidzume, A., Yamaguchi, H., and Takashima, Y. (2009) *Chem. Rev. (Washington, DC)*, **109**, 5974−6023.

88. Harada, A., Takashima, Y., and Yamaguchi, H. (2009) *Chem. Soc. Rev.*, **38**, 875−882.

89. Ooya, T. and Yui, N. (1999) *J. Controlled Release*, **58**, 251−269.

90. Okumura, Y. and Ito, K. (2001) *Adv. Mater. (Weinheim)*, **13**, 485−487.

91. Osaki, M., Takashima, Y., Yamaguchi, H., and Harada, A. (2007) *J. Am. Chem. Soc.*, **129**, 14452−14457.

10
Glycopolymers via Post-polymerization Modification Techniques

James A. Burns, Matthew I. Gibson, and C. Remzi Becer

10.1
Introduction

Synthetic carbohydrate-containing macromolecules or glycopolymers have attracted increasing attention in various fields as synthetic mimics of natural oligosaccharides, glycoproteins, or glycolipids, because of their specific recognition properties [1–4]. The actual binding affinity between carbohydrates and their protein target is very weak, with dissociation constants on the order of $10^3 – 10^6$ M [5]. In nature, this is overcome through presentation of multiple copies of the same carbohydrate residue on the surface of cells, which leads to an enhancement in the binding affinity, which is greater than the simple linear sum of the binding affinities of individual sugars. This enhanced binding is due to the so-called cluster glycoside effect, which is distinct from simple polyvalency, which gives a linear increase in binding as more ligands are expressed. The exact mechanisms of these are still a topic of intense debate [6, 7]. Considering the avidity enhancement associated with multiple carbohydrates, it is no surprise that glycopolymers have emerged as attractive candidates for new biomaterials, as tens, or hundreds, of individual sugars are incorporated onto a single polymer backbone. It has also emerged that the nature of the polymer chain, that is, architecture, length, and linkers, can strongly affect the binding characteristics [8]. Therefore, the advent of modern controlled polymerization processes has opened the doors to access a plethora of potential structures with an aim of optimizing the protein–polymer interaction.

Direct polymerization of glycomonomers is a convenient route to glycopolymers, but represents challenges when structure–property relationships are desired. Considering the strong link between the valency (i.e., degree of polymerization) and lectin binding affinity, it is essential to have identical polymer lengths when comparing two different carbohydrates for multivalent binding. Despite the challenges in controlled radical polymerization, obtaining two batches with identical molecular weight and molecular weight distribution is very challenging. To address this, Mammen *et al.* [9] first used poly(*N*-acryloyl succinimide), which is a reactive polymeric precursor that can be functionalized with

aminoglycosides. Using this, they demonstrated the effect of polymer structure and carbohydrate density on the binding affinity of glycopolymers to influenza virus.

Active esters are useful precursors, but the addition of bulky functional groups, such as carbohydrates, leads to nonquantitative conversion and hence statistical copolymers, rather than homogeneous glycopolymers [10]. Considering this fact, this chapter focuses on the use of highly efficient reactions (click reactions) that have been used for the synthesis of well-defined glycopolymers. The applications of synthetic glycopolymers have been discussed elsewhere, and readers are pointed to several reviews on the topic [11–15].

10.2
Synthesis and Controlled Polymerization of Glycomonomers

The most obvious route to synthetic glycopolymers is through the direct polymerization of carbohydrate-bearing vinyl monomers for radical polymerization, as demonstrated by Horejsi *et al.* [16]. In their work, they copolymerized allyl mannoside with acrylamide to obtain glycopolymers capable of specifically recognizing plant lectins. Despite this early breakthrough, the main challenge associated with direct polymerization of carbohydrate-functional monomers lies in monomer synthesis and the tolerance of the polymerization methodology to the functional groups present [17]. In order to obtain homogeneous glycopolymers, it is essential to either polymerize unprotected monomers, or to be able to quantitatively remove all protecting groups post polymerization in the absence of any competing side reaction. This was demonstrated by Ambrosi *et al.* [18] who obtained poly[β-ᴅ-gluco- or β-ᴅ-galacto-(methacrylates)] by direct polymerization of the unprotected monomer or polymerization/deprotection of the acylated derivatives (Scheme 10.1). Deprotection of the acylated polymer using sodium methoxide resulted in poorly defined copolymers because of competing hydrolysis of the methacrylic ester, whereas the deprotected monomer route gave homogeneous glycopolymers.

The second, and perhaps more important, challenge in glycomonomer synthesis is the requirement for stereoselective synthetic methods. As carbohydrate–protein recognition events are dictated by the relative stereochemistry of the carbohydrate, the stereochemistry of the linker is also a key consideration. It should be noted that the same considerations apply later in this chapter to the synthesis of "clickable" carbohydrates. In order to obtain anomerically pure carbohydrate derivatives, acylated glycosyl donors are often employed. The presence of an acetate group at the 2-hydroxyl blocks one face of the carbohydrate from nucleophilic attack – known as *neighboring group participation* [19]. Scheme 10.1 shows the case for carbohydrates with galacto configuration, with the 2-acetate preventing formation of the α-anomer. For the synthesis of glycomonomers, the most common strategies are those based on the Koenigs–Knorr reaction: the displacement of anomeric halogens or other leaving groups with a good nucleophile [19, 20], enzymatic synthesis
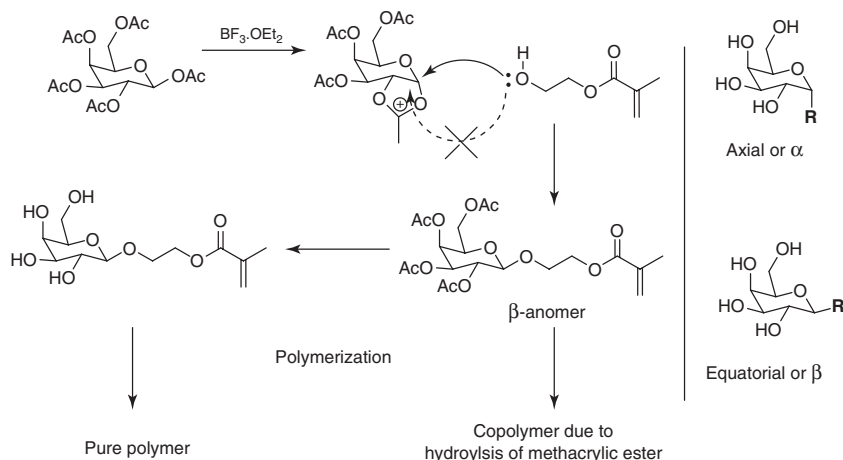
Scheme 10.1 Synthesis and polymerization of protected or unprotected glycosylated monomers. Right side shows anomeric stereochemistry for pyranosides.

[21], lactone derivatives [22], or using aminoglycosides to obtain (meth)acrylamides [23], which are of limited use to the non-native glycosidic linkage. It is essential to use fully protected carbohydrates for this, which does increase the synthetic burden. Despite these methods, there is still a major interest in developing techniques for stereoregular formation of glycoside linkages [24]. With these synthetic routes to glycomonomers at hand, several controlled polymerization methodologies have been applied to them. In particular, reversible addition fragmentation chain transfer (RAFT) polymerization has been used to obtain a wide range of glycopolymers (Scheme 10.2).

RAFT chemistry provides control over the molecular weight, polydispersity, and functionality by changing the thiocarbonylthio chain transfer agent (RAFT agent), which can polymerize a wide range of monomers. The RAFT agent has also been shown to be an effective route to introducing both α and ω functionality to polymers made by this technique [38]. Fleury *et al.* synthesized azide-functional glycomonomers, *N*-[2-((6-deoxy-6-azido-α-D-glucopyranosyloxy) acetamido)ethyl] acrylamide and *N*-[2-((2-deoxy-2-azido-α-D-mannopyranosyloxy) acetamido)ethyl] acrylamide, which were then polymerized using RAFT chemistry [30]. A water-soluble RAFT agent, 3-benzylsulfanylthiocarbonyl sulfanylpropionic acid, was used with (4,4-azobis(4-cyanopentanoic acid) as the thermal initiator. The RAFT polymerization was seen to control the polymerization, achieving target molecular weights with narrow PDIs (<1.15).

Transition-metal-mediated living radical polymerization (TMM-LRP), also known as atom transfer radical polymerization (ATRP), is a well-established route to synthesize polymers that are well-defined with precise functionality [39–42]. This method relies on the deactivation of the propagating radicals carried out by the copper(II) bromide–ligand complex and is particularly useful to obtain α-chain
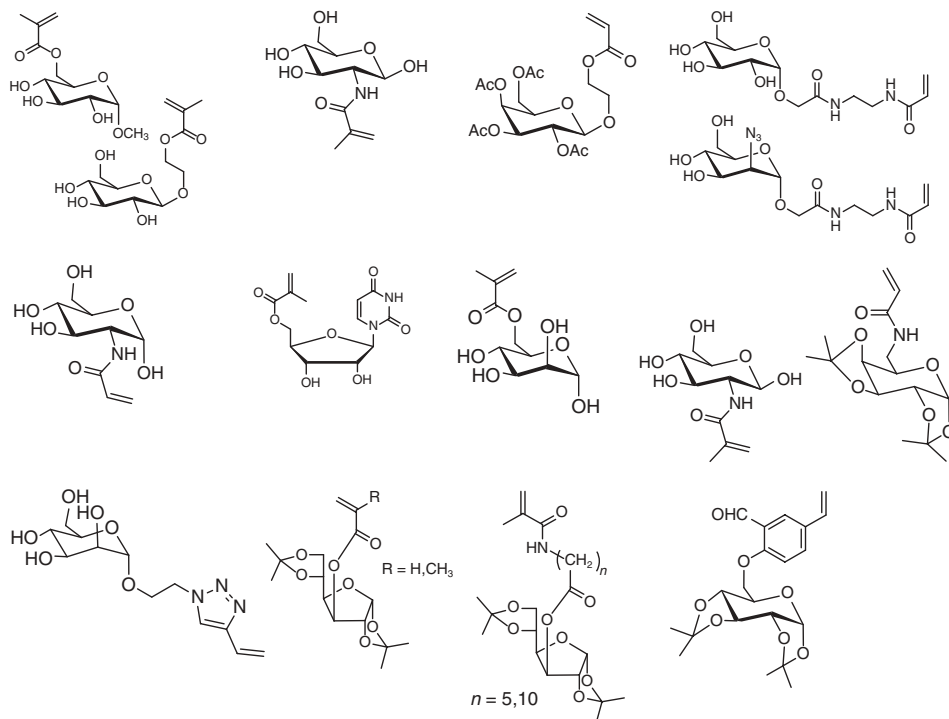
Scheme 10.2 Selected examples of glycomonomers utilized in RAFT polymerization.

end-functional polymers. ATRP has been used to polymerize a variety of protected and unprotected glycomonomers (Scheme 10.3).

Other polymerization techniques such as free radical polymerization (FRP), nitroxide-mediated polymerization (NMP), and ring-opening polymerization (ROP) have been employed for the polymerization of glycomonomers (Scheme 10.4). FRP and NMP do not require any thiol-based chain transfer agents or metal/ligand complexes. However, NMP requires polymerization temperatures above 90 °C, which might be a problem because of the thermal stability of glycomonomers.

Synthesis of glycopolymers using glycomonomer approach is still a very active area of research. However, the multistep synthesis of glycomonomers, incompatibility of unprotected glycomonomers with certain polymerization methods, and difficulty in characterizing the glycopolymers has meant that a post-polymerization technique is becoming increasingly popular.

10.3
Post-polymerization Modification of Polymer Scaffolds to Synthesize Glycopolymers

The concept of "click chemistry" was introduced by Sharpless in 2001 and has revolutionized all fields of synthetic chemistry [56, 57]. According to the criteria
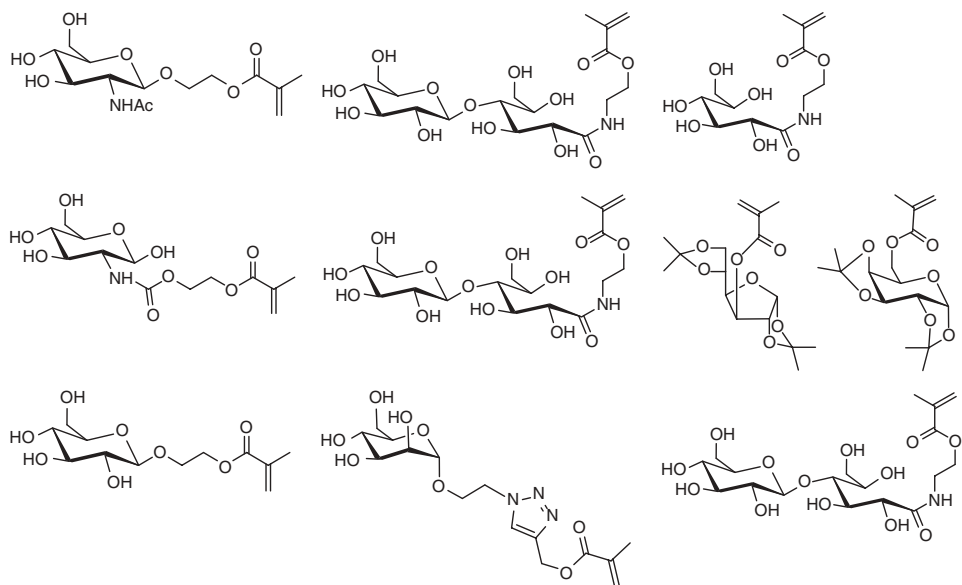
Scheme 10.3 Selected examples of glycomonomers utilized in ATRP polymerization.

R = H, X = O,
R = MO$_3$S, X = O,
R = H, X = CH$_2$,
R = MO$_3$S, X = CH$_2$,

R = H, Ac
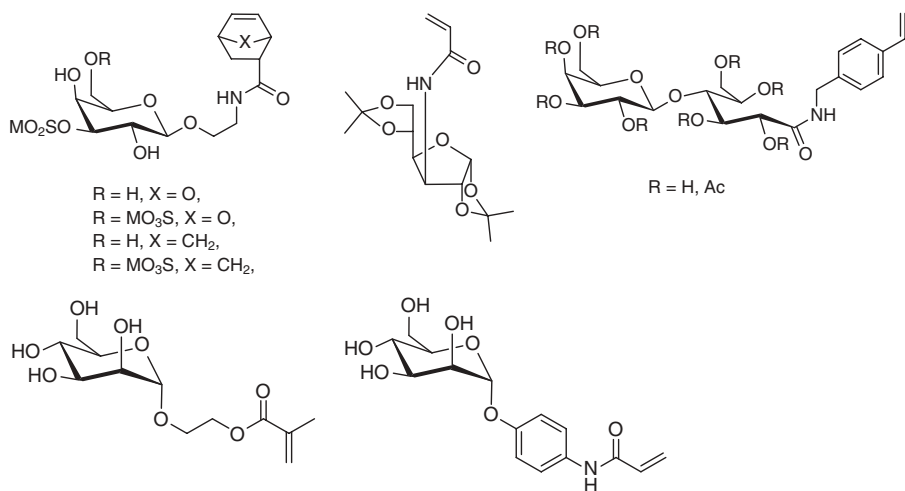
Scheme 10.4 Selected examples of glycomonomers utilized in ROP, NMP, and FRP.

drawn by Sharpless, a click reaction should be modular and wide in scope, highly efficient, generate inoffensive or no by-products, be stereospecific, use readily available starting materials, use benign or no solvent, and require simple purification techniques. One of the most widely employed click reactions has been the copper-catalyzed azide-alkyne cycloaddition (CuAAC) reaction [58–60]. The principle of a simple and highly efficient click reaction is advantageous toward post-polymerization modification; a route that has been proved to be effective in the synthesis of glycopolymers.

The combination of the CuAAC reaction and metal-mediated living radical polymerization has been inevitable since they both use a similar catalyst and could even be conducted in a one-pot reaction [61, 62]. Synthesis of glycomonomers using CuAAC click reaction have been demonstrated by Haddleton *et al.* and Stenzel *et al.*, which is discussed further in this chapter [34,62–64]. In general, a well-defined and functional backbone has been prepared using controlled polymerization techniques and azido sugars have been clicked on the backbone. This allows for the preparation of glycopolymers in a more controlled manner by means of backbone length or comonomer ratios. In a practical sense, it is usually more challenging to structurally characterize a glycopolymer because of their bulky carbohydrate groups, therefore this method provides added benefit.

Moreover, thiol-based click reactions have attracted attention in the past five years because of the commercial availability of a wide range of thiols [65, 66]. The versatility of thiol click reactions has been demonstrated by preparing tailor-made macromolecular architectures varying from telechelic homopolymers to highly complex dendritic structures [67–74]. Glycopolymers have been synthesized from reactions of thiols with various functional groups such as alkenes, alkynes, *para*-fluorophenyl, and halides [75, 76]. Most of these reactions are highly efficient and provide high yields under the employed reaction conditions (Scheme 10.5). In the case of thiol–ene click reactions, it is possible to use UV light and photoinitiator to provide a sufficient radical source. The remaining thiol click reactions are either catalyzed by base or are nucleophilic and proceed under ambient conditions. In terms of synthesis, preparation of thiol sugars seems to be more demanding than that of azido sugars. Nevertheless, selected thiol sugars (glucose and mannose) are commercially available, which helps to reduce the number of synthetic steps required for the preparation of glycopolymers. Moreover, it is relatively easy and versatile to obtain polymers with alkene, alkyne, *para*-fluoro, and halide pendant groups, which can then undergo thiol click reaction.

Selected examples of the various combinations of click reactions and polymerization techniques that are used to prepare glycopolymers have been listed in Table 10.1. Some selected examples have been discussed, where clickable sugars are used either to synthesize glycomonomers, which will lead to a glycopolymer, or to directly click onto a polymeric backbone. The combination of different polymerization techniques, that is, FRP, RAFT polymerization, NMP, ATRP, cobalt-catalyzed chain transfer polymerization (CCTP), and ROP, with selected click reactions are discussed further.

Copper catalyzed azide-alkyne cyclosddition (CuAAC)

$R_1-N_3 +$ ≡ $-R_2$ $\xrightarrow[\text{Solvent or neat}]{\text{[Cu]}}$ $R_1-N\begin{smallmatrix}N=N\\ \\R_2\end{smallmatrix}$

Thiol-ene Click: Radical mechanism

$RS-H +$ R_2 $\xrightarrow{R^\bullet}$ R_2 RS

Thiol-ene Click: hetero-Miahael addition

$RS-H +$ EWG $\xrightarrow{\text{Base/Nu}^\ominus}$ EWG RS $+$ B

Thiol-yne Click: Radical mechanism

$RS-H +$ R_2 $\xrightarrow{2R^\bullet}$ RS R_2 RS

Thiol-halogen Click: Nu$^\ominus$ Substitution

$R_1-S^\ominus$ R_2-X $\xrightarrow{\text{Base}}$ R_1-S-R_2 $X^\ominus$

Thiol-para Fluoro Click: Nu$^\ominus$ Substitution

$R_1-S^\ominus$ $\underset{F}{\overset{F}{\underset{F}{\overset{F}{\bigcirc}}}}$ $\xrightarrow{\text{Base}}$ $R_1-S-C_6F_4$ $F^\ominus$

Scheme 10.5 Various click reactions that are employed in the synthesis of glycopolymers.

10.4
Azide–Alkyne Click Reactions

The CuAAC reaction has been influential in improving synthetic strategies, not only in polymer chemistry but also in other research fields, such as biochemistry, medicinal chemistry, and surface chemistry. The reaction is simple to perform, tolerates various conditions and functional groups, is highly stereospecific, and provides near-quantitative conversions that expedite the purification process. The copper catalyst has a crucial role in the ''click'' process. Before copper was used in the reaction, Huisgen and coworkers studied the azide–alkyne cycloaddition [82]. However, this reaction is slow and results in a mixture of both 1,4- and

Table 10.1 Selected examples on different combinations of click reactions and polymerization techniques to synthesize glycopolymers.
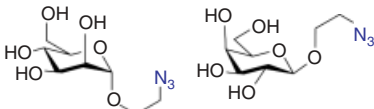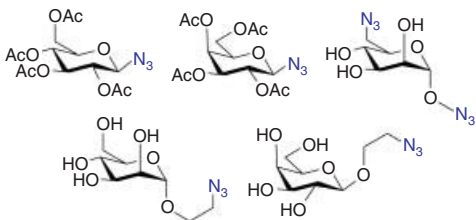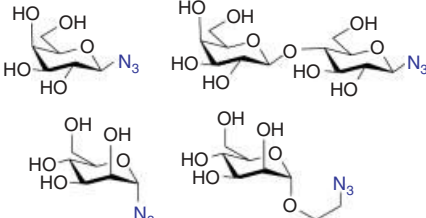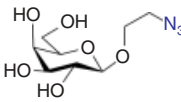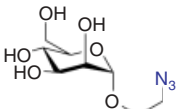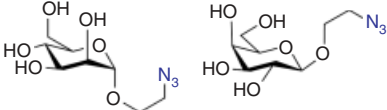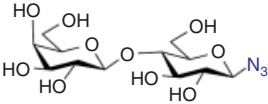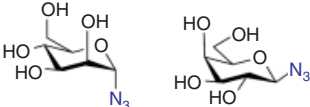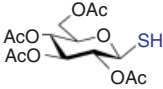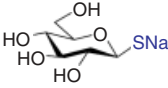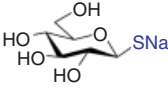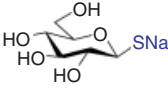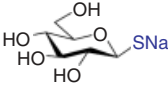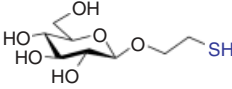
Click reaction	Polymerization method	Backbone	Saccharide	References
CuAAC	ATRP	Methacrylate		[3]
CuAAC	ATRP	Methacrylate		[63]
CuAAC	ATRP	Methacrylate		[48]
CuAAC	RAFT	Acrylate/ Methacrylate		[77]
CuAAC	RAFT	4-Vinyl-1, 2,3-triazole		[34]
CuAAC	ROP	ε-Caprolactone		[78]

Table 10.1 (continued)

Click reaction	Polymerization method	Backbone	Saccharide	References
CuAAC	CCTP (cobalt)	Methacrylate		[74]
p-Fluoro-thiol	NMP	Pentafluoro-styrene		[75]
Thiol–ene	Cationic	N-acylalkylene imine		[79]
Thio–halogen	RAFT	Styrene		[80]
Thiol–ene	RAFT	Acrylate/methacrylate		[77]
Thiol–yne	RAFT	Acrylate/methacrylate		[77]
Thiol–ene	ROP	Ester		[81]

1,5- disubstituted 1,2,3-triazole regioisomers being formed with unsymmetrically substituted alkynes. Meldal and Sharpless independently investigated and introduced copper as a catalyst for this reaction, which solved these problems associated with this reaction [83, 84]. Through the use of a copper catalyst, the reactions proceed faster at and below ambient temperature and with complete conversion to the 1,4-disubstituted 1,2,3-triazole product. An excellent tutorial review has been recently published by Fokin and Hein, which provides extensive details of the CuAAC reaction and mechanism [85]. This type of click reaction has a major role in polymer chemistry, since it provides a variety of new routes to synthesizing glycopolymers.

Haddleton *et al.* reported a versatile synthetic strategy to obtain poly(propargyl methacrylates) suitable for "clicking" with glycosyl azides. This methodology generates a library of glycopolymers with exactly the same molar mass, polydispersity index (PDi), and polymer architecture and also allows the introduction of further orthogonal end groups for conjugation to proteins [3]. Using this general methodology, three different synthetic concepts have been developed (Scheme 10.6). The
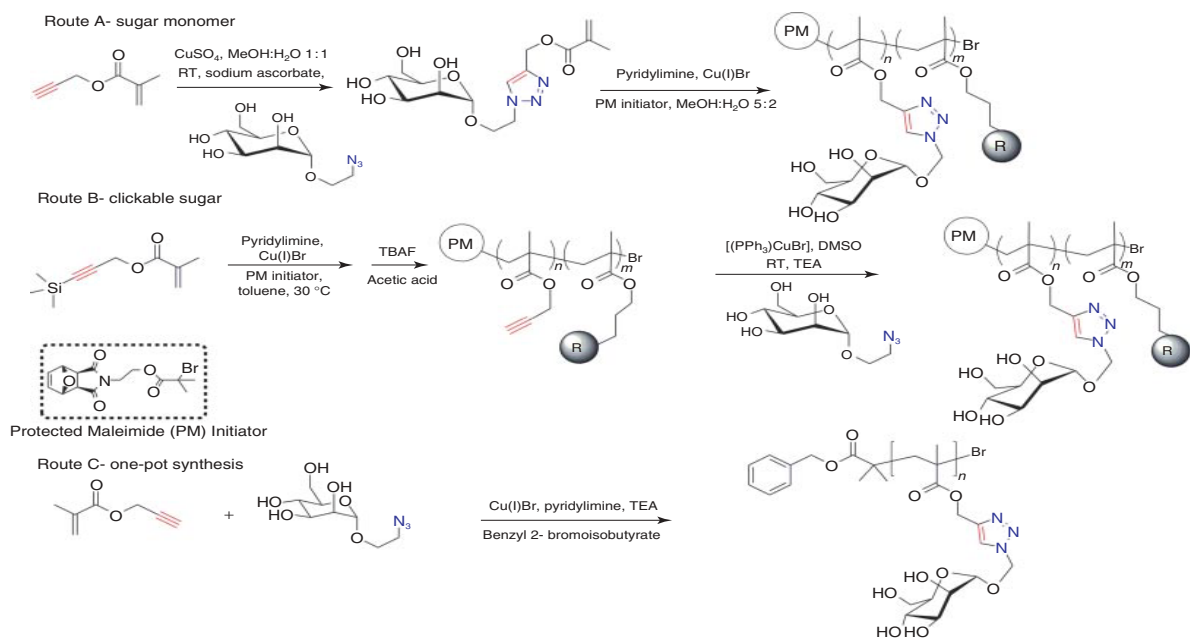
Scheme 10.6 Preparation of glycopolymers using different approaches.

first route (A) produces a glycosyl methacrylate monomer *via* CuAAC click reaction. This monomer is then polymerized by ATRP without the need to protect the hydroxyl groups present on the sugar molecule, which is typically required in glycopolymer synthesis [86]. The second route to glycopolymers (B) reveals the advantages of using click chemistry. First, trimethylsilyl (TMS)-protected propargyl methacrylate is polymerized. The use of the TMS group is essential to prevent radical-induced cross-linking reactions of the alkyne side chain. After polymerization via ATRP, a deprotection step generates the reactive propargyl units, providing a ''clickable'' scaffold, with which a variety of glycosyl azides can be reacted. A final retro-Diels–Alder deprotection of the maleimide end group, installed by the ATRP initiated, allowed site-specific protein conjugation. In essence, it is possible to generate a library of polymers, all containing the same macromolecular characteristics, with the only difference being the sugar chosen to be ''clicked'' onto the scaffold. Haddleton *et al.* successfully conjugated the glycopolymers onto bovine serum albumin (BSA) to create a glycoprotein mimic, which was shown to induce immunological behavior *via* interaction with mannose binding lectin (MBL). A third route has been investigated in which glycopolymers were synthesized *via* a one-pot process with simultaneous CuAAC and living radical polymerization [64]. The mechanism for both of these processes is not yet fully understood; however, Haddleton *et al.* have demonstrated that it is possible to have both reactions proceeding at the same time in the same reaction mixture. Furthermore, by changing experimental conditions such as solvent, temperature, and catalyst concentration, it was possible to influence the rate of each process. This is an important feature of this work since any unclicked alkyne group may undergo side reactions *in situ*, which would lead to less-controlled polymerization. An additional advantage of this one-pot system is that there is no need to use sugar-functional methacrylate monomers that are prone to self-polymerize. This method is useful, as it reduces the number of synthetic steps involved in preparing well-defined glycopolymers.

Synthesis of ω-terminal end-functional polymers with high fidelity has been challenging for polymer chemists. In the case of metal-mediated living radical polymerization, the polymer chain carries a terminal halide atom, which undergoes several activation–deactivation cycles, which may lead to loss of the halogen end group. CCTP, an alternative method, is a versatile technique to produce ω end-functional polymers with high chain end fidelity and controlled molecular weight, albeit with larger polydispersity. This technique benefits from the stability of the bis(boron difluorodimethylglyoximate) cobalt(II) (CoBF) catalyst in neutral aqueous media, allowing polymerizations of acidic monomers, which are unsuitable for anionic polymerization [87]. In anionic polymerization, these acidic monomers would react rapidly with carbanions and eventually terminate the polymerization. With monomers containing an α-methyl group, termination and initiation occur principally by chain transfer reaction from CoBF to the active center. Thus, products contain, invariably, an unsaturated end group. A vinyl-terminated chain end allows facile modification of the polymer chain by a thiol–ene click reaction. The combination of CCTP and click chemistry to synthesize glycopolymers
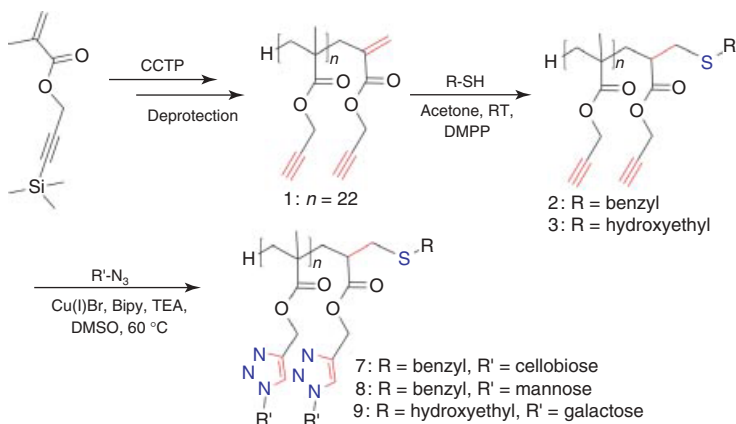
Scheme 10.7 The synthesis of glycopolymers via CCT polymerization and double click reactions.

has been recently reported, in which a protected alkyne monomer is homopolymerized in the presence of CoBF and 2,2′-azobis(2-methylpropionitrile) (AIBN) to yield protected alkyne polymers with vinyl end groups (Scheme 10.7) [74]. Various azide sugars, that is, mannose, galactose, and cellobiose, were reacted with the alkyne groups of the glycopolymer after the removal of the deprotection groups. An attractive feature of this work is the ability of these polymers to undergo further functionalization because of the ω-terminal vinyl group. It is well known that activated vinyl groups can undergo hetero-Michael reaction with thiols. This reaction has been termed *base-catalyzed thiol−ene* click reaction [88, 89]. Moreover, the sugar azides can be clicked onto the polymer scaffold before or after the thiol−ene click chemistry has been performed. This allows a wide array of functionality to be introduced to the glycopolymers.

RAFT polymerization, used in a number of examples, is a well-established, versatile route to the synthesis of well-defined polymer architectures [90−92]. In particular, it has been shown to be an effective route to hyperbranched polymers [93−95]. Stenzel *et al.* [34] have reported the synthesis and RAFT polymerization of a novel glycomonomer *via* CuAAC, belonging to an uncommon monomer class (Scheme 10.8). The 4-vinyl-1,2,3-triazole monomers are a relatively new class of monomers with good thermal properties [96]. They showed the facile synthesis of 2′-(4-vinyl-1,2,3-triazol-1-yl)ethyl-*O*-α-D-mannoside, from 2′-azidoethyl-*O*-α-D-mannoside and 4-trimethylsilyl-1-buten-3-yne. The azide-functional saccharide was easily synthesized without protecting groups. A disadvantage of this glycomonomer synthesis, however, is the complex synthesis of 4-trimethylsilyl-1-buten-3-yne, which requires harsh conditions and led to low yields. To synthesize the glycomonomer, the deprotection of the alkyne by tetra-*n*-butylammonium fluoride (TBAF) and CuAAC click reaction were carried out in a one-pot reaction, in which copper(I) was produced *in situ* by the reduction of $CuSO_4$ by sodium ascorbate.
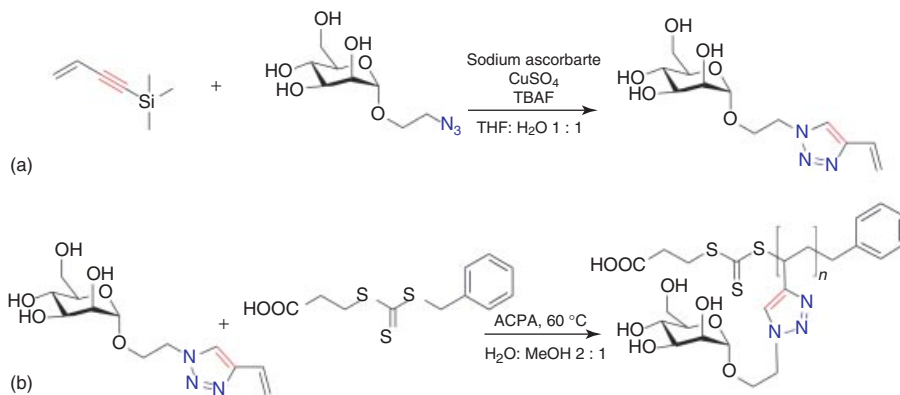
Scheme 10.8 The synthesis of a 4-vinyl-1,2,3-triazole glycomonomer (a) and RAFT polymerization (b).

The 4-vinyl-1,2,3-triazole monomer was polymerized by RAFT in water, with 4,4-azobis(4-cyanovaleric acid) used as the water-soluble thermal initiator. The reactions were carried out in the presence of 3-(benzylsulfanylthiocarbonylsulfanyl) propionic acid (BSPA) as RAFT agent, to yield high-molecular-weight polymer with PDI < 1.25. Poly[2′-(4-vinyl-1,2,3-triazol-1-yl)ethyl-*O*-α-D-mannoside)] macro-RAFT agent was used to synthesize an AB block copolymer with *N*-isopropylacrylamide p(NIPAAm), which reversibly formed micelles above the lower critical solution temperature (LCST) of the p(NIPAAm) block. The micelles formed were seen to have higher rates of binding to Con A in comparison to their linear counterparts, indicating the importance of architecture.

Furthermore, Whittaker *et al.* [97] demonstrate another efficient route to hyperbranched glycopolymers through the use of RAFT polymerization and click chemistry (Scheme 10.9). They modify the chain transfer agent to incorporate alkyne groups into the polymer at the α-chain end. The polymer formed is a statistical copolymer of *N,N*-dimethylaminoethyl acrylate (DMAEA) and trifluoroethyl acrylate (tFEA) with ethylene glycol dimethacrylate (EGDMA) as a branching agent to give an alkyne functionalized hyperbranched polymer network. The CuAAC reaction was implemented to click azide-functionalized sugars onto the polymer network. An elegant feature of this work was the successful incorporation of ^{19}F magnetic resonance imaging contrast agent into the glycopolymer. Another striking feature was that the polymerization was carried out without protection of the alkyne group on the RAFT agent. As has been discussed previously in this chapter, alkynes are typically protected during polymerization, with TMS groups. This is to avoid undesired side reactions; however, in this work, no side reactions were reported. This enables synthesis of glycopolymers in only two steps, with the added benefit of defined macromolecular properties because of the polymerization method as well as incorporation of the MRI contrasting agent.

All the above-mentioned strategies rely on having high-purity glycosyl azides. The most convenient and commonly employed route to stereopure glycosyl azides
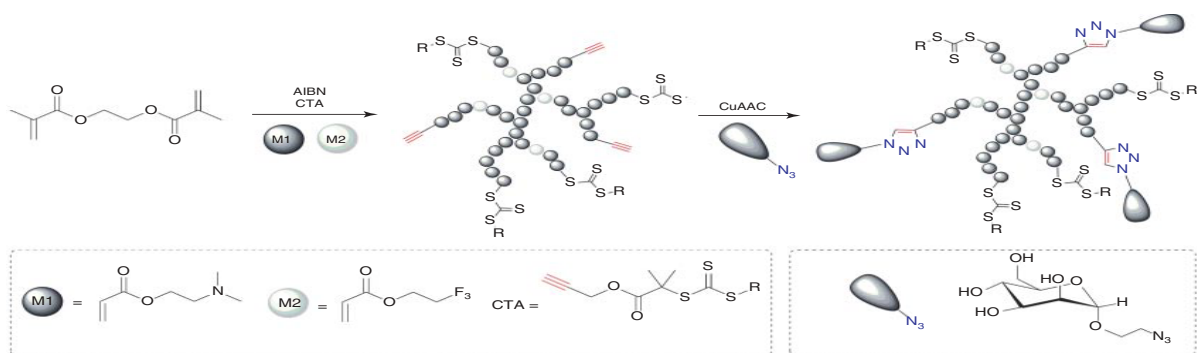
Scheme 10.9 Synthesis of hyperbranched glycopolymers by RAFT using an alkyne-functional RAFT agent and CuAAC click.
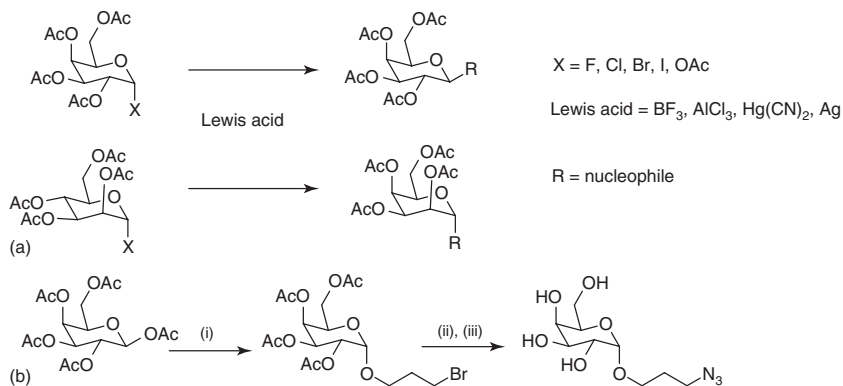
Scheme 10.10 (a) Synthesis of sugar azides under different reaction conditions. (b) an example of sugar azide synthesis, 2′-azoethyl-*O*-a-D- mannopyranoside (i) Bromoethanol, BF$_3$OEt$_2$, −20°C to ambient temperature (ii) NaN$_3$, Reflux in acetone (iii) Sodium methoxide, methanol, ambient temperature.
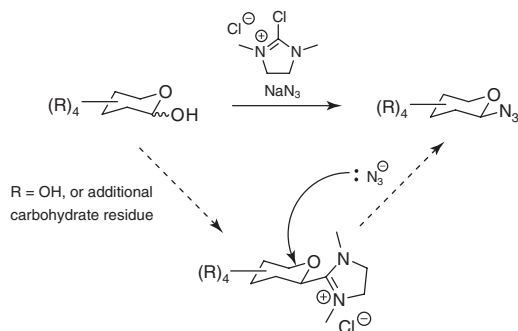
Scheme 10.11 One-step synthesis of glycosyl azides from unprotected carbohydrates as described by *Tanaka et al.*

are based on the Koenigs-and-Knorr-type chemistry [20] and are based on two possible strategies: (i) direct addition of the azide to the carbohydrate and (ii) a two-step process through use of a linker [63]. The advantage of the latter is that it allows the possibility to install a native O-linkage rather than the unnatural triazole.

The routes shown in Scheme 10.10 are the most commonly used methods to obtain glycosyl azides, but it is still preferable to obtain these directly from unprotected carbohydrates and in aqueous media, especially for low-abundance or expensive sugars.

Tanaka *et al.* [98] have demonstrated the use of 2-chloro-1,3-dimethylimida-zolinium chloride (DMC) to specifically activate the anomeric center toward nucleophilic attack by sodium azide in aqueous solution (Scheme 10.11). This method is convenient, applicable to mono-/di-/trisaccharides, and provides excellent stereo control (>90% anomeric purity), with the absolute configuration controlled by the strereochemistry of the 2-hydroxyl adjacent to the anomeric position.
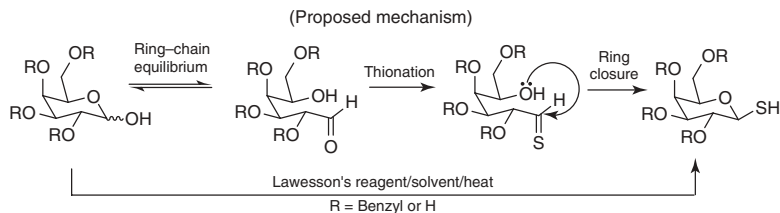
Scheme 10.12 Synthesis of anomeric thioglycosides using Lawesson's reagent [102].

Axial hydroxyl groups result in α-azides, and equatorial hydroxyl groups result in β-azides. This methodology was used to prepare a library of glycopolymers bearing short oligosaccharides by Gibson *et al.* [99].

10.5
Utilizing Thiol-Based Click Reactions

The use of thiols as orthogonal coupling units has been used extensively in organic and peptide chemistry. For example, the low natural abundance of cysteine residues on native proteins allows the incorporation of unique ''handles'' for conjugation reactions via recombinant expression of proteins and has been studied in detail for the chemical synthesis of glycoproteins [100, 101]. Several reaction classes have been developed for this including Michael addition to acrylic or maleimides, radical additions, nucleophilic substitutions, and native chemical ligation, all of which do not require the addition of transition metal catalysts, along with cross-metathesis. Therefore, it is no surprise that these reactions can also be applied to materials science.

Similar to glycosyl azides, it is essential to use stereopure glycosyl thiols to obtain well-defined glycopolymers by post-polymerization modification. A particularly useful method to obtain glycosyl thiols from both protecting and unprotecting carbohydrates was introduced by Davis *et al.* [102]. They exploited Lawesson's reagent, which is a common thionation reagent for converting carbonyls into thiocarbonyls, along with the ring–chain equilibria of reducing sugars. When in the chain form, the carbonyl can be thionated, pushing the equilibrium toward the thionated product, which can then undergo an irreversible ring closure (Scheme 10.12). In most cases, good to excellent anomeric selectivity and yields of 80% were observed.

Owing to the increased nucleophilicty of thiols compared to, for example, alcohols or azides it is possible to directly substitute anomeric bromides without the use of a Lewis acid catalyst in a Koenigs-Knorr-type reaction. The most common routes for this are thioureas, which allow hydrolysis of the urea under mild conditions, retaining other protecting groups, and thioacetate salts, which are removed using methanolic base [103]. Sodium thiohydride can also be used to generate the free thiol (Scheme 10.13). Phase transfer conditions have also been employed to generate protected thioglycosides in a multistep, one-pot reaction starting with unprotected carbohydrates [104].
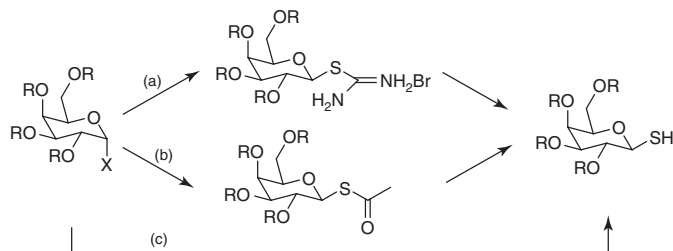
Scheme 10.13 Generalized synthesis of glycosylthiols from anomeric halides via (a) thioureas or (b) thioacetate intermediates (c) direct synthesis.
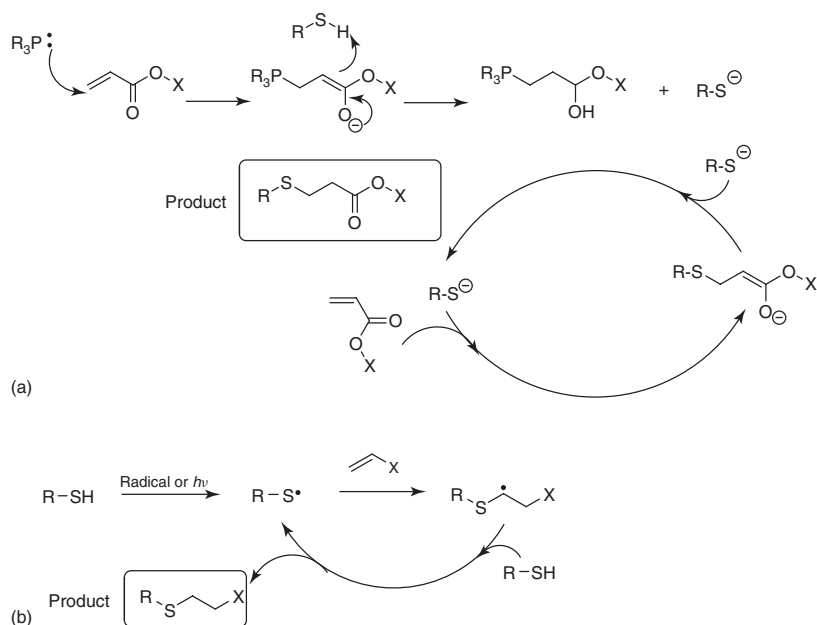

Scheme 10.14 Mechanism of thiol–ene reactions. (a) Phosphine-catalyzed Michael addition to conjugated alkenes. (b) Radical-catalyzed addition of thiols to alkenes.

10.6
Thiol–ene Click Reactions

Thiol-containing compounds are capable of reacting with unsaturated bonds in a variety of efficient, and orthogonal, manners, depending on the nature of the substituents adjacent to the alkene [67]. Two reaction mechanisms are possible, as shown in Scheme 10.14. Route (a) shows the radical-induced addition of thiols onto alkenes, and route (b) shows the phosphine-catalyzed addition of thiols onto electron-deficient alkenes. The use of catalyst drives the latter reaction forward, ensuring its click reaction characteristics.
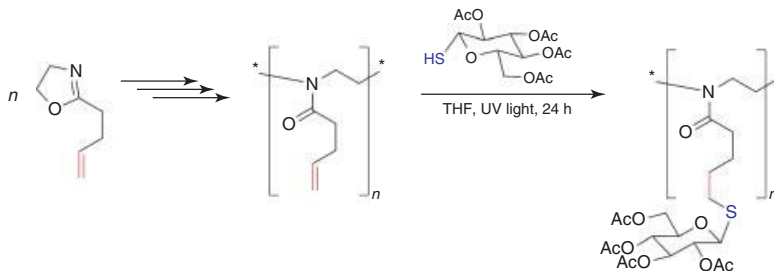
Scheme 10.15 Synthesis of glycopolymers by combination of cationic ring-opening polymerization of 2-oxazoline and thiol–ene click reaction.

In 2001, Fulton and Stoddart [105] used glycosyl thiols to functionalize allylated cyclodextrins, with reported conversions of ∼70%. You and Schlaad [106] first extended this to synthetic polymers by the functionalization of poly(1,2 butadienes) as a route to obtain glycosylated vesicles. Subsequent work demonstrated that well-defined poly[2(-3-isobutenyl)-2-oxazoline] that was synthesized via cationic ring-opening polymerization (CROP) was a better scaffold, as the increased distance between alkene and backbone reduced cross-linking side reactions [107]. This functionalization strategy can be initiated both using a thermal radical initiator or a photoinitiator (Scheme 10.15). Photoaddition of thiols was performed in a 4 wt% solution of polymer in dry THF=tetrahydrofuran NCA=N-carboxyanhydride:methanol (1 : 1) under argon atmosphere and exposed to UV light for a day.

A further study was reported by Stenzel *et al.* [108] on the synthesis of thiol-linked neoglycopolymers by a combination of RAFT polymerization and thiol–ene click reaction. Block copolymerization of di(ethyleneglycol) methylether methacrylate (DEGMA) and 2-hydroxyethyl methacrylate (HEMA) was performed and followed by a post-polymerization modification of the hydroxyl groups of HEMA to clickable vinyl units. This report also highlights the challenges that remain in obtaining well-defined alkene-functional polymers by direct controlled radical polymerization because of the incompatibility of the alkene-functional group. A further glycopolymer synthesis utilized unreacted pendant methacrylate groups present after the polymerization of EGDMA in the absence of a monofunctional monomer. 2-Cyanoisopropyl dithiobenzoate RAFT agent was used to control the polymerization, and dimethyl phenyl phosphine (DMPP) was used to catalyze the hetero-Michael addition of thioglucose to the unreacted pendant methacrylate groups. This reaction yielded a hyperbranched glycopolymer with high conversion of click reaction in a relatively simple manner.

10.7
Thiol–yne Click Reactions

As with alkenes, alkynes can undergo two sequential radical additions to give disubstitution. Perrier *et al.* [77] have reported the synthesis of hyperbranched

glycopolymers using RAFT and a number of "click" reactions. Propionic acidyl butyl trithiocarbonate (PABTC), a RAFT agent, was used to control the polymerization of a protected alkyne acrylate in the presence of difunctional monomer, EGDMA. Following deprotection, the "clickable" scaffold was modified by two different routes (Scheme 10.16). The first was by CuAAC reaction of 2-azidoethyl-β-D-galactopyranoside with the alkyne functionality on the polymer, which reached 85% conversion. The second route was via radical addition of the thioglucose to the alkyne to yield bisglucose functionality. The radical addition reaction was seen to reach 90% conversion, with a small amount of C=C bonds visible in the infrared analysis and vinyl protons present in the NMR analysis. While this is an effective route to obtain hyperbranched glycopolymers, optimization of the click reactions is necessary to avoid the possibility of cross-linking occurring between unreacted vinyl groups.

10.8
Thiol–Halogen Substitution Reactions

Owing to the increase in nucleophility of thiols compared to other functional groups, such as amines, alcohols, and carboxylic acids, they can be used for highly orthogonal nucleophilic substitution reactions. When the leaving group is a sufficiently activated halogen, this reaction can proceed to near-quantitative yields. Schubert *et al.* [75] have demonstrated the polymerization of pentafluorostyrene by NMP (Scheme 10.17). NMP is less commonly used compared to other controlled radical polymerization techniques (RAFT and ATRP) because of the high reaction temperatures necessary for polymerization. However, it is desirable because of the simplicity of the reaction and because the lack of a metal catalyst is appealing for many applications [71, 109]. Poly(pentafluorostyrene) obtained by NMP was specifically functionalized at the para position by addition of tetra-acetyl (β-D-1-thio)glucose with base. Using ^{19}F NMR spectroscopy, quantitative conversion was obtained in less than an hour at 40 °C. Although in essence it is a nucleophilic substitution reaction, the versatility and efficiency of the amine or thiol substitution at the para position of C_6F_5 has been demonstrated by Schubert *et al.* to comply with most of the "click" chemistry requirements [110].

Boyer *et al.* [111] utilized a thio–chloro substitution reaction to yield well-defined glycopolymers, using the modification of preformed polymers synthesized by RAFT. Polymerization of poly(*tert*-butyl acrylate-*co*-chloromethylstyrene) was carried out in the presence of BSPA as RAFT agent and AIBN to yield well-defined polymers with pendant chloro-functional moieties (Scheme 10.18). The reaction of the chloro moieties with thioglucose, in the presence of triethylamine, proceeded to completion in 16 h to yield glucose-functional polymers. An additional approach was utilized by Boyer *et al.* through the copolymerization of 2-hydroxyethyl acrylate with butyl acrylate; however, this approach requires rigorous reaction conditions.
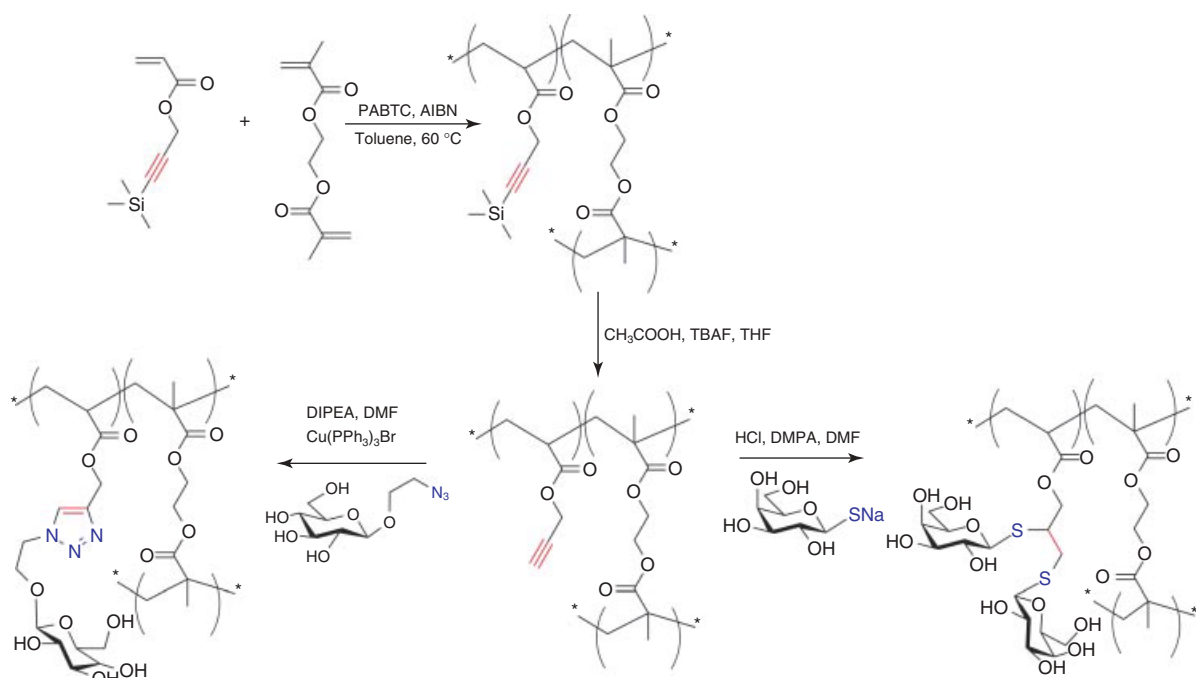
Scheme 10.16 Synthesis of hyperbranched glycopolymers using RAFT polymerization and CuAAC click reactions (left) or thiol-yne click reactions (right).
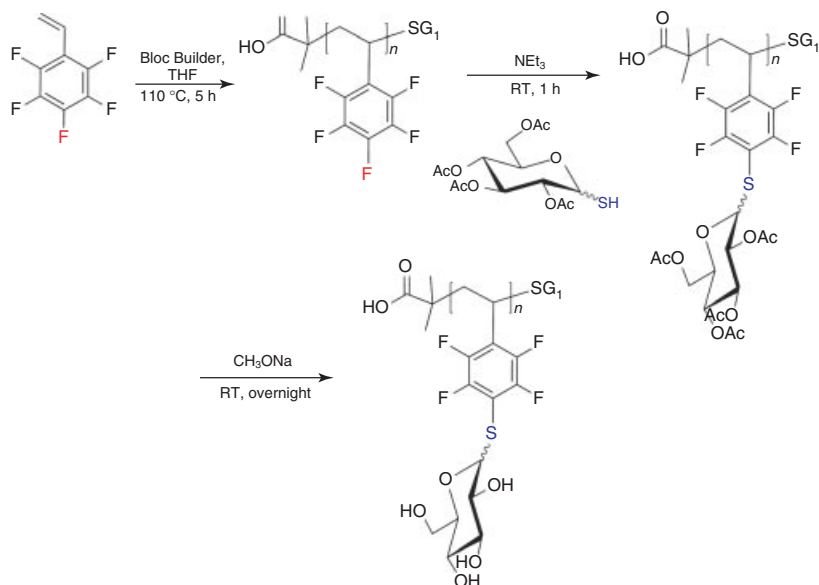
Scheme 10.17 Synthesis of glycopolymers using nitroxide-mediated polymerization (NMP) and thiol-*para*-fluoro click reaction.
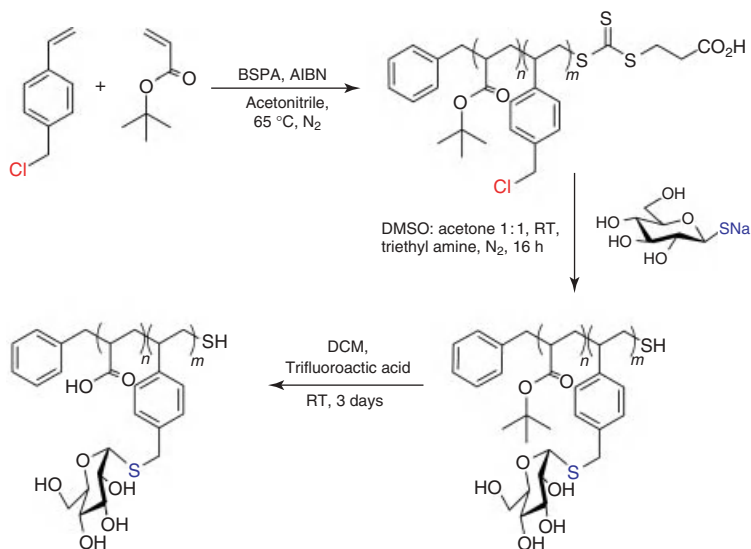
Scheme 10.18 Synthesis of glycopolymer by RAFT polymerization of *tert*-butyl acrylate-*co*-chloromethyl-styrene and thiol–chloro click.
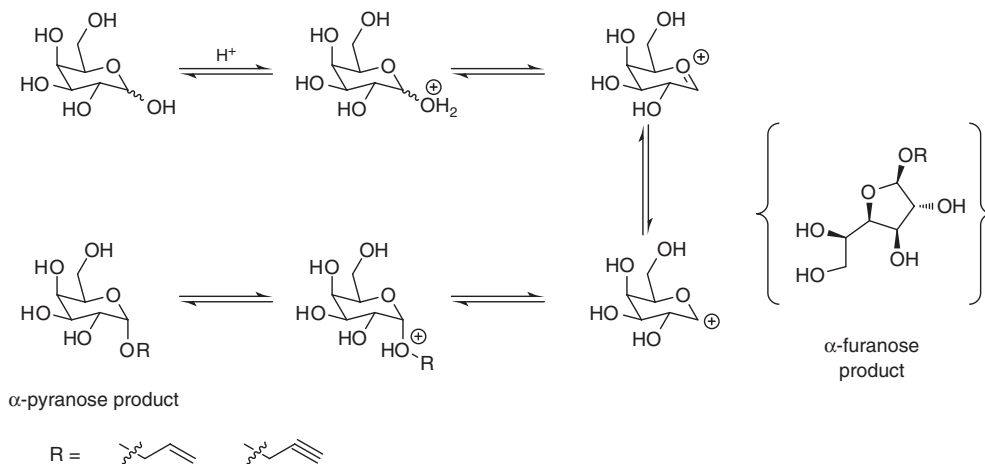
Scheme 10.19 Synthesis of glycosyl alkynes/alkenes by Fischer glycosidation.

For instance, the hydroxyl groups of poly(2-hydroxyethyl methacrylate) were converted to tosyl groups and protected galactose was reacted in the presence of sodium hydride.

10.9
Alkyne/Alkene Glycosides: "Backward" Click Reactions

Most research in this field has focused on materials in which alkenes or alkynes are present on the polymer backbone, which can be reacted with azido/thio glycosides. However, there are several reports of the opposite strategy being used, that is, for peptides [112], which in some cases has several benefits including removing the problems of side reactions during radical or ionic polymerization of alkene/alkynes. Furthermore, the synthesis of alkyne/alkene glycosides is relatively straightforward, employing the Koenigs–Knorr chemistry. A second strategy involves a classic Fischer glycosidation, whereby a reducing sugar is dissolves in an alcoholic solvent in the presence of acid (Scheme 10.19) [113]. Acid-catalyzed dehydration leads to the formation of an oxycarbocation, which is captured by the nucleophilic attack. This reaction is an equilibrium process and therefore requires the nucleophilic solvent to drive the reaction forward. Alcohols can proceed to quantitative yield with relatively short reaction times in the range of several hours. However, a special care should be taken because of the ring–chain equilibrium of reducing sugars. Furthermore, this reaction is under thermodynamic control, which for pyranosides results in the preferential formation of α-glycosides because of the anomeric effect.

10.10
Post-polymerization Glycosylation of Nonvinyl Backbone Polymers

This chapter has focused mostly on vinyl-derived glycopolymers, which covers the vast majority of the literature in this field. However, there is also a need to develop functional polymers based on degradable polymer backbones, which includes poly(amides) and poly(esters). Both of these polymer classes are typically accessed by ROP of cyclic monomers. A challenge of ROP is that it is typically intolerant of protic functionalities, that is, alcohol, amine, acid, sulfate, phosphate. Therefore, the synthesis of poly(esters/amides) from functional cyclic monomers is limited. Compared to radical polymerization methods, ROPs have a specific advantage in that alkene and alkyne functional groups can be directly incorporated into the monomers, as these do not typically interfere with the polymerization process.

NCA polymerization is a particularly attractive method to obtain well-defined homopolypeptides, block polypeptides, or copolypeptides, which display precise secondary structures (typically α-helices and β-sheets) similar to proteins (Scheme 10.20) [114–116]. However, NCA polymerization is intolerant to almost any functional group, meaning that fully protected monomers must be synthesized. Several groups have reported the synthesis of glycosylated NCAs [117, 118], but these are multistep syntheses, which require extensive purification. Schlaad polymerized DL-allylglycine *N*-carboxyanhydride, which was subsequently functionalized with 1-thio β-D-glucose to give well-defined glycopolypeptides [119]. Huang *et al.* [120] used a similar strategy to obtain poly-DL-propargylglycine, which could then be functionalized with 1-azido,β-D-galactose.
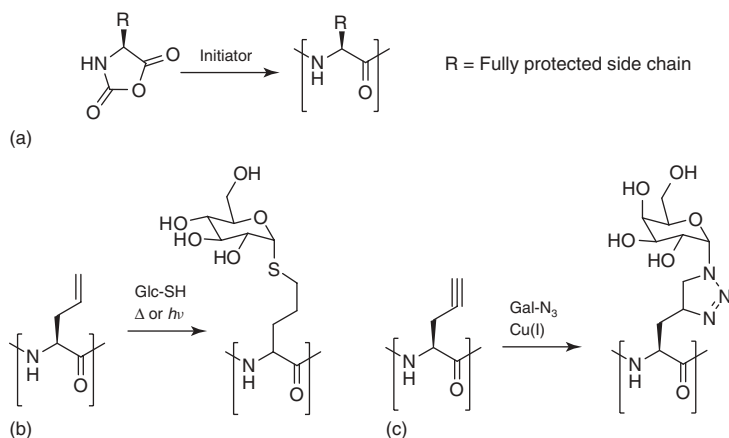
Scheme 10.20 Polypeptides obtained by ring-opening polymerization of *N*-carboxyanhydrides. (a) NCA polymerization, (b) thiol−ene reaction of poly(allylglycine), and (c) alkyne/azide cycloadditon onto poly(propargylglycine).

Well-defined poly(esters) can be obtained by ROP of cyclic esters, but as with NCAs, incorporation of functional groups is very challenging. Owing to their tunable hydrolytic degradability, poly(ester) biomaterials are very appealing. Zi-Chen *et al.* [121] demonstrated that amphiphilic biodegradable glycopolymers can be successfully synthesized via combination of ROP and click chemistry. They synthesized a functional monomer, 2-bromo-ε-caprolactone (BrCL), derived from successive modifications of cyclohexene. Addition of *N*-bromosuccinimide to the alkene was carried out to introduce bromine and alcohol functionalities. The alcohol group was initially converted to a ketone and then to an ester via Baeyer–Villiger oxidation. The effort devoted to the synthesis and polymerization of this type of monomer is worthwhile since the resulting glycopolymer is biodegradable. Block copolymerization with poly(ε-caprolactone) macroinitiator is illustrated in Scheme 10.21. Several more steps were required to introduce sugars and hence produce an amphiphilic block copolymer, involving the conversion of bromide groups to azides and then utilizing the CuAAC click reaction to attach alkyne functional sugars. Proof of aggregation as a result of interaction with lectin Con A was shown using atomic force microscopy (AFM) and transmission electron microscopy (TEM).

10.11
Conclusions and Outlook

The main aim of this chapter was to summarize the breadth of synthetic methodologies that are available to obtain glycopolymers by post-polymerization modification techniques. This synthetic route is gaining increased importance because of the developing understanding between valency of glycopolymers and their biological properties. Only post-polymerization modification allows for the generation of glycopolymer libraries with identical molecular weights, but different densities of carbohydrates.

Before the application of the "click" chemistry philosophy, direct polymerization of glycosyl monomers was the route of choice to obtain these materials, as modification of preformed polymer backbones was inefficient. In this chapter, a selection of synthetic routes to glycopolymers that combine the advantages of click chemistry and controlled polymerization techniques have been discussed.

The CuAAC click reaction has been shown to be a versatile and effective route to glycopolymers, although the removal of copper catalyst still remains a challenge for biological applications. This reaction has been utilized to prepare polymers with different topologies and carbohydrate content. It has also been demonstrated to be a facile route to glycomonomers as well as a promising class of monomer based on vinyltriazole. Alternatively, thiol-based reactions provide a new platform because of their reactivity and orthogonality with alkenes, Michael acceptors, and alkyenes. Furthermore, the nucleophilicity of the thiol group has been exploited to functionalize polymers with thiosugars via chloro- and *para*-pentafluoro groups to yield glycopolymers. There are still several thiol-based reactions that have not been employed for glycopolymer synthesis. For instance, thio–bromo, thiol-epoxide, and
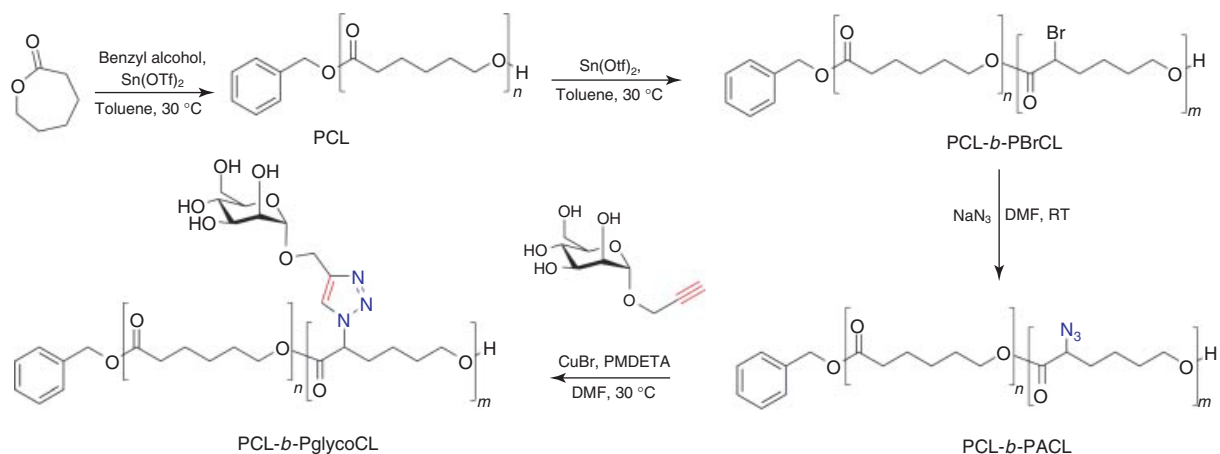
Scheme 10.21 Synthesis of glycopolymers *via* ROP of ε-caprolactone (CL) and 2-bromo-ε-caprolactone (BrCL) blocks, modification of the bromo moieties to azides, and CuAAC click.

thiol-isocyanate reactions could be potentially investigated for their applicability in the glycopolymer field.

The ongoing search for reactions, that meet the criteria of click chemistry, will present opportunities to polymer chemists looking for new and simple methods to well-defined glycopolymers. These advances in the synthesis of glycopolymers will open new avenues toward understanding the role of multivalent interactions in biological systems and, perhaps, the development of new therapeutics, diagnostics, and materials that exploit these interactions.

References

1. Bertozzi, C.R. and Kiessling, L.L. (2001) *Science*, **291**, 2357.
2. Gestwicki, J.E., Cairo, C.W., Strong, L.E., Oetjen, K.A., and Kiessling, L.L. (2002) *J. Am. Chem. Soc.*, **124**, 14922.
3. Geng, J., Mantovani, G., Tao, L., Nicolas, J., Chen, G., Wallis, R., Mitchell, D.A., Johnson, B.R.G., Evans, S.D., and Haddleton, D.M. (2007) *J. Am. Chem. Soc.*, **129**, 15156.
4. Kiessling, L.L., Gestwicki, J.E., and Strong, L.E. (2006) *Angew. Chem. Int. Ed.*, **45**, 2348.
5. Ambrosi, M., Cameron, N.R., and Davis, B.G. (2005) *Org. Biomol. Chem.*, **3**, 1593.
6. Lee, Y.C., Townsend, R.R., Hardy, M.R., Lonngren, J., Arnarp, J., Haraldsson, M., and Lonn, H. (1983) *J. Biol. Chem.*, **258**, 199.
7. Spain, S.G. and Cameron, N.R. (2011) *Polym. Chem.*, **2**, 1552.
8. Cairo, C.W., Gestwicki, J.E., Kanai, M., and Kiessling, L.L. (2002) *J. Am. Chem. Soc.*, **124**, 1615.
9. Mammen, M., Dahmann, G., and Whitesides, G.M. (1995) *J. Med. Chem.*, **38**, 4179.
10. Gibson, M.I., Frohlich, E., and Klok, H.A. (2009) *J. Polym. Sci., Part A: Polym. Chem.*, **47**, 4332.
11. Spain, S.G. and Cameron, N.R. (2012) *Polym. Chem.*, **2**, 60.
12. Roy, R. (1996) *Trends Glycosci. Glycotechnol.*, **8**, 79.
13. Imberty, A., Chabre, Y.M., and Roy, R. (2008) *Chem. Eur. J.*, **14**, 7490.
14. Ladmiral, V., Melia, E., and Haddleton, D.M. (2004) *Eur. Polym. J.*, **40**, 431.
15. Slavin, S., Burns, J., Haddleton, D.M., and Becer, C.R. (2011) *Eur. Polym. J.*, **47**, 435.
16. Horejsi, V., Smolek, P., and Kocourek, J. (1978) *Biochim. Biophys. Acta*, **538**, 293.
17. Spain, S.G., Gibson, M.I., and Cameron, N.R. (2007) *J. Polym. Sci., Part A: Polym. Chem.*, **45**, 2059.
18. Ambrosi, M., Batsanov, A.S., Cameron, N.R., Davis, B.G., Howard, J.A.K., and Hunter, R. (2002) *J. Chem. Soc., Perkin Trans. 1*, **1**, 45.
19. Banoub, J., Boullanger, P., and Lafont, D. (1992) *Chem. Rev.*, **92**, 1167.
20. Koenigs, W. and Knorr, E. (1901) *Chem. Ber.*, **34**, 957.
21. Albertin, L., Stenzel, M.H., Barner-Kowollik, C., Foster, L.J.R., and Davis, T.P. (2005) *Macromolecules*, **38**, 9075.
22. Narain, R. and Armes, S.P. (2003) *Biomacromolecules*, **4**, 1746.
23. Bernard, J., Hao, X., Davis, T.P., Barner-Kowollik, C., and Stenzel, M.H. (2005) *Biomacromolecules*, **7**, 232.

24. Zhu, X. and Schmidt, R.R. (2009) *Angew. Chem. Int. Ed.*, **48**, 1900.

25. Cameron, N.R., Spain, S.G., Kingham, J.A., Weck, S., Albertin, L., Barker, C.A., Battaglia, G., Smart, T., and Blanazs, A. (2008) *Faraday Discuss.*, **139**, 359.

26. Spain, S.G., Albertin, L., and Cameron, N.R. (2006) *Chem. Commun.*, 4198.

27. Smith, A.E., Sizovs, A., Grandinetti, G., Xue, L., and Reineke, T.M. (2011) *Biomacromolecules*, **12**, 3015.

28. Pearson, S., Allen, N., and Stenzel, M.H. (2009) *J. Polym. Sci., Part A: Polym. Chem.*, **47**, 1706.

29. Escale, P., Ting, S.R.S., Khoukh, A., Rubatat, L., Save, M., Stenzel, M.H., and Billon, L. (2011) *Macromolecules*, **44**, 5911.

30. Abdelkader, O., Moebs-Sanchez, S., Queneau, Y., Bernard, J., and Fleury, E. (2011) *J. Polym. Sci., Part A: Polym. Chem.*, **49**, 1309.

31. Granville, A.M., Quémener, D., Davis, T.P., Barner-Kowollik, C., and Stenzel, M.H. (2007) *Macromol. Symp.*, **255**, 81.

32. Ting, S.R.S., Min, E.H., Zetterlund, P.B., and Stenzel, M.H. (2010) *Macromolecules*, **43**, 5211.

33. Gody, G., Boullanger, P., Ladavière, C., Charreyre, M.T., and Delair, T. (2008) *Macromol. Rapid Commun.*, **29**, 511.

34. Hetzer, M., Chen, G., Barner-Kowollik, C., and Stenzel, M.H. (2010) *Macromol. Biosci.*, **10**, 119.

35. Özyürek, Z., Komber, H., Gramm, S., Schmaljohann, D., Müller, A.H.E., and Voit, B. (2007) *Macromol. Chem. Phys.*, **208**, 1035.

36. Liu, L., Zhang, J., Lv, W., Luo, Y., and Wang, X. (2010) *J. Polym. Sci., Part A: Polym. Chem.*, **48**, 3350.

37. Xiao, N.Y., Li, A.L., Liang, H., and Lu, J. (2008) *Macromolecules*, **41**, 2374.

38. Bertrand, A., Chen, S., Souharce, G.W., Ladavière, C., Fleury, E., and Bernard, J. (2011) *Macromolecules*, **44**, 3694.

39. Kato, M., Kamigaito, M., Sawamoto, M., and Higashimura, T. (1995) *Macromolecules*, **28**, 1721.

40. Kamigaito, M., Ando, T., and Sawamoto, M. (2001) *Chem. Rev.*, **101**, 3689.

41. Ouchi, M., Terashima, T., and Sawamoto, M. (2009) *Chem. Rev.*, **109**, 4963.

42. Wang, J.S. and Matyjaszewski, K. (1995) *J. Am. Chem. Soc.*, **117**, 5614.

43. Vazquez-Dorbatt, V., Tolstyka, Z.P., Chang, C.W., and Maynard, H.D. (2009) *Biomacromolecules*, **10**, 2207.

44. Narain, R. and Armes, S.P. (2003) *Macromolecules*, **36**, 4675.

45. León, O., Bordegé, V., Muñoz-Bonilla, A., Sánchez-Chaves, M., and Fernández-García, M. (2010) *J. Polym. Sci., Part A: Polym. Chem.*, **48**, 3623.

46. Ladmiral, V., Monaghan, L., Mantovani, G., and Haddleton, D.M. (2005) *Polymer*, **46**, 8536.

47. Gupta, S.S., Raja, K.S., Kaltgrad, E., Strable, E., and Finn, M.G. (2005) *Chem. Commun.*, 4315.

48. Geng, J., Lindqvist, J., Mantovani, G., Chen, G., Sayers, C.T., Clarkson, G.J., and Haddleton, D.M. (2007) *QSAR Comb. Sci.*, **26**, 1220.

49. Yang, Q. and Ulbricht, M. (2011) *Macromolecules*, **44**, 1303.

50. Manning, D.D., Hu, X., Beck, P., and Kiessling, L.L. (1997) *J. Am. Chem. Soc.*, **119**, 3161.

51. Gordon, E.J., Gestwicki, J.E., Strong, L.E., and Kiessling, L.L. (2000) *Chem. Biol.*, **7**, 9.

52. Shinde, V.S. and Pawar, V.U. (2009) *J. Appl. Polym. Sci.*, **111**, 2607.

53. Miura, Y., Koketsu, D., and Kobayashi, K. (2007) *Polym. Adv. Technol.*, **18**, 647.

54. Obata, M., Shimizu, M., Ohta, T., Matsushige, A., Iwai, K., Hirohara, S., and Tanihara, M. (2010) *Polym. Chem.*, **2**, 651.

55. Yu, L., Huang, M., Wang, P.G., and Zeng, X. (2007) *Anal. Chem.*, **79**, 8979.

56. Kolb, H.C., Finn, M.G., and Sharpless, K.B. (2001) *Angew. Chem. Int. Ed.*, **40**, 2004.

57. Kolb, H.C. and Sharpless, K.B. (2003) *Drug Discovery Today*, **8**, 1128.

58. Wang, Q., Chittaboina, S., and Barnhill, H.N. (2005) *Lett. Org. Chem.*, **2**, 293.

59. Sharpless, W.D., Wu, P., Hansen, T.V., and Lindberg, J.G. (2005) *J. Chem. Educ.*, **82**, 1833.

60. Binder, W.H. and Kluger, C. (2006) *Curr. Org. Chem.*, **10**, 1791.

61. Lutz, J.F., Borner, H.G., and Weichenhan, K. (2006) *Macromolecules*, **39**, 6376.

62. Chen, G.J., Tao, L., Mantovani, G., Geng, J., Nystrom, D., and Haddleton, D.M. (2007) *Macromolecules*, **40**, 7513.

63. Ladmiral, V., Mantovani, G., Clarkson, G.J., Cauet, S., Irwin, J.L., and Haddleton, D.M. (2006) *J. Am. Chem. Soc.*, **128**, 4823.

64. Geng, J., Lindqvist, J., Mantovani, G., and Haddleton, D.M. (2008) *Angew. Chem. Int. Ed.*, **47**, 4180.

65. Hoyle, C.E., Lowe, A.B., and Bowman, C.N. (2010) *Chem. Soc. Rev.*, **39**, 1355.

66. Kade, M.J., Burke, D.J., and Hawker, C.J. (2010) *J. Polym. Sci., Part A: Polym. Chem.*, **48**, 743.

67. Campos, L.M., Killops, K.L., Sakai, R., Paulusse, J.M.J., Damiron, D., Drockenmuller, E., Messmore, B.W., and Hawker, C.J. (2008) *Macromolecules*, **41**, 7063.

68. Killops, K.L., Campos, L.M., and Hawker, C.J. (2008) *J. Am. Chem. Soc.*, **130**, 5062.

69. Pounder, R.J., Stanford, M.J., Brooks, P., Richards, S.P., and Dove, A.P. (2008) *Chem. Commun.*, 5158.

70. ten Brummelhuis, N., Diehl, C., and Schlaad, H. (2008) *Macromolecules*, **41**, 9946.

71. Becer, C.R., Kokado, K., Weber, C., Can, A., Chujo, Y., and Schubert, U.S. (2010) *J. Polym. Sci., Part A: Polym. Chem.*, **48**, 1278.

72. Xu, J., Tao, L., Boyer, C., Lowe, A.B., and Davis, T.P. (2009) *Macromolecules*, **43**, 20.

73. Jones, M.W., Mantovani, G., Ryan, S.M., Wang, X., Brayden, D.J., and Haddleton, D.M. (2009) *Chem. Commun.*, 5272.

74. Nurmi, L., Lindqvist, J., Randev, R., Syrett, J., and Haddleton, D.M. (2009) *Chem. Commun.*, 2727.

75. Becer, C.R., Babiuch, K., Pilz, D., Hornig, S., Heinze, T., Gottschaldt, M., and Schubert, U.S. (2009) *Macromolecules*, **42**, 2387.

76. Boyer, C. and Davis, T.P. (2009) *Chem. Commun.*, 6029.

77. Semsarilar, M., Ladmiral, V., and Perrier, S.W. (2010) *Macromolecules*, **43**, 1438.

78. Xu, N., Wang, R., Du, F.S., and Li, Z.C. (2009) *J. Polym. Sci., Part A: Polym. Chem.*, **47**, 3583.

79. Gress, A., Volkel, A., and Schlaad, H. (2007) *Macromolecules*, **40**, 7928.

80. Boyer, C., Bousquet, A., Rondolo, J., Whittaker, M.R., Stenzel, M.H., and Davis, T.P. (2009) *Macromolecules*, **43**, 3775.

81. Hu, Z., Fan, X., and Zhang, G. (2010) *Carbohydr. Polym.*, **79**, 119.

82. Huisgen, R. (1968) *Angew. Chem. Int. Ed. Engl.*, **7**, 321.

83. Tornoe, C.W., Christensen, C., and Meldal, M. (2002) *J. Org. Chem.*, **67**, 3057.

84. Rostovtsev, V.V., Green, L.G., Fokin, V.V., and Sharpless, K.B. (2002) *Angew. Chem. Int. Ed.*, **41**, 2596.

85. Hein, J.E. and Fokin, V.V. (2010) *Chem. Soc. Rev.*, **39**, 1302.

86. Besenius, P., Slavin, S., Vilela, F., and Sherrington, D.C. (2008) *React. Funct. Polym.*, **68**, 1524.

87. Heuts, J.P.A. and Smeets, N.M.B. (2011) *Polym. Chem.*, **2**, 2407.

88. Li, G.Z., Randev, R.K., Soeriyadi, A.H., Rees, G., Boyer, C., Tong, Z., Davis, T.P., Becer, C.R., and Haddleton, D.M. (2010) *Polym. Chem.*, **1**, 1196.

89. Soeriyadi, A.H., Li, G.Z., Slavin, S., Jones, M.W., Amos, C.M., Becer, C.R., Whittaker, M.R., Haddleton, D.M., Boyer, C., and Davis, T.P. (2011) *Polym. Chem.*, **2**, 815.

90. Moad, G., Rizzardo, E., and Thang, S.H. (2006) *Aust. J. Chem.*, **59**, 669.

91. Moad, G., Rizzardo, E., and Thang, S.H. (2009) *Aust. J. Chem.*, **62**, 1402.

92. Moad, G. and Thang, S.H. (2009) *Aust. J. Chem.*, **62**, 1379.

93. Tao, L., Liu, J., Tan, B.H., and Davis, T.P. (2009) *Macromolecules*, **42**, 4960.

94. Luzon, M., Boyer, C., Peinado, C., Corrales, T., Whittaker, M., Tao, L., and Davis, T.P. (2010) *J. Polym. Sci., Part A: Polym. Chem.*, **48**, 2783.

95. Liu, B., Kazlauciunas, A., Guthrie, J.T., and Perrier, S. (2005) *Macromolecules*, **38**, 2131.

96. Thibault, R.J., Takizawa, K., Lowenheilm, P., Helms, B., Mynar, J.L., Fréchet, J.M.J., and Hawker, C.J. (2006) *J. Am. Chem. Soc.*, **128**, 12084.

97. Thurecht, K.J., Blakey, I., Peng, H., Squires, O., Hsu, S., Alexander, C., and Whittaker, A.K. (2010) *J. Am. Chem. Soc.*, **132**, 5336.

98. Tanaka, T., Nagai, H., Noguchi, M., Kobayashi, A., and Shoda, S.I. (2009) *Chem. Commun.*, 3378.

99. Vinson, N., Gou, Y., Becer, C.R., Haddleton, D.M., and Gibson, M.I. (2011) *Polym. Chem.*, **2**, 107.

100. Gamblin, D.P., Scanlan, E.M., and Davis, B.G. (2009) *Chem. Rev.*, **109**, 131.

101. Gauthier, M.A. and Klok, H.A. (2008) *Chem. Commun.*, 2591.

102. Bernandes, G.J.L., Gamblin, D.P., and Davis, B.G. (2006) *Angew. Chem. Int. Ed.*, **45**, 4007.

103. Pachamuthu, K. and Schmidt, R.R. (2006) *Chem. Rev.*, **106**, 160.

104. Kumar, R., Tiwari, P., Maulik, P.R., and Misra, A.K. (2006) *Eur. J. Org. Chem.*, 74.

105. Fulton, D.A. and Stoddart, J.F. (2001) *J. Org. Chem.*, **66**, 8309.

106. You, L. and Schlaad, H. (2006) *J. Am. Chem. Soc.*, **128**, 13336.

107. Gress, A., Välkel, A., and Schlaad, H. (2007) *Macromolecules*, **40**, 7928.

108. Chen, G., Amajjahe, S., and Stenzel, M.H. (2009) *Chem. Commun.*, 1198.

109. Hawker, C.J., Bosman, A.W., and Harth, E. (2001) *Chem. Rev.*, **101**, 3661.

110. Becer, C.R., Hoogenboom, R., and Schubert, U.S. (2009) *Angew. Chem. Int. Ed.*, **48**, 4900.

111. Boyer, C., Bousquet, A., Rondolo, J., Whittaker, M.R., Stenzel, M.H., and Davis, T.P. (2010) *Macromolecules*, **43**, 3775.

112. Dondoni, A. and Marra, A. (2012) *Chem. Soc. Rev.*, **41**, 573.

113. Fischer, E.H. (1893) *Chem. Ber.*, **26**, 2400.

114. Gibson, M.I. and Cameron, N.R. (2009) *J. Polym. Sci., Part A: Polym. Chem.*, **47**, 2882.

115. Deming, T.J. (1997) *Nature*, **390**, 386.

116. Alferis, T., Iatrou, H., and Hadkichristidis, N. (2004) *Biomacromolecules*, **5**, 1653.

117. Gibson, M.I., Hunt, G.J., and Cameron, N.R. (2007) *Org. Biomol. Chem.*, **5**, 2756.

118. Kramer, J.R. and Deming, T.J. (2010) *J. Am. Chem. Soc.*, **132**, 15068.

119. Sun, J. and Schlaad, H. (2010) *Macromolecules*, **43**, 4445.

120. Huang, J., Habraken, G., Audouin, F., and Heise, A. (2010) *Macromolecules*, **43**, 6050.

121. Ning, X., Rui, W., Fu-Sheng, D., and Zi-Chen, L. (2009) *J. Polym. Sci., Part A: Polym. Chem.*, **47**, 3583.

11
Design of Polyvalent Polymer Therapeutics

Jacob T. Martin and Ravi S. Kane

11.1
Introduction

Polymer scientists admire living systems for the precise control over macromolecular structure and function that they exhibit. Biomacromolecules such as proteins and nucleic acids are naturally synthesized to be monodisperse and to contain a specific sequence of multiple different monomers. Using various combinations of a limited assortment of monomers, they can exhibit an immensely wide variety of defined structures and functions, including catalysis and recognition. Furthermore, they are often precisely modified post-polymerization, leading to designed changes in secondary, tertiary, and quaternary structures that fine-tune the exact function of the biopolymer for the specific living requirements. On the other hand, these elegant features can be sensitive to environmental damage coming from temperature, pH, oxidation, and degradation by other biomolecules. Furthermore, the use of biomolecules in therapeutic applications is often hampered by pharmacological issues such as low solubility, short residence time in the body, and the propensity to elicit an undesired immune response.

When designing any therapeutic, it is important to minimize the propensity for unplanned function, or "side effects," because these could be detrimental in ways that could override any designed therapeutic benefit. Accordingly, maximizing the specificity of a therapeutic for a target is the primary goal. In living systems, this is often achieved through polyvalency [1]. Polyvalency is characterized by the use of an arrangement of multiple binding elements (various biomolecules) to enhance the binding of one entire (often biological) entity to another. Relative to the binding strength of an individual ligand–receptor pair (a monovalent interaction), the corresponding polyvalent interaction is frequently many orders of magnitude stronger [1, 2], and there have been a multitude of reviews in the past 15 years highlighting the potential benefits of utilizing polyvalency [1, 3–10]. However, the value of polyvalency is not merely in the enhancement of binding strength, as it can also play a role in a wide variety of biological interactions. For example, polyvalent interactions can affect biological signaling [1, 7, 11] by establishing scaled interactions, by creating combinations of biological interactions,

and by maintaining contact between two surfaces over a large area. In addition, polyvalency can be used to inhibit undesired interactions such as viral attachment to cells [12–18] and bacterial toxin assembly [19–32]. Many of or all these kinds of interactions have therapeutic implications, and there has been growing interest in implementing polyvalency for therapeutic purposes [8–10].

Some of the structures that have been used to support polyvalent displays include nanoparticles, often gold or iron oxide, and derivatives of naturally occurring constructs, such as viral particles and liposomes. However, synthetic polymers have advantages, in that they can be used in a broad range of structures (scaffolds) to manipulate the presentation of biomolecules, and the details of the presentation can be sequentially modified, thus resulting in the optimization of activity through polyvalency. The synthetic polymer can also introduce new properties, such as self-assembly and phase behavior, and sometimes can even be used to improve biomolecule stability, solubility, and biocompatibility. There are a multitude of good reviews on the synthesis of such polymer conjugates [33–42], but the main strategies relevant for synthesis of *polyvalent* polymer therapeutics are ''grafting through'' and ''grafting to.'' The ''grafting-through'' strategy involves the polymerization of monomers that have been preconjugated with the desired ligand, which can yield polymers that display a high density of ligands along the polymer backbone. However, this strategy has several disadvantages. Lack of reaction modularity and lack of reproducibility are the major disadvantages of this strategy that arise from the need to tune the reaction conditions of each polymerization and the difficulty in handling and accurately measuring the minuscule quantities of precious modified biomolecule ligands, respectively. Furthermore, the difficulties involved in characterization and analysis of qualities, such as polydispersity and ligand composition, can hinder the optimization of the product polyvalent presentation. In contrast, the ''grafting-to'' strategy involves the attachment of ligands to the polymer scaffold post-polymerization. By using controlled polymerization and traditional polymer characterization techniques to reveal accurate descriptors of the pieces involved before conjugation, the resulting product analysis is much easier. That information can then be used in turn to guide subsequent polyvalent designs, which can often be synthesized without modification of reaction conditions.

11.2
Polyvalent Polymer Therapeutics

One of the first examples of a polymeric polyvalent inhibitor that was effective *in vivo* was the anthrax toxin inhibitor reported by Mourez *et al.* [22]. The polyvalent polymer therapeutic inhibited the assembly of anthrax toxin, which is composed of nontoxic monomeric proteins called protective antigen (PA), lethal factor (LF), and edema factor (EF), which assemble into toxic complexes after being released by the bacteria [43–45]. The receptor binding protein PA is cleaved by a cell surface protease into a 63 kDa fragment (PA_{63}), which subsequently forms a heptamer ($[PA_{63}]_7$) [46]. The heptamer binds and transports LF and EF into the host cell cytosol,

where they exhibit their cytotoxic functions [47, 48]. The researchers used phage display to identify a peptide sequence (HTSTYWWLDGAP) that binds the $[PA_{63}]_7$ heptamer and inhibits toxin assembly with a half-maximal inhibitory concentration (IC_{50}) of 150 µM (i.e. weakly). Multiple copies of a modified peptide containing the $[PA_{63}]_7$ binding sequence and a C-terminal lysine, Ac-HTSTYWWLDGAPK-Am, were attached pendant to a polyacrylamide polymer backbone. The polyvalent conjugation was performed by reacting poly(*N*-acryloyloxysuccinimide) (pNAS), an activated ester form of polyacrylic acid (pAA), with the amine-functionalized peptide ligand. This protocol was based on previous reports [1, 14–16] on the synthesis of polyvalent displays of sialic acid along polyacrylamide backbones. The polyvalent anthrax toxin inhibitor thus created was 7500-fold more potent than the monovalent peptide at inhibiting anthrax toxin complex formation *in vitro*, on a per-peptide basis. Furthermore, the polyvalent inhibitor was shown to have *in vivo* efficacy, preventing symptoms in a rat intoxication model.

The successful inhibition of the toxin *in vivo* demonstrated that the therapeutic design strategy was sound. The study by Mourez *et al.* [22] showed that it is possible to construct a therapeutically effective conjugate from weakly binding, previously unknown ligands without extensive modification or optimization. Ligands that have been screened from a random library for a desired target molecule can be made significantly more efficacious by polyvalent display on a suitable scaffold. Our group has placed a particular emphasis on controlling the architecture of polyvalent scaffolds in order to better understand the influence of the design parameters on the efficacy of polyvalent therapeutics. Here, we primarily highlight our studies on polymer-based scaffolds. Specifically, we discuss designing self-assembling polymeric micelles for use as polyvalent therapeutics [49, 50], controlling the molecular weight and pendant ligand spacing for linear polymeric scaffolds [27, 51, 52] and matching the architecture of the scaffold to that of the target [53]. We also include some discussion on the use of polypeptide-based scaffolds [28], both in the context of synthetic polymers and with scaffolds designed by protein engineering methods. While there have been many studies on the structure–activity relationships of potential polyvalent therapeutics (see [54, 55], and [56–59] for more general reviews of polymer therapeutics), this chapter focuses primarily on our own group's work toward developing polyvalent inhibitors of anthrax toxin, as well as providing a few examples of other works which are likely to be important for the future of this field.

11.2.1
Polymer Micelles

Micelles are useful in therapeutic applications due to their ease of preparation, their ability to store molecules, and the ability to include functional molecules on their surface. Micelles created from amphiphilic block copolymers often exhibit greater stability and have lower critical micellar concentrations relative to analogous micelles formed from low-molecular-weight surfactants, making them good candidates for therapeutics (Scheme 11.1).
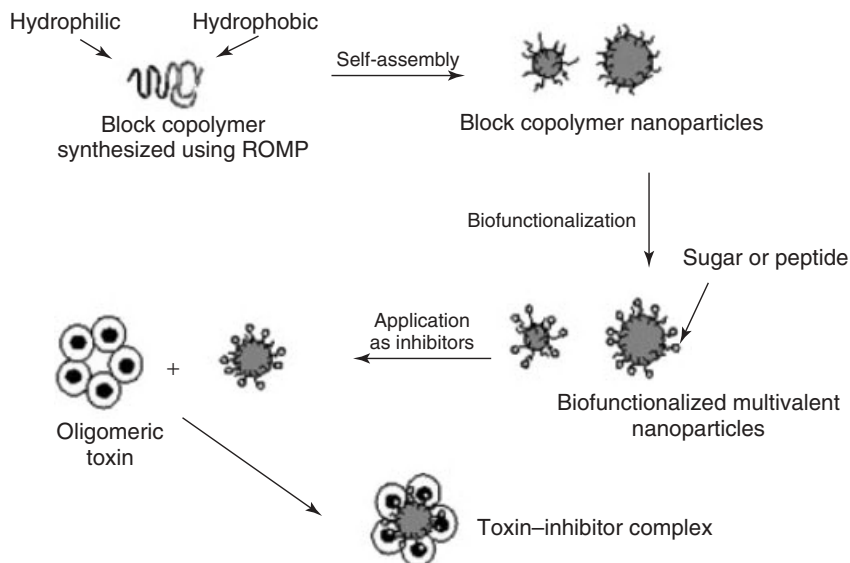
Scheme 11.1 Schematic representation of the block copolymer nanoparticle-based approach to the synthesis of multivalent ligands. (Source: Reprinted with permission from [50]. Copyright 2006 Wiley Periodicals, Inc.)

Carrillo and Kane [49] demonstrated the preparation of self-assembling polymer micelles of controlled size by ring-opening metathesis polymerization (ROMP) to synthesize an amphiphilic block copolymer. The living polymerization technique, depicted in Scheme 11.2, first allowed for the synthesis of a hydrophobic homopolymer with good control over the degree of polymerization (DP) by varying the ratio of monomer to initiator (Figure 11.1). The second stage of polymerization, in tetrahydrofuran (THF), added a hydrophilic block to the end of the hydrophobic block. The block copolymers then self-assembled in an aqueous solvent such that the hydrophobic block was contained within the hydrophilic exterior, and the hydrodynamic radii of the resulting micelles were dependent on the DP of the various block copolymer samples [49]. Being on the exterior, the hydrophilic block could also be potentially conjugated with a polyvalent display of ligands via the repeating carboxyl functionality. For example, in a related study, Carrillo *et al.* [50] used a similar copolymerization strategy to attach blocks of activated NHS (*N*-hydroxysuccinimide) esters to the hydrophobic core. The activated esters were then reacted with oligo(ethylene glycol) chains, as shown in Scheme 11.3. Chloroacetylation of the ends of these short ethylene glycol branches rendered them thiol-reactive, and dihydroxylation of the carbon–carbon double bonds along the backbone of that block increased its hydrophilicity. After these modifications, and assembly of the copolymer into micelles, the peptide ligand of anthrax [PA$_{63}$]$_7$, was conjugated via a thiol (the C-terminal Lys of the Ac-HTSTYWWLDGAPK-Am peptide was replaced with cysteine to impart thiol functionality). The presence of the peptide on the nanoparticle surface (as opposed to the interior) was confirmed
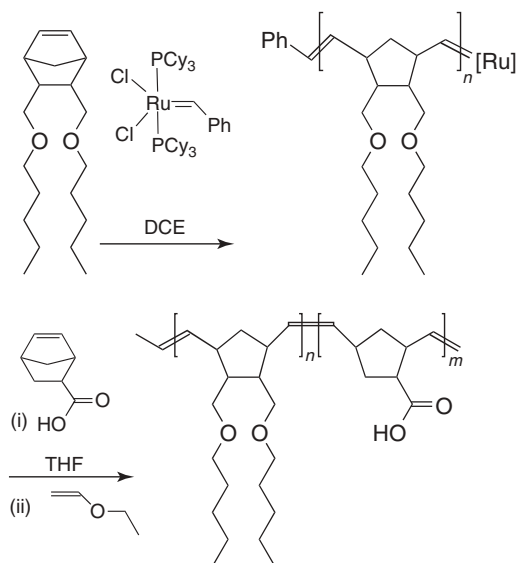
Scheme 11.2 Procedure used for the synthesis of hydrophobic homopolymers and amphiphilic diblock copolymers. (Source: Reprinted with permission from [49]. Copyright 2004 Wiley Periodicals, Inc.)
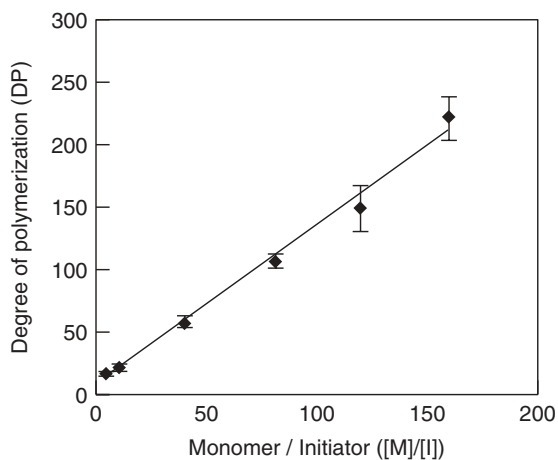
Figure 11.1 Plot of degree of polymerization (DP), as measured by gel permeation chromatography (GPC), versus [M]/[I] ratios for homopolymer. (Source: Reprinted with permission from [49]. Copyright 2004 Wiley Periodicals, Inc.)
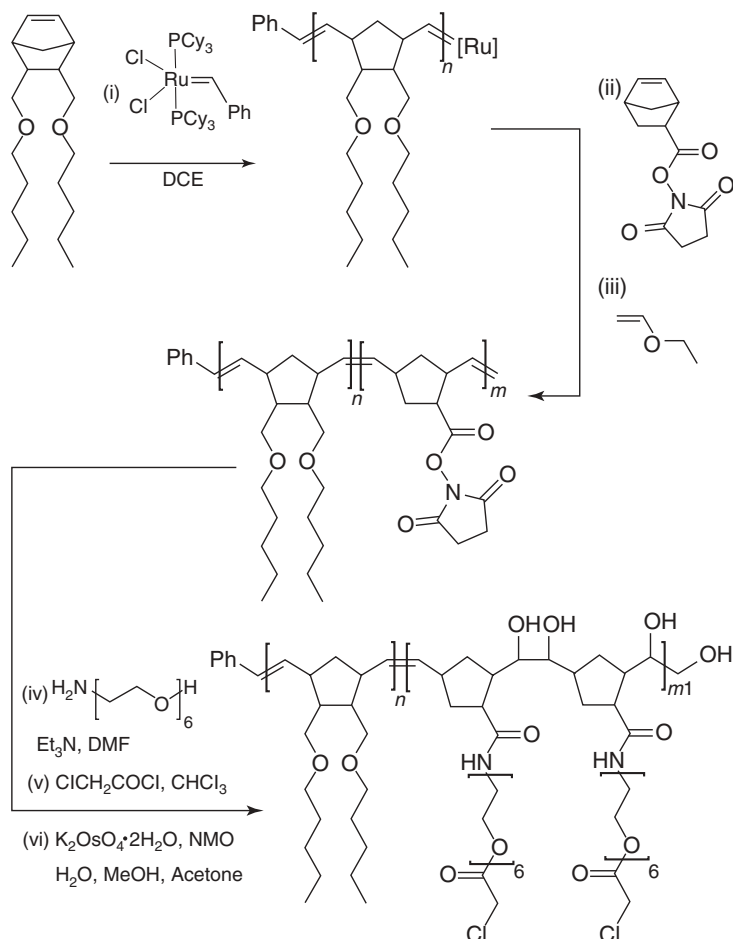
Scheme 11.3 Procedure used for the synthesis of amphiphilic, thiol-reactive block copolymers: (i) ROMP of the hydrophobic block with Grubbs' catalyst, (ii) polymerization of the second block, (iii) termination of the polymerization with an excess of ethyl vinyl ether, (iv) coupling of hexaethylene glycol side chains to the second block, (v) chloroacetylation of terminal hydroxyl group on hexaethylene glycol chains, and (vi) dihydroxylation of the double bonds along the polymer backbone. (Source: Reprinted with permission from [50]. Copyright 2006 Wiley Periodicals, Inc.)

via observation of the fluorescence emission spectrum (Figure 11.2). The peak at a wavelength of 350 nm confirmed the presence of water-solvated tryptophan, suggesting that the peptide ligand was accessible on the surface in a polyvalent display. Considering that liposomes exhibiting comparable polyvalent displays of the same ligand have shown significant efficacy as anthrax toxin inhibitors [26, 30, 32, 60], the preparation of these polymeric micelles and the post-polymerization modifications demonstrated on them should represent a sound strategy for crafting polymeric nanoparticles with potential therapeutic applications.
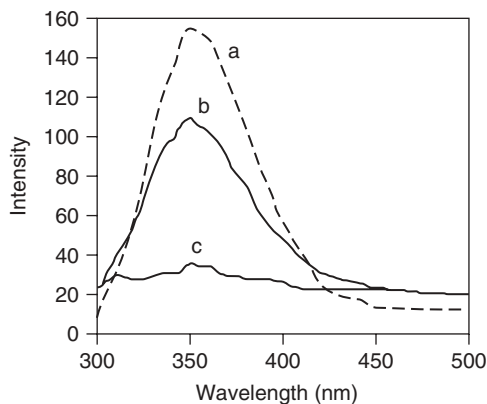
Figure 11.2 Fluorescence emission spectra for (a) an aqueous solution of peptide Ac-HTSTYWWLDGAPC-Am, (b) peptide-functionalized block copolymer nanoparticles, and (c) a control (thioglycerol-functionalized nanoparticles). (Source: Reprinted with permission from [50]. Copyright 2006 Wiley Periodicals, Inc.)

11.2.2
Controlled-Molecular-Weight Linear Polymers

While polymeric micelles and polymersomes are good candidates for therapeutic delivery applications, in the interest of investigating the role of the geometry of a polyvalent display (such as the arrangement and spacing between ligands) on its efficacy, we pursued linear polymer modification. For all types of linear polymer therapeutics (including end-functional, side-chain-functional linear polymers, or branched (brush) polymers), the molecular weight of the polymer backbone is one of the primary variables in the scaffold design. When using presynthesized polymers or controlled polymerization techniques for custom synthesis, the molecular weight, the DP, and the polydispersity index (PDI) are measures of how well-defined the polymer sample is. These factors affect the hydrodynamic radius and therapeutically relevant qualities such as the enhanced permeation and retention (EPR) effect in tumors, other pharmacokinetic and biodistribution effects, and biodegradability or toxicity. In the context of polyvalent therapeutic design, the molecular weight of a polymer scaffold is particularly important for determining the potential valency and density of a conjugated ligand. Moreover, with greater precision over DP and PDI, the degree of uncertainty in conjugate characterization can be reduced so that structure–activity relationships and optimized therapeutic properties can be elucidated with greater confidence. For these reasons, we [27, 51] and others [16, 61] have investigated the effects of scaffold molecular weight on post-polymerization functional polymers by minimizing the effects of PDI.

The work by Gujraty *et al.* [27] took advantage of the fact that poly(tert-butyl acrylate) (pTBA) was commercially available in a range of molecular weights (e.g., 28.4, 69, 100, and 150 kDa) with low PDIs (ranging from 1.03 to 1.2). For each sample, the pTBA was hydrolyzed in acid to make pAA, which was subsequently treated
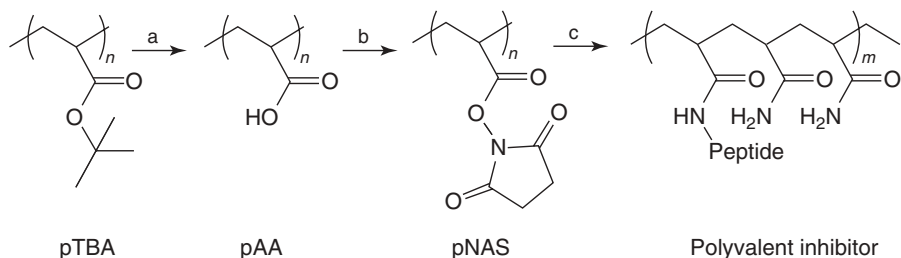
Scheme 11.4 Synthesis of a polyvalent inhibitor (PVI) of controlled molecular weight. (a) TFA/CH$_2$Cl$_2$ (trifluoroacetic acid). (b) N,N'-Carbonyldiimidazole, N-hydroxysuccinimide, and pyridine, 110 °C. (c) (i) peptide, dimethylformamide (DMF) and (ii) NH$_4$OH. (Source: Reprinted with permission from [27]. Copyright 2006 American Chemical Society.)
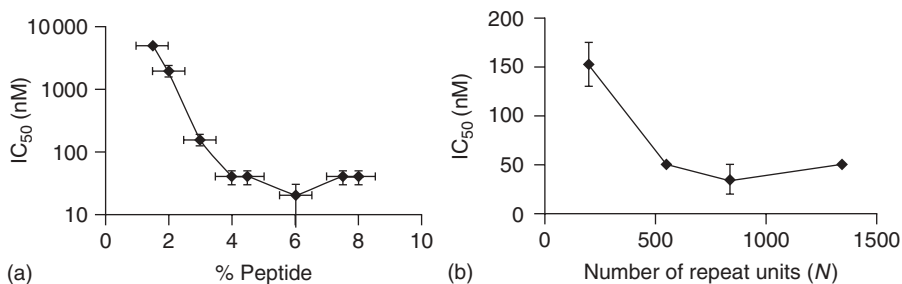
Figure 11.3 (a) Influence of peptide density on the potency of a polyvalent anthrax toxin inhibitor. Number of monomer repeat units in the backbone, N, about 200. (b) Influence of number of monomer repeat units on the inhibitory potency (peptide density, about 3%). IC$_{50}$ values are reported on a per-peptide basis. (Source: Reprinted with permission from [27]. Copyright 2006 American Chemical Society.)

with N,N'-carbonyldiimidazole followed by NHS to produce pNAS (Scheme 11.4). The resulting polymer contained the same activated esters and polymer backbone that were used to make the anthrax toxin inhibitor reported by Mourez *et al.* [22], except that in this case, the starting materials had molecular weights that were more well defined, leading to products that could be compared with greater confidence. This characteristic of the resulting activated polymers was exploited to compare the efficacies of a range of polyvalent inhibitors that varied in both the density of the conjugated ligands on the backbone and the backbone molecular weight. The results (Figure 11.3) revealed that for polyvalent inhibitors prepared from the same size backbone and various degrees of ligand conjugation, there existed a ligand coupling percentage corresponding to a peak in potency and that higher ligand density led to a plateau in potency (Figure 11.3a). Furthermore, a similar pattern was observed when comparing a range of backbone sizes for a specified ligand density. That is, potency increased with increasing backbone length up to a point, beyond which the potency stabilized (Figure 11.3b). For this set, the increase in backbone length at constant peptide density basically meant there was a greater number of ligands
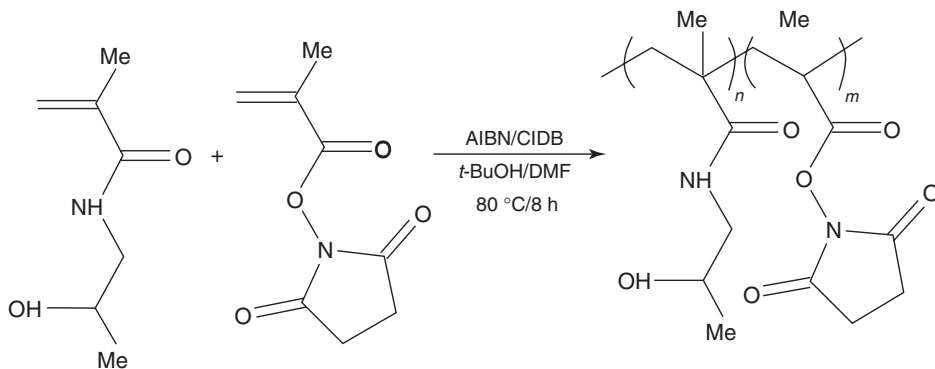
Scheme 11.5 Copolymerization of HPMA and NMS by RAFT. The product is a random copolymer. (Source: Reprinted with permission from [51]. Copyright 2006 American Chemical Society.)

per chain on average but that the average spacing between ligands along the chain was the same. These results showed that although polyvalency can provide orders of magnitude enhancements of potency over monovalent ligands, beyond a certain point, increasing the valency may not correlate with further increases in potency.

While the use of commercially available pTBA allowed for the synthesis of low-PDI homopolymers of pNAS, an alternative approach by Yanjarappa *et al.* [51] relied on the controlled polymerization techniques known as reversible addition-fragmentation chain transfer (RAFT) polymerization to create an activated polymer backbone with controlled molecular weight. In this case, the reaction was a copolymerization between the monomers *N*-methacryloyloxysuccinimide (NMS) and *N*-(2-hydroxypropyl)methacrylamide (HPMA), with 2-cyanoisopropyl dithiobenzoate as the chain transfer agent (CTA) and azobisisobutyronitrile (AIBN) as the radical initiator (Scheme 11.5). HPMA was used as a monomer because it is biocompatible and forms nontoxic, nonimmunogenic polymers. Polymers of HPMA have been used in several studies related to drug delivery and gene delivery [62, 63], but in most of these cases, the polymer was synthesized via free radical polymerization and thus had a broad molecular weight distribution. In contrast, RAFT is a controlled, living polymerization technique, and it was used in this study to synthesize an activated copolymer as a route toward an HPMA-based therapeutic. Owing to the higher reactivity of the NMS relative to the HPMA and the desire to create a copolymer in which the compositional ratio remained consistent throughout each polymer chain, a semibatch reaction was used. NMS was added gradually throughout the first 6 h, and the concentrations of NMS and HPMA were monitored by sampling over a period of 8 h (Figure 11.4). Characterization of the resulting heteropolymers by ^{1}H NMR spectroscopy and size exclusion chromatography (SEC) confirmed the ability to control the composition (Figure 11.5) and size (Figure 11.6) of the polymer chains. Furthermore, the activated esters of the NMS monomers enabled polymer biofunctionalization by further reaction with the Ac-HTSTYWWLDGAPK-Am peptide in DMSO. The conjugation reaction yielded
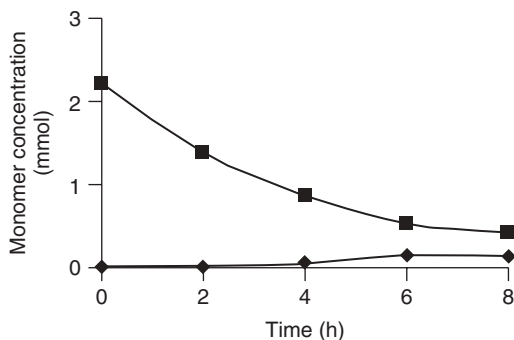
Figure 11.4 Kinetics of semibatch copolymerization of HPMA and NMS ([M]/[CTA] = 320). NMS was continuously added over a period of 6 h. The concentrations of HPMA (squares) and NMS (diamonds) in the Schlenk tube were monitored over a period of 8 h. (Source: Reprinted with permission [51]. Copyright 2006 American Chemical Society.)
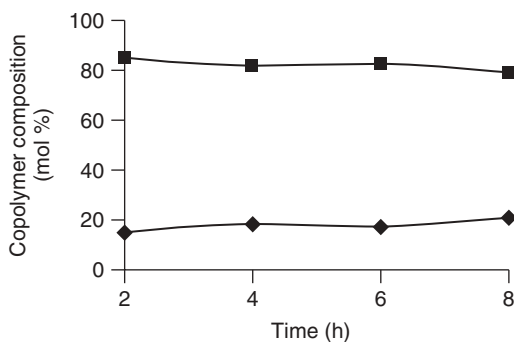
Figure 11.5 Variation in copolymer composition with time. The mole percentage of HPMA (squares) and NMS (diamonds) was determined by ^{1}H NMR spectroscopy at periodic intervals. (Source: Reprinted with permission from [51]. Copyright 2006 American Chemical Society.)

a polyvalent inhibitor that protected RAW264.7 cells from the anthrax lethal toxin with an inhibition IC_{50} of 150 nM on a per-peptide basis. This work demonstrated not only the potential for using RAFT to create activated copolymers of controlled molecular weight and PDI but also that various polymer backbones are generally effective for use in polyvalent therapeutics.

11.2.3
Controlled Ligand Spacing

Well-defined polymer scaffolds with low PDI were needed to accurately characterize the polyvalent inhibitors described in the previous section. The studies used homo- and heteropolymers containing activated esters to draw conclusions on the effects of ligand density and polymer backbone length on polyvalent potency. However,
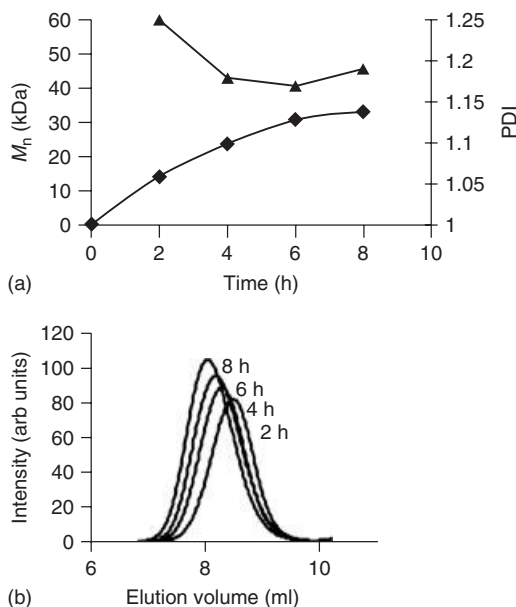
Figure 11.6 Characterization of polymers at various time intervals during semibatch RAFT copolymerization. Samples were removed at periodic intervals, converted to pHPMA by aminolysis, and characterized by SEC. (a) Variation of M_n (diamonds) and PDI (triangles) with time. (b) SEC traces of pHPMA at 2, 4, 6, and 8 h. (Source: Reprinted with permission from [51]. Copyright 2006 American Chemical Society.)

owing to the nature of the subsequent ligand-grafting reactions, irrespective of backbone homo- or heterogeneity, the grafted ligands on all the inhibitors were randomly distributed along the portions of the scaffold that had been preactivated. While statistical interpretations of the characterization data could lead to deductions about valency and interligand spacing on average, it was hypothesized that more precise control over the placement of the activated monomers would help to gain an even more comprehensive understanding of the relationship between structure and activity in polyvalent systems. With this goal in mind, the semibatch RAFT polymerization approach described previously was modified to construct polymers with defined spacing between reactive monomers [52].

The first step was to determine the distances between ligands that are likely to provide a reasonable range of activity in the designed polyvalent inhibitor. To solve this problem, a range of homopolymers of NAS with low PDIs were prepared by RAFT. The samples differed in their DP as determined by SEC (Table 11.1). The Ac-HTSTYWWLDGAPK-Am peptide was conjugated with each polymer sample such that the number of copies of the ligand that were attached was controlled, and the remainder of the activated esters along the polymer backbone were "quenched" by reaction with ammonium hydroxide. An average of three copies of the peptide were conjugated to each individual polymer chain (as determined by ^{1}H NMR spectroscopy), but due

Table 11.1 Polymerization of NAS at various [M]/[CTA] ratios.[a]

Run no.	[M]/[CTA]	[CTA]/[Initiator]	Polymerization time (h)	Conversion[b] (mol%)	DP theoretical[c]	ASEC results[d]			
						M_n (kDa)	M_w (kDa)	PD	DP[e]
1	100	10	1.5	77	77	5.97	6.27	1.05	84
2	200	10	2.0	60	120	8.96	9.85	1.10	126
3	300	5	2.5	48	144	1.12	1.28	1.14	158
4	400	5	3.5	48	192	1.45	1.62	1.12	204

[a]Polymerization conditions: NAS (1.34 g) in DMF (4 ml, 2 M solution), temperature = 70°C.
[b]NAS conversion determined by ^{1}H NMR.
[c]Determined based on conversion.
[d]Determined by aqueous size exclusion chromatography (ASEC) after ammonolysis.
[e]Calculated based on M_n.
Source: Reprinted with permission from [52]. Copyright 2008 Wiley Periodicals, Inc.

to the differences in the backbone chain length of each sample, it was inferred that the resulting polyvalent inhibitors would have different averages for the number of unconjugated monomers separating each attached peptide. As illustrated in Figure 11.7, the difference in ligand spacing could conceivably lead to a measurable variation in sample efficacy. Indeed, for the inhibitor sample with DP = 120, the inhibition IC_{50} of the binding of LF to $[PA_{63}]_7$ was over an order of magnitude lower than the IC_{50} of the polyvalent inhibitor with DP = 80 (Figure 11.8a). Furthermore, as shown in Figure 11.8b, the polyvalent inhibitor with DP = 120 was able to inhibit the cytotoxicity of anthrax lethal toxin on RAW264.7 cells *in vitro* with an IC_{50} of 36 nM, yet the inhibitor with DP = 80 was unable to inhibit cytotoxicity even at

(a) (b)
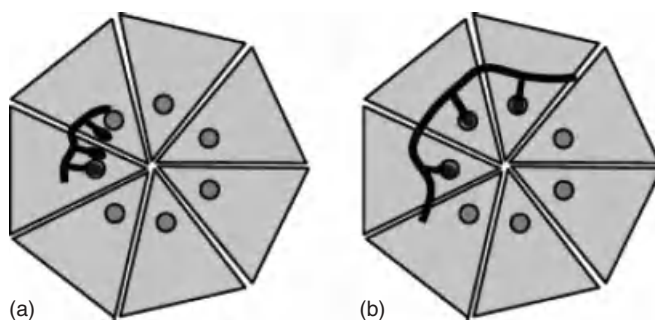
Figure 11.7 Design of polyvalent inhibitors with control over molecular weight and ligand spacing. The linear polyvalent inhibitors displaying peptides (black ovals) are shown bound to the PA_{63} heptamer at the peptide binding sites (circles). The spacing between peptides on the linear scaffold is either too short (a) or sufficient (b) to allow a polyvalent interaction. (Source: Reprinted with permission from [52]. Copyright 2008 Wiley Periodicals, Inc.)
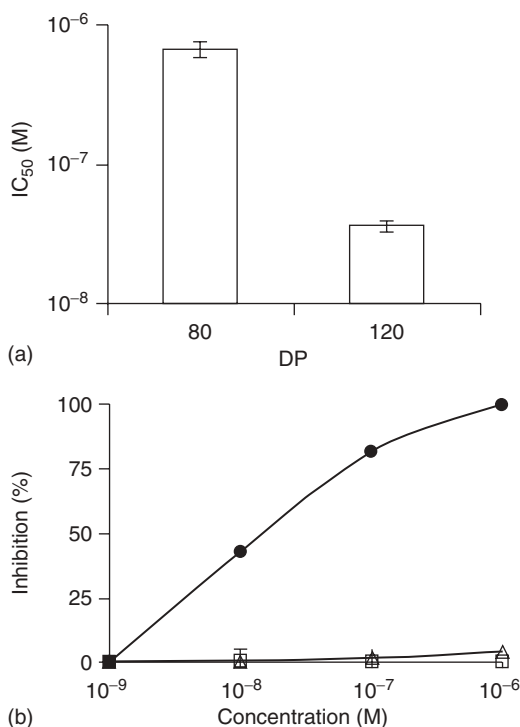
Figure 11.8 Inhibitory activity of polyvalent inhibitors of anthrax toxin derived from controlled molecular weight homopolymer, pNAS. (a) Inhibition of the binding of the anthrax lethal factor. (b) Inhibition of toxin-induced cytotoxicity at various concentrations of polymeric inhibitors with DP = 80 (open squares) and DP = 120 (filled circles). Control polymer (polyacrylamide) did not show any inhibitory activity at the concentrations tested (open triangles). (Source: Reprinted with permission from [52]. Copyright 2008 Wiley Periodicals, Inc.)

concentrations as high as 1 μM on a per-peptide basis. With these results in hand, it was possible to design the polymers with controlled spacing between reactive monomers so that the spacing matched that of the average spacing achieved by the homopolymer conjugation protocol. For a polyvalent inhibitor with a number of peptides "i" conjugated randomly along the polymer backbone, the average spacing between adjacent conjugated peptides was calculated by $DP/(i+1)$. Accordingly, for the polyvalent inhibitor with DP = 120 and $i = 3$, the average number of monomers of separation was estimated to be roughly 30. This spacing thus served as the target number of nonactive acrylamide (AAm) monomers to incorporate between reactive NAS monomers in a controlled RAFT polymerization of a heteropolymer, poly(AAm-*co*-NAS).

After analysis of the homopolymers was complete, the procedure that was used to synthesize controlled heteropolymers of NMS and HPMA [51] was adapted for the purpose of creating a specific arrangement of reactive NAS monomers

within a low-PDI poly(AAm) scaffold. Exploiting the knowledge of the rate of homopolymerization of AAm and the fact that the NAS monomers have much faster reaction kinetics of attachment to the growing polymer chain during RAFT than the AAm monomers, small injections of NAS were made at calculated time points during the RAFT polymerization of AAm. As can be seen in Figure 11.9a, the NAS was added to the reaction 90, 126, and 162 min into the polymerization in order to generate a spacing of about 31 AAm monomers between each pair of NAS monomers. In a second sample (Figure 11.9b), the time interval between successive additions of NAS was shorter, leading to a spacing of about 18 AAm monomers. Using the reactive NAS monomers to conjugate the amine-functional Ac-HTSTYWWLDGAPK-Am peptide, polyvalent inhibitors with controlled ligand spacing were created. The effect of this controlled ligand display on inhibitor performance is shown in Figure 11.9c; in the *in vitro* cytotoxicity assay, the polyvalent inhibitor with about 31 AAm monomers between peptide ligands exhibited an IC_{50} that outperformed the inhibitor with a spacing of about 18 AAm monomers by 2 orders of magnitude.

The polyvalent inhibitor with increased space between ligands presumably had better performance because of a combination of the following attributes: more adequate matching of the distance between the ligands along the polymer backbone and the distance between binding sites on $[PA_{63}]_7$ (as illustrated in Figure 11.7) and increased steric blocking of LF from binding $[PA_{63}]_7$ due to increased polymer presence at the heptamer surface. Although the steric stabilization of surfaces bound by a polyvalent inhibitor is expected to play a role in the inhibition of biological interactions [15], factors that enhance the binding strength of the inhibitor account for the majority of the inhibitor's efficacy [1]. Thus, it is desirable to adjust the architecture of the polyvalent inhibitors such that the complementarity to the target's binding epitopes is maximized. As an additional example, the target of the anthrax toxin inhibitors described thus far has been $[PA_{63}]_7$, a heptameric protein oligomer with seven binding sites for the peptide ligand containing the sequence HTSTYWWLDGAP. For the polyvalent inhibitors of varying controlled molecular weights that were prepared by modifying pTBA, the sample that displayed the greatest inhibitory activity was the one that had an average of 6 ± 2 peptide ligands per polymer chain [27], which means the valency of the inhibitor and the target was nearly matched.

11.2.4
Matching Valency to the Target

Inspired by the efforts of several other groups to design oligovalent inhibitors with architectures that matched the geometry of binding epitopes on various bacterial toxins [19, 20, 24, 25, 64, 65], our group investigated the construction of an anthrax toxin inhibitor by modifying a β-cyclodextrin (βCD) scaffold with the $[PA_{63}]_7$ binding peptide [53]. Cyclodextrins are cyclic oligomers of glucopyranose [66] that have a defined molecular weight and a given symmetry, and they are commercially available in a highly pure form. βCD, with its sevenfold symmetry,
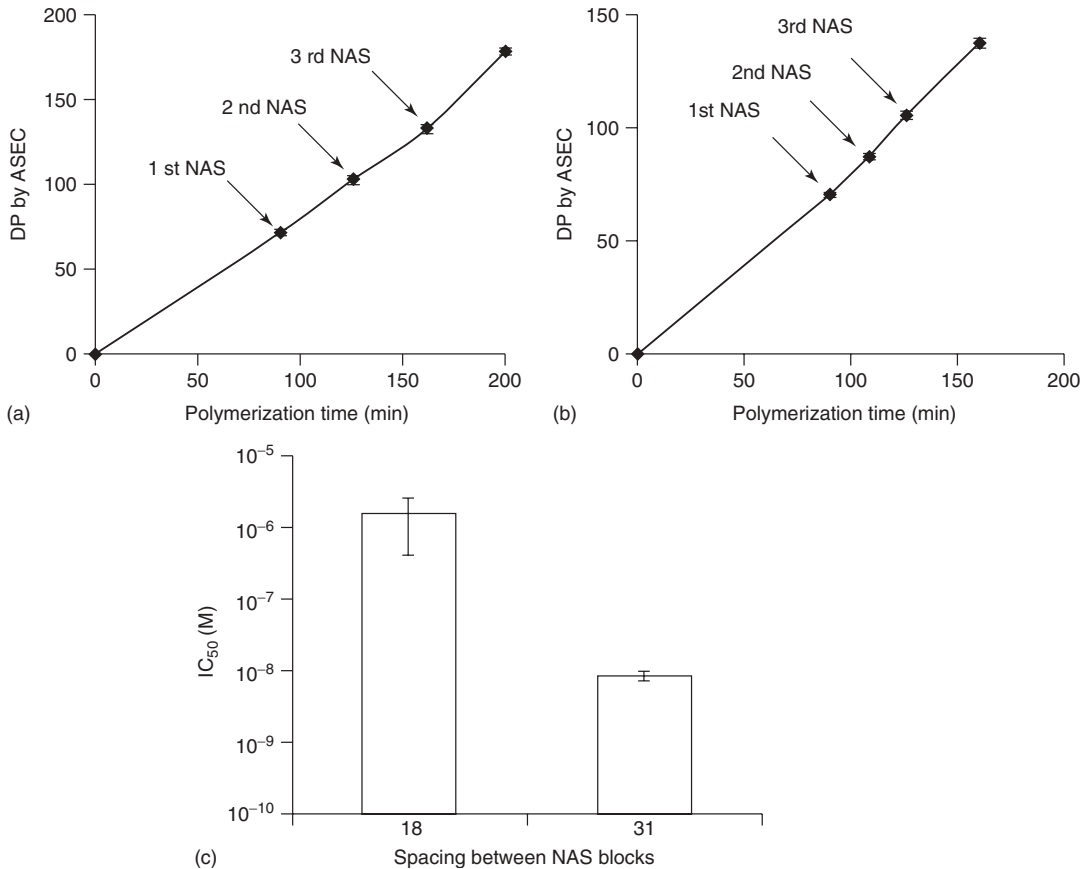
Figure 11.9 Characterization of polyvalent inhibitors based on poly(AAm-*co*-NAS) copolymers. Characterization of molecular weight during semibatch RAFT copolymerization of polymers with an average spacing of (a) 31 and (b) 18 units between adjacent blocks. (c) The inhibitory activity of the resulting peptide-functionalized polyvalent inhibitors in a cytotoxicity assay. (Source: Reprinted with permission from [52]. Copyright 2008 Wiley Periodicals, Inc.)

(a)   (b)   (c)

= Linker
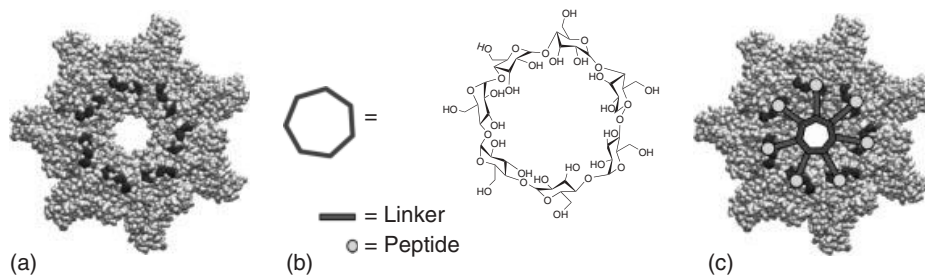
= Peptide

Figure 11.10 Structure-based design of heptavalent anthrax toxin inhibitors. (a) Structure of the LF-binding face of $[PA_{63}]_7$. Residues 184, 187, 197, and 200, which form part of the peptide binding site, are shown in dark gray. (b) Structure of the core, β-cyclodextrin. (c) Binding to $[PA_{63}]_7$ of a heptavalent inhibitor synthesized by the attachment of seven inhibitory peptides to the β-cyclodextrin core via an appropriate polyethylene glycol linker. (Source: Reprinted with permission from [53]. Copyright 2011 American Chemical Society.)

was thus much more conducive to creating a heptavalent inhibitor than using a controlled polymerization approach like the one described in the previous section. As shown in Figure 11.10, the design involved connecting the peptide Ac-HTSTYWWLDGAPC-Am to the βCD scaffold via bifunctional poly(ethylene glycol) (PEG) linkers in a hub-and-spoke geometry. It was hypothesized that a well-designed βCD inhibitor would span the pore of the $[PA_{63}]_7$ heptamer, with PEG linkers of sufficient length to allow all seven of the peptide ligands to bind simultaneously and to block the binding of LF and EF. In order to synthesize such an inhibitor, the βCD scaffold was first modified so that the secondary hydroxyls were methylated and the primary hydroxyls were propargylated, as depicted in Scheme 11.6. A range of inhibitor sizes were prepared using various lengths of bifunctional azido-PEG-amine or azido-PEG-hydroxyl linkers. Chloroacetylation of the terminal amine/hydroxyl on the PEG linker allowed for subsequent conjugation with the peptide ligand via the thiol of the cysteine at the C-terminus. This resulted in the formation of heptavalent inhibitors that were able to inhibit anthrax toxin in a RAW264.7 cell cytotoxicity assay differentially depending on the linker length, as shown in Figure 11.11. The inhibitors with the shortest PEG linkers, corresponding to dimers, trimers, and hexamers of ethylene glycol, showed no measurable activity, presumably because the linkers were not long enough to allow the inhibitors to span all the $[PA_{63}]_7$ binding sites. For the inhibitor composed of linkers with eight ethylene glycol repeats, some measurable inhibition of cytotoxicity was observed, but the quality of the oligovalent binding may have been poor (i.e., the linkers were stretched and thus conformational entropy was a constraint, or a low number of the peptide ligands bound their epitopes), thus leading to less effective inhibition. The best inhibitors were constructed from linkers having 11–15 ethylene glycol repeats; estimation of the root-mean-square distance from the core to ligand for inhibitors within this range of linker lengths also matched the calculated distances from the lumen of $[PA_{63}]_7$ to the binding epitopes [53]. This correlation suggests that these linker lengths were thermodynamically the most favorable for allowing
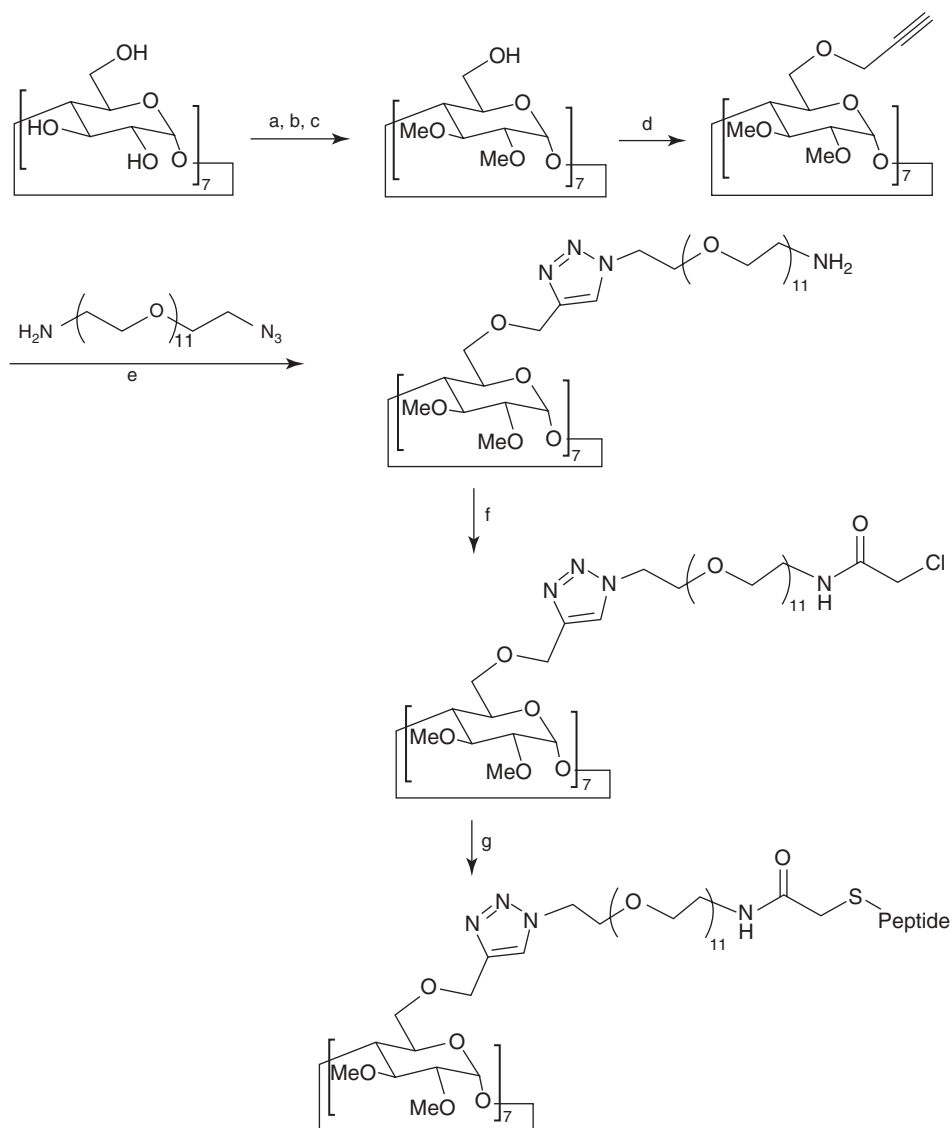
Scheme 11.6 Synthesis of a heptavalent anthrax toxin inhibitor: (a) TBDMSCl, pyridine, 0 °C-rt; (b) NaH, MeI, THF; (c) NH$_4$F, MeOH, reflux; (d) NaH, propargyl bromide, DMF, 0 °C-rt; (e) CuSO$_4$, sodium ascorbate, THF/H$_2$O/*t*-BuOH (0.5 : 1 : 1), 80 °C; (f) chloroacetic anhydride, triethylamine; and (g) peptide, DMF, 1,8-diazabicyclo[5.4.0]undec-7-ene (DBU), triethylamine. (Source: Reprinted with permission from [53]. Copyright 2011 American Chemical Society.)
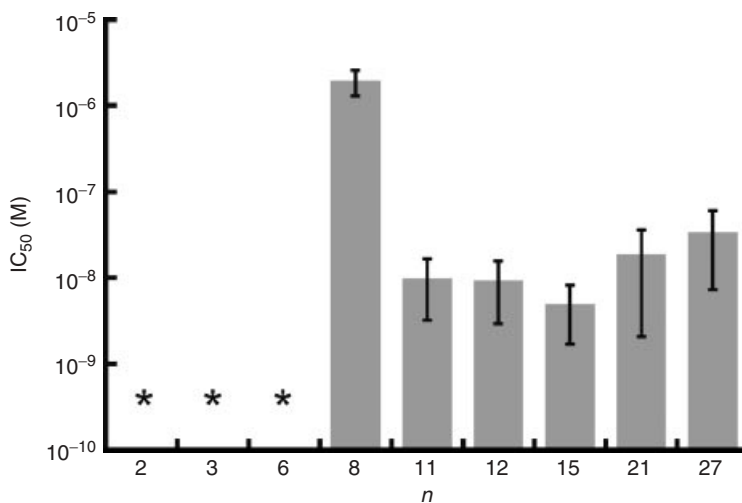
Figure 11.11 Influence of linker length on the activity of heptavalent inhibitors. The indicated PEG linkers were used to join the HTSTYWWLDGAP peptide to β-cyclodextrin, and the IC_{50} values of the resulting inhibitors were measured in a RAW264.7 cell cytotoxicity assay. The error bars represent the standard deviation from four separate experiments. Asterisks indicate that the inhibitory activity was not detected. (Source: Reprinted with permission from [53]. Copyright 2011 American Chemical Society.)

the βCD inhibitors to bind to $[PA_{63}]_7$ and block the binding of LF [21, 67–70]. Indeed, further increases in linker length resulted in inhibitors of slightly lower potency.

11.2.5
Biocompatible Polymer Scaffolds

When designing a polymeric substance to be administered within the human body or within the environment, some of the primary concerns are biocompatibility and biodegradability. For a polymer therapeutic to be biocompatible, the polymer and all its metabolites should be nontoxic, and administration should not induce excessive immunological reactions. Biodegradability describes the ability of a material to be decomposed naturally due to either natural chemical or enzymatic processes, and is desirable in the context of most therapeutics because the ability of a material to be naturally cleared from the body is correlated with good biocompatibility. The ability to use pHPMA, a proven biocompatible polymer [62, 63], as an effective polyvalent scaffold has already been described [51]. However, HPMA is not biodegradable. On the other hand, the polypeptide-based polymer poly(L-glutamic acid) (pGA) has been shown to be both biocompatible and biodegradable [71], and it has been used to prepare a variety of polyvalent displays [17, 29, 72, 73]. Joshi *et al.* [28] used an ester activation strategy similar to that used for pAA (Scheme 11.7) to modify the carboxyl groups on the side chains of this polypeptide with the

PGA sodium salt   Activated PGA   Polyvalent inhibitor
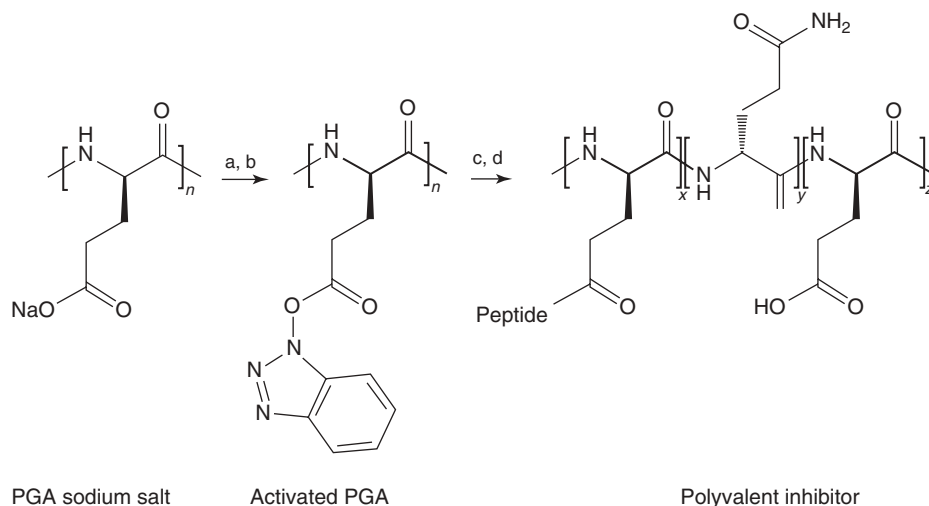
Scheme 11.7 Synthesis of pGA-based polyvalent inhibitor. (a) 1-ethyl-3-(3-dimethylaminopropyl)carbodiimide (EDC), H_2O; (b) HOBt, DMF; (c) peptide, DMF, triethylamine (TEA); and (d) NH_4OH, dialysis. The polyvalent inhibitor is a random copolymer composed of peptide conjugates (*x* repeat units), glutamine (*y* repeat units), and glutamic acid (*z* repeat units). (Source: Reprinted with permission from [28]. Copyright 2006 American Chemical Society.)

amine-functional $[PA_{63}]_7$ binding peptide ligand. The resulting pGA polyvalent inhibitors not only had similar activity to the corresponding pAA-based inhibitors in an *in vitro* cytotoxicity assay (Figure 11.12) but also were shown to be 100% effective in preventing the intoxication symptoms of anthrax lethal toxin *in vivo* in Fisher 344 rats. The advantage over the pAA-based inhibitors, which also exhibited *in vivo* efficacy, is in the inherent biodegradability of the polypeptide scaffold, which decreases the probability of long-term side effects from the administration of the polymer-based inhibitor.

11.2.6
Bioengineered Polymer Scaffolds

The use of polypeptides as scaffolds is especially attractive from a therapeutic standpoint because catabolism should result in amino acid products, which would be easily handled by the body. However, the use of polypeptides as scaffolds is not limited to homopolymers. Monodisperse, functional polymer scaffolds are readily available from nature in the form of proteins. Amine (lysine), carboxylic acid (aspartic acid and glutamic acid), thiol (cysteine), and hydroxyl (serine and threonine) are naturally occurring functional handles on the side chains of peptides. The research of Yang *et al.* [74] demonstrated as a proof of concept the ability to acylate lysine side chains with acetic anhydride in three different proteins: ubiquitin (8.6 kDa, 7 lysines, 1 N-terminal amine), lysozyme (14.3 kDa, 6 lysines,
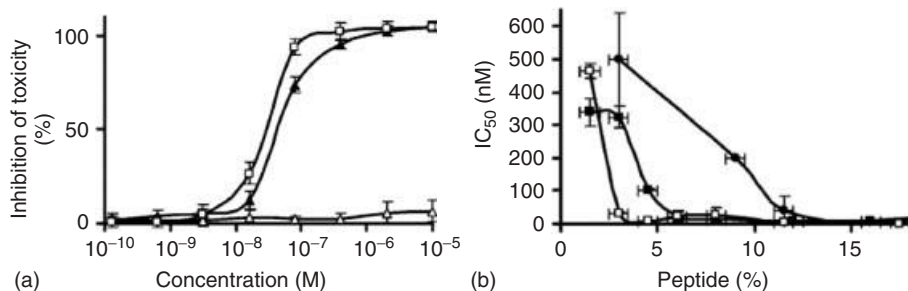
Figure 11.12 (a) Inhibition of cytotoxicity in cell culture by pGA-based polyvalent inhibitor (open squares), polyacrylamide-based polyvalent inhibitor (filled triangles), and control polymer (ammonium hydroxide quenched activated pGA) (open triangles). (b) Influence of peptide density on the potency of polyvalent inhibitors with different molecular weights $M_w = 4.5$ kDa (filled circles), 12 kDa (filled squares), and 29 kDa (open squares); average number of repeat units about 27, 70, and 170, respectively. (Source: Reprinted with permission from [28]. Copyright 2006 American Chemical Society.)

1 N-terminal amine), and bovine carbonic anhydrase II (BCA) (29 kDa, 18 lysines, posttranslationally acetylated N-terminal amine). The ability to acylate the lysine side chains depended on the size of the protein; denaturation with SDS was required for complete acylation of the lysine residues in BCA, but there was no reported difference between the native and denatured reactivities of the lysine residues in ubiquitin. Furthermore, the ability to react ubiquitin with hydrophilic triethylene glycol carboxylate, hydrophobic benzoate, anionic glutarate, and chemically reactive iodoacetate demonstrated both the generality of the procedure and the range of chemical properties that might be introduced into protein scaffolds. The approach is interesting, but the propensity for the proteins to fold into tertiary structures should still be considered. On the other hand, recombinant protein engineering methods can be used to take advantage of nature's polymer synthesis machinery in order to create scaffolds that are both monodisperse and designed to have functional handles at predetermined locations [75]. The Kiick research group has employed these methods [31, 76, 77] to make well-defined scaffolds into polyvalent inhibitors of the cholera toxin B pentamer subunit. The researchers demonstrated that by altering the composition of the polypeptide, they could control the interligand spacing, the valency, and even the conformation (α-helical vs random coil) of the inhibitors. In addition to observing improvements in inhibitors with interligand spacing and valency that matched that of the target toxin, the results revealed more potent inhibition using α-helical scaffolds than random coil scaffolds. The authors hypothesized that the α-helical conformation may have increased the accessibility of the pendant ligands and/or reduced the loss of conformational entropy on binding, thus leading to the measured improvement in potency. Using oligovalent proteins as supramolecular templates for prearranging the displays of heterobifunctional ligands on a polyvalent polymer scaffold has also been shown to yield vast improvements in potency [78, 79]. Further research is warranted, as

these methods for controlling all aspects of scaffold architecture are promising advancements for the future of polyvalent therapeutic design.

11.3
Conclusions

Conjugates of natural and synthetic polymers may be prepared to synergistically combine their properties and overcome the limitations of each component for potential therapeutic applications. For the past two decades, such benefits have been exemplified in polyvalent displays of ligands on polymer scaffolds. Although there are clearly advantages of polyvalent interactions over monovalent interactions in specific applications, progress toward gathering a detailed understanding of the determinants of efficacy in polyvalent systems has been slow due to the existence of several challenges. For instance, a synthetic polymer sample is always composed of many different macromolecules, leading to uncertainty when trying to relate characterization data to the structure of individual polymer chains. Thus, it has been difficult to discern exactly how factors such as ligand spacing, valency, linker length, and scaffold flexibility and size affected polyvalent potency. In addition, these challenges prevented comparison between different polyvalent systems. Many of these challenges have been increasingly met by controlled polymerization techniques such as atom transfer radical polymerization (ATRP), RAFT, and ROMP. However, samples prepared using these strategies are still remarkably unrefined when compared to natural polymers such as nucleic acids and proteins. In this regard, protein engineering represents a promising pathway toward further advancements. The advantages of using hub-and-spoke scaffolds, such as the βCD-based anthrax toxin inhibitor previously described, have also been recognized; matching the valency of the therapeutic to that of the target is more economical, and the resulting potency can be greater on a per-ligand basis [77]. Other polymeric scaffolds such as dendrimers [23], polymeric micelles [49, 50], and polymersomes [80] are also amenable to polyvalent functionalization and may expand the therapeutic potential of polyvalent polymer scaffolds, as they have the added benefit of being able to transport cargo. It should be noted that the therapeutic potential of polyvalent systems is not limited to preventing undesired biological interactions (such as in inhibition of viral infection and bacterial toxin assembly) but can also include increasing the potency of signaling proteins such as Sonic hedgehog [81]. However, there are still difficulties in the construction of polyvalent therapeutics that can arise when the ligands of interest are themselves macromolecules. In these cases, steric hindrance between ligands and reductions in solubility coinciding with ligand conjugation may lead to low conjugation efficiency and efficacy. When this happens, the final product is susceptible to contamination with starting materials. Indirect functionalization in which a heterobifunctional spacer is reacted first can be used to introduce a more reactive secondary functionality and can alleviate some of the problems associated with the lack of reactivity when bringing two large molecules together.

Still, when ligands are not available in bulk and must be specially synthesized and purified, utilizing high or even moderate concentrations to achieve the desired coupling percentages may not be a feasible option. Fortunately, there has been an increasing interest among polymer scientists in developing and taking advantage of ''click'' chemistry reactions [82] for modifying polymers [41, 83, 84]. Some of these methods are the topic of other chapters within this book. Further advancements in adapting click chemistry for polymer modification will be extremely beneficial for the construction of polyvalent polymer therapeutics in the future because conjugation schemes that are facile, high yielding, and involve simple purification schemes become particularly important as the size of pendant ligands is increased. Furthermore, the ability to use mild reaction conditions and orthogonally reactive functionalities will surely increase the scope of how polyvalent displays might be prepared, including allowing for the attachment of more sensitive biomolecules and the combination of multiple different types of ligands along one backbone. These new capabilities will be important for tailoring the interactions of a polyvalent polymer therapeutic to a desired target.

References

1. Mammen, M., Choi, S.-K., and Whitesides, G.M. (1998) *Angew. Chem. Int. Ed.*, **37**, 2754–2794.
2. Rao, J., Lahiri, J., Isaacs, L., Weis, R.M., and Whitesides, G.M. (1998) *Science (New York)*, **280**, 708–711.
3. Kiessling, L.L. and Pohl, N.L. (1996) *Chem. Biol.*, **3**, 71–77.
4. Kiessling, L.L., Strong, L.E., and Gestwicki, J.E. (2000) in *Annual Reports in Medicinal Chemistry*, Elsevier, pp. 321–330.
5. Mulder, A., Huskens, J., and Reinhoudt, D.N. (2004) *Org. Biomol. Chem.*, **2**, 3409–3424.
6. Badjiæ, J.D., Nelson, A., Cantrill, S.J., Turnbull, W.B., and Stoddart, J.F. (2005) *Acc. Chem. Res.*, **38**, 723–732.
7. Kiessling, L.L., Gestwicki, J.E., and Strong, L.E. (2006) *Angew. Chem. Int. Ed.*, **45**, 2348–2368.
8. Joshi, A., Vance, D., Rai, P., Thiyagarajan, A., and Kane, R.S. (2008) *Chemistry (Weinheim an der Bergstrasse, Germany)*, **14**, 7738–7747.
9. Vance, D., Shah, M., Joshi, A., and Kane, R.S. (2008) *Biotechnol. Bioeng.*, **101**, 429–434.
10. Vance, D., Martin, J., Patke, S., and Kane, R.S. (2009) *Adv. Drug Delivery Rev.*, **61**, 931–939.
11. Maheshwari, G., Brown, G., Lauffenburger, D.A., Wells, A., and Griffith, L.G. (2000) *J. Cell Sci.*, **113** (Pt. 1), 1677–1686.
12. Matrosovich, M.N., Mochalova, L.V., Marinina, V.P., Byramova, N.E., and Bovin, N.V. (1990) *FEBS Lett.*, **272**, 209–212.
13. Spevak, W., Nagy, J.O., Charych, D.H., Schaefer, M.E., Gilbert, J.H., and Bednarski, M.D. (1993) *J. Am. Chem. Soc.*, **115**, 1146–1147.
14. Mammen, M., Dahmann, G., and Whitesides, G.M. (1995) *J. Med. Chem.*, **38**, 4179–4190.
15. Choi, S.K., Mammen, M., and Whitesides, G.M. (1996) *Chem. Biol.*, **3**, 97–104.
16. Sigal, G.B., Mammen, M., Dahmann, G., and Whitesides, G.M. (1996) *J. Am. Chem. Soc.*, **118**, 3789–3800.
17. Kamitakahara, H., Suzuki, T., Nishigori, N., Suzuki, Y., Kanie, O., and Wong, C.-H. (1998) *Angew. Chem. Int. Ed.*, **37**, 1524–1528.
18. Honda, T., Yoshida, S., Arai, M., Masuda, T., and Yamashita, M.

(2002) *Bioorg. Med. Chem. Lett.*, **12**, 1929–1932.

19. Fan, E., Zhang, Z., Minke, W.E., Hou, Z., Verlinde, C.L.M.J., and Hol, W.G.J. (2000) *J. Am. Chem. Soc.*, **122**, 2663–2664.

20. Kitov, P.I., Sadowska, J.M., Mulvey, G., Armstrong, G.D., Ling, H., Pannu, N.S., Read, R.J., and Bundle, D.R. (2000) *Nature*, **403**, 669–672.

21. Gargano, J.M., Ngo, T., Kim, J.Y., Acheson, D.W., and Lees, W.J. (2001) *J. Am. Chem. Soc.*, **123**, 12909–12910.

22. Mourez, M., Kane, R.S., Mogridge, J., Metallo, S., Deschatelets, P., Sellman, B.R., Whitesides, G.M., and Collier, R.J. (2001) *Nat. Biotechnol.*, **19**, 958–961.

23. Nishikawa, K., Matsuoka, K., Kita, E., Okabe, N., Mizuguchi, M., Hino, K., Miyazawa, S., Yamasaki, C., Aoki, J., Takashima, S., Yamakawa, Y., Nishijima, M., Terunuma, D., Kuzuhara, H., and Natori, Y. (2002) *Proc. Natl. Acad. Sci.*, **99**, 7669–7674.

24. Mulvey, G.L., Marcato, P., Kitov, P.I., Sadowska, J., Bundle, D.R., and Armstrong, G.D. (2003) *J. Infect. Dis.*, **187**, 640–649.

25. Karginov, V.A., Nestorovich, E.M., Moayeri, M., Leppla, S.H., and Bezrukov, S.M. (2005) *Proc. Natl. Acad. Sci.*, **102**, 15075–15080.

26. Basha, S., Rai, P., Poon, V., Saraph, A., Gujraty, K., Go, M.Y., Sadacharan, S., Frost, M., Mogridge, J., and Kane, R.S. (2006) *Proc. Natl. Acad. Sci.*, **103**, 13509–13513.

27. Gujraty, K.V., Joshi, A., Saraph, A., Poon, V., Mogridge, J., and Kane, R.S. (2006) *Biomacromolecules*, **7**, 2082–2085.

28. Joshi, A., Saraph, A., Poon, V., Mogridge, J., and Kane, R.S. (2006) *Bioconjugate Chem.*, **17**, 1265–1269.

29. Polizzotti, B.D. and Kiick, K.L. (2006) *Biomacromolecules*, **7**, 483–490.

30. Rai, P., Padala, C., Poon, V., Saraph, A., Basha, S., Kate, S., Tao, K., Mogridge, J., and Kane, R.S. (2006) *Nat. Biotechnol.*, **24**, 582–586.

31. Polizzotti, B.D., Maheshwari, R., Vinkenborg, J., and Kiick, K.L. (2007) *Macromolecules*, **40**, 7103–7110.

32. Rai, P.R., Saraph, A., Ashton, R., Poon, V., Mogridge, J., and Kane, R.S. (2007) *Angew. Chem. Int. Ed.*, **46**, 2207–2209.

33. Lutz, J.-F. and Börner, H.G. (2008) *Prog. Polym. Sci.*, **33**, 1–39.

34. Hartmann, L. and Börner, H.G. (2009) *Adv. Mater. (Deerfield Beach, FL.)*, **21**, 3425–3431.

35. Hawker, C.J. and Wooley, K.L. (2005) *Science (New York)*, **309**, 1200–1205.

36. Börner, H.G. (2011) *Macromol. Rapid Commun.*, **32**, 115–126.

37. Dehn, S., Chapman, R., Jolliffe, K., and Perrier, S. (2011) *Polym. Rev.*, **51**, 214–234.

38. Canalle, L.A., Löwik, D.W.P.M., and van Hest, J.C.M. (2010) *Chem. Soc. Rev.*, **39**, 329–353.

39. Gauthier, M.A. and Klok, H.-A. (2008) *Chem. Commun. (Cambridge, England)*, 2591–2611.

40. Klok, H.-A. (2009) *Macromolecules*, **42**, 7990–8000.

41. Le Droumaguet, B. and Nicolas, J. (2010) *Polym. Chem.*, **1**, 563.

42. Gauthier, M.A., Gibson, M.I., and Klok, H.-A. (2009) *Angew. Chem. Int. Ed.*, **48**, 48–58.

43. Collier, R.J. and Young, J.A.T. (2003) *Annu. Rev. Cell Dev. Biol.*, **19**, 45–70.

44. Rainey, G.J.A. and Young, J.A.T. (2004) *Nat. Rev. Microbiol.*, **2**, 721–726.

45. Dixon, T.C., Meselson, M., Guillemin, J., and Hanna, P.C. (1999) *N. Engl. J. Med.*, **341**, 815–826.

46. Petosa, C., Collier, R.J., Klimpel, K.R., Leppla, S.H., and Liddington, R.C. (1997) *Nature*, **385**, 833–838.

47. Duesbery, N.S., Webb, C.P., Leppla, S.H., Gordon, V.M., Klimpel, K.R., Copeland, T.D., Ahn, N.G., Oskarsson, M.K., Fukasawa, K., Paull, K.D., and Vande Woude, G.F. (1998) *Science (New York)*, **280**, 734–737.

48. Bradley, K.A., Mogridge, J., Mourez, M., Collier, R.J., and Young, J.A. (2001) *Nature*, **414**, 225–229.

49. Carrillo, A. and Kane, R.S. (2004) *J. Polym. Sci. Part A: Polym. Chem.*, **42**, 3352–3359.

50. Carrillo, A., Yanjarappa, M.J., Gujraty, K.V., and Kane, R.S. (2006) *J. Polym. Sci. Part A: Polym. Chem.*, **44**, 928–939.

51. Yanjarappa, M.J., Gujraty, K.V., Joshi, A., Saraph, A., and Kane, R.S. (2006) *Biomacromolecules*, **7**, 1665–1670.

52. Gujraty, K.V., Yanjarappa, M.J., Saraph, A., Joshi, A., Mogridge, J., and Kane, R.S. (2008) *J. Polym. Sci. Part A, Polym. Chem.*, **46**, 7246–7257.

53. Joshi, A., Kate, S., Poon, V., Mondal, D., Boggara, M.B., Saraph, A., Martin, J.T., McAlpine, R., Day, R., Garcia, A.E., Mogridge, J., and Kane, R.S. (2011) *Biomacromolecules*, **12**, 791–796.

54. Pieters, R.J. (2009) *Org. Biomol. Chem.*, **7**, 2013–2025.

55. Top, A. and Kiick, K.L. (2010) *Adv. Drug Delivery Rev.*, **62**, 1530–1540.

56. Duncan, R. (2003) *Nat. Rev. Drug Discovery*, **2**, 347–360.

57. Twaites, B., de las Heras Alarcǧn, C., and Alexander, C. (2005) *J. Mater. Chem.*, **15**, 441–455.

58. Kiick, K.L. (2007) *Science*, **317**, 1182–1183.

59. Liu, S., Maheshwari, R., and Kiick, K.L. (2009) *Macromolecules*, **42**, 3–13.

60. Rai, P., Vance, D., Poon, V., Mogridge, J., and Kane, R.S. (2008) *Chemistry (Weinheim an der Bergstrasse, Germany)*, **14**, 7748–7751.

61. Gordon, E.J., Gestwicki, J.E., Strong, L.E., and Kiessling, L.L. (2000) *Chem. Biol.*, **7**, 9–16.

62. Kopecek, J., Kopecková, P., Minko, T., and Lu, Z. (2000) *Eur. J. Pharm. Biopharm.: Off. J. APV e.V*, **50**, 61–81.

63. Kopecek, J. and Kopecková, P. (2010) *Adv. Drug Delivery Rev.*, **62**, 122–149.

64. Moayeri, M., Robinson, T.M., Leppla, S.H., and Karginov, V.A. (2008) *Antimicrob. Agents Chemother.*, **52**, 2239–2241.

65. Ragle, B.E., Karginov, V.A., and Bubeck Wardenburg, J. (2010) *Antimicrob. Agents Chemother.*, **54**, 298–304.

66. Szejtli, J. (1998) *Chem. Rev.*, **98**, 1743–1754.

67. Kramer, R.H. and Karpen, J.W. (1998) *Nature*, **395**, 710–713.

68. Kitov, P.I. and Bundle, D.R. (2003) *J. Am. Chem. Soc.*, **125**, 16271–16284.

69. Diestler, D. and Knapp, E. (2008) *Phys. Rev. Lett.*, **100**, 1–4.

70. Kane, R.S. (2010) *Langmuir*, **26**, 8636–8640.

71. Li, C. (2002) *Adv. Drug Delivery Rev.*, **54**, 695–713.

72. Totani, K., Kubota, T., Kuroda, T., Murata, T., Hidari, K.I.-P.J., Suzuki, T., Suzuki, Y., Kobayashi, K., Ashida, H., Yamamoto, K., and Usui, T. (2003) *Glycobiology*, **13**, 315–326.

73. Zeng, X., Murata, T., Kawagishi, H., Usui, T., and Kobayashi, K. (1998) *Biosci. Biotechnol. Biochem.*, **62**, 1171–1178.

74. Yang, J., Gitlin, I., Krishnamurthy, V.M., Vazquez, J.A., Costello, C.E., and Whitesides, G.M. (2003) *J. Am. Chem. Soc.*, **125**, 12392–12393.

75. Davis, N.E., Karfeld-Sulzer, L.S., Ding, S., and Barron, A.E. (2009) *Biomacromolecules*, **10**, 1125–1134.

76. Wang, Y. and Kiick, K.L. (2005) *J. Am. Chem. Soc.*, **127**, 16392–16393.

77. Liu, S. and Kiick, K.L. (2008) *Macromolecules*, **41**, 764–772.

78. Kitov, P.I., Mulvey, G.L., Griener, T.P., Lipinski, T., Solomon, D., Paszkiewicz, E., Jacobson, J.M., Sadowska, J.M., Suzuki, M., Yamamura, K.-I., Armstrong, G.D., and Bundle, D.R. (2008) *Proc. Natl. Acad. Sci.*, **105**, 16837–16842.

79. Cui, L., Kitov, P.I., Completo, G.C., Paulson, J.C., and Bundle, D.R. (2011) *Bioconjugate Chem.*, **22**, 546–550.

80. Egli, S., Nussbaumer, M.G., Balasubramanian, V., Chami, M., Bruns, N., Palivan, C., and Meier, W. (2011) *J. Am. Chem. Soc.*, **133**, 4476–4483.

81. Wall, S.T., Saha, K., Ashton, R.S., Kam, K.R., Schaffer, D.V., and Healy, K.E. (2008) *Bioconjugate Chem.*, **19**, 806–812.

82. Kolb, H.C., Finn, M., and Sharpless, K.B. (2001) *Angew. Chem. Int. Ed.*, **40**, 2004–2021.

83. Le Droumaguet, B. and Velonia, K. (2008) *Macromol. Rapid Commun.*, **29**, 1073–1089.

84. Golas, P.L. and Matyjaszewski, K. (2010) *Chem. Soc. Rev.*, **39**, 1338–1354.

12

Posttranslational Modification of Proteins Incorporating Nonnatural Amino Acids

Haresh More, Ching-Yao Yang, and Jin Kim Montclare

The ability to posttranslationally modify proteins is becoming increasingly important to not only further gain insight into protein interactions in biology but also fabricate novel protein materials. While there are naturally existing enzymatic approaches to posttranslational modifications (PTMs), recent advances in molecular and chemical biology have led to the development of powerful methods that allow the incorporation of virtually any nonnatural amino acid (NAA). In this chapter, we describe the *in vitro* and *in vivo* methodologies for PTMs and highlight applications for NAA incorporation.

12.1
Posttranslational Modification of Existing Amino Acids within Protein Chain

While proteins are composed of a natural set of 22 amino acid building blocks, nature has developed processes to modify such residues posttranslationally. These PTMs are performed by a host of enzymes and proteins to transform natural amino acids into NAAs. PTMs include phosphorylation, acetylation, methylation, glycosylation, hydroxylation, sulfation, and ubiquitination [1]. All these modifications add a chemical moiety to the amino acid with the exception of ubiquitination that adds an entire protein domain. In biology, PTMs regulate the cellular activity and modify the nascent protein under physiological conditions [1]. The chemical moiety is either covalently attached to or removed from a designated side chain. These covalent modifications are mainly carried out by different enzymes that act on the particular amino acids. As this review is centered on PTMs, we focus on the regulatory proteins that modify natural amino acids without discussing those that remove the modifications.

12.1.1
Phosphorylation

Protein phosphorylation mainly occurs on threonine (Thr), tyrosine (Tyr), or serine (Ser) in eukaryotes and histidine (His) or aspartic acid (Asp) in prokaryotes
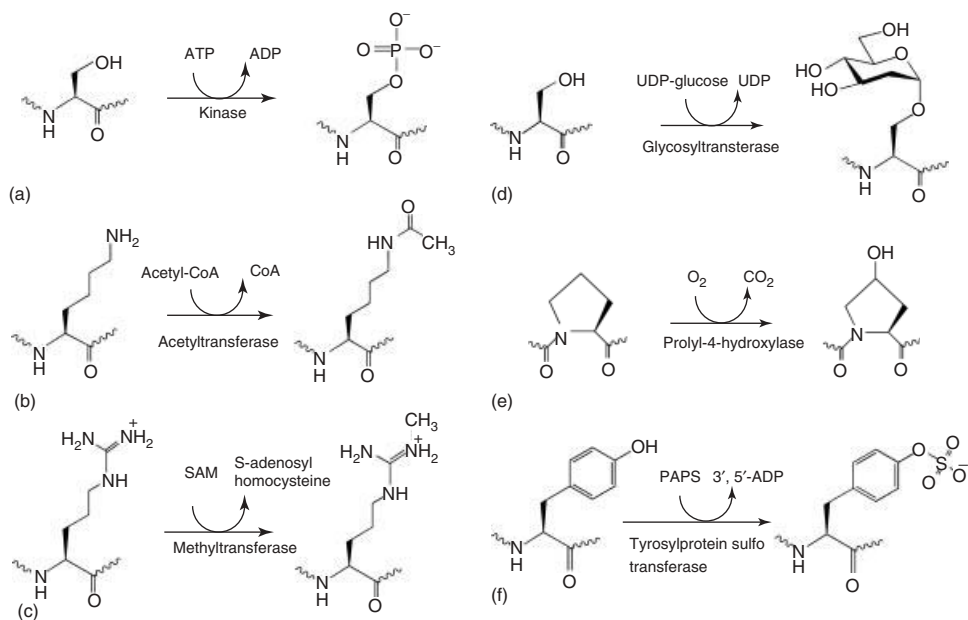
Scheme 12.1 Five major types of PTMs of proteins. (a) Phosphorylation, (b) acetylation, (c) methylation, (d) glycosylation, (e) hydroxylation, and (f) sulfation.

by the addition of phosphate from adenosine-5′-triphosphate (ATP) by kinases (Scheme 12.1a) [2]. It can cause the activation and deactivation of enzyme activity and also take part in a signal transduction pathway [3]. For example, the addition of a tetrahedral anionic phosphate group to the aforementioned amino acid residues can lead to the interaction with positively charged arginine (Arg) residues, leading to signal transduction [4].

12.1.2
Acetylation

The ε-amino group of lysine (Lys) is also an important site for acetylation as a PTM [5]. The histone acetyl transferase (HAT) [6] or acetyl transferase (AT) [7] acetylates the Lys residues on the N-terminal tail of histones or other proteins with the help of acetyl coenzyme A (AcCoA), which leads to the alteration of charge distribution (Scheme 12.1b). Histone and non-histone proteins can be acetylated, leading to regulation of genes and proteins [6, 7].

12.1.3
Methylation

The amino acids Lys, Arg, and glutamic acid (Glu) are posttranslationally methylated by a class of methyltransferases enzymes, which transfer a methyl group

from *S*-adenosylmethionine (SAM) (Scheme 12.1c) [8]. Arg and Lys methylation are the most prevalent PTMs that occur on acetylated histone tails by a family of histone methyltransferases enzymes [9]. These modifications play an important role in chromatin remodeling and transcriptional regulation [10]. Arg methylation is catalyzed by a family of protein arginine methyltransferases (PRMT), which add one or two methyl groups to the guanidino nitrogen [11] to generate monomethyl-larginine (MMA), symmetric dimethylarginine (sDMA), and asymmetric dimethyl arginine (aDMA). The proteins with the glycine- and arginine-rich (GAR) motif are targets of PRMT. PRMTs methylate histone H3 and many non-histone proteins including the RNA-binding proteins, transcriptional coregulators, DNA-binding transcription factors, and signal transducers [12–14]. Similar to Arg methylation by PRMT, histone lysine methyl transferases (HKMTs) perform methylation on the ε-amino group of Lys to generate mono-, di-, and trimethylated forms.

12.1.4
Glycosylation

Glycosylation is a PTM that attaches a carbohydrate moiety to a set of specific amino acid residues including asparagine Asn (N-glycosylation), Ser or Thr (O-glycosyla-tion), and tryptophan Trp (C-mannosylation) (Scheme 12.1d) [15, 16]. For N-glycosylation, *N*-acetylglucosamine (GlcNAc) is linked to Asn via an amide bond (GlcNAc−β-Asn) [17]. In the glycosylation process, the precursor oligosaccharide $Glc_3Man_9(GlcNAc)_2$ gets assembled on the dolichol-pyrophosphate by the membrane-associated glycosyltransferases in the endoplasmic reticulum (ER), which then serves as a substrate for the oligosaccharyltransferase to transfer onto Asn usually within the context of Asn-Xaa-Ser/Thr [15, 17]. This N-linked $Glc_3Man_9(GlcNAc)_2$ undergoes a series of trimming processes by different glucosidase and mannosidase enzymes [18]. O-Glycosylation is less complex than N-glycosylation and the monosaccharide unit GlcNAc is added to the hydroxyl group of Ser or Thr by specific O-GlcNAc transferases to form GlcNAc-α-Ser/Thr [19]. Other monosaccharides including *N*-acetylgalactosamine (GalNAc), xylose, mannose, and fucose also get attached to the Ser using GalNAc transferase, xylose transferase, mannose transferase, and fucose transferase, respectively [15]. Unlike the O- and N-glycosylation, C-mannosylation involves the attachment of α-mannopyranosyl to indole C-2 carbon atom of Trp via C−C linkage [20, 21]. This linkage has been found in human ribonuclease from urine [21], interleukin-12 [6], and properdin protein [22]. The enzyme C-mannosyltransferase mainly recognizes the Trp-X-X-Trp sequence and glycosylates the first Trp residue [23].

12.1.5
Hydroxylation

Protein hydroxylation is an irreversible PTM that occurs on the nonnucleophilic aminoacyl side chain of Pro and Lys to generate 3-hydroxy Pro, 4-hydroxy Pro,

and 5-hydroxy Lys [24] (Scheme 12.1e). Hydroxylation is predominant in collagen substrates bearing the Xaa-Pro/Lys-Gly sequence and is important for proper folding and stability of the triple helical conformation. Prolyl-4-hydroxylase, prolyl-3-hydroxylase, and lysyl hydroxylase catalyze the hydroxylation reaction in the presence of Fe^{2+}, 2-oxoglutarate, O_2, and ascorbate [24, 25]. Hydroxylated Lys residue further undergoes glycosylation at the hydroxyl group through an O-glycosidic linkage [26].

12.1.6
Sulfation

Tyr sulfation is facilitated by a tyrosylprotein sulfotransferase (TPST), which catalyzes the transfer of a sulfate group from 3′-phosphoadenosine-5′-phosphosulfate (PAPS) to the hydroxyl group of Tyr residues forming Tyr O-sulfate esters and adenosine 3′,5′-diphosphate (Scheme 12.1f) [27–29]. Tyr sulfation is involved in various biological processes including hemostatis regulation [30], inflammatory responses, hormonal regulation, and infectious diseases [29, 31]. More recently, sulfo-Thr and sulfo-Ser have been identified; however, the enzymes and their biological implications are yet to be identified [32].

12.2
Exploiting Biosynthetic Machinery: Cotranslational Approach

As PTMs are performed by enzymes, the protein substrates are often very specific and require a particular amino acid sequence. Thus, the utilization of such enzymes for the synthesis of modified amino acids cannot be achieved on any desired protein. To overcome this obstacle, the scientists have developed approaches that exploit the biosynthetic machinery for the incorporation of NAAs. In order to integrate modified amino acids into proteins biosynthetically, two critical criteria ought to be met [33]. First, there needs to be a place holder in the mRNA sequence for the NAA. Second, a method for conjugating the NAA onto the tRNA recognizing the place holder in the mRNA is required. Several different approaches have been developed to address these two criteria, leading to site-specific and residue-specific incorporation (RSI) of NAAs.

12.2.1
Site-Specific Incorporation (SSI)

12.2.1.1 *In vitro* SSI

Chemical Aminoacylation of tRNA, Suppressor Codon With the development of chemical aminoacylation of tRNA, scientists devised a strategy to incorporate the misacylated tRNA with NAA; however, this method resulted in NAA incorporation at multiple sites [34–37]. In order to enable the site-specific incorporation (SSI) of
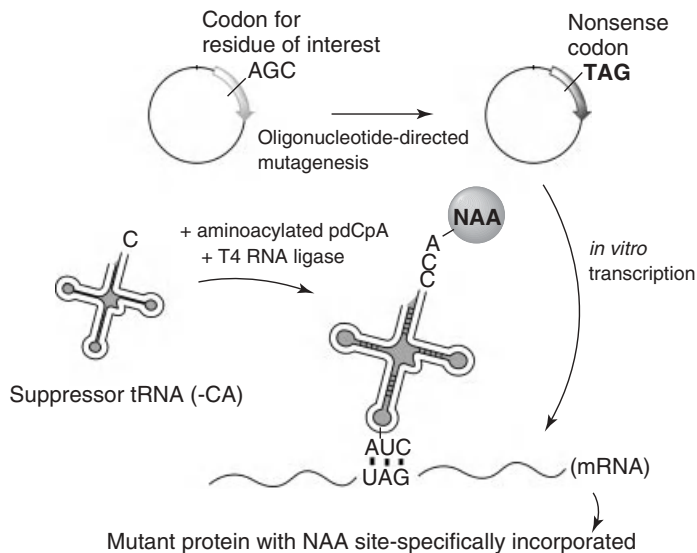
Figure 12.1 Schematic representation of *in vitro* SSI via amber suppression.

NAAs, a codon that would not encode for any of the 20 amino acids was required. In 1985, Bayley and Shih announced their intention of the *in vitro* incorporation of NAA at the amber stop codon using the suppressor tRNA. Afterward, the Schultz group developed a method where a hybrid dinucleotide pdCpA was synthesized with the NAA in which the amine was protected with the easily removable *o*-nitrophenylsulfenyl chloride (Figure 12.1) [38]. The aminoacylated pdCpA was ligated to a truncated amber suppressor tRNA$_{CUA}$^{Phe} using the T4 RNA ligase, which was used for the SSI of the phenylalanine (Phe) analogs: *p*-fluorophenylalanine (*p*FF), *p*-nitrophenylalanine (*p*NO$_2$F), homophenylalanine (hF), 3-amino-2-benzylpropionic acid (ABPA), and 2-hydroxy-3-phenylpropionic acid (PA) into β-lactamase [38]. The analogs *p*FF, *p*NO$_2$F, and hF showed 7–15% incorporation efficiency, while the ABPA and PA were not incorporated [38].

A similar strategy was used by Chamberlin and coworkers to incorporate iodotyrosine into a 16-residue polypeptide. However, the acylated tRNA (^{125}I-Tyr-tRNA$_{CUA}$Gly-dCA) was prepared without any modifications to avoid the tedious procedures of isolation from the cellular mixture. Using this acylated tRNA, ^{125}I-Tyr-tRNA$_{CUA}$Gly-dCA, the suppression efficiency was 30% [38, 39]. Subsequently, they employed runoff transcription [40] to generate the semisynthetic nonsense suppressor tRNA for *in vitro* incorporation of L-3-[^{125}I] iodotyrosine (^{125}I-Tyr) into the 16-mer polypeptide (Met-Gly-Leu-Tyr-Leu-Gly-Leu-Phe-Stop-Gly-Leu-Tyr-Leu-Gly-Leu-Phe-Stop-Stop) [41]. The suppression efficiency was 65% for ^{125}I-Tyr; in the case of the other NAAs, it was 72% for *N*-methylphenylalanine and 46% for phenyllactic acid. Using this approach, a variety of NAAs have been incorporated into proteins *in vitro* with suppression efficiencies of up to 72% [42].
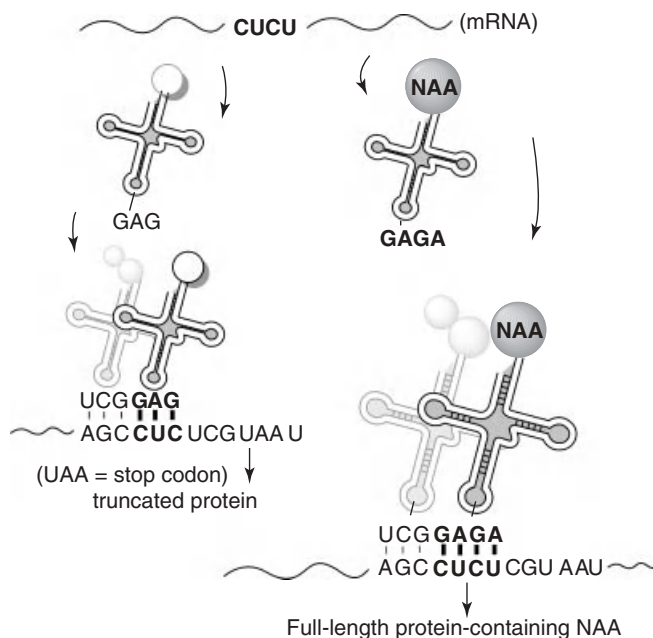
Figure 12.2 Schematic representation of SSI of NAAs using frameshift suppression.

Chemical Aminoacylation of tRNA, Four-Base Codon Of the 64 codons, all except for the three stop codons are assigned to a particular natural amino acid. While this leaves three possible trinucleotide stop codons for assignment to the NAA, suppression efficiency is a problem because of the dominance by the releasing factor (RF-1) [43]. To address this issue, Hohsaka and coworkers developed a frameshift suppression strategy in which four-base codons are employed for incorporation of NAA using an *Escherichia coli* cell-free translation system [44, 45]. The chemically aminoacylated tRNA, which contains a four-base anticodon translates the four-base codon on the mRNA.

Sisido and coworkers [44, 45] reported the incorporation of different Phe analogs into streptavidin, including 1-naphthylalanine (1-Nap), 2-naphthylalanine (2-Nap), *p*-(phenylazo)phenylalanine, *p*-dimethylaminophenylalanine, 2-anthryl-phenylalanine, 2-anthraquinonylalanine, *p*-benzoylphenylalanine (Bpa), pNO_2F, and 7-azatryptophan (7AzW) using the four-base codon AGGN (N = C,U,A, or G) and the corresponding NCCU anticodon system (Figure 12.2, Table 12.1).

In this approach, Tyr83 was mutated into AGGN and, on translation by the $tRNA_{NCCU}$ anticodon, the target protein streptavidin was synthesized; however, when the mRNA codon was read by endogenous $tRNA_{CCU}$, protein synthesis was terminated, confirming the specificity of the four-base codon system [45]. To increase the yield of protein, a fresh aminoacyl-$tRNA_{NCCU}$ was added 5 min after protein synthesis was started to maintain its concentration, which led to 45% yield

Table 12.1 Frameshift base codon and anticodons.

Frameshift base	Anticodon	References
AGGU	ACCU	[44, 46–48]
CGGG	CCCG	[44, 46–49]
CGGU	ACCG	[50]
CCCU	AGGG	[46]
CCCG	CGGG	[45, 47, 51]
CUCU	AGAG	[46]
CUAU	AUAG	[46]
CGGUA	UACCG	[52]

in case of 1-Nap and 90% yield for 2-Nap [53]. Using steady-state fluorescence spectroscopy, its binding ability to *N*-biotin-L-1-pyrenylalanine and photoinduced electron transfer from the excited pyrenyl group to the nitrophenyl group was observed. Subsequent studies showed that other four-base codon–anticodon systems, namely, AGGU–ACCU, CGGG–CCCG, CGGU–ACCG, CGCU–AGCG, CCCU–AGGG, CCCG–CGGG, CUCU–AGAG, and CUAU–AUAG, work efficiently (Table 12.1) [44–47, 49, 50].

Employing this four-base codon approach, Hohsaka *et al.* [48] were able to incorporate *two different* NAAs at the same time in same protein. Employing AGGU and CGGG, they effectively added ε-(7-nitrobenz-2-oxa-1,3-diazol-4-yl)-L-lysine (Lys(NBD)) and 2-Nap in a cell-free *E. coli* system with a yield of 41 and 22%, respectively [48]. In another study, they synthesized the streptavidin mRNA with the CGGG codon at the Tyr54 position and GGGU at the Tyr83 position and expressed in the presence of tRNA$_{CCCG}$ and mutated tRNA$_{ACCC}$ (with mutations G2-C71, C3-G70, C4-G69, and G73) aminoacylated with 2-Nap and *p*NO$_2$F, respectively. The yield of the full-length streptavidin was 64% relative to the wild-type protein and, when the AGGU and CGGG codons were used, the yield decreased to 19%, demonstrating the higher efficiency of the CGGG over the AGGU codon [49].

Hecht and coworkers [51] developed an efficient method to incorporate *two different* NAAs using a four-base codon and a stop codon into the dihydrofolate reductase (DHFR) having an HIV protease cleavage sequence in between the two NAA incorporation sites. 7AzW as fluorescence donor and dabcyl-1,2-diaminopropionic acid (Dap) derivative as a fluorescence acceptor were chemically aminoacylated to the tRNA$_{CCCG}$^{Tyr} and tRNA$_{CUA}$^{Tyr}, respectively, and incorporated into DHFR fusion protein using the *E. coli* S-30 *in vitro* translation system. The excitation of intact DHFR fusion protein containing 7AzW and Dap showed emission somewhat greater than the wild-type DHFR protein; however, when the DHFR fusion protein was treated with HIV protease, it showed a significant increase in fluorescence because of the cleavage of the protease sequence and separation of the fluorescence acceptor and donor [51].

In addition to four-base codon, a five-base codon–anticodon CGGUA–UACCG system was employed to effectively incorporate pNO$_2$F and Lys(NBD) at the Tyr54 position in streptavidin. While pNO$_2$F exhibited a yield of 16% compared to wild-type streptavidin, and the incorporation of Lys(NBD) was confirmed by tryptic digestion and high-performance liquid chromatography (HPLC), no yields were provided [52]. In addition to this, another 15 five-base codons CGGN$_1$N$_2$ (N$_1$ and N$_2$ indicate one of the four bases) were designed, which showed effective incorporation of pNO$_2$F with the yields ranging from 5 to 30% relative to that of wild-type streptavidin [52].

12.2.1.2 *In vivo* SSI

Microinjection of NAA-tRNA and mRNA   While the approaches mentioned so far enable the SSI of NAAs into polypeptides, they are limited by the amount of mRNA template and charged tRNA. As cell-free extracts are employed, the protein yields are often low. Thus efforts toward *in vivo* strategies have become increasingly important. Initially, *in vivo* SSI of NAAs was accomplished via microinjection of the amber stop codon bearing chemically aminoacylated tRNA and mRNA. [54, 55]. Lummis and coworkers [54] used suppressor tRNA from *Tetrahymena thermophila* G73 (THG73) to incorporate several analogs of Tyr and Phe into the 5-hydroxytryptamine$_3$ receptor using *Xenopus* oocytes to evaluate the importance of Tyr residues in the agonist binding and gating. This powerful approach was utilized by Chollet *et al.* [56] to incorporate the fluorescent 3-*N*-(7-nitrobenz-2-oxa-1,3-diazol-4-yl)-2,3-diaminopropionic acid (NBD-Dap) into the G-protein-coupled receptor tachykinin NK2 using *Xenopus* oocytes to study the ligand–receptor interaction. For this study, the suppressor tRNA was derived from yeast tRNA$_{CUA}$^{Phe} in which the G20U and A37G mutations were performed at the stem loop and the acceptor stem, respectively, to prevent the incorporation of a natural amino acid at the UAG amber codon site.

Frameshift suppression was exploited by Dougherty and coworkers [57] for use in *Xenopus* oocytes, in which α-aminobutyric acid (aBA), 5-fluorotryptophan (5-FW), and norvaline (NV) were incorporated into the nicotinic acetylcholine receptor (nAChR). In this study, the yeast phenylalanine frameshift suppressor (YFFS) tRNA$_{CCCG}$^{Phe} and YFFS with mutation in acceptor step (YFaFS$_{ACCC}$), which recognized two different codons CGGG and GGGU in the nAChR mRNA, were injected into *Xenopus* oocytes. These tRNAs were less effective compared to the amber suppressor tRNA from THG73, which was used extensively for NAA incorporation. However, the two YFFS tRNAs were more orthogonal to the *Xenopus* oocytes system than THG73 in terms of their recognition from the endogenous aminoacyl tRNA synthetase (AARS) [57]. They showed the simultaneous incorporation of 5-FW and aBA or NV by microinjecting both THG73 tRNA$_{CUA}$ and YFFS tRNA$_{CCCG}$^{Phe} or YFaFS$_{ACCC}$^{Phe}, respectively. Also, for the incorporation of three NAAs, they utilized 5-FW THG73 tRNA$_{CUA}$, aBA-tRNA$_{CCCG}$^{Phe}, and NV-tRNA$_{ACCC}$^{Phe} [57].

Orthogonal AARS, tRNA: Positive and Negative Selection for E. coli, Yeast, and Mammalian Cells   In the aforementioned cases for *in vivo* SSI, the protein yields are dependent on the amount of charged tRNA provided. Thus, the ability to constantly supply tRNA charged with NAA is critical for not only improving the protein yield but also developing an *in vivo* biosynthetic approach. In order to accomplish this, two important criteria need to be met: (i) an AARS that can exclusively aminoacylate the designated tRNA (usually suppressor tRNA) and (ii) the endogenous AARS that cannot cross-react with the suppressor tRNA [58]. Essentially, an orthogonal AARS/tRNA pair is necessary for biosynthetic *in vivo* SSI.

In the first ever approach, Furter [59] introduced a phenylalanyl-tRNA synthetase (PheRS)/suppressor tRNA$_{CUA}$^{Phe} pair from *Saccharomyces cerevisiae* into *E. coli* for SSI of *p*FF (Table 12.2). Since then, several strategies have beeen developed to engineer an orthogonal pair of AARS/tRNA that would not be aminoacylated by endogenous AARSs. In one approach, Schimmel *et al.* investigated species-specific tRNA recognition by analyzing the tRNA contact residues on *Bacillus stearothermophilus* tyrosyl-tRNA synthetase (TyrRS) and extended these

Table 12.2   Orthogonal amber suppressor AARS/tRNA pair for *in vivo* SSI of NAA.

Organism	AARS/tRNA pair	Derived from	NAA	References
Escherichia coli	PheRS/tRNA$_{CUA}$^{Phe}	*Saccharomyces cerevisiae*	*p*FF	[59]
	TyrRS/tRNA$_{CUA}$^{Tyr}	*Methanocaldococcus jannaschii*	β-GlcNAc-L-serine	[65]
	TyrRS/tRNA$_{CUA}$^{Tyr}	*M. jannaschii*	*p*-azido-L-phenylalanine, *p*AcF, *p*-aminophenylalanine, naphthylalanine, *p*-benzoylphenylalanine, *p*-methyoxyphenylalanine, *p*-aminomethylphenylalanine, *p*-methylphenylalanine, *p*-trifluoromethylphenylalanine, *p*-nitrophenylalanine	[66–71]
S. cerevisiae	TyrRS/tRNA$_{CUA}$^{Tyr}	*E. coli*	*p*AzF, *p*-benzoylphenylalanine, *p*-aminophenylalanine, *p*-isopropyl-phenylalanine, *m*-acetylphenylalanine, *p*-acetylphenylalanine, *O*-methyltyrosine, *O*-allyl-tyrosine, 3-(2-naphthyl)alanine, *p*-iodo-ʟ-tyrosine, BiaF	[72, 73]
Mammalian cells	TyrRS/tRNA$_{CUA}$^{Tyr}	*Bacillus sterothermophilius*, *E. coli*	OmeTyr, Bpa, Dan(Ala)	[74, 75]

studies to *Mycobacterium tuberculosis* TyrRS to investigate cross-species aminoacylation [60]. Schultz and coworkers [61, 62] performed three different mutations on $tRNA_2^{Gln}$ and several mutations on glutaminyl-tRNA synthetase (GlnRS) and screened a library for their orthogonality toward a derived $tRNA_2^{Gln}$. An orthogonal suppressor tRNA derived from *S. cerevisiae* was imported into *E. coli*, where it showed complete inactivity toward suppression by endogenous AARS while the yeast GlnRS was able to suppress it [63]. Using this approach, two different orthogonal pairs $GlnRS/tRNA_{CUA}^{Gln}$ and aspartyl-tRNA synthetase $(AspRS)/tRNA_{CUA}^{Asp}$ from *S. cerevisiae* were generated [63, 64].

Schultz and coworkers [66] developed an orthogonal pair from *Methanococcus jannaschii* $(Mj\ TyrRS/MjtRNA_{CUA}^{Tyr})$ that showed higher aminoacylation activity toward its cognate tRNA using *E. coli*. However, the orthogonality was not as high as $ScGlnRS/SctRNA_{CUA}^{Gln}$ [63]. Using a semirational design strategy, Wang and Schutlz developed an excellent orthogonal pair of $MjTyrRS/MjtRNA_{CUA}^{Tyr}$, which they used to incorporate a variety of NAAs in *E. coli* (Table 12.2) [67–71]. Directed evolution was employed in which a $MjtRNA_{CUA}^{Tyr}$ mutant library was generated and orthogonality was established through extensive *positive* and *negative selection* (Figure 12.3a). Specifically, the 11 nucleotides of $MjtRNA_{CUA}^{Tyr}$ that were not directly involved with $MjTyrRS$ recognition were randomly mutated to generate the suppressor tRNA library [58, 76]. For the *negative selection*, $MjtRNA_{CUA}^{Tyr}$ variants were coproduced with a gene-bearing barnase containing three stop codons in *E. coli* (Figure 12.3a). When endogenous AARS from *E. coli* activated the $MjtRNA_{CUA}^{Tyr}$,
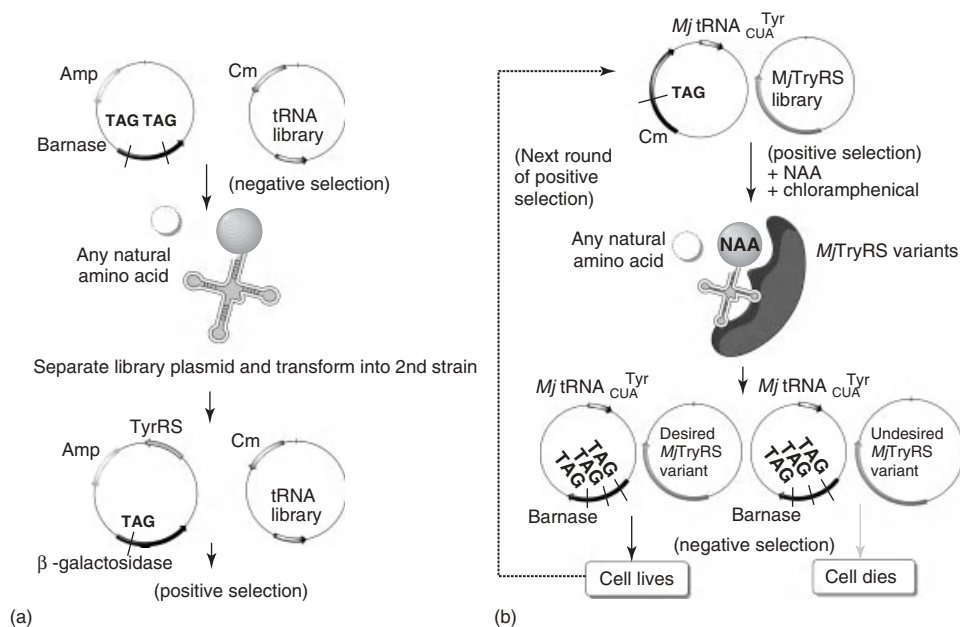
Figure 12.3 A *positive* and *negative selection* scheme for the generation of an orthogonal $MjTyrRS/MjtRNA_{CUA}^{Tyr}$ pair for SSI to develop (a) a tRNA library and (b) TyrRS library.

cell death occurred because of barnase production. The surviving cells bearing the remaining MjtRNA$_{CUA}$^{Tyr} library were selected for a round of *positive selection* (Figure 12.3a). The purified MjtRNA$_{CUA}$^{Tyr} were transformed into *E. coli* bearing the β-lactamase gene with an amber codon. Cells surviving on ampicillin (Amp) indicated that the MjtRNA$_{CUA}$^{Tyr} was charged with MjTyrRS.

The specificity of the orthogonal MjTyrRS for charging of MjtRNA$_{CUA}$^{Tyr} with particular NAA was developed through saturation mutagenesis of the five selected residues in the active site of MjTyrRS to generate a large library of mutants ($\approx$10^9 mutants) (Figure 12.3b) [77–79]. Initially, *positive selection* was performed in the presence of the NAA, MjtRNA$_{CUA}$^{Tyr}, and MjTyrRS library bearing the chloramphenicol acetyltransferase (CAT) gene with an amber TAG codon. Those cells surviving in the presence of chloramphenicol (Cm) were able to acylate the tRNA with NAA or a natural amino acid (Figure 12.3b). A *negative selection* was performed using the toxic barnase gene with in-frame nonsense codon and the natural set of 20 amino acids. Variants capable of acylating the NAA onto the orthogonal MjtRNA$_{CUA}$^{Tyr} survived (Figure 12.3b). After several rounds of *positive* and *negative selection*, MjTyrRS variants were evolved for various NAAs (Figure 12.3) [76, 80]. Using this selection scheme, many different AARS/suppressor tRNA pairs were developed for expanding the number of different NAAs into proteins, with suppression efficiencies ranging from 25 to 75% of that of wild-type protein (Table 12.2) [72, 81]. To mimic the PTM of protein sulfation, Schultz *et al.* incorporated a sulfotyrosine and *p*-carboxymethyl-L-phenylalanine into Z-domain protein in response to the amber suppression codon in *E. coli* using an evolved orthogonal pair of MjTyrRS/MjtRNA$_{CUA}$^{Tyr} [82, 83]. Similarly, glycoprotein mimetics were developed by encoding GlcNAc-Ser in *E. coli* using an evolved orthogonal pair MjTryRS/MjtRNA$_{CUA}$^{Tyr} (Table 12.2) [65].

A similar strategy was implemented by the Schultz group for the SSI of NAA in yeast using an orthogonal EcTyrRS/EctRNA$_{CUA}$^{Tyr} pair (Table 12.2) [73]. On the basis of the crystal structure of TyrRS from *B. stearothermophilus*, a library of EcTyrRS was synthesized and transformed into *S. cerevisiae* in which transcriptional activator GAL4 possessed two amber suppression codons. A *positive selection* was performed where the cells were grown in the presence of NAA and 3-aminotriazole (3-AT), lacking histidine (HIS3) and uracil (URA3). While the biosynthesis of GAL4 can lead to the production of HIS3, URA3, and lacZ, 3-AT serves as a competitive inhibitor of HIS3p (Figure 12.4). When a mutant EcTyrRS charged the EctRNA$_{CUA}$^{Tyr} with an NAA, leading to the suppression of amber codon, the cell survived because of the production of histidine and uracil. The LacZ gene, which encodes for β-galactosidase, caused the bacteria to produce a blue color when grown on a medium-containing substrate analog X-gal, serving as a colorimetric indicator to identify the active synthetase. For *negative selection*, the clones that incorporated the endogenous amino acid were removed by growing the cells in the presence of 5-fluorootic acid (5-FOA). 5-FOA could be converted into the toxic product 5-fluorouracil (5-FU) by URA3, which was expressed because of the amber suppression of GAL4 by a natural amino acid (in the absence of NAA) leading to cell death. Using this approach, five different amino acids, namely,
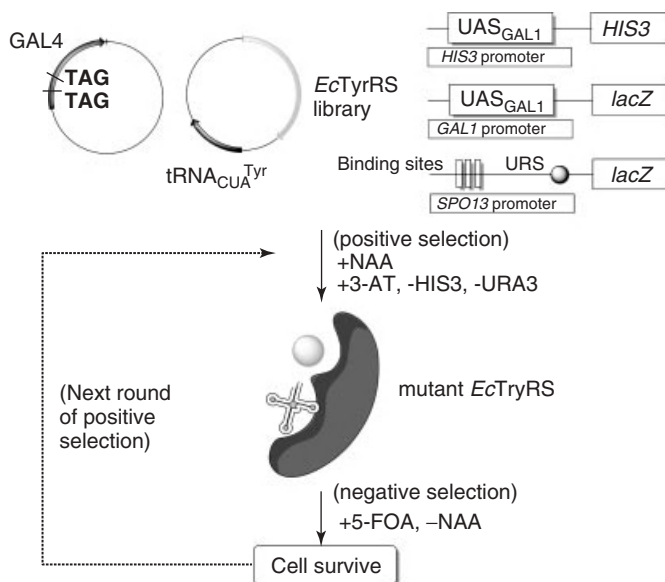
Figure 12.4 General *positive* and *negative selection* for the development of an orthogonal EcTyrRS/EctRNA$_{CUA}^{Tyr}$ pair for SSI of NAAs using *S. cerevisiae*.

p-acetylphenylalanine (pAcF), p-azidophenylalanine (pAzF), Bpa, O-methyltyrosine (OmeTyr), and p-iodophenylalanine, were incorporated using *S. cerevisiae* at a particular site with 20% yield as compared to wild-type protein [73].

Utilizing a mutant EcTyrRS evolved in *S. cerevisiae* [84] and the amber suppressor tRNA (BstRNA$_{CUA}^{Tyr}$), Schultz and coworkers [74] incorporated p-methoxy, p-acetyl, p-benzoyl, p-azido, p-iodo, and p-propargyloxyphenylalanine into the green fluorescent protein (GFP) in chinese hamster ovary (CHO) and 239T cells with the yield of up to 1 μg of protein per 2×10^7 cells with >95% fidelity (Table 12.2). The critical modifications were that (i) the anticodon of BstRNA^{Tyr} was changed to CUA (BstRNA$_{CUA}^{Tyr}$) and (ii) the 5′ flanking sequence of human tRNA^{Tyr} was added to BstRNA$_{CUA}^{Tyr}$ for efficient transcription in mammalian cells [85].

To enhance translation, three tandem repeats of BstRNA$_{CUA}^{Tyr}$ were inserted into the PUC18 vector to generate PUC18-3BstRNA$_{CUA}^{Tyr}$. The gene for EcTyrRS was inserted into a mammalian expression vector pcDNA4/TO/myc-HisA to produce (pcDNA4-EcTyrRS) in which a tetracycline-regulated cytomegalovirus (CMV) promoter controlled the expression. The orthogonality of BstRNA$_{CUA}^{Tyr}$/EcTyrRS was assayed by its efficiency in the suppression of TAG amber codon mutation at the Tyr37 position of GFP (GFP37TAG) in mammalian cells. The charging of amber codon by suppressor BstRNA$_{CUA}^{Tyr}$ led to the expression of GFP. When the CHO and 239T cells were transfected with pcDNA4-GFP37TAG and pcDNA4-EcTyrRS or PUC18-3BstRNA$_{CUA}^{Tyr}$, they did not show fluorescence, indicating that BstRNA$_{CUA}^{Tyr}$ was aminoacylated only by EcTyrRS, functioning as an effective pair for nonsense suppression in mammalian cells [74].

Wang *et al.* [75] incorporated *O*meTyr, Bpa, and 2-amino-3-(5-(dimethylamino)-naphthalene-1-sulfonamido)propanoic acid (DanAla) in mammalian HeLa cells using the *Ec*TyrRS/*Ec*tRNA$_{CUA}^{Tyr}$ pair evolved in yeast (Table 12.2). The H1 promoter was used to enhance the expression of functional tRNA; it was effectively used for biosynthesis of *E. coli* tRNAs regardless of the internal promoter. While *O*meTyrRS was specific for *O*meTyr, demonstrating 41% incorporation into GFP, BpaRS and DanAlaRS incorporated Bpa and DanAla with 13% incorporation for both.

Orthogonal Ribosomal Engineering: Positive and Negative Selection   While the development of orthogonal AARS/tRNA has led to the expansion of the genetic code for SSI in *E. coli*, yeast, and mammalian cells, the levels of NAA incorporation and protein yields vary. This is in part due to the burden that the ribosome has for not only synthesizing the target protein bearing the NAA but also producing all the proteins required for the sustenance of the cell. To address this, orthogonal ribosomes have been developed. The bacterial ribosome is a complex of rRNA and the protein that translates the mRNA into the protein. The ribosome binding site on mRNA, or the Shine–Dalgarno (SD) sequence, plays an important role in the initiation of protein synthesis [86]. The SD sequence GGAGG interacts with the complementary sequence CCUCC on the 3′ end of the 16S rRNA anti-Shine–Dalgarno sequence (ASD).

The specificity of the ribosome for a particular mRNA was achieved by Hui and de Boer [87], who synthesized a ribosome-specific mutated mRNA by changing the 5′ GGAGG SD sequence to CCUCC or GUGUG and the ASD sequence from CCUCC to GGAGG or CACAC. These complementary pairs of mRNA and 16S rRNA showed good expression of the human growth hormone (hGH) in *E. coli*. However, these specialized ribosomes with mutant SD sequence led to rapid cell lysis and death [88]. To overcome this limitation, the Chin group engineered O-ribosome/O-mRNA pairs (Figure 12.5) [89–91]. They chose −7 to −13 upstream residues on mRNA, which provided the highest information content ribosome binding and mutated all seven nucleotides to all possible sequence combinations containing all five bases of the SD sequence. An mRNA library ($4^7 = 16\,834$) was created in which more than 10^7 independent transformants were isolated. These mRNAs were transformed into GH371 cells, and ribosome binding was observed by plating the cells on agar plates containing Cm. Approximately 8000 distinct sequences were identified that did not employ endogenous ribosome. The rRNA library was created by mutating eight nucleotides in the 16S rRNA encompassing the region 1536–1541 at the 3′ end. Of the six nucleotides, five were involved in the SD–ASD interactions necessary for the translation of the mRNA. The other two mutated bases 722 and 723 protruded toward the minor groove of the SD helix. The library provided a theoretical diversity of $4^8 = 65\,536$ with more than 10^7 independent transformants of the rRNA library (Figure 12.5a).

A *positive* and *negative selection* was performed by incorporating the CAT and uracil phosphoribosyltransferase (UPRT) fusion gene downstream of a constitutive promoter and ribosome binding site (Figure 12.5b) [89]. In the first step, the
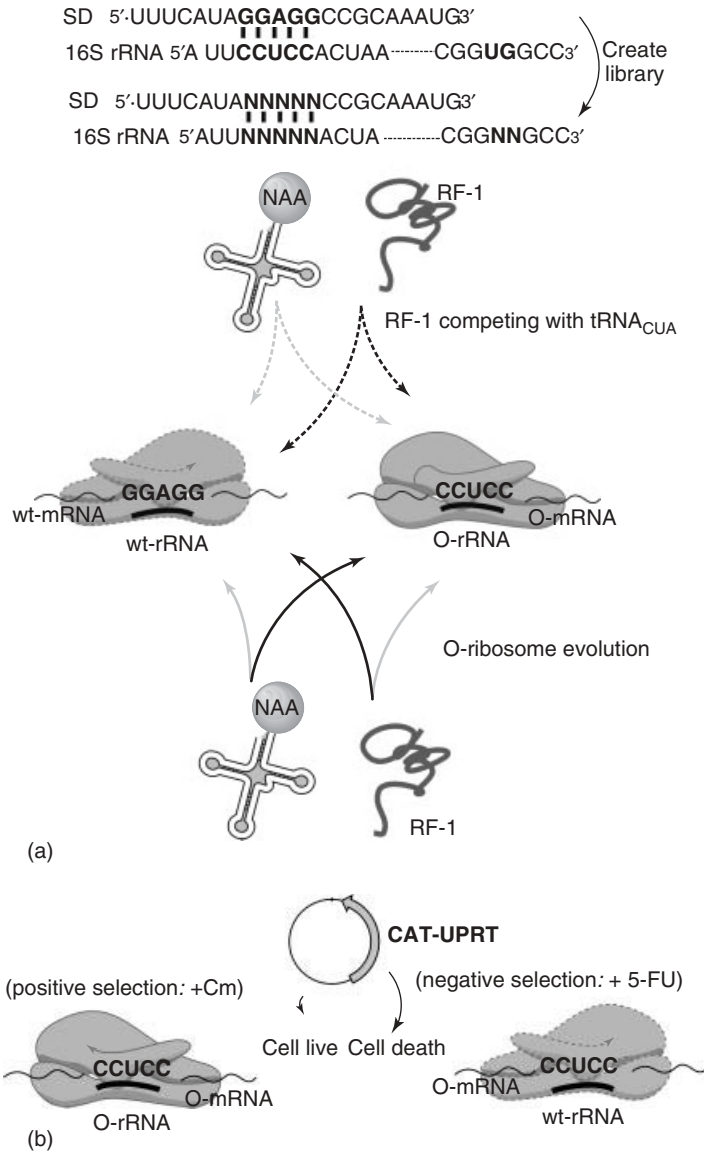
Figure 12.5 Illustration of (a) an rRNA library for O-rRNA generation and (b) development of an O-mRNA/O-ribosome via positive and negative selection.

negative selection was performed to obtain an O-mRNA, which was not translated by endogenous ribosomes. In the *negative selection,* the mutated mRNA library was grown in the presence of 5-FU. When an endogenous ribosome bound to the O-mRNA, UPRT was produced and converted the 5-FU to the toxic product 5-fluoro-dUMP, inhibiting thymidylate synthetase and causing cell death. In the

second step, *positive selection* was performed to obtain an O-ribosome by transforming the cells containing O-mRNA with a library of mutant ribosomes in the presence of chloramphenicol. When an O-ribosome bound to an O-mRNA at the ribosome binding site, the gene for *cat* was translated, leading to cell growth.

Subsequently, they generated an O-ribosome library for the SSI of NAAs at the amber codon engineered in the O-mRNA [90]. A key issue of using the amber suppression methodology to incorporate NAAs site specifically is that there is a strong competition with RF-1, which terminates the peptide before the amber codon is read by the suppressor tRNA. To overcome this limitation, the 16S rRNA, which is involved in the binding to tRNA and RF-1, was randomized at seven nucleotides in the 530 loop to create the A-site mutant library. Mutants were identified that effectively suppressed the amber codon by inhibiting the RF-1. These mutant ribosomes were transformed into *E. coli* cells with a plasmid bearing a CAT gene with a UAGA amber codon at the ribosome binding site. The UAGA-containing reporter with $tRNA^{Ser2}$ was used to select a ribosome with improved activity. The cells containing the O-CAT gene (UAGA103, UAGA146/$tRNA_{UCUA}^{Ser2}$) and the O-ribosome were grown in the presence of Cm. A variant with U531G and U534A mutations on the 16S rRNA was effective in the suppression of the UAGA codon. In this way, an orthogonal pair of O-ribosome/O-mRNA was selected.

This evolved orthogonal O-ribosome/O-mRNA pair was used to incorporate Bpa into the glutathione *S*-transferase–maltose binding protein (GST–MBP) using Bpa-tRNA synthetase/$tRNA_{CUA}^{Tyr}$ (BpaRS/$tRNA_{CUA}^{Tyr}$) developed from the $MjTyrRS/tRNA_{CUA}^{Tyr}$ pair [90, 92]. The incorporation efficiency of Bpa was increased to 62% in the presence of the O-ribosome/O-mRNA pair from 24% using the wild-type ribosome. For two amber codons suppression, the incorporation efficiency was 38% compared to the wild-type ribosome, which exhibited 6% incorporation [90]. They further expanded this approach by using a quadruplet-decoding ribosome [93]. The O-ribosome evolved from previous studies (ribo-X) [90] was mutated at 16S rRNA by saturation mutagenesis, and the O-ribosome library was cotransformed with the reporter construct (O-cat (AAGA 146)–$tRNA_{UCUU}^{Ser2}$) containing the AAGA quadruplet codon. From all the mutations, the ribo-Q1 that possessed A1196G and A1197G mutations showed greater efficiency than triplet (CUA) decoding without the evolved ribosome. When the ribo-Q1 was tested for Bpa incorporation in response to amber codon, it exhibited comparable efficiency to ribo-X. The incorporation efficiency of ribo-Q1 for the quadruplet codon was evaluated by incorporating *p*AzF into a recombinant GST–MBP fusion in *E. coli* with the use of the *p*AzFTyrRS/$tRNA_{UCCU}^{Tyr}$ pair derived from the $MjTyrRS/MjtRNA_{CUA}^{Tyr}$ [67]. The simultaneous incorporation of *p*AzF and N^6-[(2-propynyloxy)carbonyl]-ʟ-lysine into the GST–calmodulin protein was demonstrated by using the $MbPylRS/MbtRNA_{CUA}^{Pyl}$ pair [94] and the *p*AzFTyrRS/$tRNA_{UCCU}^{Tyr}$ pair in the presence of ribo-Q1 [93]. By using these orthogonal ribosomes and different AARS/suppressor tRNA pairs, it was demonstrated that a vast variety of NAAs could be incorporated with an independent and parallel coding system without affecting the cellular machinery.

12.2.1.3 **Applications**

With the development of all these approaches for SSI, a variety of NAAs have been explored. In this section, we provide examples that apply the technology of SSI to further investigate protein behavior.

Photoreactive NAAs Photoreactive NAAs are analogs that bear a photochemical cage that, on interaction with light, can be liberated to present the natural amino acid side chain [95–97]. In one of the earliest approach, Schultz and coworkers [98] reported the *in vitro* SSI of phocaged aspartyl β-nitrobenzyl ester in T4 lysozyme at Asp20 via amber suppression to confirm its significance on the binding cleft floor of T4 lysozyme. T4 lysozyme with caged Asp was catalytically inactive but, on the irradiation, it regained the activity up to 32% as that of wild-type protein.

Lester and coworkers [99] incorporated a caged Tyr (*o*-nitrobenzyl tyrosine) at three different positions into the α subunit of muscle nAChR expressed in *Xenopus* oocyte. On photolysis, Tyr was formed, and the agonist–receptor interaction was studied in real time in the presence of steady ACh concentrations. To study the kinase-dependant modulation of ion channels, a caged Tyr was incorporated via nonsense suppression at the conserved site in the potassium channel. The photolysis of this residue led to a decrease in K^+ current and activity because of kinase-initiated endocytosis and also because of the activation of the channels [100].

The Schultz group reported the SSI of photocaged *o*-nitrobenzyl-*O*-tyrosine (ONBY) using evolved orthogonal *Mj*TyrRS/*Mj*tRNA$_{CUA}$^{Tyr} in myoglobin initially using *E. coli* (Table 12.2). To develop the specificity of *Mj*TyrRS for ONBY, a library of *Mj*TyrRS mutants was developed by randomizing the six residues in its binding pocket. The screened library showed a mutant *Mj*TyrRS with residues Tyr32Gly, Leu65Gly, Phe108Glu, Asp158Ser, and Leu162Glu at the binding pocket, which were able to accommodate the bulky ONBY. The use of ONBY to control the protein function was also demonstrated by incorporating it at the catalytically active residue Tyr503 of β-galactosidase; it showed 5% activity relative to wild-type enzyme. However, after irradiation, the activity was increased up to 67% of that of the wild-type [101].

Photocross-linkable NAAs Photocross-linkable NAAs bearing a photoreactive azido or benzoyl group can be covalently cross-linked to any nearby macromolecule on UV irradiation at 365 nm. These properties of photocross-linkable NAAs have made it possible to investigate protein–protein interactions [92, 102]. Chin and Schultz demonstrated the *in vivo* incorporation of Bpa via amber suppression using the evolved *Mj*TyrRS/*Mj*tRNA$_{CUA}$^{Tyr} pair into dimeric GST protein to investigate protein–protein interactions (Table 12.2). They demonstrated that Bpa incorporation into Phe52, which was buried in the dimer interface, resulted in cross-linking on irradiation, while the control experiment with wild-type protein or the Bpa at solvent-exposed residue Tyr198 did not lead to cross-linking [92, 103].

More recently, Schultz *et al.* [104] confirmed the interaction between cyclin-dependent kinase 5 (Cdk5) and its substrate using the photocross-linkable 3′-azibutyl-*N*-carbamoyllysine (AbK). An *Mb*PylRS library was developed by

randomizing the residues Leu270, Tyr271, Leu274, Cys313, and an additional Tyr349Phe [105] to obtain a mutant that could effectively charge AbK (Table 12.2). A *positive* and *negative selection* was performed in *E. coli* as before. A mutant *Mb*TyrRS (Leu274Met, Cys313Ala, and Tyr349Phe) with *Mb*tRNA$_{CUA}$^{Pyl} showed effective amber suppression in GFP in mammalian cells. The RacGTP-dependent kinase-catalyzed phosphorylation of Pak1 by Cdk5 and its activator p35 was evaluated by coexpressing the Rac mutant, p35, Pak1, and Cdk5 with Asp144TAG in the presence of AbK. After the expression of the proteins and exposure to UV light, Cdk5 and Pak1 were cross-linked, confirming their interactions [104].

Biophysical Studies Using NAAs   The SSI of NAAs has made it possible to directly engineer biophysical probes to study the protein–protein and protein–ligand interactions. Schultz and colleagues studied the effect of several NAAs via *in vitro* amber suppression including α,α-disubstituted and *N*-alkyl amino acids, lactic acid, and an isoelectric analog of Alanine (Ala) on the thermal stability of T4 lysozyme at the Ala82 position [106]. In another study, they showed that the specific replacement of the buried residue Leu133 of T4 lysozyme with NV, ethylglycine, *O*-methyl serine, *S*,*S*-2-amino-4-methylhexanoic acid, and *S*-2-amino-3-cyclopentylpropanoic acid affected the protein stability by modulating the hydrophobicity, packing density, and side-chain conformational entropy [107].

   More recently, Hecht and coworkers employed *in vitro* amber suppression to incorporate 2-naphthylglycine (2NG), *p*-aminophenylalanine (*p*NH$_2$F), N^γ-methylarginine (MeR), N^γ-nitroarginine (NO$_2$R), citrulline (Cit), homoarginine (HR), and three conformationally constrained proline analogs at the Trp22 in DHFR with 2–27% efficiency. These analogs at Trp22 resulted in the decrease in enzymatic activity by two- to threefold compared to the wild-type protein. They also confirmed the importance of Arg218 and Arg437 in *Photinus pyralis* luciferase by incorporating MeR, NO$_2$R, Cit, and HR at that position with suppression yields of 21–36% at Arg218 and 17–50% at Arg437. The resultant proteins bearing the Arg218 substitution emitted light with less efficiency and at longer wavelength, while those bearing the Arg437 substitution showed no effect on the wavelength. This confirmed the essential role of Arg218 for maintaining the rigidity and polarity of the luciferin binding site [108].

   Using *in vivo* SSI, Dougherty and coworkers probed the role of different Tyr residues at the ligand binding site of nAChR by substituting with 3-fluorotyrosine, homotyrosine, tetrafluorotyrosine, 2-fluorotyrosine, 4-caboxyphenylalanine, 4-methylphenylalanine, 4-aminophenylalanine, 4-methoxyphenylalanine, 4-chlorophenylalanine, 4-fluorophenylalanine, 4-acetylphenylalanine, 3-hydroxyphenylalanine 3-methoxyphenylalanine, and their analogs creating an electronic perturbation in the phenol ring of Tyr. By evaluating the EC$_{50}$ values as a means of monitoring the electronic perturbation, they found that the hydroxyl group was not necessary for perturbation; rather it served as a steric placeholder [109]. For further structure/function studies of nAChR, many of the same analogs were used to probe possible cation–π interaction of the quaternary ammonium group of the ACh with several aromatic amino acids that were present near the

ligand binding site [55]. A series of fluorinated amino acids were used because they were known to have an additive effect on the cation−π interaction [110]. Using SSI, the Trp149 in the α-subunit of nAChR was identified to be important for Ach binding [110] and this was further established by using a Tyr (Tyr-O3Q) attached to the quaternary ammonium group [111]. They incorporated Tyr-O3Q at the α149 position that resulted in a constitutively active receptor in which its activation was dependent on the length of the tether group [111].

Bio-orthogonal NAAs Genetically incorporated NAAs bearing unique reactive groups such as alkynes, azides, and ketones can provide bio-orthogonal handles to selectively conjugate fluorescent tags or affinity ligands [112, 113]. In one such approach, Schultz and coworkers [114] incorporated (*S*)-2-amino-3-(4-(2-oxopropoxy)phenyl)propanoic acid into T4 lysozyme via the *in vitro* amber suppression methodology. Subsequently, it was selectively conjugated to fluorescein hydrazide for visualization by fluorescence spectroscopy.

The conjugation of fluorescent labels was recently demonstrated by Zhang and coworkers using *in vivo* incorporation of *m*-acetylphenylalanine (*m*AcF) and *p*AcF into the cytosolic *Z*-domain protein in *E. coli* via amber suppression using a mutant *Mj*TyrRS/*Mj*tRNA$_{CUA}^{Tyr}$ (Table 12.2) [115]. They also showed *in vivo* labeling of *m*AcF-incorporated membrane protein LamB with fluorescein hydrazide, Cascade blue hydrazide, Alexa568 hydrazide, and Alexa647 hydrazide in the GS20 strain of *E. coli*. A mutant *Mj*TyrRS was generated for *m*AcF by randomizing Ala67, His70, Gln155, and Ala67 residues and for *p*AcF by randomizing Tyr32, Asp158, Ile159, and Leu162 residues. Both libraries were subjected to *positive* and *negative selection* [115].

The Francis group incorporated *p*NH$_2$F into bacteriophage MS2 via the amber suppression methodology [116] using the orthogonal pair *Mj*TyrRS/ *Mj*tRNA$_{CUA}^{Tyr}$ (Table 12.2) [77]. MS2 was conjugated to three different target peptides bearing the *N,N*-diethyl-*N′*-acylphenylene diamine group at the N-terminus of each peptide via oxidative coupling reaction to develop a tumor-targeting assembly. As a further extension, they used this *p*NH$_2$F-incorporated MS2 for the development of a multivalent targeted drug delivery vehicle. They installed tyrosine kinase receptor-specific DNA aptamer that targets the Jurkat T cells and other cancer cell lines via periodate-mediated reaction with a *p*NH$_2$F aniline group. The interior Cys residues of the Asn87Cys mutant of MS2 were conjugated to Alexa Fluor 488 maleimide to observe the cellular internalization of MS2 capsid [117]. Thus simultaneous targeting and visualization was achieved.

12.2.2
Residue-Specific Incorporation (RSI)

While SSI enables the integration of NAAs at a designated position in the protein chain, RSI essentially replaces a natural amino acid for an NAA [118]. RSI is achieved by the use of auxotrophic bacteria that cannot biosynthesize one or more of the natural amino acids [118]. The NAA is added to the growth medium and

endogenous AARS will recognize the analog for subsequent incorporation [118]. The resulting protein may display completely different physicochemical properties because of the global NAA incorporation (Figure 12.6a) [118, 119].

The first ever experiment by Cohen and Munier set the stage for RSI by replacing the Met with selenomethionine, which facilitated the determination of protein structure by X-ray crystallography [120, 121]. In the recent years, many different NAAs have been incorporated into proteins using auxotrophic *E. coli*, yeast, and mammalian cells [122–124]. In a protein translation machinery, the aminoacylation of tRNA with cognate amino acid is achieved by the AARS, and the ability of the AARS to accommodate NAAs has been exploited in several ways.
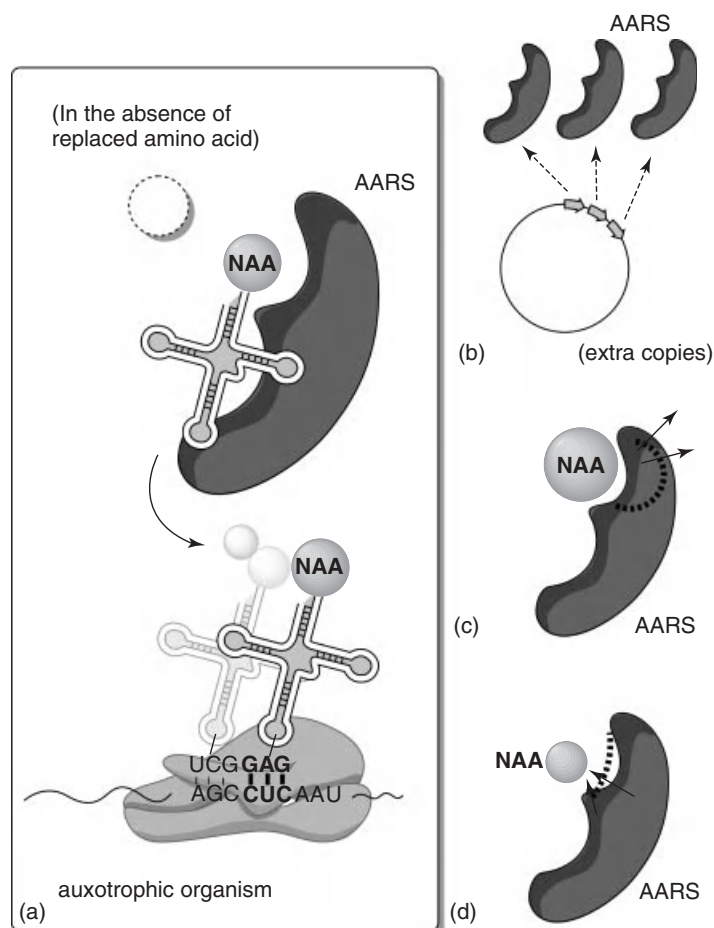
Figure 12.6 Illustration of NAA incorporation via (a) RSI using auxotrophic strain, (b) engineering additional copies of endogenous AARS, (c) expanding the AARS binding pocket, and (d) shrinking the AARS editing pocket.

12.2.2.1 Endogenous AARS

Many endogenous AARSs are known to activate the closely related analogs of natural amino acids and attach them to cognate tRNA. By using RSI, selenomethionine [120], difluoromethionine [125], trifluoromethionine [126], norleucine [123, 127], homopropargylglycine (Hpg) [128], azidohomoalanine (Aha) [129], homoallylglycine (Hag) [130], and methoxinine [127] have been incorporated using methionyl-tRNA synthetase (MetRS); per-thiaproline, 3-fluoroproline, (2S,4S)-4-fluoroproline, (2S,4R)-4-fluoroproline, (2S)-3,4-dehydroproline, (2S, 4S)-4-hydroxyproline, (2S,4R)-4-hydroxyproline, (2S)-4,4-difluoroproline, (2S)-azetidine-2-carboxylic acid, (2S)-piperidine-2-carboxylic acid, and (4R)-1,3-thiazolidine-4-carboxylic acid have been incorporated using prolyl-tRNA synthetase (ProRS) [131, 132]; trifluorovaline (TfV), 2-amino-3-methyl-4-pentenoic acid have been incorporated using isoleucyl-tRNA synthetase (IleRS) [133–135]; *o*-fluorophenylalanine, *m*-fluorophenylalanine, *p*FF [136], 2-pyridylalanine, 3-pyridylalanine, and 4-pyridylalanine [137] have been incorporated using PheRS; 4-aminotryptophan (4AW), 5-aminotryptophan (5AW), 4-fluorotryptophan (4FW), 6-fluorotryptophan (6FW), 5-hydroxytryptophan (5HW), 7AzW have been incorporated using TyrRS [138–141]; and trifluoroleucine has been incorporated using leucyl-tRNA synthetase (LeuRS) [142, 143] in *E. coli* (Table 12.3). Budisa and coworkers have explored RSI for the integration of Hpg and norleucine into the superoxide dismutase (SOD) protein in yeast [123]. The RSI of Hpg [124], azidohomoalanine [144, 145], photo-leucine, and photo-methionine [146] into mammalian cells has also been reported (Table 12.3).

Although endogenous AARSs can incorporate analogs that are structurally similar, the efficiency can be enhanced by (i) the overexpression of the corresponding AARS [130, 147, 148], (ii) shrinking the editing domain [118, 149, 150], and (iii) enlarging the amino acid binding pocket (Figure 12.6) [151–154]. By these strategies, an expanded set of NAAs have been integrated via RSI.

12.2.2.2 Overexpression of Endogenous AARS

While the inherent permissiveness of the aforementioned AARSs, that is, LeuRS, MetRS, PheRS, ProRS, TrpRS, TyrRS, and IleRS, has made it possible to incorporate predominantly isosteric analogs, certain NAAs are not integrated. A simple approach to facilitate incorporation has been to overexpress the AARS, producing extra copies for aminoacylation of the tRNA with NAAs (Figure 12.6b).

The MetRS was overexpressed in *E. coli* to incorporate the bulkier analogs 2-butynylglycine, *trans*-crotylglycine, *cis*-crotylglycine, 2-aminoheptanoic acid, NV, and allylglycine into murine dihydrofolate reductase (mDHFR) (Table 12.3) [130, 147, 148]. In addition, the reduced activity of LeuRS and IleRS for hexafluoroleucine and D,L-2-amino-5,5,5-trifluoro-3-methyl pentanoic acid, respectively, was overcome by presenting multiple copies (Table 12.3) [134, 155]. The studies on the incorporation of 4,4,4-TfV stereoisomers using endogenous ValRS or IleRS failed; however, when cells bearing either extra copies of either ValRS and IleRS were used, the incorporation of 2S,3R-TfV was observed (Table 12.3) [156].

Table 12.3 Residue-specific incorporation of NAA cells.

	AARS	NAA	References
Escherichia coli	MetRS	Selenomethionine	[120]
		Difluoromethionine	[125]
		Trifluoromethionine	[126]
		Norleucine	[123, 127]
		Aha	[129]
		Hag	[130]
		Hpg	[130]
		Methoxinine	[127]
	ProRS	per-Thiaproline	[131, 132]
		3-Fluoroproline	[131, 132]
		(2*S*,4*S*)-4-Fluoroproline	[131, 132]
		(2*S*,4*R*)-4-Fluoroproline	[131, 132]
		(2*S*)-3,4-Dehydroproline	[131, 132]
		(2*S*,4*S*)-4-Hydroxyproline	[131, 132]
		(2*S*,4*R*)-4-Hydroxyproline	[131, 132]
		(2*S*)-4,4-Difluoroproline	[131, 132]
		(2*S*)-Azetidine-2-carboxylic acid	[131, 132]
		(2*S*)-Piperidine-2-carboxylic acid	[131, 132]
		(4*R*)-1,3-Thiazolidine-4-carboxylic acid	[131, 132]
	IleRS	Trifluorovaline	[133–135]
		2-Amino-3-methyl-4-pentenoic acid	[133–135]
	PheRS	*o*-Fluorophenylalanine	[136, 137]
		pFF	[136]
		m-Fluorophenylalanine	[136]
		2-Pyridylalanine	[137]
		3-Pyridylalanine, 4-Pyridylalanine	[137]
	TyrRS	4AW, 5AW, 4FW, 6FW, 5HW, 7AzW	[138–141]
	LeuRS	Trifluoroleucine	[142, 143]
Saccharomyces cerevisiae	MetRS	Hpg	[123]
		Norleucine	[123]
Mammalian cells	MetRS	Hpg	[124]
		Aha	[144, 145]
		Photo-leucine and photo-methionine	[146]

12.2.2.3 **Shrinking the AARS Editing Pocket**

The specificity of AARS toward its cognate tRNA is very important in terms of translational fidelity, which is in part dependent on the editing pathway of the AARS. Mutation of the editing domain of AARSs has made it possible to incorporate NAAs through the unchecked misacylation with the NAAs (Figure 12.6c) [151–154].

Initially, Schimmel and coworkers [151] described that the mutation in the *E. coli* ValRS Thr222Pro effectively incorporated aminobutyrate in place of Val. In the case of LeuRS, the editing function was important to correct the misacylation of tRNA^{Leu} by Ile and Met. Toward this study, Martinis *et al.* [152] identified Thr252

as an important residue for the LeuRS editing pathway, which was effectively utilized by Tirrell and Tang for the incorporation of NAAs [153]. Three different point mutations, namely, Thr252Tyr, Thr252Leu, and Thr252Phe, that disabled the proofreading activity of LeuRS were generated. This allowed the incorporation of NV, norleucine, allylglycine, propargylglycine, homoallylglycine, homopropargyl-glycine, and 2-butynylglycine in place of Leu (Table 12.3). In a subsequent study, Tirrell and coworkers generated two LeuRS variants Thr252Ile and Thr252Val in addition to Thr252Tyr, which enabled the incorporation of oxonorvaline (Oxn) and NV (Nor) (Table 12.3). While Nor was incorporated by wild-type LeuRS, Oxn was incorporated only when the above three variants were introduced. This suggested that the hydrogen bonding between side-chain hydroxyl group of Thr252 was important in the binding of Oxn in the editing cavity of LeuRS [154].

12.2.2.4 Enlarging the AARS Binding Pocket
The charging of tRNA with a cognate amino acid is dependent on the effective binding of the amino acid to its respective AARS, and the fidelity of this process is determined by the substrate recognition. To accommodate bulkier NAAs, mutation of the amino acid side-chain recognition pocket represents an alternative strategy for facilitating incorporation (Figure 12.6d) [118, 149, 150].

Mutagenesis of the α-subunit part of the *E. coli* PheRS at Ala294Gly and Ala294Ser was employed by Kast and Hennecke [157] to enable NAA incorporation. The Ala294Gly mutation presumably enlarged the binding pocket and was capable of charging the tRNA^{Phe} with *p*FF, *p*-chlorophenylalanine, and *p*-bromo-phenylalanine (Table 12.3) [149, 150]. The Tirrell group [137] also utilized the Ala294Gly PheRS to effectively incorporate *p*-iodo-, *p*-cyano-, *p*-ethynyl-, and *p*AzF and 2-,3-,4-pyridylalanine into DHFR (Table 12.3). On the basis of the crystal structure of PheRS from *T. thermophilus* [158], the PheRS was modified further to produce a double mutant bearing Thr251Gly and Ala294Gly for the incorporation of keto functional *p*AcF (Table 12.3) [159]. Mutation of the binding pocket at Cys433Gly of ProRS facilitated the incorporation of a ring-expanded proline analog (2*S*)-piperidinyl-2-carboxylic acid into a recombinant elastinlike polypeptide (ELP) (Table 12.3) [132].

12.2.2.5 Applications
The promiscuity of wild-type AARS to accommodate several structurally similar analogs and the genetic manipulation of AARSs with compromised editing and binding activity have made it possible to globally incorporate several NAAs into proteins via RSI. In this chapter, we focus on the application of RSI of NAAs into proteins. In particular, NAAs that are photocross-linkable undergo bio-orthogonal reactions and can serve as biophysical probes.

Photocross-linkable NAAs   While SSI of photocross-linkable NAAs has been employed exclusively for the investigation of protein–protein interactions, RSI of NAAs bearing a photocross-linkable functionality has made it possible to also immobilize

the proteins on surfaces. The Tirrell group [160] developed a thin film of an artificial extracellular matrix (ECM) protein-containing CS5 cell-binding domain and an ELP containing *p*AzF. The *p*AzF was incorporated via RSI [160] using an *Ec*PheRS bearing Ala294Gly mutation [157]. UV irradiation resulted in the cross-linking of the ECM. The elastic moduli of the films were tuned by the level of *p*AzF incorporation and UV exposure time [160]. Using photolithographic techniques, a patterned surface of the cell-binding protein (CS5 or RGD) was developed and cross-linked via *p*AzF. Cell adhesion and growth studies with Rat-1 fibroblast demonstrated specific cell binding to the azide cross-linked RGD protein [161]. The reactivity of the azido group was effectively utilized for the immobilization of a protein polymer comprising an acidic component of the leucine zipper (ZE) and ELP [162]. RSI of *p*AzF into ZE-ELP polymer was immobilized on a modified glass support via photocross-linking. The ZE of the fusion was then exploited for binding to the complementary basic leucine zipper (ZR)-tagged proteins [162]. Purified GFP-ZR and GST-ZR proteins showed a specific binding to ZE. Moreover, this immobilized ZE-ELP scaffold was also sensitive to ZR-fusion proteins under denatured conditions, making it feasible to produce high-throughput protein arrays for the detection of specific proteins, thereby eliminating complex and costly purification procedures [162].

Thiele and coworkers incorporated photo-leucine and photo-methionine into caveolin-1 in COS7 cells via RSI. On UV irradiation, cross-linked caveolin-1 dimer was observed [146]. In addition, the specificity of these two photo-amino acids was investigated by cross-linking the subunits of the 19S proteosome regulatory particle. Antibodies for the two 19S subunits, Rpt4 and Rpt1, were used to analyze the cytosol of the photocross-linked HeLa cells. Rpt4 exhibited three distinct cross-linked bands, which was consistent with the reported interactions with other proteosome subunits [163]. However, Rpt1 did not show any cross-linking band with other proteosome subunits or with Rpt4. Finally, they confirmed the interaction of the progesterone-binding membrane protein PGRMC1 of the ER and a membrane protein Insig-1 in COS7 [146].

Bio-orthogonal NAAs The global analysis of protein synthesis, localization, and identification can be achieved by RSI of NAAs bearing bio-orthogonal azides and selective labeling with affinity or fluorescence tags. Both the Bertozzi and Tirrell groups [129, 164] employed the RSI of Aha using endogenous MetRS in *E. coli* to subsequently conjugate a Flag peptide-bearing triarylphosphine or alkyne biotin to proteins via Staudinger ligation or [3 + 2] cycloaddition, respectively. Tirrell and coworkers [164] also demonstrated the cell-selective metabolic labeling of proteins using Anl. An *E. coli* MetRS [165] bearing Leu13Asp, Thr260Leu, and His301Leu mutations in the binding pocket was utilized. In a complex cellular mixture, the cells that expressed the mutant MetRS were able to incorporate Anl and were conjugated to biotin-FLAG-alkyne for selective enrichment or to fluorescent dyes for visualization via Cu (I)-catalyzed cycloaddition.

Link and Tirrell [166] reported cell-surface labeling by incorporating Aha into the OmpC in *E. coli*, which was conjugated to an alkyne–biotin reagent and then to a

fluorescent dye. Flow cytometry analysis readily differentiated the Aha-bearing cells from the wild-type cells. This technique of bio-orthogonal conjugation using endogenous AARS within cells was exploited to develop bio-orthogonal noncanonical amino acid tagging (BONCAT) [124, 144, 167, 168] and fluorescent noncanonical amino acid tagging (FUNCAT) [169]. In BONCAT, newly synthesized proteins were labeled with Aha through metabolic labeling, and these proteins were covalently coupled to an alkyne-bearing biotin. The resulting conjugates were purified via avidin affinity resin and subsequently analyzed via tandem mass spectrometry after trypsinization. This approach was employed on bacteria [164], neuronal cells [169], and mammalian cells [124, 144, 168]. In a similar study, Bertozzi and coworkers [170] employed an azide-reactive cyclooctyne resin for selective enrichment of Aha-containing proteins. In FUNCAT, the labeling of the azide-containing protein was achieved by fluorescent tagging of both Aha and Hpg using endogenous MetRS from mammalian [167] or rat neuronal cells [169]. Both NAAs were exclusively incorporated into newly synthesized proteins, which could be visualized *in situ* by fluorescence microscopy [169]. Recently, Brittis *et al.* used a similar approach and incorporated Aha into the newly synthesized proteins in axons and dendrites. Fluorescence tagging of Aha showed that the transmembrane receptor DCC, which regulated axon growth, colocalized in the same region as that of newly synthesized protein and mediated the translational regulation in response to its ligand netrin [171].

Bio-orthogonal handles have been employed to decorate proteins with sugars for application in drug delivery and imaging. Davis and coworkers [172] demonstrated the glycosylation of different proteins via free radical hydrothiolation of Hag, which was incorporated via RSI (Table 12.3). A β-glycosidase mutant protein with Met43 was used for RSI of Hag using endogenous MetRS. 1-Thio-β-D-glucose (GlcSH) was selectively conjugated with 95% yield using a water-soluble initiator Vazo44 (VA044, 2,2′-azobis[2-(2-imidazolin-2-yl)propane]dihydrochloride) and UV light (365 nm). They extended the glycoconjugation to the self-assembled multimeric viruslike particle Qβ displaying 180 Hag at predetermined sites. The hydrothiolation with GlcSH exhibited complete glycosylation at all 180 Hag residues [172]. In addition, the Davis group conjugated the azide-bearing fluorosugar 2-deoxy-2-fluoroglucose to the Hpg-incorporated β-glycosidase and viruslike particle Qβ via Cu-catalyzed [3 + 2] cycloaddition reaction. This homogeneously fluorinated glycoprotein under mild conditions could be effectively used as a biophysical probe for NMR and MRI [173].

Biophysical Studies Using NAAs   NAAs can serve as biophysical probes, offering a unique opportunity to study the structure and function of protein using different spectroscopic techniques. Wong and Eftink [174] employed RSI of 5HW, 7AzW, 4FW, 5-fluorotryptophan (5FW), and 6FW into Staphylococcal nuclease (Table 12.3). 5HW showed both a redshifted absorbance and fluorescence compared to the wild-type protein, while incorporation of 6FW showed similar behavior to wild-type. The 4FW-bearing protein exhibited a blue shift in absorbance and fluorescence with comparable quantum yield, rendering it a suitable candidate for

forming fluorescence ''knock-out'' proteins. The 7AzW had a redshifted absorbance spectrum, and the fluorescence was very sensitive to the environment. In addition, the fluorotryptophans enabled biophysical investigation via ^{19}F NMR through the enhanced chemical shift [174].

The Budisa group demonstrated the usefulness of 4AW and 5AW by incorporating them into barstar protein and performed pH-responsive studies for the absorption and emission maxima (Table 12.3) [175]. The UV absorbance spectra of 4AW and 5AW were pH sensitive. At pH 3.0, 4AW–barstar and 5AW–barstar showed similar spectra. However, at pH 7 and 9, the main absorption peak at 281 nm was blueshifted, while the spectral shoulder was redshifted for both 4AW–barstar and 5AW–barstar. Also, the pH-dependent fluorescence studies demonstrated a blueshifted emission maximum in case of 4AW and a redshift for 5AW. This pH sensitivity of 4AW– and 5AW–barstar was entirely due to the intramolecular charge migration that occurred as a result of cation to anion transition of aminoindoles around pH 6. RSI of 4AW in place of Trp chromophore site of the enhanced cyan fluorescent protein (ECFP) resulted in a red shift in the emission by 50 nm with respect to the parent ECFP, resulting in a golden fluorescent protein (GdFP). Surprisingly, aggregation was negligible in case of GdFP relative to ECFP at 4 °C for up to six months [176]. Subsequently, Kurschus and coworkers [177] fused the GdFP to human annexin A5 (anxA5) to generate an apoptosis-detecting agent. The GdFP–anxA5 bound membrane phosphotidylserine patches of apoptotic cells, leading to visualization via flow cytometry. The RSI of Tyr analogs 2-fluorotyrosine (2FY) and 3-fluorotyrosine (3FY) into *Agriocnemis Victoria* green fluorescent proteins (avGFPs) produced ''enhanced green'' and ''enhanced yellow'' variants with modified spectral properties [178]. The incorporation of 3FY resulted in a red shift, while 2FY caused a blue shift in the fluorescence. In another study, the Budisa group developed a blue fluorescence anxA5 protein by the RSI of 4-azatryptophan (4AzW) and 5-azatryptophan (5AzW). The fluorescence emission maximum of 4AzW–anxA5 was more redshifted than 5AzW–anxA5 (Table 12.3) [179].

12.3
Intein-Inspired Ligation Approach

An alternative approach for the incorporation of NAAs exploits intein-mediated ligation in which a peptide with an NAA is ligated to another peptide (expressed/synthesized) with or without an NAA. Inteins are internal segments of precursor proteins that splice themselves during the posttranslational process via intramolecular rearrangement, leading to the ligation of two external flanking portion termed *exteins* [180]. In the first step of protein splicing mechanism, the N-extein is transferred to the -SH or -OH group of Cys/Ser residues located immediately at the N-terminus of the intein (N to S or N to O acyl shift). In the second step, the N-terminal extein is transferred to the Cys/Ser/Thr residue at the +1 position of C-extein, leading to the branch intermediate. In the final step, the conserved Asn residue at the C-terminus of the intein cyclizes and excises the

intein as a C-terminal succinimide derivative. The peptide bond is formed between two exteins through S to N acyl shift (Scheme 12.2) [181]. Inteins are found in all phylogenic domains: eukaryotes, bacteria, and archaea, with more than 115 inteins listed in the intein database InBase [182, 183]. Inteins are predominantly found in enzymes including DNA and RNA polymerase, metabolic enzymes, proteases, and vacuolar-type ATPase [183].

12.3.1
Native Chemical Ligation (NCL)

Inspired by inteins, native chemical ligation (NCL) involves the chemoselective reaction between an N-terminal Cys or selenocysteine (Sec) residue of one peptide fragment and another peptide with C-terminal α-thioester group (Scheme 12.2a) [184]. This transthioesterification reaction is followed by a spontaneous intramolecular S/Se to N acyl shift, which results in an amide bond at the site of ligation leading to a full-length polypeptide bearing a Cys or Sec at the conjugation site. Using this method, it is possible to incorporate NAAs by essentially having either peptide fragment bear the NAA.

12.3.1.1 Sulfur-Based N-Terminal Residue

In order for the initial transthioesterification to occur, a side chain bearing a thiol is needed at the N-terminus [184]. Commonly, Cys is employed, but, as Cys is rarely present in proteins, an alternative method has been developed in which the Cys is replaced with the NAA homocysteine (Hcy). Hcy at the N-terminus reacts in the same way as Cys with the peptide-bearing Cα-thioester [185]. After NCL, the Hcy is converted into Met by methylation. In another approach, an auxiliary groups 2-mercaptobenzylamine (2MB) [186] and oxyethanethiol (OET) [187] have been used to overcome the requirements of N-terminal Cys. These groups mimic the Cys thiol group allowing for NCL, but they can be removed. A photoremovable 2-mercapto-1-(2-nitrophenyl)ethylamine was attached to the N-terminal amino acid of a peptide via periodate oxidation of the N-terminal Ser. After ligation, this group was removed by UV irradiation, producing the native peptide bond [188]. The major limitation of using auxiliary groups is that they need to be synthesized [189].

12.3.1.2 Selenocysteine-Based N-Terminal Residue

While sulfur-bearing residues have been employed at the N-termini for NCL, the selenium-containing amino acid Sec has been successfully used for NCL. With an understanding of reactivity, Hilvert *et al.* demonstrated the NCL synthesis of the bovine pancreatic trypsin inhibitor (BPTI) using Sec [190]. Two fragments of BPTI, in which one possessed a C-terminal amino acid thioester and the other contained an N-terminal Sec in place of Cys38, were synthesized by solid-phase peptide synthesis (SPPS). The ligated Cys38Sec−BPTI protein exhibited the same inhibition activity toward trypsin and chymotrypsin as that of wild-type BPTI [190]. Raines and coworkers [191] reported the use of N-terminal Sec for NCL and compared the rate of conjugation to that of Cys. A model thioester peptide
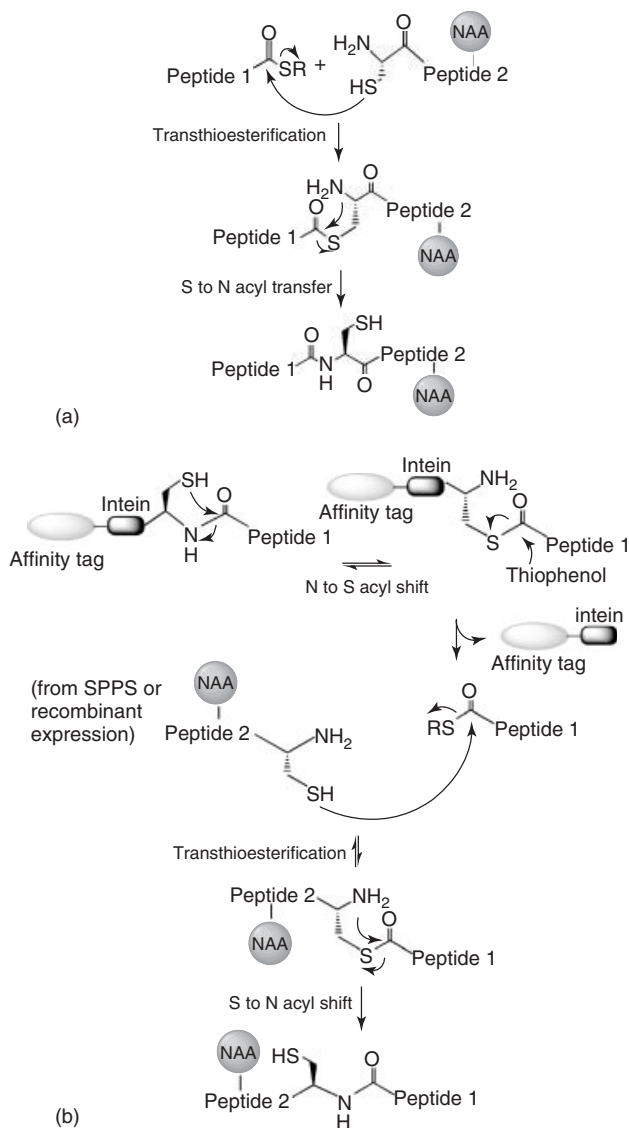
Scheme 12.2 Intein-inspired mechanisms of (a) NCL and (b) EPL.

AcGlySCHC(O)NHCH$_3$ was reacted with cysteine (CysOH)$_2$ in the presence of the reducing agent tris-(2-carboxyethyl)phosphine, which resulted in the formation of AcGlyCysOH and (AcGlyCysOH)$_2$. When (SecOH)$_2$ was used, (AcGlySecOH)$_2$ was formed (Scheme 12.2d). As Se was easier to ionize than S, the pK_a of RSeH was lower than that of RSH, suggesting that the selenolate (RSe-) was more nucleophilic than thiolate (RS-). Owing to this property of Se, the reaction rate of NCL was higher

for Sec, which was confirmed by the chromogenic thioester $AcGlySC_6H_4$-p-NO_2 as a function of pH.

12.3.2
Expressed Protein Ligation (EPL)

As an extension of NCL, expressed protein ligation (EPL) has been developed in which a recombinant protein bearing C-terminal thioester is ligated to either a chemically synthesized or another expressed protein/peptide containing an N-terminal Cys or Sec (Scheme 12.2b) [192, 193]. In the first step of EPL, the purified recombinant protein with a C-terminal intein fusion is reacted with thiophenol or 2-mercaptoethanesulfonic acid, which promotes intein-mediated transthioesterification to produce the Cα-thioester. The N-terminal Cys/Sec can be synthesized through standard SPPS or recombinantly generated in which the N-terminal of Cys is fused to an intein that can be cleaved by thiols, pH change, or temperature [194].

In order to incorporate NAAs, the fragment that is synthetically produced can bear the NAAs. For example, Muir and coworkers [192] ligated a synthetic peptide carrying the NAA phosphotyrosine to the C-terminus Src kinase (Csk), which was expressed as an intein fusion to generate the Cα-thioester Csk. The resultant fusion protein showed an increased catalytic phosphoryl transfer to a substrate compared to the nonphosphorylated control. The effect of phosphorylation at two Tyr residues on the protein tyrosine phosphtase (PTPase) SH-2 was monitored by introducing phosphonomethylene-phenylalanine at the phosphorylation sites of SH-2 using EPL [195]. The phosphorylation at Tyr542 resulted into the inhibition of PTPase activity, while phosphorylation at Tyr580 enhanced PTPase activity by interacting with the C-terminal SH-2 domain.

More recently, Lu and coworkers [196] synthesized an azurin metalloprotein variant containing Sec at the active site Cys using EPL. A peptide with C-terminal 17 residues of azurin was synthesized by SPPS with Sec at the N-terminal of the peptide and the remaining truncated azurin expressed as an intein fusion. EPL was carried out in the presence of mercaptoethane sulfonic acid. The resulting variant exhibited altered spectroscopic properties compared to wild-type protein, perhaps due to change in metal coordination geometry; however, the reduction potential was same as that of wild-type [196].

The Stubbe group [197, 198] replaced Tyr356 with 2,3-difluorotyrosine (DFT) and pNH$_2$F to probe the role of the tyrosine radical in the catalytic activity of the ribonucleotide reductase (RNR) enzyme. The R2 subunit of RNR (1−353) was expressed recombinantly and ligated to synthetic peptide with residues 354−375 containing DFT and pNH$_2$F at Tyr356 position. At pH > 8.0, the DFT-bearing R2 having pK_a of 7.4 was completely deprotonated, supporting the mechanism of proton-coupled transfer for RNR activity. The pNH$_2$F-containing R2 showed a decrease in activity with increase in pH, suggesting that proton transfer before electron transfer is not necessary for radical transfer through Tyr356 position.

The major advantage of EPL is that it does not require the complex genomic synthesis of the AARS specific for NAA, as it is entirely dependent on the ligation to a synthetic peptide bearing an NAA. Using SPPS, any NAA can be integrated into the peptide at a specific position. In addition, multiple peptides can be coupled to each other to generate a full-length protein or then can be coupled to the expressed protein via NCL. Although the EPL serve as an excellent tool to modify the protein by attaching versatile sets of synthetic peptides containing NAAs at specific positions, arguably it still requires the N-terminal Cys or Sec. For those that employ auxiliaries groups that have been introduced in place of Cys/Sec, devising methods for the removal of those groups are needed. As the NAA incorporation occurs synthetically, the size of the peptide fragment is limited to the capabilities of SPPS.

12.4
Combined Approach

All the previous approaches facilitate the incorporation of NAAs in different ways, and these strategies can be combined with each other to generate modified proteins. In particular, RSI and SSI have been merged to intein-mediated EPL and NCL to produce domain-specific labels, photoreactive splicing, cyclic peptides, and PTMs.

12.4.1
RSI and EPL

RSI of NAAs into one domain has been combined with NCL as a means of ligating a labeled fragment to the remainder of a protein. In one such approach, Muir and coworkers [199] modified a multidomain c-Crk-I adapter protein. The protein consisted of a Src homology 2 domain (SH2) and a Src homology 3 domain (SH3) possessing two Trp residues. To study the folding and thermodynamic properties of SH3 domain in the context of full-length protein, they incorporated 7AzW via RSI into the SH3 domain (C125−G206). The SH2 domain (A1−G124) was expressed separately in *E. coli* by using gyrase A intein fusion, and thiolysis of the fusion protein yielded the SH2 α-thioester protein. Ligation of 7AzW-labeled SH3 domain with SH2 domain via EPL generated a native c-Crk-I protein with a domain-specific label [199].

12.4.2
SSI and Intein-Mediated Ligation

Photoreactive intein splicing was demonstrated by Noren *et al.*, in which a caged serine (2-nitrobenzylether of serine) was incorporated via *in vitro* SSI at the splice

junction of intein-2 from *T. litoralis* DNA polymerase via amber suppression in presence of chemically aminoacylated $tRNA_{CUA}^{Ser}$. Upon irradiation at 300–350 nm, the caged serine underwent rapid conversion, generating free serine and the spliced intein [200].

Split-intein-catalyzed ligation of proteins and peptides (SICLOPPS) was effectively utilized by the Schultz group to develop a therapeutic cyclic peptide. Diverse set of hexapeptides were inserted between the split inteins and cotransformed with a plasmid vector encoding an orthogonal pair of $MjTyrRS/MjtRNA_{CUA}^{Tyr}$ to incorporate Bpa via amber suppression. A vector comprising HIV protease gene and a tetracycline resistance gene bearing the HIV protease recognizing sequence was coexpressed with the hexapeptide-containing plasmid and a plasmid vector encoding $MjTyrRS/MjtRNA_{CUA}^{Tyr}$. Cells were grown on LB agar plates containing tetracycline, and those that exhibited tetracycline resistance resulted from the inhibition of HIV protease by the expressed cyclic peptide. The resultant cyclic peptides with the sequence GIXVSL (X – TAG codon for Bpa), VVIPXI, and ILLGYN without any amber codon were able to inhibit the HIV protease. For the peptide-bearing, Bpa the inhibition was due to a Schiff-base formation between Bpa and the ε-amino group of Lys14 on protease [201].

Site-specific ubiquitination was effectively achieved by ligating a pyrrolysine analog incorporating calmodulin (CaM) and Ubiquitin (Ub) [202]. Chan and workers demonstrated the SSI of *tert*-butylN^2-(*tert*-butoxycarbonyl)-N^6-((*S*)-(−)-2-*tert*-butoxycarbonylamino-3-(tritylthio) propanoyl)lysinate, a D-cysteine-based analog of (*S,S*)-D-Cys-ε-Lys, into CaM via amber suppression at Lys21 using the $MbPylRS/MbtRNA_{CUA}^{Pyl}$ pair in *E. coli* (Table 12.2). The truncated ubiquitin Ub75 was produced as an intein fusion and converted into Ub75 thioester by thiolysis using 2-mercaptoethane sulfonate. The Ub75 thioester was ligated to (*S,S*)-D-Cys-ε-Lys of CaM (UbΔ-CaM) via NCL. The NCL-synthesized UbΔ-CaM showed 85% decrease in its ability to modulate the PK as compared to wild-type CaM and these results were comparable to the enzymatically generated Ub-CaM.

12.5
Protein and Polymer Conjugates

The inherent specificity and specialized biological function of proteins make them a suitable candidate as a therapeutic agent and for other biotechnological applications. The conjugation of protein to different synthetic polymers has shown promising results with increase in the stability, solubility, biocompatibility, and modulation of their activity [203–207]. Protein–polymer conjugates have been extensively studied, and many smart polymer bioconjugates have been developed with a variety of applications including biosensing and molecular switches [208, 209], affinity purification [210, 211], microfluidics [212], and enzyme bioprocessing [213–215].

12.5.1
PEGlyation of Proteins via NAA

The PEGlyation of proteins enhances *in vivo* stability through increase in plasma half-life, resistance to proteolytic cleavage, and reduction in immunogenicity. Hohsaka and coworkers [216] demonstrated polyethylene-conjugated amino acid (PEGylated) incorporation via the CCCG–CGGG codon–anticodon into streptavidin using the *E. coli* cell-free translation system. The PEGylated pNH$_2$F (PEG$_n$$pNH_2$F) and Lys (PEG$_n$Lys) derivative were developed with varying length of polyethylene glycol (PEG) ($n = 4, 8, 12$). The PEGlyated aminoacyl-pdCpAs of pNH$_2$F and Lys were ligated to the yeast tRNA^{Phe} that encode for CCCG anticodon. PEG$_4$$pNH_2F, PEG_8$$pNH_2$F, and PEG$_{12}$$pNH_2$F were incorporated at the Tyr83 position in streptavidin with an efficiency of 46, 18, and 4%, respectively. However, the PEG$_n$Lys was not incorporated at that position. Incorporation at the N-terminal region of protein was further explored; while PEG$_4$$pNH_2$F and PEG$_{12}$$pNH_2$F demonstrated 80 and 50% incorporation, respectively, PEG$_4$Lys and PEG$_8$Lys surprisingly exhibited only 30% incorporation [216].

The introduction of reactive bio-orthogonal handles via NAA has been studied extensively. In particular, NAAs have been effectively used to conjugate synthetic polymers such as PEGs. The Schultz lab performed SSI of pAzF into SOD-1 protein via amber suppression using an orthogonal *Mj*TyrRS/mutant *Mj*tRNA$_{CUA}$^{Tyr} pair from *E. coli* into an *E. coli* expression system (Table 12.2). It was conjugated to an alkyne-derivatized PEG via [3 + 2] cycloaddition reaction [217]. More recently, Cho and coworkers [218] developed a PEGylated hGH which is in clinical Phase I–II trial for the treatment of pathological short stature and other growth-associated abnormalities. A total 20 amino acids on hGH were selected for SSI of pAcF via amber suppression using an orthogonal *Mj*TyrRS/*Mj*tRNA$_{CUA}$^{Tyr} in *E. coli*. A linear 30 kDa PEG with an amino-oxy group was conjugated to pAcF-hGH, and the resulting oxime bond was stable at physiological pH over a one-year period. The potency of the pAcF-hGH was evaluated *in vitro* in a human IM-9 cell to confirm Signal transducers and activators of transcription 5 (STAT5) phosphorylation in response to the hGH receptor binding. From this, six PEGylated derivatives were selected for *in vivo* studies in rats, which showed that the site of PEGylation significantly affected the pharmacokinetics and pharmacodynamics of the conjugated derivative. Clinical studies with hGH-Y35pAcF-PEG on GH-deficient patients showed an enhanced half-life of 89–102 h, leading to rapid normalization of insulin-like growth factor 1 (IGF-1) level [218].

Using RSI, Carrico *et al.* demonstrated the integration of Aha into human adenovirus type 5 (hAd5) in HEK293 mammalian cells, and the surface-exposed azide moiety was effectively conjugated to the alkyne-PEG-folate for targeted delivery to the cancer cells [219]. A 18- to 20-fold increase in transgene expression of the reporter luciferase gene was observed compared to the unmodified virus particle [219]. The C-terminal site-specific PEGylation of a truncated thrombomodulin (TM) mutant was reported via RSI of Aha that was conjugated to PEG-triarylphosphine via

Staudinger ligation [220]. PEG–TM showed similar bioactivity to that of wild-type TM toward the thrombin-catalyzed activation of protein C [220].

The van Hest group performed RSI of Aha into *Candida antarctica* lipase B (CalB) consisting of five Met residues out of which four were buried into protein. The Aha-labeled CalB was conjugated to alkyne-functionalized PEG5000 via Cu-catalyzed [3 + 2] cycloaddition reaction. The resultant PEG–CalB exhibited hydrolytic activity similar to that of wild-type CalB [221]. To avoid the issue of Cu (I) binding to the active site of CalB, in addition to toxicity to cells, they subsequently used aza-dibezocyclooctyne-modified PEG2000 which was conjugated to CalB via strain-promoted [3 + 2] cycloaddition reaction [222].

12.6
Modulating the Physicochemical Properties of Protein Polymers via NAA Incorporation

The vast diversity of NAAs, in addition to the different methods for the integration of several analogs, has made it possible to synthesize tailored protein materials with versatile functionalities [122]. Many functional groups including alkyne, alkene, ketone, and azides have been incorporated into the proteins via NAA, providing an orthogonal handle for protein modifications [122, 223, 224]. Halogenated NAAs, especially fluorinated amino acids, have made a significant impact on protein engineering [133, 155, 225–232]. Repetitive protein polymers with fluorinated amino acid have shown distinct physicochemical properties, including an increase in thermal and chemical stability [155, 228], as a result of the electronegativity and hydrophobicity of the fluorine atom [233, 234]. For example, fluoroprolines incorporated into the elastinlike peptide (ELP) containing a repeat unit of (Val-Pro-Gly-Val-Gly) was explored by Conticello and coworkers [235]. To assess the stereoelectronic effect, RSI of (2*S*,4*S*)-4-fluoroproline (2*S*4*S*FP) and (2*S*,4*R*)-4-fluoroproline (2*S*4*R*FP) into ELP was conducted. The studies revealed that 2*S*4*R*FP favored type II β-turn population in protein, decreasing the lower critical solution temperature (LCST); however, 2*S*4*S*FP exhibited the opposite effects [235]. Recently, they showed that, when (2*R*,3*R*)-3-fluoroproline was incorporated in to ELP via RSI, the LCST increased as also the type II β-turn conformation. However, the RSI of (2*R*,3*S*)-3-fluoroproline decreased the LCST and it showed a characteristic type I β-turn structure. These studies confirmed that the stereoelectronic and steric effect altered the conformational energetics of ELP [236].

12.7
Future in Combined Technologies to Fabricate Tailored Protein-Polymer Conjugates as New Materials

The unrivaled diversity of protein structures and functions, in addition to the developments in the field of NAA incorporation, has made it possible to fabricate tailored

protein materials with a range of applications. While research in exploring protein function and labeling has been extensively developed, efforts in the fabrication of protein materials exploiting NAA have been limited.

Van Hest and coworkers [237] developed a clickable ELP via RSI of Aha and Hpg. A fluorescent protein–polymer hybrid was synthesized by reacting a coumarin-functionalized PEG2000-bearing azide with Hpg-ELP via Cu (I)-catalyzed azide–alkyne cycloaddition. In addition, the azide-functionalized CalB generated via RSI of Aha [221] was conjugated to Hpg-ELP, shifting the LCST behavior from the ELP to the CalB, while maintaining 50% of its hydrolytic activity relative to the conjugated Aha–CalB [237].

Many different protein–polymer conjugates have been developed by chemically conjugating synthetic polymers to proteins via functional groups provided by natural amino acids [238, 239]. Researchers have effectively utilized the reversible addition-fragmentation chain transfer (RAFT) or the atom-transfer radical polymerization (ATRP) via coupling the reactive initiator to the protein [240]. However, this method failed to produce homogeneous proteins with reactive polymer initiator at specific sites of the protein. To overcome these difficulties, Mehl and coworkers [241] developed a genetic approach in which 4-(2′-bromoisobutyramido)-phenylalanine (BiaF) was incorporated in response to the amber codon using the evolved orthogonal pair MjTyrRS/MjtRNA$_{CUA}^{Tyr}$ (Table 12.2). A GFP with amber codon at 134 showed effective incorporation of BiaF. A GFP with BiaF (which served as an initiator) was mixed with a monomer oligo (ethylene oxide) monomethyl ether methacrylate (OEO300MA) and the ATRP reaction was initiated by adding 2,2′-bipyridine and Cu^+/Cu^{+2}. The polymer growth from GFP–BiaF was confirmed, as an increase in molecular weight was observed while the wild-type GFP showed no change. Size-exclusion chromatography showed that 93% of GFP–BiaF was converted into the high-molecular-weight polymer within a reaction time of 180 min. The resultant polyMPEG-GFP exhibited similar fluorescence as that of the wild-type with the expected molecular weight increase (120 kDa) when characterized by SDS-PAGE. This method provided access to the diverse sites on the protein via SSI of the polymer initiator, and the initiator incorporation could be further reacted to fabricate novel protein–polymer hybrid biomaterials with unprecedented properties.

12.8
Conclusion and Future Perspectives

In vitro and *in vivo* approaches have proven to be very effective in incorporating a wide range of structurally diverse sets of NAAs. The development of selection and screening methods has remarkably improved the ability to genetically encode NAAs. This, coupled with the recent advances in intein-inspired methods, certainly makes NAA incorporation more accessible for scientists. Indeed, these methods have been extremely valuable tools to further investigate protein structure and function in addition to produce protein materials with application in drug delivery

and medicine [116, 161, 162, 173, 219]. While considerable efforts have been made for the incorporation of NAA into proteins, some of the challenges that remain are to expand the incorporation capabilities in other multicellular organisms and increase the yields of the resultant proteins for future applications.

Acknowledgments

References

1. Walsh, C.T., Garneau-Tsodikova, S., and Gatto, G.J. (2005) *Angew. Chem. Int. Ed.*, **44**, 7342–7372.

2. Manning, G., Whyte, D.B., Martinez, R., Hunter, T., and Sudarsanam, S. (2002) *Science*, **298**, 1912–1934.

3. Pawson, T. (2002) *Eur. J. Cancer*, **38** (Suppl.5), S3–S10.

4. Johnson, L.N. and Lewis, R.J. (2001) *Chem. Rev.*, **101**, 2209–2242.

5. Allfrey, V.G. (1966) *Proc. Can. Cancer Conf.*, **6**, 313–335.

6. Doucey, M.A., Hess, D., Blommers, M.J., and Hofsteenge, J. (1999) *Glycobiology*, **9**, 435–441.

7. Gu, W. and Roeder, R.G. (1997) *Cell*, **90**, 595–606.

8. Lee, Y.H. and Stallcup, M.R. (2009) *Mol. Endocrinol.*, **23**, 425–433.

9. Khorasanizadeh, S. (2004) *Cell*, **116**, 259–272.

10. Kouzarides, T. (2007) *Cell*, **128**, 693–705.

11. Gary, J.D. and Clarke, S. (1998) *Prog. Nucleic Acid Res. Mol. Biol.*, **61**, 65–131.

12. Paik, W.K., Paik, D.C., and Kim, S. (2007) *Trends Biochem. Sci.*, **32**, 146–152.

13. Lee, D.Y., Teyssier, C., Strahl, B.D., and Stallcup, M.R. (2005) *Endocrinol. Rev.*, **26**, 147–170.

14. Bedford, M.T. and Richard, S. (2005) *Mol. Cell*, **18**, 263–272.

15. Spiro, R.G. (2002) *Glycobiology*, **12**, 43R–56R.

16. Furmanek, A. and Hofsteenge, J. (2000) *Acta Biochim. Pol.*, **47**, 781–789.

17. Helenius, A. and Aebi, M. (2004) *Annu. Rev. Biochem.*, **73**, 1019–1049.

18. Moremen, K.W., Trimble, R.B., and Herscovics, A. (1994) *Glycobiology*, **4**, 113–125.

19. Clausen, H. and Bennett, E.P. (1996) *Glycobiology*, **6**, 635–646.

20. Hofsteenge, J., Muller, D.R., de Beer, T., Loffler, A., Richter, W.J., and Vliegenthart, J.F. (1994) *Biochemistry*, **33**, 13524–13530.

21. de Beer, T., Vliegenthart, J.F., Loffler, A., and Hofsteenge, J. (1995) *Biochemistry*, **34**, 11785–11789.

22. Hartmann, S. and Hofsteenge, J. (2000) *J. Biol. Chem.*, **275**, 28569–28574.

23. Krieg, J., Hartmann, S., Vicentini, A., Glasner, W., Hess, D., and Hofsteenge, J. (1998) *Mol. Biol. Cell*, **9**, 301–309.

24. Vranka, J.A., Sakai, L.Y., and Bachinger, H.P. (2004) *J. Biol. Chem.*, **279**, 23615–23621.

25. Myllyharju, J. (2003) *Matrix Biol.*, **22**, 15–24.

26. Oikarinen, A., Anttinen, H., and Kivirikko, K.I. (1976) *Biochem. J.*, **156**, 545–551.

27. Baeuerle, P.A. and Huttner, W.B. (1987) *J. Cell Biol.*, **105**, 2655–2664.

28. Lee, R.W. and Huttner, W.B. (1983) *J. Biol. Chem.*, **258**, 11326–11334.

29. Stone, M.J., Chuang, S., Hou, X., Shoham, M., and Zhu, J.Z. (2009) *Nat. Biotechnol.*, **25**, 299–317.

30. Leyte, A., van Schijndel, H.B., Niehrs, C., Huttner, W.B., Verbeet, M.P., Mertens, K., and van Mourik, J.A. (1991) *J. Biol. Chem.*, **266**, 740–746.

31. Seibert, C. and Sakmar, T.P. (2008) *Biopolymers*, **90**, 459–477.

32. Medzihradszky, K.F., Darula, Z., Perlson, E., Fainzilber, M., Chalkley, R.J., Ball, H., Greenbaum, D., Bogyo, M., Tyson, D.R., Bradshaw, R.A., and Burlingame, A.L. (2004) *Mol. Cell Proteomics*, **3**, 429–440.

33. Voloshchuk, N. and Montclare, J.K. (2010) *Mol. Biosyst.*, **6**, 65–80.

34. Hecht, S.M., Alford, B.L., Kuroda, Y., and Kitano, S. (1978) *J. Biol. Chem.*, **253**, 4517–4520.

35. Heckler, T.G., Chang, L.H., Zama, Y., Naka, T., Chorghade, M.S., and Hecht, S.M. (1984) *Biochemistry*, **23**, 1468–1473.

36. Johnson, A.E., Woodward, W.R., Herbert, E., and Menninger, J.R. (1976) *Biochemistry*, **15**, 569–575.

37. Baldini, G., Martoglio, B., Schachenmann, A., Zugliani, C., and Brunner, J. (1988) *Biochemistry*, **27**, 7951–7959.

38. Noren, C.J., Anthony-Cahill, S.J., Griffith, M.C., and Schultz, P.G. (1989) *Science*, **244**, 182–188.

39. Bain, J.D., Diala, E.S., Glabe, C.G., Dix, T.A., and Chamberlin, A.R. (1989) *J. Am. Chem. Soc.*, **111**, 8013–8014.

40. Noren, C.J., Anthony-Cahill, S.J., Suich, D.J., Noren, K.A., Griffith, M.C., and Schultz, P.G. (1990) *Nucleic Acids Res.*, **18**, 83–88.

41. Bain, J.D., Diala, E.S., Glabe, C.G., Wacker, D.A., Lyttle, M.H., Dix, T.A., and Chamberlin, A.R. (1991) *Biochemistry*, **30**, 5411–5421.

42. Bain, J.D., Wacker, D.A., Kuo, E.E., and Chamberlin, A.R. (1991) *Tetrahedron*, **47**, 2389–2400.

43. Sisido, M. and Hohsaka, T. (2001) *Appl. Microbiol. Biotechnol.*, **57**, 274–281.

44. Hohsaka, T., Ashizuka, Y., Murakami, H., and Sisido, M. (1996) *J. Am. Chem. Soc.*, **118**, 9778–9779.

45. Hohsaka, T., Kajihara, D., Ashizuka, Y., Murakami, H., and Sisido, M. (1999) *J. Am. Chem. Soc.*, **121**, 3440.

46. Taki, M., Tokuda, Y., Ohtsuki, T., and Sisido, M. (2006) *J. Biosci. Bioeng.*, **102**, 511–517.

47. Murakami, H., Hohsaka, T., Ashizuka, Y., and Sisido, M. (1998) *J. Am. Chem. Soc.*, **120**, 7520–7529.

48. Hohsaka, T., Ashizuka, Y., Sasaki, H., Murakami, H., and Sisido, M. (1999) *J. Am. Chem. Soc.*, **121**, 12194–12195.

49. Hohsaka, T., Ashizuka, Y., Taira, H., Murakami, H., and Sisido, M. (2001) *Biochemistry*, **40**, 11060–11064.

50. Taira, H., Fukushima, M., Hohsaka, T., and Sisido, M. (2005) *J. Biosci. Bioeng.*, **99**, 473–476.

51. Anderson, R.D., Zhou, J., and Hecht, S.M. (2002) *J. Am. Chem. Soc.*, **124**, 9674–9675.

52. Hohsaka, T., Ashizuka, Y., Murakami, H., and Sisido, M. (2001) *Nucleic Acids Res.*, **29**, 3646–3651.

53. Yamanaka, K., Nakata, H., Hohsaka, T., and Sisido, M. (2004) *J. Biosci. Bioeng.*, **97**, 395–399.

54. Beene, D.L., Price, K.L., Lester, H.A., Dougherty, D.A., and Lummis, S.C. (2004) *J. Neurosci.*, **24**, 9097–9104.

55. Nowak, M.W., Kearney, P.C., Sampson, J.R., Saks, M.E., Labarca, C.G., Silverman, S.K., Zhong, W., Thorson, J., Abelson, J.N., and Davidson, N. (1995) *Science*, **268**, 439–442.

56. Turcatti, G., Nemeth, K., Edgerton, M.D., Meseth, U., Talabot, F., Peitsch, M., Knowles, J., Vogel, H., and Chollet, A. (1996) *J. Biol. Chem.*, **271**, 19991–19998.

57. Rodriguez, E.A., Lester, H.A., and Dougherty, D.A. (2006) *Proc. Natl. Acad. Sci. U.S.A.*, **103**, 8650–8655.

58. Xie, J. and Schultz, P.G. (2006) *Nat. Rev. Mol. Cell Biol.*, **7**, 775–782.

59. Furter, R. (1998) *Protein Sci.*, **7**, 419–426.

60. Nair, S., Ribas de Pouplana, L., Houman, F., Avruch, A., Shen, X., and Schimmel, P. (1997) *J. Mol. Biol.*, **269**, 1–9.

61. Liu, D.R., Magliery, T.J., Pastrnak, M., and Schultz, P.G. (1997) *Proc. Natl. Acad. Sci. U.S.A.*, **94**, 10092–10097.

62. Liu, D.R., Magliery, T.J., and Schultz, P.G. (1997) *Chem. Biol.*, **4**, 685–691.

63. Liu, D.R. and Schultz, P.G. (1999) *Proc Natl. Acad. Sci. U.S.A.*, **96**, 4780–4785.

64. Pastrnak, M., Magliery, T.J., and Schultz, P.G. (2000) *Helv. Chim. Acta*, **83**, 2277–2286.

65. Zhang, Z., Gildersleeve, J., Yang, Y.Y., Xu, R., Loo, J.A., Uryu, S., Wong, C.H., and Schultz, P.G. (2004) *Science*, **303**, 371–373.

66. Wang, L., Magliery, J., Liu, D.R., and Schultz, P.G. (2000) *J. Am. Chem. Soc.*, **122**, 5010–5011.

67. Chin, J.W., Santoro, S.W., Martin, A.B., King, D.S., Wang, L., and Schultz, P.G. (2002) *J. Am. Chem. Soc.*, **124**, 9026–9027.

68. Wang, L., Zhang, Z., Brock, A., and Schultz, P.G. (2003) *Proc. Natl. Acad. Sci. U.S.A.*, **100**, 56–61.

69. Santoro, S.W., Wang, L., Herberich, B., King, D.S., and Schultz, P.G. (2002) *Nat. Biotechnol.*, **20**, 1044–1048.

70. Jackson, J.C., Duffy, S.P., Hess, K.R., and Mehl, R.A. (2006) *J. Am. Chem. Soc.*, **128**, 11124–11127.

71. Xie, J., Wang, L., Wu, N., Brock, A., Spraggon, G., and Schultz, P.G. (2004) *Nat. Biotechnol.*, **22**, 1297–1301.

72. Santoro, S.W., Anderson, J.C., Lakshman, V., and Schultz, P.G. (2003) *Nucleic Acids Res.*, **31**, 6700–6709.

73. Chin, J.W., Cropp, T.A., Anderson, J.C., Mukherji, M., Zhang, Z., and Schultz, P.G. (2003) *Science*, **301**, 964–967.

74. Liu, W., Brock, A., Chen, S., and Schultz, P.G. (2007) *Nat. Methods*, **4**, 239–244.

75. Wang, W., Takimoto, J.K., Louie, G.V., Baiga, T.J., Noel, J.P., Lee, K.F., Slesinger, P.A., and Wang, L. (2007) *Nat. Neurosci.*, **10**, 1063–1072.

76. Wang, L. and Schultz, P.G. (2001) *Chem. Biol.*, **8**, 883–890.

77. Wang, L., Brock, A., Herberich, B., and Schultz, P.G. (2001) *Science*, **292**, 498–500.

78. Kobayashi, T., Nureki, O., Ishitani, R., Yaremchuk, A., Tukalo, M., Cusack, S., Sakamoto, K., and Yokoyama, S. (2003) *Nat. Struct. Biol.*, **10**, 425–432.

79. Zhang, Y., Wang, L., Schultz, P.G., and Wilson, I.A. (2005) *Protein Sci.*, **14**, 1340–1349.

80. Wang, L., Xie, J., and Schultz, P.G. (2006) *Annu. Rev. Biophys. Biomol. Struct.*, **35**, 225–249.

81. Kowal, A.K., Kohrer, C., and RajBhandary, U.L. (2001) *Proc. Natl. Acad. Sci. U.S.A.*, **98**, 2268–2273.

82. Liu, C.C. and Schultz, P.G. (2006) *Nat. Biotechnol.*, **24**, 1436–1440.

83. Xie, J., Supekova, L., and Schultz, P.G. (2007) *ACS Chem. Biol.*, **2**, 474–478.

84. Deiters, A., Cropp, T.A., Mukherji, M., Chin, J.W., Anderson, J.C., and Schultz, P.G. (2003) *J. Am. Chem. Soc.*, **125**, 11782–11783.

85. Zhang, Z., Alfonta, L., Tian, F., Bursulaya, B., Uryu, S., King, D.S., and Schultz, P.G. (2004) *Proc. Natl. Acad. Sci. U.S.A.*, **101**, 8882–8887.

86. Kozak, M. (1999) *Gene*, **234**, 187–208.

87. Hui, A. and de Boer, H.A. (1987) *Proc. Natl. Acad. Sci. U.S.A.*, **84**, 4762–4766.

88. Wood, T.K. and Peretti, S.W. (1991) *Biotechnol. Bioeng.*, **38**, 891–906.

89. Rackham, O. and Chin, J.W. (2005) *Nat. Chem. Biol.*, **1**, 159–166.

90. Wang, K., Neumann, H., Peak-Chew, S.Y., and Chin, J.W. (2007) *Nat. Biotechnol.*, **25**, 770–777.

91. Rackham, O. and Chin, J.W. (2006) *Biochem. Soc. Trans.*, **34**, 328–329.

92. Chin, J.W., Martin, A.B., King, D.S., Wang, L., and Schultz, P.G. (2002) *Proc. Natl. Acad. Sci. U.S.A.*, **99**, 11020–11024.

93. Neumann, H., Wang, K., Davis, L., Garcia-Alai, M., and Chin, J.W. (2010) *Nature*, **464**, 441–444.

94. Polycarpo, C., Ambrogelly, A., Berube, A., Winbush, S.M., McCloskey, J.A., Crain, P.F., Wood, J.L., and Soll, D. (2004) *Proc. Natl. Acad. Sci. U.S.A.*, **101**, 12450–12454.

95. Philipson, K.D., Gallivan, J.P., Brandt, G.S., Dougherty, D.A., and Lester, H.A. (2001) *Am. J. Physiol. Cell Physiol.*, **281**, C195–C206.

96. Adams, S.R. and Tsien, R.Y. (1993) *Annu. Rev. Physiol.*, **55**, 755–784.

97. Ellis-Davies, G.C. (2007) *Nat. Methods*, **4**, 619–628.

98. Mendel, D., Ellman, J.A., and Schultz, P.G. (1991) *J. Am. Chem. Soc.*, **113**, 2758–2760.

99. Miller, J.C., Silverman, S.K., England, P.M., Dougherty, D.A., and Lester, H.A. (1998) *Neuron*, **20**, 619–624.

100. Tong, Y., Brandt, G.S., Li, M., Shapovalov, G., Slimko, E., Karschin, A., Dougherty, D.A., and Lester, H.A. (2001) *J. Gen. Physiol.*, **117**, 103–118.

101. Deiters, A., Groff, D., Ryu, Y., Xie, J., and Schultz, P.G. (2006) *Angew. Chem. Int. Ed.*, **45**, 2728–2731.

102. Beatty, K.E. and Tirrell, D.A. (2009) *Nucleic Acids Mol. Biol.*, **22**, 127–153.

103. Chin, J.W. and Schultz, P.G. (2002) *Chembiochem*, **3**, 1135–1137.

104. Ai, H.W., Shen, W., Sagi, A., Chen, P.R., and Schultz, P.G. (2011) *Chembiochem*, **12**, 1854–1857.

105. Groff, D., Chen, P.R., Peters, F.B., and Schultz, P.G. (2010) *Chembiochem*, **11**, 1066–1068.

106. Ellman, J.A., Mendel, D., and Schultz, P.G. (1992) *Science*, **255**, 197–200.

107. Mendel, D., Ellman, J.A., Chang, Z., Veenstra, D.L., Kollman, P.A., and Schultz, P.G. (1992) *Science*, **256**, 1798–1802.

108. Choudhury, A.K., Golovine, S.Y., Dedkova, L.M., and Hecht, S.M. (2007) *Biochemistry*, **46**, 4066–4076.

109. Kearney, P.C., Nowak, M.W., Zhong, W., Silverman, S.K., Lester, H.A., and Dougherty, D.A. (1996) *Mol. Pharmacol.*, **50**, 1401–1412.

110. Zhong, W., Gallivan, J.P., Zhang, Y., Li, L., Lester, H.A., and Dougherty, D.A. (1998) *Proc. Natl. Acad. Sci. U.S.A.*, **95**, 12088–12093.

111. Li, L., Zhong, W., Zacharias, N., Gibbs, C., Lester, H.A., and Dougherty, D.A. (2001) *Chem. Biol.*, **8**, 47–58.

112. Sletten, E.M. and Bertozzi, C.R. (2009) *Angew. Chem. Int. Ed.*, **48**, 6974–6998.

113. Best, M.D. (2009) *Biochemistry*, **48**, 6571–6584.

114. Cornish, V.W., Hahn, K.M., and Schultz, P.G. (1996) *J. Am. Chem. Soc.*, **118**, 8150–8151.

115. Zhang, Z., Smith, B.A., Wang, L., Brock, A., Cho, C., and Schultz, P.G. (2003) *Biochemistry*, **42**, 6735–6746.

116. Carrico, Z.M., Romanini, D.W., Mehl, R.A., and Francis, M.B. (2008) *Chem. Commun.*, 1205–1207.

117. Tong, G.J., Hsiao, S.C., Carrico, Z.M., and Francis, M.B. (2009) *J. Am. Chem. Soc.*, **131**, 11174–11178.

118. Link, A.J. and Tirrell, D.A. (2005) *Methods*, **36**, 291–298.

119. Rennert, O.M. and Anker, H.S. (1963) *Biochemistry*, **2**, 471–476.

120. Cohen, G.N. and Munier, R. (1956) *Biochim. Biophys. Acta*, **21**, 592–593.

121. Hendrickson, W.A., Horton, J.R., and LeMaster, D.M. (1990) *EMBO J.*, **9**, 1665–1672.

122. Johnson, J.A., Lu, Y.Y., Van Deventer, J.A., and Tirrell, D.A. (2010) *Curr. Opin. Chem. Biol.*, **14**, 774–780.

123. Wiltschi, B., Wenger, W., Nehring, S., and Budisa, N. (2008) *Yeast*, **25**, 775–786.

124. Beatty, K.E., Liu, J.C., Xie, F., Dieterich, D.C., Schuman, E.M., Wang, Q., and Tirrell, D.A. (2006) *Angew. Chem. Int. Ed.*, **45**, 7364–7367.

125. Walasek, P. and Honek, J.F. (2005) *BMC Biochem.*, **6**, 21.

126. Duewel, H.S., Daub, E., Robinson, V., and Honek, J.F. (2001) *Biochemistry*, **40**, 13167–13176.

127. Wolschner, C., Giese, A., Kretzschmar, H.A., Huber, R., Moroder, L., and Budisa, N. (2009) *Proc. Natl. Acad. Sci. U.S.A.*, **106**, 7756–7761.

128. Beatty, K.E., Xie, F., Wang, Q., and Tirrell, D.A. (2005) *J. Am. Chem. Soc.*, **127**, 14150–14151.

129. Kiick, K.L., Saxon, E., Tirrell, D.A., and Bertozzi, C.R. (2002) *Proc. Natl. Acad. Sci. U.S.A.*, **99**, 19–24.

130. Kiick, K.L., van Hest, J.C., and Tirrell, D.A. (2000) *Angew. Chem. Int. Ed.*, **39**, 2148–2152.

131. Budisa, N., Minks, C., Medrano, F.J., Lutz, J., Huber, R., and Moroder, L. (1998) *Proc. Natl. Acad. Sci. U.S.A.*, **95**, 455–459.

132. Kim, W., George, A., Evans, M., and Conticello, V.P. (2004) *Chembiochem*, **5**, 928–936.

133. Son, S., Tanrikulu, I.C., and Tirrell, D.A. (2006) *Chembiochem*, **7**, 1251–1257.

134. Wang, P., Tang, Y., and Tirrell, D.A. (2003) *J. Am. Chem. Soc.*, **125**, 6900–6906.

135. Mock, M.L., Michon, T., van Hest, J.C., and Tirrell, D.A. (2006) *Chembiochem*, **7**, 83–87.

136. Minks, C., Huber, R., Moroder, L., and Budisa, N. (2000) *Anal. Biochem.*, **284**, 29–34.

137. Kirshenbaum, K., Carrico, I.S., and Tirrell, D.A. (2002) *Chembiochem*, **3**, 235–237.

138. Rubini, M., Lepthien, S., Golbik, R., and Budisa, N. (2006) *Biochim. Biophys. Acta*, **1764**, 1147–1158.

139. Zhang, Q.S., Shen, L., Wang, E.D., and Wang, Y.L. (1999) *J. Protein Chem.*, **18**, 187–192.

140. Parsons, J.F., Xiao, G., Gilliland, G.L., and Armstrong, R.N. (1998) *Biochemistry*, **37**, 6286–6294.

141. Katragadda, M. and Lambris, J.D. (2006) *Protein Expr. Purif.*, **47**, 289–295.

142. Tang, Y., Ghirlanda, G., Petka, W.A., Nakajima, T., DeGrado, W.F., and Tirrell, D.A. (2001) *Angew. Chem. Int. Ed.*, **40**, 1494–1496.

143. Montclare, J.K. and Tirrell, D.A. (2006) *Angew. Chem. Int. Ed.*, **45**, 4518–4521.

144. Dieterich, D.C., Link, A.J., Graumann, J., Tirrell, D.A., and Schuman, E.M. (2006) *Proc. Natl. Acad. Sci. U.S.A.*, **103**, 9482–9487.

145. Dieterich, D.C., Lee, J.J., Link, A.J., Graumann, J., Tirrell, D.A., and Schuman, E.M. (2007) *Nat. Protoc.*, **2**, 532–540.

146. Suchanek, M., Radzikowska, A., and Thiele, C. (2005) *Nat. Methods*, **2**, 261–267.

147. Kiick, K.L., Weberskirch, R., and Tirrell, D.A. (2001) *FEBS Lett.*, **502**, 25–30.

148. van Hest, J., Kiick, K.L., and Tirrell, D.A. (2000) *J. Am. Chem. Soc.*, **122**, 1282–1288.

149. Ibba, M., Kast, P., and Hennecke, H. (1994) *Biochemistry*, **33**, 7107–7112.

150. Ibba, M. and Hennecke, H. (1995) *FEBS Lett.*, **364**, 272–275.

151. Doring, V., Mootz, H.D., Nangle, L.A., Hendrickson, T.L., de Crecy-Lagard, V., Schimmel, P., and Marliere, P. (2001) *Science*, **292**, 501–504.

152. Mursinna, R.S., Lincecum, T.L. Jr., and Martinis, S.A. (2001) *Biochemistry*, **40**, 5376–5381.

153. Tang, Y. and Tirrell, D.A. (2002) *Biochemistry*, **41**, 10635–10645.

154. Tang, Y., Wang, P., Van Deventer, J.A., Link, A.J., and Tirrell, D.A. (2009) *Chembiochem*, **10**, 2188–2190.

155. Tang, Y. and Tirrell, D.A. (2001) *J. Am. Chem. Soc.*, **123**, 11089–11090.

156. Wang, P., Fichera, A., Kumar, K., and Tirrell, D.A. (2004) *Angew. Chem. Int. Ed.*, **43**, 3664–3666.

157. Kast, P. and Hennecke, H. (1991) *J. Mol. Biol.*, **222**, 99–124.

158. Reshetnikova, L., Moor, N., Lavrik, O., and Vassylyev, D.G. (1999) *J. Mol. Biol.*, **287**, 555–568.

159. Datta, D., Wang, P., Carrico, I.S., Mayo, S.L., and Tirrell, D.A. (2002) *J. Am. Chem. Soc.*, **124**, 5652–5653.

160. Nowatzki, P.J., Franck, C., Maskarinec, S.A., Ravichandran, G., and Tirrell, D.A. (2008) *Macromolecules*, **41**, 1839–1845.

161. Carrico, I.S., Maskarinec, S.A., Heilshorn, S.C., Mock, M.L., Liu, J.C., Nowatzki, P.J., Franck, C., Ravichandran, G., and Tirrell, D.A. (2007) *J. Am. Chem. Soc.*, **129**, 4874–4875.

162. Zhang, K., Diehl, M.R., and Tirrell, D.A. (2005) *J. Am. Chem. Soc.*, **127**, 10136–10137.

163. Ferrell, K., Wilkinson, C.R., Dubiel, W., and Gordon, C. (2000) *Trends Biochem. Sci.*, **25**, 83–88.

164. Ngo, J.T., Champion, J.A., Mahdavi, A., Tanrikulu, I.C., Beatty, K.E., Connor, R.E., Yoo, T.H., Dieterich, D.C., Schuman, E.M., and Tirrell, D.A. (2009) *Nat. Chem. Biol.*, **5**, 715–717.

165. Tanrikulu, I.C., Schmitt, E., Mechulam, Y., Goddard, W.A. III, and Tirrell, D.A. (2009) *Proc. Natl. Acad. Sci. U.S.A.*, **106**, 15285–15290.

166. Link, A.J. and Tirrell, D.A. (2003) *J. Am. Chem. Soc.*, **125**, 11164–11165.

167. Beatty, K.E., Szychowski, J., Fisk, J.D., and Tirrell, D.A. (2011) *Chembiochem*, **12**, 2137–2139.

168. Beatty, K.E. and Tirrell, D.A. (2008) *Bioorg. Med. Chem. Lett.*, **18**, 5995–5999.

169. Dieterich, D.C., Hodas, J.J., Gouzer, G., Shadrin, I.Y., Ngo, J.T., Triller, A., Tirrell, D.A., and Schuman, E.M. (2010) *Nat. Neurosci.*, **13**, 897–905.

170. Nessen, M.A., Kramer, G., Back, J., Baskin, J.M., Smeenk, L.E., de Koning, L.J., van Maarseveen, J.H., de Jong, L., Bertozzi, C.R., Hiemstra, H., and de Koster, C.G. (2009) *J. Proteome Res.*, **8**, 3702–3711.

171. Tcherkezian, J., Brittis, P.A., Thomas, F., Roux, P.P., and Flanagan, J.G. (2010) *Cell*, **141**, 632–644.

172. Floyd, N., Vijayakrishnan, B., Koeppe, J.R., and Davis, B.G. (2009) *Angew. Chem. Int. Ed.*, **48**, 7798–7802.

173. Boutureira, O., D'Hooge, F., Fernandez-Gonzalez, M., Bernardes, G.J., Sanchez-Navarro, M., Koeppe, J.R., and Davis, B.G. (2010) *Chem. Commun.*, **46**, 8142–8144.

174. Wong, C.Y. and Eftink, M.R. (1998) *Biochemistry*, **37**, 8938–8946.

175. Budisa, N., Rubini, M., Bae, J.H., Weyher, E., Wenger, W., Golbik, R., Huber, R., and Moroder, L. (2002) *Angew. Chem. Int. Ed.*, **41**, 4066–4069.

176. Bae, J.H., Rubini, M., Jung, G., Wiegand, G., Seifert, M.H., Azim, M.K., Kim, J.S., Zumbusch, A., Holak, T.A., Moroder, L., Huber, R., and Budisa, N. (2003) *J. Mol. Biol.*, **328**, 1071–1081.

177. Kurschus, F.C., Pal, P.P., Baumler, P., Jenne, D.E., Wiltschi, B., and Budisa, N. (2009) *Cytometry A*, **75**, 626–633.

178. Pal, P.P., Bae, J.H., Azim, M.K., Hess, P., Friedrich, R., Huber, R., Moroder, L., and Budisa, N. (2005) *Biochemistry*, **44**, 3663–3672.

179. Lepthien, S., Hoesl, M.G., Merkel, L., and Budisa, N. (2008) *Proc. Natl. Acad. Sci. U.S.A.*, **105**, 16095–16100.

180. Perler, F.B. and Adam, E. (2000) *Curr. Opin. Biotechnol.*, **11**, 377–383.

181. Muir, T.W. (2003) *Annu. Rev. Biochem.*, **72**, 249–289.

182. Perler, F.B. (2002) *Nucleic Acids Res.*, **30**, 383–384.

183. Gogarten, J.P., Senejani, A.G., Zhaxybayeva, O., Olendzenski, L., and Hilario, E. (2002) *Annu. Rev. Microbiol.*, **56**, 263–287.

184. Dawson, P.E., Muir, T.W., Clark-Lewis, I., and Kent, S.B. (1994) *Science*, **266**, 776–779.

185. Tam, J.P. and Yu, Q. (1998) *Biopolymers*, **46**, 319–327.

186. Offer, J. and Dawson, P.E. (2000) *Org. Lett.*, **2**, 23–26.

187. Canne, L.E., Bark, S.J., and Kent, S.B.H. (1996) *J. Am. Chem. Soc.*, **118**, 5891–5896.

188. Kawakami, T. and Aimoto, S. (2003) *Tetrahedron Lett.*, **44**, 6059–6061.

189. Macmillan, D. (2006) *Angew. Chem. Int. Ed.*, **45**, 7668–7672.

190. Quaderer, R., Sewing, A., and Donald, H. (2001) *Helv. Chim. Acta*, **84**, 1197–1206.

191. Hondal, R.J., Nilsson, B.L., and Raines, R.T. (2001) *J. Am. Chem. Soc.*, **123**, 5140–5141.

192. Muir, T.W., Sondhi, D., and Cole, P.A. (1998) *Proc. Natl. Acad. Sci. U.S.A.*, **95**, 6705–6710.

193. Severinov, K. and Muir, T.W. (1998) *J. Biol. Chem.*, **273**, 16205–16209.

194. Evans, T.C. Jr., Benner, J., and Xu, M.Q. (1999) *J. Biol. Chem.*, **274**, 3923–3926.

195. Lu, W., Gong, D., Bar-Sagi, D., and Cole, P.A. (2001) *Mol. Cell*, **8**, 759–769.

196. Berry, S.M., Gieselman, M.D., Nilges, M.J., van Der Donk, W.A., and Lu, Y. (2002) *J. Am. Chem. Soc.*, **124**, 2084–2085.

197. Yee, C.S., Chang, M.C., Ge, J., Nocera, D.G., and Stubbe, J. (2003) *J. Am. Chem. Soc.*, **125**, 10506–10507.

198. Chang, M.C., Yee, C.S., Nocera, D.G., and Stubbe, J. (2004) *J. Am. Chem. Soc.*, **126**, 16702–16703.

199. Muralidharan, V., Cho, J., Trester-Zedlitz, M., Kowalik, L., Chait, B.T., Raleigh, D.P., and Muir, T.W. (2004) *J. Am. Chem. Soc.*, **126**, 14004–14012.

200. Cook, S.N., Jack, W.E., Xiong, X., Danley, L.E., Ellman, J.A., Schultz, P.G., and Noren, C.J. (2003) *Angew. Chem. Int. Ed.*, **34**, 1629–1630.

201. Young, T.S., Young, D.D., Ahmad, I., Louis, J.M., Benkovic, S.J., and Schultz, P.G. (2011) *Proc. Natl. Acad. Sci. U.S.A.*, **108**, 11052–11056.

202. Li, X., Fekner, T., Ottesen, J.J., and Chan, M.K. (2009) *Angew. Chem. Int. Ed.*, **48**, 9184–9187.

203. Caliceti, P. and Veronese, F.M. (2003) *Adv. Drug Deliv. Rev.*, **55**, 1261–1277.

204. Leader, B., Baca, Q.J., and Golan, D.E. (2008) *Nat. Rev. Drug Discovery*, **7**, 21–39.

205. Vandermeulen, G.W. and Klok, H.A. (2004) *Macromol. Biosci.*, **4**, 383–398.

206. Hoffman, A.S. and Stayton, P.S. (2004) *Macromol. Symp.*, **207**, 139–152.

207. Hoffman, A.S. (2000) *Clin. Chem.*, **46**, 1478–1486.

208. Ladaviere, C., Delair, T., Domard, A., Novelli-Rousseau, A., Mandrand, B., and Mallet, F. (1998) *Bioconjug. Chem.*, **9**, 655–661.

209. Shimoboji, T., Ding, Z., Stayton, P.S., and Hoffman, A.S. (2001) *Bioconjug. Chem.*, **12**, 314–319.

210. Chen, J.P. and Hoffman, A.S. (1990) *Biomaterials*, **11**, 631–634.

211. Takei, Y.G., Matsukata, M., Aoki, T., Sanui, K., Ogata, N., Kikuchi, A., Sakurai, Y., and Okano, T. (1994) *Bioconjug. Chem.*, **5**, 577–582.

212. Pennadam, S.S., Firman, K., Alexander, C., and Gorecki, D.C. (2004) *J. Nanobiotechnol.*, **2**, 8.

213. Fujimura, M., Mori, T., and Tosa, T. (1987) *Biotechnol. Bioeng.*, **29**, 747–752.

214. Sharma, S., Kaur, P., Jain, A., Rajeswari, M.R., and Gupta, M.N. (2003) *Biomacromolecules*, **4**, 330–336.

215. Ding, Z., Chen, G., and Hoffman, A.S. (1996) *Bioconjug. Chem.*, **7**, 121–126.

216. Shozen, N., Iijima, I., and Hohsaka, T. (2009) *Bioorg. Med. Chem. Lett.*, **19**, 4909–4911.

217. Deiters, A., Cropp, T.A., Summerer, D., Mukherji, M., and Schultz, P.G. (2004) *Bioorg. Med. Chem. Lett.*, **14**, 5743–5745.

218. Cho, H., Daniel, T., Buechler, Y.J., Litzinger, D.C., Maio, Z., Putnam, A.M., Kraynov, V.S., Sim, B.C., Bussell, S., Javahishvili, T., Kaphle, S., Viramontes, G., Ong, M., Chu, S., Becky, G.C., Lieu, R., Knudsen, N., Castiglioni, P., Norman, T.C., Axelrod, D.W., Hoffman, A.R., Schultz, P.G., DiMarchi, R.D., and Kimmel, B.E.

219. Banerjee, P.S., Ostapchuk, P., Hearing, P., and Carrico, I.S. (2011) *J. Virol.*, **85**, 7546–7554.

220. Cazalis, C.S., Haller, C.A., Sease-Cargo, L., and Chaikof, E.L. (2004) *Bioconjug. Chem.*, **15**, 1005–1009.

221. Schoffelen, S., Lambermon, M.H., van Eldijk, M.B., and van Hest, J.C. (2008) *Bioconjug. Chem.*, **19**, 1127–1131.

222. Debets, M.F., van Berkel, S.S., Schoffelen, S., Rutjes, F.P., van Hest, J.C., and van Delft, F.L. (2010) *Chem. Commun.*, **46**, 97–99.

223. Young, T.S. and Schultz, P.G. (2010) *J. Biol. Chem.*, **285**, 11039–11044.

224. Magliery, T.J. (2005) *Med. Chem. Rev. Online*, **2**, 303–323.

225. Tang, Y., Ghirlanda, G., Vaidehi, N., Kua, J., Mainz, D.T., Goddard, I.W., DeGrado, W.F., and Tirrell, D.A. (2001) *Biochemistry*, **40**, 2790–2796.

226. Baker, P.J. and Montclare, J.K. (2011) *Chembiochem*, **12**, 1845–1848.

227. Holzberger, B., Rubini, M., Moller, H.M., and Marx, A. (2010) *Angew. Chem. Int. Ed.*, **49**, 1324–1327.

228. Montclare, J.K., Son, S., Clark, G.A., Kumar, K., and Tirrell, D.A. (2009) *Chembiochem*, **10**, 84–86.

229. Mehta, K.R., Yang, C.Y., and Montclare, J.K. (2011) *Mol. Biosyst.*, **7**, 3050–3055.

230. Voloshchuk, N., Zhu, A.Y., Snydacker, D., and Montclare, J.K. (2009) *Bioorg. Med. Chem. Lett.*, **19**, 5449–5451.

231. Voloshchuk, N., Lee, M.X., Zhu, W.W., Tanrikulu, I.C., and Montclare, J.K. (2007) *Bioorg. Med. Chem. Lett.*, **17**, 5907–5911.

232. Panchenko, T., Zhu, W.W., and Montclare, J.K. (2006) *Biotechnol. Bioeng.*, **94**, 921–930.

233. Yoder, N.C. and Kumar, K. (2002) *Chem. Soc. Rev.*, **31**, 335–341.

234. Neil, E. and Marsh, G. (2000) *Chem. Biol.*, **7**, R153–R157.

235. Kim, W., McMillan, R.A., Snyder, J.P., and Conticello, V.P. (2005) *J. Am. Chem. Soc.*, **127**, 18121–18132.

236. Kim, W., Hardcastle, K.I., and Conticello, V.P. (2006) *Angew. Chem. Int. Ed.*, **45**, 8141–8145.

(2011) *Proc. Natl. Acad. Sci. U.S.A.*, **108**, 9060–9065.

237. Teeuwen, R.L., van Berkel, S.S., van Dulmen, T.H., Schoffelen, S., Meeuwissen, S.A., Zuilhof, H., de Wolf, F.A., and van Hest, J.C. (2009) *Chem. Commun.*, 4022–4024.

238. Heredia, K.L. and Maynard, H.D. (2007) *Org. Biomol. Chem.*, **5**, 45–53.

239. Broyer, R.M., Grover, G.N., and Maynard, H.D. (2011) *Chem. Commun.*, **47**, 2212–2226.

240. Grover, G.N. and Maynard, H.D. (2010) *Curr. Opin. Chem. Biol.*, **14**, 818–827.

241. Peeler, J.C., Woodman, B.F., Averick, S., Miyake-Stoner, S.J., Stokes, A.L., Hess, K.R., Matyjaszewski, K., and Mehl, R.A. (2010) *J. Am. Chem. Soc.*, **132**, 13575–13577.

13
Functionalization of Porous Polymers from High-Internal-Phase Emulsions and Their Applications

Linda Kircher, Patrick Theato, and Neil R. Cameron

13.1
Introduction

This chapter focuses on the functionalization of porous materials prepared via the high-internal-phase emulsion (HIPE) techniques. These so-called polyHIPEs are highly porous, open-pore, cross-linked polymers. The concept of cross-linked polymers was introduced in the early 1940s as ion exchangers and became widely spread after Merrifield developed the solid-phase peptide synthesis using a cross-linked polystyrene-based support in the 1960s [1].

Preparation of porous cross-linked polymers based on the emulsion-templated method was first described by Lissant and Mayhan in the early 1970s [2]. This area of research was then intensively studied. In 1982, Unilever produced the first patent in which the term polyHIPEs was pioneered [3]. A large variety of polyHIPEs have been developed using HIPEs as templates for the porous structure. These materials include hydrophobic [4] and hydrophilic [5] polymers, hydrophobic–hydrophilic bicontinuous polymers [6], biocompatible polymers [7–11], interpenetrating polymer networks (IPNs) [12, 13], nanocomposites [14], or organic–inorganic hybrids [13, 15].

The wide range of monomers that can be used in emulsion templating as well as the large number of methods available to functionalize polyHIPEs have enhanced their utilization for many interesting applications such as tissue engineering [8], electrodes [16], separation media [17], and catalytic surfaces and supports [18–22].

HIPEs are formed by mixing two immiscible liquids in the presence of an emulsifier. They are highly viscous emulsions with a dispersed-phase content higher than 74% of the emulsion volume, which causes the droplets to form a polyhedral shape [2]. Although HIPEs are both kinetically and thermodynamically unstable, it is still possible to produce metastable systems. Accordingly, the unstable structure of the HIPE can be preserved if one uses one monomer/cross-linker-rich – mostly organic – phase during the emulsification process. Polymerization of the monomer phase results then in a stable porous polymer derived from HIPEs, hence called polyHIPEs.
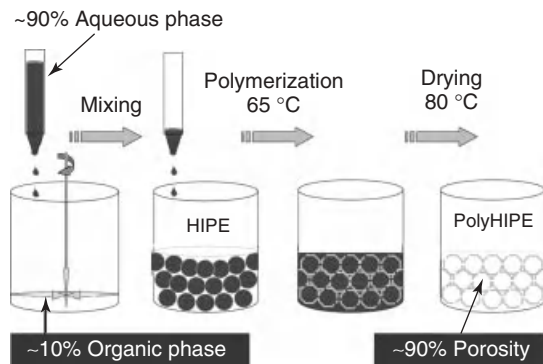
Figure 13.1 Preparation of polyHIPEs [23]. (Source: Reproduced with permission of John Wiley & Sons, Inc.)

13.1.1
Preparation Method of polyHIPEs

The preparation of polyHIPEs requires a phase consisting of a monomer, a cross-linker, an appropriate surfactant, and an initiator to trigger the polymerization, and an immiscible phase, which is usually added dropwise under constant agitation to prevent phase separation. The process is illustrated in Figure 13.1. Once the HIPE is formed, polymerization can be initiated. The polymerized emulsion, termed *polyHIPE*, is then washed – typically by Soxhlet extraction – to remove unreacted monomers and surfactant.

During the process of polymerization, small interconnecting windows can develop at the thinnest points of the continuous-phase envelope surrounding the dispersed internal phase [24]. Many parameters affect the formation of these interconnecting windows, including volume fraction of the internal phase, the concentration of the surfactant, the droplet size, the nature of the polymer formed throughout the polymerization, and the tendency for Ostwald ripening [25].

Drying of polyHIPE removes the dispersed internal phase and yields an open-pore void with highly interconnected structure. An example of the typical polyHIPE structure is shown in Figure 13.2.

HIPEs can be water-in-oil (w/o), oil-in-water (o/w), oil-in-oil (o/o) [26], or supercritical CO_2-in-water (c/w) [27] phase in nature; the first phase mentioned refers to the discontinuous phase and the last phase is the continuous phase. Well-established polymerization techniques offer different ways to cure the HIPE. The most common way is free radical polymerization with thermally activated initiators such as azobisisobutyronitrile (AIBN) or potassium persulfate.

Alternatively, the faster photopolymerization has also been utilized in the formation of polyHIPEs. This method requires only a few seconds for complete curing of the HIPE. Another advantage of photoinitiation over thermal initiation is that polymerization can be conducted at lower temperatures. This is advantageous
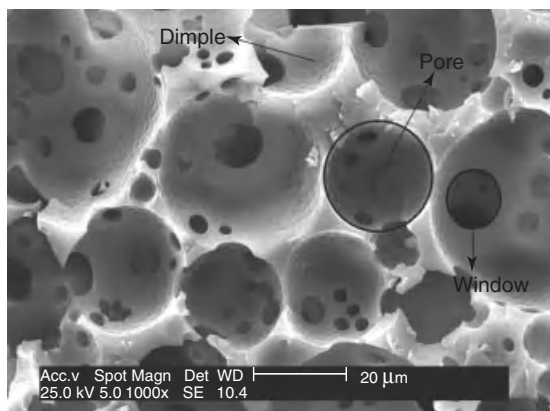
Figure 13.2 SEM image of a typical polyHIPE showing its characteristic features.

when polymerizations of emulsions that are unstable under thermal polymerization conditions need to be performed. Accordingly, photopolymerization of HIPEs has been applied to many multiacrylate monomers and showed promising results especially for industrial applications [28]. Aromatic ketones, such as Darocur 4265, are often used to generate free radicals that can initiate either the polymerization of acrylates [29] or the coupling of thiol–ene groups by a step-growth addition mechanism [30].

Photopolymerization led to a new approach to prepare porous polymer beads, which could so far only be prepared from suspension polymerization using a porogen to obtain the required porosity [31]. For instance, once the HIPE had been formed, it can be dropped in a water phase containing a surfactant under continuous flow, and subsequent solidifying of the polymer beads by photopolymerization results in a continuous preparation of porous polymer beads, as illustrated in Figure 13.3.

This microfluidic approach enables the production of polyHIPE particles with controlled diameter and shape via the adjustment of the emulsion viscosity. The main advantage of this method is the formation of beads with porous skin (Figure 13.4), which permits reagents to penetrate into the porous particles. This provides the possibility to functionalize the beads selectively and thus enables them to be used in a wide range of applications [32].

13.2
Functionalization of polyHIPEs

Apparently, the great interest in a versatile functionalization of polyHIPEs has led to the investigation of various approaches, which is documented by the large number of publications in this field. To date, the various functionalization methods for polyHIPEs can be organized and consequently divided into three different types: (i)

Continuous aqueous carrier phase
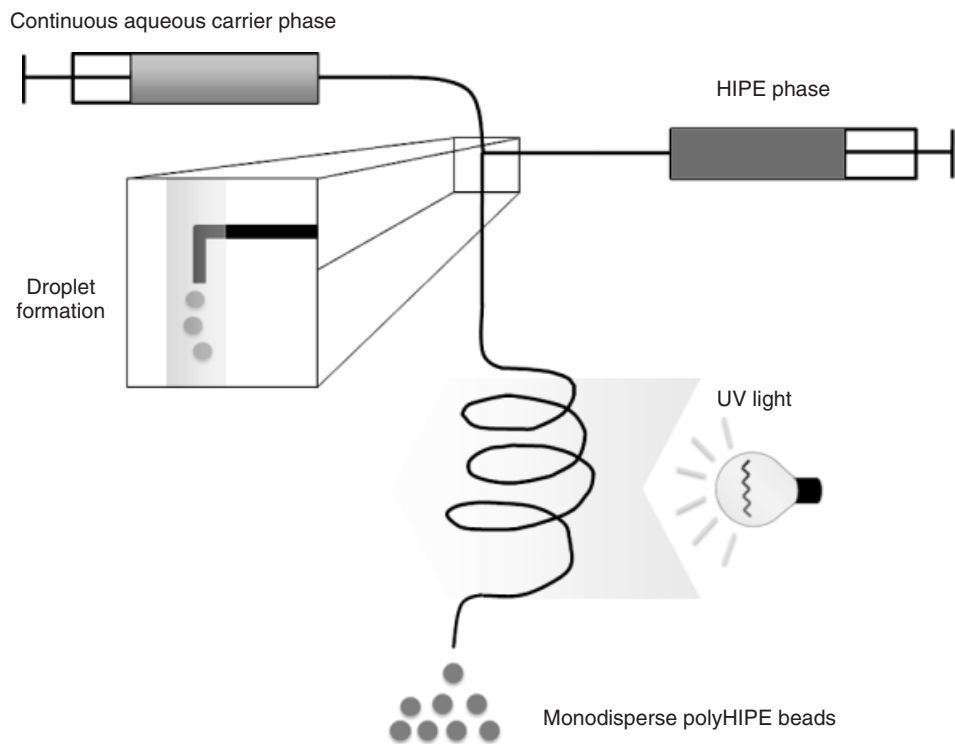
Figure 13.3 Microfluidic approach to prepare polyHIPE beads.
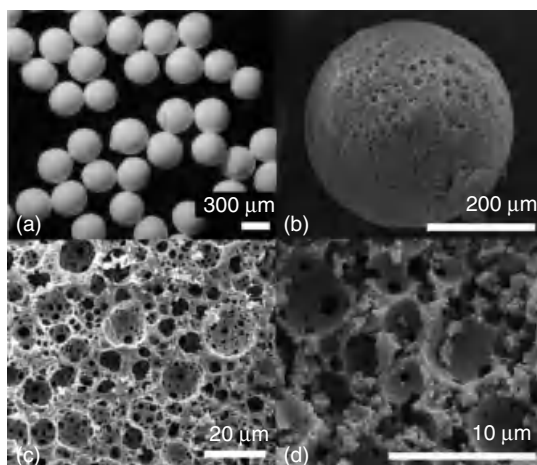
Figure 13.4 Porous polyHIPE beads. (a) Optical microscopy image showing size monodispersity. SEM images of (b) a whole bead, (c) surface of a bead, and (d) inner part of a broken bead. (Source: Reprinted with permission from [32]. Copyright 2009 American Chemical Society.)

incorporating a comonomer, bearing the desired functional group, into the HIPE; (ii) post-polymerization modification of the preformed polyHIPE by reaction with small organic molecules; and (iii) grafting functionalized macromolecular chains to the previously prepared polyHIPE. Of course, in some cases, more than one of these methods are used.

Copolymerization with a functional monomer seems to be the most convenient method because it is an easy one-step reaction yielding the desired functional polyHIPE in a direct way. However, there are some drawbacks that should be considered. Using HIPE templating techniques implies a sufficient polarity difference between the two phases to obtain a stable emulsion. Therefore, when working with a w/o emulsion, which is the most commonly used, problems can occur with comonomers containing polar functional groups, which are more hydrophilic and are therefore likely to destabilize the emulsion. This leads to larger droplet sizes or, in the worst case, to phase separation. One possible solution to tackle this problem is to decrease the hydrophilicity of these functional groups by means of protecting groups, which can be removed after polymerization. Hence, this method is limited to comonomers containing hydrophobic functional groups. Table 13.1 shows some selected examples of polyHIPEs, which have been prepared by copolymerization and their applications.

The second method is based on a two-step process. First, preparation of the polyHIPE and subsequently functionalization are conducted to achieve the desired functional polyHIPE. While the morphology can be changed by different well-studied factors such as surfactant concentration, stirring rate, and temperature, it is important to enable a post-polymerization functionalization afterward that does not change the previously installed morphological structure. An overview of different post-polymerization modifications on polyHIPEs and their applications is given in Table 13.2.

Finally, the third method, which also falls into the category of a post-polymerization modification, involves grafting functional macromolecules from the preformed polyHIPE. Selected examples are highlighted in Table 13.3. It is worth mentioning that this method provides high loading yields and good accessibility of the functional groups compared to method 1, the copolymerization of functional monomers, because functionalization occurs predominantly on the internal surface of the structure.

13.2.1
Functionalization of polyHIPEs Based on Copolymerization with Functional Comonomers

Various examples have been presented in the literature that utilize copolymerization with functional comonomers to prepare functional polyHIPEs. Apparently, various comonomers allow also a post-polymerization modification afterward and particular attention is paid to these systems. Highly porous monolithic columns with chloromethyl functionalities were obtained from styrene (ST)/divinylbenzene(DVB)-HIPEs that were prepared in the presence

Table 13.1 PolyHIPEs made by copolymerization techniques and their applications.

Constitutional monomer	Functional comonomer	Application	References
ST/DVB	VBC	Catalytic and scavenger support	[4, 21, 33–36]
ST/DVB or ST/EGDMA	TCPA	Scavenger resins	[2237–39]
ST/DVB or ST/EGDMA	NPA	Scavenger resins, removal of atrazine from aqueous solutions	[22, 37, 38, 40]
DVB or EGDMA	GMA	Monolithic supports for protein separation	[41–43]
DVB	VDMA	Scavenger resins	[44]
ST/DVB	EHA	Reduction of Tg	[12, 45, 46]
ST/DVB	Organotin	Catalytic support	[47]
DCPD	PETMP	—	[48]
EGDMA, MBAM	HEMA	—	[49–51]
TMPTA or octadiyne	TMPTMP	Tissue engineering	[30]
ST, tBA, or MMA	PCL	Biodegradable materials, tissue engineering	[7, 52]
ST or MMA	PLA	Biodegradable materials, tissue engineering	[8]
MBAM	AM	Support for chromatography, catalysis, and tissue engineering	[51, 53]
MBAM	AA	Support for chromatography, catalysis, and tissue engineering	[51, 53, 54]
MBAM	NIPAM	Drug delivery, thermoresponsive pump for organic nanoparticles	[51, 55]
ST/DVB	Aryl ether sulfone	—	[56]
ST/DVB	Alkylmaleimide	—	[57]

PETMP, pentaerythritol tetrakis-(3-mercaptopropionate); TMPTMP, trimethylolpropane tris(3-mercaptopropionate); *t*-BA, *tert*-butyl acrylate; AM, acrylamide; AA, acrylic acid; NIPAM, *N*-isopropylacrylamide.

of the comonomer 4-vinylbenzyl chloride (VBC). Potential functionalization could be achieved by a flow-through method immobilizing tris(2-aminoethyl) amine, diethanolamine, and 4-bromophenylboronic acid [35]. In addition, VBC/DVB-polyHIPEs were postfunctionalized with various amines and used as monolithic polymer supports and scavengers [21]. It could be shown that the pore size of VBC/DVB-polyHIPEs can be varied with the VBC content [4].

N-(*p*-Vinylbenzyl)-4,4-dimethylazlactone (VDMA) with the cross-linker DVB has been used to synthesize azlactone-functionalized polyHIPEs. Azlactone features an electrophilic ring, which can be used to scavenge primary amines in a batch

Table 13.2 Post-polymerization modification of polyHIPEs and their applications.

Monomer/cross-linker/comonomer	Postfunctionalization	Application	References
ST/DVB	Nitration, bromination, sulfonation	Catalyst for the hydration of cyclohexene, ion exchange modules	[18, 19, 58]
ST/DVB	Addition of thiols, HBr, BH$_3$	—	[20, 59, 60]
ST/DVB/VBC	Nucleophilic substitution	Catalytic support, scavenger resins	[4, 21, 33–36]
ST/DVB/VBC	4-Iodobenzoic acid	Support material in Suzuki cross-coupling reactions, yielding pure biaryl products	[61]
ST/DVB or EGDMA/TCPA	Nucleophilic substitution	Scavenger resins	[2237–39]
ST/DVB or EGDMA/NPA	Reacted to possess acid chloride and amino or hydroxy functionality	Scavenger resins, removal of atrazine from aqueous solutions	[22, 37, 38, 40]
DVB or EGDMA/GMA	Hydrolysis	Monolithic supports for protein separation	[41–43]
IBOA/EHA/TMPTA/NASI	Nucleophilic addition	Immobilization of the enzyme CAL-B	[28]
DCPD	Thiol–ene reaction, oxidation followed by hydrazone formation	—	[48]
MBAM/AA	Chlorination	Scavenger resins	[51, 53, 54]

Table 13.3 PolyHIPEs with different grafts and their applications.

Monomer/cross-linker/comonomer	Grafting	Application	References
DVB/VPBMP	GMA, MMA	Scavenger resins	[62, 63]
PEGMA/EGDMA	EBPs	Bioanalytical devices, preparation of rewritable peptide and protein arrays	[64]
VBC/DVB	VDMA, AEMA, GMA, VBC	Scavenger resins	[65]

VPBMP, 4-vinylphenyl 2-bromo-2-methylpropanoate; PEGMA, poly(ethylene glycol) methacrylate; AEMA, 2-aminoethyl methacrylate.

and a flow-through process [44]. A series of monolithic cross-linked polymers with 2,4,6-trichlorophenyl acrylate (TCPA) as a reactive component were prepared by free radical polymerization of ST by varying the cross-linkers, such as DVB or ethylene glycol dimethacrylate (EGDMA), and the porogenic solvents and thus the porosities. Monolithic supports could then be functionalized by reaction of the activated ester moieties with, for example, tris(2-aminoethyl)amine derivative and by hydrolysis of the ester groups yielding carboxylic acids [39]. Krajnc *et al.* [22] studied intensively the effect on emulsion stability in ST/DVB-HIPEs when two functional comonomers, namely, *p*-nitrophenyl acrylate (NPA) and TCPA (both activated esters), were introduced.

As discussed before, the first problem to solve when introducing a functional comonomer is obtaining a stable emulsion in the presence of the new monomer. Thus, the surfactant is the critical factor. It should be completely soluble only in the continuous phase to prevent phase separation and/or phase inversion. Surfactants are classified by their hydrophilic–lipophilic balance (HLB) value of 0–30, where 0 represents a very hydrophobic surfactant. Changing the monomer content of an HIPE requires adjusting the HLB value of the surfactant, which can be easily achieved by blending two surfactants [66]. For example, a mixture of sorbitan monooleate and sorbitan trioleate in a ratio that resulted in a surfactant with an HLB value of 3.4 has been used to stabilize an emulsion with NPA up to 65 °C.

In contrast, when TCPA was used as a comonomer instead of NPA, the salt concentration in the aqueous phase needed to be changed. Increasing the salt concentration increases the density of the aqueous phase toward the presumably higher density of the oil phase, which results in a reduced phase separation. Therefore, the presence of salt in the aqueous phase plays an important role in tuning the stability of the emulsions. Accordingly, an ST-based emulsion with TCPA or NPA as functional monomers using DVB as a cross-linker could be stabilized by varying the HLB value of the surfactant as well as the salt concentration in the aqueous phase. Free radical polymerization was used to achieve the accordant polyHIPE [22].

Both the activated ester groups can be used to modify the polyHIPE by post-polymerization steps. Different functional groups can be introduced via nucleophilic substitution of amines. This versatility in chemical functionalizations is very important for materials used in reactive supports. Alcohol as a functional group with a loading of 10.9 mmol of OH groups per gram polyHIPE has also been introduced using tris(hydroxymethyl)aminomethane derivative. Moreover, a polymeric scavenger for acid and sulfonyl chlorides, isocyanates, isothiocyanates, and acids [67], namely, tris(2-aminoethyl)amino derivative has been introduced [22].

Hydrolysis of the activated ester on polyHIPEs is another possible way to functionalize these materials. Complete conversion of NPA-based polyHIPE into the corresponding carboxylic acid with 1.5 M aqueous NaOH has been achieved. Further modification with thionyl chloride yielded the corresponding acid chloride, allowing functionalization with weaker nucleophiles. TCPA-based polyHIPE has also been successfully converted into the acid chloride. Furthermore, the porosity

of the polyHIPEs plays a major role in the success of the post-polymerization modification. The rate of hydrolysis of the NPA-based polyHIPEs was found to be dependent on their porosity. The highest porosity resulted in the fastest hydrolysis [22]. Beaded polyHIPEs with the reactive comonomers NPA and TCPA acrylates have also been prepared using water-in-oil-in-water multiple emulsions [38].

Maleimides were copolymerized with ST and cross-linked with either DVB or bis(3-ethyl-5-methyl-4-maleimide-phenyl)methane. All maleimide modifiers increased the foam glass-transition temperature (T_g) as a function of the maleimide concentration [57]. Poly(aryl ether sulfone)-polyHIPEs could be synthesized using maleimide-terminated aryl ether sulfone as a comonomer in ST/DVB-HIPEs [56].

A new type of organotin chloride catalyst supported on a polyHIPE has been prepared. This polymer-supported organotin chloride showed good activity for the catalytic reduction of 1-bromoadamantane [47]. Polyester-based polyHIPE foams containing poly(ε-caprolactone) (PCL) [7] or poly(lactic acid) (PLA) [8] were synthesized from the corresponding macromonomers mixed with ST, methyl methacrylate (MMA), or toluene. The produced materials were also reported to be biodegradable and accordingly found application in tissue engineering.

Hydrophilic polyHIPEs have been synthesized in o/w or c/w emulsion with monomers such as acrylic acid, acrylamide, *N*-isopropylacrylamide, 2-hydroxyethyl acrylate (HEA), and 2-hydroxyethyl methacrylate (HEMA) [49–51, 54]. In addition, (meth)acrylate comonomers such as 2-ethylhexyl (meth)acrylate [45] and isobornyl acrylate (IBOA) [68] have been used to synthesize functionalized polyHIPEs.

Photoinitiation was investigated to allow the use of less thermally stable monomers such as *N*-acryloxysuccinimide (NASI) (an activated ester), which was incorporated into a 2-ethylhexyl acrylate (EHA)- and IBOA-based polyHIPE using trimethylolpropane triacrylate (TMPTA) as the cross-linker. The monolith from this material showed excellent qualities for the immobilization of enzymes [28].

Krajnc *et al.* [54] prepared ''reversed'' polyHIPEs from oil-in-water emulsion. Acrylic acid as a hydrophilic monomer with *N,N'*-methylene bisacrylamide (MBAM) as a cross-linker formed the continuous aqueous phase and the oil phase consisting of toluene formed the droplet phase. In this case, the surfactant needed a higher HLB value to be soluble only in the aqueous phase. Triton X-405 (HLB = 17.9) turned out to be a good choice to stabilize this o/w emulsion, and the polymerization provided a hydrophilic polyHIPE with pore sizes around 10 μm.

One significant disadvantage of o/w emulsion is the large amount of organic solvent required to form an HIPE. For instance, synthesis of 1 kg of hydrophilic porous polymer required 20 kg of organic solvent, even if one disregards any additional solvents that may be used in the washing steps after polymerization [69]. This problem has to be addressed especially when thinking about industrial applications. One possible solution, which has recently been explored and is well known in ''*green chemistry*,'' is the use of supercritical carbon dioxide as a solvent [70]. Inversed emulsion polymerization was also used to prepare hydrophilic porous copolymers of acrylic acid and acrylamide cross-linked by methylene bisacrylamide. The acrylic acid was functionalized with thionyl chloride to yield acid chloride. Because of site-site dehydration reactions of the carboxylic groups,

conversion to the chloride is higher with less acrylic acid content [53]. These chloride-functionalized polyHIPEs are useful as scavengers for amines [21].

Recently, different reactive monomers have been introduced within step-growth reactions. For example, base-catalyzed polycondensation of 2-nitroresorcinol with cyanuric chloride [71], reaction of an isocyanate with a polyol to produce polyurethane [72], and resorcinol–formaldehyde polymerization in an o/w emulsion [73] were studied. Another step-growth polymerization used for polyHIPEs is based on thiol–ene and thiol–yne click reactions [30].

Despite its simplicity, copolymerization results in two problems: (i) only a small number of functional groups on the pore surface are available for further use and (ii) a major part of the functional monomer located in the interior is wasted and also leads to unfavorable mechanical properties [74].

13.2.2
Functionalization of polyHIPEs by Post-polymerization Modification

The success of post-polymerization modification is based on excellent conversions achievable under mild conditions and the possibility to functionalize the prepared materials using numerous reactions that have been described in the literature [75], notably, the so-called click reactions [76]. To obtain good chemical modifications of polyHIPEs, the solvent used should have good swelling properties for the unmodified as well as the modified polyHIPEs [58].

In principle, there are two possible routes for postfunctionalizations of poly-HIPEs. The challenge is to penetrate the polyHIPE with the reagent as quickly as possible to prevent a reaction gradient within the polyHIPE, which would lead eventually to a nonhomogeneous functionalization.

The batch method [20, 59] is based on diffusion of reactants into the polyHIPE. In this method, small cubes of polyHIPE are used, so that diffusion into the cubes is quick and the reaction is uniform throughout the polyHIPE. Also, polyHIPEs can be used as a powder, which should enhance the diffusion into the polyHIPEs [61] The batch method needs only elementary equipment, as illustrated in Figure 13.5a; therefore, it is very useful for an initial testing of functionalization. However, there are some drawbacks with this method, such as the stirring of the cubes leads to constant mechanical grinding against each other, the stirrer bar, and the reaction vial, which leads to undesired degradation of the polyHIPE cubes.

The more promising method is the continuous flow method [35], in which a monolith of polyHIPE is placed in a column and the reactants are passed through the column with an applied vacuum, as shown in Figure 13.5b.

The structure of polyHIPEs is particularly favorable for use in flow-through methods because the large pore size and the interconnecting windows offer optimal conditions. For application in flow-through methods, monoliths are better than beads because they are more stable and therefore do not compress when pressure is applied to pump the reactants through the column. The continuous flow method facilitates the automatization of the functionalization, which makes it more interesting for industrial applications. The drawback of this method is
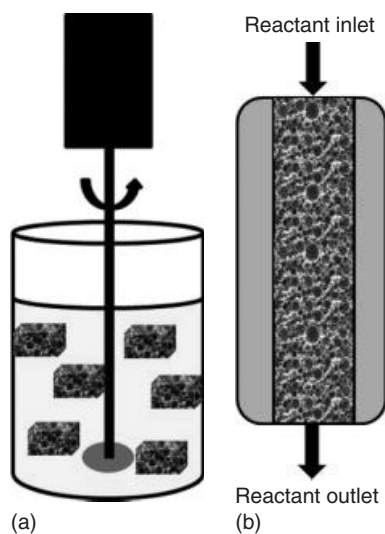
Figure 13.5 Methods of polyHIPE functionalization: (a) batch method and (b) continuous flow method.

the large amount of solvents required, which needs to be used because of the large pore volume in polyHIPEs. Nevertheless, Mercier *et al.* [59] found that the functionalization rate is generally the same for both methods.

More important than the method is the selection of the right solvent because good swelling of the cross-linked polymer is required to afford a good diffusion of the reagents into the polymer. A big challenge is that the functionalization can alter the swelling behavior dramatically. Therefore, a solvent with good swelling behavior for the unfunctionalized and functionalized polyHIPEs is required. This is, for example, the case for the functionalization of chloromethylated polystyrene with tertiary amines, where the polarity of the polyHIPE changes from relatively hydrophobic to a very hydrophilic polyHIPE possessing ionic groups [58].

The most studied polyHIPEs are ST/DVB-polyHIPEs, which have been functionalized by bromination, sulfonation, and nitration [58]. Functionalization has also been carried out via pendant unreacted DVB vinyl groups in ST/DVB-polyHIPES. Free radical addition of thiols and HBr provided selectively the β-addition products. Hydroboration with BH_3 followed by oxidation with H_2O_2 and then hydrolysis has also been investigated [20]. As highlighted in Figure 13.6, a wide range of different functional groups can be introduced via thiols [59, 60].

13.2.3
Functionalization of polyHIPEs Based on Grafting Modification of Porous Materials

PolyHIPEs based on poly(ethylene glycol) methacrylate have been used for the reversible immobilization of stimuli-responsive polymers. Elastin-based side chain polymers (EBPs), a stimuli-responsive carbon-backbone polymer composed of a
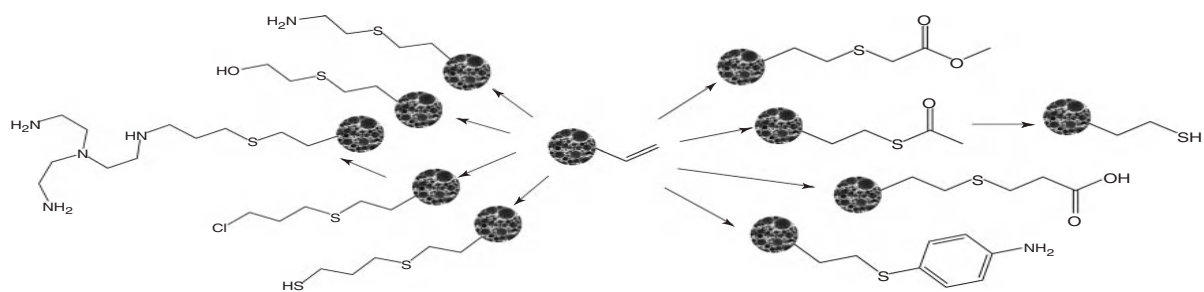
Figure 13.6 Functionalization of (vinyl)polystyrene polyHIPEs by thiols. (Redrawn after Ref. [60].)

pendant pentapeptide consisting of the amino acids valine, proline, glycine, valine, and glycine (VPGVG), have been synthesized via reversible addition-fragmentation chain transfer (RAFT) polymerization [77]. EBPs, which are known to have a lower critical solution temperature (LCST) depending on their molecular weight [78], could be immobilized onto PEGylated polyHIPEs, using their unreacted double bonds and coupling them with the thiol of the modified RAFT chain end by thiol–ene reaction. When an EBP with a high molecular weight was immobilized on the polyHIPE, the coassembly of a complementary EBP with lower molecular weight could be achieved by reducing the pH to 1.5. This was reversible by increasing the pH to 3.2 where it could be washed out again [64].

13.2.3.1 ATRP to Functionalize polyHIPEs

Atom transfer radical polymerization (ATRP) is a controlled radical polymerization technique, which offers the advantages to control the molecular weight while achieving low polydispersities and, because of the ''living'' character, it provides the possibility to synthesize block copolymers [79]. Incorporating an ATRP initiating site within a comonomer into an HIPE gives the great possibility to graft various polymeric branches with a wide range of functionalities from the previously prepared polyHIPE. The use of ATRP for grafting glycidyl methacrylate (GMA) and MMA from polyHIPEs was first investigated by Moine *et al.* [62]. The influence of various parameters, such as feed ratio and the concentration of immobilized ATRP initiator groups in the polyHIPE and spacer groups in the initiator to advance the availability, on the surface grafting of MMA was studied [63].

Barbetta *et al.* [41] studied the hydrolysis of epoxy groups in GMA/DVB-poly HIPEs and found that the percentage of the exposed epoxy groups that underwent hydrolysis depends on the pore size.

Instead of using thermally cured ST-based polyHIPEs, Cummins *et al.* [29] combined fast photopolymerization of acrylate-based polyHIPEs with ATRP surface grafting. They also showed that postfunctionalization using ATRP enables the grafting of block copolymers of MMA and HEMA on polyHIPEs. Grafting GMA additionally offers the feasibility to perform further modification on the epoxy group, which could be used to change the wettability of the sample. Simple acid-catalyzed ring opening of the epoxy group produced a hydrophilic surface, and further modification with pentafluorobenzoyl chloride changed the surface wettability to hydrophobic [29].

These materials have established their usability in many applications because of their wide functionalization possibilities. For example, they have all the requirements for a good scavenger, that is, high loading and good accessibility given by the mobility of the grafted chains and a porous interconnected structure that allows the rapid diffusion of fluids [63].

An interesting grafting approach has been achieved by Tripp *et al.* using VBC/DVB-polyHIPE disks. This approach involved the immobilization of the radical initiator 4,4′-azobis(4-cyanovaleric acid) (ACVA) on the porous surface through the chloride functionality followed by adding a functional monomer and then the thermally initiated grafting reaction. Different reactive monomers could
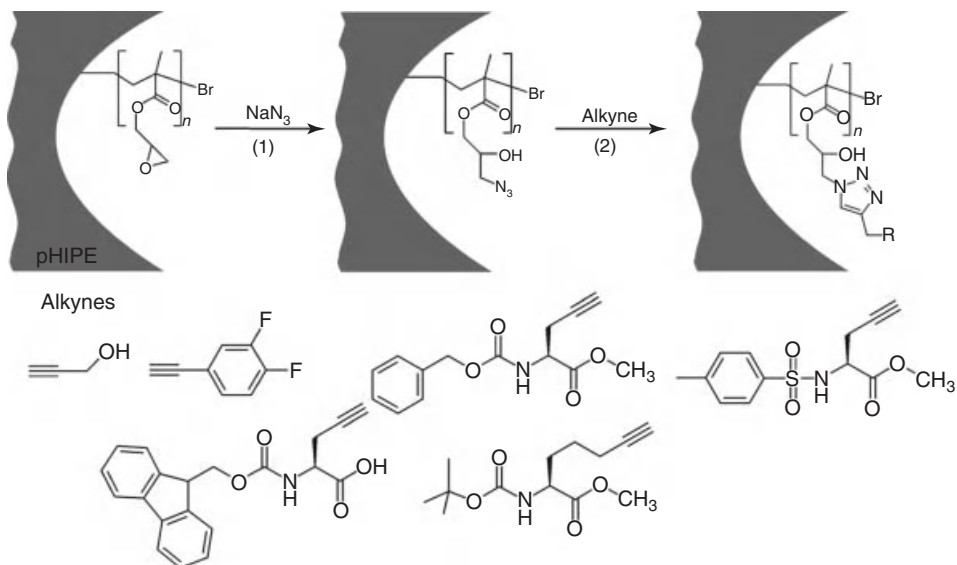
Scheme 13.1 Schematic illustration of azidation of GMA grafted from polyHIPEs (1), followed by Huisgen-type click reaction (2) with various alkynes on polyHIPE support [83].

be grafted on the porous surface, such as VDMA, 2-aminoethyl methacrylate, GMA, and VBC. In a comparison study of the scavenging reactivity between a copolymerized and a grafted functionality of VDMA on a polyHIPE disk, it was found that the reactivity of the former was 37% and the latter scavenged as much as 75% of the benzylamine in tetrahydrofuran (THF) within 8 min residence time [63, 65].

13.2.4
Click Chemistry for Functionalization of polyHIPEs

Click chemistry is a chemical philosophy introduced by Barry Sharpless in 2001, which has grown in popularity ever since. Sharpless defined click chemistry as a class of reactions for the generation of complex substances by bringing together smaller units via heteroatoms. The copper(I)-catalyzed Huisgen azide-alkyne cycloadditions (CuAACs) have rapidly become the most popular click reaction to date [80] and have been intensively used in materials modification because of their high efficiency and tolerance toward functional groups [76, 81]. CuAACs have also found broad applications in materials science and have been highlighted in several reviews [82].

Cummins *et al.* [29] achieved the first surface functionalization of macroporous polyHIPEs by Huisgen-type click reaction. As previously reported, poly(glycidyl methacrylate) (PGMA) was grafted from the polyHIPE surface by ATRP. As illustrated in Scheme 13.1, ring opening reaction of the epoxy group with sodium azide (1) resulted in a nearly quantitative azidation throughout the 600–800 nm thick

layer of PGMA. The success of the following azide-alkyne cycloaddition (2) could be visualized with a fluorescence dye. More interestingly, the biofunctionalization of the polyHIPEs' interior and exterior could be achieved with various amino acids with both the N- and C-termini available for further modification or interaction [83]. CuAACs have also been successfully used to functionalize polyHIPE beads [32].

13.2.5
Thiol-ene-based polyHIPEs

Another type of click reaction is the thiol–ene and thiol–yne reactions [84, 85]. Novel, highly porous polymeric materials have been prepared by thiol–ene and thiol–yne photopolymerization of the continuous phase of HIPEs. The investigated polyHIPEs have well-defined morphologies, and their mechanical properties are dependent on the porosity and the type of network formed by either thiol–ene or thiol–yne reactions [30]. Recently, this approach for polymer formation has attracted intense interest because of its ease and versatility leading to the production of a wide range of functional macromolecular materials [85, 86]. Detailed information about the thiol–ene and thiol–yne photoinitiated reaction mechanisms has been described extensively in the literature [87, 88].

13.2.6
Dicyclopentadiene polyHIPEs

Recently, a different approach using ring opening metathesis polymerization (ROMP) to cure an HIPE was investigated. The ROMP of dicylcopentadiene (DCPD) leads to polyHIPEs with advanced mechanical properties, compared to polyHIPEs cured by free radical polymerization. The Young's moduli of DCPD-polyHIPEs are about 145–159 MPa, which is much higher than those typically obtained for polyHIPEs (3–6 MPa). The unreacted double bonds in the DCPD-polyHIPEs are a good platform for further functionalization. Oxidation occurred on the double bonds, which could be detected by IR spectroscopy. Functionalization with aqueous hydrazine solution was performed and yielded hydrazones. Moreover, functionalization via click chemistry, such as the thiol–ene reaction, was conducted. Together with the good mechanical properties, these materials are very promising for applications in separation or catalysis chemistry [48].

13.3
Applications

The majority of applications take advantage of three beneficial characteristics of polyHIPEs: (i) the fully interconnected porous structure of the polyHIPE, induced by the physical properties of the emulsion, which allows the easy flow of fluids through the monolith; (ii) the relatively large surface area compared to

nonporous materials; and (iii) the ability to introduce functional surface groups, which previously has been described in depth in this review.

13.3.1
Tissue Engineering

PolyHIPEs with large void sizes caused by destabilization of HIPEs are good candidates as scaffolds for tissue engineering because they create a three-dimensional environment for cell growth and differentiation. Cells cultured *in vitro* in a 3D environment exhibit distinct differences in their physiology and resemble cells *in vivo* more closely [88, 89].

The classical ST/DVB-polyHIPEs have been used as scaffolds to culture hepatocyte cells *in vitro* [90]. 3D cultured HepG2 cells were shown to have a more similar morphology to hepatocyte cells *in vivo* and to be much more resilient to the cytotoxic drug methotrexate in comparison to those cells cultured on 2D plastic tissue culture [91].

PolyHIPE polymers containing hydroxyapatite, with pore sizes of 40, 60, and 100 μm, were evaluated as materials for osteoblast growth and bone formation. Modification with hydroxyapatite to improve cell adhesion and osteoconductive properties was studied, and investigations showed that there is a significant increase in osteoblast numbers penetrating into the polymer [92].

In another study, porous ST/DVB-polyHIPE matrices were coated with aqueous-based solutions including poly-D-lysine and laminin. The growth of human-stem-cell-derived neurons on these porous matrices has been investigated [9].

Biodegradable polyHIPEs have also been investigated as tissue engineering scaffolds. Polyester-based polyHIPE foams containing PCL [7] or PLA [8] were studied for tissue growth. The results showed excellent biocompatibility for both types of foam. Comparative studies indicated that cells adhered more rapidly to PCL-based materials than to the PLA-containing counterparts [8]. Hydrophilic polysaccharide-based polyHIPEs prepared from vinyl-functionalized dextran were shown to support neuronal migration [93]. Highly porous biodegradable gelatin-based polyHIPEs were prepared by both free radical polymerization and enzymatic cross-linking [94]. Polycaprolactone-polystyrene semi-IPNs have been synthesized. Myoblasts were successfully attached to the surface of a semi-IPN poly-HIPE, resulting in the formation of a monolayer and spontaneous differentiation of the cells, with the development of myotubes [10].

13.3.2
Support Materials

Functionalized polyHIPEs are often used as a support material. The two forms of the polyHIPEs, monolith and beads, can be used. Beads are more commonly used because of their commercial availability and it is more suitable for the

batch method. However, continuous flow-through techniques gain more attention because of their feasibility in automatic reactions.

Monolithic supports have better characteristics because of their simple preparation procedure, excellent performance, good permeability, large surface area, and high concentration of functional groups [63, 95]. However, both beads and monoliths have been functionalized with different chemical groups for the support of reagents, scavengers, and catalysts.

Chloromethyl functionalities prepared by copolymerization with VBC are well established for further functionalization and used in reactive supports [21, 35]. However, in some cases, a more reactive support was needed. Therefore, preparation of polyHIPEs bearing NPA groups and postmodification into an acid chloride was a possible route. Alternatively the direct copolymerization with acrylic acid and functionalization to the acid chloride was suggested [53].

Poly(glycidyl methacrylate-*co*-ethylene glycol dimethacrylate) monolithic supports were prepared by radical polymerization. They were modified to bear weak anion-exchange groups and tested on the separation of standard protein mixtures. A dynamic binding capacity close to $9 \, \mathrm{mg \, ml^{-1}}$ was achieved for bovine serum albumin [42, 43].

PolyHIPE supports have found many applications including the separation of heavy metals [34], the purification of water from atrazine [37], ion exchange resins [19], supports for reactions [18], and amine-functionalized 4-chlorobenzoyl chloride scavengers [21].

13.4
Conclusions

Emulsion-templated porous polymers (polyHIPEs) have been functionalized by three different approaches, leading to a wide variety of functional porous materials. Each method has its advantages and disadvantages. The use of comonomers ensures homogeneous functionalization throughout the monolith; however, polar functionalities can severely destabilize the emulsion leading to inhomogeneous samples and emulsion breakdown before curing. Functionalizing a preformed monolith overcomes this problem, but uniform chemical modification throughout the bulk of the sample can be difficult to achieve, and the density of functional groups can be quite low. This problem of low-density functional groups can be overcome by grafting polymer chains to the internal surface of the material. In all postcure functionalization processes, reactions should be as efficient as possible to ensure the maximum extent of chemical modification. The resulting functional porous polymers have been found to be applicable in biomedicine and chemical process technologies, with advantages over existing materials demonstrated. Improvements in the manufacturing processes of polyHIPEs, using alternative curing methods such as photopolymerization, will increase the range of materials available and the format in which they can be obtained (for example, beads, disks,

and membranes). These new materials will undoubtedly continue to be applied in different areas of advanced materials science.

References

1. Merrifield, R.B. (1963) *J. Am. Chem. Soc.*, **85**, 2149–2154.
2. Lissant, K. (1973) *J. Colloid Interface Sci.*, **42**, 201–208.
3. Barby, D. and Haq, Z. (1982) European Patent E Pat. 60, 138.
4. Barbetta, A., Cameron, N.R., and Cooper, S.J. (2000) *Chem. Commun.*, 221–222.
5. Zhang, H. and Cooper, A.I. (2003) *Macromolecules*, **36**, 5061–5064.
6. Gitli, T. and Silverstein, M.S. (2011) *Polymer*, **52**, 107–115.
7. Busby, W., Cameron, N.R., and Jahoda, C.A.B. (2001) *Biomacromolecules*, **2**, 154–164.
8. Busby, W., Cameron, N.R., and Jahoda, C.A. (2002) *Polym. Int.*, **51**, 871–881.
9. Hayman, M.W., Smith, K.H., Cameron, N.R., and Przyborski, S.A. (2005) *J. Biochem. Biophys. Methods*, **62**, 231–240.
10. Lumelsky, Y., Zoldan, J., Levenberg, S., and Silverstein, M.S. (2008) *Macromolecules*, **41**, 1469–1474.
11. Christenson, E.M., Soofi, W., Holm, J.L., Cameron, N.R., and Mikos, A.G. (2007) *Biomacromolecules*, **8**, 3806–3814.
12. Tai, H., Sergienko, A., and Silverstein, M.S. (2001) *Polym. Eng. Sci.*, **41**, 1540–1552.
13. Silverstein, M., Tai, H., Sergienko, A., Lumelsky, Y., and Pavlovsky, S. (2005) *Polymer*, **46**, 6682–6694.
14. (a) Normatov, J. and Silverstein, M.S. (2008) *J. Polym. Sci., Part A: Polym. Chem.*, **46**, 2357–2366; (b) Menner, A., Haibach, K., Powell, R., and Bismarck, A. (2006) *Polymer*, **47**, 7628–7635.
15. Tai, H., Sergienko, A., and Silverstein, M. (2001) *Polymer*, **42**, 4473.
16. (a) Brown, I.J., Clift, D., and Sotiropoulos, S. (1999) *MRS Bull.*, **34**, 1055–1064; (b) Sotiropoulos, S., Bronw, I.J., Akay, G., and Lester, E. (1998) *Mater. Lett.*, **35**, 383–391.
17. Bhumgara, Z. (1995) *Filtr. Sep.*, **32**, 245–251.
18. Ottens, M., Leene, G., Beenackers, A.A.C.M., Cameron, N., and Sherrington, D.C. (2000) *Ind. Eng. Chem. Res.*, **39**, 259–266.
19. Wakeman, R., Bhumgara, Z., and Akay, G. (1998) *Chem. Eng. J.*, **70**, 133–141.
20. Mercier, A., Deleuze, H., and Mondain-Monval, O. (2000) *React. Funct. Polym.*, **46**, 67–79.
21. Krajnc, P., Brown, J.F., and Cameron, N.R. (2002) *Org. Lett.*, **4**, 2497–2500.
22. Krajnc, P., Stefanec, D., Brown, J.F., and Cameron, N.R. (2005) *J. Polym. Sci., Part A: Polym. Chem.*, **43**, 296–303.
23. Silverstein, M.S., Cameron, N.R., and Hillmyer, M.A. (2011) *Porous Polymers*, John Wiley & Sons, Inc., Hoboken, NJ.
24. Menner, A., Powell, R., and Bismarck, A. (2006) *Macromolecules*, **39**, 2034–2035.
25. Lissant, K. (1966) *J. Colloid Interface Sci.*, **22**, 462–468.
26. Cameron, N.R. and Sherrington, D.C. (1996) *Faraday Trans.*, **92**, 1543.
27. (a) Butler, R., Davies, C.M., and Cooper, A.I. (2001) *Adv. Mater.*, **13**, 1459; (b) Butler, R., Hopkinson, I., and Cooper, A.I. (2003) *J. Am. Chem. Soc.*, **125**, 14473–14481.
28. Pierre, S.J., Thies, J.C., Dureault, A., Cameron, N.R., van Hest, J.C.M., Carette, N., Michon, T., and Weberskirch, R. (2006) *Adv. Mater.*, **18**, 1822–1826.
29. Cummins, D., Wyman, P., Duxbury, C.J., Thies, J., Koning, C.E., and Heise, A. (2007) *Chem. Mater.*, **19**, 5285–5292.
30. Lovelady, E., Kimmins, S.D., Wu, J., and Cameron, N.R. (2011) *Polym. Chem.*, **2**, 559.
31. Poschalko, A., Rohr, T., Gruber, H., Bianco, A., Guichard, G., Briand, J.-P., Weber, V., and Falkenhagen, D. (2003) *J. Am. Chem. Soc.*, **125**, 13415–13426.
32. Gokmen, M.T., van Camp, W., Colver, P.J., Bon, S.A.F., and Du Prez, F.E. (2009) *Macromolecules*, **42**, 9289–9294.

33. Pulko, I., Wall, J., Krajnc, P., and Cameron, N.R. (2010) *Chem.-Eur. J.*, **16**, 2350–2354.

34. Benicewicz, B.C., Jarvinen, G.D., Kathios, D.J., and Jorgensen, B.S. (1998) *J. Radioanal. Nucl. Chem.*, **235**, 31–35.

35. Kovacic, S. and Krajnc, P. (2009) *J. Polym. Sci., Part A: Polym. Chem.*, **47**, 6726–6734.

36. Stefanec, D. and Krajnc, P. (2005) *React. Funct. Polym.*, **65**, 37–45.

37. Pulko, I., Kolar, M., and Krajnc, P. (2007) *Sci. Total Environ.*, **386**, 114–123.

38. Stefanec, D. and Krajnc, P. (2007) *Polym. Int.*, **56**, 1313–1319.

39. Leber, N., Fay, J.D.B., Cameron, N.R., and Krajnc, P. (2007) *J. Polym. Sci., Part A: Polym. Chem.*, **45**, 4043–4053.

40. Pulko, I. and Krajnc, P. (2005) *Acta Chim. Slov.*, **52**, 215–223.

41. Barbetta, A., Dentini, M., Leandri, L., Ferraris, G., Coletta, A., and Bernabei, M. (2009) *React. Funct. Polym.*, **69**, 724–736.

42. Yao, C., Qi, L., Jia, H., Xin, P., Yang, G., and Chen, Y. (2009) *J. Mater. Chem.*, **19**, 767–772.

43. Krajnc, P., Leber, N., Stefanec, D., Kontrec, S., and Podgornik, A. (2005) *J. Chromatogr. A*, **1065**, 69–73.

44. Lucchesi, C., Pascual, S., Dujardin, G., and Fontaine, L. (2008) *React. Funct. Polym.*, **68**, 97–102.

45. Cameron, N.R. and Sherrington, D.C. (1997) *J. Mater. Chem.*, **7**, 2209–2212.

46. Sergienko, A.Y., Tai, H., Narkis, M., and Silverstein, M.S. (2004) *J. Appl. Polym. Sci.*, **94**, 2233–2239.

47. Mercier, A., Deleuze, H., Maillard, B., and Mondain-Monval, O. (2002) *Adv. Synth. Catal.*, **344**, 33–36.

48. Kovacic, S., Krajnc, P., and Slugovc, C. (2010) *Chem. Commun.*, **46**, 7504.

49. Kovacic, S., Stefanec, D., and Krajnc, P. (2007) *Macromolecules*, **40**, 8056–8060.

50. Kulygin, O. and Silverstein, M.S. (2007) *Soft Matter*, **3**, 1525.

51. Zhang, H. and Cooper, A.I. (2002) *Chem. Mater.*, **14**, 4017–4020.

52. Lumelsky, Y., Lalush-Michael, I., Levenberg, S., and Silverstein, M.S. (2009) *J. Polym. Sci., Part A: Polym. Chem.*, **47**, 7043–7053.

53. Majer, J. and Krajnc, P. (2009) *Acta Chim. Slov.*, **56**, 629–634.

54. Krajnc, P., Stefanec, D., and Pulko, I. (2005) *Macromol. Rapid Commun.*, **26**, 1289–1293.

55. Zhang, H. and Cooper, A.I. (2007) *Adv. Mater.*, **19**, 2439–2444.

56. Cameron, N.R. and Sherrington, D.C. (1997) *Macromolecules*, **30**, 5860–5869.

57. Duke, J. (1998) *Polymer*, **39**, 4369–4378.

58. Cameron, N.R., Sherrington, D.C., Ando, I., and Kurosu, H. (1996) *J. Mater. Chem.*, **6**, 719–726.

59. Mercier, A., Deleuze, H., and Mondain-Monval, O. (2001) *Macromol. Chem. Phys.*, **202**, 2672–2680.

60. Deleuze, H., Maillard, B., and Mondain-Monval, O. (2002) *Bioorg. Med. Chem. Lett.*, **12**, 1877–1880.

61. Brown, J.F., Krajnc, P., and Cameron, N.R. (2005) *Ind. Eng. Chem. Res.*, **44**, 8565–8572.

62. Moine, L., Deleuze, H., and Maillard, B. (2003) *Tetrahedron Lett.*, **44**, 7813–7816.

63. Moine, L., Deleuze, H., Degueil, M., and Maillard, B. (2004) *J. Polym. Sci., Part A: Polym. Chem.*, **42**, 1216–1226.

64. Fernández-Trillo, F., van Hest, J.C.M., Thies, J.C., Michon, T., Weberskirch, R., and Cameron, N.R. (2009) *Adv. Mater.*, **21**, 55–59.

65. Tripp, J.A., Stein, J.A., Svec, F., and Fréchet, J.M.J. (2000) *Org. Lett.*, **2**, 195–198.

66. Zupan, M., Krajnc, P., and Stavber, S. (1996) *Polymer*, **37**, 5477–5481.

67. Ault-Justus, S.E., Hodges, J.C., and Wilson, M.W. (1998) *Biotechnol. Bioeng.*, **61**, 17–22.

68. Thunhorst, K.L., Gehlsen, M.D., Wright, R.E., Nelson, E.W., Koecher, S.D., and Gold, D. (2001) WO Pat. 2001/021693.

69. Zhang, H. and Cooper, A.I. (2005) *Soft Matter*, **1**, 107.

70. Noyori, R. (2005) *Chem. Commun.*, 1807.

71. Audouin, F., Birot, M., Pasquinet, É., Deleuze, H., Besnard, O., and Poullain, D. (2008) *J. Appl. Polym. Sci.*, **108**, 2808–2813.

72. David, D. and Silverstein, M.S. (2009) *J. Polym. Sci., Part A: Polym. Chem.*, **47**, 5806–5814.

73. Elmes, A.R., Hammond, K., and Sherrington, D.C. (1994) *Eur. Pat. Appl.* EP Pat. 289238.

74. (a) Peters, E.C., Svec, F., and Fréchet, J.M.J. (1999) *Adv. Mater.*, **11**, 1169–1181; (b) Preinerstorfer, B., Bicker, W., Lindner, W., and Lammerhofer, M. (2004) *J. Chromatogr. A*, **1044**, 187–199.

75. Gauthier, M.A., Gibson, M.I., and Klok, H.-A. (2009) *Angew. Chem. Int. Ed.*, **48**, 48–58.

76. Kolb, H.C., Finn, M.G., and Sharpless, K. (2001) *Angew. Chem. Int. Ed.*, **40**, 2004–2021.

77. Fernández-Trillo, F., Duréault, A., Bayley, J.P.M., van Hest, J.C.M., Thies, J.C., Michon, T., Weberskirch, R., and Cameron, N.R. (2007) *Macromolecules*, **40**, 6094–6099.

78. Fernández-Trillo, F., van Hest, J.C.M., Thies, J.C., Michon, T., Weberskirch, R., and Cameron, N.R. (2008) *Chem. Commun.*, 2230.

79. (a) Wang, J.-S. and Matyjaszewski, K. (1995) *Macromolecules*, **28**, 7901–7910; (b) Braunecker, W.A. and Matyjaszewski, K. (2007) *Prog. Polym. Sci.*, **32**, 93–146.

80. Kolb, H.C. and Sharpless, K. (2003) *Drug. Discov. Today*, **8**, 1128–1137.

81. (a) Huisgen, R. (1984) in *13-Dipolar Cycloaddition Chemistry* (ed. A. Padwa), John Wiley & Sons, Inc., New York, pp. 1–176; (b) Bock, V.D., Hiemstra, H., and van Maarseveen, J.H. (2006) *Eur. J. Org. Chem.*, **2006**, 51–68.

82. (a) Goodall, G.W. and Hayes, W. (2006) *Chem. Soc. Rev.*, **35**, 280; (b) Lutz, J.-F. (2007) *Angew. Chem. Int. Ed.*, **46**, 1018–1025.

83. Cummins, D., Duxbury, C.J., Quaedflieg, P.J.L.M., Magusin, P.C.M.M., Koning, C.E., and Heise, A. (2009) *Soft Matter*, **5**, 804.

84. Hoyle, C.E. and Bowman, C.N. (2010) *Angew. Chem. Int. Ed.*, **49**, 1540–1573.

85. Lowe, A.B. (2010) *Polym. Chem.*, **1**, 17.

86. (a) Hoyle, C.E., Lowe, A.B., and Bowman, C.N. (2010) *Chem. Soc. Rev.*, **39**, 1355; (b) Kade, M.J., Burke, D.J., and Hawker, C.J. (2010) *J. Polym. Sci., Part A: Polym. Chem.*, **48**, 743–750; (c) Prasath, R.A., Gokmen, M.T., Espeel, P., and Du Prez, F.E. (2010) *Polym. Chem.*, **1**, 685.

87. Fairbanks, B.D., Scott, T.F., Kloxin, C.J., Anseth, K.S., and Bowman, C.N. (2009) *Macromolecules*, **42**, 211–217.

88. Abbott, A. (2003) *Nature*, **424**, 870–872.

89. (a) Justice, B.A., Badr, N.A., and Felder, R.A. (2009) *Drug. Discov. Today*, **14**, 102–107; (b) Cukierman, E. (2001) *Science*, **294**, 1708–1712.

90. Bokhari, M., Carnachan, R.J., Cameron, N.R., and Przyborski, S.A. (2007) *Biochem. Biophys. Res. Commun.*, **354**, 1095–1100.

91. Bokhari, M., Carnachan, R.J., Cameron, N.R., and Przyborski, S.A. (2007) *J. Anat.*, **211**, 567–576.

92. Akay, G., Birch, M., and Bokhari, M. (2004) *Biomaterials*, **25**, 3991–4000.

93. Barbetta, A., Dentini, M., de Vecchis, M.S., Filippini, P., Formisano, G., and Caiazza, S. (2005) *Adv. Funct. Mater.*, **15**, 118–124.

94. Barbetta, A., Massimi, M., Conti Devirgiliis, L., and Dentini, M. (2006) *Biomacromolecules*, **7**, 3059–3068.

95. Zou, H., Huang, X., Ye, M., and Luo, Q. (2002) *J. Chromatogr. A*, **954**, 5–32.

14
Post-polymerization Modification of Polymer Brushes

Sara Orski, Gareth Sheppard, Rachelle Arnold, Joe Grubbs, and Jason Locklin

14.1
Introduction

Polymer thin films are a highly specialized class of polymers on surfaces that range in thickness from several nanometers to micrometers. The chemical composition and conformation of the polymer chains at the surface can dictate interfacial properties such as adhesion, friction, wetting, and absorption of molecules from the environment. Ultimately, techniques that afford polymer coatings that are easily tunable provide the most versatility to develop a wide array of surfaces. Specialized surfaces such as arrays and sensors provide an insight into the development of small-scale sensors and devices for fields such as biomaterials science and nanotechnology [1–7].

Polymeric thin films are attached to the surface in one of the two ways: through physical deposition of a thin film (physisorption) or by covalent attachment of the polymer chains to the surface (chemisorption). Weak intermolecular forces between the polymer thin film and the substrate govern surface modification by physisorption. Physisorption can lead to failure of the thin film under nonideal conditions by delamination, dewetting, desorption, and displacement [8]. In contrast, covalent attachment of a polymer thin film to the surface provides enhanced stability to polymer surface modification over physical absorption methods. Polymer brushes consist of macromolecular chains, in which covalent bonds tether the chains to the surface with a large grafting density to alter the unperturbed solution dimensions of the chains [9]. Films generated from polymer brushes exhibit unique surface phenomena that are advantageous in controlling physical properties such as wetting, phase segregation, absorption of molecules and macromolecules, lubrication, and diffusion control [7].

These unique properties of polymer brushes are dictated by the extended conformation of the dense, ordered grafting on the surface. The polymer chains extend to balance the free energy associated with chain stretching and chain–solvent interactions. The entropic energy associated with a random walk configuration of the polymer chains favors short, low grafting density brushes. In contrast, a brush will extend to be energetically favorable in a highly solvated,

nonoverlapping configuration [10]. The extended conformation of the brush creates a polymer thin film with a larger volume, allowing for a greater number of functional groups per unit area. The presence of accessible pendant groups, such as *N*-hydroxysuccinimide (NHS) esters, for postfunctionalization allows for a greater influence on interfacial properties of the substrate [7].

The degree to which polymer chains in the brush regime interact with each other to exhibit these surface phenomena is largely determined by their method of formation. Polymer brushes can be formed in a ''grafting-to'' (Figure 14.1) approach by synthesizing a polymer in solution with a reactive functional group at one end of the chain [11, 12]. The polymer is then covalently attached to a complementary functional group on the surface. This process, however, keeps the polymer brush grafting density low and limits the degree of chain extension because the lack of chain interaction does not provide sufficient energy to extend the polymer away from the surface [8]. As polymer chains are more likely to be in their entropically favored random coil configuration in solution, they remain coiled once attached to the surface, forming a blocking layer to the surrounding reaction sites. These random coils are referred to as the *mushroom regime*. After the film is formed, properties such as thickness are proportional to the radius of gyration of the polymer in solution.

Polymer brushes can also be synthesized by the direct polymerization from an immobilized initiator species on the surface in a ''grafting-from'' approach [10, 13]. Chains grown by surface-initiated polymerizations are formed in a confined environment, which forces them to extend away from the surface, increasing the grafting density. Grafting density is the number of polymeric units bound to the surface per unit area, σ (chains per square nanometers), defined by Eq. (14.1),

(a)

(b)
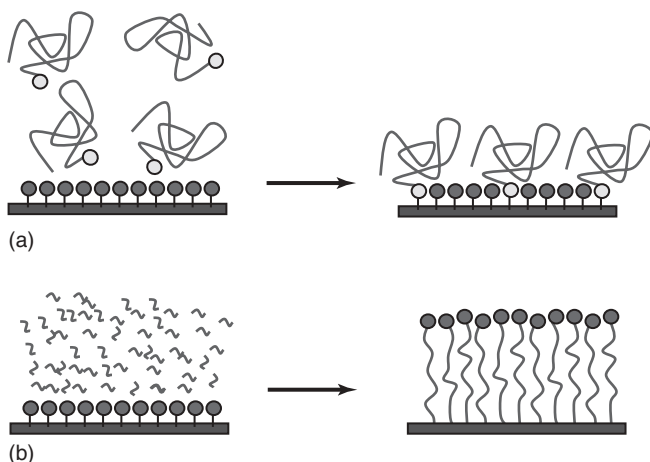
Figure 14.1 Depiction of polymer brushes grown from a ''grafting-to'' versus a ''grafting-from'' approach. (a) ''Grafting-to'' polymerization: reaction of an end-group functional polymer with complementary surface functionality. (b) ''Grafting-from'' polymerization: monomer in solution is polymerized by a surface-bound initiator.

where h is the brush thickness, ρ is polymer bulk density, N_A is Avogadro's number, and M_n is the number average molecular weight of the polymer. Reduced tethering density (Σ) describes the extent of chain extension relative to the grafting density and the polymer's radius of gyration (R_g) as described by Eq. (14.2).

$$\sigma = \frac{h\rho N_A}{M_n} \tag{14.1}$$

$$\Sigma = \sigma \pi R_g^2 \tag{14.2}$$

$$h \propto N\sigma^{\frac{1}{3}} \tag{14.3}$$

The highly extended polymer chain configuration is known as the *brush regime*, where the brush thickness (h) is proportional to the degree of polymerization (N) (Eq. (14.3)) [13]. Polymer chains will orient in an extended conformation as the polymerization proceeds, as the effects of excluded volume interactions overcome the entropic energy loss related to chain stretching. In this geometry, selective control of the polymer brush environment, brought about by conformational changes using stimuli such as temperature, pH, light, electrochemical, electromagnetic field, or polymer solvation, can dramatically alter film properties such as thickness and morphology.

Several polymerization mechanisms have been used to generate polymer brushes, including free radical polymerization and living polymerizations. These reactions include, but are not limited to, atom transfer radical polymerization (ATRP), nitroxide-mediated polymerization (NMP), and ring-opening metathesis polymerization (ROMP) reactions [6, 14–22]. Mediating agents are utilized in living polymerizations to control the build of molecular weight with reaction time [23]. Living polymerizations add a degree of control over surface morphology, as the extended polymer chains will have a decreased molecular weight distribution. Low polydispersities obtained with living radical polymerization yield well-defined high-density polymer brushes [24].

Designing specialized functionality along the backbones of polymer chains requires one of two strategies: synthesis of a monomer containing a desired functionality, or a multistep modification of polymer chains after polymerization. If the functionality is already incorporated into the monomer, no post-polymerization modification is necessary [25]. However, functional group tolerance toward reaction conditions or the optimization of the polymerization conditions must be determined for each monomer, which may not produce the desired characteristics, such as thickness and grafting density. Multistep polymer modification may not need as much initial experimentation, but the use of a single polymer brush scaffold to get the desired functionality requires several permutations that are often not quantitative and prone to side reactions [26].

Polymerization of a functional monomer containing a pendant group designed for single-step derivatization is a straightforward method to overcome functional group incompatibilities. It can also be used to quickly introduce new types of moieties onto the repeat units of polymer chains. This is especially pertinent to

polymer brush generation, as the confined dimensions from the surface make the optimization of the polymerization reaction increasingly difficult with a multistep approach. Single-step polymer modification is preferred over multistep to reduce side reactions and to produce homogeneous functionalization. Modification utilizing rare or costly functionalities, such as biomolecules and functionalized nanostructures, can limit the formation of specialized surfaces. However, using the reactive polymer brush approach allows for facile post-polymerization modification and can reduce the loss of precious materials.

Polymer brushes amenable to single-step post-polymerization modifications exist, the most common of which are polymers containing activated ester functional groups. Activated esters contain an excellent leaving group, prompting the rapid and quantitative functionalization with amine nucleophiles under mild conditions. Several classes of polymeric active esters such as NHS [27–35], pentafluorophenol [36–40], *p*-nitrophenol [41–44], and dicarboxyimide [45] functionalized esters have previously been investigated. NHS esters are commonly used for biological post-polymerization modification, where the conjugation of biomolecules occurs between the amine functional groups on peptides and the activated ester [46–55]. Minimization of hydrolysis and side reactions of the activated ester can be achieved by using aqueous solutions with a pH of 7 or by performing the aminolysis reaction in an organic solvent in the presence of a proton acceptor [46]. The Rühe group [56] has polymerized *n*-methacryloyl-β-alanine succinimide ester from a surface-bound free radical initiator and demonstrated the functionalization of the activated ester with small molecules and oligomers with 80 nm polymer brushes. Cullen *et al.* [57] used ATRP to grow polymer brushes of 2-vinyl-4,4-dimethyl azlactone on a surface to immobilize RNase A. They showed that the enzyme maintained activity while covalently attached to the polymer matrix. Polymer brushes bearing an azlactone group can also be quantitatively functionalized in aqueous environments without competitive hydrolysis [57–59].

Other functional polymer brushes, in addition to active esters, have been synthesized for post-polymerization modification, such as epoxides [60–66], activated alkenes [67–69], thiols [70, 71], pyridyldisulfides [32, 72–74], aldehydes and ketones [75–79], and alkyne/azide cycloaddition [80–90]. The use of alkyne/azide cycloaddition chemistry in the post-polymerization modification of polymer brushes is an additional functionalization strategy to active esters [91, 92]. The alkyne/azide Huisgen 1,3-dipolar cycloaddition is very selective, tolerant of other functional groups, and compatible with protic, aprotic, and aqueous solvent conditions [85]. Known as *click* chemistry, these cycloaddition reactions proceed with high quantitative yields at a rapid reaction rate [85, 93–95]. Click chemistry reactions are especially appealing for biological attachment due to incorporation of azides into biomolecules through postsynthetic modification [96, 97], enzymatic transfer [98, 99], and selective nutrition of metabolites [100]. Conventional alkyne/azide cycloaddition requires a metal catalyst such as copper and is ideal for many applications [101–103]. However, use of a metal catalyst can limit the incorporation of alkyne/azide cycloaddition into biological conjugation because of the cytotoxicity

of the metal [104]. An alternative to using copper-catalyzed alkyne/azide cycloaddition (CuAAC) involves using a highly strained and polarized alkyne such as dibenzocyclooctyne to lower the activation energy of the cycloaddition reaction, which circumvents the necessity of a catalyst. These high-energy alkynes can be incorporated into polymer brushes by post-polymerization through aminolysis of active ester brushes with amine-functionalized alkynes [105].

Post-polymerization modification of polymer brushes with photoactivated compounds allows for the formation of multifunctional, orthogonal surfaces. Two or more types of functionalized polymer pendant groups can be utilized in a well-defined spatially oriented domain for use in biochips, microfluidic devices, targeted drug delivery, and microelectronic devices. Specifically, the use of poly(propargyl methacrylate) brushes to functionalize thiol-terminated molecules in the radical-mediated thiol–yne click reaction generated by ultraviolet light photopatterning was demonstrated by Patton *et al.* [106]. Gleason and coworkers [93] used capillary force lithography to create nanodomains of amine- and alkyne-functionalized polymers for one-pot functionalization of NHS esters and azides. The applications involving incorporation of alkyne/azide chemistry into polymer brushes by a photoactivated precursor (Section 14.3) are elucidated later.

14.2
Synthesis and Strategies for Functional Polymer Brushes

14.2.1
Preparation of Active Ester Polymer Brushes by SI-ATRP

Silicon wafer substrates (orientation <100>, native oxide, University Wafer) were cut to the appropriate size and cleaned by sonication in acetone, isopropanol, and deionized water (18.2 MΩ), and then dried under a stream of nitrogen. The surfaces were further cleaned by argon plasma (Harrick Plasma, PDC-32-G, 0.8 mbar, 18 W) for 5 min. The initiator, 11-(2-bromo-2-methyl)propionyloxy undecyl trichlorosilane [107], was deposited on the SiO$_2$ surface in a dry, nitrogen-filled glove box by submerging the substrates in a 10 mM solution in toluene overnight, yielding an average monolayer thickness of 2.5 nm. An atomic force microscopy (AFM) topographic image of the monolayer was featureless, with a root-mean-square (RMS) roughness of 1.2 nm. The active ester monomer, *n*-hydroxysuccinimide 4-vinyl benzoate (NHS4VB), was prepared according to procedures listed in the literature (Figure 14.2) [108–111]. This styrenic monomer has been shown to polymerize with high reaction rates [112].

The initiator substrate was placed in a dry, flat-bottom Schlenk flask in an inert atmosphere. The polymerization was performed in anhydrous dimethyl sulfoxide (DMSO) to ensure the solubility of both the NHS4VB monomer and the polymer brush. The use of polar solvents in ATRP has also been demonstrated to have a significant enhancement on polymerization reaction rate [113, 114]. The active ester monomer (0.662 g, 2.7 mmol) was dissolved in 0.5 mL DMSO in a Schlenk flask. About 93 μL of stock solution containing 0.5 mL DMSO, copper

Figure 14.2 Scheme of SI-ATRP of NHS4VB with post-polymerization modification of the active ester with primary amines.
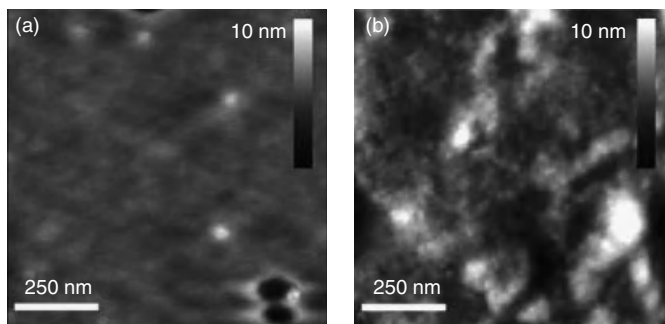
Figure 14.3 AFM topography images of 20 nm poly(NHS4VB) brushes polymerized (a) with and (b) without CuCl$_2$. (Source: Reprinted with permission from [111]. Copyright 2010 American Chemical Society.)

catalyst (CuBr, 39 mg, 0.27 mmol), N,N,N',N',N''-pentamethyldiethylenetriamine (PMDETA)-coordinating ligand (423 μL, 2.03 mmol), and copper(II) deactivator (CuCl$_2$, 7.26 mg, 0.05 mmol) was then added to the Schlenk flask, which was sealed and stirred in a 50 °C oil bath for 1 h. The substrates were rinsed thoroughly with dimethylformamide (DMF) and dried under a stream of nitrogen. Average polymer brush thicknesses were 50 nm as measured by ellipsometry, with an RMS roughness of 0.5 nm as measured by AFM. This very smooth surface is attributed to the controlled polymerization, especially the copper(II) deactivator, which lowers the propagating radical concentration, evident from the comparison of two poly(NHS4VB) brushes, one with deactivator (Figure 14.3a) and one without (Figure 14.3b).

Polymer film thickness can be controlled through polymerization time (Figure 14.4). Samples were polymerized for various time intervals, and film thickness increased linearly with time for the first 50 nm of brush growth. Without
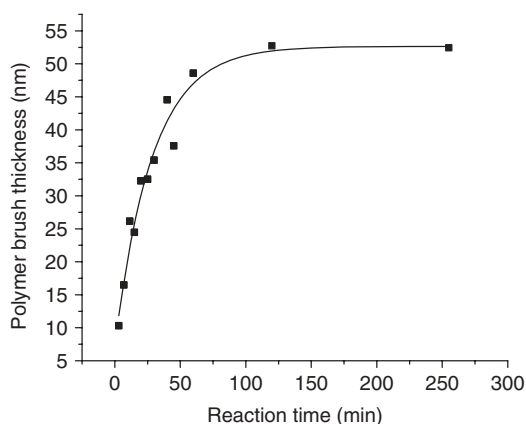
Figure 14.4 Kinetic curve for poly(NHS4VB) thickness. Solid line is to guide the eye. (Source: Reprinted with permission from [111]. Copyright 2010 American Chemical Society.)

the use of a deactivator (CuCl$_2$), the polymer films generated by surface-initiated polymerization had a rougher surface morphology, with an RMS roughness of 2 nm. Early termination is more prevalent due to the larger concentration of propagating radicals, resulting from a faster, less controlled rate of polymerization. Polymerization with CuCl$_2$ afforded better control due to halogen exchange of the alkyl bromide initiator with CuCl$_2$, which provided faster initiation relative to propagation [115]. The copper(II) also lowers the equilibrium concentration of propagating radicals, which slows propagation and affords better control over the polymerization rate.

14.2.2
Synthesis of Poly(NHS4VB) Block Copolymer Brushes with 2-Hydroxyethyl Acrylate, tert-Butyl Acrylate, or Styrene

In using ATRP, the alkyl halide initiator remains at the end of the polymer chains, allowing the poly(NHS4VB) substrates to function as macroinitiators for a secondary polymerization. Block copolymers of NHS4VB with 2-hydroxyethyl acrylate and styrene were used to create hydrophilic and hydrophobic microenvironments for the polymer brush, respectively. The silicon wafer containing the poly(NHS4VB) macroinitiator and a micro stir bar were placed in a dry, flat-bottom Schlenk flask in a glove box. The monomer (2.7 mmol) was dissolved in DMSO (50 wt%), along with 93 μL of the previously described stock solution. The Schlenk flask was sealed, brought outside the glove box, and stirred in a 50 °C oil bath for 16 h. The wafer was removed, rinsed with copious amounts of DMF, and dried with nitrogen. The incorporation of block copolymers allows for layering functionalities within the brush to control the polymer microenvironment. Block copolymers provide a means to create multifunctional brushes for tailoring surface properties via post-polymerization techniques.

14.2.3
Functionalization of Poly(NHS4VB) Brushes with Primary Amines

Polymer brushes of poly(NHS4VB) were converted to functionalized amide derivatives of 4-vinyl benzoic acid using primary amines (100 mM in dry DMF, 50 °C). 1-Aminomethylpyrene (Py-N) was used for quantitation of active ester sites, and a cyclopropenone–amine conjugate [111] was used as a masked cyclic octyne. Triethylamine (2 : 1 mol equivalents to amine) was also added as a proton acceptor [56].

Formation of the active ester polymer brush and conversion to the functionalized amide were confirmed by grazing-angle attenuated total reflection FTIR (GATR-FTIR). Figure 14.5a shows the self-assembled monolayer of the ATRP initiator, which is indicated by absorbance bands representing methyl and carbonyl stretches at 1963 and 1737 cm^{-1}, respectively. Characteristic C=O stretching of the NHS ester appears at 1801, 1769, and 1738 cm^{-1} in poly(NHS4VB) (Figure 14.5b). These bands disappear upon functionalization of the brush with primary amine,
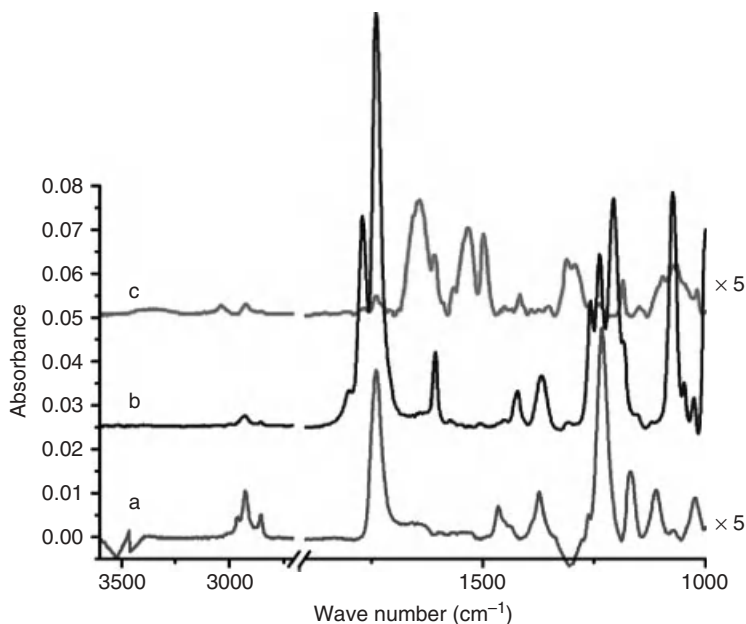
Figure 14.5 GATR-FTIR of the (a) ATRP initiator, (b) poly(NHS4VB) brush, and (c) poly(NHS4VB) brush functionalized with Py-N. (Source: Reprinted with permission from [111]. Copyright 2010 American Chemical Society.)

such as aminomethylpyrene (Py-N) (Figure 14.5c). Amide I and II regions from Py-N functionalization are observed at 1642 and 1542 cm^{-1}, respectively [111].

14.2.4
Quantification of Active Ester Post-polymerization Modification

The numbers of active esters accessible to different brush thicknesses were determined by polymerization of NHS4VB films on glass slides, which were then functionalized with Py-N. The Py-N absorbance for each slide was measured using a UV–vis spectrometer with a slide holder accessory with a sample window area of 19.6 mm^2. A calibration curve using Py-N in DMF solution was created with concentrations between 5.0×10^{-6} and 3.3×10^{-5} M to calculate the extinction coefficient (ε) for Py-N as 32204 cm^{-1} M^{-1}.

$$A = lc \tag{14.4}$$

$$d_{\text{surf}} = \frac{A}{\varepsilon} \tag{14.5}$$

Using the Beer–Lambert law (Eq. (14.4)), one can calculate the surface coverage (d_{surf}) using Eq. (14.5), where A, ε, l, and c are the absorbance, extinction coefficient, film thickness, and concentration, respectively [116]. This calculation includes the assumption that the difference in extinction coefficient between Py-N in solution
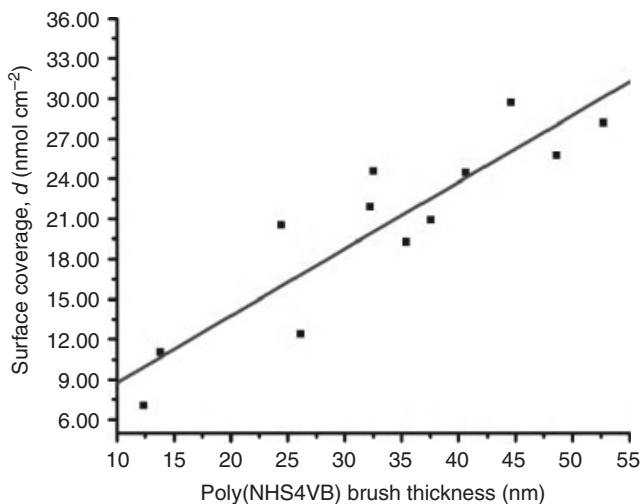
Figure 14.6 Surface coverage of Py-N on poly(NHS4VB) with increasing film thickness. (Source: Reprinted with permission from [111]. Copyright 2010 American Chemical Society.)

and Py-N in the polymer film is negligible. The linear relationship between surface coverage (nmol cm^{-2}) and polymer brush thickness is shown in Figure 14.6. The linear fit shown in the plot has a standard deviation of 3.2 nmol cm^{-2}, indicating that Py-N functionalization occurs through the brush layers for all thicknesses studied. Furthermore, the 50 nm poly(NHS4VB) film can be functionalized with 25.7 nmol cm^{-2} of Py-N, which is three times the amount of accessible active sites on polymer brushes than previously reported [111] and is 3 orders of magnitude greater than two-dimensional self-assembled monolayers containing activated ester functional groups [117, 118].

14.3
Applications of Polymer Brush Modification: Multifunctional Surfaces via Photopatterning

14.3.1
Polymer Brush Functionalization with Photoactivated Dibenzocyclooctyne for Catalyst-Free Azide Cycloaddition

The use of alkyne/azide chemistry for bioorthogonal conjugation to polymer surfaces has been limited by the toxicity of metal catalysts [104]. Recently, alkyne/azide cycloadditions have been developed that circumvent the need for a metallic catalyst by using a reactive, high-energy, strained cycloalkyne to promote the cycloaddition with comparable reaction rates to CuAAC [119–123]. The driving force for copper-free click is the high distortion energy of the cycloalkyne, which lowers

the total activation energy required to undergo the cycloaddition by 8.2 kcal mol^{-1} [124]. Different cyclooctyne derivatives have different rates of reaction based on the substituents that change the polarization of the alkyne bond, thereby lowering the activation energy of the reaction [119, 125–129]. Furthermore, the cyclooctyne can be generated *in situ* from a cyclopropenone-functionalized precursor molecule, which is readily converted to the high-energy alkyne [111, 130]. The photodecarbonylation of cyclopropenones to alkynes in solution (L) and in the solid, crystalline state (S) proceeds quantitatively on the order of picoseconds with high quantum efficiency ($\Phi_L = 0.2$–1.0, $\Phi_S > 1$) [131, 132]. In masking the reactive alkyne with cyclopropenone, copper-free click chemistry can be photodirected to react only where photodecarbonylation forms the reactive cyclooctyne when immobilized at the surface.

The copper-free click surface immobilization strategy is shown in Figure 14.7. Poly(NHS4VB) coatings (125 nm) were prepared using surface-initiated ATRP and then functionalized with a cyclopropenone amine conjugate, as shown in
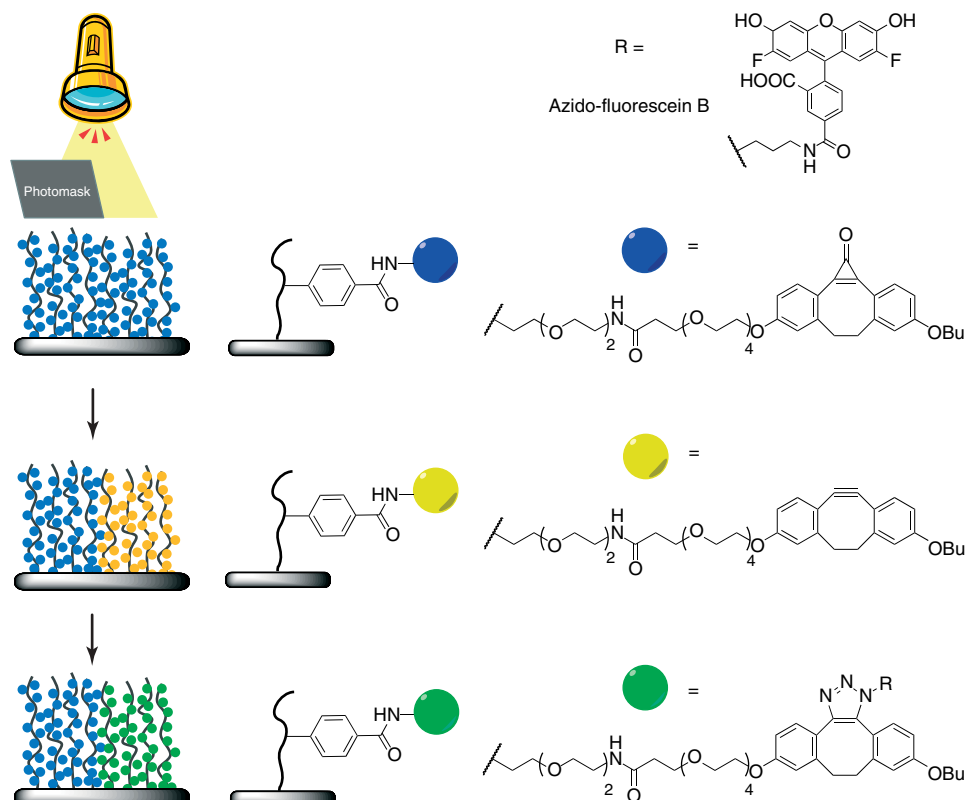
Figure 14.7 Attachment of cyclopropenone to poly(NHS4VB) brushes by photoactivation and functionalization of the polymer brush pendant groups with azide-derived fluorescent dyes such as azido-fluorescein.

Figure 14.2. The cyclopropenone-modified polymer brushes underwent decarbonylation to form dibenzocyclooctyne using UV irradiation (Rayonet UV bulb, 350 nm, 3.5 mW cm^{-2}) for 150 s. The conversion rate of cyclopropenone to dibenzocyclooctyne was monitored using a polymer brush on a quartz slide. A rate constant of $k = 0.022$ s^{-1} was determined by UV–vis absorbance of the cyclopropenone ($\lambda = 353$ nm). Near-quantitative conversion (95%) was complete within 90 s of irradiation. After irradiation of the dibenzocyclooctyne, the slide was submerged in a 5 mg ml^{-1} solution of azido-fluorescein (azido-FL) [111] in methanol at room temperature for 1 h. The substrate was rinsed thoroughly with methanol. The masked cyclopropenone-functionalized polymer brushes did not react with the azides and remained thermally stable at 60 °C for 12 h without decomposition [130, 131]. Unreacted cyclopropenone was still viable for future photoactivation, as demonstrated in the subsequent section.

The post-polymerization modification of the brush was characterized using GATR-FTIR. Figure 14.7 shows the progression from poly(NHS4VB) brush to the covalent attachment of an azido-FL conjugate via photoactivated click chemistry. The characteristic NHS peaks disappear after functionalization with the cyclopropenone–amine conjugate (Figure 14.8a,b), and a C=O stretch and ring
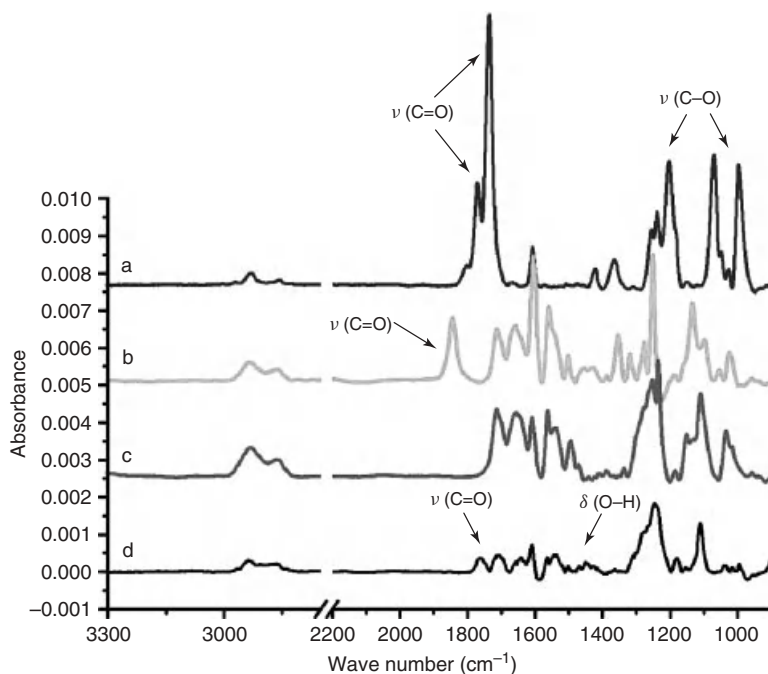
Figure 14.8 GATR-FTIR of (a) poly(NHS4VB) brush, (b) postfunctionalization with cyclopropenone, (c) conversion of cyclopropenone to dibenzocyclooctyne, and (d) functionalization with azido-fluorescein. (Source: Reprinted with permission from [105]. Copyright 2010 American Chemical Society.)

conjugation for cyclopropenone appear at 1846 and 1608 cm^{-1}, respectively. Upon irradiation, the cyclopropenone C=O stretch disappears, yielding the dibenzocyclooctyne (Figure 14.8c). Functionalization of the azido-FL is indicated by carboxylic acid stretches at 1757 and 1447 cm^{-1} (Figure 14.8d).

14.3.2
Copper-Free Click of Dibenzocyclooctyne and Azido-FL/Azido-RB

The masked cyclopropenone surface can be activated to a reactive alkyne by subsequent irradiation. In order to generate a bifunctional surface, cyclopropenone-functionalized substrates were irradiated through a shadow mask to form multicomponent surfaces with spatially resolved chemical functionality. A square-patterned transmission electron microscope (TEM) grid (12 μm pitch) was used to mask the polymer brush. The polymer brush substrate was placed on a piece of poly(dimethylsiloxane) (PDMS) with the TEM grid on top of the substrate. A quartz slide was used to create intimate contact between the grid and the substrate. The four layers were held together tightly by clamps to eliminate space between the grid mask and silicon wafer substrate in order to photopattern the grid without distortion. The wafer was irradiated through the shadow mask and then immersed in a solution of lissamine rhodamine B–azide conjugate [111] (azido-RB, 5 mg mL^1 in methanol, 20 min). Rhodamine B was only functionalized on the polymer brush where the film had been irradiated. The entire substrate was irradiated again without the TEM grid to activate the remaining cyclooctynes. Azido-FL was then immobilized (5 mg mL^1 in methanol, 20 min) to generate a bifunctional, patterned substrate. Figure 14.9 shows a fluorescence microscopy image of the photopatterned substrates. There is negligible cross-contamination between the two dyes, with segregation between the selectively activated regions. This indicates quantitative conversion of the first irradiation, as no fluorescein appeared in the areas where rhodamine B was attached.

(a)   (b)   (c)
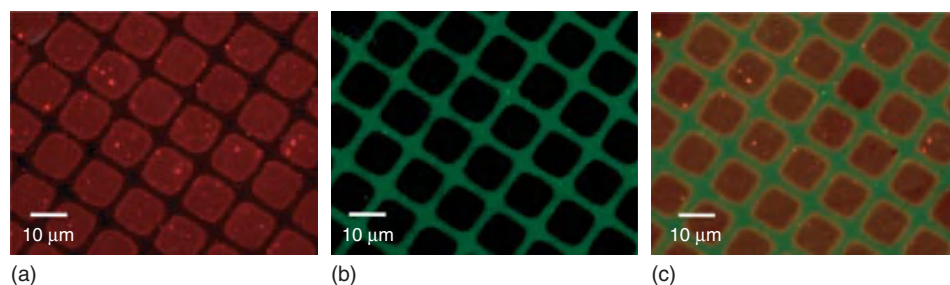
Figure 14.9 Fluorescence microscopic images of a photopatterned surface fabricated by sequential photoactivation of dibenzocyclooctynes: (a) click-functionalized azido-RB excited at λ = 550 nm, (b) azido-FL excited at λ = 477 nm, and (c) both dyes imaged under wide UV excitation (λ = 350 nm). (Source: Reprinted with permission from [105]. Copyright 2010 American Chemical Society.)

14.4
Conclusions and Future Outlook

The use of activated ester-containing polymer scaffolds is a simple and efficient way to perform post-polymerization functionalization in the brush regime. This allows for the incorporation of moieties that are not compatible with specific polymerization techniques. NHS4VB was used to determine the quantitative conversion of the active ester with primary amines in a homopolymer and in various block copolymers. The utility of the NHS4VB brush was demonstrated in conjunction with copper-free alkyne/azide click to create photopatterned surfaces. Spatially organized, multifunctional surfaces were created with this system that showed little to no cross-contamination. With the increase in specialized polymer functionality, new platforms and unique surface-bound polymer architectures will lead to tailored interfaces with tunable physical properties.

References

1. Grest, G.S. (1999) *Polymers in Confined Environments*, Springer, vol. 138.
2. Klein, J., Kumacheva, E., Mahalu, D., Perahia, D., and Fetters, L.J. (1994) *Nature*, **370**, 634.
3. Ratner, B.D., Hoffmann, F.J., and Lemons, J.E. (1996) *Biomaterials Science, An Introduction to Materials in Medicine*, Academic Press, San Diego.
4. Senaratne, W., Andruzzi, L., and Ober, C.K. (2005) *Biomacromolecules*, **6**, 2427.
5. Ayres, N. (2010) *Polym. Chem.*, **1**, 769.
6. Barbey, R., Lavanant, L., Paripovic, D., Schüwer, N., Sugnaux, C., Tugulu, S., and Klok, H.A. (2009) *Chem. Rev.*, **109**, 5437.
7. Orski, S.V., Fries, K.H., Sontag, S.K., and Locklin, J. (2011) *J. Mater. Chem.*, **21**, 14135.
8. Rühe, J. (2004) *Polymer Brushes*, Wiley-VCH Verlag GmbH & Co. KGaA, p. 1.
9. Brittain, W.J. and Minko, S. (2007) *J. Polym. Sci., Part A: Polym. Chem.*, **45**, 3505.
10. Milner, S.T. (1991) *Science*, **251**, 905.
11. Ionov, L., Zdyrko, B., Sidorenko, A., Minko, S., Klep, V., Luzinov, I., and Stamm, M. (2004) *Macromol. Rapid Commun.*, **25**, 360.
12. Minko, S., Patil, S., Datsyuk, V., Simon, F., Eichhorn, K.J., Motornov, M., Usov, D., Tokarev, I., and Stamm, M. (2002) *Langmuir*, **18**, 289.
13. Zhou, F. and Huck, W.T.S. (2006) *Phys. Chem. Chem. Phys.*, **8**, 3815.
14. Chen, K., Liang, D., Tian, J., Shi, L., and Zhao, H. (2008) *J. Phys. Chem. B*, **112**, 12612.
15. Liu, X., Guo, S., and Mirkin, C.A. (2003) *Angew. Chem. Int. Ed.*, **42**, 4785.
16. Senkovskyy, V., Khanduyeva, N., Komber, H., Oertel, U., Stamm, M., Kuckling, D., and Kiriy, A. (2007) *J. Am. Chem. Soc.*, **129**, 6626.
17. Sontag, S.K., Marshall, N., and Locklin, J. (2009) *Chem. Commun.*, 3354.
18. Tomlinson, M.R. and Genzer, J. (2003) *Chem. Commun.*, 1350.
19. Wang, X., Tu, H., Braun, P.V., and Bohn, P.W. (2006) *Langmuir*, **22**, 817.
20. Wu, T., Gong, P., Szleifer, I., Vlček, P., Šubr, V., and Genzer, J. (2007) *Macromolecules*, **40**, 8756.
21. Zhao, B. (2004) *Langmuir*, **20**, 11748.
22. Edmondson, S., Osborne, V.L., and Huck, W.T.S. (2004) *Chem. Soc. Rev.*, **33**, 14.
23. Hawker, C.J., Bosman, A.W., and Harth, E. (2001) *Chem. Rev.*, **101**, 3661.
24. Tsujii, Y., Ohno, K., Yamamoto, S., Goto, A., and Fukuda, T. (2006) in *Surface-Initiated Polymerization I*,

vol. 197 (ed. R. Jordan), Springer, Berlin/Heidelberg, p. 1.

25. Jain, P., Dai, J., Baker, G.L., and Bruening, M.L. (2008) *Macromolecules*, **41**, 8413.

26. Huang, W., Kim, J.B., Bruening, M.L., and Baker, G.L. (2002) *Macromolecules*, **35**, 1175.

27. Arisumi, K., Feng, F., Miyashita, T., and Ninomiya, H. (1998) *Langmuir*, **14**, 5555.

28. Hu, Z., Liu, Y., Hong, C., and Pan, C. (2005) *J. Appl. Polym. Sci.*, **98**, 189.

29. Wong, S.Y. and Putnam, D. (2007) *Bioconjugate Chem.*, **18**, 970.

30. Desai, A., Atkinson, N., Rivera, F., Devonport, W., Rees, I., Branz, S.E., and Hawker, C.J. (2000) *J. Polym. Sci., A: Polym. Chem.*, **38**, 1033.

31. Favier, A., D'Agosto, F., Charreyre, M.T., and Pichot, C. (2004) *Polymer*, **45**, 7821.

32. Ghosh, S., Basu, S., and Thayumanavan, S. (2006) *Macromolecules*, **39**, 5595.

33. Mammen, M., Dahmann, G., and Whitesides, G.M. (1995) *J. Med. Chem.*, **38**, 4179.

34. Pedone, E., Li, X., Koseva, N., Alpar, O., and Brocchini, S. (2003) *J. Mater. Chem.*, **13**, 2825.

35. Vosloo, J.J., Tonge, M.P., Fellows, C.M., D'Agosto, F., Sanderson, R.D., and Gilbert, R.G. (2004) *Macromolecules*, **37**, 2371.

36. Arnold, R., Sheppard, G., and Locklin, J. (2012) **45**(13), 5444–5450.

37. Günay, K., Schüwer, N., and Klok, H.-A. (2012) *Polym. Chem.*, **3**, 2186–2192.

38. Eberhardt, M., Mruk, R., Zentel, R., and Théato, P. (2005) *Eur. Polym. J.*, **41**, 1569.

39. Nilles, K. and Theato, P. (2007) *Eur. Polym. J.*, **43**, 2901.

40. Vogel, N. and Théato, P. (2007) *Macromol. Symp.*, **249–250**, 383.

41. Ye, L., Cormack, P.A.G., and Mosbach, K. (2001) *Anal. Chim. Acta*, **435**, 187.

42. Liu, Y., Wang, L., and Pan, C. (1999) *Macromolecules*, **32**, 8301.

43. Hu, Y.C., Liu, Y., and Pan, C.Y. (2004) *J. Polym. Sci., Part A: Polym. Chem.*, **42**, 4862.

44. Li, R.C., Hwang, J., and Maynard, H.D. (2007) *Chem. Commun.*, 3631.

45. Subr, V. and Ulbrich, K. (2006) *React. Funct. Polym.*, **66**, 1525.

46. Hermanson, G.T. (2008) *Bioconjugate Techniques*, 2nd edn, Academic Press, New York.

47. Wood, K.C., Azarin, S.M., Arap, W., Pasqualini, R., Langer, R., and Hammond, P.T. (2008) *Bioconjugate Chem.*, **19**, 403.

48. Pasut, G., Mero, A., Caboi, F., Scaramuzza, S., Sollai, L., and Veronese, F.M. (2008) *Bioconjugate Chem.*, **19**, 2427.

49. Chen, G., Huynh, D., Felgner, P.L., and Guan, Z. (2006) *J. Am. Chem. Soc.*, **128**, 4298.

50. Theato, P. and Zentel, R. (1999) *Langmuir*, **16**, 1801.

51. Theato, P. (2008) *J. Polym. Sci., Part A: Polym. Chem.*, **46**, 6677.

52. Hausch, M., Zentel, R., and Knoll, W. (1999) *Macromol. Chem. Phys.*, **200**, 174.

53. Buck, M.E., Breitbach, A.S., Belgrade, S.K., Blackwell, H.E., and Lynn, D.M. (2009) *Biomacromolecules*, **10**, 1564.

54. Buck, M.E., Zhang, J., and Lynn, D.M. (2007) *Adv. Mater.*, **19**, 3951.

55. Barringer, J.E., Messman, J.M., Banaszek, A.L., Meyer, H.M., and Kilbey, S.M. (2008) *Langmuir*, **25**, 262.

56. Murata, H., Prucker, O., and Ruhe, J. (2007) *Macromolecules*, **40**, 5497.

57. Cullen, S.P., Mandel, I.C., and Gopalan, P. (2008) *Langmuir*, **24**, 13701.

58. Barringer, J.E., Messman, J.M., Banaszek, A.L., Meyer, H.M., and Kilbey, S.M. (2009) *Langmuir*, **25**, 262.

59. Fournier, D., Pascual, S., Montembault, V., Haddleton, D.M., and Fontaine, L. (2006) *J. Comb. Chem.*, **8**, 522.

60. Tsyalkovsky, V., Klep, V., Ramaratnam, K., Lupitskyy, R., Minko, S., and Luzinov, I. (2007) *Chem. Mater.*, **20**, 317.

61. Edmondson, S. and Huck, W.T.S. (2004) *J. Mater. Chem.*, **14**, 730.

62. Jones, R.G., Yoon, S., and Nagasaki, Y. (1999) *Polymer*, **40**, 2411.

63. Grubbs, R.B., Dean, J.M., Broz, M.E., and Bates, F.S. (2000) *Macromolecules*, **33**, 9522.

64. Benoit, D., Chaplinski, V., Braslau, R., and Hawker, C.J. (1999) *J. Am. Chem. Soc.*, **121**, 3904.

65. Yin, H., Zheng, H., Lu, L., Liu, P., and Cai, Y. (2007) *J. Polym. Sci., A: Polym. Chem.*, **45**, 5091.

66. Rebizant, V., Abetz, V., Tournilhac, F., Court, F., and Leibler, L. (2003) *Macromolecules*, **36**, 9889.

67. París, R. and de la Fuente, J.L. (2007) *J. Polym. Sci., A: Polym. Chem.*, **45**, 3538.

68. Stranix, B.R., Gao, J.P., Barghi, R., Salha, J., and Darling, G.D. (1997) *J. Org. Chem.*, **62**, 8987.

69. Justynska, J. and Schlaad, H. (2004) *Macromol. Rapid Commun.*, **25**, 1478.

70. Wong, L., Boyer, C., Jia, Z., Zareie, H.M., Davis, T.P., and Bulmus, V. (2008) *Biomacromolecules*, **9**, 1934.

71. Justynska, J., Hordyjewicz, Z., and Schlaad, H. (2005) *Polymer*, **46**, 12057.

72. Wang, L., Kristensen, J., and Ruffner, D.E. (1998) *Bioconjugate Chem.*, **9**, 749.

73. Bulmus, V., Woodward, M., Lin, L., Murthy, N., Stayton, P., and Hoffman, A. (2003) *J. Controlled Release*, **93**, 105.

74. El-Sayed, M.E.H., Hoffman, A.S., and Stayton, P.S. (2005) *J. Controlled Release*, **101**, 47.

75. Sun, G., Cheng, C., and Wooley, K.L. (2007) *Macromolecules*, **40**, 793.

76. Schilli Christine, M., Müller Axel, H.E., Rizzardo, E., Thang San, H., and Chong, Y.K. (2003) *Advances in Controlled/Living Radical Polymerization*, vol. **854**, American Chemical Society, p. 603.

77. Mittal, A., Sivaram, S., and Baskaran, D. (2006) *Macromolecules*, **39**, 5555.

78. Cheng, C., Sun, G., Khoshdel, E., and Wooley, K.L. (2007) *J. Am. Chem. Soc.*, **129**, 10086.

79. Yang, S.K. and Weck, M. (2007) *Macromolecules*, **41**, 346.

80. Binder, W.H. and Kluger, C. (2004) *Macromolecules*, **37**, 9321.

81. Sessions, L.B., Mîinea, L.A., Ericson, K.D., Glueck, D.S., and Grubbs, R.B. (2005) *Macromolecules*, **38**, 2116.

82. Tsuda, K., Tsutsumi, K., Yaegashi, M., Miyajima, M., Ishizone, T., Hirao, A., Ishii, F., and Kakuchi, T. (1998) *Polym. Bull.*, **40**, 651.

83. Zhang, K., Lackey, M.A., Wu, Y., and Tew, G.N. (2011) *J. Am. Chem. Soc.*, **133**, 6906.

84. Gao, H. and Matyjaszewski, K. (2007) *J. Am. Chem. Soc.*, **129**, 6633.

85. Binder, W.H. and Sachsenhofer, R. (2007) *Macromol. Rapid Commun.*, **28**, 15.

86. Lutz, J.F. (2007) *Angew. Chem. Int. Ed.*, **46**, 1018.

87. Johnson, J.A., Lewis, D.R., Díaz, D.D., Finn, M.G., Koberstein, J.T., and Turro, N.J. (2006) *J. Am. Chem. Soc.*, **128**, 6564.

88. Fournier, D. and Du Prez, F. (2008) *Macromolecules*, **41**, 4622.

89. Sumerlin, B.S., Tsarevsky, N.V., Louche, G., Lee, R.Y., and Matyjaszewski, K. (2005) *Macromolecules*, **38**, 7540.

90. Riva, R., Schmeits, S., Stoffelbach, F., Jerome, C., Jerome, R., and Lecomte, P. (2005) *Chem. Commun.*, 5334.

91. Lee, B.S., Lee, J.K., Kim, W.J., Jung, Y.H., Sim, S.J., Lee, J., and Choi, I.S. (2007) *Biomacromolecules*, **8**, 744.

92. Soto-Cantu, E., Lokitz, B.S., Hinestrosa, J.P., Deodhar, C., Messman, J.M., Ankner, J.F., and Kilbey, S.M. II (2011) *Langmuir*, **27**, 5986.

93. Im, S.G., Bong, K.W., Kim, B.S., Baxamusa, S.H., Hammond, P.T., Doyle, P.S., and Gleason, K.K. (2008) *J. Am. Chem. Soc.*, **130**, 14424.

94. White, M.A., Johnson, J.A., Koberstein, J.T., and Turro, N.J. (2006) *J. Am. Chem. Soc.*, **128**, 11356.

95. Iha, R.K., Wooley, K.L., Nyström, A.M., Burke, D.J., Kade, M.J., and Hawker, C.J. (2009) *Chem. Rev.*, **109**, 5620.

96. Weisbrod, S.H. and Marx, A. (2008) *Chem. Commun.*, 5675.

97. Gramlich, P.M.E., Wirges, C.T., Manetto, A., and Carell, T. (2008) *Angew. Chem. Int. Ed.*, **47**, 8350.

98. Ochiai, H., Huang, W., and Wang, L.X. (2008) *J. Am. Chem. Soc.*, **130**, 13790.

99. Fernandez-Suarez, M., Baruah, H., Martinez-Hernandez, L., Xie, K.T., Baskin, J.M., Bertozzi, C.R., and Ting, A.Y. (2007) *Nat. Biotech.*, **25**, 1483.

100. Baskin, J.M. and Bertozzi, C.R. (2007) *QSAR Comb. Sci.*, **26**, 1211.

101. Sumerlin, B.S. and Vogt, A.P. (2009) *Macromolecules*, **43**, 1.

102. Canalle, L.A., Berkel, S.S., Haan, L.T., and Hest, J.C.M. (2009) *Adv. Funct. Mater.*, **19**, 3464.

103. Bernardin, A., Cazet, A., Guyon, L., Delannoy, P., Vinet, F., Bonnaffé, D., and Texier, I. (2010) *Bioconjugate Chem.*, **21**, 583.

104. Gaetke, L.M. and Chow, C.K. (2003) *Toxicology*, **189**, 147.

105. Orski, S.V., Poloukhtine, A.A., Arumugam, S., Mao, L., Popik, V.V., and Locklin, J. (2010) *J. Am. Chem. Soc.*, **132**, 11024.

106. Hensarling, R.M., Doughty, V.A., Chan, J.W., and Patton, D.L. (2009) *J. Am. Chem. Soc.*, **131**, 14673.

107. Matyjaszewski, K., Miller, P.J., Shukla, N., Immaraporn, B., Gelman, A., Luokala, B.B., Siclovan, T.M., Kickelbick, G., Vallant, T., Hoffmann, H., and Pakula, T. (1999) *Macromolecules*, **32**, 8716.

108. Nozaki, K., Sato, N., Tonomura, Y., Yasutomi, M., Takaya, H., Hiyama, T., Matsubara, T., and Koga, N. (1997) *J. Am. Chem. Soc.*, **119**, 12779.

109. Angiolini, L., Caretti, D., Mazzocchetti, L., Salatelli, E., Willem, R., and Biesemans, M. (2006) *J. Organomet. Chem.*, **691**, 3043.

110. Aamer, K.A. and Tew, G.N. (2007) *J. Polym. Sci., Part A: Polym. Chem.*, **45**, 5618.

111. Orski, S.V., Fries, K.H., Sheppard, G.R., and Locklin, J. (2010) *Langmuir*, **26**, 2136.

112. Matyjaszewski, K. and Davis, T.P. (2002) *Handbook of Radical Polymerization*, John Wiley and Sons, Inc., Hoboken, NJ.

113. Perrier, S. and Haddleton, D.M. (2002) *Macromol. Symp.*, **182**, 261.

114. Percec, V., Guliashvili, T., Ladislaw, J.S., Wistrand, A., Stjerndahl, A., Sienkowska, M.J., Monteiro, M.J., and Sahoo, S. (2006) *J. Am. Chem. Soc.*, **128**, 14156.

115. Matyjaszewski, K., Shipp, D.A., Wang, J.L., Grimaud, T., and Patten, T.E. (1998) *Macromolecules*, **31**, 6836.

116. Li, D., Swanson, B.I., Robinson, J.M., and Hoffbauer, M.A. (1993) *J. Am. Chem. Soc.*, **115**, 6975.

117. Lockett, M.R., Phillips, M.F., Jarecki, J.L., Peelen, D., and Smith, L.M. (2007) *Langmuir*, **24**, 69.

118. Gooding, J.J. and Hibbert, D.B. (1999) *Trends Anal. Chem.*, **18**, 525.

119. Baskin, J.M., Prescher, J.A., Laughlin, S.T., Agard, N.J., Chang, P.V., Miller, I.A., Lo, A., Codelli, J.A., and Bertozzi, C.R. (2007) *Proc. Natl. Acad. Sci.*, **104**, 16793.

120. Jewett, J.C. and Bertozzi, C.R. (2010) *Chem. Soc. Rev.*, **39**, 1272.

121. Lallana, E., Fernandez-Megia, E., and Riguera, R. (2009) *J. Am. Chem. Soc.*, **131**, 5748.

122. Bernardin, A., Cazet, A., Guyon, L., Delannoy, P., Vinet, F., Bonnaffé, D., and Texier, I. (2010) *Bioconjugate Chem.*, **21**, 583.

123. Canalle, L.A., van Berkel, S.S., de Haan, L.T., and van Hest, J.C.M. (2009) *Adv. Funct. Mater.*, **19**, 3464.

124. Ess, D.H., Jones, G.O., and Houk, K.N. (2008) *Org. Lett.*, **10**, 1633.

125. Codelli, J.A., Baskin, J.M., Agard, N.J., and Bertozzi, C.R. (2008) *J. Am. Chem. Soc.*, **130**, 11486.

126. Debets, M.F., van Berkel, S.S., Schoffelen, S., Rutjes, F.P.J.T., van Hest, J.C.M., and van Delft, F.L. (2010) *Chem. Commun.*, **46**, 97.

127. Jewett, J.C., Sletten, E.M., and Bertozzi, C.R. (2010) *J. Am. Chem. Soc.*, **132**, 3688.

128. Kuzmin, A., Poloukhtine, A., Wolfert, M.A., and Popik, V.V. (2010) *Bioconjugate Chem.*, **21**, 2076.

129. Ning, X., Guo, J., Wolfert, M.A., and Boons, G.J. (2008) *Angew. Chem. Int. Ed.*, **47**, 2253.

130. Poloukhtine, A.A., Mbua, N.E., Wolfert, M.A., Boons, G.J., and Popik, V.V. (2009) *J. Am. Chem. Soc.*, **131**, 15769.

131. Poloukhtine, A. and Popik, V.V. (2003) *J. Org. Chem.*, **68**, 7833.

132. Kuzmanich, G., Gard, M.N., and Garcia-Garibay, M.A. (2009) *J. Am. Chem. Soc.*, **131**, 11606.

15
Covalent Layer-by-Layer Assembly Using Reactive Polymers

Adam H. Broderick and David M. Lynn

15.1
Introduction

Methods for the fabrication of nanostructured thin films provide powerful and practical approaches to defining the interfacial properties of materials. Approaches to fabrication that are substrate independent are particularly versatile because they can be used to coat a wide variety of surfaces, often without regard for surface composition or the need for specific preparative treatments. For an increasing number of applications, however, it is also important that the thin films and coatings themselves be versatile in terms of the degree to which new chemical functionalities can be introduced to tune or modify surface properties during subsequent downstream processing steps. Methods for the fabrication of *reactive* thin films and coatings are attractive in this context because they provide access to interfaces that can be modified to present or pattern new functionalities on surfaces *after* fabrication (including chemical or biological functionalities that may not otherwise survive environmental conditions present during film fabrication). While the ''ideal/universal'' process for the fabrication of reactive, nanostructured coatings does not exist, there are currently many useful laboratory-scale and commercial-scale options from which to choose [1–5]. This chapter focuses on a discussion of relatively new – and increasingly popular – approaches to the reactive or covalent layer-by-layer (LbL) assembly of cross-linked and reactive thin films that address several of these practical issues and provide useful alternatives to other methods.

15.2
Overview of Layer-by-Layer Assembly: Conventional versus Covalent Assembly

Approaches to the LbL assembly of multicomponent polymer films [6, 7] have had an enormous impact on the design of new materials and functional interfaces. Many approaches to LbL assembly involve the stepwise and alternating (i.e., ''layer-by-layer'' Figure 15.1a) deposition of oppositely charged polymers on a surface to form multilayered films called polyelectrolyte multilayers (PEMs) composed of

(a)

(b) Polyelectrolytes — Ionically cross-linked

(c) Reactive polymers — X + Y → X–Y — Covalently cross-linked

(d)
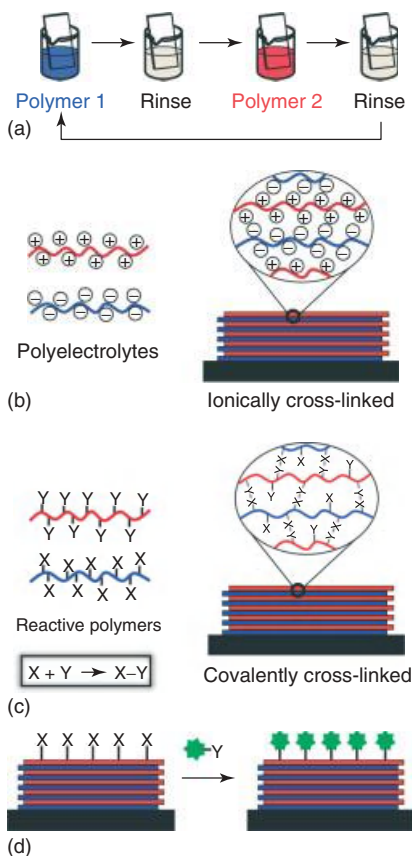
Figure 15.1 (a) Schematic illustration of a typical dipping-based approach to the LbL assembly of polymer multilayers. (b,c) Idealized illustration showing fundamental differences between (b) ionically cross-linked polyelectrolyte multilayers (PEMs) assembled by the LbL assembly of charged polymers, and (c) covalently cross-linked polymer multilayers fabricated by covalent/reactive LbL assembly. (d) The presence of residual reactive groups in multilayers fabricated by covalent LbL assembly can be used as a platform for further functionalization.

interpenetrating layers of positively and negatively charged polymers (Figure 15.1b) [6–9]. This approach can be used to design thin, ionically cross-linked multilayers with thicknesses, compositions, and morphologies that can be varied at the nanoscale by changing (i) the number of different polymer "layers" that are deposited, (ii) the structures of the polymers that are used to form the films, or (iii) other experimental or environmental conditions used during assembly.

In general, LbL methods are technically straightforward; they require no expensive equipment and can be performed on a laboratory bench top under mild conditions (e.g., in water and at ambient room temperature). Two additional practical advantages of this approach are that it can be used (i) to fabricate uniform,

conformal thin films on the surfaces of topologically and topographically complex substrates (including planar, curved, and porous/rough surfaces) and (ii) to coat the surfaces of objects fabricated from a wide variety of materials (including inorganic and organic materials, and both ''hard'' and ''soft'' substrates). Additional information on the structures, properties, and wide-ranging potential applications of PEMs can be found in several recent comprehensive reviews [8,10–17].

Although LbL assembly confers many practical advantages relative to some other methods for the fabrication of thin films and coatings, the ionically cross-linked nature of conventional PEMs (Figure 15.1b) can limit the usefulness of these materials in certain contexts. For example, some PEMs can exhibit limited stability upon changes in pH, ionic strength, and temperature (or upon exposure to other ''harsh'' environments) that can disrupt the weak ionic interactions that stitch these materials together [18–24]. Several groups have sought to address this limitation by developing approaches to the covalent cross-linking of PEMs by postfabrication thermal treatment [25–29], exposure to UV radiation [27, 30–32], or by treatment of preassembled PEMs with chemical cross-linking agents [33–38]. These approaches can lead to PEMs with increased stability, but thermal treatment can also alter other important film properties and these approaches are, in general, limited to the cross-linking of PEMs with appropriate combinations of mutually reactive functional groups (e.g., amine and carboxylic acid functionalities) that may or may not be present depending on the structure of the polyelectrolytes used to fabricate a film.

As an alternative to these postfabrication approaches to cross-linking, several groups have developed more direct approaches to the LbL fabrication of cross-linked multilayers [39, 40]. These ''reactive'' or ''covalent'' methods exploit interfacial covalent-bond-forming reactions between *mutually reactive materials* to drive film assembly (as opposed to ionic interactions between oppositely charged species), and thus lead to thin polymer multilayers that are inherently covalently cross-linked (Figure 15.1c). These new approaches retain many of the desirable features of conventional LbL assembly noted above, including the ability to control film thickness and composition and the ability to fabricate films on the surfaces of complex objects. However, these new methods also introduce several additional practical advantages. Foremost among these is that the introduction of covalent cross-links during assembly can lead to multilayers with increased stabilities without the need for additional postfabrication treatment. In addition, while conventional LbL processes for the assembly of PEMs are generally restricted to the use of aqueous solutions (owing to the limited solubility of many polyelectrolytes in solvents other than water), many materials useful for covalent LbL assembly are compatible with the use of organic solvents, including aprotic and less polar solvents, which can expand the range of substrates and interfaces on which films can be deposited. Finally, a particularly useful feature of these covalent approaches is that they often result in polymer multilayers containing residual, unreacted functional groups (either on the surface or in the interior of a film; e.g., Figure 15.1c) that can be exploited postfabrication, and under mild conditions, to covalently attach and/or create patterns of other functionalities using a wide range

Table 15.1 Reactive groups and cross-linking chemistry used for covalent LbL assembly.

Reactive group X	Reactive group Y	Type of cross-link	References
Alkyne	Azide	Triazole	[41–53]
Azlactone	Amine	Amide–amide	[54–65]
Anhydride	Amine	Amide	[66–73]
Activated ester	Amine	Amide	[74–77]
Carboxylic acid	Amine	Amide	[78–80]
Acid chloride	Amine	Amide	[81, 82]
Isocyanate	Amine	Urea	[81, 82]
Dichlorophosphazene	Amine	Phosphazene	[83]
Acrylate	Amine	Amino-ester	[84, 86, 147]
Alkyl halide	Amine	Alkyl amine	[87, 88]
Epoxide	Amine	Alkyl amine	[89]
Aldehyde	Amine	Schiff base (imine)	[90–98]
Dihydroxybenzene	Amine	Schiff base (imine)	[99]
Acid chloride	Hydroxyl	Ester	[81, 82, 100–102]
Isocyanate	Hydroxyl	Urethane	[81, 82]
Boronic acid	Hydroxyl	Boronate ester	[103–106]
Epoxide	Hydroxyl	Ether	[81]
Aldehyde	Alkoxyamine	Oxime	[107–109]
Vinylsulfone	Thiol	Sulfonethioether	[110]
Phenyl	Diazonium salt	Azo	[31, 111]
Metal complexes	Various ligands	Metal coordination	[112–123]

of different chemical and biological agents (Figure 15.1d). Although it is certainly not impossible to chemically functionalize or pattern the surfaces of conventional PEMs, the combination of increased film stability and chemical reactivity afforded by these reactive approaches can greatly facilitate postfabrication modification and, in general, opens the door to new opportunities for the design of functional surfaces and interfaces. Many specific examples highlighting these general features and practical advantages are discussed in greater detail in the following sections.

The most fundamental and obvious material-based requirement for covalent LbL assembly is the need for two film components (or ''layers'') that contain two different functional groups that can react with each other to form a covalent bond (Figure 15.1c) [39, 40]. Although it is not an explicit requirement, these reactive processes are, of course, facilitated tremendously if the reactions chosen are robust, occur rapidly, and proceed to completion under mild reaction conditions (e.g., in either the presence or the absence of a catalyst, but at ambient pressure and manageable temperatures). A wide variety of reactive materials can be used as components of covalently assembled multilayer films, including synthetic polymers, small molecules, nanospheres and colloids, carbon nanotubes, and proteins in various combinations. In the broader context of this book as a whole, we restrict our discussion to examples of covalent or reactive LbL assembly where at least one of the ''building blocks'' used during assembly is a reactive polymer. Table 15.1

provides an overview of the different reactive groups and the resulting types of interlayer cross-links that are discussed in the following sections.

15.3
Scope and Organization

This chapter provides an overview and account of recent approaches to reactive LbL assembly. It also endeavors to provide some broader perspective on the development of these materials as well as insight into currently unresolved issues and opportunities for further development in view of several potential applications. In the broader context of LbL assembly, approaches to ''covalent'' assembly are relatively new. This chapter is not intended, however, to serve as a comprehensive review – as noted above, the discussion in this chapter is limited, in large measure, to examples involving the use of readily reactive polymers. Although details related to polymer reactivity are included where additional context is helpful, readers interested in fundamental aspects of the chemistry of a given reactive polymer will find additional details and broader context on many of these points in other chapters of this book.

The following discussion is not organized chronologically. Rather, it is organized, in general, around groups of reactions (or groups of similar approaches) that have been used for covalent LbL assembly. Although many different types of reactions have been investigated, some general reaction platforms have been investigated more extensively than others. The discussion below begins with consideration of approaches based on ''click chemistry'' that have been investigated broadly by several different groups. Subsequent sections focus on approaches developed in our laboratory based on the chemistry of azlactones and on several other approaches developed by other groups. This collection of examples highlights both the versatility of this covalent approach to assembly and the range of different ways in which it can prove useful.

15.4
Covalent LbL Assembly Based on "Click Chemistry"

As mentioned above, one of the most basic requirements for covalent LbL assembly is the need for two polymers with side-chain or main-chain functionalities that can react with each other to form a covalent bond. Although there are no particular limits on the types of reactions that can be used, from a practical point of view these processes are more accessible, and ultimately more useful, if the chemical reactions that are selected are rapid and irreversible, occur under mild conditions, and do not participate in unwanted side reactions or lead to the generation of reaction by-products that could remain in a film after assembly. For these and other practical reasons, many groups have exploited click chemistry – specifically, the Huisgen 1,3-dipolar cycloaddition of azides and alkynes to form 1,2,3-triazoles

using Cu(I) as a catalyst [124] (Eq. (15.1)) – as a general, convenient, and model platform for the assembly of cross-linked multilayers.

$$R_1 \!-\!\!\equiv\ +\ \underset{R_2}{N}\!=\!\overset{\oplus}{N}\!=\!\overset{\ominus}{N} \longrightarrow \underset{R_1}{\overset{N=N}{\diagup}}\!\!\diagdown\!\!\overset{N}{\diagdown}\!\!-R_2 \tag{15.1}$$
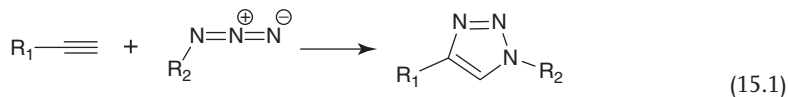
The applications of click chemistry in the broader contexts of polymer synthesis and materials science have been reviewed comprehensively [124–128], but a short discussion of the general features of this reaction that render it attractive for covalent LbL assembly is useful here. Click reactions of the type outlined above (Eq. (15.1)) generally proceed rapidly and under mild conditions [124] which permits them to be performed in the types of open vessels (e.g., beakers or flasks) that are commonly used in immersion- or dipping-based LbL assembly protocols. These azide/alkyne coupling reactions are also very selective and can be performed in the presence of a wide variety of other functional groups without unwanted side reactions [125]. Furthermore, the resulting triazole linkages that are formed are generally resistant to hydrolysis, oxidation, or reduction reactions, and this approach can therefore be used to introduce robust and stable chemical cross-links [124]. Finally, these reactions proceed in aqueous media, which, in addition to facilitating the development of bench top assembly protocols, renders this approach well suited for use with biomacromolecular species (such as proteins) or with other charged polymers that may only be soluble in water (as discussed below). Although click chemistry coupling reactions were not the first types of reactions to be used for covalent LbL assembly, these and other practical advantages have rendered this reaction platform a popular choice in a broad range of studies. In the following sections, we highlight several reports that illustrate further many of the attractive features of this approach.

The first example of the use of click chemistry for the covalent assembly of LbL films was reported by Caruso and coworkers, and this approach has since been developed extensively by this group. In a seminal report, Such *et al.* demonstrated that the Huisgen 1,3-dipolar cycloaddition reaction could be used to build up cross-linked polymer multilayers by the alternating and repetitive immersion of planar silicon, quartz, or gold-coated substrates into solutions of alkyne- and azide-functionalized poly(acrylic acid) (PAA) copolymers (Figure 15.2) [41]. In addition to being the first example of the use of click reactions for the covalent assembly of cross-linked multilayers, this approach is also notable because it demonstrated an approach to the fabrication of ''single-component'' multilayers (that is, multilayers composed entirely of layers of anionic PAA, as opposed to alternating layers of cationic and anionic polymers) that cannot be prepared using conventional (i.e., electrostatic) approaches to LbL assembly.

Additional studies demonstrated that this click-based approach to assembly proceeds with many of the features and practical advantages of conventional LbL processes, including the ability to exert control over film thickness by varying the number of click layers deposited during assembly. Film growth was found to proceed in a linear manner with respect to the number of polymer layers deposited
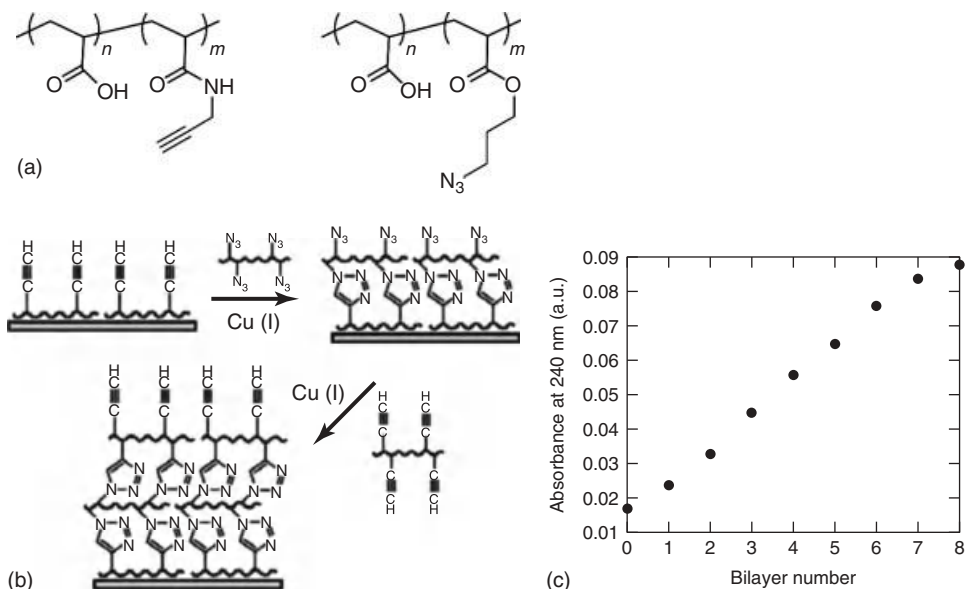
Figure 15.2 (a) Structures of alkyne- and azide-functionalized PAA derivatives (PAA-Alk (left) and PAA-Az (right)). (b) Schematic showing a "click chemistry" approach to LbL assembly. (c) Plot of UV–vis absorption peak intensity at 240 nm (corresponding to the absorption of copper/PAA complexes) versus the number of (PAA-Az/PAA-Alk) bilayers deposited on a quartz substrate. (Reprinted with permission from [41]. Copyright 2006 American Chemical Society.)

(Figure 15.2c), similar to what is observed during the assembly of many ionically cross-linked PEMs [41]. A subsequent report demonstrated that film thickness and morphology could be tailored further by varying the conditions under which assembly was performed, including (i) changing the ionic strength of the aqueous dipping solutions, (ii) adjusting the length of polymer deposition/reaction times, and (iii) changing the density of click-functional side chains (i.e., the number of alkyne or azide functional groups) on the PAA polymer backbones [42]. Finally, these covalently cross-linked PAA-based films were demonstrated to be physically stable (that is, they did not erode or disintegrate significantly) on exposure to aqueous solutions over a broad range of pH (from 3.5 to 9.5) or to a range of organic solvents including ethanol, acetone, and dimethylformamide (DMF) [41]. Tang *et al.* [43] also reported independently on the click assembly of PAA-based multilayers and used a quartz crystal microbalance to characterize extents to which these cross-linked films exhibit reversible swelling behavior on changes in pH.

Following their initial report on the covalent assembly of PAA-based multilayers on macroscopic planar surfaces, Such *et al.* [44] demonstrated that this click approach could be extended to the design of cross-linked hollow microcapsules (Figure 15.3). The motivation for this work arose from numerous past reports [12, 16, 129–132] demonstrating that the fabrication of ionically cross-linked PEMs on sacrificial colloidal substrates can provide convenient template-assisted routes

Hollow
capsule
(e)

Coated
sphere
(d)
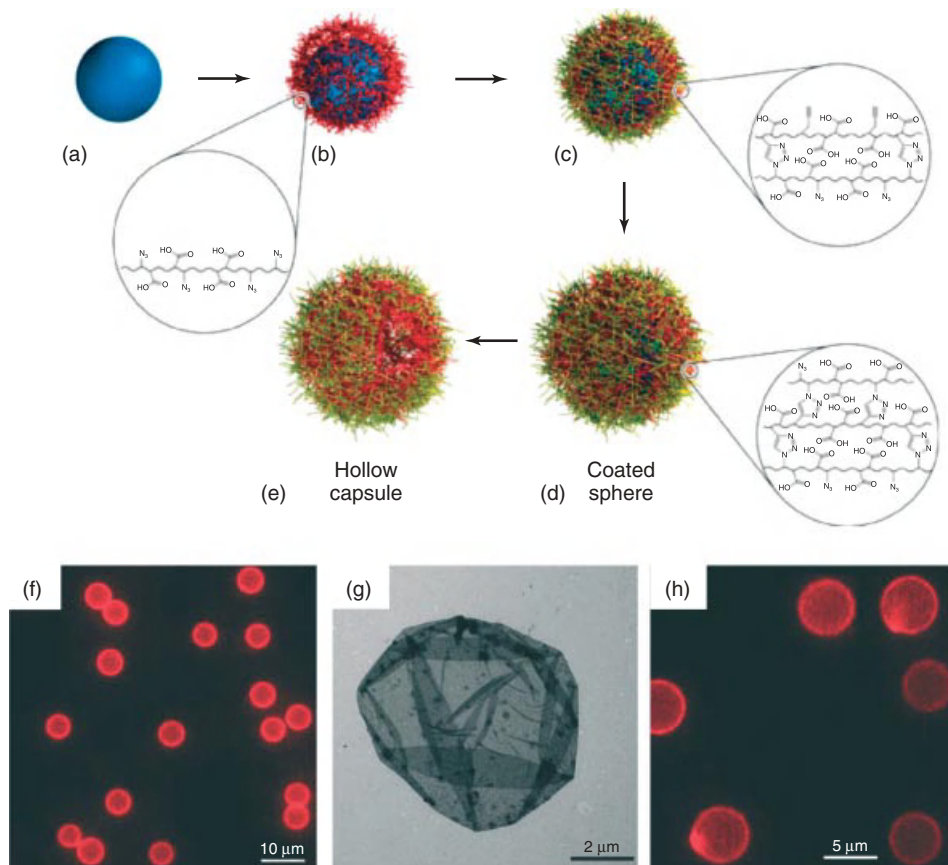
Figure 15.3 (a–e) Schematic showing the process used to fabricate hollow capsules using click-based LbL assembly. The images show (a) template particle, (b) PAA-Az electrostatically adsorbed to the surface, and (c) PAA-Alk ''clicked'' onto the PAA-Az layer. (d) Steps (b) and (c) are repeated until the desired number of layers is deposited. (e) Removal of the sacrificial core forming a hollow click capsule. (f) Fluorescence microscopy image of silica particles coated with a click film fabricated using PAA-Alk that was fluorescently labeled with rhodamine. (g) TEM image of a hollow click capsule. (h) Fluorescence microscopy image of microspheres coated with click films and then subsequently functionalized by treatment with an azide-functionalized fluorescent dye in the presence of a copper catalyst. (Adapted with permission from [44]. Copyright 2007 American Chemical Society.)

to making hollow polymer capsules that are useful in catalysis, drug delivery, and many other applications (e.g., by depositing films on solid microparticle substrates that can subsequently be removed by dissolution or etching). This report investigated the covalent, click-assisted assembly of PAA-based multilayers (using components similar to those described above; Figure 15.2a) on the surfaces of poly(ethyleneimine) (PEI)-coated silica microparticles $\sim$5 µm in diameter (Figure 15.3a–d) [44]. Characterization of film growth using films fabricated from
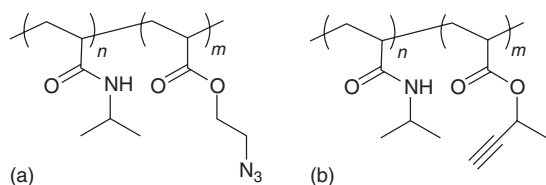
Figure 15.4 Structures of (a) azide- and (b) alkyne-functionalized poly(*N*-isopropylacrylamide) (PNIPAm) derivatives.

fluorescently labeled polymers confirmed stepwise linear growth and that the particles were uniformly coated (Figure 15.3f). Removal of the silica cores using hydrofluoric acid (Figure 15.3d,e) provided hollow microcapsules with walls ∼5 nm thick for films composed of 12 polymer layers (as determined by characterization of dried capsules using AFM and transmission electron microscopy (TEM; Figure 15.3g)). Cross-linked multilayer capsules exposed repeatedly to solutions ranging from pH 2 to 10 were observed to shrink and swell in response to high and low pH, respectively, but the capsules otherwise remained intact under these conditions.

Another important outcome of this study was the demonstration that the residual unreacted alkyne functionality present in the walls of these capsules (that is, the pendant alkyne functionality that was not consumed to form triazole-based cross-links during covalent assembly) could be used to covalently attach other azide-functionalized molecules to the films [44]. For example, treatment of the film-coated microparticles described above with an azide-modified rhodamine dye (in the presence of Cu(I) as a catalyst) resulted in immobilization of the dye in the film (Figure 15.3h). While this initial study demonstrated the proof of concept using a model fluorescent agent, the ability to readily conjugate other functionalities could prove particularly useful in the context of developing these hollow capsules for biological applications (e.g., to attach ligands that promote targeted drug delivery, or to prevent particle aggregation, etc.) [16, 129, 130, 132].

Several other groups have reported examples of the click-assisted assembly of covalently cross-linked multilayers using non-PAA-based building blocks. In another early example, Bergbreiter *et al.* [45] reported the fabrication of single-component multilayers using water-soluble poly(*N*-isopropylacrylamide) (PNIPAm) copolymers functionalized with alkyne or azide groups (Figure 15.4). This work provided additional fundamental insight into important aspects of film structure and reactivity. For example, treatment of films using a solution containing an alkyne-containing dansyl fluorescent label (and Cu(I) as a catalyst) resulted in immobilization of the dye (as characterized by fluorescence microscopy). However, additional studies demonstrated that equivalent levels of fluorophore could be immobilized independent of the identity of the topmost layer of the film (i.e., equivalent fluorescence was observed regardless of whether alkyne- or azide-functionalized PNIPAm was deposited as the last polymer layer during assembly). These results provided evidence that residual unreacted functional groups (in this case, azide groups) were present and available for further reaction in the interiors of these

materials (and not just on their surfaces) [45]. These observations are interesting, and have potential implications for materials design, because they suggest that the ability to perform postfabrication chemical modifications is not limited to modification of film surface properties alone. More broadly, these results suggest opportunities to use this approach to tailor and define the bulk (internal) and interfacial (surface) properties of these materials independently. In a separate study, Huang *et al.* demonstrated that the thermoresponsive behavior of PNIPAm [133, 134] could also be used to control the properties of click-assembled PNIPAm multilayer capsules [46].

More complex (e.g., nonlinear) polymer architectures can also be used as components for click-assisted LbL assembly and, in some cases, can provide new levels of molecular-level control over film thickness and uniformity. Vestberg *et al.* [47] used alkyne- or azide-functionalized 2,2-bis(methylol)propionic acid dendrimers (Figure 15.5) to assemble films on planar surfaces. The thicknesses of these dendrimer-based films increased in a linear manner for the deposition of at least 30 individual layers, and the thickness of each layer could be controlled with precision by varying the generation (e.g., ranging from G2 to G5) of the dendrimer building blocks used during assembly. Increased uniformity and control over layer thicknesses in these films were attributed to the much more compact and monodisperse structures of dendrimers relative to linear polymer analogs used in other studies.

Owing to the strength of the bonds that are formed during assembly, covalent LbL is also well suited for the design of films using small bifunctional molecules and uncharged molecules as building blocks. This contrasts to some extent with conventional methods for LbL assembly driven by weak interactions, which, in general, require components capable of three or more points of interaction with other polymer layers to achieve significant film growth and/or stability [7, 8]. We limit the discussion in this chapter to examples using click chemistry to assemble films using combinations of bifunctional small molecules and mutually reactive polymers. Other examples of this approach that exploit non-click reactions are discussed in subsequent sections.

El Haitami *et al.* [48] have reported on films fabricated using end-functionalized, bifunctional PEG spacers (3–50 ethylene glycol monomer units long) and side-chain-modified PAA (each functionalized with an appropriate alkyne or azide functionality) (Figure 15.6). Characterization of these films using AFM demonstrated that they were uniform but rough (R_{rms} up to ∼60 nm), and film thickness was influenced significantly by the length of the PEG spacer and the length of the polymer side-chain functionality (with longer spacers and/or side chains, in general, leading to thicker films, with the exception of very long spacers, which resulted in decreased film growth due to steric hindrance of the reactive group).

One other interesting observation arising from this work was that the properties of films assembled using azide-functional PEG and alkyne-functional PAA were different from those assembled using alkyne-functional PEG and azide-functional PAA (i.e., upon "swapping" of functional groups) under otherwise identical conditions [48]. These differences in film properties were suggested to arise from potential differences in interactions between positively charged alkyne/Cu(I)
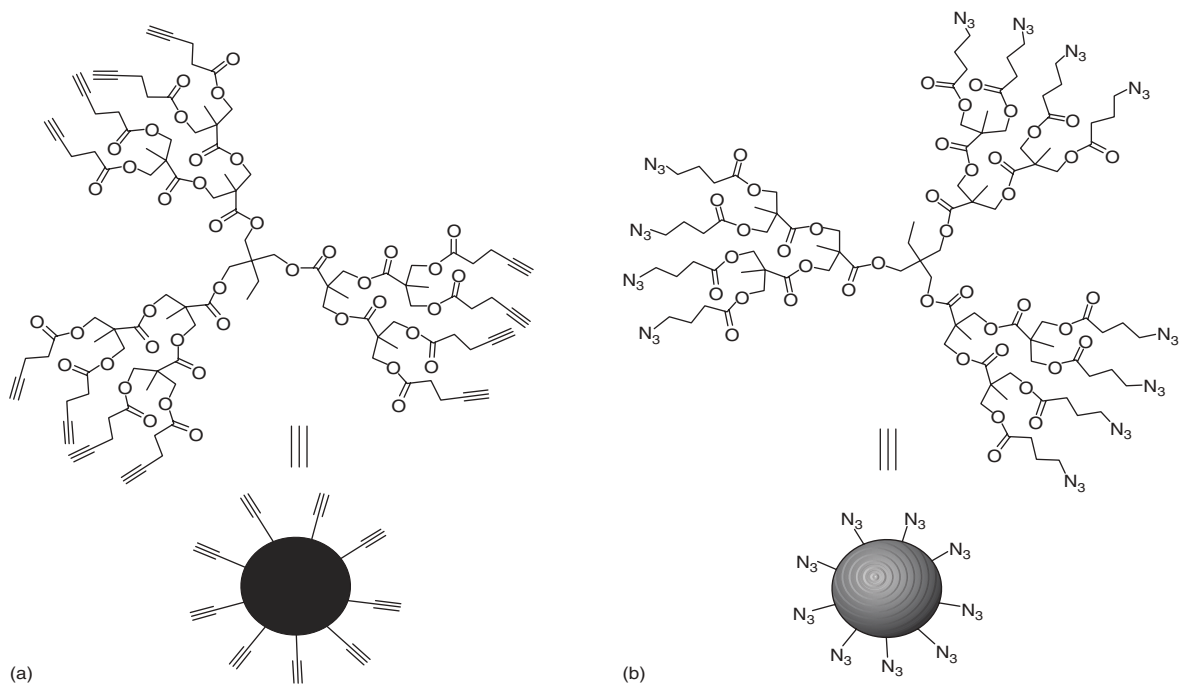
Figure 15.5 Structures of (a) alkyne- and (b) azide-functionalized dendrimers containing 12 chain-end functional groups reacted onto 2,2-bis(methylol)propionic acid (bisMPA) second-generation dendrimers with trimethylolpropane (TMP) cores. (Adapted with permission from [47]. Copyright © 2007 by John Wiley & Sons, Inc.)
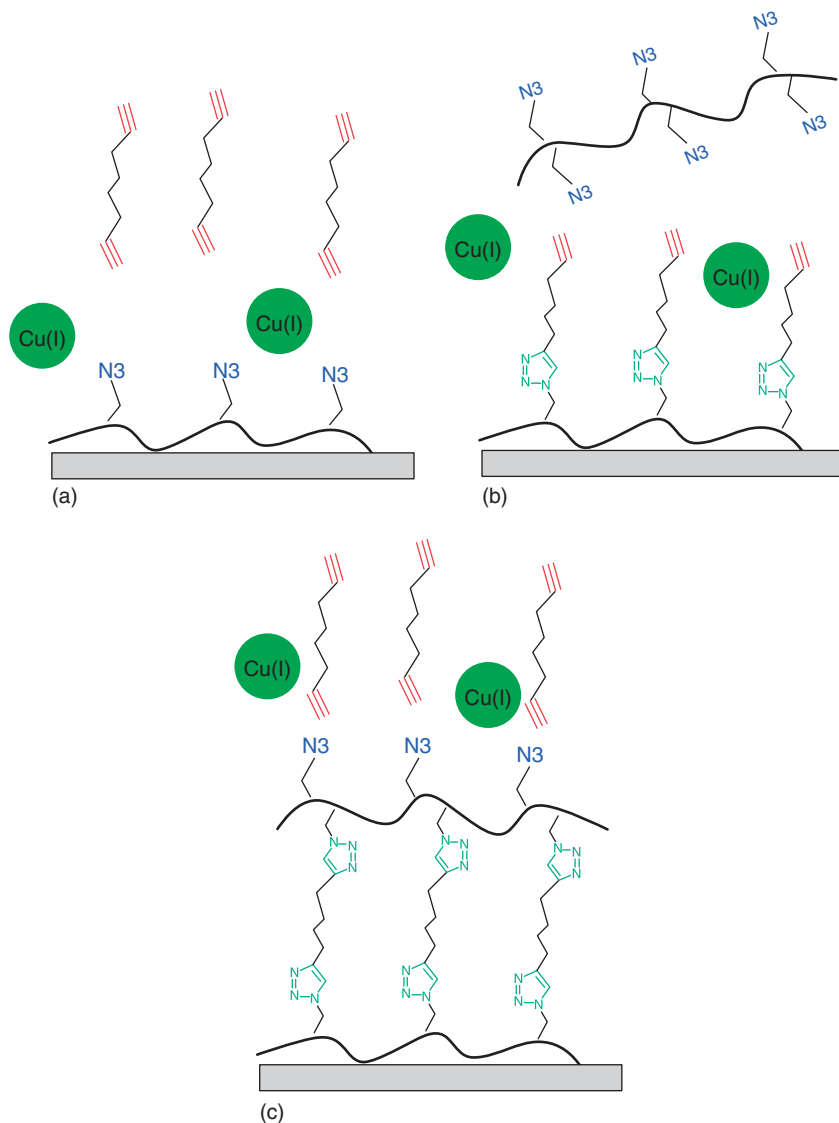
Figure 15.6 (a–c) Schematic illustration of click-based LbL assembly of multilayers using functionalized PAA and end-functionalized, bifunctional oligoethylene glycol spacers. (Reprinted with permission from [48]. Copyright 2010 American Chemical Society.)

complexes and negatively charged carboxylic acid groups on PAA. In a follow-up study, Jierry *et al.* reported differences in film growth during click-based assembly using combinations of neutral and charged (either positively or negatively charged) copolymers (polymers **1**–**6** in Figure 15.7), which provided additional insight into the roles that electrostatic interactions and alkyne/Cu(I) intermediates
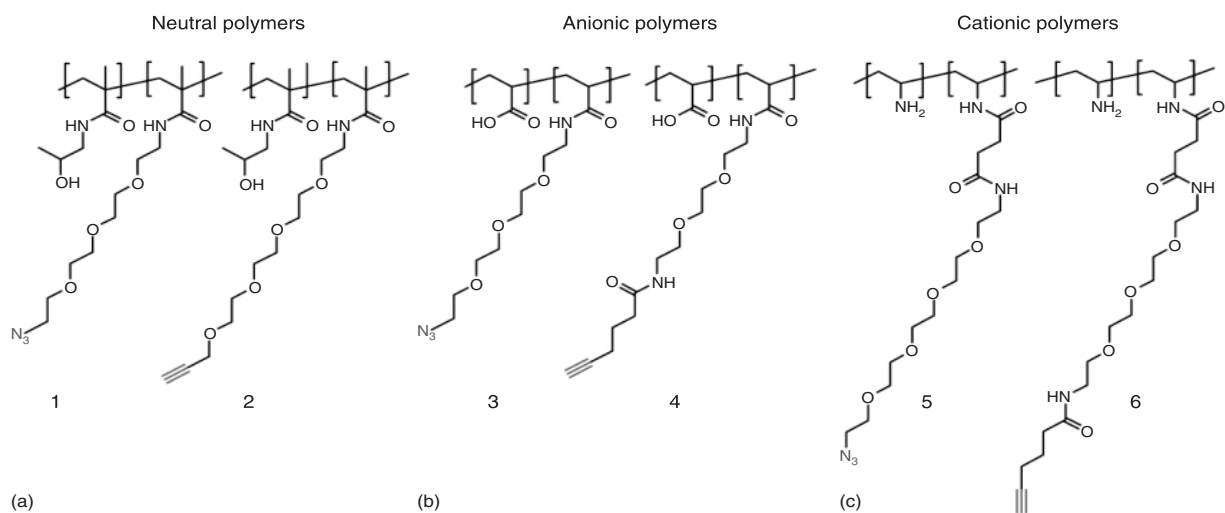
Figure 15.7 (a–c) Structures of neutral polymers PHPMA-azide (**1**) and PHPMA-alkyne (**2**), and modified polyelectrolytes PAA-azide (**3**) and PAA-alkyne (**4**) (anionic polymers) and PAH-azide (**5**) and PAH-alkyne (**6**) (cationic polymers) used to investigate the effects of ionic interactions during click-assembly. (Adapted with permission from [49]. Copyright 2010 American Chemical Society.)

might play during assembly [49]. For example, films assembled using a neutral alkyne-functionalized poly(*N*-hydroxypropylmethacrylamide) (PHPMA) derivative (**2**) and an azide-functionalized anionic PAA derivative (**3**) increased in thickness an order of magnitude faster than films fabricated using two appropriately functionalized neutral polymers (**1** and **2**) or when the functionality of the neutral and anionic polymers was reversed (**1** and **4**). Conversely, fabrication of films using a cationic poly(allylamine hydrochloride) (PAH) derivative (**5** and/or **6**) as a component resulted in decreased growth in all cases (consistent with unfavorable electrostatic interactions between positively charged alkyne/Cu(I) complexes and the cationic polymer). These results suggest additional means by which film properties might be tuned by the choice of polymer structure or by changing solution properties (e.g., pH or ionic strength) during film assembly.

As discussed above, another practical advantage of covalent assembly is the direct introduction of chemical cross-links that can confer added stability to a film (e.g., films that may swell, but that do not erode or fall apart on exposure to changes in pH, etc.). For certain types of applications, however, it may be necessary or desirable for a film or surface coating to degrade over time (e.g., Figure 15.8a), so as to release an encapsulated component or to facilitate the elimination of materials used for drug delivery or other biomedical applications. De Geest and coworkers [50] reported the covalent assembly of hydrolytically degradable film architectures using click chemistry and appropriately functionalized dextran polymers (Figure 15.8b). Because the triazole linkages formed by click chemistry are themselves hydrolytically stable, they introduced degradable carbonate ester linkages between the backbone of dextran and either azide- or alkyne-functionalized side chains.

Films fabricated on planar quartz substrates using this approach eroded over a period of 24 h when incubated at pH 9, consistent with the gradual hydrolysis of the covalent cross-links introduced during assembly [50]. These investigators also demonstrated that this approach was suitable for the fabrication of hollow, degradable microcapsules by fabrication of films on the surfaces of removable calcium carbonate microparticles (similar to approaches described above for the design of nondegradable click capsules). These capsules degraded and dissolved rapidly (e.g., within 15 s) upon the addition of sodium hydroxide, and more slowly (e.g., over the course of one week) when incubated under more physiologically relevant conditions (pH 7.4; as observed by optical microscopy).

Ochs *et al.* [51] reported a different approach to the click-based assembly of degradable microcapsules. Rather than introducing degradable functionality to polymer cross-links as described above (e.g., Figure 15.8b), they used alkyne- and azide-functionalized poly(L-lysine) (PLL) and poly(L-glutamic acid) (PGA), two biodegradable polymers, as building blocks for the assembly of PLL-based or PGA-based films on colloidal silica supports. Capsules fabricated by dissolution of the templates exhibited pH-induced swelling behavior. The surfaces of these capsules were modified postfabrication by the conjugation of PEG-based agents to the primary amine groups of PLL to confer resistance to nonspecific adsorption
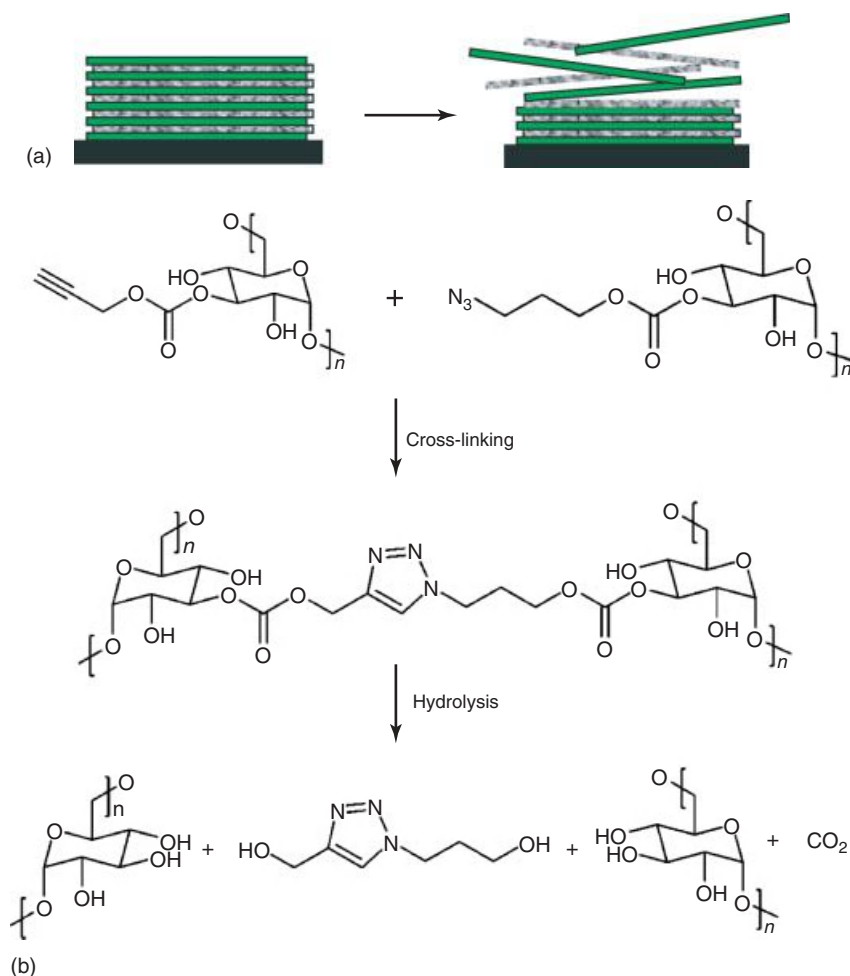
Figure 15.8 (a) Idealized scheme showing the physical erosion of a polymer multilayer. (b) Schematic of click-based cross-linking reaction involving propargyl carbonate-functionalized dextran azidopropylcarbonate-functionalized dextran. Hydrolysis of the carbonate esters after LbL assembly results in degradation of the multilayers with the formation of dextran chains, carbon dioxide, and a low-molecular-weight triazole compound as degradation products. (Images in part (b) reproduced with permission from [50].)

of proteins, although residual azide or alkyne groups could also potentially be used as described above. When combined, these approaches to the covalent assembly of cross-linked and reactive – but ultimately degradable – films open new opportunities for the design of films, coatings, and capsules with properties appropriate for a broader range of biomedical and biotechnological applications.

Several of the examples discussed above for the design of hollow microcapsules have highlighted the extent to which covalent LbL assembly is well
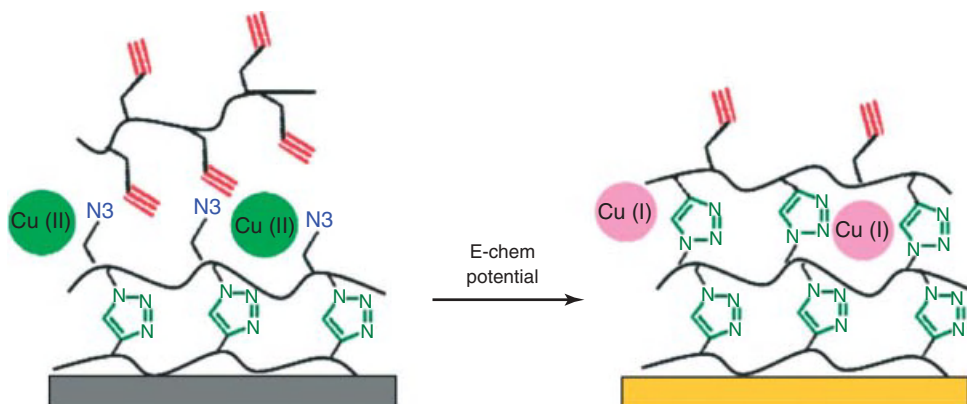
Figure 15.9 Schematic illustration of electrochemically controlled click-based LbL assembly of multilayers on electrode surfaces. (Reprinted with permission from [53]. Copyright 2010 American Chemical Society.)

suited for the fabrication of films on complex surfaces (e.g., on the curved surfaces of colloids). Zhang and coworkers [52] have also demonstrated the click-based formation of cross-linked multilayers on the surfaces of multiwalled carbon nanotubes (MWNTs). Following an initial treatment to introduce alkyne groups on the surfaces of the MWNTs, poly(2-azidoethyl methacrylate) and poly(propargyl methacrylate) were used to assemble the multilayers (again, using Cu(I) as a catalyst). The formation of films was confirmed using several methods, and postassembly functionalization using an alkyne-modified dye was demonstrated as an initial step toward the design of functionalized nanotube/polymer assemblies [52].

We note here that, in all the examples discussed above, Cu(I) species were used as catalysts to promote the "clicking" of azide and alkyne functionalities. These reactions were generally performed in the presence of a chemical reducing agent, such as sodium ascorbate, to convert Cu(II) to Cu(I) and regenerate the active species *in situ*. Recent work by Rydzek and coworkers has demonstrated that electrochemical methods can also be used to reduce Cu(II) and promote click-based LbL assembly directly at electrode surfaces (Figure 15.9) [53]. This approach eliminates the need for chemical reducing agents and localizes the formation or regeneration of the click catalyst at the surface of the electrode where film assembly takes place. This report demonstrated the feasibility of this approach for the assembly of films using alkyne- or azide-functionalized PAA alone (e.g., to fabricate "single-component" multilayers), or in combination with azide-grafted branched PEI. Film growth was reported to be independent of applied voltages more negative than a critical value (50–150 mV), but changes in other parameters, including the concentration of Cu(II), the structure of the polymers used, and the length of time that reducing potentials were applied could be used to manipulate important aspects of film growth.
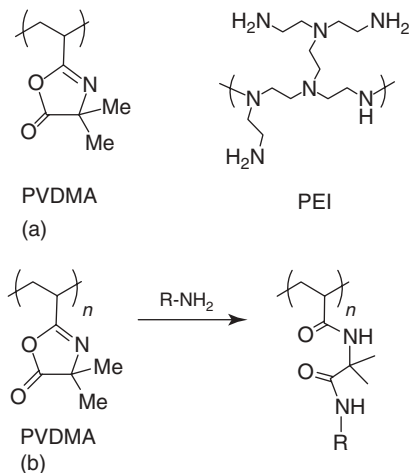
Figure 15.10 (a) Structures of poly(2-vinyl-4,4-dimethylazlactone) (PVDMA) and branched poly(ethylene imine) (PEI). (b) Post-polymerization reaction of the pendant azlactone functionality with a nucleophilic species (here, a primary amine) yielding a side-chain-functionalized poly(acrylamide)-type polymer. (Reprinted with permission from Ref. [59] (copyright 2012 American Chemical Society) and [143] (reproduced by permission of The Royal Society of Chemistry).)

15.5
Reactive LbL Assembly Using Azlactone-Functionalized Polymers

The increasing use of click reactions for covalent LbL assembly tracks the popularity of this reaction in many other areas of materials science and is, in general, a reflection of the practical advantages offered by the rapid, selective, and mild nature of this reaction platform. Other reaction schemes that share these general features also make good candidates for reactive LbL assembly and can introduce new opportunities and additional practical advantages over click-based methods. In this section, we highlight reports from our research group that demonstrate the utility of reactive azlactone-functionalized polymers as building blocks for the covalent assembly of cross-linked polymer multilayers.

Azlactones (or oxazolones) are lactone-based functional groups that undergo ring-opening reactions with nucleophiles such as primary amines, alcohols, or thiols (examples of a representative azlactone group and the reaction of an azlactone functionality with a primary amine are shown in Figure 15.10) [135, 136]. Although these reactions are not explicitly "click" reactions [137], they can, in certain cases, proceed with several of the same practical advantages. In particular, reactions of the azlactone functionality with primary amines generally proceed rapidly at room temperature, in a variety of solvents, and without the production of reaction by-products or the need for a catalyst (reactions with hydroxyl groups and thiol groups are also useful but proceed more slowly and generally require a catalyst) [135, 136]. These and other features of these reactions have been gainfully exploited

in the context of polymer chemistry, particularly with respect to the design of platforms for the rapid synthesis of side-chain-functionalized poly(acrylamide)-type polymers [138–142]. The chemistry and other fundamental aspects of azlactones and azlactone-functionalized polymers have been reviewed comprehensively and are not discussed in additional detail in this chapter [136, 143].

Our group has leveraged the reactivity of azlactone-functionalized polymers with polymers bearing primary amine functionality to develop reactive routes to LbL assembly. A schematic illustration of this general approach is shown in Figure 15.11a. In general, this process preserves many of the useful features of the click-assisted processes outlined above, including (i) precise control over film thickness, (ii) the ability to coat the surfaces of complex substrates, (iii) the ability to introduce stable covalent cross-links (in this case, by formation of robust amide/amide-type linkages; e.g., Figures 15.10b and 15.11a), and (iv) the ability to use residual reactive functionalities to further modify film properties after fabrication (Figure 15.11b).

This azlactone-based approach, however, also provides some additional practical advantages relative to click-based methods. First, as noted above, reactions between azlactones and primary amines occur very rapidly in the absence of a catalyst [135, 136] (dipping times required for azlactone-based LbL assembly processes are typically between 15 and 30 s, and times as short as 1 s can also be used [54]). While the need for copper catalysts in click-based LbL protocols has not yet proved to be a limitation, catalyst-free processes can, in general, decrease the complexity of fabrication procedures and eliminate the potential need to remove catalyst material for certain applications. Second, this approach can be used to fabricate films in organic solvents (including polar-aprotic media), and it thus expands the range of materials (in terms of both substrates and polymer-based building blocks) that can be used relative to aqueous-based click protocols. Finally, the general reactivity of azlactone functionality provides opportunities for postfabrication modification by treatment with a broader range of commercially available amine-, alcohol-, and thiol-based agents. These and other practical advantages of this azlactone-based approach are highlighted in the following discussion.

In an initial report, Buck *et al.* [54] demonstrated that multilayers could be fabricated by the alternating immersion of silicon substrates into organic solutions of branched PEI and the azlactone-functionalized polymer poly(2-vinyl-4,4-dimethylazlactone) (PVDMA; see structures in Figure 15.10). Characterization using ellipsometry demonstrated that film growth occurred in a linear manner to yield films ~100 nm thick after the deposition of 10 PEI/PVDMA layer pairs (or ''bilayers'') (Figure 15.12a). Further characterization by reflective IR spectroscopy revealed the presence of a residual unreacted azlactone functionality (Figure 15.12b). Treatment of these films with solutions of a small-molecule primary-amine-containing fluorophore (Figure 15.12c) demonstrated that these residual groups were available for the immobilization of an additional functionality. Additional proof-of-concept studies demonstrated that this approach could be used to modify and tailor important interfacial properties of film-coated surfaces (e.g., water contact angles) by simple treatment of these
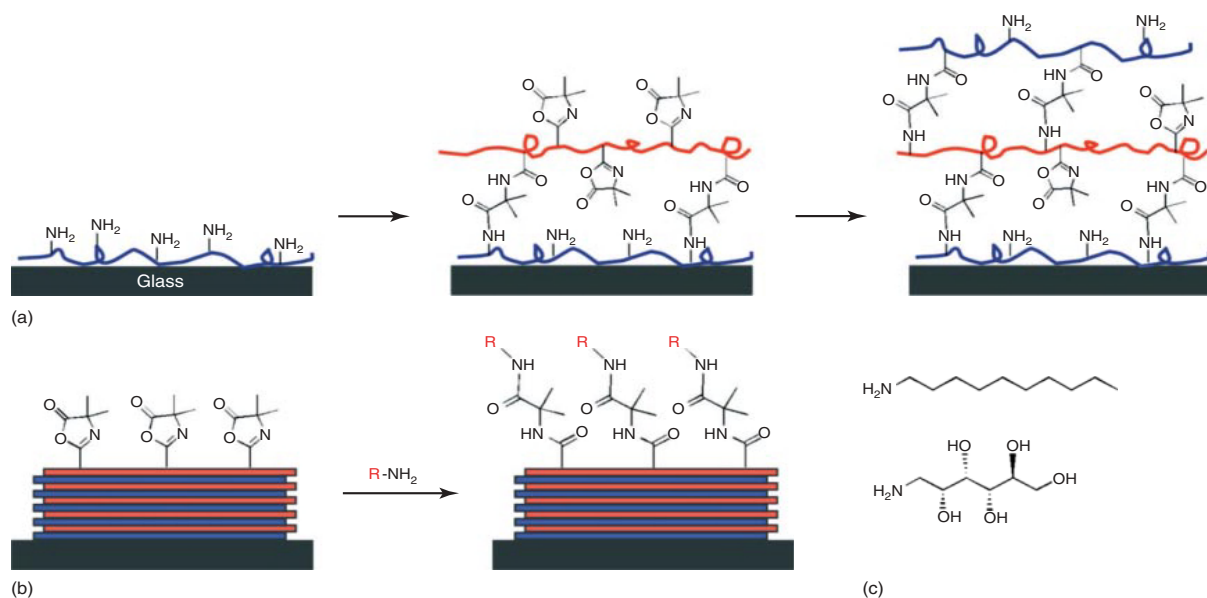
Figure 15.11 Schematic illustration showing LbL assembly and the subsequent chemical functionalization of reactive covalently cross-linked films fabricated by covalent LbL assembly of PVDMA and PEI. (a) PEI is first adsorbed onto a substrate followed by treatment with a solution of an azlactone-containing polymer (PVDMA). Repetition of this process results in the LbL buildup of covalently cross-linked multilayers containing residual azlactone functionality. (b) A broad range of surface functionalities can be imparted by postfabrication modification of residual azlactone functionality by exposure of the films to primary amine-containing nucleophiles. (c) Chemical structures of the amine-functionalized small molecules decylamine (top) and D-glucamine (bottom) used to modify the surfaces of azlactone-containing films. (Reprinted with permission from [55]. Copyright 2010 American Chemical Society.)
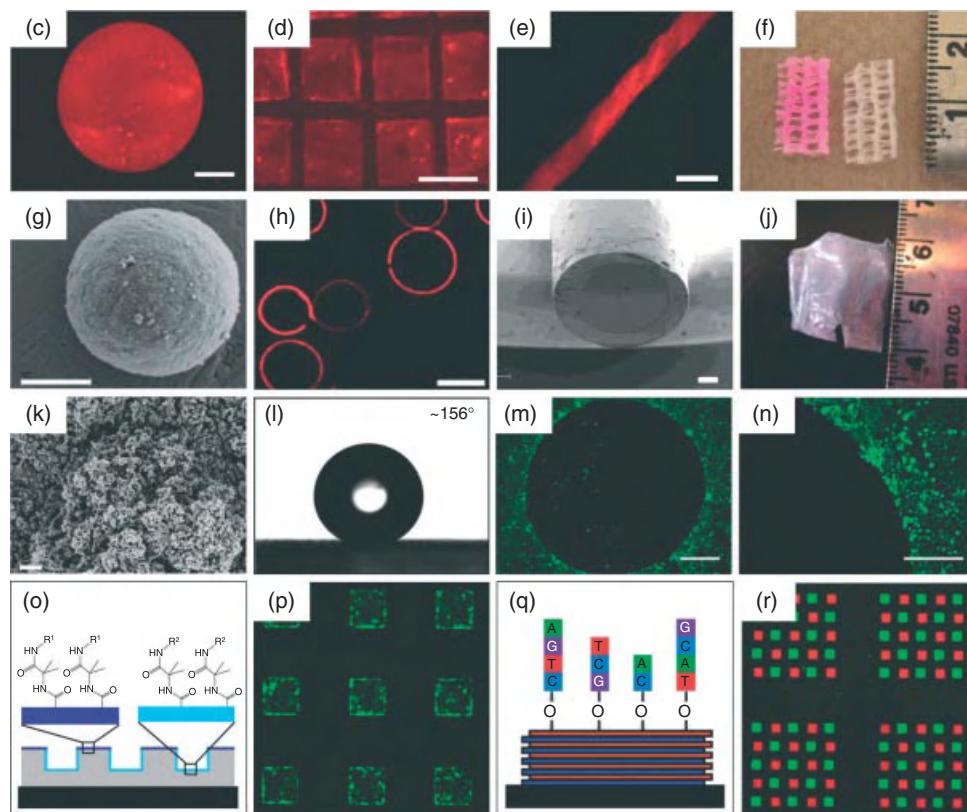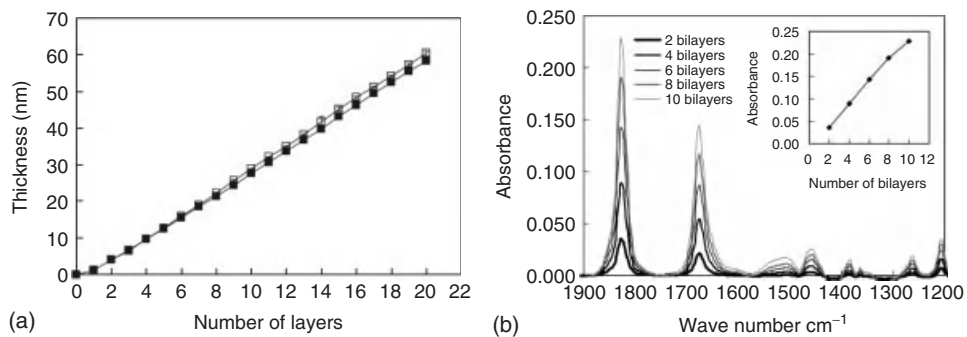
reactive films with hydrophobic amines or by using conventional methods such as microcontact printing to covalently immobilize patterns of amine-functionalized fluorescent molecules on film-coated surfaces (Figure 15.12d) [54].

Subsequent work demonstrated the versatility of this azlactone-based approach as a means to coat and modify the interfacial properties of a variety of different materials and more complex substrates, including the surfaces of glass [54–60, 143], soft materials (e.g., polymer-based substrates) [59, 61], paper [62], cotton thread and commercial wound dressings (Figure 15.12e,f) [62], protein-based surfaces (e.g., horsehair) [62], inorganic microparticles (for the fabrication of hollow microcapsules Figure 15.12g,h) [63], and, owing to the ability to perform covalent assembly in organic solvents that are immiscible with water, liquid/liquid interfaces formed between organic and aqueous phases (for the fabrication of suspended membranes; Figure 15.12i) [64]. In each of these studies, the presence of amine-reactive azlactone functionality on the surface (or within the bulk) of the films provided a convenient and straightforward platform for further postfabrication modification of surface properties by exposure to a broad range of different amine-functionalized molecules (including amine-functionalized small molecules [54, 55, 57–63], proteins [55, 61], peptides [65], functional

---

Figure 15.12 (a) Plot of film thickness versus the number of PVDMA/PEI layers deposited for two films deposited on a silicon substrate. (b) IR spectra of a PVDMA/PEI film as a function of the number of layers of PVDMA/PEI deposited. Inset: Absorbance of the peak at 1828 cm^{-1} (corresponding to the carbonyl of unreacted azlactone groups) versus the number of layers deposited. (c,d) Fluorescence micrographs of PVDMA/PEI films treated with (c) a drop of a solution of tetramethylrhodamine cadaverine (TMR-cad) or (d) patterned by reactive microcontact printing of TMR-cad using a polydimethylsiloxane (PDMS) stamp. (e,f) Fluorescence microscopy images of a cotton thread (e) and a strip (left) of commercial gauze (f) coated with reactive films and then treated with TMR-cad. (g) SEM image of a calcium carbonate microparticle coated with a reactive film. (h) Confocal microscopy image of hollow microcapsule reacted with TMR-cad. (i) SEM image of the end of a hollow glass capillary coated with a suspended PEI/PVDMA film. (j) Digital picture of a reactive freestanding film obtained by removal of a PEI/PVDMA film from an underlying substrate. (k) SEM image of the surface of a 100-bilayer film treated with heptadecafluoroundecylamine (see text). (l) Image of a water droplet (4 μl) on the surface of a film similar to that shown in (k). (m,n) Fluorescence microscopy images of COS-7 cells on chemically treated PEI/PVDMA films. Image (m) shows cells seeded on a film treated with a small drop of a solution of D-glucamine. Image (n) shows a higher magnification portion of the edges of the glucamine-treated region shown in (m). (o) Diagram of film-coated microwell array showing ability to exert spatial control over the functionalization of topographically patterned substrates. (p) Fluorescence microscopy images of cells seeded on a microwell array substrate patterned to restrict cell attachment inside wells (microwell dimensions are 300 μm per side). (q,r) Schematic (q) and merged fluorescence microscopy image (r) of an oligonucleotide array synthesized on the surface of a PVDMA/PEI film using maskless array synthesis (the image in (r) showing an array consisting of two different oligonucleotide sequences synthesized in an alternating pattern and hybridized with fluorescein (green) or Cy3 (red) labeled complement sequences. Each block of 25 array elements is 1.2 mm wide. Scale bars for other images are (c) 500 μm, (d) 300 μm, (e) 500 μm, (f) scale in centimeter, (g) 2 μm, (h) 30 μm, (i) 200 μm, (j) scale in centimeter, (k) 2 μm, (m) 500 μm, and (n) 300 μm. (Reproduced with permission from Refs. [54, 55, 57–59, 61–64, 143].)

polymers [61], and amine-functionalized droplets of thermotropic liquid crystals [56]).

The majority of our work has made use of branched PEI and PVDMA as reactive building blocks for film assembly (e.g., Figure 15.10), but this general approach provides several other opportunities for the selection and incorporation of materials that can influence film structure and function significantly. For example, the use of azlactone-containing copolymers can influence film thickness and provide control over the relative densities of the residual azlactone functionality available for further functionalization after assembly. We demonstrated that the assembly of films fabricated using PEI and poly(2-vinyl-4,4-dimethylazlactone-*co*-methyl methacrylate) (poly(VDMA-*co*-MMA)) depended significantly on copolymer composition [60]. Decreasing the content of the reactive azlactone functionality of the copolymer (i.e., by increasing MMA content) resulted in general decreases in film thickness relative to films fabricated using the homopolymer PVDMA. In addition, changing the overall number of reactive groups in the film (e.g., by increasing or decreasing the VDMA:MMA ratio in the copolymers) influenced the extents to which postfunctionalization treatment with primary amine-containing small molecules affected surface properties (e.g., contact angles or extents of cell attachment).

Although changes in the MMA content of these films also likely played a role in defining overall surface properties, these studies demonstrated that surface reactivity could be modulated by changes in the density of the reactive azlactone functionality in the copolymers used during LbL assembly. More generally, we note that VDMA can be readily copolymerized with many other vinyl monomers (e.g., styrene, acrylates and methacrylates, vinylpyrolidone, etc.) [135, 143]. In combination with the compatibility of this particular LbL approach with the use of organic solvents, this reactive-copolymer approach could therefore present additional opportunities to design multilayers with a much broader range of surface and/or bulk film properties. More broadly, it should also be possible to expand the range of film compositions and material properties that can be achieved by using other types of primary-amine-containing polymers.

As discussed above, PEI/PVDMA films have been demonstrated to grow in a linear manner on planar silicon substrates [54], and this affords levels of control over film thickness that are similar to those associated with many other conventional LbL approaches. Past studies have also demonstrated that this approach could be used to fabricate thin conformal films that are uniform, smooth, and optically clear [54]. A recent study, however, demonstrates that film morphology can change considerably depending on the solvents and polymers used and, in particular, on variation in the number of PEI/PVDMA bilayers that are deposited during fabrication [58]. For example, films fabricated from ∼50 to 100 bilayers were demonstrated to be optically opaque, to present significant microscale and nanoscale roughness (e.g., Figure 15.12k), and to have advancing water contact angles in excess of 150°.

Investigations into the origin of these surface features revealed them to result, at least in part, from the presence of cyclic azlactone-containing oligomers that were present during the polymerization of the samples of PVDMA used to fabricate the

films [58]. Although the specific ways in which these cyclic oligomers contribute to these changes in film structure are not understood, this work underscores (i) the complexity of this reactive assembly procedure and, just as importantly, (ii) ways that changes in assembly protocols and/or polymer structure can be used to design films with entirely new, and potentially useful, properties. For example, the synthesis of PVDMA in the presence of intentionally added cyclic oligomers leads to polymers that could be used to fabricate "superhydrophobic" films (Figure 15.12l) [58]. An interesting and potentially useful outcome of this reactive LbL approach is that it also produced superhydrophobic surfaces that were *reactive* and that could be further functionalized. For example, these as-fabricated superhydrophobic films gradually became hydrophilic on exposure to water, presumably a result of the hydrolysis of the surface-exposed azlactone functionality. However, treatment of these reactive films with hydrophobic primary amines resulted in films that retained their superhydrophobic properties after being submerged in water for at least six weeks [58]. The relative ease with which these superhydrophobic coatings can be modified chemically after fabrication could prove useful in a variety of applications.

Additional studies will be required to understand the molecular-level structures of these PEI/PVDMA films. It is not likely, however, that they present azlactone functionality at densities sufficient to allow immobilized groups to self-organize and produce dense and structured surfaces similar to those typically associated with self-assembled monolayers (SAMs) [1]. Nevertheless, recent reports have demonstrated that design principles and chemical/structural motifs arising from past studies of SAMs on gold-coated surfaces can, in some cases, be used to design film-coated surfaces that capture or recapitulate some of the important functions of these more ordered surfaces. A cluster of reports describing the reactive immobilization of two small hydrophilic and hydrophobic amines (D-glucamine and *n*-decylamine; see structures in Figure 15.11c) on PEI/PVDMA films provides several illustrative examples. Schematic illustrations of films functionalized with glucamine and decylamine are shown in Figure 15.13.

Glucamine was selected as a hydrophilic amine for use in these studies based on the demonstration that this carbohydrate motif can be used to design antifouling surfaces (e.g., surfaces that prevent the adhesion of mammalian cells or the adsorption of protein) when used as functional elements of SAMs [144, 145]. Decylamine was chosen as a model hydrophobic motif similar to those used in past studies on SAMs to prepare hydrophobic surfaces and surfaces that promote protein adsorption and/or cell adhesion [146]. Initial investigations demonstrated that the reactive immobilization of these two amine-based agents on PEI/PVDMA films modified the wetting behavior of the films considerably [55]. For example, whereas untreated (i.e., azlactone-containing) films exhibited contact angles of $\sim 62°$, the angles increased to $\sim 100°$ after treatment with decylamine and decreased to below $10°$ on treatment with glucamine. Additional experiments demonstrated that decylamine-functionalized films promoted the nonspecific adhesion and growth of mammalian fibroblast cells, as well as the nonspecific adsorption of the model protein bovine serum albumin (BSA) [55]. In stark contrast, glucamine-functionalized
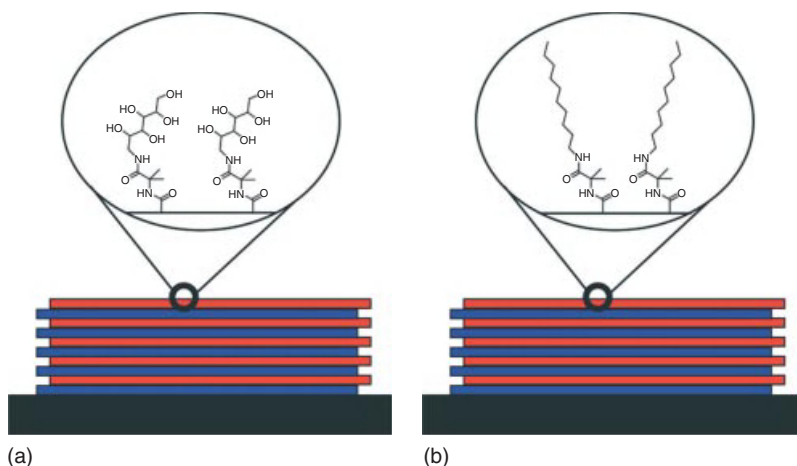
Figure 15.13 Schematic illustrations of PEI/PVDMA films functionalized postfabrication by treatment with the small-molecule amines D-glucamine (a) or decylamine (b).

films prevented the nonspecific adsorption of protein and the attachment and growth of cells almost completely.

Further experiments demonstrated that PEI/PVDMA films fabricated on planar glass slides could be patterned with regions that promoted cell adhesion and regions that remained resistant to the attachment, migration, or in-growth of cells during incubation in cell culture media (Figure 15.12m,n) for at least one month [55]. More recent experiments demonstrated that the coimmobilization of glucamine and amine-terminated peptide sequences containing RGD (arginine-glycine-aspartic acid; a commonly used cell-binding motif) can be used to design surfaces that promote the attachment and proliferation of cells via specific (as opposed to nonspecific) interactions with film-coated surfaces [65]. This postfabrication approach to functionalization was also used to create patterns of cell-adhesive and cell-resistant regions on the surfaces of film-coated polyurethane microwell cell culture arrays (Figure 15.12o,p) [61]. This permitted the design of 3D microwell arrays that confined the growth of cuboidal clusters of cells (e.g., with glucamine-treated regions between/outside the microwells preventing or resisting the outgrowth of cells; Figure 15.12p) for up to three weeks. In addition to contributing new approaches to the design of chemically and topographically patterned culture environments, these three reports also serve to highlight the stability of these cross-linked multilayers in an important practical context (e.g., long-term incubation in cell culture media at 37 °C).

The ability to immobilize glucamine and other hydroxyl functionalities on film-coated surfaces can also be useful in other ways. Recently, we demonstrated that cross-linked PEI/PVDMA multilayers can be used as platforms for the multistep maskless array synthesis (MAS) of oligonucleotide arrays (an iterative and automated process based on phosphoramidite chemistry that requires reactive hydroxyl-functionalized surfaces for the initial covalent attachment

of nucleoside bases) (Figure 15.12q) [59]. Glucamine-functionalized films fabricated on aminosilane-treated glass substrates supported the synthesis of arrays of oligonucleotides (Figure 15.12r) with fluorescence intensities and S/N ratios (after hybridization with fluorescent complementary strands) that were comparable to those of arrays fabricated on conventional silanized glass. However, the versatile nature of LbL assembly also permitted array synthesis directly on other unconventional substrates (e.g., thin sheets of film-coated poly(ethylene terephthalate) (PET)) to yield flexible arrays that could be bent and cut into smaller arrays. The ability to fabricate functional microarrays on arbitrary (e.g., soft, flexible, or topographically complex) surfaces could offer practical manufacturing and point-of-use advantages over arrays on rigid substrates. We emphasize, however, that this work also serves to highlight again the stable nature of the cross-linked multilayers that arise from this covalent assembly approach. For example, during the MAS array synthesis process, substrates are exposed to over 450 individual chemical processing steps, including both flow-based and static exposure to different organic solvents, base-pair solutions, photoirradiation steps, and oxidation procedures [59]. The results of this study demonstrated that these films did not crack, peel, or delaminate from their underlying substrates significantly during this process or during manipulations required to hybridize and dehybridize the arrays (including prolonged exposure to 8 M urea).

We attribute the stability of the PEI/PVDMA multilayers in all the examples above – including their ability to resist physical erosion or deconstruction upon exposure to a range of different conditions (i.e., acidic media, alkaline media, denaturing media, organic solvents, and solutions of high ionic strength) – to the formation of stable amide/amide-type cross-links that result from the reaction of azlactones with primary amine functionality (e.g., Figure 15.11a). These amide/amide linkages are also formed during postfabrication immobilization of amine-functionalized compounds (e.g., Figure 15.11b). Although we have not investigated this aspect of these systems specifically, many of the long-term cell culture-based experiments described in the examples above suggest that the amide/amide functionality used to immobilize functional groups (e.g., glucamine; Figure 15.13a) do not hydrolyze readily (e.g., on extended incubation in cell culture media, on contact with cells, etc.).

One other important aspect of stability that was also mentioned, but not discussed explicitly, above relates to the potential to tune stability at the film/substrate interface. For example, because the polymers that are used for these (and other) covalent LbL processes are reactive, they can be used to form covalent linkages to appropriately designed substrates to improve film adhesion and prevent film delamination. The resistance to delamination during oligonucleotide synthesis and exposure to solutions of 8 M urea in the MAS-based example [59] above is likely a consequence of bond-forming reactions between PVDMA (deposited as a first layer during LbL assembly) and amine groups on the aminosilane-treated glass substrates used in those experiments. This level of stability is, of course, likely to be useful in a range of contexts and is, in general, something that is more

difficult to achieve using ionically cross-linked PEMs fabricated using conventional (noncovalent) LbL methods.

Finally, in closing this section, we note that the presence of weaker noncovalent interactions at film/substrate interfaces can be exploited to fabricate covalently cross-linked freestanding films by intentional delamination of films fabricated on solid surfaces. Buck *et al.* [57] demonstrated that PEI/PVDMA films fabricated on untreated (nonsilanized) silicon substrates could be induced to delaminate and lift off to yield cross-linked, stable, and amine-reactive freestanding thin films (Figure 15.12j) that can be postfunctionalized and physically transferred onto the surfaces of other objects. Other examples of this approach using other reactive polymers are discussed in the following section.

15.6
Other Reactions and Other Approaches

This final section provides discussion of many of the other types of bond-forming reactions that have been used to assemble covalently cross-linked multilayers. Although none of the types of individual reactions discussed below has been investigated as broadly as approaches based on click or azlactone-based chemistry, the combined total of reports using these other reaction types currently exceeds the combined number of reports discussed in Sections 15.4 and 15.5 above. We note again that Table 15.1 provides a summary of all the different reactive groups and types of interlayer cross-linked structures discussed in the following section.

The particular nature of any specific chemical reaction can, of course, introduce potential practical limitations, including (i) slower rates, (ii) the need to remove reaction by-products, (iii) the need to control potential side reactions, (iv) general restrictions on types of solvents, (v) the need for catalysts, (vi) the need for anhydrous conditions, and (vii) the strength or stability of covalent bonds that are formed. In the context of LbL assembly, many of these considerations should, of course, only be regarded as ''potential'' limitations because the extent to which they are limiting in a practical sense depends entirely on the needs of a particular process or a potential application. Regardless of the potential advantages or disadvantages of a particular reaction platform, all the examples discussed below share the general features and advantages of covalent LbL assembly discussed more broadly above (e.g., stepwise growth of covalently cross-linked films, the ability to fabricate conformal films on complex surfaces, and the ability to exploit residual reactive groups to functionalize film-coated surfaces post fabrication). The discussion below is organized, in general, around groups of reactions and discussions of salient features of different reaction types rather than aspects or applications of the resulting materials that are similar to those already discussed in greater detail above (e.g., the ability to fabricate capsules or freestanding films, to pattern films post fabrication, etc.).

Many of these other approaches have made use of chemical reactions between amines and carbonyl-based functionalities that yield films with amide-based cross-links. As discussed briefly in Section 15.5, this has several general advantages. First, amide bonds are chemically robust and, in general, hydrolytically stable under a variety of conditions. Second, there exists a broad range of both basic and more sophisticated organic reactions that can be used to form amide bonds. Finally, a wide selection of amine-containing building blocks (including small molecules, polymers, nanoparticles, nanotubes, proteins, etc.) is commercially available or otherwise accessible through established synthetic processes.

Examples of amide-bond-forming reactions that have proved particularly useful for covalent LbL assembly include reactions between amine-functionalized agents and building blocks functionalized with (i) anhydrides [66–73], (ii) acid chlorides [81, 82], (iii) activated esters (e.g., polymers bearing reactive pentafluorophenyl ester groups) [74–77], and, in the presence of a carbodiimide coupling agent, (iv) carboxylic acids [78–80]. The reactivity of anhydride and acid chloride functionalities generally restricts the first two of these approaches to the use of aprotic organic solvents and film components that do not contain other protic groups that could lead to unwanted side reactions. Approaches based on carbodiimide coupling and the use of building blocks bearing pentafluorophenyl groups, however, have the advantage of being less sensitive to water and can be used for covalent assembly in aqueous or organic media and with a much broader selection of film component materials. Pentafluorophenyl ester-based approaches, as exemplified in recent reports by Wang [74, 75] and Theato and Char [76, 77] (Figure 15.14a,b), are rapid and selective, and particularly versatile from the standpoint of postfabrication functionalization. Seo *et al.* [77] demonstrated the fabrication of robust amide-cross-linked films with residual activated esters in the films that could be used to pattern amine-containing molecules (Figure 15.14c) or fabricate reactive free-standing films (Figure 15.14d). Other reports by these groups have demonstrated the assembly of functional films for photovoltaic applications [75] or for the design of transparent conducting surfaces [76]. The general ease with which activated ester groups can be introduced to a broad range of both polymeric and nonpolymeric building blocks (including photoactive nanoparticles and MWCNTs), combined with the advantages mentioned above (e.g., moisture resistance and fast reaction times), should extend the reach of this approach significantly.

Amine-functionalized polymers and small molecules have also been used in combination with reactive building blocks bearing isocyanate [81, 82], dichlorophosphazene [83], acrylate [84–86, 147], alkyl halide [87, 88], epoxide [89], or aldehyde groups [90–98] to fabricate covalent LbL films cross-linked with urea [81, 82], phosphazene [83], amino-ester [84–86, 147], alkyl amine [84–88], or Schiff base [90–98] (imine) linkages. Approaches based on reactions between amine- and aldehyde-functionalized components (to form imine or Schiff base linkages) have been particularly well studied because of the relatively fast and mild (aqueous) nature of these reactions, which also permits reactive immobilization of biomacromolecular agents such as proteins into cross-linked multilayers. As one example, Hou *et al.* [90] fabricated nanotubes composed of the enzymes glucose oxidase or

(a)

(b)

(c)

(d)
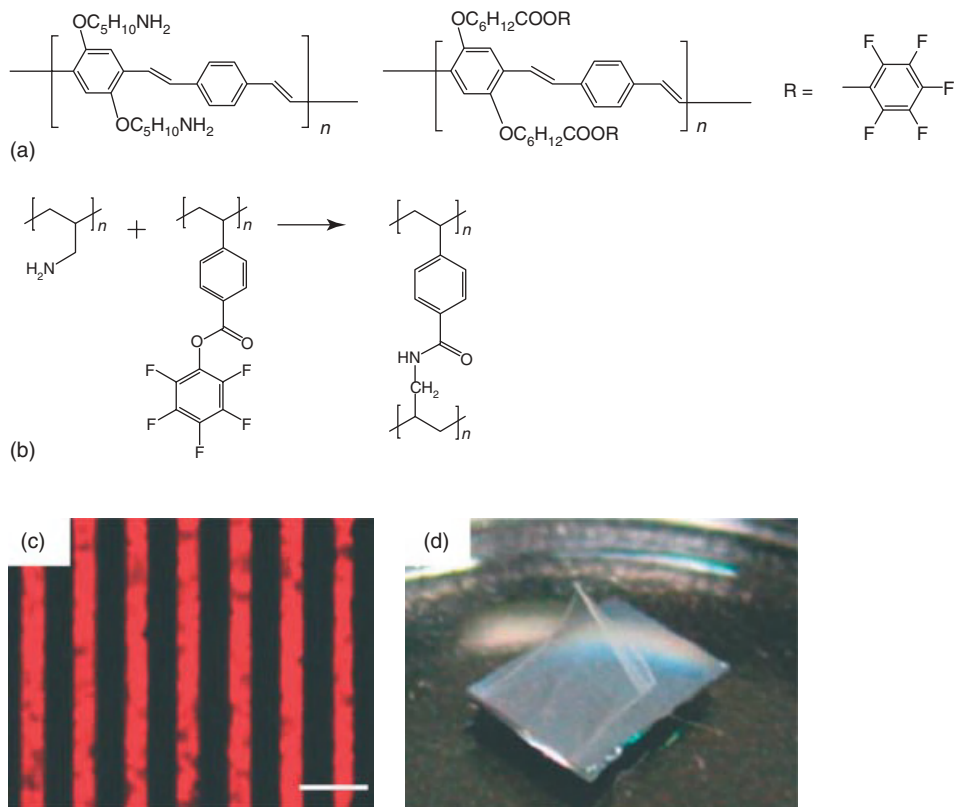
Figure 15.14 (a,b) Examples of approaches to covalent LbL assembly based on polymers functionalized with activated pentafluorophenyl ester groups (corresponding amine-functionalized polymers used for film assembly are also shown). (c) Fluorescence micrograph of a pentafluorophenyl ester-containing reactive multilayer assembled from the polymers shown in (b), followed by microcontact printing and covalent immobilization of a fluorescent dye (scale bar is 5 µm). (d) Digital picture of a reactive pentafluorophenyl ester-containing freestanding film obtained by delamination of a similar film from a silicon substrate (film dimensions are 1.5 cm by 2 cm). (Reproduced with permission from Refs. [74, 77]. Copyright 2004 and 2010 American Chemical Society.)

hemoglobin by the alternating reactive deposition of protein and the difunctional aldehyde agent glutaraldehyde inside pores of an alumina template (followed by removal of the template). LbL growth in this case was driven by cross-linking reactions between the difunctional glutaraldehyde molecules and the lysine groups on the surfaces of the proteins. Both glucose oxidase and hemoglobin were found to retain their enzymatic and electrochemical activities, respectively, demonstrating that this type of reactive assembly can be used to incorporate biomolecules into cross-linked multilayers without loss of function (a hallmark of more conventional

noncovalent approaches to the assembly of ionically cross-linked PEMs). Subsequent reports from other groups used this same Schiff-base approach to assemble hollow protein capsules as well as antibacterial coatings containing nisin, a natural antimicrobial peptide [93, 95, 99].

In each of these cases, glutaraldehyde cross-linking led to films that were stable under the various environmental conditions in which they were used. We note, however, that Schiff base functionality is reversible under certain conditions (e.g., in acidic media). The use of this approach therefore introduces the potential to design cross-linked multilayers that degrade under certain conditions. In this particular context, we also note that this approach differs fundamentally from the click-based examples of approaches to degradable films discussed above [50, 51]. While in those cases it was necessary to introduce additional degradable functionality into polymer backbones or side-chains (because triazole linkages themselves are not readily degradable), the covalent Schiff-base linkages formed during assembly are reversible. Examples of reactive assembly based on the conjugate addition of primary amines to acrylate groups also inherently provide LbL routes to films containing ester-functionalized cross-links [84–86, 147]. This approach could, thus, also provide a basis for the design of cross-linked multilayers that degrade in aqueous environments (e.g., by hydrolysis of ester functionality) and open the door to additional applications of these materials in biomedical contexts.

Other groups have exploited hydroxyl-functionalized polymers as non-amine-based building blocks for covalent assembly. Examples of these approaches include schemes based on reactions between alcohols and acid chlorides [81, 82, 100–102], isothiocyanates [81, 82], boronic acids [103–106], and epoxides [81] to fabricate covalent LbL films containing ester-, urethane-, boronate ester-, and ether-based interlayer cross-links, respectively. These approaches expand significantly the range of materials that can be used for reactive LbL assembly to include a variety of synthetic and natural (e.g., carbohydrate-based) hydroxyl-containing materials.

Several of these hydroxyl-based reactions lead to the formation of cross-links that are reversible either by general hydrolysis (as discussed above) or in response to other specific environmental cues. One example of the latter is films formed by the LbL assembly of polyols and building blocks containing boronic acid groups (e.g., Figure 15.15). Films assembled in this manner have been demonstrated to disassemble gradually on exposure to aqueous media (at rates that vary according to pH and ionic strength), but they also degrade much more rapidly in the presence of added small-molecule carbohydrates (e.g., glucose) [104, 105]. For example, Levy *et al.* demonstrated that films fabricated using phenylboronic acid-grafted PAA and the polysaccharide mannan dissolve rapidly when placed in contact with solutions of several different sugars (with high selectivity for fructose) [104]. Ding *et al.* [105] have also demonstrated that multilayers assembled from poly(vinyl alcohol) (PVA) and poly(acrylamide-*co*-3-(acrylamido)phenylboronic acid) (Figure 15.15) disassemble at an accelerated rate on the addition of glucose. In both studies, disassembly was attributed to competitive interactions (e.g., boronate ester exchange) in the films on addition of small-molecule sugars, which resulted in a reduction of intrachain
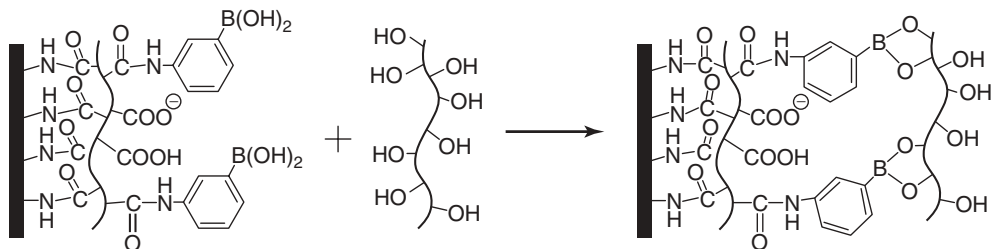
Figure 15.15 Schematic showing covalent LbL assembly mediated by reactions between phenyl boronic acid-functionalized polymers and alcohol-functionalized polymers. (Adapted with permission from Ref. [105]. Reproduced by permission of The Royal Society of Chemistry).

cross-linking. The study by Levy *et al.* also demonstrated the ability of boronate ester-cross-linked microcapsules to release an encapsulated model protein (BSA) in response to added sugars [104], demonstrating the basis of a potential new covalent LbL platform for the release of therapeutic agents, such as insulin, in a glucose-responsive manner.

While these latter examples demonstrate the potential of this approach, we note that the chemistry of boronic acids can be complex, and the nature and extents of reactions between polyols and boronic acids can depend strongly on changes in pH, ionic strength, and the structure of the reactants [148–150]. As is also generally true for most other reaction platforms described above (with the possible exceptions of highly specific click-type reactions), the potential for side reactions and/or important contributions arising from other noncovalent interactions during or after film assembly should be borne in mind with respect to the further development of these covalent LbL approaches.

Finally, we note that several other types of chemical reactions have been used to promote covalent LbL assembly. Examples of these approaches include reactions between aldehydes and alkoxyamines [107–109], sulfones with thiols [110], and aromatic substitution chemistry [31, 111] (e.g., coupling reactions between phenyl diazonium salts and phenyl functionality to form azobenzene-based linkages). In addition, several recent reports also demonstrate the utility of metal–ligand interactions as a means of promoting LbL assembly. For example, interactions of various metal complexes with polymers bearing amine [112], carboxylic acid [113, 114], salicylidene [115, 116], and pyridine-containing [117–121] and palladium pincer-type [122, 123] groups have been used to assemble metal complex crosslinked polymer films under a variety of different conditions. The metal–ligand bonds formed in these examples should be regarded as coordinate bonds rather than as covalent bonds. However, these approaches, and the materials that result, are included here at the close of this section because they differ significantly from approaches to assembly based on ionic interactions or hydrogen bonding and share many of the same behaviors and benefits of many of the reactive/covalent LbL examples discussed above.

As one example, South *et al.* reported linear growth of LbL films composed of poly(vinyl pyridine) and poly(norbornene) derivatives containing Pd(II)-pincer complex-functionalized side chains (e.g., Eq. (15.2)) [122, 123]. These coordination-cross-linked films were stable to high temperatures and resisted degradation in polar solvents (e.g., EtOH, tetrahydrofuran (THF), and DMF) up to an order of magnitude longer than other common PEM films but could be disassembled in response to the addition of pyridine or other ligands via ligand/metal exchange. Maier *et al.* demonstrated that films fabricated from terpyridine-functionalized polymers and one of several divalent metal salts displayed electrochromic behavior (e.g., where the color of the film was dependent on the metal ion in the film and could be quickly and reversibly switched between different colors by changing oxidation state) [121]. In general, the ability to incorporate metal centers into the structures of these films in well-defined ways (e.g., as stoichiometrically defined components of individual cross-links, as opposed to the ill-defined or random incorporation of metal complexes in an otherwise cross-linked multilayer) can provide unique opportunities for the design of responsive or erasable materials (e.g., films that disassemble in response to other metals or ligands), catalytic materials and membranes, electrical and photoelectric devices, and sensors.

(15.2)
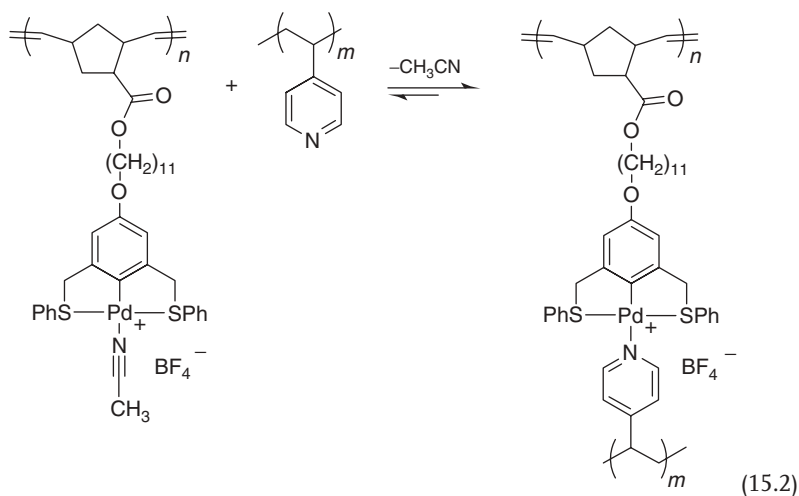
15.7
Concluding Remarks

Approaches to covalent or reactive LbL assembly are driven by covalent-bond-forming reactions between mutually reactive polymers. The iterative and stepwise nature of these processes confers several practical advantages typical of other approaches to LbL assembly, but these reactive methods also introduce new, interesting, and potentially useful features, including the ability to fabricate covalently

cross-linked multilayers (to improve film stability) and design thin films that contain residual reactive functionality (to design films that can be readily functionalized and patterned with new functionality after fabrication).

The sections above highlighted many of the different reaction platforms that have been used for covalent LbL assembly, as well as some of the ways that the various advantages of these platforms have enabled new coating processes and the design of reactive thin films, coatings, and other materials with enhanced properties and new functionalities. It is clear from these examples that the potential impact of these covalent/reactive approaches is both broad and diverse. It is also clear from the rapidly growing number of reports in the literature that there is an increasing awareness of, and interest in, these new covalent approaches. As the field of covalent LbL assembly continues to expand, we expect that new types of reactive polymers and other types of chemical reactions will be exploited to enable more sophisticated control over the structures and properties of polymer multilayers. Further development of the covalent/reactive methods that have already been developed should also lead to the development of practical approaches to the fabrication of reactive thin films that can be practiced outside the laboratory and on larger scales.

Acknowledgments

References

1. Ulman, A. (1996) *Chem. Rev.*, **96**, 1533–1554.
2. Choy, K.L. (2003) *Prog. Mater. Sci.*, **48**, 57–170.
3. Chattopadhyay, D.K. and Raju, K.V.S.N. (2007) *Prog. Polym. Sci.*, **32**, 352–418.
4. Hall, D.B., Underhill, P., and Torkelson, J.M. (1998) *Polym. Eng. Sci.*, **38**, 2039–2045.
5. Tracton, A.A. (ed.) (2005) *Coatings Technology Handbook*, 3rd edn, CRC Press, Bridgewater.
6. Decher, G. (1997) *Science*, **277**, 1232–1237.
7. Decher, G. and Schlenoff, J.B. (2003) *Multilayer Thin Films: Sequential Assembly of Nanocomposite Materials*, Wiley-VCH Verlag GmbH, Weinheim.
8. Bertrand, P., Jonas, A., Laschewsky, A., and Legras, R. (2000) *Macromol. Rapid Commun.*, **21**, 319–348.
9. Schonhoff, M. (2003) *Curr. Opin. Colloid Interface Sci.*, **8**, 86–95.
10. Ai, H., Jones, S.A., and Lvov, Y.M. (2003) *Cell Biochem. Biophys.*, **39**, 23–43.
11. Hammond, P.T. (2004) *Adv. Mater.*, **16**, 1271–1293.
12. Sukhishvili, S.A. (2005) *Curr. Opin. Colloid Interface Sci.*, **10**, 37–44.
13. Tang, Z.Y., Wang, Y., Podsiadlo, P., and Kotov, N.A. (2006) *Adv. Mater.*, **18**, 3203–3224.
14. Lynn, D.M. (2007) *Adv. Mater.*, **19**, 4118–4130.

15. Jewell, C.M. and Lynn, D.M. (2008) *Curr. Opin. Colloid Interface Sci.*, **13**, 395–402.

16. De Geest, B.G., De Koker, S., Sukhorukov, G.B., Kreft, O., Parak, W.J., Skirtach, A.G., Demeester, J., De Smedt, S.C., and Hennink, W.E. (2009) *Soft Matter*, **5**, 282–291.

17. Boudou, T., Crouzier, T., Ren, K.F., Blin, G., and Picart, C. (2010) *Adv. Mater.*, **22**, 441–467.

18. Sukhishvili, S.A. and Granick, S. (2000) *J. Am. Chem. Soc.*, **122**, 9550–9551.

19. Schüler, C. and Caruso, F. (2001) *Biomacromolecules*, **2**, 921–926.

20. Gao, C.Y., Leporatti, S., Moya, S., Donath, E., and Mohwald, H. (2001) *Langmuir*, **17**, 3491–3495.

21. Dubas, S.T., Farhat, T.R., and Schlenoff, J.B. (2001) *J. Am. Chem. Soc.*, **123**, 5368–5369.

22. Dubas, S.T. and Schlenoff, J.B. (2001) *Langmuir*, **17**, 7725–7727.

23. Kovacevic, D., van der Burgh, S., de Keizer, A., and Cohen Stuart, M.A. (2002) *Langmuir*, **18**, 5607–5612.

24. Antipov, A.A., Sukhorukov, G.B., Leporatti, S., Radtchenko, I.L., Donath, E., and Mohwald, H. (2002) *Colloid Surf. A*, **198**, 535–541.

25. Harris, J.J., DeRose, P.M., and Bruening, M.L. (1999) *J. Am. Chem. Soc.*, **121**, 1978–1979.

26. Mendelsohn, J.D., Barrett, C.J., Chan, V.V., Pal, A.J., Mayes, A.M., and Rubner, M.F. (2000) *Langmuir*, **16**, 5017–5023.

27. Yang, S.Y. and Rubner, M.F. (2002) *J. Am. Chem. Soc.*, **124**, 2100–2101.

28. Tong, W. and Gao, C. (2005) *Polym. Adv. Technol.*, **16**, 827–833.

29. Jang, W.-S., Jensen, A.T., and Lutkenhaus, J.L. (2010) *Macromolecules*, **43**, 9473–9479.

30. Sun, J., Wu, T., Liu, F., Wang, Z., Zhang, X., and Shen, J. (2000) *Langmuir*, **16**, 4620–4624.

31. Chen, J., Luo, G., and Cao, W. (2001) *Macromol. Rapid Commun.*, **22**, 311–314.

32. Pastoriza-Santos, I., Schöler, B., and Caruso, F. (2001) *Adv. Funct. Mater.*, **11**, 122–128.

33. Leporatti, S., Voigt, A., Mitlöhner, R., Sukhorukov, G., Donath, E., and Möhwald, H. (2000) *Langmuir*, **16**, 4059–4063.

34. Richert, L., Boulmedais, F., Lavalle, P., Mutterer, J., Ferreux, E., Decher, G., Schaaf, P., Voegel, J.-C., and Picart, C. (2003) *Biomacromolecules*, **5**, 284–294.

35. Zelikin, A.N., Quinn, J.F., and Caruso, F. (2005) *Biomacromolecules*, **7**, 27–30.

36. Zhang, Y., Guan, Y., and Zhou, S. (2005) *Biomacromolecules*, **6**, 2365–2369.

37. Francius, G., Hemmerlé, J., Ohayon, J., Schaaf, P., Voegel, J.-C., Picart, C., and Senger, B. (2006) *Microsc. Res. Tech.*, **69**, 84–92.

38. Boudou, T., Crouzier, T., Auze'ly-Velty, R., Glinel, K., and Picart, C. (2009) *Langmuir*, **25**, 13809–13819.

39. Quinn, J.F., Johnston, A.P.R., Such, G.K., Zelikin, A.N., and Caruso, F. (2007) *Chem. Soc. Rev.*, **36**, 707–718.

40. Bergbreiter, D.E. and Liao, K.-S. (2009) *Soft Matter*, **5**, 23–28.

41. Such, G.K., Quinn, J.F., Quinn, A., Tjipto, E., and Caruso, F. (2006) *J. Am. Chem. Soc.*, **128**, 9318–9319.

42. Kinnane, C.R., Such, G.K., and Caruso, F. (2011) *Macromolecules*, **44**, 1194–1202.

43. Tang, Y., Liu, G., Yu, C., Wei, X., and Zhang, G. (2008) *Langmuir*, **24**, 8929–8933.

44. Such, G.K., Tjipto, E., Postma, A., Johnston, A.P.R., and Caruso, F. (2007) *Nano Lett.*, **7**, 1706–1710.

45. Bergbreiter, D.E. and Chance, B.S. (2007) *Macromolecules*, **40**, 5337–5343.

46. Huang, C.-J. and Chang, F.-C. (2009) *Macromolecules*, **42**, 5155–5166.

47. Vestberg, R., Malkoch, M., Kade, M., Wu, P., Fokin, V.V., Barry Sharpless, K., Drockenmuller, E., and Hawker, C.J. (2007) *J. Polym. Sci., Part A: Polym. Chem.*, **45**, 2835–2846.

48. El Haitami, A.E., Thomann, J.-S., Jierry, L., Parat, A., Voegel, J.-C., Schaaf, P., Senger, B., Boulmedais, F., and Frisch, B. (2010) *Langmuir*, **26**, 12351–12357.

49. Jierry, L., Ben Ameur, N., Thomann, J.-S., Frisch, B., Gonthier, E., Voegel, J.-C., Senger, B., Decher, G., Felix,

O., Schaaf, P., Mesini, P., and
Boulmedais, F. (2010) *Macromolecules*,
43, 3994–3997.

50. De Geest, B.G., Van Camp, W.,
Du Prez, F.E., De Smedt, S.C.,
Demeester, J., and Hennink, W.E.
(2008) *Macromol. Rapid Commun.*, **29**,
1111–1118.

51. Ochs, C.J., Such, G.K., Städler, B., and
Caruso, F. (2008) *Biomacromolecules*, **9**,
3389–3396.

52. Zhang, Y., He, H., Gao, C., and Wu, J.
(2009) *Langmuir*, **25**, 5814–5824.

53. Rydzek, G., Thomann, J.-S.,
Ben Ameur, N., Jierry, L., Mésini,
P., Ponche, A., Contal, C., El Haitami,
A.E., Voegel, J.-C., Senger, B., Schaaf,
P., Frisch, B., and Boulmedais, F.
(2010) *Langmuir*, **26**, 2816–2824.

54. Buck, M.E., Zhang, J., and Lynn, D.M.
(2007) *Adv. Mater.*, **19**, 3951–3955.

55. Buck, M.E., Breitbach, A.S., Belgrade,
S.K., Blackwell, H.E., and Lynn,
D.M. (2009) *Biomacromolecules*, **10**,
1564–1574.

56. Kinsinger, M.I., Buck, M.E., Abbott,
N.L., and Lynn, D.M. (2010) *Langmuir*,
26, 10234–10242.

57. Buck, M.E. and Lynn, D.M. (2010)
Langmuir, **26**, 16134–16140.

58. Buck, M.E., Schwartz, S.C., and
Lynn, D.M. (2010) *Chem. Mater.*, **22**,
6319–6327.

59. Broderick, A.H., Lockett, M.R., Buck,
M.E., Yuan, Y., Smith, L.M., and
Lynn, D.M. (2012) *Chem. Mater.*, **24**,
938–945.

60. Buck, M.E. and Lynn, D.M. (2011) *Adv.
Eng. Mater.*, **13**, B343–BB52.

61. Broderick, A.H., Azarin, S.M., Buck,
M.E., Palecek, S.P., and Lynn,
D.M. (2011) *Biomacromolecules*, **12**,
1998–2007.

62. Buck, M.E. and Lynn, D.M. (2010) *ACS
Appl. Mater. Interfaces*, **2**, 1421–1429.

63. Saurer, E.M., Flessner, R.M., Buck,
M.E., and Lynn, D.M. (2011) *J. Mater.
Chem.*, **21**, 1736–1745.

64. Buck, M.E. and Lynn, D.M. (2010) *Adv.
Mater.*, **22**, 994–998.

65. Tocce, E.J., Broderick, A.H., Murphy,
K.C., Liliensiek, S.J., Murphy, C.J.,
Lynn, D.M., and Nealey, P.F. (2012) *J.
Biomed. Mater. Res. A*, **100**, 84–93.

66. Liu, Y., Bruening, M.L., Bergbreiter,
D.E., and Crooks, R.M. (1997) *Angew.
Chem., Int. Ed. Engl.*, **36**, 2114–2116.

67. Huck, W.T.S., Yan, L., Stroock, A.,
Haag, R., and Whitesides, G.M. (1999)
Langmuir, **15**, 6862–6867.

68. Dai, J., Sullivan, D.M., and Bruening,
M.L. (2000) *Ind. Eng. Chem. Res.*, **39**,
3528–3535.

69. Kim, Y.-S., Liao, K.-S., Jan, C.J.,
Bergbreiter, D.E., and Grunlan, J.C.
(2006) *Chem. Mater.*, **18**, 2997–3004.

70. Tian, Y., He, Q., Tao, C., Cui, Y.,
Ai, S., and Li, J. (2006) *J. Nanosci.
Nanotechnol.*, **6**, 2072–2076.

71. Puniredd, S.R. and Srinivasan, M.P.
(2007) *J. Colloid Interface Sci.*, **306**,
118–127.

72. Liao, K.-S., Wan, A., Batteas, J.D., and
Bergbreiter, D.E. (2008) *Langmuir*, **24**,
4245–4253.

73. Gill, R., Mazhar, M., Félix, O., and
Decher, G. (2010) *Angew. Chem. Int.
Ed. Engl.*, **49**, 6116–6119.

74. Liang, Z. and Wang, Q. (2004) *Langmuir*, **20**, 9600–9606.

75. Liang, Z., Dzienis, K.L., Xu, J., and
Wang, Q. (2006) *Adv. Funct. Mater.*, **16**,
542–548.

76. Park, H.J., Kim, J., Chang, J.Y.,
and Theato, P. (2008) *Langmuir*, **24**,
10467–10473.

77. Seo, J., Schattling, P., Lang, T.,
Jochum, F., Nilles, K., Theato, P.,
and Char, K. (2010) *Langmuir*, **26**,
1830–1836.

78. Serizawa, T., Nanameki, K., Yamamoto,
K., and Akashi, M. (2002) *Macromolecules*, **35**, 2184–2189.

79. Serizawa, T., Nakashima, Y., and
Akashi, M. (2003) *Macromolecules*, **36**,
2072–2078.

80. Serizawa, T., Matsukuma, D.,
Nanameki, K., Uemura, M., Kurusu, F.,
and Akashi, M. (2004) *Macromolecules*,
37, 6531–6536.

81. Major, J.S. and Blanchard, G.J. (2002)
Chem. Mater., **14**, 2574–2581.

82. Major, J.S. and Blanchard, G.J. (2002)
Chem. Mater., **14**, 4320–4327.

83. Feng, Z., Fan, G., Wang, H., Gao, C.,
and Shen, J. (2009) *Macromol. Rapid
Commun.*, **30**, 448–452.

84. Russell, R.J., Sirkar, K., and Pishko, M.V. (2000) *Langmuir*, **16**, 4052–4054.

85. Dyer, M.A., Ainslie, K.M., and Pishko, M.V. (2007) *Langmuir*, **23**, 7018–7023.

86. Ford, J., Marder, S.R., and Yang, S. (2009) *Chem. Mater.*, **21**, 476–483.

87. Bergbreiter, D.E., Simanek, E.E., and Owsik, I. (2005) *J. Polym. Sci., Part A: Polym. Chem.*, **43**, 4654–4665.

88. Yoon, M., Kim, Y., and Cho, J. (2011) *ACS Nano*, **5**, 5417–5426.

89. Feng, Z., Wang, Z., Gao, C., and Shen, J. (2007) *Adv. Mater.*, **19**, 3687–3691.

90. Hou, S., Wang, J., and Martin, C.R. (2005) *Nano Lett.*, **5**, 231–234.

91. Tian, Y., He, Q., Cui, Y., and Li, J. (2006) *Biomacromolecules*, **7**, 2539–2542.

92. Tong, W., Gao, C., and Möhwald, H. (2006) *Macromol. Rapid Commun.*, **27**, 2078–2083.

93. Duan, L., He, Q., Yan, X., Cui, Y., Wang, K., and Li, J. (2007) *Biochem. Biophys. Res. Commun.*, **354**, 357–362.

94. Tong, W., Gao, C., and Möhwald, H. (2008) *Polym. Adv. Technol.*, **19**, 817–823.

95. Duan, L., Qi, W., Yan, X., He, Q., Cui, Y., Wang, K., Li, D., and Li, J. (2009) *J. Phys. Chem. B*, **113**, 395–399.

96. Manna, U., Dhar, J., Nayak, R., and Patil, S. (2010) *Chem. Commun.*, **46**, 2250–2252.

97. Zhang, G., Dai, L., and Ji, S. (2011) *AIChE J.*, **57**, 2746–2754.

98. Mu, B., Lu, C., and Liu, P. (2011) *Colloids Surf. B Biointerfaces*, **82**, 385–390.

99. Faure, E., Lecomte, P., Lenoir, S., Vreuls, C., Van De Weerdt, C., Archambeau, C., Martial, J., Jérôme, C., Duwez, A.-S., and Detrembleur, C. (2011) *J. Mater. Chem.*, **21**, 7901–7904.

100. Major, J.S. and Blanchard, G.J. (2001) *Langmuir*, **17**, 1163–1168.

101. Zhang, F. and Srinivasan, M.P. (2005) *Colloids Surf. A: Physicochem. Eng. Aspects*, **257–258**, 509–514.

102. Zhang, F., Jia, Z., and Srinivasan, M.P. (2005) *Langmuir*, **21**, 3389–3395.

103. Ma, Y., Qian, L., Huang, H., and Yang, X. (2006) *J. Colloid Interface Sci.*, **295**, 583–588.

104. Levy, T., Déjugnat, C., and Sukhorukov, G.B. (2008) *Adv. Funct. Mater.*, **18**, 1586–1594.

105. Ding, Z., Guan, Y., Zhang, Y., and Zhu, X.X. (2009) *Soft Matter*, **5**, 2302–2309.

106. Yao, H., Chang, F., and Hu, N. (2010) *Electrochim. Acta*, **55**, 9185–9192.

107. Chan, E.W.L., Lee, D.-C., Ng, M.-K., Wu, G., Lee, K.Y.C., and Yu, L. (2002) *J. Am. Chem. Soc.*, **124**, 12238–12243.

108. Lee, D.-C., Chang, B.-J., Morales, G.M., Jang, Y.A., Ng, M.-K., Heller, S.T., and Yu, L. (2004) *Macromolecules*, **37**, 1849–1856.

109. Park, M.-K., Lee, D.-C., Liang, Y., Lin, G., and Yu, L. (2007) *Langmuir*, **23**, 4367–4372.

110. Kim, J., Wacker, B.K., and Elbert, D.L. (2007) *Biomacromolecules*, **8**, 3682–3686.

111. Zhang, Y., Yang, S., Guan, Y., Cao, W., and Xu, J. (2003) *Macromolecules*, **36**, 4238–4240.

112. Watanabe, S. and Regen, S.L. (1994) *J. Am. Chem. Soc.*, **116**, 8855–8856.

113. Kang, E.-H., Bu, T., Jin, P., Sun, J., Yang, Y., and Shen, J. (2007) *Langmuir*, **23**, 7594–7601.

114. Appoh, F.E. and Kraatz, H.-B. (2009) *J. Appl. Polym. Sci.*, **111**, 709–723.

115. Byrd, H., Holloway, C.E., Pogue, J., Kircus, S., Advincula, R.C., and Knoll, W. (2000) *Langmuir*, **16**, 10322–10328.

116. Belghoul, B., Welterlich, I., Maier, A., Toutianoush, A., Rabindranath, A.R., and Tieke, B. (2007) *Langmuir*, **23**, 5062–5069.

117. Krass, H., Papastavrou, G., and Kurth, D.G. (2003) *Chem. Mater.*, **15**, 196–203.

118. Blasini, D.R., Flores-Torres, S., Smilgies, D.-M., and Abruña, H.D. (2006) *Langmuir*, **22**, 2082–2089.

119. Zhang, G., Ruan, Z., Ji, S., and Liu, Z. (2010) *Langmuir*, **26**, 4782–4789.

120. Welterlich, I. and Tieke, B. (2011) *Macromolecules*, **44**, 4194–4203.

121. Maier, A. and Tieke, B. (2011) *J. Phys. Chem. B*, **116** (3), 925–934.

122. South, C.R., Piñón, V., and Weck, M. (2008) *Angew. Chem. Int. Ed.*, **47**, 1425–1428.

123. South, C.R. and Weck, M. (2008) *Langmuir*, **24**, 7506–7511.

124. Kolb, H.C., Finn, M.G., and Sharpless, K.B. (2001) *Angew. Chem. Int. Ed.*, **40**, 2004–2021.

125. Kolb, H.C. and Sharpless, K.B. (2003) *Drug Discovery Today*, **8**, 1128–1137.

126. Binder, W.H. and Sachsenhofer, R. (2007) *Macromol. Rapid Commun.*, **28**, 15–54.

127. Moses, J.E. and Moorhouse, A.D. (2007) *Chem. Soc. Rev.*, **36**, 1249–1262.

128. Binder, W.H. and Sachsenhofer, R. (2008) *Macromol. Rapid Commun.*, **29**, 952–981.

129. Peyratout, C.S. and Dahne, L. (2004) *Angew. Chem. Int. Ed.*, **43**, 3762–3783.

130. Angelatos, A.S., Katagiri, K., and Caruso, F. (2006) *Soft Matter*, **2**, 18–23.

131. Johnston, A.P.R., Cortez, C., Angelatos, A.S., and Caruso, F. (2006) *Curr. Opin. Colloid Interface Sci.*, **11**, 203–209.

132. De Geest, B.G., Sanders, N.N., Sukhorukov, G.B., Demeester, J., and De Smedt, S.C. (2007) *Chem. Soc. Rev.*, **36**, 636–649.

133. Schild, H.G. (1992) *Prog. Polym. Sci.*, **17**, 163–249.

134. Schmaljohann, D. (2006) *Adv. Drug Deliv. Rev.*, **58**, 1655–1670.

135. Rasmussen, J.K., Heilmann, S.M., and Krepski, L.R. (1988) in *Encyclopedia of Polymer Science and Engineering*, vol. **11**, 2nd edn, (eds H.F. Mark, N. Bikales, C.G. Overberger, G. Menges), Wiley-Interscience, New York, pp. 558–571.

136. Heilmann, S.M., Rasmussen, J.K., and Krepski, L.R. (2001) *J. Polym. Sci., Part A: Polym. Chem.*, **39**, 3655–3677.

137. Barner-Kowollik, C., Du Prez, F.E., Espeel, P., Hawker, C.J., Junkers, T., Schlaad, H., and Van Camp, W. (2011) *Angew. Chem. Int. Ed.*, **50**, 60–62.

138. Guichard, B., Noel, C., Reyx, D., Thomas, M., Chevalier, S., and Senet, J.P. (1998) *Macromol. Chem. Phys.*, **199**, 1657–1674.

139. Zhang, J. and Lynn, D.M. (2007) *Adv. Mater.*, **19**, 4218–4223.

140. Kinsinger, M.I., Buck, M.E., Campos, F., Lynn, D.M., and Abbott, N.L. (2008) *Langmuir*, **24**, 13231–13236.

141. Messman, J.M., Lokitz, B.S., Pickel, J.M., and Kilbey, S.M. II (2009) *Macromolecules*, **42**, 3933–3941.

142. Sun, B., Liu, X., Buck, M.E., and Lynn, D.M. (2010) *Chem. Commun.*, **46**, 2016–2018.

143. Buck, M.E. and Lynn, D.M. (2012) *Polym. Chem.*, **3**, 66–80.

144. Ostuni, E., Chapman, R.G., Holmlin, R.E., Takayama, S., and Whitesides, G.M. (2001) *Langmuir*, **17**, 5605–5620.

145. Orner, B.P., Derda, R., Lewis, R.L., Thomson, J.A., and Kiessling, L.L. (2004) *J. Am. Chem. Soc.*, **126**, 10808–10809.

146. Ostuni, E., Yan, L., and Whitesides, G.M. (1999) *Colloid Surf. B*, **15**, 3–30.

147. Wang, G., Fang, Y., Kim, P., Hayek, A., Weatherspoon, M.R., Perry, J.W., Sandhage, K.H., Marder, S.R., and Jones, S.C. (2009) *Adv. Funct. Mater.*, **19**, 2768–2776.

148. Kanaya, T., Takahashi, N., Nishida, K., Seto, H., Nagao, M., and Takeda, T. (2005) *Phys. Rev. E*, **71**, 011801.

149. Manna, U. and Patil, S. (2009) *J. Phys. Chem. B*, **113**, 9137–9142.

150. Sato, K., Yoshida, K., Takahashi, S., and Anzai, J.-I. (2011) *Adv. Drug Deliv. Rev.*, **63**, 809–821.

Index